UNIVERSITY OF SOUTHAMPTON

FACULTY OF ENGINEERING, SCIENCE AND MATHEMATHICS

School of Civil Engineering and the Environment

Quantification of Factors Affecting Rate and Magnitude of Secondary Settlement of Landfills

by

Lyudmila K. Ivanova

Thesis for the degree of Doctor of Philosophy

June 2007

UNIVERSITY OF SOUTHAMPTON

ABSTRACT

FACULTY OF ENGINEERING, SCIENCE AND MATHEMATICS
SCHOOL OF CIVIL ENGINEERING AND THE ENVIRONMENT

Doctor of Philosophy

QUANTIFICATION OF FACTORS AFFECTING RATE AND MAGNITUDE OF SECONDARY SETTLEMENT OF LANDFILLS

by Lyudmila Kaloianova Ivanova

The biodegradation of solid waste materials is the main cause of secondary settlement in landfills and has a significant impact on the post-closure performance of landfill capping systems. The objectives of this study were: to review previous work on secondary settlement of landfills; to provide a quantitative understanding of the influence of waste composition, depth and gas production rate on the rate of secondary settlement under constant applied load; to evaluate changes in chemical composition of the leachate as the waste degrades; and to provide data for the validation of quantitative models to explain the laboratory tests .

To accomplish this, laboratory scale experiments were conducted to estimate waste settlement rates under different operational-management practices including leachate recirculation and the addition of synthetic methanogenic mineral media and an anaerobic microbial seed culture. The effect of these practices on settlement rates and magnitude was evaluated using four purpose-designed test cells-Consolidating Anaerobic Reactors (CARs) in which a waste sample was subjected to a constant applied load to simulate the waste overburden effect. A detailed characterisation of the waste and its associated chemical and physical properties was a key component of the study. Inter-relationships between the onset of biodegradation of the waste and associated chemical parameters are discussed in the context of their influences on the degree and rate of settlement of the waste material.

Prior to the establishment of the CARs, the degradability of the waste selected for the study was quantified by means of a series of Biochemical Methane Potential (BMP) tests. Studies also allowed the determination of the most efficient proportion of anaerobically digested microbial seed to promote rapid methanogenic conditions in the CAR which was found to be 10% (v/v). In both cases, the reactors were sacrificed at various stages in the biodegradative process to allow the waste sample to be analysed for total carbon to facilitate the calculation of C mass balance for the biodegradative process.

The long-term secondary settlement was found to be dependent on waste depth. The increased stress (150kPa) led to a 20% increase in the rates of long-term secondary compression in comparison to a stress level of 50 kPa. For the fresh waste tested in this study (CARs 2, 3 & 4) secondary settlement due to biodegradation was found to be of comparable magnitude to the component of secondary settlement caused by mechanical creep. The organic content of the waste was found to directly affect the volume of the gas produced which in turn directly affected the magnitude of secondary settlement observed in the CARs. The enhanced biodegradative conditions were found to accelerate the waste biodegradation processes in the CARs and hence the establishment of methanogenic conditions. The removal of all the sulphate in the leachate resulted in a simultaneous increase in the rate of gas production. The rate of biodegradation was found to vary with depth. This was established by obtaining core samples from the CARs at the end of the test. The BMP test results indicate that changes in values for NDF, ADF, cellulose, (C+H)/L ratio and methane potential for the BMP test samples to be interrelated. The good statistical correlation between all the chemical parameters mentioned above suggests that monitoring only one of these parameters may be sufficient to provide an accurate prediction of the biodegradability of a fresh MSW sample without extensive monitoring methods. The data collected in this study is a good medium term dataset that will provide modellers with the ability to compare their predictions and promote the development of more accurate models.

List of figures

List of tables

List of equations

Acknowledgements

The work presented in this thesis was made possible with the support of many people. I would like to express my gratitude to Dr David Richards, Dr David Smallman and Dr Richard Beaven for their generous guidance, encouragement and patience throughout this period of research.

I am grateful to Prof William Powrie for his patronage throughout the development of this project.

I would also like to thank the following people: Dr John Robinson (Queen Merry, University of London) who shared his experience in the field of microbiology and for his support; Prof Stoyan Stoyanov for his encouragement and support (University of Chemical Technology and Metallurgy, Sofia, Bulgaria); Harvey Skinner, Julie Vaclavic and Ken Yates (University of Southampton) for their technical assistance in the experimental phases of the work.

Finally, I would like to thank my parents, family and friends for their love and support, and especially my beloved husband Rumen, who has made this possible for me.

The opportunity to work at the University of Southampton and to undertake this research was possible through the funding of EPSRC.

Notation

This notation only contains those symbols which have more-or-less universal meaning within the construction industry. Other terms which are used within this thesis are defined as they occur, within the section to which they are specifically applicable.

Symbol	*Parameter*	*Units*
a	Primary compressibility parameter (section 4.2.4)	1/day
b	Secondary compressibility parameter	1/day
C_c	Primary compression index	/
C_R	Modified primary compression index	/
C_s	Primary recompression index (section 4.2.1)	/
C_α	Secondary compression index	/
$C_{\alpha\varepsilon}$	Rate of secondary compression	/
$C_{\alpha\varepsilon 1}$	Intermediate secondary compression index	/
$C_{\alpha\varepsilon 2}$	Long-term secondary compression index	/
e	Void ratio. Subscripts may be used as follows: o (initial, before compression), I (after initial compression), p (after primary compression), and s (after secondary compression).	/
E	Modulus of elasticity	kPa
h	Waste height. Subscripts may be used as follows: i (after initial compression), p (after primary compression), and s (after secondary compression).	m
h_o	Initial (before loading) thickness of the waste layer under consideration	m
h_{ref}	Reference height of waste at time t_{ref}	m
k	Rate constant for mechanical creep, $k = \lambda/b$	/
k	Hydraulic conductivity	m/s
q	Biogas production rate	m^3/ m^3/year
r_s	Creep resistance (section 4.2.2 B)	/
S	Secondary compression potential constant (section 4.2.2 B)	/
s	Degree of saturation = volume of water/ volume of voids = V_w/ V_v	/
T	Median age of a fill column (section 4.2.4)	months
t	Time since load application. Subscripts may be used as follows: i (after initial compression), p (after primary compression), and s (after secondary compression).	days
t_c	Time of construction of a waste column (cover included)	month
t_k	Time to complete primary compression	
t_o	Initial time	days

t_{ref}	Reference time introduced to make time dimensionless (t_r = 1day)	
ult	Subscript denoting the ultimate value of a parameter (e.g. settlement)	/
V	Volume (total)	m^3
V_a	Volume of air voids in waste sample	m^3
V_s	Volume of waste solids in waste sample	m^3
V_d	Volume of drainable voids	m^3
V_w	Volume of water in waste sample	m^3
x	Coefficient related to degradation (section 4.2.2)	/
Y	Biomass yield	g cells COD/ g COD utilised
Δ	Prefix denoting increment (e.g., of stress, strain or height)	/
Δh	Settlement occurring in the layer under consideration	m
Δh_i	Settlement due to initial compression	m
Δh_p	Settlement due to primary compression	m
Δh_s	Settlement due to secondary compression	m
Δt	Time interval	sec
$\Delta\sigma'$	Increase in vertical stress due to the fill placement	kPa
α_b	Biocompression rate parameter (section 4.2.4)	/
α_c	Creep compression rate parameter (section 4.2.4)	/
β	Slope of the linear section	/
ε	Settlement rate. Subscripts may be used to indicate the compression: i (initial), p (primary), and s (secondary).	mm/month
ε_{bio}	Compression due to biodegradation (section 4.5.1)	kPa
λ/b	Rate of secondary compression (section 4.3.1)	1/day
ρ	Mass density. Subscripts may be used as follows: s (for the density of waste solids), w (for the density of water = 1000kg/m^3 at 4°C compression).	kg/m^3
ρ_o	Initial rate of compression (section 4.4.2)	mm/month
σ'	Change in compressive stress	kPa
σ	Effective vertical stress or total stress	kPa
σ'_o	Existing vertical effective stress at midpoint in the layer	kPa
σ'_p	Preconsolidation pressure	kPa
σ_v	Vertical stress	kPa
ω	Waste water content. Subscripts may be used as follows: i (after initial compression), p (after primary compression), and s (after secondary compression).	/

List of abbreviations

ADF	Acid detergent fibre
ADL	Acid digestible lignin
AG	Aged waste sample
AOAC	Association of Official Agricultural Chemists
ARFC	Agricultural and Food Research Council
ASTM	American Society for Testing and Materials
BMP	Biochemical methane potential
BS	British Standard
C/N	Carbon/nitrogen ratio
CANON	Completely autotrophic nitrogen-removal over nitrite
CARs	Consolidating anaerobic reactors
(C+H)/L	Cellulose plus hemicellulose to lignin ratio
COD	Chemical oxygen demand
DRI	Dynamic respiration index
DM	Dry matter content
DNRA	Dissimilatory nitrate reduction to ammonium
EDWS	European Drinking Water Standards
EPA	United States Environmental Protection Agency
EPSRC	Engineering and Physical Science Research Council
ESART	Environmental Services Association Research Trust
FID	Flame ionisation detection
FR	Fresh waste sample
GC	Gas chromatography
HDPE	High density polyethylene
IC	Inorganic carbon
ICPMS	Inductively coupled plasma mass spectroscopy
IRD	Infrared detector
ISBN	International standard book number
LDAT	Landfill degradation and transport model
LOI	Loss on ignition
MARS	Microwave accelerated reaction system
MF	Microfibres filter
MOCLA	Model for organic chemicals in landfills
MSOR	Mechanical separation organic residues
MSW	Municipal solid waste
NDF	Neutral detergent fibre
NJIT	New Jersey Institute of Technology
NREL	National Renewable Energy Laboratory
OC	Organic content

OHPAs	Obligate hydrogen oxidising acetogens
PP	Polypropylene
PSD	Particle size distribution
PVC	Polyvinyl chloride
RLS	Rate-limiting step
SRB	Sulphate-reducing bacterial
STP	Standard temperature and pressure
TC	Total carbon
TCD	Thermal conductivity detector
TDOC	Total dissolved organic carbon
TN	Total nitrogen
TOC	Total organic carbon
TS	Total solids
TVA	Total volatile acids
UUCETF	Urban Consortium Energy Foundation
VFAs	Volatile fatty acids
VS	Volatile solids

Chapter 1

Introduction

1.1. Background

Landfill is by far the most common method of disposal for waste in the UK. About 120 million tonnes of all controlled wastes per year are landfilled in the UK, and includes 90% of all household waste, 85% of all commercial waste, 63% of all construction and demolition waste and 73% of all other industrial waste (Williams, 2002). Approximately 10% (4% solid content) of wet sludge (equivalent to 3.5 million tonnes per year) is also disposed of to landfill (Williams, 2002). However, the implementation of Landfill Directive Waste Acceptance Criteria (WAC) (adopted in December 2002) had an impact on the waste management industry in terms of the acceptable materials that are allowed to go to landfills of biodegradable wastes. The Landfill Directive requires that individual landfills accept only hazardous waste or non-hazardous waste or inert waste hence ending the practice (since July 2004) of co-disposal. The move to dedicated landfills for hazardous waste has dictated tighter controls over site engineering and composition of the waste going into the sites. The Directive specifically restricts waste inputs in two ways: by explicitly banning certain wastes from landfill (e.g., sewage sludge); and by applying acceptance criteria to waste intended for landfill.

Landfilling in the UK is assisted by the fact that the underlying geology and the hydrogeological conditions provide low permeability sites for the widespread deposition of wastes. Consequently, the UK has a long and established tradition of landfilling of wastes, as a low-cost disposal option. Currently there are approximately 4000 licensed landfill sites in the UK (Williams, 2002).

A major issue affecting the operation and future reuse of landfill is waste settlement (Sowers, 1973; Wall and Zeiss, 1995). The reduction in the number of viable MSW

landfill facilities along with a gen increase in their size (related to economic viability) has made it imperative to achieve the maximum utilization of the landfill voids. In this regard, the exploitation of settlement can provide additional volume which can be utilised. On the other hand, landfill settlement is a subject that is increasing in importance as the need to understand how landfill sites behave in the long-term is required in order to allow the redevelopment of potential closed landfill sites to bring them back into beneficial use (e.g., sports, pitches and leisure parks). Predicting settlement rates and magnitudes is currently difficult analytically, as municipal fill undergoes large amounts of compression due to the combined effects of load, creep and biodegradation-induced settlement. These effects are not easily incorporated into traditional settlement calculations (Wall & Zeiss, 1995). Secondary settlement due to waste biodegradation can continue for many years following closure and can have a devastating effect on the integrity of landfills and possibly lead to localized failure of the capping system (Emberton and Parker, 1987). This may in turn lead to water ingress and enhanced leachate generation, significantly increasing the risk of harm to the environment.

This study focuses on the quantification of factors affecting settlement of landfills and the following will concentrate on the main problems arising in more detail.

A number of studies have investigated settlement processes in landfill. Sowers (1973) identified mechanisms that contribute to the settlement that occurs in landfills and that these processes are time-dependant, in some cases, extending over several decades. Sowers (1973) stated that the waste is compressed by its own-weight overburden, and external loads such as that induced by compaction, leading to a reduction in the waste voids. In addition, because of the difference in particle size of the waste materials, smaller particles migrate into the void between the larger particles, especially during compaction. A large reduction in volume also occurs due to waste degradation, through biological and chemical processes. He concluded that the degradation process is complicated involving many interactive factors, such as the waste type and composition, moisture content, temperature, etc. (further summarized by Ling *et al.*, 1998).

The mechanisms that govern waste compressibility are due to the deformability of individual waste particles as well as the heterogeneity of the material. Five main mechanisms have been identified as being involved in settlement (Edil e*t al.*, 1990):

i) *Mechanical compression*: Slip, distortion, bending, crushing and reorientation of waste particles as vertical stresses are increased, either during compaction or due to the own weight of the fill;

ii) *Ravelling*: Movement of fine particles into larger voids;

iii) *Physico-chemical changes*: Corrosion, oxidation and combustion;

iv) *Bio-chemical degradation*: Fermentation and decay; and

v) *Interaction*: The above processes interact with each other. For example, volume changes due to mechanical compression may trigger ravelling; VFAs produced during degradation of organic matter may induce corrosion.

The majority of initial settlement is due to mechanical mechanisms (i). Sowers (1973) estimated that the primary settlement due to mechanical processes is completed within a month of waste emplacement. The last four mechanisms (ii, iii, iv & v) are of particular significance in the long term. Sowers (1973) attributed the long-term settlement of refuse fills to secondary compression processes caused by the decaying waste mass within the landfill as a result of the physico-chemical (iii), bio-chemical degradation (iv) and interactive (v) mechanisms which continue until the refuse reaches a stabilized inert condition.

The rate of degradation and degradation processes within the refuse are also affected by a range of landfill management practises. The method of operation can provide increased moisture and nutrients which will enhance degradation, and also influence temperatures in the landfill. The temperature, moisture content, pH, microbial activity and landfill gas present or generated within the landfill are environmental factors that affect the magnitude of the settlement. Waste settlement can also be influenced by other factors such as:

- *Initial void ratio of the waste*: larger initial densities due to compaction reduce both the initial settlement as well as the rates of primary and secondary settlement;
- *Waste type and organic content*: the higher the organic content of the waste, the greater is the rate of long-term secondary settlement;
- *Landfill depth and rate of filling*: in general, deeper landfills would be expected to exhibit greater overall settlement values due to greater weight; rapid waste emplacement will lead to more rapid settlement in the early stages; and

- *Moisture content, temperature and landfill gas extraction*: the higher the moisture content and temperature of the waste, the greater the rate of degradation, which in turn directly affects the overall magnitude of settlement; active landfill gas extraction is known to accelerate settlement.

The five landfill settlement mechanisms put forward by Sowers (1973) are difficult to distinguish individually so are usually interpreted using a temporal classification of *initial*, *primary* and *secondary settlement*. However, Grisolia and Napoleoni (1995) further divided secondary settlement into three sub-stages (Figure 1.1):

- *Intermediate* secondary settlement;
- *Long-term* secondary settlement; and
- *Residual* settlement.

Initial settlement is instant settlement that occurs immediately after an external load is applied in the landfill i.e. emplacement of further waste, and the main mechanism is mechanical in nature. It is generally associated with the immediate compaction of void space and particle crushing due to the superimposed load. Initial settlement values of between 12 and 17% have been reported in a limited number of household waste sites (RPS Clouston and Wey College) in the UK with long term projected values of approximately 20% (Waste Management Paper, 1995). This guidance manual suggests values of 15-20% as being typical of the surcharge allowance that may need to be made when considering the void capacity and final pre-settlement contours of a household waste landfill.

Primary settlement is due to mechanical compression by crushing, distortion, reorientation, bending and/or breaking of waste particles as vertical stresses are increased, either during machine compaction or due to the self weight of the fill as further material is deposited. Primary settlement due to self weight effects would probably occur during or soon after placement, usually over a period of days (Bleiker *et al.*, 1995; Beaven & Powrie, 1995). Primary settlement would not therefore affect the post-closure behaviour of a landfill and its capping system.

Secondary settlement takes place over a longer period of time (years) and is due to both creep within the refuse skeleton which may be exacerbated by the loss of structure and the strength of waste due to biological decay (Sowers, 1973) and loss of solid mass

caused by the degradation of organic components and transformation into liquid and gas phases.

Secondary settlement was divided into three sub-stages (Grisolia and Napoleoni, 1995). In the early stages of secondary settlement (*intermediate secondary settlement*), the settlement is dominated by mechanical interactions due to delayed compression of the waste.

In the second stage of secondary settlement (*long-term secondary settlement*), the settlement rates are higher possibly due to the added effects of degradation of the readily biodegradable fraction of the waste (Bjarngard and Edgers, 1990). It is now recognized that secondary settlement due to waste biodegradation has a significant impact on the post-closure performance of landfills. Settlement due to biological processes depends upon a number of factors such as waste composition, density and waste depth, waste pre-treatment, active gas extraction, temperature, moisture content and leachate mobility (Dixon & Jones, 2004). As a process, it can continue for a considerable period after site closure. The action of microbial activity on waste, results in the production of landfill gases (methane and carbon dioxide), and considerably influences the composition of leachate. The conversion of waste mass by microbial activity will cause a significant decrease in volume of filled waste, leading to secondary settlement in landfills (Gabr *et al.*, 2000). According to a study conducted by Coduto and Huitric (1990) biological degradation can account for settlement of between 18 - 24% of the refuse thickness. Secondary compression becomes more evident when filling of the landfill is finished (Edil *et al.*, 1990).

In the last stage of secondary settlement (*residual settlement*), the settlement is induced by the residual deformation of the waste due to both delayed mechanical reorientation and delayed degradation of those organic components which are more resistant to biodegradation over the previous stages (Grisolia and Napoleoni, 1995).

Grisolia and Napoleoni's (1995) classification of secondary settlement (above) has been adopted and applied to the data generated in this study. It should be noted that the settlement observed in this study during filling and loading was considered to be caused by *initial* and *primary* compression of the waste due to a lack of adequate compaction during the sample preparation stage, and was not included in the determination of settlement.

The composition of the waste contained within a landfill is highly dependent on the local conditions. Each town or city produces different waste composition, since these waste inputs depend on socio-economic factors, types of industry and level of industrialisation, geographic location, climate, level of consumption, the collection system, population density, the extent of recycling, legislative controls and public attitudes generally. It is this variability in waste composition that makes ultimate settlement predictions extremely difficult to calculate when taking a varying waste mass as a whole. These changes also need to be taken into consideration during settlement calculations.

Typical long-term settlement values for municipal solid waste (MSW) are 15-20% reduction in height, although values of up to 40% have been reported where there is a high organic content (OC) in the waste (Tchobanoglous and O'Leary, 1994). Settlement can take place over periods of up to 50 years, but the major settlement period (up to 90%) typically occurs within the first 5 years of the final emplacement of the waste. If, some years after the completion of filling, the site is considered for building development, the stability of structures built on the surface of the reclaimed land is clearly a major concern.

There is very little guidance available for designers and regulators to assess the impact of waste settlement on cap performance and/or the post-closure maintenance requirements of landfills. This poses a serious threat to the long-term integrity of landfill sites, with potentially damaging consequences for the environment. By understanding the processes governing secondary settlement in landfills it will be possible in the future to define more easily the end of the post-closure monitoring period.

1.2. Objectives

The main deliverables of the research were:

- to review previous work on secondary settlement of landfills;
- to determine the optimum sewage seed addition to be applied in all CAR tests;
- to obtain a quantitative understanding of the influence of the organic fraction of waste, temperature, depth and gas production rate on the rate of secondary settlement under constant applied load;
- to evaluate details of the changes in chemical composition of the leachate as the waste degrades;

- to gain further information on the chemical composition of the waste material at the end of the experiment in order to be able to assess variability in the degradation of the waste body;
- to predict the rate and potential of MSW biodegradation in the CARs filled with specific type of wastes;
- to determine whether there is a correlation between settlement and biodegradation;
- to assess the performance of various settlement models by its ability to simulate settlement results from this study and the accuracy of the simulation with specific type of wastes; and
- to generate good quality data set for the validation of other quantitative models.

1.3. Thesis outline

This thesis is divided into seven chapters. In this Introduction chapter (*Chapter 1*), the main objectives of this research are outlined (section 1.2), followed by an overview of the basic mechanisms of the anaerobic biodegradation of waste organic matter that result in leachate production, highlighting the factors that influence waste degradation in landfills (*Chapter 2*).

Chapter 3 provides information on the engineering properties of waste; this is required to investigate and quantify their influence on the rate and magnitude of secondary settlement in landfills.

Chapter 4 is a detailed literature survey on the mechanisms causing settlement in landfills. Investigations carried out by other researchers were divided into settlement modelling, field observation and laboratory and pilot-scale studies.

Chapter 5 provides information on the waste samples tested and describes the design and laboratory set up of the experimental reactors used in this study. The improvements in their design made as a part of this research are also outlined. In addition, the chapter reviews the analytical methods and experimental procedures applied to investigate, understand and quantify factors affecting biodegradation and landfill settlement processes. The determination of the most efficient proportion (v/v) of anaerobically digested microbial seed to promote rapid methanogenic conditions in the experimental reactors is also described.

Chapter 6 and Chapter 7 summarise and discuss the experimental results involving both aged and fresh MSW, respectively. Waste settlement rates are estimated under different operational-management practices including leachate recirculation, the addition of a synthetic mineral media and a microbial bacterial seed. Inter-relationships between the onset of biodegradation of the waste and associated chemical parameters are discussed in the context of their influences on the degree and rate of settlement of the waste material. In addition, changes in the composition of the leachate during waste biodegradation with regard to the removal of the organic substrate and the reduction of total organic carbon (TOC), inorganic carbon (IC), dissolved organic carbon (DOC), volatile fatty acids (VFAs), heavy metals, and various cations and anions are presented to allow the inter-relationship between biodegradation and settlement to be established. The volumes of the gas produced are reported and compared with the theoretical gas generation rates. Predictions of the rate and potential of waste biodegradation in the reactors are also given. Data on the chemical composition of the waste material retrieved from the test reactors filled with fresh MSW on their dismantling is provided in *Chapter 7*.

Chapter 8 presents settlement interpretations of the experimental results using five models: the Gibson and Lo (1961) model; the Sowers (1973) model; the Power Creep Law (Edil *et al.*, 1990) model; the Hyperbolic Law (Ling *et al.*, 1998) model; and the biomechanical model (Park and Lee, 1997). The results are compared with those obtained by other researchers and a discussion on the mechanisms of secondary settlement made.

Chapter 9 presents the major conclusions drawn from this research, followed by recommendations for future work.

Figures

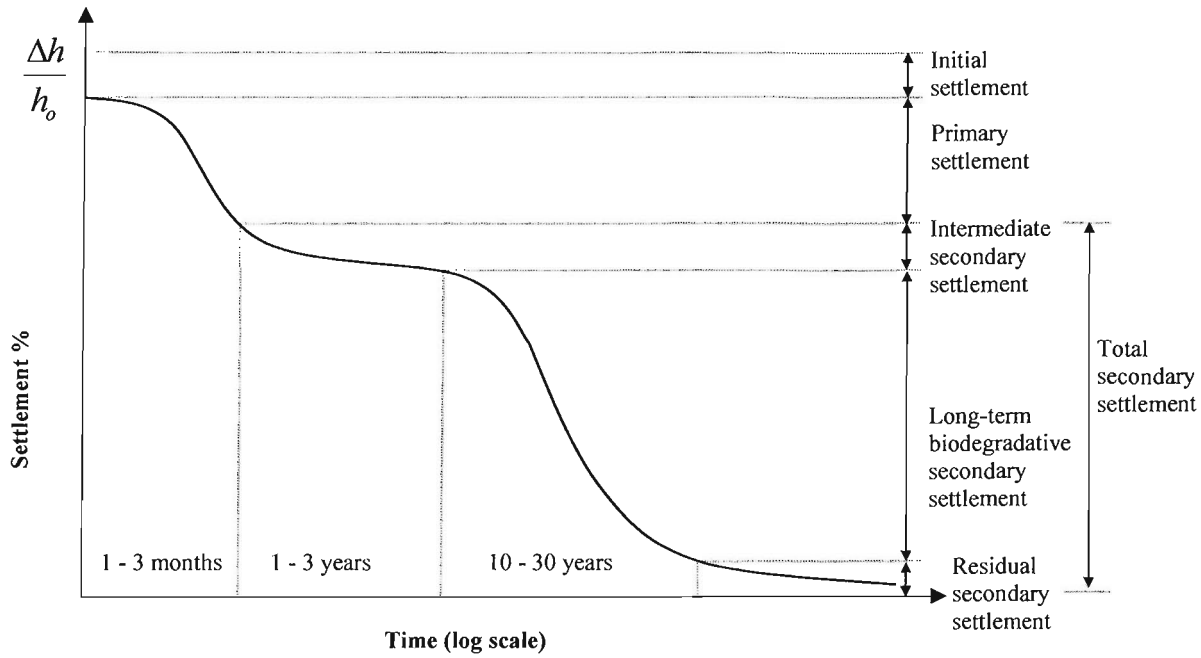

Figure 1.1. Conceptual time-settlement behaviour of waste. (modified from Grisolia and Napoleoni, 1995).

Chapter 2

Biochemical processes of anaerobic degradation

2.1. Introduction

Following emplacement, the organic fraction of MSW will undergo biodegradation by the bacterial populations present in the waste. When excess rainwater percolates through the waste layers in a landfill, leachate is generated. As the leachate moves downwards, under the influence of gravity towards the leachate collection system, the dissolved organic matter in the leachate will be degraded due to the influence of a combination of physical, chemical, and microbial processes in the waste. The biodegradability of the OC in the MSW and the compaction of the waste layers which limits oxygen transfer, makes the landfill primarily an anaerobic environment. In such environments, and those produced artificially in digester or bioreactor cells where the ingress of oxygen is prohibited, large organic molecules are converted into methane and carbon dioxide by the action of bacteria. Under ideal conditions, and in the complete absence of free oxygen, this reaction ultimately leads to methane (CH_4) and carbon dioxide (CO_2). These breakdown processes at the microscopic level are biochemically very complex, involving potentially hundreds of intermediate reactions and compounds. Many of these reactions require additional specific synergistic chemicals, catalysts or enzymes. However, in general terms, it is possible to simplify the overall biochemical reaction to:

Eq. 2.1 $$Organic\ Matter \xrightarrow[ANAEROBIC\ \ DIGESTION]{} CH_4 + CO_2 + N_2 + NH_3 + H_2S$$

This chapter reviews the basic mechanisms of the anaerobic biodegradation of waste where a consortium of microorganisms convert organic matter into methane, carbon dioxide, inorganic nutrients, and recalcitrant humic type materials.

2.2. Biochemical degradation of waste organic matter in landfill

When waste is landfilled, anaerobic biodegradation does not occur immediately. A period ranging from months to years may be necessary for anaerobic conditions to become fully established. Anaerobic waste biodegradation in landfill has been identified as a five-phase process by which solid organic particles are solubilised and converted through methanogenesis to methane and carbon dioxide. These phases are: the aerobic phase; anaerobic acid phase; acetogenic phase; methane phase; and a final aerobic phase which are described below and is summarised in Figure 2.1 (Waste Management Paper, 1995).

2.2.1. Phase I: Aerobic degradation

Aerobic degradation occurs during the initial emplacement of the waste and for a short period following emplacement, the duration of which depends on the availability of oxygen in the trapped air within the waste. The micro-organisms metabolise the available oxygen and a proportion of the organic waste fraction to produce simpler hydrocarbons, carbon dioxide, water and energy. The released energy is in the form of heat (exothermic reactions) and can raise the temperature of the waste to 70-90°C (Waste Management Paper, 1995). However, compacted waste tends to reach lower temperatures due to the lower availability of oxygen. Water and carbon dioxide are the main products, with carbon dioxide released as gas or taken into solution forming carbonic acid, which gives acidity to the leachate. The aerobic stage may last for only a matter of days or weeks depending on the availability of oxygen, which in turn depends on the amount of air trapped in the waste, the degree of waste compaction and how quickly the waste is covered.

2.2.2. Phase II: Acidogenesis

As oxygen becomes depleted, further stages of degradation develop. The aerobic micro-organisms are superseded by other micro-organisms which can tolerate low levels of oxygen (facultative anaerobes) and then, as anaerobic conditions develop, the obligate anaerobic micro-organisms, which include the methane generating organisms (methanogens), become established. These processes are dynamic, each new stage being dependent on the creation of a suitable environment by the preceding stage.

In this second stage of the process, *hydrolysis*, complex insoluble organic polymers, such as carbohydrates, cellulose, proteins and fats, are broken down and made soluble by the extracellular enzymes produced by *hydrolytic bacteria.* This makes them more readily available for use by the *acidogenic bacteria* in the next stage. In general, proteins present in the waste are converted into long-chain fatty acids and complex carbohydrates into simple sugars. The liquefication of these compounds, particularly cellulose, to simple soluble substances is often the rate-limiting step (RLS) in degradation once methanogenesis is established, since bacterial action at this stage proceeds more slowly than in either of the following stages (Boone *et al.*, 1993; Lai *et al.*, 2001 ; Noike *et al.*, 1985). The rate at which hydrolysis takes place is governed by substrate availability, the bacterial population density, temperature and pH. *Acidogenesis* is characterised by the production of acetic acid from the monomers produced in the preceding stage, and other volatile fatty acids (VFAs) which are derived from the biodegradation of protein, fat and carbohydrate components of the waste. The pH falls as the levels of these compounds increase. Carbon dioxide and hydrogen are also evolved as a result of the catabolism of carbohydrates, with the additional potential for the production of methanol and/or other simple alcohols. The production of these different by-products depends upon the environmental conditions and on the particular bacterial species present.

Eq. 2.2 $$C_6H_{12}O_6 + 2H_2O \rightarrow 2CH_3COOH\ (acetic\ acid) + 4H_2 + 2CO_2$$

Eq. 2.3 $$C_6H_{12}O_6 + 2H_2 \rightarrow 2CH_3CH_2COOH\ (propionic\ acid) + 2H_2O$$

Eq. 2.4 $$C_6H_{12}O_6 \rightarrow CH_3CH_2CH_2COOH\ (butyric\ acid) + 2CO_2 + 2H_2$$

Acidogenesis is the energy yielding stage for the hydrolytic and fermentative microorganisms. The temperature within the landfill typically falls to 30-50°C during this stage. Gas concentrations in the waste undergoing Phase II degradation may rise to levels of up to 80% carbon dioxide and 20% hydrogen (Waste Management Paper, 1995).

2.2.3. Phase III: Acetogenesis

In this phase, *acetogenic bacteria* convert the long-chain fatty acids (propionic, butyric, valeric and caproic acids) to acetate, carbon dioxide and hydrogen. The long chain fatty acids are degraded sequentially by subtraction of two-carbon fragments. Fatty acids with an even number of carbon atoms are degraded step-wise to form acetate: for example, one mole of butyric acid is degraded to form two moles of acetate:

Eq. 2.5 $CH_3CH_2CH_2COOH + 2H_2O \rightarrow 2CH_3COOH + 2H_2$

Fatty acids with odd numbers of carbon atoms are degraded to form acetate and propionate: for example, one mole of valeric acid is degraded to one mole of acetate and one mole of propionate:

Eq. 2.6 $CH_3CH_2CH_2CH_2COOH + 2H_2O \rightarrow CH_3COOH + CH_3CH_2COOH + 2H_2$

The propionate can then further broken down to acetate:

Eq. 2.7 $CH_3CH_2COOH + 2H_2O \rightarrow CH_3COOH + CO_2 + 3H_2$

During this stage the gases generated from the waste mass are predominately carbon dioxide and hydrogen. Hydrogen and carbon dioxide production decreases as Phase III progresses. The conversion of the longer chain fatty acids to acetate requires an energy input under standard conditions (25°C, 1 atmosphere pressure, pH=7.0). Acetogenesis must therefore be coupled with energy liberating reactions and to proceed hydrogen must be removed or the concentration of hydrogen maintained at a very low partial pressure (Archer, 1988). Low hydrogen levels promote the methane-generating microorganisms, the methanogens, which generate methane and carbon dioxide from the organic acids and their derivatives generated in the earlier stages. If the hydrogen concentration remains greater than 10^{-4} atmospheres partial pressure the long-chain fatty acids cannot be further degraded and under these circumstances propionic and butyric acids accumulate (acid souring). Consequently, *acetogenesis* can only be maintained if hydrogen utilising organisms such as methane-generating and sulphate-reducing bacteria are active.

The acidic conditions of the acetogenic stage can increase the solubility of metal ions and thus enhance their aqueous concentration in the leachate. In addition, organic acids, chloride ions, ammonium ions and phosphate ions, all in high concentration in the leachate, readily form complexes with metal ions, causing further increases in solubilisation of metal ions. Hydrogen sulphide may also be produced throughout the anaerobic stages as the sulphate compounds in the waste are reduced to hydrogen sulphide by sulphate-reducing bacterial (SRB) microorganisms (Christensen *et al.*, 1996). Insoluble metal sulphides may be a reaction product of the hydrogen sulphide and metal ions in solution. The harmful effects of heavy metals and their principal routes via waste management systems to the environment are discussed further in section 2.2.4.

2.2.4. Phase IV: Methanogenesis

The methanogenesis stage is the main landfill gas generation stage, with the gas composition of typical landfill gas approximately 60% methane and 40% carbon dioxide. Methanogenesis involves the production of methane from the breakdown products formed in the previous stage (Barlaz *et al.*, 2002). This is brought about by obligate anaerobes such as acetogenic bacteria, the growth rate of which is generally slower than the bacteria responsible for the preceding stages. The methane is therefore produced from a number of simple substrates: acetic acid, methanol carbon dioxide and hydrogen. Of these acetate is the most important, since around 75% of the methane produced is the aceticlastic reaction (Eq. 2.8):

Eq. 2.8 $$CH_3COOH \rightarrow CO_2 + CH_4$$

Methane-forming bacteria may also be formed using methanol (Tchobanoglous *et al.*, 2003):

Eq. 2.9 $$CH_3OH + H_2 \rightarrow CH_4 + H_2O$$

Or via carbon dioxide and hydrogen:

Eq. 2.10 $$CO_2 + 4H_2 \rightarrow CH_4 + 2H_2O$$

The hydrogen utilising type of metabolism (Eq. 2.10) releases very small amounts of free energy, that is just enough to sustain cell growth, resulting in very low growth rates (Rovers and Farquhar, 1972). The acetate utilising metabolism (Eq. 2.8) releases slightly more energy and is energetically more favourable (Rovers and Farquhar, 1972). However, under field conditions no energetic advantage has been reported for either reaction (Archer, 1988).

There are other potential substrates for methane-producing bacteria, such as formic acid, but these do not routinely occur in the anaerobic digestion of MSW.

The doubling time of methanogenic bacteria varies from 24 hours to several days (Tchobanoglous *et al.*, 2003). The bacteria also have a low biomass yield (Y), expressed as the amount of biomass produced to the amount of substrate utilised. Values for Y of only 0.046g cells COD/g COD utilised have been calculated for anaerobic systems, compared with 0.59g cells COD/g COD utilised for aerobic (Tchobanoglous *et al.*, 2003) assuming a 60% energy capture efficiency. The biomass yield is directly related with the

free energy released. As shown in Table 2.1, the free energy released during the methanogenic anaerobic process is 3.57kJ/electron equivalent compared with 105kJ/ electron equivalent for aerobic reactions. This significant difference is because when CO_2 is used as a final electron acceptor, instead of O_2, a considerable amount of energy is needed to incorporate CO_2 into the bacterial cells (Tchobanoglous *et al.*, 2003).

Table 2.1. Values for the free energy change during anaerobic and aerobic degradation of organic matter (Tchobanoglous *et al.*, 2003).

Reaction	**Energy released (kJ/mole e⁻)**
Aerobic degradation - oxygen as the electron acceptor	
$\frac{1}{8}CH_3COO^- + \frac{3}{8}H_2O \rightarrow \frac{1}{8}CO_2 + \frac{1}{8}HCO_3^- + H^+ + e^-$	-27.66
$\frac{1}{4}O_2 + H^+ + e^- \rightarrow \frac{1}{2}H_2O$	-78.14
Total: $\frac{1}{8}CH_3COO^- + \frac{1}{4}O_2 \rightarrow \frac{1}{8}CO_2 + \frac{1}{8}HCO_3^- + \frac{1}{8}H_2O$	**-105.82**
Anaerobic degradation - carbon dioxide as the electron acceptor	
$\frac{1}{8}CH_3COO^- + \frac{3}{8}H_2O \rightarrow \frac{1}{8}CO_2 + \frac{1}{8}HCO_3^- + H^+ + e^-$	-27.66
$\frac{1}{8}CO_2 + H^+ + e^- \rightarrow \frac{1}{8}CH_4 + \frac{1}{8}HCO_3^-$	+24.11
Total: $\frac{1}{8}CH_3COO^- + \frac{3}{8}H_2O \rightarrow \frac{1}{8}CH_4 + \frac{1}{4}HCO_3^-$	**-3.57**

Note: The values for the energy released are obtained for the transfer of 1 mole of electrons in oxidation-reduction reactions. The negative sign indicates a release of energy (Tchobanoglous *et al.*, 2003).

Methanogenic bacteria are very sensitive to the hydrogen concentration, the substrate for methane production, and pH, the most active pH range being 6.8-7.4 (Zehnder, 1978). The acetogenic and hydrogen oxidising bacteria form a symbiotic (mutually beneficial) relationship, where the methanogenic bacteria depend on the acetogenic bacteria to provide the acetate and H_2 required for methane generation. In turn the acetogenic bacteria depend on the methanogenic bacteria to remove H_2, the accumulation of which leads to the suppression of acetogenesis. As methanogenic bacteria are very slow growing bacteria, they are unlikely to be present in the early stages of refuse degradation. Their initial absence would lead to the increased partial pressure of hydrogen, which

would, in turn, result in the inhibition of acetogenesis and accumulation of long-chain fatty acids thus lowering the pH, leading to further inhibition of methanogenesis. The introduction of methanogenic bacteria, by the addition of sewage sludge, has been shown to encourage their early establishment. In addition pH control by buffering of the leachate may be required (Findikakis & Leckie, 1979) (section 2.4.2).

The effect of sewage sludge on landfill degradation processes is further explored in section 2.4.4.

2.2.5. Phase V: Aerobic

Recently, an additional aerobic phase of degradation has been proposed (Christensen and Kjeldsen, 1995; Bozkurt *et al.*, 2000). Thereafter, a new population of aerobic micro-organisms may develop that slowly replaces the anaerobic forms, so aerobic conditions are re-established where oxygen diffusion into the system is greater than that utilised by the aerobic microorganisms. Thus, over time the anaerobic landfill becomes an aerobic ecosystem where aerobic micro-organisms can convert residual methane to carbon dioxide and water (methane oxidation) (Spokas *et al.*, 2006).

Figure 2.1 summarizes the predominant biodegradation pathways for the degradation of major organic and inorganic components of biodegradable waste (Waste Management Paper, 1995). A schematic description of the five phases of refuse degradation is presented in Figure 2.2.

2.3. The bacterial ecology of anaerobic digestion

2.3.1. Major groups of bacteria involved in anaerobic digestion of waste

Effective biodegradation of waste organic matter requires the combined and co-ordinated metabolism of different microbial populations. At least four different types of bacteria have been isolated from landfills, and these bacteria can be recognized on the basis of the organic substrates fermented and the metabolic end products formed (Barlaz *et al.*, 1989[b]):

Group 1: *Hydrolytic bacteria* (e.g., *Cellulomonas spp. and Flavobacterium spp.*) excrete the hydrolytic extracellular enzymes which are able to break down complex insoluble organic molecules in the waste such as carbohydrates, cellulose, proteins and fats into much smaller, soluble compounds that can be absorbed into bacterial cells and

metabolised. Hydrolysis of the complex molecules is catalyzed by extracellular extracellular enzymes such as cellulases, proteases, chitinases, amylases and lipases. The soluble monomers are then directly available to the next group of bacteria. However, the hydrolytic phase is relatively slow and can be limiting in anaerobic digestion of waste such as raw cellulolytic wastes, which contain lignin. The rate of methane production is often limited by the rate of biopolymer destruction and/or effective metabolic interaction between hydrolytic bacteria and methanogens (Zeikus, 1980[a,b,c]).

Group 2: *Fermentative acidogenic bacteria (e.g. Clostridium spp. and Eubacterium spp).* Fermentative acidogenic (i.e., acid-forming) bacteria metabolise the by-products of hydrolysis such as amino acids, peptides, sugars, purines, pyrimidines to form organic acids (e.g., acetic, propionic, formic, lactic, butyric, or succinic acids), alcohols and ketones (e.g., ethanol, methanol, glycerol, acetone), ammonia (from amino acids), acetate, CO_2, and H_2. Acetate is the main product of carbohydrate fermentation. The products formed vary with the type of bacteria as well as with culture conditions (temperature, pH, redox potential) (Tchobanoglous *et al.*, 2003). The *lytic bacteria* also form part of this fermentative population, since they metabolise the products of their hydrolytic activities (Palmisano *et al.*, 1993).

Group 3: *Acetogenic bacteria* (e.g. *Clostridium thermoaceticum, Butyribacterium methylotrophicum Desulfovibrio spp., Syntrophobacter spp., Syntrophomonas spp.*). The acetogenic bacteria are usually referred to as the "Obligate Hydrogen Oxidising Acetogens" (OHPAs) and include both obligate and facultative species. The OHPAs can oxidise the products of the second group - the organic acids larger than acetic acid (e.g. propionic (C-3), butyric (C-4), valeric (C-5) and caproic (C-6) acid) and neutral compounds larger than methanol ((C-1) (e.g. ethanol (C-2), propanol(C-3)) to acetic acid (C-2), hydrogen and carbon dioxide, which are used by the methanogens. The OHPAs require low hydrogen concentrations (< 20nM) for fatty acid conversion. Under relatively high H_2 concentrations (>100nM), acetate formation is reduced and the substrate is converted to propionic acid, butyric acid and ethanol rather than methane (Mormile *et al.*, 1996). Typical reactions of the OHPAs are butyrate and propionate degradation to acetate, hydrogen and CO_2 (Eq. 2.5 to Eq. 2.7). These reactions are characterised by the absorption of heat (endothermic reactions) under standard conditions and the OHPAs can only grow in association with other bacteria capable of removing H_2. They generally form close associations with methane forming (methanogenic) bacteria of group 4. For example, acetogens can ferment a number of substrates (including formate, carbon

dioxide and hydrogen) into acetate, which leads them into direct competition with methanogens for the same substrate. The basis for this competition is suggested to consist of acetogenic bacteria that have the capability of coupling hydrogen oxidation with carbon dioxide reduction to acetate (homoacetogens) and methanogens that yield methane from hydrogen and carbon dioxide (autotrophic methanogens) or from acetate produced by homoacetogens (acetoclastic methanogens) (Carpentier *et al.*, 2006; Drake *et al.*, 2002; Chen *et al.*, 2003[b]). Most homoacetogens can make acetate from either (H_2 + CO_2) or from the fermentation of sugars. The overall stoichiometry of the homoacetogens growth mode is shown below:

1. Glucose fermentation

Eq. 2.11 $$C_6H_{12}O_6 + 2H_2O \rightarrow 2CH_3COOH + 2CO_2 + 8H^+ + 8e^-$$

2. Carbon dioxide reduction

Eq. 2.12 $$2CO_2 + 8H^+ + 8e^- \rightarrow CH_3COOH + 2H_2O$$

Homoacetogenic bacteria possess high thermodynamic efficiencies of metabolism, as a consequence of not forming H_2 and CO_2 during growth on multi-carbon compounds. *Clostridium thermoaceticum* is the most extensively studied homoacetogenic bacteria, which is generally regarded as incapable of growth on monocarbon compounds alone (Ferry, 1995). *Butyribacterium methylotrophicum* is probably the most versatile homo-acetogen, because it grows on monocarbon compounds (e.g., H_2/CO_2, methanol/CO_2) and on multi-carbon compounds (e.g., hexoses, lactic acid, pyruvate), but forms mixtures of butyrate and acetate on most substrates, except on H_2/CO_2, where acetate is the sole end product (Kerby and Zeikus, 1987; Lowe *et al.*, 1993).

Relatively little is known about the functional importance of homoacetogen metabolism in anaerobic digestion, or the metabolic interactions of homoacetogens and methanogens. Nonetheless, during growth on multiple carbon compounds (e.g., glucose), these bacteria derive more thermodynamic metabolic efficiency than hydrolytic species; and, as a consequence of not producing but consuming hydrogen, homoacetogens lower the hydrogen partial pressure during anaerobic digestion. For example, *Butyribacterium methylotrophicum* can, in co-culture with *Methanosarcina barkeri*, metabolize butyrate as the sole carbon and electron donor. Hence, *Butyribacterium methylotrophicum* can also function as a facultative hydrogen producing acetogen (Hungate, 1950). These associations, or consortia, are a key element in the degradation of organic matter under

anaerobic conditions and their formation may be the RLS in the establishment of methanogenesis in a landfill (Lowe *et al.*, 1993; Micales and Skog, 1997).

Group 4: The methanogenic bacteria are characterised, as their name suggests, by their ability to synthesise methane. They are strict obligate anaerobes unable to survive exposure to even relatively small amounts of oxygen for any length of time. Methanogenic bacteria are restricted to such environments as deep sediments, anaerobic digesters, landfills, waterlogged soils and animal guts and are able to metabolise only a restricted number of compounds as growth substrate. Virtually all of the methanogens described are capable of using H_2/CO_2 and formate as substrates to produce methane. This group of methanogens is known as the hydrogenotrophic methanogens and includes *Methanobacterium spp, Methanobrevibacterium spp, Methanofollis spp., Methanoculleus spp., Methanosaeta spp., etc.* Substrates used by methanogenic bacteria as carbon and energy source include H_2/CO_2, formate, methanol, methylamines, CO_2 and acetate. Most methanogens can grow on H_2/CO_2. However, several species are unable to metabolize H_2/CO_2. For example *Methanococcoides methylutens* grows only on methylamines or methanol (Sowers and Ferry, 1983). *Methanosarcina spp.* (Zinder and Mah, 1979), *Methanotrix soehugenii* (Huser *et al.*, 1982) and *Methanolobus tindarius* (Konig and Stetter, 1982) can grow on methanol or methylamines. About half the genera can metabolize formate, by first oxidizing it using the enzyme formate dehydrogenase to H_2+CO_2, and then by reducing CO_2 to methane (Daniels *et al.*, 1984). *Methanosarcina barker* is the most metabolically versatile species and can grow on acetate, methanol, methylamines and H_2/CO_2, but cannot grow on formate (Mah and Smith, 1981). In contrast to acetate, which was considered the major methanogenic precursor in several ecosystems (Zeikus, 1977), methanol is not considered a natural intermediate in the degradation of most organic compounds in ecosystems (Hashimoto *et al.*, 1980). Some methanogens can oxidize CO_2 and convert it to methane, and a few strains can use CO_2 as the sole growth substrate (Zeikus, 1983). The main reactions catalysed by the hydrogenotrophic methanogens are:

1. Hydrogen oxidation

Eq. 2.13 $$4H_2 + CO_2 \rightarrow CH_4 + 2H_2O$$

2. Formate oxidation

Eq. 2.14 $$4HCOOH + H_2O \rightarrow CH_4 + 3CO_2 + 3H_2O$$

Acetoclastic methanogens (e.g. *Methanosarcina barkeri, Methanosaeta concilii, Methanosaeta spp.*) are types of methanogens that can use H_2/CO_2, methanol and methylamines as electron donors to produce methane, for example methylamine metabolism (Eq. 2.15). Most can use hydrogen as well but there are some examples of obligate acetoclastic methanogens such as *Methanothrix soehngenii* that uses only acetate as an electron donor (acetate metabolism) (Eq. 2.8) (Uz *et al.*, 2003).

Eq. 2.15 $$4CH_3NH_3^+ \rightarrow 3CH_4 + CO_2 + 4NH_3$$

Methanosarcina spp. and *Methanoculleus spp.* are the most widely distributed methanogenic bacteria in landfill samples (Huang *et al.*, 2002 & 2003; Chen *et al.*, 2003[a] & 2003[c]; Mori *et al.* 2003; Uz *et al.* 2003). These results are in good agreement with a resent study conducted on MSW landfill leachate samples where *Methanosarcina spp., Methanosaeta spp., Methanoculleus spp. and Methanofollis spp.* were the key methanogens isolated (Carpentier *et al.*, 2006). In this study leachates were incubated with different methanogenic precursors which resulted in acetoclatic methanogenesis being easily induced, whereas incubations with hydrogen, formate, methanol and methylamine as substrates led to the prevalence of the homoacetogenic pathway.

Studies of anaerobic digestion have showed that in most anaerobic environments (including landfills, anaerobic digesters, deep aquatic sediments, black mud, marshes, swamps and other), 70% or more of the methane formed is derived from acetate. Thus, acetate is the key intermediate in the overall fermentation of these ecosystems (Hansen *et al.*, 1998[b]). The other 30% of methane is predominantly the result of carbon dioxide reduction by hydrogen.

Methanogenic bacteria tend to be inhibited by low pH and if the initial fermentation in landfill is too rapid then the concentration of the acidic products of fermentation can cause inhibition of the final reactions preventing the development of a methanogenic population. The temperature and water content as well as the particle size of the waste all influence the rate of development of the fermentative population and care must be taken not to accelerate the initial reactions to the point that methanogenesis fails. In a well balanced system the OHPAs: methanogenic consortia are able to remove hydrogen and volatile acids as rapidly as they are produced and so the concentration of these intermediates remain low. This interaction between H_2-oxidizing and H_2-reducing organisms has been termed "interspecies hydrogen transfer" (Iannotti *et al.*, 1973; Wolin, 1974). This term is used to describe the coupled oxidation-reduction reactions between

two or more interacting anaerobic bacteria during the fermentation of one initial substrate.

Interspecies hydrogen transfer occurs when the flow of fermentation - generated electrons is shifted from the formation of reduced organic end products to proton reduction. H_2 formation then becomes the major, if not sole, electron sink. Because of the thermodynamic or inhibitory properties of the reaction, such a shift in electron flow requires a mechanism for the continuous removal of H_2. This can be provided by the methanogenic bacteria (Iannotti *et al.,* 1973). Thus, H_2 concentration (i.e. partial pressure) plays a key role in the regulation of the proportions of various end-products produced during the overall conversion of organic matter to methane. The concentration of H_2 may be a good indicator of the course of the fermentation.

The overall process of anaerobic degradation of waste showing the manner in which various groups of anaerobes act together in the conversion of complex organic matter, ultimately producing methane and carbon dioxide is shown in Figure 2.3. This figure shows that the degradation of organic material under anaerobic conditions is a quite complex but well defined process, which is carried out by 7 different groups of bacteria constituting 3 main and 4 secondary phases. *Hydrolytic and fermentative bacteria* (group 1) hydrolyze the polymers to soluble oligomers and monomers by action of extra-cellular enzymes; then, the dissolved products are fermented by bacteria forming acetate and other short-chain fatty acids (VFA), alcohols, hydrogen and carbon dioxide. Short-chain fatty acids, longer than acetate and alcohols, are oxidized by the *hydrogen-producing acetogenic bacteria* (group 2) forming hydrogen, acetate, formate and carbon dioxide. The final products of the fermentation step are then taken up by the *methanogenic bacteria* (group 3) and finally transformed into methane (Gerrardi, 2003). Aside from this major process leading from complex organic matter to CH_4, there are several secondary sub-reactions carried out by *homoacetogenic bacteria* (group 4) which degrade different intermediate products like H_2, CO_2 or glucose producing acetate; meanwhile a special subgroup of homoacetogenic bacteria (group 5) performs exactly the opposite reaction by oxidizing the acetate to H_2 and CO_2; another group of bacteria - *acid synthesizing bacteria* (group 6) reverses the transformation of VFA when the concentration of H_2 and acetate or ethanol is too high; and finally, in anaerobic reactors containing sulphate , both sulphate reduction and methanogenesis can be performed simultaneously because of the action of *sulphate reducing bacteria* (SRB) (group 7) which is capable of oxidizing many of the intermediates formed during methanogenesis

(as H_2 and VFAs) to H_2S. The role of SRB in anaerobic environments is explained in more detail in section 2.3.3.

2.3.2. Other bacterial reactions and their consequence

Nitrate and nitrite reducing bacteria may play a role in organic matter degradation in landfills where the leachate contains high concentrations of these anions. MSW has been estimated to contain about 4% protein and therefore, any nitrate (NO_3^-)or nitrite (NO_2^-) present in the waste will be leached into the soluble fraction and reduced to nitrogen or ammonia soon after waste placement (Madigan *et al.*, 1997; Barlaz *et al.*, 1990). Because ammonia is stable under anaerobic conditions, it typically accumulates in landfill leachates from freshly deposited waste, frequently in excess of 1000mg/l (Burton and Watson-Craik, 1998; Onay and Pohland, 2001). Thus, high concentrations of ammonia persist long after the BOD and COD have decreased to concentrations representative of well-decomposed refuse. Since ammonia inhibits methanogenic bacteria, methane formation will not occur until its concentration has been reduced. Due to its toxicity the treatment of leachate to remove ammonia to an acceptable level (<10mg/l) before it is discharged (Welander *et al.*, 1997) is an important aspect of long-term landfill management. The final step in the removal of ammonia nitrogen from the system is also known as *denitrification* which occurs in environments without oxygen.

Denitrification is the dissimilatory biochemical process of reducing NO_3^- and NO_2^- to N_2O and N_2. It is performed by a group of aerobic bacteria known collectively as denitrifiers which include *Pseudomonas spp., Micrococcus spp., Archromobacter spp.,* and *Bacillus spp.* (Reynolds, 1996). The denitrifiers are capable of growth with NO_3^- and NO_2^- as electron acceptors (Tiedje, 1988). Denitrification is inhibited by the presence of oxygen and is therefore limited to anoxic environments. Even though nitrate is not typically found in landfills, some bacteria with the ability to denitrify survive (Burton and Watson-Craik, 1998). During anaerobic degradation of organic substances, the use of nitrate as a terminal electron acceptor for growth is energetically favorable for acetogenesis, sulphate reduction and methanogenesis.

Nitrate can be used by some microorganisms via two different pathways (Atlas, 1998):

(1) One pathway is a dissimilative process that can occur by the following reactions:

1. Respiratory denitrification:

Eq. 2.16 $2NO_3^- + 12H^+ + 10e^- \rightarrow N_2 + 6H_2O$

2. Dissimilatory nitrate reduction to ammonium:

Eq. 2.17 $NO_3^- + 10H^+ + 8e^- \rightarrow NH_4^+ + 3H_2O$

(2) the other pathway is an assimilative process by which nitrate is reduced to ammonia and thereafter into cell biomass:

3. Assimilatory nitrate reduction to ammonia:

Eq. 2.18 $NO_3^- \rightarrow NO_2^- \rightarrow NH_2OH \rightarrow NH_3 \rightarrow R-NH_2$

In *Path way 1* NO_3^-, used as electron acceptor, is usually reduced to NO_2^-, then to nitric oxide (NO) or nitrous oxide (N_2O), and finally to nitrogen gas (N_2) (Eq. 2.16). In some cases, because of the lack of some enzymes, the reduction procedure from NO_3^- - to N_2 can be blocked at any step such as NO_2^-, or NO, or N_2O. Some microbes can only use nitrate as an electron acceptor; some can use nitrate as both nutrient sources to set up cell structure material and as electron acceptor. When the degradable organic carbon/nitrate level is high, microbes are electron acceptor limited and *Path way 2* (Eq. 2.17) prevails which would be counterproductive in a landfill because it would lead to inhibition of methanogenesis due to the accumulation of ammonium. In contrast, when the degradable carbon/nitrate level is low, the microbes are carbon limited and *Path way 1* (Eq. 2.16) prevails as is desired in a landfill because, in this case, the methanogenesis will not be inhibited and the treatment of leachate to remove ammonium to an acceptable level before it is discharged will not be necessary. Dissimilatory nitrate reduction to ammonium (DNRA) has been reported to predominate in anaerobic sludge digesters, anoxic sediments, and the rumen, all of which are carbon-rich, nitrate poor environments (Tiedje, 1988). H^+ ions are consumed in both reactions and a pH increase during denitrification has been reported (Burton and Watson-Craik, 1999).

In *Path way 3* nitrate, used as a nutrient source, is reduced to nitrite by the enzyme *nitrate reductase* and nitrite is then reduced to hydroxylamine (NH_2OH) by the enzyme *hydroxylamine reductase* and NH_2OH is then reduced to ammonia in a series of two electron transfers. The final product is ammonia which is readily incorporated into amino acids and cell biomass (R-NH_2) (Eq. 2.18).

Nitrification is the term used to describe the two-step biological process in which ammonia (NH_4-N) is oxidized to nitrite (NO_2^-) which is then oxidized to nitrate (NO_3^-). Nitrification is performed by the group of bacteria known as nitrifiers. The nitrifying process takes place in two steps and each step is carried out by a specific group of nitrifying organisms. The two microbes involved have been identified in many studies and are the aerobic autotrophic genera *Nitrosomonas spp.* and *Nitrobacter spp.* (Reynolds, 1996). The reactions are as follows:

1. Ammonia oxidation (*Nitrosomonas spp.*):

Eq. 2.19 $$2NH_4^+ + 3O_2 \rightarrow 2NO_2^- + 4H^+ + 2H_2O$$

2. Nitrite oxidation (*Nitrobacter spp.*):

Eq. 2.20 $$2NO_2^- + O_2 \rightarrow 2NO_3^-$$

Since complete nitrification is a sequential reaction, treatment processes must be designed to produce an environment suitable for growth and survival of both groups of nitrifying bacteria (De Renzo, 1978). The oxidation of ammonia to nitrate occurs if extensive aeration is allowed in the leachate treatment processes.

Ammonia nitrogen is present in water in two forms. The first is as dissociated ammonia, NH_4^+, also referred to as the ammonium ion. The second is as undissociated ammonia, NH_3, known as ammonia gas. The equation governing the relationship between ammonia gas and the ammonium ion is as follows:

Eq. 2.21 $$NH_4^+ + OH^- \leftrightarrow NH_3 + H_2O$$

It has also been noted that as the temperature of the water increases so the amount of free ammonia gas also increases (Srinath and Loehr, 1974). The ratio of ammonia in the gas phase to the total ammoniacal nitrogen, referred to as "f", may be expressed as follows:

Eq. 2.22 $$f = \frac{[NH_3]}{[NH_3]+[NH_4^+]}$$

The relationship between pH, temperature and "f" takes the form represented in Figure 2.4.

Leachate has been successfully treated to remove ammonia by an aerobic step, to oxidise it to nitrite and nitrate (nitrification), followed by reduction of the nitrate to dinitrogen (denitrification). Knox and Gronow, 1995 described a system in which leachate ammonia was oxidised to nitrate which was subsequently reduced to dinitrogen (N_2) in a reactor containing methanogenic waste. In this system methanogenesis and nitrate reduction took place at the same time.

Completely new treatment concepts in biological ammonia removal from wastewater are *partial nitrification* and the *anaerobic ammonium oxidation* (anammox) processes. Anaerobic ammonium oxidation (anammox) is a very recent addition to our understanding of the biological nitrogen cycle (Kuenen and Jetten, 2001; Strous *et al.*, 1999). Discovered as late as 1986, it so far is the most unexplored part of the cycle. Given its basic features, the anammox process is a viable option for biological wastewater treatment (Jetten *et al.*, 1999; Jetten *et al.*, 2001; Strous *et al.*, 1997[b]). Very recently, it was discovered that anammox makes a significant (up to 70%) contribution to nitrogen cycling in the World's oceans (Thamdrup & Dalsgaard, 2002).

Nitrogen removal based on this concept consists of two treatment steps: partial nitrification followed by anaerobic ammonium oxidation. In the first step 50% of the ammonia is biologically converted to nitrite, using nitrifying bacteria. Partial nitrification requires oxygen and therefore (limited) aeration is required. In the second step, ammonia and nitrite are biologically converted into nitrogen gas. The two processes proceed as follows:

Eq. 2.23. Partial nitrification: $2NH_4^+ + 1.5O_2 \rightarrow NH_4^+ + NO_2^- + H_2O + 2H^+$

Eq. 2.24. Anammox: $NH_4^+ + NO_2^- \rightarrow N_2 + 2H_2O$

Eq. 2.25. Total: $2NH_4^+ + 1.5O_2 \rightarrow N_2 + 3H_2O + 2H^+$

Anammox needs ammonium and nitrite in a ratio of roughly one to one. For sludge digester effluents, this ratio can be achieved without control, because these effluents contain bicarbonate as the counter ion for ammonium (Jetten *et al.*, 2001).

The anammox reaction is carried out by a group of *Planctomycete bacteria spp.* Three of these have been named provisionally: *Candidatus "Brocadia anammoxidans"*, *Candidatus "Kuenenia stuttgartiensis"* and *Candidatus "Scalindua sorokinii"*. The first two have been found in wastewater treatment systems. The latter, *Scalindua spp.*, has also been detected in many marine ecosystems, such as the Black Sea. The anammox

bacteria seem to be very similar in that: they all grow at the same, very slow rate, they all have an anammoxosome and ladderane lipids. The differences that must exist between the three genera have not yet been fully evaluated.

Anammox bacteria have been described as strict autotrophs and are known to be active at temperatures between 6 and 43°C (Thamdrup & Dalsgaard, 2002). The pH range is 6.7 - 8.3 (optimum 8). The anammox process is based on energy conservation from anoxic ammonium oxidation with nitrite as the electron acceptor and hydrazine as the intermediate. CO_2 is used as the main carbon source for growth. It has been shown that CO_2 fixation is accomplished via the acetyl-CoA pathway. The necessary electrons are obtained from the anaerobic oxidation of nitrite to nitrate (Van de Graaf, 1997; Strous, 1999).

The actual biochemical mechanism of nitrite reduction remains unclear (Güven *et al.*, 2005). In principle, anammox bacteria could either make use of the denitrification pathway to produce nitrogen gas directly or first reduce nitrite to ammonium and subsequently oxidize ammonium in the anammox reaction (Figure 2.5).

Anammox was found to be inhibited completely at oxygen concentrations as low as 0.5% air saturation (Strous *et al.*, 1997[a]). Under oxygen limitation (<0.5% air saturation), a co-culture of aerobic and anaerobic ammonium oxidizers was obtained. This culture converted ammonium directly to nitrogen gas, with nitrite as the intermediate (Third *et al.*, 2001). Application of this concept in wastewater treatment could lead to complete ammonia removal in a single autotrophic reactor by performing two sequential reactions simultaneously.

The combined partial nitrification - anammox process is a very competitive and sustainable process since less energy is consumed and no chemicals are required, as compared to the conventional nitrification and denitrification process. Compared to conventional nitrification/ denitrification, this method saves 100% of the required synthetic carbon source (i.e. methanol) and 50% of the required oxygen. This leads to a reduction of operational costs of 88%, a decrease in CO_2 emissions of more than 100% (the process actually consumes CO_2) (Strous *et al.*, 1999), and a decrease in energy demand.

2.3.3. Sulphate reduction and methanogenesis

Another factor that may affect refuse methanogenesis is the availability of alternative electron donors like hydrogen and acetate (Kristjansson *et al.*, 1982). In anaerobic reactors containing sulphate, both sulphate reduction and methanogenesis can be the final steps in the degradation process because, SRB are capable of using many of the intermediates formed during methanogenesis (see Figure 2.3).
Typically in the presence of sulphate in the anoxic zone of landfills SRB will oxidise hydrogen and the fatty acid products of the fermentative phase. Substrate competition in such systems is possible on two levels:

- **competition between SRB and acetogenic bacteria for volatile fatty acids (VFA) (formation of hydrogen sulphide):**

Butyrate oxidation by acetogenic bacteria

Eq. 2.26 $$CH_3(CH_2)_2COOH + 2H_2O \rightarrow 2CH_3COOH + 2H_2$$

Butyrate oxidation by sulphate-reducing bacteria

Eq. 2.27 $$CH_3(CH_2)_2COOH + 0.5H_2SO_4 \rightarrow 2CH_3COOH + 0.5H_2S$$

Propionate oxidation by acetogenic bacteria

Eq. 2.28 $$CH_3CH_2COOH + 2H_2O \rightarrow CH_3COOH + 3H_2 + CO_2$$

Propionate oxidation by sulphate-reducing bacteria

Eq. 2.29 $$4CH_3CH_2COOH + 3H_2SO_4 \rightarrow 4CH_3COOH + 3H_2S + 4CO_2 + 4H_2O$$

- **competition between SRB and methanogenic bacteria for acetate and hydrogen (inhibition of methane formation):**

Hydrogen oxidation by methanogenic bacteria

Eq. 2.30 $$2H_2 + 0.5CO_2 \rightarrow H_2O + 0.5CH_4$$

Hydrogen oxidation by sulphate-reducing bacteria

Eq. 2.31 $$4H_2 + SO_4^{2-} + H^+ \rightarrow 4H_2O + HS^-$$

Acetate oxidation by methanogenic bacteria

Eq. 2.32 $$CH_3COOH \rightarrow CO_2 + CH_4$$

Acetate oxidation by sulphate-reducing bacteria

Eq. 2.33 $$CH_3COOH + SO_4^{2-} \rightarrow CO_2 + H_2O + HS^- + HCO_3^-$$

Various researchers have observed that SRB can successfully compete with methanogenic bacteria for acetate during the breakdown of sulphate-containing waste water (Visser *et al.*, 1996), whereas others indicate that acetate is preferentially degraded to methane (Hoeks *et al.*, 1984; Mulder, 1984). To explain these differences, factors other than pure bacterial kinetics should be taken into account. These include the COD/SO_4^{2-} ratio, the type of seed sludge used, hydrogen sulphide inhibition, pH and nutrient limitation (Kalyuzhnyi *et al.*, 1998). Based on the kinetics of VFAs (acetic, propionic and butyric acids) and hydrogen utilisation by SRB, acetogenic and methanogenic bacteria, the SRB will be able to out-compete the acetogenic and methanogenic bacteria (Oude Elferink *et al.*, 1994). This prediction has been confirmed experimentally for hydrogen (Mulder, 1984) and for long chain VFA like propionic and butyric acids (Omil *et al.*, 1996, 1997; Visser *et al.*, 1993). For utilisation of acetate in anaerobic reactors the situation is different. Various researchers have observed that during the breakdown of sulphate-containing waste water, SRB can indeed successfully compete with methanogenic bacteria for acetate (Visser *et al.*, 1996), whereas others indicate that acetate is preferentially degraded to methane (Hoeks *et al.*, 1984 and Mulder, 1984).

To explain the mechanism of methane inhibition in sulphate-reducing anaerobic environments Borowski *et al.* (1999) made the assumption that the methane oxidising bacteria are consuming methane. All of the well known methane-consuming microorganisms are aerobic bacteria, requiring oxygen to use methane. Scientists have long suspected that methane oxidation occurs in anoxic marine sediments. In such an environment, sulphate becomes depleted downwards through the sediments, matched by an upward depletion of methane, and the minimum of the two depletion curves intersect (Borowski *et al.*, 1999). Furthermore, isotopic evidence indicates that the CO_2 found near this boundary is derived largely from methane (Borowski *et al.*, 1997).

Preliminary studies have indicated that some methanogens have limited capacity to reverse their normal metabolism, thereby oxidizing methane (Eq. 2.34), rather than producing it from H_2 and CO_2 (Zehnder and Brock, 1979):

Eq. 2.34 $$CH_4 + 2H_2O \rightarrow CO_2 + 4H_2$$

This process is known as reverse methanogenesis and would be energetically favourable if the H_2 end product were rapidly removed, and so kept at a low steady-state concentration (Hoehler *et al.*, 1994). In this scheme, H_2, an end product of the methane-

oxidizing microorganisms, becomes the energy substrate for another microbial group, the hydrogen-oxidizing sulphate-reducers:

Eq. 2.35 $$H^+ + 4H_2 + SO_4^{2-} \rightarrow HS^- + 4H_2O$$

The sum of this cooperative process between methane-oxidizers and sulphate reducers is:

Eq. 2.36 $$CH_4 + SO_4^{2-} \rightarrow HCO_3^- + HS^- + H_2O$$

Boetius *et al.*, 2000 provided strong evidence that methane oxidation in anoxic marine sediments is carried out by a consortium of methanogenic bacteria and SRB. The authors presented visual evidence that one previously identified waste-associated methanogen, affiliated with the order *Methanosarcinales spp.* (section 2.3.1), is a key methane-oxidizer. Moreover, their work shows that the microorganisms are spatially organized in tight clusters, closely surrounded by SRB.

SRB have two potential effects on the degradation processes in the landfill: the formation of hydrogen sulphide and the inhibition of methane formation through competition for hydrogen and acetic acid. Formation of insoluble sulphides of iron and other metallic ions in leachate immobilises potentially toxic metals such as cadmium and chromium. Insoluble sulphides, combined with magnesium and calcium carbonate deposits resulting from metabolic carbon dioxide, may also contribute to clogging of drainage systems (Brune *et al.*, 1991 and Rowe *et al.*, 1997)

2.3.4. Leachability of heavy metals in landfills and their environmental impact

In recent years, there has been a growing movement to ban certain products from disposal in MSW landfills because of a concern for the potential release of heavy metals to the environment. The major sources of heavy metals in landfills are the co-disposed industrial wastes, incinerator ashes, mine wastes and household hazardous substances such as batteries, paints, dyes, inks, etc. (Förstner *et al.*, 1991). The most common heavy metals in landfills are iron, cadmium, copper, zinc and nickel (Flyhammar *et al.*, 1998). The concentrations of heavy metals in leachate vary over a wide range depending on a number of factors including waste composition, landfill age, and moisture availability.

The solubility of metals in leachate depends on the pH, the redox potential, and the solubility of the deposited metal species, concentration of complexing agents (NH_3/NH_4^+,

humic acids, etc.) and ionic strength (Förstner *et al.*, 1991). Metal solubility in the leachate increases as pH decreases. The highest metal concentrations are observed during the acid formation phase of waste stabilization (Phase III) when pH values are low (section 2.2.3). The solubility of metals under methanogenic conditions is different. As a result of attenuating processes (sorption and precipitation) that takes place within the disposed waste, the content of heavy metals in the leachate is generally very low under methanogenic conditions. In Phase IV of the stabilization process, reducing conditions exist, meaning that elements and compounds tend to gain electrons using organic matter as the electron donor. For example, in this phase sulphate ions (SO_4^{2-}) are reduced to sulphide ions (S^{2-}). These sulphide ions, as well as carbonate (CO_3^{2-}) and hydroxide ions (OH^-), are then available during subsequent phases to react with *Cd*, *Ni*, *Zn*, *Cu*, and *Pb* to form insoluble compounds that effectively remove these heavy metals from the leachate (Pohland *et al.*, 2003). While carbonates are abundant in landfill leachate, the solubilities of metal carbonates are generally higher than that of metal sulfides (Christensen *et al.*, 2000). In general, sulfide precipitation is expected to dominate heavy metal attenuation compared with complexation agents (Reinhart and Grosh, 1998). *Cr* is an exception to this because it does not form an insoluble sulfide precipitate (Christensen *et al.*, 2000). However, *Cr* tends to form insoluble precipitates with hydroxide (Revans *et al.*, 1999).

When organic sulfur compounds are decomposed by bacteria, the initial sulfur product is generally H_2S. Subsequently, although a fraction of sulfide escapes in anaerobic systems in the biogas, the majority of sulfide remains dissolved in solution as either $H_2S(aq)$ or $HS^-(aq)$ (McFarland and Jewell, 1989). $H_2S(aq)$ is in equilibrium with $H_2S(g)$ and when pH increases, $H_2S(aq)$ is converted to HS^-. The dissolution of H_2S in water forms the following equilibrium:

Eq. 2.37 $$H_2S \leftrightarrow H^+ + HS^- \leftrightarrow 2H^+ + S^{2-}$$

Depending on the pH, the percentage of insoluble H_2S drops from 90% at pH 6.0 to 50% at pH 7.0 and to 10% at pH 8.0 (Oleszkiewicz and Hilton, 1985).

Investigations of the sulfur content of landfilled waste have shown that the waste does not contain sufficient sulfur to bind all the heavy metals present in the waste. The landfill sampled by Martensson *et al.* (1999) contained only enough sulfur to bind 5% of metals present. Occasionally, phosphates and hydroxides will also precipitate metals (Pohland,

1991). Hydroxide precipitates form at pHs at or above neutral, which is typically the case in methanogenic leachates (Reinhart and Grosh, 1998).

Heavy metals mobilizing processes are also possible in landfills. Several processes, including complexation to inorganic and organic ligands, and sorption to colloids are capable of mobilizing heavy metals by increasing the concentration in the mobile aqueous phase. Christensen and Jensen (1999) separated leachate samples from four Danish landfills into size fractions to obtain information about size distribution of colloids and associated heavy metals (*Cd*, *Ni*, *Zn*, *Cu*, *Pb*, *Cr*). A significant but highly varying fraction of the heavy metals was associated with colloidal fractions.

In a closed aqueous anaerobic system containing certain ions (NO_3^-, Fe^{3+}, SO_4^{2-}, Mn^{4+}), biodegradation of available dissolved organic matter (CH_2O) is observed to occur in the sequence shown in Table 2.2 (Stumm and Morgan, 1996). CH_2O-oxidation is expected to occur first by reduction of O_2. As can be seen in Table 2.2, the succession of the reactions follows their thermodynamic possibility, i.e. the decreasing energy release level ($p\varepsilon^o$) in each process. The described sequence implies that denitrification will precede nitrate reduction, followed by the reduction of $FeOOH$ or $Fe(OH)_3$ to Fe^{2+}. Reduction of Mn^{4+} to Mn^{2+} (if present) should occur at about the same $p\varepsilon$ level as that of nitrate reduction. When sufficiently negative $p\varepsilon$ levels have been reached, methane fermentation and reduction of SO_4^{2-} and CO_2 may occur almost simultaneously. Non-methanogenic reactions compete with methanogenesis through preferential utilisation of hydrogen and VFAs as electron donors and under standard conditions, non-methanogenic reactions out-compete methanogenic reactions because the former are energetically more favourable.

2.4. Factors influencing waste degradation in landfills

This section outlines the principal factors that can influence the degree and the role of anaerobic degradation processes in landfills.

2.4.1. Organic fraction of municipal solid waste

Waste stabilisation is achieved by destroying the biodegradable organic fraction of MSW and through lowering the carbon/nitrogen (C/N) ratio as biogas is produced. Waste is approximately 75 to 80% organic matter, composed mainly of proteins, lipids, carbohydrates (cellulose and hemicellulose), and lignin. MSW typically contains 40-50% cellulose, 10-15% lignin, 5-12% hemicellulose, 4-5% lipids and 2% protein (Barlaz *et*

al., 1990). As outlined in section 2.5, lignin is not readily biodegradable, and hemicelluloses and proteins can take days to degrade. The other organic groups mentioned, however, break down readily. Lipids (fats, oils and grease) become fluid at temperatures slightly above ambient and proteins, containing nitrogen and sulphur, provide a useful source of nutrients (see below). Proportionally, carbohydrates and lignin comprise the major component of MSW and their biodegradation is discussed in great details in section 2.5.

Table 2.2. Sequence of microbially mediated redox processes (From: Stumm and Morgan, 1996).

Reduction reactions	**Energy released, $p\varepsilon^o(W) = -\log K(W)$**
(1) Aerobic respiration (O_2 consumption): $\frac{1}{4}\{CH_2O\}+\frac{1}{2}O_2 \rightarrow \frac{1}{4}CO_2+\frac{1}{4}H_2O$	+ 13.75
(2) Denitrification: $\frac{1}{4}\{CH_2O\}+\frac{1}{5}NO_3^- +\frac{1}{5}H^+ \rightarrow \frac{1}{4}CO_2+\frac{1}{10}NH_4^+ +\frac{1}{2}H_2O$	+ 12.65
(3) (Mn^{4+})oxide → Mn^{2+} (production of soluble Mn^{2+}): $\frac{1}{4}\{CH_2O\}+\frac{1}{2}MnO_2(s)+H^+ \rightarrow \frac{1}{4}CO_2+\frac{1}{2}Mn^{2+}\frac{1}{8}H_2O$	+ 8.90
(4) Nitrate reduction: $\frac{1}{4}\{CH_2O\}+\frac{1}{8}NO_3^- +\frac{1}{4}H^+ \rightarrow \frac{1}{4}CO_2+\frac{1}{8}NH_4^+ +\frac{1}{8}H_2O$	+ 6.50
(5) (Fe^{3+})oxide → Fe^{2+} (production of soluble Fe^{2+}): $\frac{1}{4}\{CH_2O\}+FeOOH(s)+2H^+ \rightarrow \frac{1}{4}CO_2+\frac{7}{4}H_2O+Fe^{2+}$	- 0.80
(6) Fermentation: $\frac{1}{4}\{CH_2O\}+\frac{1}{2}O_2 \rightarrow \frac{1}{4}CO_2+\frac{1}{4}H_2O$	- 3.01
(7) Sulphate reduction (production of H_2S): $\frac{1}{4}\{CH_2O\}+\frac{1}{8}SO_4^{2-} +\frac{1}{8}H^+ \rightarrow \frac{1}{8}HS^- +\frac{1}{4}CO_2+\frac{1}{4}H_2O$	- 3.75
(8) Methane fermentation: $\frac{1}{4}\{CH_2O\} \rightarrow \frac{1}{8}CH_4+\frac{1}{8}H_2O$	- 4.13

Note: $p\varepsilon^o$ gives the hypothetical electron activity at equilibrium and measures the relative tendency of a solution to accept or transfer electrons, K is the equilibrium constant for the reduction half-reaction, and W-watt.

2.4.2. Temperature and pH

Another parameter which influences the anaerobic biodegradation of waste is temperature (Misra *et al.*, 1992). The process can take place in ambient (20-25°C), mesophilic (30-40°C), or thermophilic (50-60°C) conditions. In general, the overall process kinetics doubles for every 10 degree Celsius increase in operating temperature up to a critical temperature (approximately 60°C) above which a rapid decrease in microbial activity occurs (Harmon *et al.*, 1993). The populations operating in the thermophilic range are genetically unique (Zinder, 1993), do not survive at lower temperatures, and are more sensitive to temperature fluctuations outside of their optimum range. Thermophilic bacteria exhibit some differences compared to mesophilic bacteria. For example, at thermophilic temperatures (50-60°C), acetate is oxidized by a two-step mechanism (syntrophic acetate oxidation to hydrogen and carbon dioxide followed by formation of methane) when the acetate is less than 1mM (Zinder and Koch, 1984). At higher concentrations, and at mesophilic temperatures (30-40°C), the principal acetoclastic mechanism is through direct conversion of the methyl group to methane. Also, ammonia has been shown to be more toxic in thermophilic conditions due to a higher proportion of free ammonia (Angelidaki and Ahring, 1994). Although thermophilic conditions are thought to have higher energy requirements (Srivastava, 1987), heat losses can be minimized through effective insulation and use of heat exchangers to reduce system heat losses. Most anaerobic digesters are operated at mesophilic or ambient temperatures (Pohland and Harper, 1985). Thermophilic operation is practiced under rare circumstances when the reduced reactor size justifies both the higher energy requirements and increased maintenance required to insure stable performance. In any anaerobic system, the reactor temperature must be maintained at a relatively constant level to maintain the gas production rate.

One of the most widely used formulas showing that increasing temperatures increase microbial degradation rates is the van Hoff-Arrhenius equation (Tchobanoglous *et al.*, 2003). This states that the parameter k (degradation rate constant, day^{-1}) is dependent on a temperature based relationship:

Eq. 2.38
$$\frac{k_t}{k_{20}} = \theta^{(T-20)}$$

Where k_t is the degradation rate constant at a particular temperature; k_{20} is the degradation rate constant at 20°C (typical value 0.23); θ is a constant, and for temperatures between 20°C and 30°C has a value of 1.056; T is the temperature at which k is measured. Using this equation at 30°C, the biodegradation reaction rate constant will be 0.40. This shows a 60% increase in the degradation rate constant from a temperature increase of 10°C.

Alkalinity, acidity and pH are inter-related and indicate the prevailing general environmental conditions during anaerobic biodegradation of waste. The VFA concentration is also commonly one of the most important monitoring parameters in this process. High concentrations of total VFA are often associated with an unstable anaerobic process and are the first sign of a stressed reactor. Low pH levels usually accompany high VFA concentrations and adequate alkalinity is important to buffer the effect of VFA accumulation. Addition of buffering chemicals is sometimes necessary to restore and maintain neutral pH when VFA produced exceed the buffering capacity of the reactor contents. Increased VFA concentration and reduced pH might occur as a result of overloading, organism washout, ineffective mixing, temperature upset, nutrient deficiency or toxic conditions. The breakdown of methanogenesis will allow acetate to increase in the system and this inhibits propionate and butyrate degradation. The mixed populations of bacteria involved in anaerobic degradation of organic matter have different optimum pH values. An optimum pH range for all is between 6.4 and 7.2 and a pH below or above this range can be toxic, particularly to methane-forming bacteria. Low pH can also inhibit acidogenic conversion of the substrate. The buffering capacity in anaerobic degradation is provided by the reaction of ammonium ions with bicarbonate ions to form ammonium bicarbonate near pH 7. Adequate alkalinity (>500mg/l) is the indicator of a good buffering capacity.

The buffering capacity of a system regulates the pH of the MSW leachate. Without a sufficient buffering capacity, the pH could be reduced to a level below the optimal range for the methanogens (6.8-7.4, Zehnder, 1978). Under such circumstances, methanogenesis is subject to substrate inhibition by high levels of volatile fatty acids, resulting in cessation of methane production and an inhibition of the overall process (Findikakis and Leckie, 1979).

2.4.3. Nutrients

Adequate nutrients are important for all biological waste treatment systems. Nitrogen and phosphorus are the major nutrients required for anaerobic degradation of waste. These elements are building blocks for cell synthesis and their requirements are directly related to the microbial growth. An optimal ratio between carbon, nitrogen and phosphorus of 100:24:4 has been calculated using typical values for the composition of prokaryotic cells - 50% carbon, 22% oxygen, 12% nitrogen, 9% hydrogen and 2% phosphorus (Tchobanoglous *et al.*, 2003). Sulphur is also required for cell growth and during anaerobic biodegradation it can be supplied through the degradation of sulphur containing amino acids or through the reduction of sulphate to sulphide. Other nutrients needed in intermediate concentrations include sodium, potassium, calcium, magnesium, and chlorine. Requirements for several micronutrients have also been identified, including iron, copper, manganese, zinc, molybdenum, nickel, and vanadium (Speece, 1987). Available forms of these nutrients may be limiting because of their ease of precipitation and removal by reactions with phosphate and sulphide.

The nutritional requirements of methanogens range from simple to complex. With regard to carbon assimilation, some methanogens are autotrophs (inorganic carbon source metabolizers), some heterotrophs (organic carbon source metabolizers), and some mixotrophs (organic and inorganic carbon source metabolizers). In natural habitats, methanogenic bacteria depend strongly on other bacteria to supply essential nutrient such as trace minerals, vitamins, acetate, amino acids or other growth factors (Mah and Smith, 1981).

2.4.4. Additions

Additions to MSW may be made in order to steer the degradation towards the methanogenic phase move rapidly. Although, co-disposal of hazardous waste does occur (Cossu and Serra 1989), its influence will not be considered any further in this study. Examples of additives to MSW could be methanogenic leachate, sewage sludge, organic rich sludges, and buffers. In order to avoid excessive accumulation of acid during acidogenesis, buffer substances can be added to prevent the inhibition of methanogenic activities. Calcium carbonate ($CaCO_3$), sodium carbonate (Na_2CO_3), lime and potassium carbonate (K_2CO_3) were found to be effective in maintaining buffering capacity in landfills (Augenstein *et al.*, 1976; Buivid *et al.*, 1981; Kinman *et al.*, 1987; Barlaz *et al.*, 1989[a]; West *et al.*, 1998)

Additives have three main functions: to serve as either a pH-buffering agent, an inoculum or as a source of nutrients. A combination of several factors determines the actual effect of additives on waste degradation processes. Among those factors are waste composition, degree of leachate recirculation or the use of one or several types of additions (e.g., sludge and buffer, just buffer, just sludge).

The addition of sludge to MSW has been reported in the literature to have both positive and negative effects in waste biodegradation. Anaerobically digested sewage sludge increases the nutrient level as well as adding moisture content (Blakey, 1991; Stamm and Walsh, 1988). It also provides a seed inoculum of microorganisms. However, care must be taken not to use concentrations of any sewage containing high levels of heavy metals that could be toxic to bacteria. Low pH inoculum may lead to an imbalance due to the more rapid growth rate of acid-forming bacteria (compared to methanogens) and depression of pH (Leckie *et al.*, 1979; Barlaz *et al.*, 1987; Stegmann *et al.*, 1989; Eleazer *et al.*, 1997; Wang *et al.*, 1997; Buivid *et al.*, 1981). Inocula may also become imbalanced when exposed to toxic substances or environmental stress factors (e.g., abnormal temperature) for which they are not acclimated.

According to Pohland (1975), leachate recycling with buffer addition shortened the acidogenic stage compared with simple leachate recycling. However, the addition of sewage sludge and buffer to MSW resulted in acidogenic conditions for the whole length of the experiment. The author concluded that the addition of sludge may have prevented the outset of methanogenesis.

Buivid *et al.* (1981) performed experiments to investigate the effects of several landfill decomposition enhancing techniques such as moisture, nutrients, sludge and buffers addition. Buivid *et al.* (1981) indicated that the effects of these techniques was a result of interactions between them, rather than individual effects. For example, moisture increase alone was not observed to enhance methane production but when mixed with nutrients, sludge and buffers an increase in the methane production was recorded. Buivid *et al.* (1981) also noted the importance of the type of sludge used. MSW to which anaerobically digested sewage sludge was added was found to produce three times more methane than a mixture of MSW and primary sewage sludge. Buivid *et al.* (1981) concluded that this was probably attributed to the higher population of methanogenic bacteria in the anaerobically digested sewage sludge. Other studies carried out by Stegmann (1983) and Chynoweth *et al.* (1992) also reported that inoculation helps the onset of methanogenesis by providing a balanced community of microorganisms.

Recirculation, in combination with sludge addition, and buffering has been shown to be beneficial in most cases (Knox *et al.*, 1999; Croft *et al.*, 2001; Yazdani *et al.*, 2000).

In contrast, Barlaz *et al.* (1987) observed that the addition of sewage sludge to fresh MSW caused a build-up of carboxylic acid and a decrease in pH. The results of this study indicated that sludge addition without buffer addition did not enhance methane production. This was confirmed by Barlaz *et al.* (1990) who observed that the addition of anaerobic sewage sludge without buffer to fresh MSW did not stimulate methane production, while the addition of sludge with buffer acted as stimulus.

El-Fadel *et al.* (1998) assessed gas generation characteristics from six landfill cells operated under different field conditions. The main parameters investigated were: buffer addition; sludge addition; and water addition. These parameters varied in five of the cells, while one cell was used as a control. Based on gas production data, the cells with the highest moisture content, sludge and buffer addition (cells A, B and C) were observed to have the lowest total gas production (between 74 and 104 l/kg-dry), even less than the control cell (164 l/kg-dry)

Gulec *et al.* (2000) reported that in a series of 10-liter laboratory-scale batch digesters filled with 2-year old MSW at ratios of 1:9, 1:6 and 1:4 (anaerobically digested sludge to waste on wet basis), the pH of leachate ranged from 7.0 to 8.5 compared to a sharp drop in pH levels to the acidic range in the control reactors (no sludge addition). This may be explained by the buffer capacity of sludge.

Suna Erses and Onay (2003) suggested that the introduction of leachate from old landfills (with established colonies of anaerobic microorganisms, low organic content and higher buffer capacity) into a young landfill could be a promising leachate management strategy for faster waste stabilization. In this study, old landfill leachate containing large number of methanogens served as inoculum, and helped the onset of methanogenic conditions.

Literature on sewage sludge co-disposal is contradictionary. There are four main reasons: varying proportions of sludge and refuse used; the type of sludge used; the addition of buffering agent; and varying conditions under which each experiment was carried out (e.g., temperature, moisture content, leachate recirculation, availability of nutrients). Comparing the results from various studies described in the literature, it becomes clear that conclusions are specific to each experiment and that no general trends can be identified. Various parameters of the waste and the sewage sludge seems to govern waste degradation rates. Furthermore, these parameters were considered to also have interactive

effects. The extent of interactive and individual effects is critical to the performance and stability of methanogenesis during anaerobic biodegradation and must therefore be determined experimentally using, for example, the biochemical methane potential test assay (BMP) (Godley *et al.*, 2005).

2.4.5. Toxicity

Many nutrients become toxic at high concentration. The ammonium ion, for example, is a main nitrogen source for methanogenic bacteria and an important contributor to the buffering capacity in landfills but in dry landfills, where less moisture is available for dilution, the potential for ammonia inhibition and indeed salt toxicity in general increases. Ammonium toxicity is pH related and at a pH above 7.5 the NH_3 form predominates, which is more toxic than the ammonium ion (section 2.3.2). According to McCarty and McKinney (1961) and McKarty (1964) total ammonia concentrations between 50 and 200mg/l are beneficial to anaerobic processes, whereas concentrations between 1500 and 3000mg/l are inhibitory at pH levels above 7.4, and concentrations higher than 3000mg/l are toxic at all pH values.

High salt levels cause bacterial cells to dehydrate because of the osmotic pressure effect. Some microorganisms are more susceptible to osmotic pressure than others. *Staphylococcus aureus* is able to grow in solutions containing up to 65g/l *NaCl*, while *Escherichia coli* is inhibited at much lower levels (Brock, 1970). The inhibitory effect of sodium has also been investigated by Kungelman and McCarty (1965). Compared to other metal cations, sodium proved to be the strongest inhibitor on a molar basis. Sodium showed moderate inhibition at 3.5 - 5.5g/l and strong inhibition at 8g/l.

The effect of high levels of *NaCl* and NH_4Cl on the activity and syntrophic acttivities of methanogenic bacteria in semi-continuous flow-through reactor systems was evaluated by De Baere (1984). In this, two well-functioning reactors received shock concentrations of *NaCl* and NH_4Cl, while two other reactors were adapted to increasing levels of the salts over a period of 45 days. Inhibition of the methanogens occurred upon a spontaneous treatment with 30g/l of both salts. However, the activities of the methanogenic populations in the reactors which were gradually exposed to increasing levels of the salts demonstrated tolerance levels surpassing those of the non-adapted counterparts. 50% inhibition was observed at 95g/l for adaptation to *NaCl*. 50% inhibition was observed at 45g/l for NH_4Cl. The bacterial populations in the reactors consisted mostly of *Methanosarcina spp.* (> 99% of the biomass).

In the presence of electron acceptors such as metal oxides ($Fe(OH)_3$, MnO_2), nitrogen oxides (NO_3^-, NO_2^-), or oxidized sulfur compounds (SO_4^-, SO_3^-), methanogenic activity may be inhibited and/or altered (Zehnder *et al.*, 1982). Methanogenesis usually occurs only after these alternative electron acceptors are depleted. However, Zeikus (1983) suggests that the rate of methanogenesis depends on the relative amounts of electron acceptor (e.g. acetate versus sulphate) and donor (e.g. hydrogen) present.

2.5. Anaerobic biodegradability of cellulose and hemicellulose in landfills

MSW is mainly composed of organic material, particularly cellulose and hemicellulose. It has been shown that these components can comprise 91% of the methane potential of fresh waste where 51.2% of the municipal waste was composed of cellulose, 11.9% hemicellulose and 15.2% was lignin (Barlaz & Ham, 1993). Cellulose and hemicellulose have been shown to be the principal components of MSW that are degraded in landfills (Micales & Skog, 1997, Suflita *et al.*, 1992).

Cellulose is a long chain of glucose molecules, linked to one another primarily with β (1-4) glycosidic bonds. The simplicity of the cellulosic structure, using repeated identical bonds, means that only a small number of enzymes are required to degrade this material under anaerobic conditions. The biodegradability of the cellulose can be quite variable due to variations in its degree of crystallinity and its association with lignin (Stinson & Ham, 1995). Hemicelluloses are branched polymers of xylose, arabinose, galactose, mannose, and glucose. Hemicelluloses bind bundles of cellulose fibrils to form microfibrils, which enhance the stability of the cell wall of forest products presented in landfills. They also cross-link with lignin, creating a complex web of bonds which provide structural strength, which makes their complete biodegradation difficult (Tong *et al.*, 1990).

Lignin is a complex polymer of phenylpropane units, which are cross-linked to each other with a variety of different chemical bonds. This complexity has thus far proven as resistant to detailed biochemical characterization as it is to microbial degradation. Lignin degradation in landfills is primarily an aerobic process, and in an anaerobic environment lignin can persist for years and can significantly reduce the bioavailability of the other plant cell wall constituents such as cellulose and hemicellulose (Rees, 1980; Young & Frazer, 1987; Ham *et al.*, 1993[a,b]; Wang *et al.*, 1994; Baldwin *et al.*, 1998). This effect is thought to be either due to a physical restriction, with lignin molecules reducing the surface area available to enzymatic penetration and activity (Stinson *et al.*, 1995) or to

chemical restrictions where lignin is covalently linked to cellulose/hemicellulose through bonds that cannot be degraded by cellulolytic bacteria present in methanogenic environments (Tong *et al.*, 1990).

Three groups of bacteria are involved in cellulose and hemicellulose biodegradation in acetogenic/methanogenic landfills: the hydrolytic and fermentative bacteria, the acetogenic bacteria and the methanogenic bacteria. The first group of bacteria hydrolyze polymers and ferment the resulting sugars to carboxylic acids and alcohols, the second group of bacteria convert these acids and alcohols to acetate, hydrogen and carbon dioxide and the third group convert the end-products of the acetogenic reactions to methane and carbon dioxide.

In Waste Management Paper (1993) it was suggested that the gas potential of a solid waste could be determined by carrying out fibre tests which provides values for cellulose, hemicellulose and lignin content in the waste. The major methods used to determine fibre concentration in feeds are the Neutral Detergent Fibre (NDF), Acid Detergent Fibre (ADF) and Acid Digestible Lignin (ADL) tests. The analyses were originally formulated for forage and animal feeds (Van Soest *et al.* 1991; Rosentrater *et al.,* 1999; Jung, 1997). The NDF test dissolves readily degradable material such as pectins, sugars starch and fats and leaves behind cell wall components of plant material, cellulose, hemicellulose and lignin. The test involves a chemical extraction with a neutral detergent solution under reflux followed by gravimetric determination of the fibre residue (Van Soest *et al.*, 1991). Although widely used for fibre analysis of ruminant feeds, the NDF procedure is not recognized as an official method by the Association of Official Agricultural Chemists (AOAC). The ADF test in contrast, digests the less degradable hemicellulose and some proteins leaving a residue of cellulose, lignin and bound nitrogen. The ADF procedure is an AOAC-approved method of analysis (AOAC, 1984). The ADL test is the most common lignin method in ruminant nutrition analysis (Effland, 1977). ADL is determined when the insoluble material remaining after the ADF test is treated with 72% sulphuric acid.

The components which are determined by these tests can be summarised as follows:

Eq. 2.39 NDF = Cellulose + Hemicellulose + Lignin + Mineral Ash

Eq. 2.40 ADF = Cellulose + Lignin + Mineral Ash

Eq. 2.41 ADL = Lignin + Mineral Ash

Van Soest & Robertson (1980) have stated that cellulose and hemicellulose can be determined according to the following equations:

Eq. 2.42 Cellulose = ADF - ADL

Eq. 2.43 Hemicellulose = NDF - ADF

However, cellulose concentrations have been shown to be overestimated by Eq. 2.42 where xylans present in ADF are underestimated due to heat-damaged protein contamination of ADL (Jung, 1997). Similarly, hemicellulose estimates based on Eq. 2.43 can be overestimated due to non-extracted protein in NDF determinations, and underestimated due to residual xylans remaining in the ADF (Jung, 1997). It has been also shown that the ADL test underestimates lignin content due to solubilization of some of the lignin during the ADF step in the procedure (Lowry *et al.*, 1994).

Because it is difficult to control a number of parameters under actual landfill conditions, laboratory studies are needed to assess the effects of various parameters on waste degradation and to determine the biodegradability of MSW. Furthermore, in determining the biodegradability of the waste materials, proper waste characterisation is also necessary. Laboratory studies that evaluate the biodegradability of waste are reviewed in the following paragraphs.

The effect of lignin on the anaerobic degradation of cellulose was assessed through the use of a BMP test (Stinson and Ham, 1995). Results indicated that the anaerobic biodegradation of cellulose in newspapers could be enhanced by the separation of lignin from the cellulose by physical (ballmilling) or chemical (acid chlorite) treatment. After ballmilling, almost all the cellulose in the newspapers was reported to become available for degradation, even though the lignin was not removed from the sample. In contrast, the authors reported that only about 50% of the cellulose in untreated newspapers was degradable. Stinson and Ham (1995) stated that partial delignification with acid chlorite significantly increased the amount of cellulose available for degradation in newspaper. Finally, the authors concluded that the inhibition of cellulose degradation in newspapers was not due to chemical effects of lignin (e.g., enzyme adsorption) but was mainly due to the physical association of lignin with cellulose.

Eleazer *et al.* (1997) assessed the anaerobic biodegradability of the major components of MSW in 2-litres reactors operated under conditions designed to stimulate enhanced degradation in landfill (e.g., shredding, seeding, incubation at 40°C, leachate recirculation and neutralization). Measured methane production for grass, leaves, branches, food waste, coated paper, old newsprints, old corrugated containers and office paper were 144.4, 30.6, 62.6, 300.7, 84.8, 74.3, 152.3 and 217.3 litres CH_4/kg dry wt. The following parameters were introduced by Eleazer *et al.* (1997) to evaluate the degradation:

- the extent of degradation which was the measured methane production divided by the methane production calculated assuming conversion of 100% of the cellulose, hemicellulose and protein to CH_4 and CO_2; and
- MC, MH and ML which were the ratio of cellulose, hemicellulose and lignin, respectively recovered from a reactor divided by the initial mass.

A substantial variation in the range of methane production (30.6 -300.7 l/kg dry wt.) and the extent of degradation (28-94%) was reported. Eleazer *et al.* (1997) analysed the following relationships: between (cellulose + hemicellulose) concentration and methane production (R^2=0.49); between (cellulose + hemicellulose)/lignin ((C+H)/L) ratio and MC (R^2=0.28); and between (C+H)/L) ratio and the extent of degradation (R^2=0.02). However, the relationships were weak and statistically insignificant. Eleazer *et al.* (1997) also concluded that the lignin concentration alone is not a good indicator of cellulose bioavailability based on cellulose degradation in grass and paper. In particular, grass and office paper exhibited the most extensive cellulose degradation while newsprints exhibited the least. Data associated with this work have also been reported in Barlaz (1998).

Godley *et al.* (2005) identified several methods that might be used to assess the biodegradability of organic wastes using a variety of organic materials typically found in MSW. These included a mixture of physical, chemical and biological test methods that were used in a study to determine which could provide a rapid surrogate measure of waste biodegradability. They concluded that dry matter content (DM) and organic matter content (LOI) were from their study the best advised obligatory methods. However, determination of the waste content was also recommended. Godley *et al.* (2005) reported that the cellulase hydrolysis test might also provide an indication of biodegradability as a rapid non-biological test. It was also found that the tests for ADF, cellulose and ADL

provided some useful information with regards to the waste composition, but did not provide a reliable indication of the waste biodegradability and recommended that these methods should not be used as surrogate tests for biodegradability. However, the ADF contents of the wastes tested by Godley *et al.* (2005) were generally smaller than the sum of the cellulose and lignin contents (Eq. 2.40). This could be due to the fact that the ADF, cellulose and lignin contents were analysed in independent analyses involving several procedures which are subject to systematic errors associated with transfer of samples between extraction vessels, filtration and sample homogenization. The BMP test was found to be the most reliable estimate of organic waste biodegradability although very time-consuming. The authors finally concluded that they cannot yet recommend a non-biological test that would provide a reliable and rapid indication of waste biodegradability, although the cellulase hydrolysis test showed the most promise.

An improved procedure for fibre determination has been described by Kitcherside *et al.*, (2000) and is in accordance with the AOAC (1984), Van Soest (1991) and other recognized methods. The procedure uses a novel cylindrical capsule (FiberCap) with porous walls having the same filtration characteristics as Whatman 541 filter paper. The FiberCap capsule system was specifically designed to minimise systematic errors associated with extraction and filtration commonly observed in more common techniques, offering substantial improvement in analytical precision and reproducibility for fibre analyses.

In this study, the FibreCap method for fibre determination was chosen both to speed up the procedures and reduce variability and systematic error associated with extractions and filtration.

Figures

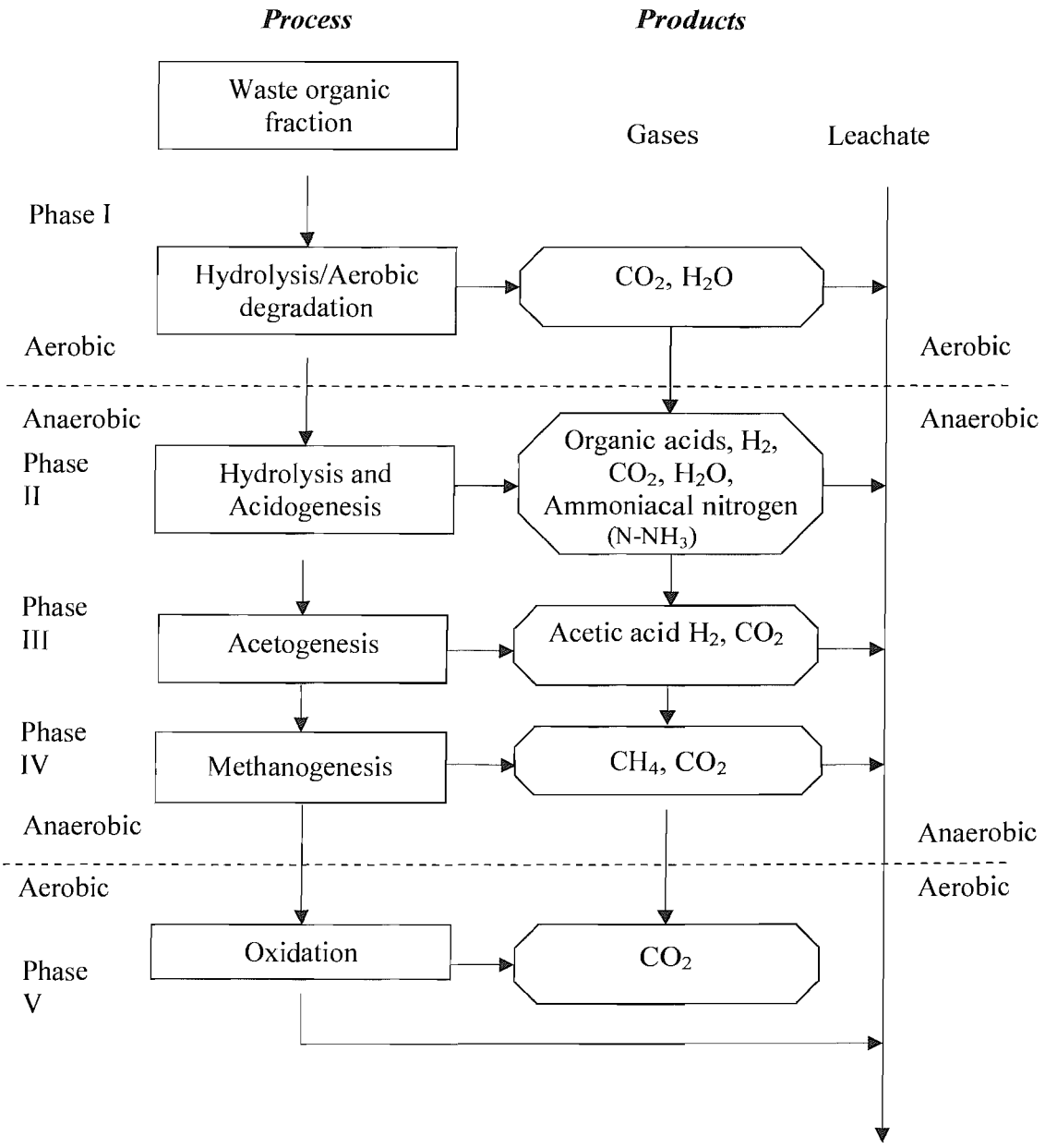

Figure 2.1. Major stages of waste degradation in landfills. Source: Waste Management Paper (1995).

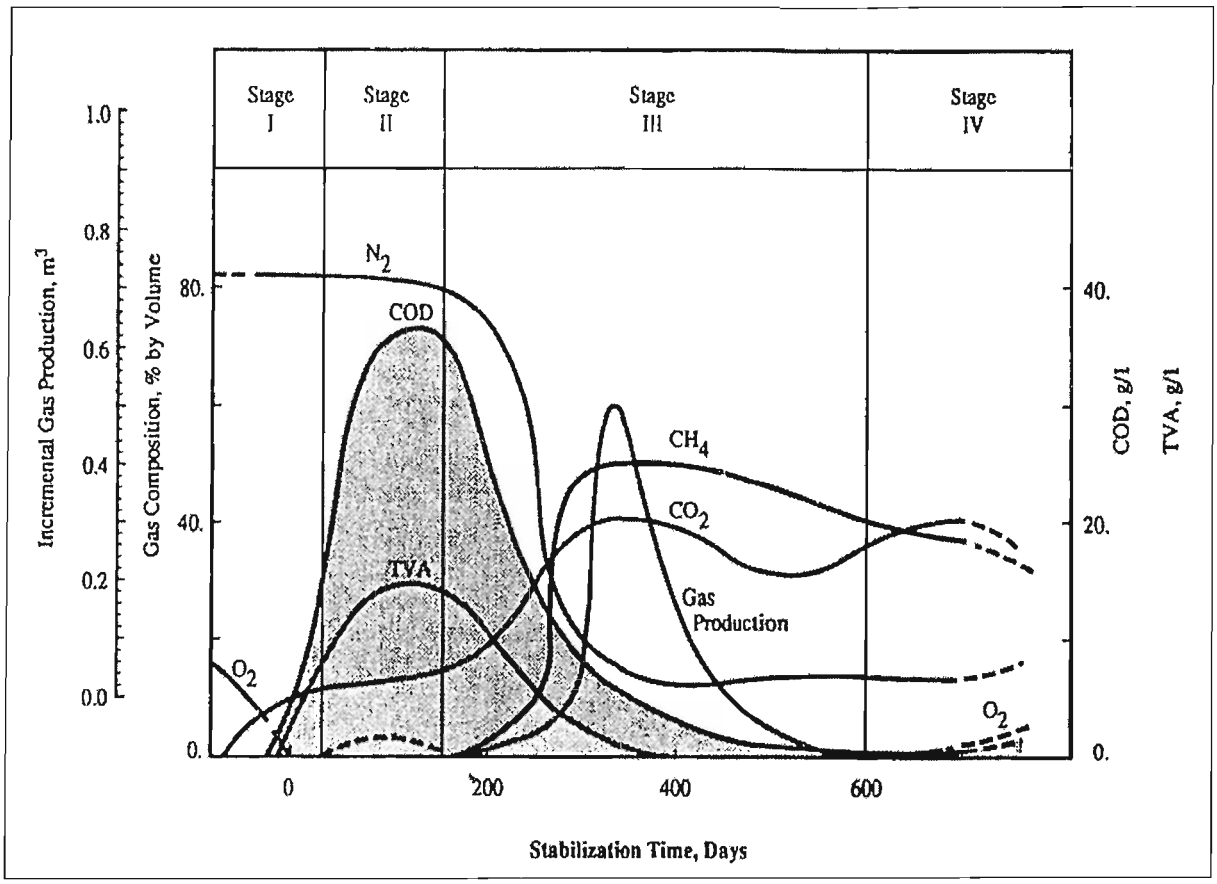

Figure 2.2. Changes in selected parameters during anaerobic degradation in a typical landfill (Pohland and Harper, 1985).

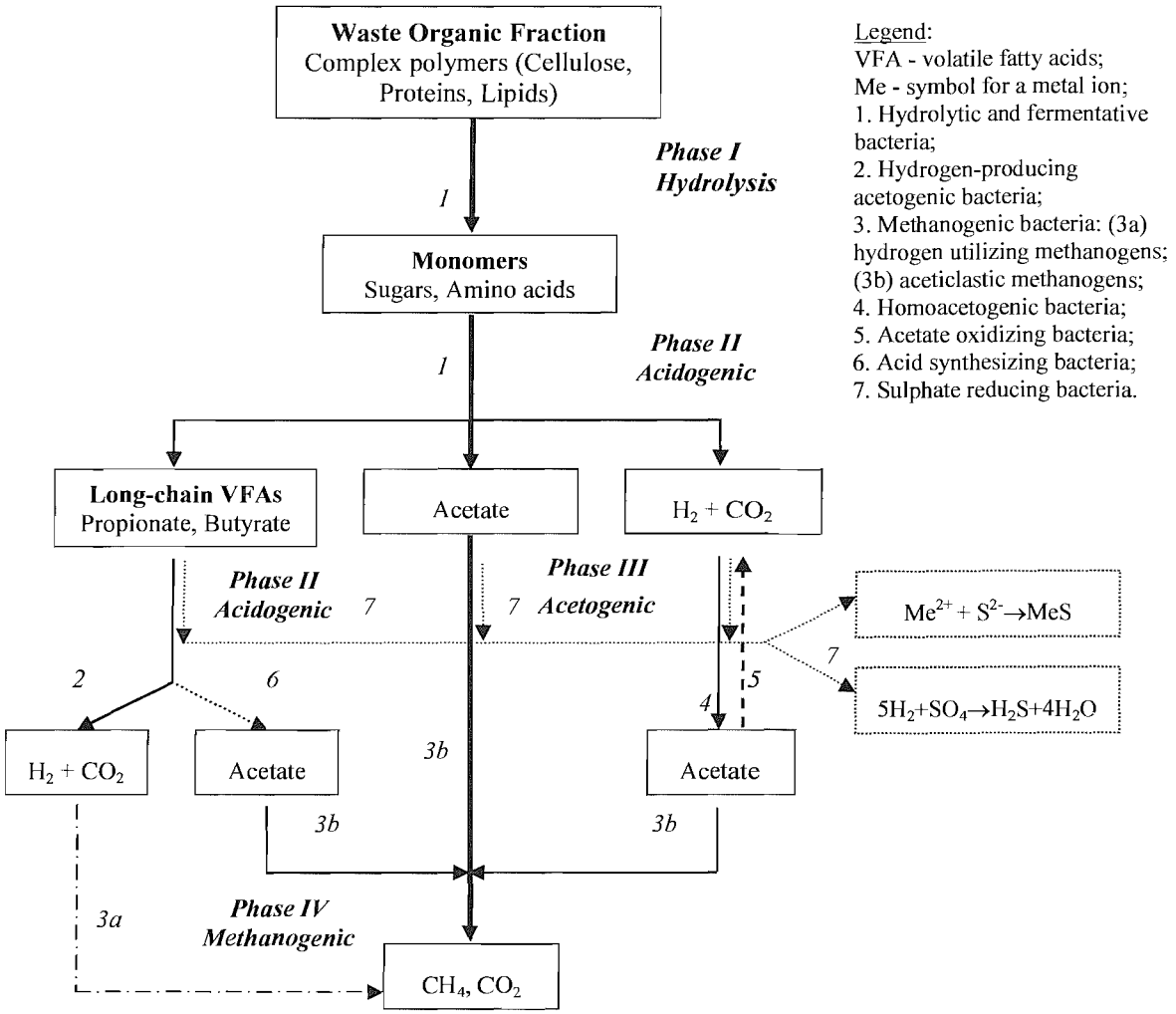

Figure 2.3. Major groups of bacteria involved in anaerobic degradation of waste organic fraction (adapted from Waste Management Paper, 1995).

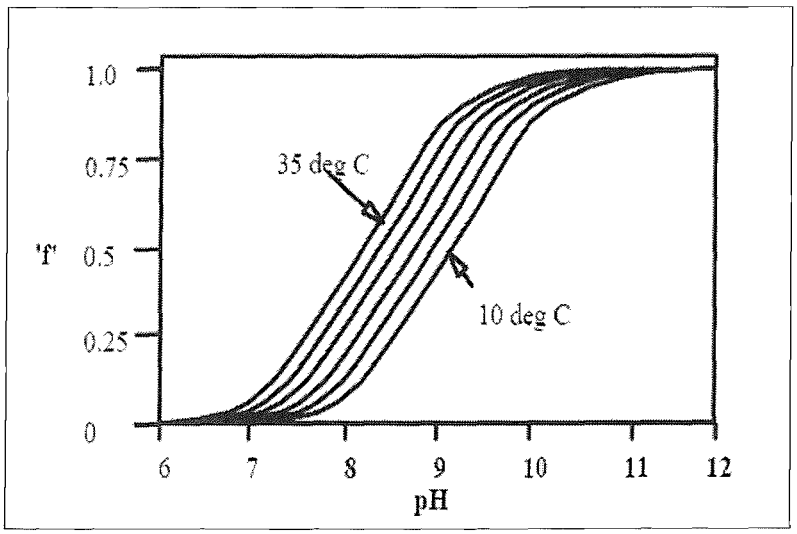

Figure 2.4. The effect of ph and temperature on "f"

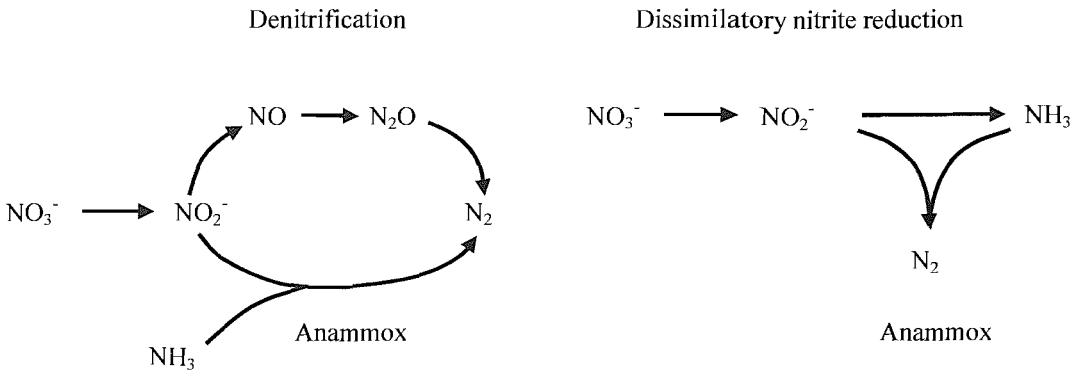

Figure 2.5. Schematic model describing the combination of anammox, denitrification, and dissimilatory nitrate reduction to ammonia by anammox cells based on Eq. 2.24 & Eq. 2.25 (Güven *et al.*, 2005).

Chapter 3

Engineering properties of waste

3.1. Introduction

Typically, MSW consists of garden and food wastes, plastics, paper products, rubber, textiles, wood, ashes, and soils (both waste products and material used as cover material). The percentage proportion of waste constituencies varies from one landfill site to another and also within a site. Legislation changes, seasonal factors and resource management practices (e.g., pretreatment and recycling activities) have a significant impact on the waste stream over time. The composition of MSW in Britain, for example, has changed noticeably over the past few decades with increasing plastic and decreasing ash content (Figure 3.1). In addition, a reduction in biodegradable fraction of waste in landfills will occur in EU member states through the introduction of the EU Landfill Directive (99/31/EC). The Directive requires a reduction in the amounts of biodegradable MSW being disposed of to landfills in the UK to 75% of 1995 levels by 2010, 50% by 2013 and 35% by 2020. These variations lead to significant differences in the mechanical properties of waste and they must be taken into consideration when using results from the literature. Quantification of these properties can obviously be very difficult, particularly in the case of heterogeneous materials such as MSW. In common with soils, the important engineering properties of waste are considered to be particle size distribution, moisture content, porosity, unit weight, field capacity, hydraulic conductivity, compressibility, and stiffness. Individual waste components have a wide range of particle sizes and these also can change over time. However, waste components may have voids within them in addition to those between components. This results in a significant percentage of waste particles behaving differently to soil particles due to their high

compressibility. Further, as waste degradation occurs these properties are liable to change.

3.2. Particle size and size distribution of waste components

The size distribution of waste components has a significant effect on the engineering properties such as hydraulic conductivity, compressibility, and shear strength. A general indication of the particle size distribution of the various components (by longest dimension and ability to pass a sieve) is presented in Figure 3.2. Typical data on the % size distribution of the individual components in MSW are presented in Figure 3.3. The average size of the individual components found in residual MSW was reported to be between 180-200mm (Tchobanoglous *et al.*, 1993). Biodegradation of the organic fraction of MSW is likely to result in a loss of mass, structure, changes in particle size and alteration of the engineering properties of MSW (i.e. density, unit weight, compressibility and shear strength) (Dixon *et al.*, 2005).

3.3. Phase relationships for waste

A number of fundamental definitions, known as phase relationships can be used to characterize the state of the refuse (Powrie, 1997) (Figure 3.4). They are:

i) the *void ratio* (e), which is defined as the ratio of the volume of the voids to the volume of solids: $e = V_v/V_s$;

ii) the *specific volume* (v), which is defined as the actual volume occupied by a unit volume of refuse solids: $v = (V_s+V_v)/V_s = 1 + e = 1/[1-(\omega_{vol} + n_e)]$, where ω_{vol} is the water content (Eq. 3.4); n_e is the drainable porosity (section 3.4);

iii) the *porosity* (n), which is defined as the volume of voids per unit total volume. Porosity (n) can be related to the void ratio (e) by the relationship: $n = e/(1+ e)$. At 100 percent saturation, we can define porosity as the ratio of total volume of water to total volume (Eq. 3.1):

Eq. 3.1. $$n = V_v/(V_s + V_v) = e/(1 + e) = (v - 1)/v;$$

iv) the *saturation ratio* (S), which is defined as the ratio of the volume of water to the volume of voids: $S = V_w/V_v$;

v) the *water content* (or moisture content) (ω), which is defined as the ratio of the mass of water to the mass of refuse solids (Eq. 3.2 to Eq. 3.3).

In general, fresh refuse when emplaced will contain some water but will not be saturated. The water content (ω_{dry}) of the refuse as deposited is referred to as the *original water content*, and is defined and determined in the conventional soil mechanics way as the ratio of the mass of water to the dry mass of solids (Eq. 3.2). Water contents are also sometimes expressed in terms of the ratio of the mass of water to the total mass of water and solids (ω_{wet}) (Eq. 3.3) or as the ratio of the volume of water to the total volume of air, water and solids (ω_{vol}) (Eq. 3.4).

Eq. 3.2 $$\omega_{dry}(\%) = \left(\frac{a-b}{b}\right)100;$$

Eq. 3.3 $$\omega_{wet}(\%) = \left(\frac{a-b}{a}\right)100;$$

where: a = initial mass of sample as delivered;
b = mass of sample after drying at 105 °C.

Eq. 3.4 $$\omega_{vol}(\%) = \left(\frac{V_w}{V_a + V_w + V_s}\right)100.$$

3.4. Field capacity and hydraulic conductivity of waste

After landfilling, the water content of the waste may increase through the absorption of water by components such as paper, cardboard and textiles. Beyond a certain limit, known as the *total absorptive capacity* of the waste, the addition of any other water leads to the production of an equivalent volume of free-draining pore fluid, which will tend to move down through the waste under the influence of gravity towards a water table below which (in the absence of landfill gas production) the waste is substantially saturated.

The infiltration or flow of leachate through the waste depends on the waste *field capacity* and its *hydraulic conductivity (coefficient of permeability)* of waste. Waste is referred to as being at *field capacity* when its total absorptive capacity has been fully utilised and conditions of free downward drainage are established. The field capacity varies with the height of waste, state of compaction, and state of degradation. Typically, the field capacity of uncompacted waste from residential and commercial sources varies from 50 to 60%. In the tests described in this study, the total absorptive capacity and the field

capacity were determined by flooding the waste from the bottom of the sample, and then allowing it to drain. This procedure also enables the *drainable porosity of the refuse* (n_e) (defined as the volume of drainable voids (V_d) per unit total volume) at field capacity to be determined (Eq. 3.5).

Eq. 3.5. $$n_e = V_d/(V_s + V_v)$$

The *hydraulic conductivity (k)* of compacted waste is an important physical property because it governs the movement of liquids and gases in a landfill and represents in this case the ease with which a fluid such as leachate will flow through the liner material. Hydraulic conductivity depends on the other properties of the solid material in the waste including pore size distribution, surface area, and porosity. Hydraulic conductivity can be determined by the application of Darcy's Law, which is an empirical law describing the flow of a fluid through a porous material:

Eq. 3.6 $$Q = -k.A\frac{dh}{dz}$$

where, Q = volumetric flow rate, m/s;
k = hydraulic conductivity, m/s;
A = flow area perpendicular to z (cross sectional area), m^2 (πr^2);
h = hydraulic head, m;
z = flow path length, m; and
d = denotes the change in h over the path z.

The term $\frac{dh}{dz}$ is known as the *hydraulic gradient* (i), which gives the pressure difference between the top and bottom of the layer of material. Thus, the hydraulic conductivity can be expressed using the hydraulic gradient i as follows:

Eq. 3.7 $$k = -\frac{Q}{A.i}$$

Typical hydraulic conductivities of saturated waste obtained by other researchers are given in Table 3.1.

Table 3.1. Waste saturated hydraulic conductivity.

Material	Hydraulic conductivity, m/s	Source
Shredded MSW	$1 \times 10^{-4} - 10^{-6}$ (not given)*	Williams, 2002
Large scale test on excavated MSW	$4 \times 10^{-4} - 1 \times 10^{-5}$ (3.5-5.5)*	Landva and Clark, 1990
MSW as placed	1×10^{-5} (not given)*	Williams, 2002
Baled MSW	7×10^{-6} (not given)*	Williams, 2002
Large scale compression test on crude domestic waste	$1.5 \times 10^{-4} - 3.4 \times 10^{-5}$ (3.8)* $8.2 \times 10^{-5} - 1.9 \times 10^{-5}$ (4.1)* $2.8 \times 10^{-5} - 3.1 \times 10^{-6}$ (4.8)* $8.9 \times 10^{-6} - 4.4 \times 10^{-7}$ (5.8)* $2.7 \times 10^{-7} - 3.7 \times 10^{-8}$ (7.0)*	Powrie and Beaven, 1999

* The number in brackets is the dry unit weight in kN/m^3 as determined *in situ*.

As waste density increases with increased depth (compression), drainable porosity and vertical hydraulic conductivity will decrease, suggesting that liquid movement may be restricted in deeper landfills, and therefore may limit processes such as leachate flushing. In deep landfills, the heavily compressed waste may have a hydraulic conductivity approaching that of "impermeable" liner materials. For landfills, hydraulic conductivity of the liner must be 1×10^{-9} m/s or less (Sarsby, 2000). Also the increased rates of gas production or gas accumulation can further reduce hydraulic conductivity.

3.5. Unit weight

Unit weight (γ) is the weight per unit volume, in kN/m^3, whereas the *bulk density* (ρ_b) is the mass per unit volume (Kg/m^3), multiplied by the gravitational constant $g = 9.81$ m/s^2. In practice, however, the unit weight is usually used in preference to the mass density. This is because it facilitates the calculation of vertical stress at depth, which often arises primarily as a result of the weight of overlying refuse. The *dry density* (ρ_{dry}) is sometimes used as an indication of the degree of compaction of the refuse. Dry density is the density that the refuse would have at the same total (gas + liquid) void ratio but zero water content. The dry density can be calculated as follows:

Eq. 3.8 $$\rho_{dry} = \frac{\rho_b}{1 + \omega_{dry}}$$

where ω_{dry} is the actual water content (section 3.3).

Waste density in landfills is difficult to determine since it is dependent upon the waste type, water content, type of daily cover and time since placement. The waste at the bottom of deep landfills compacts immediately upon placement due to mechanical compaction as well as over time, as waste filling progresses vertically. This results in a greater waste density of the waste at the bottom of the landfill as compared to the top. In bioreactor type landfills (Williams, 2002), organic waste is rapidly stabilized by practices such as leachate recirculation which promotes degradation. The process of adding this additional moisture to the waste also affects its density until the waste reaches its optimum moisture content.

Hater (2000) measured unit weight of MSW at four landfills where leachate recirculation was used. Based on these measurements, the average in-place unit weight was found to be 1790kg/m^3 or about 60% denser than for conditions where leachate circulation was not practiced, which had the average unit weight of 1070kg/m^3. The increase in unit weight depends on the initial moisture content of the waste, leachate generation or recirculation rates, waste field capacity, and the void ratio available for the liquids.

3.6. Compressibility and stiffness

Compressibility of MSW has to be quantified to enable predictions of total and differential settlement, and of the distribution of these with time during the life of the landfill facility. This information is needed to optimise capping system design. To characterize the compressibility of waste a compressibility index is often defined and is a process similar to that used for soils (Reddy and Bogner, 2003). The compressibility of the waste depends on the leachate head, moisture content, density, composition, and biodegradation phase. The compressibility of the refuse landfill also depends on a number of factors, including placement compaction, existing stress level and the magnitude of the additional stress increment. The variations in these properties together with the heterogeneous, anisotropic and often unsaturated nature of waste in most landfills limit the use of classical soil mechanics approaches to predict landfill settlements.

The principal source of loading is self-weight, which results in waste settlement during the construction period. Compression of the fill caused by additional loading can most easily be predicted by means of a compressibility parameter related to one-dimensional

compression (e.g. waste is placed over a large area in relation to the thickness of the fill). Stresses are assumed to be effective for fresh waste due to its low moisture content and for this reason strains are assumed to occur immediately after load application. If, in one dimensional compression, an increment of vertical effective stress $\Delta\sigma_v^{'}$ produces an increase in vertical strain $\Delta\varepsilon_v$, then the *stiffness* $E_o^{'}$ (also called the *constrained modulus*) is defined as:

Eq. 3.9. $$E_o^{'} = \frac{\Delta\sigma_v^{'}}{\Delta\varepsilon_v}$$

The settlement during construction (i.e. primary settlement) can be predicted using:

Eq. 3.10. $$\Delta h_p = \sum_{i=1}^{n} \frac{H_i \, \Delta\sigma_v^{'}}{E_{o,i}^{'}}$$

where $\Delta\sigma_v^{'}$ is the change in vertical effective stress, H_i is the thickness of the sub-layer *i* of waste, $E_{o,i}^{'}$ is the constrained modulus of layer *i*. As the thickness of the waste increases the stiffness of the waste will also increase with depth depending upon the level of mean stress in the waste layer under consideration. The total primary settlement is calculated as the sum of the settlement of each individual layer of waste using the relevant $E_o^{'}$ value (Eq. 3.10).

Beaven and Powrie (1995) carried out large-scale compression tests on waste samples to investigate variations in waste density, stiffness, absorptive capacity, effective porosity and hydraulic conductivity. One of their findings was that the constrained modulus varied with the stress and strain levels in tests on four waste samples (Figure 3.5 & Figure 3.6). It can be assumed that the bulk stiffness of waste increases with the stress level but decreases with the strain level, which is the same as that observed in soil behaviour. A summary of constrained moduli values found in the literature for MSW related to stress level is shown in Figure 3.7.

In several bioreactor landfill studies (El-Fadel & Al-Rashed, 1998; Augenstein *et al.*, 1999, 2005[a,b]) settlement was observed to vary significantly, both spatially and temporally. Accordingly, the information gained, highlighted that a comprehensive model for settlement analysis of bioreactor landfill waste should take into consideration the decrease in void ratio due to the solid to gas conversion process, the changes in the

degree of saturation, as well as the physical changes in particle sizes and distribution as the waste structure changes.

Hossain *et al.* (2003) attributed the total settlement of waste in bioreactor landfills to the following three components: (1) compression of the waste due to its own weight; (2) compressibility of waste caused by physicochemical processes originating in waste and its consequent variation of the waste components and their arrangement distribution; and (3) compression of the waste as mass is transformed to biogas leading to a corresponding decrease in void space. On the basis of laboratory scale one-dimensional consolidation experiments, Hossain *et al.* (2003) reported that the compressibility of waste increases with time when the conversion of solid matter to gas phase was enhanced by degradation and leachate recycling. The compressibility parameter (C_c), similar to the compression index defined for soils , was correlated to biodegradation factors such as the ratio of (cellulose + hemicellulose)/lignin or (C+H)/L. For decreasing ratios of (C+H)/L, C_c values were found to increase. For similar ratios however, the creep index (C_α), which is similar to the coefficient of secondary compression for soils, showed a certain independency to the degree of degradation. A biological compression index (C_β) was defined to describe the compression due to biodegradation and it was found to vary, depending on the state of degradation, and yielded the highest values when waste samples were actively decomposing but had a substantial remaining methane potential, typically found in the accelerated methanogenic phase (section 2.2.4).

The aim of the next chapter is to identify mechanisms that contribute to the settlement that occurs in landfills and make a comparison between the main group of models which use a single equation to express both primary and secondary settlement. In order to achieve this objective, existing classical data are taken as a basis.

Figures

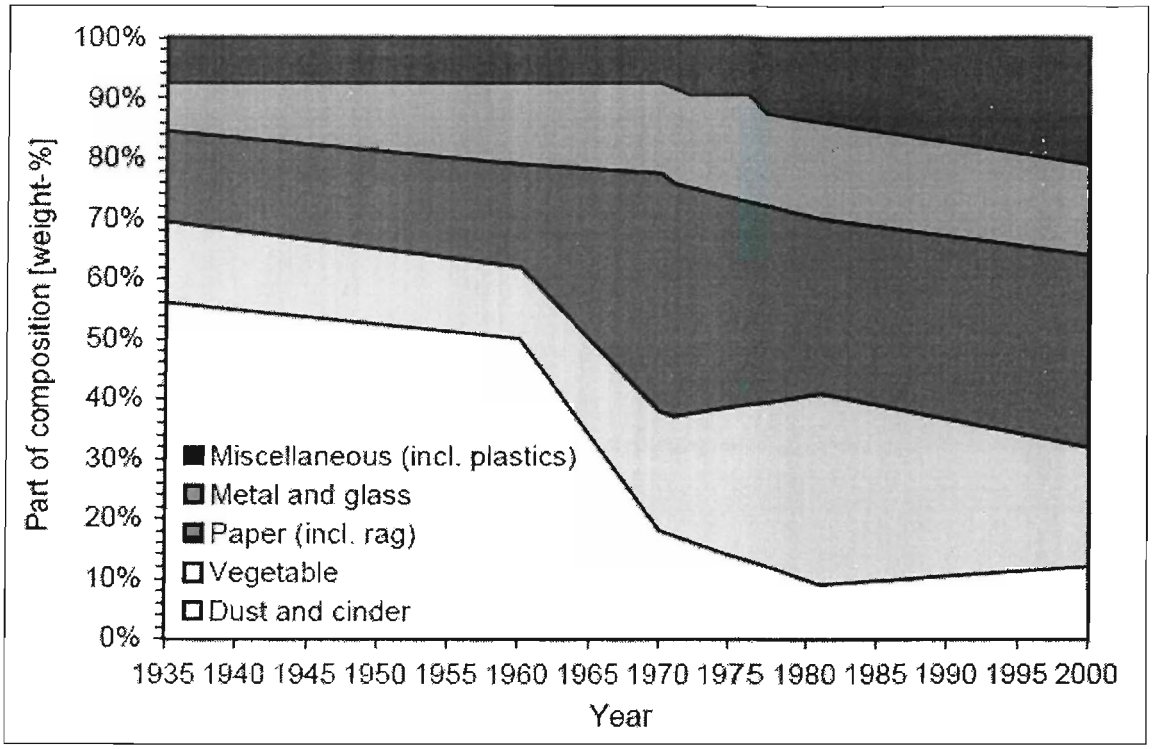

Figure 3.1. Composition of UK MSW 1935–2000 (Dixon *et al.*, 2005).

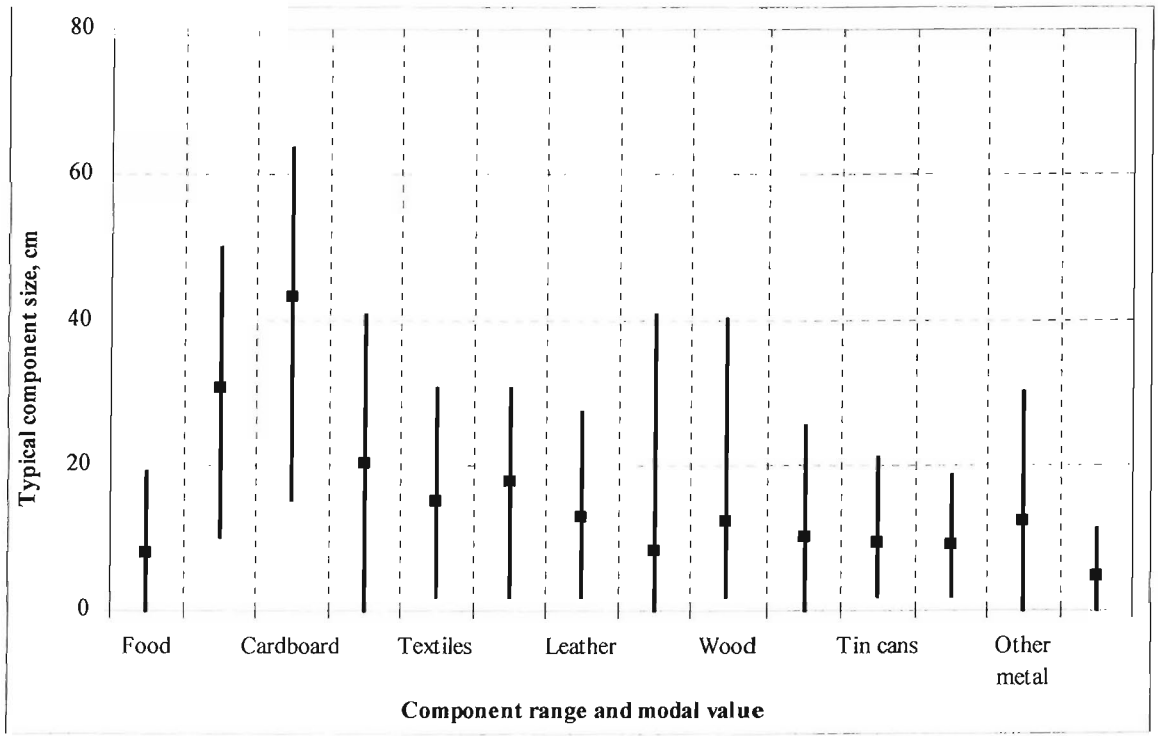

Figure 3.2. Typical size distribution of the components found in residential MSW (Tchobanoglous *et al.*, 1993).

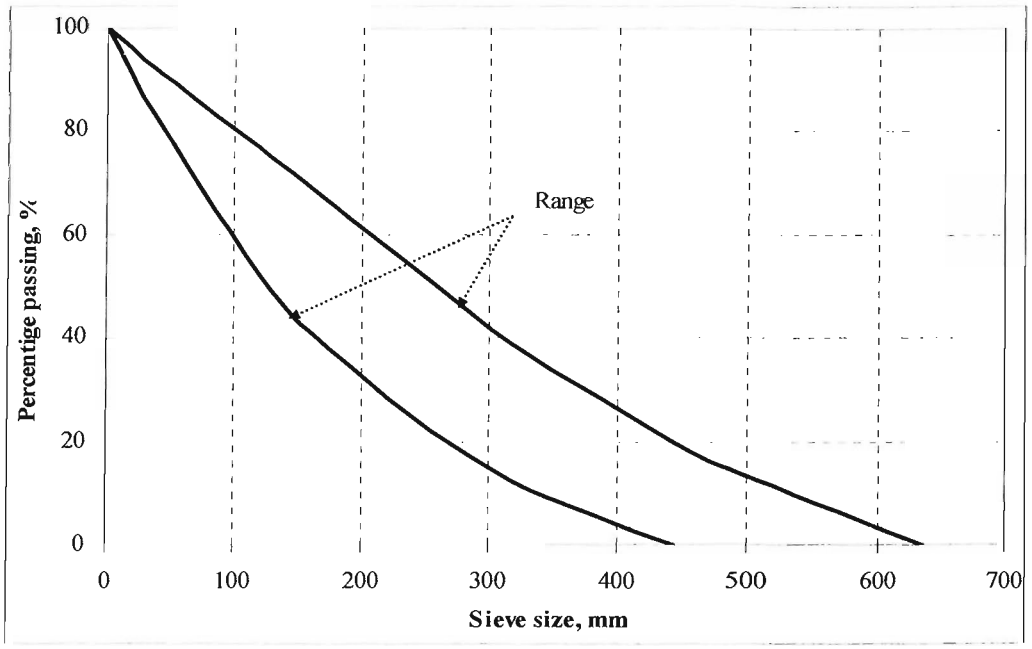

Figure 3.3. Percentage of total mass of residential and commercial MSW as a function of sieve size (adapted from Tchobanoglous *et al.*, 1993).

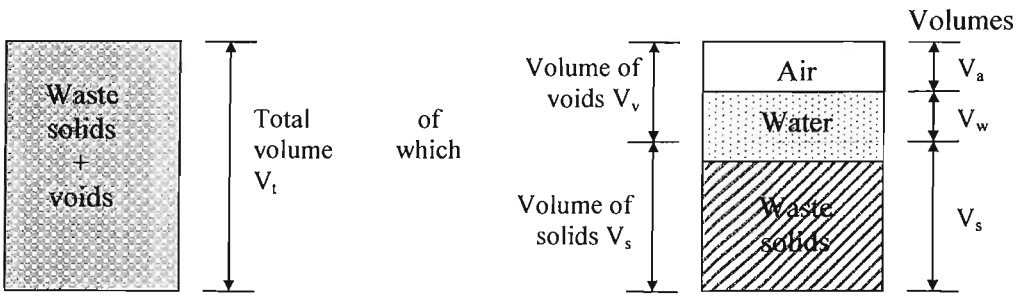

Figure 3.4. Waste as a three phase material.

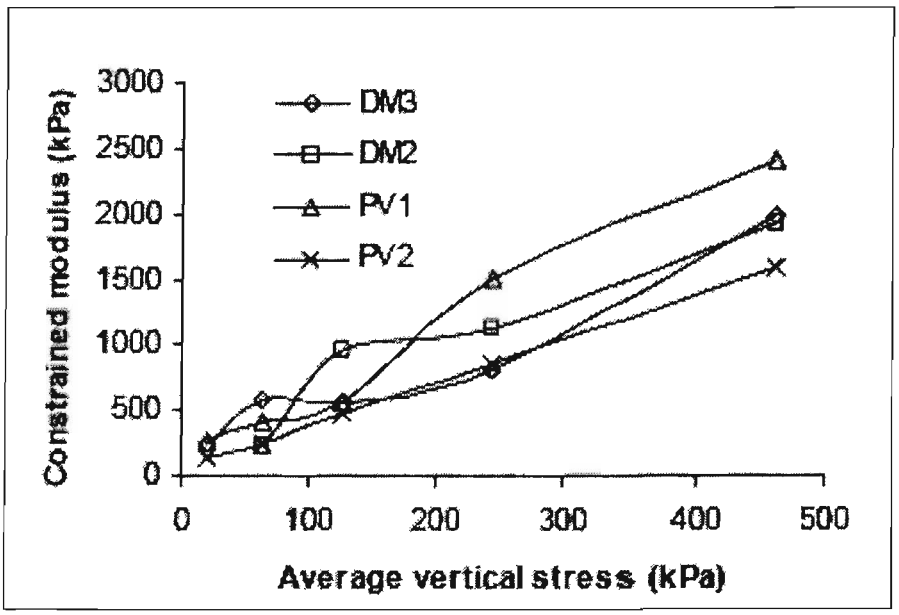

Figure 3.5. Stress dependent constrained modulus of waste (Beaven and Powrie, 1995).

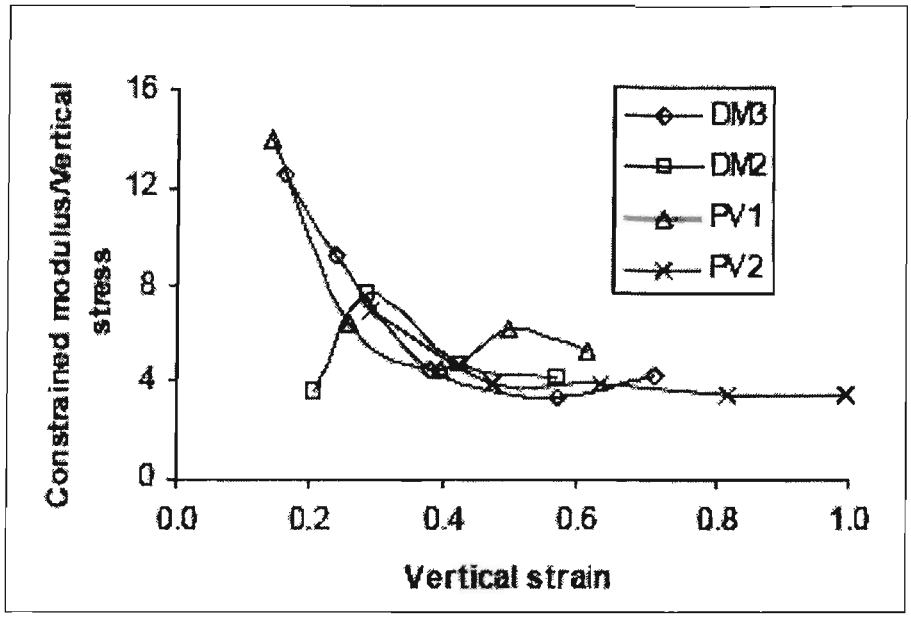

Figure 3.6. Strain dependent constrained modulus of waste (Beaven and Powrie 1995).

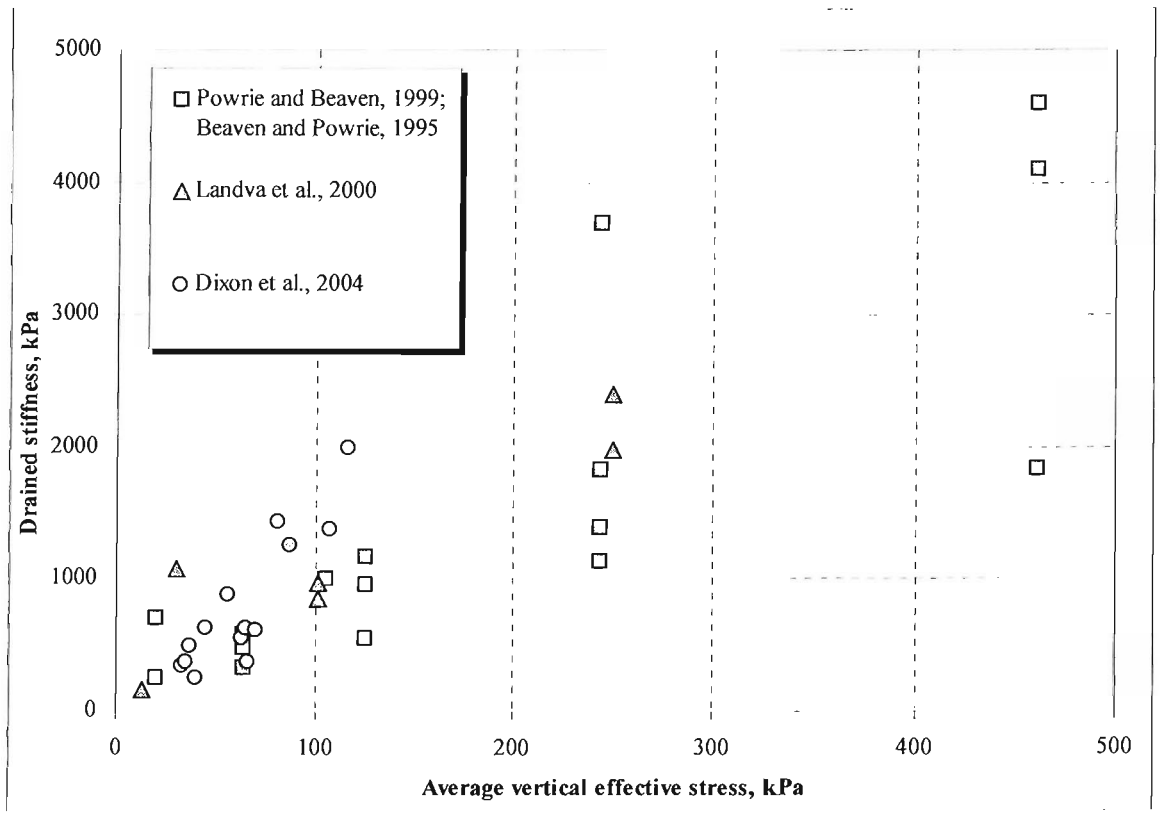

Figure 3.7. Drained stiffness values for MSW (adapted form Dixon *et al.*, 2004).

Chapter 4

Settlement of MSW

4.1. Introduction

The literature contains a wide range of models developed to predict waste settlement. These models can be classified according to:

- their formulation (logarithmic curve, exponential, hyperbolic, etc.);
- their origin (models based on soil mechanics, rheological models, empirical models); and
- their mode of resolution (analytical, geometrical, numerical).

Research conducted into the mechanisms causing landfill settlement can be divided into settlement modelling, field observation and laboratory studies. The following sections provide a review on the four main types of models which attempt to describe both primary and secondary settlement using a single equation.

4.2. Models based on logarithmic functions

4.2.1. Background of the existing models

MSW, like soil, is basically a particulate material and it is therefore not surprising that attempts to quantify its mechanical behaviour have generally been based on conventional soil mechanics principals. However, there are certain assumptions involved in many of the traditional models used in soil mechanics, such as incompressibility of the solid constituents and the pore water, which may make these models inapplicable for MSW. More specifically in the analysis of compression processes in saturated soils any change

in overall volume is only due to a rearrangement of the soil skeleton and the dissipation or taking in of pore fluid and not to degradation of and chemical reactions within the particles which is typical for long term settlement processes in waste.

Terzaghi (1925) first elaborated a comprehensive framework to describe the mechanics of behaviour of soils which defined much of the field of knowledge we currently know as geotechnical engineering. Terzaghi (1943) formulated the principle of effective stress and its importance in describing the behaviour of granular materials cannot be overstated.

Primary compression occurring in a waste layer due to imposed stress can be described by Terzaghi's theory of consolidation (1943), according to the following equation:

Eq. 4.1 $$\frac{\Delta h_p}{h_o} = \frac{C_c}{1+e_o}\log\frac{\sigma'_o+\Delta\sigma'}{\sigma'_o} = C_R.\log\frac{\sigma'_o+\Delta\sigma'}{\sigma'_o}$$

Equivalent to: $\Delta e = C_c.\log\frac{\sigma'_o+\Delta\sigma'}{\sigma'_o}$, with $\frac{\Delta h_p}{h_o} = \frac{\Delta e}{1+e_o}$ and $C_R = C_c\frac{1}{1+e_o}$

where Δh_p = primary settlement, m;

h_o = original layer thickness, m;

C_c = primary compression index;

C_R = modified primary compression index;

σ'_o = existing vertical effective stress at midpoint in the layer, kPa;

$\Delta\sigma'$ = increase in vertical stress due to the fill placement;

Δe = increment of void ratio;

e_o = initial void ratio.

This is valid only for normally consolidated soil samples which have never been subjected to effective vertical stress higher than the present effective overburden pressure (σ'_o). In this case if σ'_p is the preconsolidation pressure, then σ'_o should be higher than σ'_p ($\sigma'_o > \sigma'_p$). Only very young soil deposits, or those that have just completed primary consolidation in response to a recent loading, can be expected to lack a recompression behaviour and to have values of $\sigma'_o > \sigma'_p$.

For a soil sample which has undergone a preconsolidation higher than the effective stress $\sigma'_o + \Delta\sigma'$, i.e. $\sigma'_o + \Delta\sigma' < \sigma'_p$, the slope $\frac{\Delta e}{\Delta\log\Delta\sigma'}$ in an e_o vs $\log\sigma'$ plot is termed the recompression index C_s , then Eq. 4.1 can be presented as:

Eq. 4.2 $$\frac{\Delta h_p}{h_o} = C_s.\log\frac{\sigma'_o+\Delta\sigma'}{\sigma'_o}$$

where C_s is the primary recompression index.

In the general case of a waste sample undergoing preconsolidation under an effective stress σ'_{pc} but subjected to an increment of pressure such as: $\sigma'_o < \sigma'_{pc}$ and $\sigma'_o+\Delta\sigma' > \sigma'_{pc}$ the primary compression can be calculated by the following equation:

Eq. 4.3 $$\frac{\Delta h_p}{h_o} = C_s.\log\frac{\sigma'_{pc}}{\sigma'_o} + C_R.\log\frac{\sigma'_o+\Delta\sigma'}{\sigma'_o}$$

The coefficients of primary recompression C_s and primary compression C_R are material parameters which do not depend on the state of stress. For models based on oedometric deformation (i.e. one-dimensional compression) the following equation is valid:

Eq. 4.4 $$\Delta\sigma' = E_{eod}\frac{\Delta h_p}{h_o}$$

where E_{oed} is the modulus of elasticity, which for a normally consolidated soil varies with the stress by the primary compression index C_R:

Eq. 4.5 $$E_{eod} = \frac{\Delta\sigma'}{C_R.\log\left(\frac{\sigma'_o+\Delta\sigma'}{\sigma'_o}\right)}$$

Illustration of primary consolidation theory according to Terzaghi theory (1943) is shown in Figure 4.1.

In addition, the laboratory tests on soils carried out by Buisman (1936) showed the effect of time on the compressibility of fine grained soils. Buisman (1936) highlighted the fact that the compression of clays and peats increased linearly with the logarithm of time under constant effective load. He called the further compression *secular effects* after the latin name for century *sæculum*. Buisman (1936) reported long duration settlement curves and concluded that further settlement associated with constant effective stress occurred. Theoretically, the settlement curve has an asymptote z_∞, but experimentally the settlement continues even when the excess pore water pressure has dissipated, at constant effective stress (Figure 4.2). This has led to the definition of primary and secondary settlement in the geotechnical engineering field.

In order to take the secondary compression into account (Figure 4.2), Buisman (1936) proposed the following law:

Eq. 4.6 $$\frac{\Delta h}{h_1} = \left(\alpha_p + \alpha_s \log \frac{t}{t_1} \right) \Delta \sigma'$$

in which Δh represents the settlement, h_1 is the thickness of the soil horizon at time t_1 corresponding to the end of the primary consolidation (usually 1 day), σ_o' the effective stress increment, α_p, α_s are respectively the primary compression constant and the secondary compression constant at t_1. There are difficulties of accessing h_1 under applied load and for practical purposes h_1 is assumed to be equal to the initial layer thickness, h_o. Measurements showed that the compression constants are stress dependent as increasing stresses result in smaller compression constants. Some typical values for clay are 0.4 x 10^{-3} to 1.0 x 10^{-3} m^2/kN for α_p and 0.1 x 10^{-3} to 0.5 x 10^{-3} m^2/kN for α_s.

Koppejan (1948) combined the equations of Terzaghi (1943) and Buisman (1936):

Eq. 4.7 $$\frac{\Delta h}{h_o} = \left(\frac{1}{C_p} + \frac{1}{C_s} \log t \right) \ln \frac{\sigma_o' + \Delta \sigma'}{\sigma_o'}$$

where C_p and C_s are dimensionless constants dependent on the chosen unit of time, but are independent of the stress. The use of logarithms of different bases in Eq. 4.7 has been adopted in order to adhere to the basic formula as much as possible, but might be avoided by calculating $\ln \frac{\sigma_o' + \Delta \sigma'}{\sigma_o'} = 2.3 \log \frac{\sigma_o' + \Delta \sigma'}{\sigma_o'}$

After substitution, another form of the Eq. 4.7 is obtained:

Eq. 4.8 $$\frac{\Delta h}{h_o} = 2.3 \left(\frac{1}{C_p} + \frac{1}{C_s} \log t \right) \log \frac{\sigma_o' + \Delta \sigma'}{\sigma_o'}$$

Typical values for clay are 10 to 25 for C_p and 50 to 250 for C_s with time in days. For example, sands do not show secular effects such that $\frac{1}{C_s} = 0$. By setting $\frac{1}{C_s} = 0$ and $2.3 \frac{1}{C_p} = C_R$ Eq. 4.8 changes to Terzaghi's formulation (Eq. 4.1).

A major progress in the understanding about time dependent behaviour of soils was made by Bjerrum (1967) who formulated the concepts of instant and delayed compression and their relation to primary and secondary compression. This qualitative improvement was stimulated by the estimate of plastic Drammen clay (Norway) by means of a system of curves, each corresponding to a different duration of sustained loading. Bjerrum (1967) assumed that any given overburden pressure and void ratio corresponds to an equivalent time of constant loading and a certain rate of delayed compression. The volume change in a clay is divided into two components:

- Instant compression which occurs simultaneously with the increase in effective stress and causes a reduction in void ratio until an equilibrium value is reached at which the structure effectively supports the overburden pressure; and
- Delayed compression which represents the reduction in volume at unchanged effective stress.

These concepts are conflicting to the expressions of primary and secondary compression (Figure 4.2), which separate the compression into two processes before and after the dissipation of excess pore water pressure. The concepts of instant and delayed compression are clarified in Figure 4.3. The effective stress increases gradually due to the viscosity of water and compression occurs as represented by the solid line. The dashed line at the origin ($t = 0$) represents instant compression and is to be considered as a rather conceptual idea of an immediate application of effective stress which practically cannot be achieved. The division of the compression into a primary and a secondary contribution is considered to be rather unspecified, as the time required for the dissipation of the excess pore water pressures is dependent on factors such as the thickness of the clay layer, its permeability and the drainage conditions. Bjerrum (1967) stated this division to be inappropriate to describe the behaviour of the soil structure with respect to effective stress.

After the formulations on creep by Bjerrum (1967), several models have been developed describing this behaviour using time lines. The state of a soil is entirely described on a double logarithmic void ratio - effective stress plot with compression lines corresponding to a tenfold increase of time, as can be seen in Figure 4.4 and Figure 4.5

Hansen (1969) calibrated the settlement estimated for the Norwegian Drammen clay (Bjerrum, 1967) using the following equation:

Eq. 4.9 $$\frac{e}{e_o} = b\log\frac{\sigma_o' + \Delta\sigma'}{\sigma_o'} + c\log\frac{t_i + t}{t_i}$$

Where e_o is the initial (before compression) void ratio, e is the void ratio at time t, σ_o' and $\Delta\sigma'$ are as in Eq. 4.1, t_i corresponds to the instant compression line, b the slope of the compression line and c the spacing between adjacent tenfold increases of time. Figure 4.4 and Figure 4.5 illustrate how a soil is loaded by $\Delta\sigma'$ following the instant compression and then afterwards experiences delayed compression.

As the void ratio decreases under a constant effective stress, the soil structure becomes increasingly more stable and is capable of supporting an additional load (if it does not exceed a certain critical value) with little additional change in void ratio. If the critical pressure σ_{pc}' (also known as preconsolitation pressure) is exceeded the void ratio decreases along the instant line until the soil structure is capable of carrying the excess pressure, i.e. the pressure in excess of the critical pressure σ_{pc}'. Garlanger (1972) modified Eq. 4.9 to calculate the compression at any time t for loading above σ_{pc}' and suggested the following equation:

Eq. 4.10 $$\frac{e}{e_o} = C_s.\log\frac{\sigma_{pc}'}{\sigma_o'} + C_R.\log\frac{\sigma_o' + \Delta\sigma'}{\sigma_o'} + C_{\alpha\varepsilon}.\log\frac{t_i + t}{t_i}$$

With σ_{pc}' the preconsolidation pressure, which is considered a material property where C_s is the primary recompression index, C_R and $C_{\alpha\varepsilon}$ replaces, b and c in Eq. 4.9, e_o, e, t, t_i, σ_o' and $\Delta\sigma'$ are as in Eq. 4.9, respectively.

4.2.2. Variations of the Sowers model (1973)

A. The Sowers (1973) model

Sowers (1973) first adopted a conventional soil mechanic approach to the development of a model for the prediction of waste settlement. The Sowers model has been extensively used in the literature and has been used successfully in a number of cases (Oweis and Khera, 1986; Wall and Zeiss, 1995; Yen and Scanlon, 1975). Its formulation is simple and the number of parameters that need to be determined minimal. Moreover,

the coefficients can be deduced from an observation of a waste fill for over a significantly shorter period of time (15 months).

Sowers (1973) showed that the settlement of MSW was similar to that observed in peat, with large initial consolidation and substantial secondary compression. Peat has a high organic content that is highly compressible and susceptible to degradation in the long term. Waste settlement was divided into two phases. The first is the initial and primary compression phase, which is completed within 1 month, and illustrates a linear relationship between the observed settlement strain and the effective vertical stress. The second phase is due to secondary compression processes, such as waste degradation, where the strain is linear with the logarithm of time. This phase is complete in about thirty years.

i) Primary settlement

The relationship between stress and settlement during the first phase can be expressed using the following equation:

Eq. 4.11 $$\frac{\Delta h_p}{h_o} = C_R.\log\frac{\sigma_o' + \Delta\sigma'}{\sigma_o'},$$

where Δh_p is the primary settlement in metres. The compression index C_R for primary settlement is a function of the initial void ratio e_o ($C_R = \frac{C_c}{1+e_o}$). C_c can be expressed by the initial void ratio and a coefficient x related to degradation ($C_c = x.e_o$), where x was estimated to range between 0.15 and 0.55 (the lower value is for fills low in organic matter) (Figure 4.6) (Sowers, 1973).

ii) Secondary settlement

The Sowers model (1973) assumes that the secondary settlement curve is linear with respect to the logarithm of time as expressed by Eq. 4.12.

Eq. 4.12 $$\frac{\Delta h_s(t)}{h_{ref}} = C_{\alpha\varepsilon}.\log\frac{t}{t_{ref}},\ \text{with}\ C_{\alpha\varepsilon} = \frac{C_\alpha}{1+e_o}\ \text{and}\ C_\alpha = x'.e_o.$$

where, t = elapsed time, months;

t_{ref} = time for secondary compression to start, months;

Δh_s = secondary settlement at time t_{ref}, m;

h_{ref}= height of waste at time t_{ref} upon completion of primary settlement, m; and

$C_{\alpha\varepsilon}$= secondary compression index.

The secondary compression index $C_{\alpha\varepsilon}$ can be presented using the initial porosity of waste n_o: $C_{\alpha\varepsilon} = x' \frac{e_o}{1+e_o} = x' n_o$. The material coefficient x' ranged between 0.03 and 0.09 (the lower value is for conditions unfavourable to biodegradation). However, these relations were obtained based on measurements up to 15 months only.

Sowers (1973) suggested that the primary and secondary compression indices are functions of the initial void ratio (Figure 4.6). For any given void ratio there is a large range in C_c and $C_{\alpha\varepsilon}$, related to the potential for biodegradation. However, determination of the initial void ratio remains a difficult task, especially when waste composition is heterogeneous.

Table 4.1. Published waste compressibility parameters, complied from Fassett *et al.* (1994) and Landva *et al.* (2000).

Primary C_R	Secondary $C_{\alpha\varepsilon}$	Reference
0.13-0.47	0.02-0.07	Sowers (1973) (for e_o= 3)[a]
0.15-0.33	0.013-0.03	Zoino (1974)[b]
0.25-0.3	0.7	Converse (1975)[b]
-	0.013	Chang and Hannon (1976)
0.16-0.235	0.012-0.046	Rao *et al.* (1977)[b]
0.08-0.21	0.02-0.04	York *et al.* (1977)
0.2-0.5	0.0005-0.029	Landva *et al.* (1984)
0.15-0.35	0.04	Burlingame (1985)
0.08-0.217	-	Oweis and Khera (1986)
0.05 - 0.26	0.004-0.04	Bjarngard & Edgers (1990)[c]
-	0.001-0.024	Lukas (1992)
0.21-0.25	0.033-0.056	Wall and Zeiss (1995)
0.2-0.225	0.015-0.023	Gabr and Valero (1995)
0.09-0.19	0.006-0.012	Boutwell and Fiore (1995)
0.16	0.02	Stulgis *et al.* (1995)
-	0.01-0.08	Green and Jamenjad (1997)
0.17-0.24	0.01-0.016	Landva *et al.* (2000)
0.17-0.23	0.024-0.029	Andersen *et al.* (2004)

[a] The lower value represents low organic content and the higher value high organic content; [b] From Wall and Zeiss, 1995; [c] From Stulgis *et al.*, 1995.

It should be noted that the values available for $C_{\alpha\varepsilon}$ in the literature must be viewed with caution. The lack of information related to study sites (i.e. details of waste composition, waste height and duration of construction period) often makes these data difficult to apply. Table 4.1 gives some values for C_R and $C_{\alpha\varepsilon}$ found in the literature.

When long-term settlement is monitored, it is not usually possible to distinguish between the two processes - physical creep compression and biodegradation. In order to estimate the amount of secondary settlement it is necessary to separate the two components of settlement. Two approaches are possible in practice according to whether the exploitation time t_c is equal or higher than the consolidation time t_1. It should be noted that in the majority of the settlement studies, t_o and t_1 are assumed to be equal to t_c and t_c+1 respectively. Table 4.2 gives some values of time parameters found in the literature.

Table 4.2. Values of time parameters according to Sowers model (1973) found in the literature.

Phase	Time parameters	Reference
Initial time t_o	$t_o = t_c$ $t_o < t_c$ ($t_o = t_c/2$ or $t_o = \frac{3}{4}t_c$)	Majority of settlement studies Watts and Charles (1999)
Duration of secondary settlement phase t_1	$t_1 = t_c+125$ days $t_1 = t_c+1$ month $t_1 = t_c+1, 2, 3$ months	Sanchez - Alciturri *et al.* (1993) El Fadel and Khoury (2000) Yuen and Styles (2000)

Despite capturing the major elements of primary and secondary compression in degradable material there are numbers of disadvantages to the Sowers model (1973), these include:

- lack of standardization of time parameters, which makes it difficult for any comparison between other similar models to be made;
- unsatisfactory model calibration in case of waste fill with a complex history (rest period, late expansion); and
- considerable variation of the secondary compression index $C_{\alpha\varepsilon}$.

B. The Janbu *et al.* (1989) method

Janbu *et al.* (1989) re-analyzed a number of available settlement observations made over a period of 5 to 60 years to propose a method for the determination of settlement rates in landfills. It was found that the back-calculated, full-scale *in situ* creep (also known as secondary compression) parameters were comparable to the values usually found in laboratory tests on similar soils and on soft sedimentary rocks.

The authors defined the secondary compression potential S as the product of the observed rate of settlement (ε) and time (t). For an idealized layer of thickness h_o, laboratory and field experience over a 20 year period has shown that:

Eq. 4.13 $$S = \varepsilon.t = \frac{h_o}{r_s}$$

To determine the settlement potential S, Janbu *et al.* (1989) introduced a parameter r_s known as creep resistance which ranges in values from 10 to 100 for peat and organic clays and from 100 to 300 for clays and silts.

Eq. 4.13 may be rewritten as:

Eq. 4.14 $$\varepsilon = \frac{h_o}{r_s\, t}$$

Once S is known the rate of settlement (ε) can be obtained from Eq. 4.13. Assuming t_i to be the time of load application, when $\varepsilon = \varepsilon_i$, the settlement rate can be calculated as:

Eq. 4.15 $$\varepsilon = \int_{t_i}^{t} \frac{S}{t}\, dt + \varepsilon_i$$

if creep dominates from $t \geq t_c$ with a creep potential S_c = constant, Eq. 4.15 leads to:

Eq. 4.16 $$\varepsilon_c = S_c \ln \frac{t}{t_c}$$

where S_c represents the creep potential until $t = t_c$. In reality, primary compression and creep overlap over a long period. Since total settlement is the sum of both primary and secondary settlements, $\varepsilon = \varepsilon_p + \varepsilon_c$, the total potential at any time is equal to $S = S_p + S_c$.

The advantage of the Janbu *et al.* (1989) approach is the potential to represent the average *in situ* creep potential from deep deposits into a dimensionless creep resistance. For a layered system such as a landfill, Eq. 4.14 can be presented as follows:

Eq. 4.17 $$\overline{r_{se}} = \frac{h_o}{\sum_{i=1}^{n} \frac{\Delta h_i}{r_{s_i}}}$$

where $\overline{r_{se}}$ is the equivalent, average creep resistance.

For a column of waste with initial height h_o Eq. 4.14 leads to: $\varepsilon = \frac{h_o}{\overline{r}_{se}(t - t_c)}$ from where, after integration with respect to time, the secondary settlement can be expressed as:

Eq. 4.18 $$\frac{\varepsilon(t)}{h_o} = \frac{1}{\overline{r}_{se}} \ln\left(\frac{t}{t_c}\right) = \frac{\ln 10}{\overline{r}_{se}} \log\left(\frac{t}{t_c}\right)$$

Following the approach of Buisman (1936) and Sowers (1973), after differentiation of Eq. 4.18 with respect to time allows the creep resistance to be calculated as: $\overline{r_{se}} = \frac{\ln 10}{C_{\alpha\varepsilon}}$, where $\overline{r_{se}}$ is equal to $\frac{1}{C_{\alpha\varepsilon}} = \frac{h_o}{\sum_{i=1}^{n} C_{\alpha\varepsilon} \Delta h_i}$. The published values for secondary compression indices $C_{\alpha\varepsilon}$ ranged from 0.0005 to 0.056 (Table 4.1) and correspond to creep resistance values ranging from 7 to 4605.

C. The Coumoulos and Koryalos method (1997)

Because of the complexity of the processes that take place in the landfill and the heterogeneous nature of the waste, it has not been possible to introduce a universal model which would be able to predict settlement behaviour of any waste fill. The Sowers model (1973) was developed to predict settlement that results from both primary and secondary compression. The basic Sowers approach (1973) was evaluated by Coumoulos and Koryalos (1997) to predict the attenuation of landfill long-term settlement rates under self weight. It is based on the observation that a landfill which is placed rapidly would yield higher settlement rates than a landfill with a longer construction period. Coumoulos and Koryalos (1997) suggested a methodology to determine $C_{\alpha\varepsilon}$ from the secondary compression part of the settlement curve, if time-settlement data were available and the date of closure known. The basic assumption made was that long-term settlement can be approximated by a straight line when plotted against logarithm of time. The vertical strain rate due to long-term settlement is the slope of the curve expressed by Eq. 4.12 which can be rewritten in the following way:

Eq. 4.19 $$\varepsilon(t) = \frac{d(\Delta h_s(t)/H_c(t_c))}{dt} = \frac{C_{\alpha\varepsilon}}{t\ln 10} = \frac{0.434 C_{\alpha\varepsilon}}{t}$$

The principle of the Coumoulos and Koryalos (1997) method is illustrated in Figure 4.7. If the date of closure is not known, as it happens with old landfills, the general attenuation equation would be:

Eq. 4.20. $$\varepsilon(t) = \frac{0.434 C_{\alpha\varepsilon}}{\Delta t + t}$$

For three different topographical surveys carried out at three arbitrary times t_o, t_1 and t_2, the following attenuation equations can be written as:

- Attenuation curve $t = \frac{t_1}{2}$ Eq. 4.21 $$y_1 = \frac{\varepsilon_1 - \varepsilon_o}{t_1 - t_o} = \frac{0.434 C_{\alpha\varepsilon}}{\Delta t + \frac{t_1}{2}}$$

- Attenuation curve $t = \frac{t_2}{2}$ Eq. 4.22 $$y_1 = \frac{\varepsilon_2 - \varepsilon_o}{t_2 - t_o} = \frac{0.434 C_{\alpha\varepsilon}}{\Delta t + \frac{t_2}{2}}$$

The two unknown parameters in the system above are $C_{\alpha\varepsilon}$ and Δt. Knowing $C_{\alpha\varepsilon}$ and Δt it is then possible to trace the branch of the rectangular hyperbola asymptotic to the time axis and obtain a picture of the attenuation of vertical strain rates, and hence the attenuation of settlement rates with time: $y(t) = \frac{0.434 C_{\alpha\varepsilon}}{\Delta t + t}$

To validate their method, Coumoulos and Koryalos (1997) reanalyzed published settlement data from landfills in Europe and the United States (Figure 4.8). Figure 4.8 also shows the attenuation curves which correspond to values of coefficients of secondary compression equal to 0.02 (curve A), 0.07 (curve B) and 0.25 (curve C). All three curves were traced with the aid of attenuation Eq. 4.19. The authors concluded that the plotted settlement data clearly demonstrates the attenuation effect of vertical strain rates with time. The majority of the plotted points are close to the attenuation curve (B) (C_a = 0.07), with the exception of the data of Gasparini *et al.* (1995) and Coduto and Huitric (1990). It should be noted that the plots of Figure 4.8 were compiled on the basis of limited information about the rate of construction and the previous history of the waste fills. Furthermore, no records were available in most cases about the initial waste density, the density after placement, leachate levels and temperature variations.

4.2.3. The Yen and Scanlon (1975) model

Yen and Scanlon (1975) conducted a study of field observation of three completed sanitary landfills located in Los Angeles County, California. The objectives of their study was to deduce from field data the factors that influence the settlement process in landfills and to provide a real database against which future theoretical models might be tested. The survey periods ranged up to 9 years after completion of the landfills. The studied sites were constructed mainly of residential waste. Minor amounts of brush and construction waste were also included. The landfills varied in thickness (6-38m) and were constructed over a period ranging from less than 1 year to 7 years. The wastes were placed on compacted concessive layers (sites 1 & 2: terraces of 6m; site 3: layers of 1.5m). The average waste density for all sites after compaction was 640kg/m^3.

In an approach similar to that of Coumoulos and Koryalos (1997), the method suggested by Yen and Scanlon (1975) also considers the change in elevation (m) of the survey fill for each site against the median age (t) of a fill column:

Eq. 4.23 $$m = \frac{1}{H(t_c)} \frac{d(\Delta h_s(t))}{dt}$$

Where m is the settlement rate, $\Delta h_s(t)$, $H(t_c)$ and t are as in Eq. 4.12 (p. 66). The median age was measured as the elapsed time between the date of settlement survey and the time when the fill column was half completed. A parameter "total fill construction time period", t_c, was introduced to accommodate the importance of construction or filling period over landfill settlement rates. The median age of fill column T can be estimated as $T = t - \frac{t_c}{2}$ (Figure 4.9).

The analysis of the topographical surveys led Yen and Scanlon (1975) to divide the studied waste columns into subgroups based on a range of the initial waste height $H(t_c)$ and the construction time t_c values:

- $H(t_c)$: < 12m; 12-25m; 25-31m; > 31m;
- t_c: < 12 months; 24-50 months; 70-82 months.

Settlement was plotted against the logarithm of the median time T:

Eq. 4.24 $$m = a - b \log T, \qquad T \text{ (in months)} > t_c/2$$

where, m is the settlement rate and "a" and "b" are the settlement rate parameters. In order to determine the settlement rate from Eq. 4.24, the two settlement parameters must be known.

The linear relationship between m and T was determined by the method of least squares applied to the survey settlement data. Figure 4.10(a) represents relationships obtained by Yen and Scanlon (1975) between the settlement rate and the fill age, designated as (A), (B), (C), and (D). Figure 4.10(a) also represents a settlement rate vs. fill age relationship determined by using settlement data obtained by Rao *et al.*(1977) from an experiment cell filled with 1.5 metres of household waste, designated as curve (E). As can be seen from (E) the linearity develops beyond the age of 12 months.

Yen and Scanlon (1975) concluded that the rate of settlement appears to decrease linearly in proportion to the logarithm of median fill age and to increase with fill depth in general, until it reached a limit. The median age has a limiting value ($T = t - t_c/2 = 10^{(a/b)}$), after which settlement rates become negative that cannot happen in reality. Thus for practical purposes, the prediction must be stopped at time $T_{ult} = 10^{(a/b)}$. However, this method consistently overpredicted settlement for shallow landfills, and underpredicted settlement for very deep landfills. The major advantage of the model lies in its relative simplicity. Eq. 4.24 suggested by Yen and Scanlon (1975) can be compared with Sowers (1973) Eq. 4.12 if it is expressed in its differential form (between the moments t and $(t + dt)$ following the current assumption that $t_{ref} = t - t_c$.

Eq. 4.25
$$d\varepsilon = \varepsilon(t+dt) - \varepsilon(t) = C_{\alpha\varepsilon} \log\left[\frac{(t-dt)-t_c}{t-t_c}\right]$$

When the average settlement rate over a considered period of time is expressed as $m = d\varepsilon / dt$ the secondary compression index may be presented in the following form:

Eq. 4.26
$$C_{\alpha\varepsilon} = m(t)\frac{dt}{\log\left[\frac{(t-dt)-t_c}{t-t_c}\right]}$$

Eq. 4.24 allows the values of the coefficient $C_{\alpha\varepsilon}$ to be related to settlement rates determined by Yen and Scanlon model (1975).

Sohn and Lee (1994) re-analyzed the Yen-Scanlon (1975) data and showed that the settlement rate is linearly proportional to the fill height:

Eq. 4.27 $$a = 0.00095H(t_c) + 0.0323$$

Eq. 4.28 $$b = 0.00035H(t_c) + 0.0167$$

The settlement of a given landfill for the time span of interest (Δt) can be obtained by integrating the settlement rate over that time span (Sohn and Lee, 1994):

Eq. 4.29 $$\frac{\Delta h_s(T)}{H(t_c)} = \int m dt = \int_T^{T+\Delta t} (a - b\log T)dT = T\left[a - \frac{b}{\ln 10}(\ln T - 1)\right]_T^{T+\Delta t}$$

Since the settlement rate must be greater than zero, it should be noted that the time span in the above integration should be limited to $T + \Delta t \leq 10^{(a/b)}$. After integration of Eq. 4.29 with respect to the absolute time t the settlement rate can be presented in the following form:

Eq. 4.30 $$\frac{\Delta h_s(t)}{H(t_c)} = (t - t_c)\left(a + \frac{b}{\ln 10}\right) + \frac{t_c}{2}.\frac{b}{\ln 10}\ln\left(\frac{t_c}{2}\right) - \left(t - \frac{t_c}{2}\right)\frac{b}{\ln 10}\ln\left(t - \frac{t_c}{2}\right)$$

4.2.4. The Bjarngard and Edgers (1990) model

As a part of a research program at the Tufts University Centre for Environmental Management, funded by the U.S. EPA, Bjarngard and Edgers (1990) collected and analyzed landfill settlement data using 24 case histories to establish engineering parameters for the prediction of landfill settlement. Some of the studied fills were full-size landfills, others were surcharged landfills test sections and a few were large research test cells. The studied sites were monitored for a period ranging between 35 days and 7000 days (19 years). The field data were analysed using geotechnical parameters which include the initial settlement, the compression ratio C_R and the secondary compression index $C_{\alpha\varepsilon}$. The compression ratio is defined as the amount of strain which occurs per log cycle of stress applied to a soil and is a measure of the amount of settlement caused by the application of an external load. $C_{\alpha\varepsilon}$ is defined as the slope of a plot of percent compression vs. log-time, at large times after completion of primary compression.

Bjarngard and Edgers (1990) stated that most of the settlement curves do not show the classic "S" shape indicative of primary compression (Figure 4.11). Rather, the curves show approximately linear, relatively flat slopes over small times scales. Over larger scales, i.e. 100 days $< t \leq$ 6000 days, some of the curves develop much greater slopes. It was also stated that the long-term field settlement can be divided into two phases. As

presented in Figure 4.12, in the early stage of long-term compression, the settlement is dominated by mechanical interaction such as reorientation and delayed compression of the wastes. However, in the last stage of compression, the logarithmic compression rates are higher possibly due to the effects of biodegradation. With reference to Figure 4.12, the long-term settlement rates can be determined as follows:

Eq. 4.31 $$\frac{\Delta h_s(t)}{H(t_c)} = C_{\alpha\varepsilon 1} \log \frac{t - t_o}{t_1 - t_o}, \text{ when } t \le t_k$$

Eq. 4.32 $$\frac{\Delta h_s(t)}{H(t_c)} = C_{\alpha\varepsilon 1} \log \frac{t_k - t_o}{t_1 - t_o} + C_{\alpha\varepsilon 2} \log \frac{t - t_o}{t_k - t_o}, \text{ when } t > t_k$$

where, $C_{\alpha\varepsilon 1}$ is the intermediate secondary compression index, $C_{\alpha\varepsilon 2}$ is the long-term secondary compression index and t_k is the time when the slope of the log-time - settlement curve becomes much greater than in the early stages of secondary compression (Figure 4.12).

Bjarngard and Edgers (1990) observed in their study the following measures of landfill settlement:

- Initial settlement up to about 12% of the original fill height (average of 6.3%);
- For early time periods the intermediate secondary compression index ($C_{\alpha\varepsilon 1}$) varied from 0.003 to 0.038 (average of 0.019); and
- For later time periods the long-term secondary compression index ($C_{\alpha\varepsilon 2}$) ranged from 0.017 to 0.51 (average of 0.125).

Other published results have shown accelerated logarithmic settlement rates than those reported by Bjarngard and Edgers (1990) (Table 4.3). In Table 4.3, the slope values of the settlement results of site A are similar to $C_{\alpha\varepsilon 1}$ values of the previous stage, before the accelerated compression. Since the landfills are very young (less than 2 years), it is anticipated that these wastes may settle more at some future time and at an accelerated logarithmic compression rate ($C_{\alpha\varepsilon 2}$) due to waste biodegradation.

The drawback in Bjarngard and Edgers (1990) model lies in the fact that the time scales shown in Figure 4.11 are not consistent with typical biological events in landfills, such as gas production and infiltration, that can lead to increased secondary compression indices. Landfill gas production may begin 1 to 3 months following emplacement and continue for upwards of 20 years (Noble *et al.*, 1988). Time scales for infiltration of moisture in

landfills with typical capping systems can also be tens of years (Noble *et al.*, 1989). Furthermore, the $C_{\alpha\varepsilon}$ indices and t_k value were determined only by back-analyses starting from time periods higher than t_k (in some cases more than 10 years), which makes the determination of these parameters difficult.

Table 4.3. Literature values for long-term settlement rates.

Site	Location	Average $C_{\alpha\varepsilon 1}$	Average $C_{\alpha\varepsilon 2}$
A	24 landfill cases (Bjarngard and Edgers, 1990)	0.019	0.125
B	Large scale laboratory test (Gandolla *et al.*, 1992)	0.063	0.340
C	Large scale laboratory test (Lee *et al.*, 1995)	0.063	0.149
D	Large scale field test (El-Fadel *et al.*, 1999[b])	0.019	0.216

In a partially saturated fill under conditions of constant applied load and constant moisture content, there will be some long-term compression due to loss of structure of the waste. The linear relationship between creep compression and the log-time that has elapsed since the load was applied can be expressed using the parameter α_c. The settlement which is due to biodegradation can be described using the parameter α_b which is analogous to α_c but may be much larger and is likely to be affected not only by change in effective stress, but also by changes in the biochemical conditions within the landfill. Watts and Charles (1990) defined the creep compression rate parameter α_c and the biocompression rate parameter α_b in a similar manner to primary and secondary compression indices proposed by Sowers (1973). If the basic Sowers equation (Eq. 4.12) is differentiated with time then the settlement rate can be presented in the following form:

Eq. 4.33
$$\frac{d\varepsilon}{dt} = \frac{d\left(\Delta h_s(t) / H(t_c)\right)}{dt} = C_{\alpha\varepsilon} \frac{1}{t \ln 10} = \frac{C_{\alpha\varepsilon}}{2.303\, t}$$

Watts and Charles (1990) applied the above equation for different time periods to describe α_c and α_b:

Eq. 4.34
$$\alpha_c = \left(2.303 t \frac{\Delta\varepsilon}{\Delta t}\right)_{t<t_k}$$

Eq. 4.35 $$\alpha_b = \left(2.303t\frac{\Delta\varepsilon}{\Delta t}\right)_{t>t_k}$$

Where t_k is the time when the slope of the log-time-settlement curve becomes much greater than the early stages of compression, $\Delta\varepsilon/\Delta t$ in Eq. 4.34 & Eq. 4.35 is the rate of vertical compression due to physical and biodegradation processes, respectively. However, the determination of both coefficients α_c and α_b is not straight forward. In practice, Watts and Charles (1999) calculated α-type logarithmic compression parameters after geometrical determination of the slope values of the settlement curve ($\Delta\varepsilon/\Delta t$) presented in a semi-logarithmic scale. The settlement results were obtained from field data using an instrumentation monitoring system. As can be seen in Eq. 4.34 & Eq. 4.35 the parameters α_b and α_c are analogues to the intermediate secondary compression index ($C_{\alpha\varepsilon 1}$) and the long-term secondary compression index ($C_{\alpha\varepsilon 2}$), previously described in this section. It can be concluded that the models presented by Bjarngard and Edgers (1990) and Watts and Charles (1999) make the same classical assumption in identifying two stages of secondary settlement.

4.3. Models based on exponential functions

4.3.1. The Gibson and Lo (1961) model

Gibson and Lo (1961) proposed a model to represent the consolidation for soils undergoing simple one-dimensional compression. The model is shown in Figure 4.13[a], and represents the average compression of the refuse fill shown in Figure 4.13[b]. When a stress increment σ' acts on the model, the Hookean spring, with a spring constant of a, it compresses instantaneously. This is analogous to what occurs during primary compression. The compression of the Kelvin element, with a spring constant of b, parallel to a dashpot (viscosity of λ/b) is retarded by the Newtonian (linear) dashpot. This is similar to the continuous process of secondary compression under sustained effective stress.

The time-dependent settlement is expressed as:

Eq. 4.36 $$\varepsilon(t) = \frac{\Delta h(t)}{h_o} = \sigma'\left[a + b\left(1 - e^{-\lambda/b(t)}\right)\right] = a\sigma' + b\sigma'\left(1 - e^{-\lambda/b(t)}\right)$$

Where, σ' = effective stress, kPa

a = primary compressibility parameter, 1/kPa

b = secondary compressibility parameter, 1/kPa

λ/b = rate of secondary compression, 1/day

The model proposed by Gibson and Lo (1961) for the long-term (secondary) consolidation of soils was found to be particularly useful in predicting the settlement of peats (Edil and Mochtar, 1981) and is similar to waste as it involves similar compression mechanisms. Encouraged by the simplicity and usefulness of the rheological model proposed by Gibson and Lo (1961), Edil *et al.* (1990) decided to apply the same model to landfill settlement data records.

Edil *et al.* (1990) simulated waste settlement at four different landfill sites using the Gibson and Lo rheological model (1961) and the Power Creep Law model (Edil *et al.*, 1990). All four of these fills are existing municipal landfills situated in the USA. It was assumed that the waste in each of these four sites was of similar composition. The sites that violated the assumption of constant stress change could not be analyzed using these models.

The three empirical parameters required for the Gibson and Lo models derived for the four studied sites (Edil *et al.*, 1990) are plotted in Figure 4.14 [a,b,c]. As can be seen in Figure 4.14 [a], the amount of primary compressibility, a, decreases with an increase in stress. The secondary compressibility, b, is shown to decrease with increasing stress (Figure 4.14 [b]). As expected, as the average strain rate increases, so does the rate of secondary compression, λ/b (Figure 4.14 [c]). In order to develop a data bank of ranges for the empirical parameters a more comprehensive set of data from other landfills in different degradation stages is needed.

For the secondary part of the settlement-time curve, when $t \rightarrow \infty$, equation Eq. 4.36 can be transformed to:

Eq. 4.37 $$\frac{\varepsilon(t)}{\sigma'} = (a+b)$$

From Eq. 4.37 the parameters b and λ may be found in the following way (Gibson and Lo, 1961):

Eq. 4.36 can be written in the form

Eq. 4.38 $$\frac{\varepsilon(\infty)-\varepsilon(t)}{\sigma'} = b e^{-\lambda/b(t)}$$

Taking the logarithm of both sides

Eq. 4.39 $$\log\frac{\varepsilon(\infty)-\varepsilon(t)}{\sigma'}=\log b-0.434\frac{\lambda}{b}t$$

Eq. 4.39 represents a linear relationship between $\log\frac{\varepsilon(\infty)-\varepsilon(t)}{\sigma'}$ and t. From the slope (-0.434(λ/b)) and intercept (log b) of the straight line, b and λ/b can be determined. Then, the parameter a can be calculated from the equation Eq. 4.36 or from the relation:

Eq. 4.40 $$a=\frac{\varepsilon(t)}{\sigma'}-b\left(1-e^{-\lambda/b(t)}\right)$$

Park *et al.* (2002) determined the three empirical parameters (a, b and λ/b) by using a logarithmic plot of strain rate versus time:

Eq. 4.41 $$\frac{d\varepsilon(t)}{d(t)}=\sigma'\lambda e^{-(\lambda/b)t}$$

The slope and intercept of the best-fit line yield values of b and λ as follows:

- Intercept of line = $\sigma'\lambda$
- Slope of line = $-\frac{\lambda/b}{\ln 10}$

The primary compressibility parameter a is obtained by substituting the value of t_k and the corresponding strain $\varepsilon(t_k)$ in Eq. 4.36 and solving for a as:

Eq. 4.42 $$a=\varepsilon(t_k)/\sigma-b\left(1-e^{-(\lambda/b)t_k}\right)$$

where t_k is the time when the primary compression is completed.

A major drawback in the Edil *et al.* (1990) study lies in the fact the parameters largely depend on the applied stress, and extrapolations to other fills must be exercised with care, even when waste composition is similar. Overall, the Power Creep Law, which considers the total deformation response with time, provides better representation of the settlement data in 65% of the cases, while in the remaining cases the models were comparable to each other. Similar conclusions were reached by Lee *et al.* (1994). These studies suggest that the division of settlement into primary and secondary components may not be realistic for landfills. Thus, methods for landfill stabilisation might be better evaluated by considering total settlement behaviour.

Bleiker *et al.* (1995) proposed an alternative approach for calculating the settlement at different depths using different loading histories. By calculating the strain for individual layers and treating the upper refuse layers as additional sequential surcharges, the strain response of each layer can be individually predicted. This in turn, allows for the prediction of the permeability of each refuse layer as a separate entity.

The Gibson and Lo (1961) approach (Edil *et al.*, 1990) was applied to waste by Bleiker *et al.* (1995) to express the time-dependent strain due to mechanical creep:

Eq. 4.43 $$\varepsilon(t) = \sigma\left\{a + b\left(1 - e^{k(t-t_o)}\right)\right\}$$

where $\varepsilon(t)$ is the strain as a function of time, σ *is* the effective vertical stress, k is the rate constant for mechanical creep ($k = \frac{\lambda}{b}$) (Edil *et al.* 1990) and $(t\text{-}t_o)$ is the time since application of the stress.

However, in contrast to the Gibson and Lo (1961) model where the compressibility parameters a and b are constant with time, Bleiker *et al.* (1995) suggested that a and b values decrease with an increase in stress. Figure 4.15 shows the parameters a and b derived from the data published by Rao *et al.* (1977). These parameters are not perfect Hookean elements since their values decrease as the effective stress increases. Although Rao *et al.* (1977) used synthetic waste in laboratory conditions, their data adequately illustrate the trend, and the work of Edil *et al.* (1990) also confirmed this trend. Effectively, the more the waste has been compressed, the more difficult additional compression becomes. Due to the non-linear relationship of the parameters a and b with effective stress, and the variation of effective stress in soils with respect to depth, the model is only accurate over the stress ranges and waste thickness from which the parameters were developed.

Ideally, the strain in element a due to an effective stress increment from σ_o to σ_1 is calculated as the shaded area under the curve (A) shown in Figure 4.15, and the strain in element b is the product of the area under the curve (B) and the potential term $\left[1 - e^{k(t-t_o)}\right]$ in Eq. 4.43.

The definition of a start time (exactly when initial conditions exist, i.e. $t = 0$) is a common geotechnical problem since consolidation models often assume an instantaneous load application whilst construction of most structures actually occurs over a discrete period of time. The authors treat each additional waste layer or surcharge as if it is the

only surcharge, and then superimpose the strain from each incremental surcharge (Figure 4.16).

El-Fadel and Al-Rashed (1998), El-Fadel *et al.* (1999[a,b]) and Sadek *et al.* (2000) used the Gibson and Lo (1961), Power Creep (Edil *et al.*, 1990) and one-dimensional consolidation models to simulate laboratory and field settlement data. The Gibson and Lo model rapidly reached constant settlements, and exhibited limitations if the settlements persisted at a significant level. In contrast, the Power Creep model did not allow the determination of a time at which settlement rate stabilized. The one-dimensional model had a greater application potential as it allowed for a second stage of compression to describe secondary long-term settlement. In general, it provided a better representation of laboratory and field measurements than other models.

4.3.2. The Asaoka (1978) model

Settlement predictions based on monitoring and observational procedures have been used to monitor deformations in geotechnical constructions, such as excavations and embankments. Asaoka (1978) proposed a simple method to predict the final settlement based on settlement observations at fixed time intervals by plotting consecutive settlement readings $\varepsilon(t_{i-1})$ against $\varepsilon(t)$ to produce a line which over a large interval can be represented by the linear function:

Eq. 4.44 $$\varepsilon(t_i) = \beta_o + \beta_1 \varepsilon(t_{i-1})$$

in which: β_o = intersection of the extrapolated section of the linear fit with the Y-axis; and
β_1 = slope of the linear section of the best fit.

A few so-called Asaoka lines, representing various loading stages are depicted in Figure 4.17. Using the graphical approach of Asaoka's method (1978), the ultimate settlement at the moment full compression has been reached ($\varepsilon(t_{i-1}) = \varepsilon(t_i)$) can be calculated by:

Eq. 4.45 $$\varepsilon_{ult}(t) = \frac{\beta_o}{1-\beta_1}$$

Where coefficient β_o and β_1 can be obtained from the plot (ε_{i-1} vs. ε_i) of measured settlement described below:

i) The observed time-settlement curve plotted to an arithmetic scale is divided into equal time intervals Δt (usually between 30 and 100 days; longer Δt yields better

predictions). The settlements, ε_1, ε_2, ... corresponding to times t_1, t_2, ...($\{t_i = t_o + i\Delta t\}_{i=1,2,...}$) are read off and tabulated.

ii) The settlement values ε_1, ε_2, ...are plotted as points $(\varepsilon_{i-1}, \varepsilon_i)$ in a coordinate system with axis ε_{i-1} and ε_i. A 45° straight line with $\varepsilon_i = \varepsilon_{i-1}$ is also drawn.

iii) The plotted points are fitted by a straight line (A) whose corresponding slope is read as β_1 and its intercept with the ordinate axis is β_o. The point of intersection with the 45° line gives the final settlement ε_{ult}.

The slope of the fitted straight line (A) can be related to the mean compression coefficient β_1' by applying the following formula:

Eq. 4.46 $$\beta_1' = -\frac{5}{12} H^2 \frac{\ln \beta_1}{\Delta t}$$

in which H is the fill thickness in m and Δt is time interval in s.

It has been observed in practice that points $(\varepsilon_{i-1}, \varepsilon_i)$ always define one or more straight lines, each of them corresponding to either primary compression or secondary compression under constant loading (Magnan, 1981).

Asaoka's method has been widely used in projects where conventional consolidation theory is less applicable due to the heterogeneous layered soils, sites having large deformations, and the three-dimensional configuration of the problem (Tan *et al.*, 1991). MSW is to a certain extent similar to peat in that if exhibits large secondary compression. The applicability of Asaoka's procedure to predict peat settlement has been investigated by Edil *et al.* (1991), but was found to be unreliable because secondary compression was not completely considered.

4.3.3. The Gandolla et al. (1992) model

Gandolla *et al.* (1992) carried out experiments using three open topped cylindrical concrete lysimeters (lysimeters L1, L2 and L3) having dimensions of 1 m internal diameter and 3 m height. The lysimeters were filled with fresh shredded refuse and then mixed with sewage sludge that had been previously digested for 30 days and amounted to 6.8% of the total filling refuse. The filled refuse contained 55% waste and a 60% organic content based on the proportion of solids.

The lysimeters were initially subjected to a vertical compression of 57kPa for 314 days and then, the third lysimeter, L3, was topped up with 0.3 tons of MSW (Figure 4.18). After five years of the test, L2 was subjected to an additional surface loading of 0.5kPa, whereas the first lysimeter L1 was left undisturbed for the whole duration of the test. The experiment began on 31/5/83 and measurements were taken up to 28/11/89. The authors noticed that the settlement measured in the experimental lysimeters showed a seasonal effect, with a settlement rate much higher in the summer seasons than during the winters, which leads to the conclusion of dependence on specific local conditions. The total settlement in L1 at the end of the experiment reached a value of about 45%.

In order to obtain a result with practical applications, Gandolla *et al.* (1992) interpolated analytically the settlement data in lysimeters L1 to establish a mathematical function that expressed the evolution of secondary settlement in time with respect to the initial and final conditions (no settlement at time t = 0 and then tending to an asymptotic value). The settlement curve shows a linear portion with a small slope in plots of strain versus log-time and then it developed a much greater slope at approximately 300 days after the measurement started:

Eq. 4.47 $$\frac{\Delta h}{h_o} = a\left(1 - e^{-k(t-t_c)}\right)$$

where a and k are two constants equal to 44.1610 and 0.0077 respectively, and t is the time in months.

As can be seen in Figure 4.19, when time $t \to \infty$, the settlement tends towards a constant value equivalent to the coefficient a (in fact 44.16% of the initial waste height). In comparison with the maximum deformations generally observed in landfills (from 10 to 35%), the value suggested by Gandolla *et al.* (1992) appears excessively high. This may possibly be due to the fact that this model does not take into account the applied stress.

4.4. Other models based on existing laws

4.4.1. The Edil et al. (1990) model: the Power Creep Law

The Power Creep Law (Edil *et al.*, 1990) model and the Gibson and Low model (1961) are two models used extensively to assess the transient creep behaviour of many engineering materials and have been used successfully to assess waste settlement (Edil *et*

al., 1990; Lee *et al.*, 1994; El-Fadel & Al-Rashed, 1998; Bleiker *et al.*, 1995; El-Fadel *et al.*, 1999[b]). They are also known as rheological (stress-strain-time) models that evaluate the mechanical behaviour of materials which are considered to be continuous, and homogeneous. Even though the material may consist of various phases, only statistical averages of its microscopic behaviour are considered.

The Power Creep Law model estimates the rate and magnitude of settlement under constant stress as a function of time and the initial refuse thickness. According to the model the time-related settlement can be expressed as:

Eq. 4.48
$$\frac{\Delta h}{h_o} = \varepsilon(t) = \sigma' m \left(\frac{t}{t_{ref}} \right)^n$$

where Δh = settlement, m;

h_o = original layer thickness, m;

$\varepsilon(t)$ = strain;

σ' = effective stress, kPa;

t = time duration of interest in days;

t_{ref} = reference time introduced into the equation to make time dimensionless (t_{ref} = 1 day in general);

m = waste reference compressibility (kPa^{-1}); and

n = rate of compression at the end of loading.

Equation Eq. 4.48 can also be transformed to:

Eq. 4.49
$$\log \varepsilon = n \log \left(\frac{t}{t_r} \right) + \log \sigma' + \log m$$

Eq. 4.49 also represents a linear relationship between log ε and log t. From the slope and intercept of the straight line portion of an observed time-settlement curve, values of parameters m and n can be obtained.

Edil *et al.* (1990) determined two empirical parameters of the Power Creep Law, m and n, from four different landfill sites (Table 4.4). These parameters did not indicate any noticeable trends with respect to applied stress or average strain in each site within the range of variation of these factors. The reference compressibility parameter, m, showed no discernible pattern with respect to placement conditions of the waste, but it was found to be about 1.7 times higher for old waste than fresh waste. The rate of compression, n,

was influenced with respect to age and placement conditions, old waste relocated refuse had the lowest n (0.366) and, in general fresh waste had the highest n (1.021).

Results showed that the Power Creep Law model, which considers the total deformation response with time, better represents the settlement of MSW landfills (Edil *et al.*, 1990).

Table 4.4. Power Creep Law parameters (Edil *et al.*, 1990).

Waste age (years)	Waste condition	Test duration (years)	n_{avrage} (kPa^{-1})	m_{avrage} (t_r=1day)
Fresh waste (0)	No filling (h_o= 0m)	1.6	$4.02x10^{-5}$	0.713
	Min filling (h_o<1m)	1.5	$4.18x10^{-7}$	1.021
	Active filling (h_o<6m)	1.2	$2.16x10^{-5}$	0.626
Old waste (16)	No filling	1.2	$1.52x10^{-6}$	0.769
Old waste (40-50)	Relocated/compacted	3.9	$3.09x10^{-5}$	0.366
Old waste (not stated)	Additional surcharge	0.9	$6.04x10^{-5}$	0.582

Similar conclusions were reached by Lee *et al.* (1994). The authors pointed out that the Gibson & Lo model and Power Creep Law had been successfully applied to the estimation of actual settlement of landfill site. Furthermore, the determination of the model parameters was relatively simple.

4.4.2. The Ling et al. (1998) model: the Hyperbolic Law

Ling *et al.* (1998) first proposed a hyperbolic function as an improved tool to relate settlement and time, as well as to detect final settlement:

Eq. 4.50
$$\varepsilon(t) = \frac{S(t)}{H_o} = \frac{t}{\frac{H_o}{\rho_o} + \frac{H_o}{S_{ult}} t}$$

where $\varepsilon(t)$= strain;

t = time duration of interest in days;

$S(t)$= settlement at time t;

ρ_o= initial rate of compression;

S_{ult} = ultimate settlement of the fill when $t \rightarrow \infty$; and

H_o = Initial thickness of the waste layer under consideration, m.

Eq. 4.50 can be transformed into $t/\varepsilon(t)$ versus t relationships in order to determine the empirical parameters H_o/ρ_o and H_o/S_{ult}. The plot of $t/\varepsilon(t)$ versus t results in a straight line, and the slope and intercept of the best-fit line provide values of H_o/ρ_o and H_o/S_{ult} respectively:

Eq. 4.51
$$\frac{t}{\varepsilon(t)} = \frac{H_o}{\rho_o} + \frac{H_o}{S_{ult}} t$$

The time required to reach 95% of the ultimate value of settlement is calculated as $t_f = 19 S_{ult}/\rho_o$.

The hyperbolic function presented by Ling *et al.* (1998) offers flexibility and can be started at any time of interest, which is particularly useful if there is a change in loading conditions, such as waste surcharging.

Ling *et al.* (1998) emphasized the advantage of empirical functions such as the logarithmic function (Yen and Scanlon, 1975), the power function (Edil *et al.*, 1990) and the previously presented hyperbolic function, over functions based on conventional soil mechanics theory to examine the time-dependent settlement of MSW. The empirical relationships were used to simulate settlement data in three landfills: Southeastern Wisconsin (Edil *et al.*, 1991); Meruelo landfill, Spain (Sanchez-Alciturri *et al.*, 1993); and the Spadra landfill, California (Merz and Stone, 1962). The authors found that the hyperbolic function provided better results than the logarithmic and power functions. The Ling *et al.* (1998) model however needs to be further validated against field measurements.

4.5. Biomechanical models

Biomechanical models have been developed to predict compression due to microbial degradation and are based on the assumption that compression is directly proportional to the quantity of solid compounds converted into gas or liquid form. The production of biogas is generally expressed according to first order kinetics. In this context, four models have been proposed to represent the contribution of biodegradation to settlement (Edgers *et al.*,1992; Guasconi, 1995; Wall and Zeiss, 1995; Park and Lee, 1997).

Other models of the same type have been proposed (Leonard *et al.*, 2000; Meissner, 1996) but their applicability is questionable. Lastly, the idea to develop a new generation of integrated models (or multiphase) which accounts for changes in material characteristics as a function of the waste degradation rate and the production and the transfer of fluid (biogas + leachate) was suggested by El Fadel and Khoury (2000) and such an approach is proposed in the Landfill Degradation and Transport (LDAT) numerical model (White *et al.*, 2004).

4.5.1. The Edgers et al. (1992) model

Edgers *et al.* (1992) reviewed available MSW landfill settlement data from 22 landfill studies collected by Bjarngard and Edgers (1990) (section 4.2.4) and made comparisons with a mathematical model based on soil creep rate processes and biological degradation. In the model, Edgers *et al.* (1992) identified two stages of delayed compression, the first stage being dominated by mechanical interaction with an average compression coefficient of 0.04, and the second stage by biological processes with an average compression coefficient of 0.01 (Figure 4.20).

A. Mechanical approach ($t < t_k$):

A three parameter model (A, α, m), based on rate process theory Glasstone *et al.* (1941) was used to model landfill settlement due to mechanical compression. Primary compression was represented by the following equations:

Eq. 4.52
$$\varepsilon(t) = \varepsilon_1(t) + \frac{Ae^{\alpha.\sigma_v}}{1-m}\left[\left(\frac{t}{t_1}\right)^{1-m} - 1\right] \qquad \text{for } m \neq 1;$$

Eq. 4.53
$$\varepsilon(t) = \varepsilon_1(t) + Ae^{\alpha.\sigma_v} t_1 \ln\left(\frac{t}{t_1}\right) \qquad \text{for } m = 1.$$

Where, ε is strain, σ_v is stress level, t is time, $\varepsilon_1$and t_1 are known reference values, and A, α, and m are rate process parameters. The compression curves predicted by Eq. 4.52 and Eq. 4.53 are shown in Figure 4.21[a].

B. Biological approach ($t > t_k$):

Edgers *et al.* (1992) noticed that some field cases showed increasing settlement rates at very large times ($t > t_k$), and could not be modelled effectively by Eq. 4.52 and Eq. 4.53. For these cases the authors proposed the following equation:

Eq. 4.54 $$\varepsilon_{bio}(t) = B\left[e^{\beta(t-t_k)} - 1\right]$$

where the added effects of degradation is modelled based on the assumption of exponential bacterial growth (Figure 4.21[b]). In Eq. 4.54, β represents an average value of biological activity for all the microorganisms in a specific landfill and B serves as a scale factor relating the settlements in a landfill due to the effect of degradation to bacterial growth kinetics. The parameter β calculated from the field cases ranges between 0.1223 and 1.2666 per year. The low values are related to low rates of biological activity.

The effect of waste degradation on settlement was modelled based on the following assumptions:

i) The effect of degradation is small until a critical time, t_k, at which time settlement rates increase. This delay may be related to the lag phase of Figure 4.21[b];

ii) Degradation and associated gas generation is expressed by a linear exponential bacterial growth curve (Figure 4.21[b]); and

iii) The settlement due to degradation is directly proportioned to the change in the number of bacteria.

The drawback of this model is that the bacterial population is actually an ecosystem, yet the model can only incorporate the growth kinetics of a single species of that population, the methanogens, and therefore underestimates the role of hydrolysis which is considered to be the RLS in degradation. Edgers *et al.* (1992) effectively simulated the long term settlement of landfills, based on a limited comparison with available field data. However, determination of empirical parameters remains a difficult task, especially after time (t_k) where settlement rates start to increase due to degradation. Additional work is needed to relate model parameters to waste composition, density, moisture content, temperature fluctuations and applied stress.

4.5.2. The Guasconi (1995) model

The model developed by Guasconi (1995) at the New Jersey Institute of Technology (NJIT) comprises a two phase system to represent gas production:

i) *a first phase of ten years* (after landfilling has commenced) where the gas production is represented by a zero order mathematical equation, which increases linearly with time:

Eq. 4.55 $$q = \frac{at}{T} \qquad (0 \le t \le T)$$

Where, q =annual production of biogas (m^3/ m^3 of waste/ year);
a = average amount of gas production per year for T;
T = total duration of the initial phase (years); and
t = time period of total gas production.

ii) *a second phase of 30 years* average duration of biodegradation during which the annual production of biogas is represented by a first order mathematical model which is an inverse exponential function of time:

Eq. 4.56 $$q' = a.e^{[-k(t-T)]} \qquad (t \ge T)$$

where, q' = annual production of biogas (m^3/ m^3 of waste/ year);
t = time period of total gas production;
k = constant; and
T = total duration of the initial phase (years).

By integrating the above equation with respect to time *(q'' (t) = q(t) + q'(t))*, the area under the curve can be found. This area represents the total gas production in m^3 per m^3 of disposed waste basis for time T. The equation for the area under the curve is as follows:

Eq. 4.57 $$V = (aT/2) + (aT/b)\left(1 - e^{[-k(t-T)]}\right) \qquad (t > T)$$

The author assumed that the gas generated by the biodegradation of the waste would be collected by the venting system of the landfill. The final amount of gas being generated as a result of biodegradation was estimated by means of analysis carried out on reconstituted waste sample which was assumed to be representative of a real waste sample. Once the total value of gas generated was found, the value of the parameter a was determined by setting q to be equal to 0.95. This means that by the end of the second phase (10+30=40 years) the modeled gas production was equivalent to 95% of the total gas production. The value of a was computed to be 0.43 in this study.

In calculating the settlement of the landfill Guasconi (1995) assumed that volumetric strain was equal to the vertical strain i.e. the thickness of the landfill was considered to be quite small compared to its length and width. Since 19.7% of the volume of solid waste was considered to be converted into biogas, this would correspond to 19.7% of

settlement occurring in a landfill. These estimates agree with those of Coduto and Huitric (1990) who state that the settlement due to biodegradation alone was probably between 18 percent to 24 percent of waste thickness. associate

4.5.3. The Wall and Zeiss (1995) model

Wall and Zeiss (1995) conducted a laboratory study to evaluate the effects of biodegradation on settlement and to study time reduction though leachate recirculation in the landfills. They applied the available models to enhanced cells to assess settlement and other parameters affecting settlement such as rate of gas production, gas composition, leachate composition, and total organic carbon (TOC) content. The authors used different approaches to determine the magnitude of waste settlement at each identifiable stage:

i) Initial compression

The initial compression is generally associated with the elastic compression that occurs in soils and its calculation requires the assumption or measurement of the modulus of elasticity of a waste, E_s (kPa). Since the amount of settlement was measured in the Wall and Zeiss (1995) study, values for the modulus of elasticity can be determined as follows:

Eq. 4.58 $$E_s = \frac{\Delta\sigma\, h_o}{\Delta h_i}$$

where $\Delta\sigma$ = increase in vertical stress due to fill placement, kPa;
h_o = initial height of refuse, m; and
Δh_i = settlement due to initial compression, m.

ii) Primary compression

The magnitude of secondary compression is calculated by the following equations, which assume a linear relationship between settlement and the logarithm of time.

Eq. 4.59 $$\Delta h_p = h_i C_R \log\frac{\sigma_o' + \Delta\sigma'}{\sigma_o'}$$

iii) Secondary compression

Wall and Zeiss (1995) used Sowers's approach to calculate secondary compression:

Eq. 4.60 $$\Delta h_s = h_p C_{\alpha\varepsilon} \log \frac{t}{t_p}$$

In an attempt to find a link between secondary compression and waste degradation the authors applied first order kinetics on the carbon mass balance data to calculate the rate constant (k):

Eq. 4.61 $$M_C(t) = M_C(0)e^{-kt}$$

Where $M_C(0)$ and $M_C(t)$ are the carbon mass available in the waste at time 0 and t, respectively.

Wall and Zeiss (1995) compared degradation and settlement data obtained from their study to other available settlement models. They found that the one-dimensional consolidation theory simulates settlement better than the Gibson and Lo and the Power Creep Low models. Wall and Zeiss (1995) observed that settlement occurs initially at a faster rate than biodegradation but then slows considerably. Secondary settlement was found to be linear with the logarithm of time and could be represented well by Eq. 4.60. Degradation was found to be adequately represented by a first order kinetic model (Eq. 4.61). The authors observed that biodegradation had very little effect on the secondary settlement rates. The total mass of solids decomposed during the test period (250 days) was 1% whereas the secondary settlement at the same period accounted for 4% of the deformation. By using the first-order model and the measured rate constants, the authors predicted that the organic carbon lost in five years would amount to 5.5-8.0% of the initial waste solid mass, which suggests that the contribution of degradation to settlement will become increasingly significant over time.

4.5.4. The Park and Lee (1997) model

Park and Lee (1997) defined the concept of settlement that occurs due to degradation of biodegradable refuse. The authors proposed a mathematical model that considers the compression process of waste due to the degradation of organic solids. Long-term settlement was divided into two parts: one associated with mechanical compression, the other with degradation. The first part was estimated using classical mechanical theory, and the second using first-order kinetics. The mechanical secondary compression was expressed by:

Eq. 4.62 $$\Delta\varepsilon(t)_{mec} = C_{\alpha,mec} \log\left[\left(\frac{t+\Delta t}{t}\right)\right]$$

where $C_{\alpha,mec}$ is the rate of secondary compression not yet due to biodegradation at time t.

The degradation process was then expressed in terms of first order kinetics as follows:

Eq. 4.63 $$\frac{dS}{dt} = \bar{k} - S(t) \quad \rightarrow \quad \frac{dS}{dt} = -\bar{k}S(t)$$

where $S(t)$ is the biodegradable waste solid mass at time t, and $\bar{k}$ the first order degradation rate constant (t^{-1}). The variable $\bar{k}$ implies that the degradation rate is affected by the degradation conditions. For example, Hoeks (1983) and Ham (1988) reported that the value of $\bar{k}$ could be estimated as 0.046, 0.028 - 0.139 and 0.462 - 1.386 years^{-1} when the degradation conditions were slow, moderate and rapid, respectively.

The main geotechnical concern is concentrated on the hydrolysis of complex insoluble organic polymers found in the biodegradable part of the wastes. As biodegradable solid mass decomposes, it converts into a liquid form (and eventually to gas). The total volume reduction is believed to depend upon the amount of biodegradable solid mass ($S_{tot-dec}$). Since biodegradable solids continue to decompose for a very long period, the completion of biological compression may also take a long time. $S(0) = S_{tot-dec}$ stands for the total amount of biodegradable solid mass included in refuse landfills.

Since the solubilisation process of biodegradable solid mass can be expressed as a first order kinetic, it can be supposed that the compression process due to the solubilisation can also be characterised by the same kinetic. Then, the equation related to the compression process due to the solubilisation can be expressed as follows:

Eq. 4.64 $$\bar{\varepsilon}_{dec}(t) = \varepsilon_{tot-dec}.e^{-kt_{bio}}, \quad t_{bio} = t - t_c$$

where $\bar{\varepsilon}_{dec}$ is the amount of strain that additionally occurs due to the degradation of biodegradable solids that is not yet decomposed at time t which is a first order biological strain rate constant (t^{-1}), $\varepsilon_{tot-dec}$ stands for the total amount of compression that will occur due to the degradation of biodegradable wastes and is dependent upon the total amount of biodegradable organic solids (Wardwell & Nelson 1981), and t_{bio} represents the time lapse from the starting point (t_c) at which the compression due to degradation starts. For fresh MSW landfills, this is assumed to be the time when the slope of settlement in plots

of strain versus log-time increases. For older MSW landfills, however, it is not necessary to determine t_c since the biological strain has already occurred when the settlement monitoring started.

Thus, the strain at time t_{bio} caused by biodegraded waste solids can be obtained by:

Eq. 4.65 $$\varepsilon(t_{bio})_{dec} = \varepsilon_{tot-dec} - \bar{\varepsilon}_{dec} = \varepsilon_{tot-dec}(1 - e^{-kt_{bio}})$$

The Park & Lee (1997) model was applied to the settlement data of landfills having various fill ages (Park & Lee, 2002). In the case of young MSW landfills (Site A, B and C) the total amount of biological strain was estimated at 11~25% and the biological compression of fresh landfills would be completed within 10~20 years. The relationship between the fill age and total amount of biological strain seems to be unique for the behaviour of biological compression in fresh MSW landfills. However, for fill ages of 2~10 years, the total amount of biological strain is highly dependent on the fill age. Park & Lee (2002) also reported that long-term settlement due to degradation was seldom complete for fill ages that are greater than 20 years. The duration for the stabilisation of biological compression was also concluded to be dependent upon the degradation condition.

4.6. Selected historic and current demonstration projects

Several historic field scale projects have been completed in the U.S. and Europe, and a number of current landfills are being operated as bioreactors equipped with monitoring systems to collect adequate field data for the development of rational guidelines for landfills with accelerated biodegradation. Some significant projects are discussed in the following three sections.

4.6.1. Field observations of landfill settlement behaviour

Brogborough and Calvert Landfill Projects, UK

Watts and Charles (1990, 1993) carried out field studies of the settlement of recently placed domestic refuse at two large disposal sites in the south of England (Table 4.5). At first, landfill operation at both sites filled the clay pits with domestic refuse after which the waste disposal sites were used to monitor the settlement of recently placed waste. The filling at both sites consisted of domestic refuse in plastic bin liners which were

compacted with a steel wheel compactor and covered with a thin layer of clay at the end of the day. Compression caused by the addition of extra fill was monitored over several years to determine long-term behaviour of the waste. When filling was complete the surface was sealed by a clay cap. Data concerning both sites are given in Table 4.5.

Stiffness (definition given in section 3.6) results from the two sites are similar and are generally just smaller than 1000 kN/m^2 which lead the authors to conclude that the refuse landfills were highly compressible. Considering the similarity in stiffness at the two sites, the difference in settlement values between them was surprising (Table 4.5). At the Brogborough site the waste landfill compressed by 11% over a period of 42 months, and at Calvert, in contrast, the corresponding compression was 4% only 11 months after landfill completion. This might be due to the fact that the stiffness represents only physical behaviour under additional load, whereas the total settlement values also take into consideration the compression due to biodegradation. It should also be noted that there were differences in the length of time during which additional fill was placed on the refuse landfill.

Table 4.5. Summary of data for Brogborough and Calvert landfill sites, UK.

Parameter	Brogborough	Calvert
Period of monitoring	42 months after landfill completion	11 months after landfill completion
Age of fill	1983 to 1987	1982 to 1986
Initial refuse height, m	16	22
Surface area, m^2	1 200 000	not given
In situ bulk density including cover material (as placed)	640kg/m^3	800kg/m^3
Type of waste	MSW	MSW
Enhancement techniques	none	none
Total settlement, %	11%	4%
References	Watts and Charles (1990 & 1999)	Watts and Charles (1990 & 1999)

On the basis of their results Watts and Charles (1990, 1993) concluded that recently placed domestic refuse landfill was subject to large reductions in volume as a result of

biodegradation, and that it is highly compressible under applied load. The compressibility of the refuse landfill was similar at the two sites. The measurements suggest that large movements will continue for many years. The authors observed that long-term movement resulting from physical creep compression is difficult to distinguish from settlement resulting from biodegradation.

4.6.2. Large scale test cells

Waste Management Paper (1995) advanced the concept of making landfills more sustainable by the development of a Bioreactor Landfill which aims to remove the pollution potential of a landfill over a period of one generation. The more rapid conversion of greater quantities of solid waste to gas reduces the volume of the waste. Volume reduction translates into either landfill life extension and/or less landfill use. Thus Bioreactor Landfills are able to accept more waste over their working lifetime whereby and/or fewer landfills are needed to accommodate the same inflows of waste from a given population. The controlled bioreactor landfill has received global attention and acceptance as an appropriate, cost effective and superior technological innovation (Pohland *et al.*, 2002). Several large test cells have been constructed in attempts to optimise factors affecting waste degradation and their relative importance.

A. Mountain View Landfill Project, USA

El Fadel and Al-Rashed (1998) used data from the Mountain View Landfill which is located approximately 15 miles Northwest of San Jose, California, USA to carry out a project in response to the need to optimize energy recovery from landfills, accelerate stabilization, and control gas migration and explosion hazards in the vicinity of landfills. Field scale experiments were conducted to measure waste settlement rates and to employ these data to calibrate mathematical models that are traditionally used in soil consolidation analyses.

The field experiment included six landfill cells (Table 4.6). Each was 30 by 30 meters and 15 meters deep and was deposited in 15 equal layers of 1 meter. The base and the side walls of each cell were isolated with a thick compacted clay liner to avoid groundwater intrusion and lateral gas and leachate movement from one cell to the other. The six cells were then filled with approximately equal amounts of MSW obtained from San Francisco at the same time. Calcium carbonate buffer, water, and/or sludge from an anaerobic digester were added to various cells to test their effect on biodegradation and

stabilization processes. The monitoring spanned over a period of approximately four years (1576 days). Parameters monitored included cell settlement, total volumetric gas production and gas composition, internal refuse temperature and leachate level within the cell.

Table 4.6. Summary of cell characteristics.

Landfill Cell	Total gas produced, 10^3 m^3	Total average settlement, %
Cell A with leachate recirculation, sludge and buffer addition	345	13.5
Cell B with addition of sludge and buffer	302	13.7
Cell C with addition of sludge, buffer and water	370	12.5
Cell D with addition of buffer and water	820	7.8
Cell E with addition of sludge and water	261	15.3
Cell F control cell - none additions	693	11.7

During the experiment, the wet test cells settled approximately 13-15%, while the dry control cell settled only 11.7% over a 4 year period. The researchers reported that the average settlement rate was affected primarily by the increased moisture content in the form of leachate recirculation or direct water addition, with the exception of cell D. They assumed that the addition of buffer and microbial seed did not appear to have a significant effect on ultimate settlement which leads to the conclusion that Cell D did not respond as expected to the addition of water. The authors correlated biodegradation and settlement assuming that the volume settled in each cell corresponds to the actual amount of solid waste converted to gas. The extent of settlement that can be attributed primarily to biocompression can be evaluated by converting to landfill gas an organic mass equivalent to the average settlement observed.

Estimates of the theoretical production of landfill gas from MSW with a typical biodegradable composition indicate that between 0.3 and 0.5m^3/kg would be generated throughout the lifetime of the landfill site (McBean *et al.*, 1995). Following this approach, researchers calculated that at least in two cells (D and F), the resulting gas yield exceeded this maximum, indicating that the settlement in these cells cannot be attributed totally to biodegradation. The gas yields from the remaining four cells ranged from between 0.23 to 0.42m^3/kg of refuse (Table 4.6), which are less than the maximum ultimate yield and a total correlation between settlement and biocompression can be

made in these cases (A, B, C, and E). It is not clear how El Fadel and Al-Rashed (1998) arrived at the last conclusion since there was no data on waste composition and TOC depletion in the waste mass during the experiment.

A subsequent study of waste biodegradation data at the Mountain View landfill concluded that there was a large degree of inconsistency between measured methane yields and the methane expected based on the weight loss of cellulose (Mehta *et al.*, 2002). In addition, leachate level data indicated that surface water and/or groundwater had entered all the cells, suggesting that landfill gas may have leaked by the same pathways as the water that infiltrated into the cells.

B. Brogborough Test Cells

Brogborough test cells were set up during 1986-88 at the Shanks & McEwan landfill (Brogborough, Bedfordshire, England) to evaluate the effects of pre and post-emplacement management techniques on methane production rates (Knox *et al.*, 1999; Croft *et al.*, 2001). Six cells were constructed each measuring 40m x 25m x 20m deep, containing 15,000 tonnes of waste each. A different management technique was applied to each cell such as leachate re-circulation, air injection and sewage sludge addition. The dimensions and characteristics of Brogborough test cells are reported in Table 4.7.

Leachate, gas and solid waste were monitored at Brogborough between 1986 and 2000, making it the longest field scale landfill study in the world. Within a few years of application of the enhancement techniques, the water addition and air injection cells exhibited the highest gas yields. Rates as high as 22 litres biogas/kg/yr were reached in Cell 4, which had air injection into it. Similarly high rates were developed in Cell 3, to which large volumes of water were added. Gas production rates in the control cell reached 13 litres/kg/yr. After about 7 years, cumulative gas production of 60–125 litres gas/wet-kg waste were reported (Figure 4.22). This is approximately double the expectation from a conventional landfill.

Gas flow through landfills is highly variable, dependant on a number of factors such as moisture content, temperature, inoculation, recirculation, atmospheric pressure, design and operational parameters and fluctuates daily and monthly (Knox, 2000; Kjeldsen & Christensen, 2001; Croft *et al.*, 2001; Young, 1992; Christopherson & Kjeldsen, 2001).

Most laboratory-scale studies observe an exponential decline in gas production rate after reaching a peak within a short time of waste deposition. In contrast, at Brogborough, gas

generation rates increased steadily for 7 years (Figure 4.22). Although this can almost certainly be attributed to the conditions of the waste (too dry), where there was not enough moisture within the waste to promote maximal degradation.

However, no data have been found in the literature concerning waste settlement behaviour and temperature within the waste at the Brogborough test cells but the gas production data and physical characteristics of the cells (Table 4.7) provide a valuable data set. As an example, test Cell 1 can be taken as being typical of most UK landfill sites accepting MSW.

Another large-scale project that produced valuable results was Landfill 2000 (section 4.6.2 C) which was intended to develop a bioreactor cell rotation approach to landfill, in which stabilized solid residues could be recovered and the cell reused after three years.

C. Landfill 2000 Test Cells

The landfill 2000 study was begun in 1991 in order to assess a number of techniques that promote Sustainable Landfill. Two 1,000 tonne cells were constructed, a test cell and a control cell, each measuring 36m x 23m x 5m maximum depth. Enhancement techniques investigated were: addition of 12% sewage sludge to the test cell and the control cells during filling; addition of sewage effluent after filling to both cells; and recirculation of leachate in the test cell to give approximately a one year hydraulic retention in the waste mass. Gas flow measurements were undertaken only occasionally until late 1993, when continuous monitoring was installed in the control cell.

Knox *et al.* (1999) found in their study that methanogenesis became established within one year in both cells. Enhanced rates of up to $17m^3$ gas/t/annum developed in the cell in which leachate was recirculated at a rate equivalent to a hydraulic retention time of approximately 1 year in the waste mass. It was found that even in the non-recirculation cell a gas generation rate of approximately $8m^3$ gas/t/annum developed. In the Landfill 2000 study, gas flow rates reached almost three times higher values ($60m^3$/t/annum in the test cell) than those observed in the Brogborough study (Figure 4.23). This is more than double the gas yield expected from a conventional landfill.

As can be seen in Figure 4.23 the gas generation curve was similar to the early peaks observed in many laboratory-scale studies, although these high gas rates were achieved at unusually low temperatures (range 7-17°C, mean 12°C) due to shallow depths in both cells (below 5m).

In practice, neither the Landfill 2000 test cells nor any of the Brogborough test cells were optimized enough: the Brogborough cells were too dry, while the wetter Landfill 2000 cells were too cold (<17°C).

Two more recent sets of large scale test cells came closer to optimising conditions which led to respectively higher rates of degradation. They are at Yolo County in California (120km from San Francisco), USA (Augenstein *et al.*, 1999) and at the VAM landfill in the Netherlands (Woelders and Oonk, 1999).

D. Yolo County Test Cells

The Yolo County Project began operation in 1996 to evaluate the costs and benefits of Bioreactor Landfills (Yazdani *et al.*, 2000). Two 11,000m^3 test cells, a control cell and an enhanced cell, were constructed and filled with 8000t of mixed MSW (Table 4.7). The performance of each cell was estimated with respect to waste degradation, methane production, moisture content and settlement. The enhanced cell was accelerated by the addition of leachate and groundwater to field capacity from 14 injection pits, followed by leachate recirculation. The control cell operated with no added moisture.

Over a 10 year period the generated methane from the cells was 72.8 l/kg-dry wt. waste for the enhanced cell and 32.1 l/kg-dry for the control cell (Figure 4.24). At 50% methane in the biogas composition this would be equivalent to 145.6 and 64.2 l/kg-dry wt., respectively. The data showed that approximately two times more methane gas was generated by the enhanced cell than by the control cell and confirmed that waste degradation can be accelerated by leachate recirculation in a bioreactor cell.

The maximum theoretical methane production ranged between 200-270 l/kg of dry waste. But in the literature measured yield lies often between 60-170 l/kg dry waste (El-Fadel *et al.*, 1996). In case of field measurements (with possible leaks during biogas collection and management), methane yields appears to be not higher than 14 l/kg/year (El-Fadel *et al.*, 1996).

The enhanced test cell settled by 15.5% in just under three years (data are given only until Feb 2000) whereas the control cell settled only by 3.0% over the same period (Figure 4.25).

The research study conducted at the Yolo County landfill site represents perhaps the most complete set of data available to date on a field-scale leachate recirculation landfill

with respect to settlement, cumulative methane production and the volume of leachate recirculated. Recorded data illustrate the effect of leachate recirculation to enhance waste biodegradation, methane production and settlement rate and showed evidence of the potential of bioreactor landfills to gain additional space by increased settling.

E. VAM test cell, Netherlands

At one of the largest waste management companies in the Netherlands (ESSENT) a bioreactor study (formerly called VAM) (Woelders and Oonk, 1999) was initiated in 1996 to evaluate factors that affected biodegradation of a Mechanically Separated Organic Residue (MSOR) from a MSW separation plant and to assess the ultimate quality of the end product from the bioreactor for possible reuse.

The construction of an 8 metre deep 49,000 tonne cell was completed by the end of 1997. Leachate addition, recirculation and active gas extraction were started at the beginning of 1998 (described in detail by Oonk *et al.*, 2000; Woelders and Oonk, 1999; Oonk and Woelders, 1999). In 16 months a gas volume of 1.85 x $10^6 m^3$ with a gas content of 56% CH_4, was extracted. This is equivalent to $37 m^3$gas/t MSOR, or $64 m^3$gas/t dry matter (the MSOR has a relatively high initial moisture content at 42%). Woelders and Oonk (1999) estimated that this was 30% of the total gas potential of the waste released in less than a year and half. Massive acceleration of gas generation rates is therefore readily achievable. It is equally important to know how long gas generation will continue at rates that can be used for energy recovery and conversely what proportion of the gas yield requires active management but with no prospect of recovering energy. It is also important to know whether these proportions can be influenced by landfill operational techniques.

Table 4.7. Some representative and current large scale test cells.

Parameter	Mountain View, USA	Brogborough, UK	Landfill 2000, UK	Yolo County, USA	VAM, Netherlands
1. Period of monitoring	1981-1985 (1576)	1986-2000	1991-1995	1995-2005	1997-1999
2. Cells	1 Control cell 5 Test cells	1 Control cell 5 Test cells	1 Control cell 1 Test cell	1 Control cell 1 Test cell	1 Test cell
3. Initial refuse height, m	15	20	up to 5	12	8
4. Initial refuse density, kg/m^3	694-765	600-700; 850 (Cell 5)	890-940		800-1000 (dry); 1200-1600 (wet)
5. Surface area, m^2	6 x 900	6 x 1000	2 x 828	2 x 1094	7062
6. Initial waste mass, tonnes	6 x 8000	6 x 15000	2 x 1000	2 x 8000	49500
7. Type of waste	MSW	MSW, Mixture of MSW, Industrial & Commercial waste	MSW	MSW	Mechanically Separated Organic Residue (MSOR)
8. Enhancement techniques	leachate recirculation (Cell A); sludge and buffer addition (Cell B& Cell C); and sludge and water addition (Cell D & Cell E).	low density (Cell 2); water addition (Cell 3); air injection (Cell 4); and 7% sludge addition (Cell 5).	12% sewage sludge addition during filling(both cells); sewage effluent addition after filling (both cells); and leachate recirculation (test cell).	leachate and groundwater addition to field capacity	Leachate recirculation; particle size reduction (~45mm); and water and buffer addition.
9. Gas flow rates, l/kg/yr	n/d *	*during methanogenic phase:* 13-22 for all cells *at closure:* 2.6-7.0 for all cells	*during methanogenic phase:* Test cell-20-60; Control cell-4-25. *at closure:* Test cell-17; Control cell-8.	*during methanogenic phase:* Test cell-20-60; Control cell-10-30. *at closure:*Test cell-2-10; Control cell-0.5-3.	*during methanogenic phase:* Test cell-32; *at closure:* Test cell-nd;
10. Cumulative gas production, litres/kg	Test cells-32-100; Control cell-90.	Control cell: 1-65; Test cells: 62-100.	Control cell-48; Test cell-201.	Control cell-64; Test cell-144.	64
11. Average methane content, %	n/d	n/d	Control cell-52 Test cell-58	Control cell-27 ; Test cell-39 between 5/96-5/97	56
12. Total settlement, %	Test cells-7.8-15.3 Control cell-11.7	n/d	n/d	Test cell-15.5% Control cell-3.0%	n/d
References	El Fadel and Al-Rashed (1998)	Knox *et al.* (1999); Knox *et al.* (2005).	Knox *et al.* (1999)	Augenstein *et al.* (1999); Mehta *et al.* (2002); Augenstein *et al.* (2005[a,b]).	Woelders and Oonk (1999); Oonk and Woelders (1999); Oonk *et al.* (2000).

* n/d - not determined

4.6.3. *Laboratory and pilot-scale studies on waste degradation and settlement*

A. Wall and Zeiss (1995) study

Wall and Zeiss (1995) studied the biological enhancement augmented leachate recycle to reduce the time to reach biological stabilization of waste and to determine the effects of biodegradation on overall settlement. The study included six test cells that were monitored for 250 days (Table 4.8). Three cells were designed to simulate bioreactor landfills (enhanced cells) while another three were designed to simulate dry-vault landfill (inhibited cells).

Wall and Zeiss (1995) reported that prior to load application, the addition of water to the refuse resulted in an initial settlement of 30%. Initial compression was observed to take place immediately upon load application and accounted for a 26% and 17% decrease in the initial refuse height for enhanced and inhibited test cells respectively. Primary compression occurred within the first 30 days and resulted in a further refuse compression of 15% in the enhanced cell and 12% in the inhibited cells (Wall and Zeiss, 1995). Secondary compression was not significantly increased by the addition of water and accounted for an additional compression of 4% in the biologically enhanced test cells and 2% in the inhibited cells in the first 225 days. Results demonstrate that secondary settlement was linear with the logarithm of time and that degradation was well represented by a first-order model. The authors reported that cumulative gas production increased to over 12 l/kg, where over 25% of the total gas production was methane in the most active cell. The gas production rate at the end of the period for the most active cell was 1.9 l/kg /month

Wall and Zeiss (1995) concluded that calculated settlement parameters from the test cells resemble values seen in actual landfills. The authors observed that during the first period of secondary settlement, biodegradation had very little effect on the secondary settlement rates. To determine the effect of solids removal on settlement, the percentage of the total carbon (TC) used during degradation, over the test period of 250 days, was used to estimate a five-year prediction of settlement. The total mass of solids decomposed during the test period was 1% whereas the secondary settlement over the same period accounted for a deformation of 4%. The authors concluded that degradation did not significantly affect the rate of secondary settlement within that test period and predicted that the

contribution of degradation to settlement would become significant over a greater period of time (approximately 5-10% over five years).

B. Beaven and Powrie (1995) study

Tests on various types of household waste were undertaken in a large-scale (2m dia. by 3m high) purpose-built compression cell located at the Cleanaway Ltd waste disposal site in Pitsea, Essex (Beaven & Powrie, 1995; Powrie & Beaven, 1999; Beaven, 2000; Hudson *et al.,* 2001) (Figure 4.26). The test cell was set up to evaluate factors affecting the hydraulic conductivity of domestic waste by quantifying the effects of overburdened pressure on the mechanical and hydraulic properties of different types of waste under different loadings.

In the compression cell, samples were subjected to vertical stress which typically was increased in five or six stages up to a maximum of 600kPa, representing landfill depths of up to 60m. Water was allowed to flow upward through the sample, from two 450 litre water header tanks mounted on a scaffold tower upto 3m above the top of the test cell. The compression of the refuse was monitored as a function of time by measuring the downward movement of the upper platen of the cell. Load was applied to the upper surface of waste samples in the compression cell through the hydraulically operated platen. Sidewall friction between the cylinder walls and the waste caused a reduction of 20% with depth in the average vertical stress transmitted to the waste (Powrie & Beaven, 1999). Bulk density, drainable porosity and saturated hydraulic conductivity of the waste samples were assessed after each compression stage. Detailed descriptions of the compression cell are given by Powrie & Beaven (1999) and Beaven (2000).

Tests were carried out on four different samples of domestic waste (Table 4.9) to investigate the effects of particle size reduction, degradation and compression on the vertical hydraulic conductivity.

Beaven and Powrie (1995) reported that waste density increased with increasing compression (Figure 4.27), whereas drainable porosity and vertical hydraulic conductivity decreased significantly (Figure 4.28.[a]). Figure 4.27 shows the variation in dry density, saturated density and density at field capacity of the waste with vertical effective stress. According to Figure 4.27 the final waste dry density was found to be720kg/m^3 at an average effective stress of 463kPa. One of the implications of the work of Powrie *et al.* (1998) achieved in terms of the waste density, is that compaction at the

Table 4.8. Some representative laboratory and pilot-scale studies.

Parameter	Pitsea test cell, UK	Sadek *et al.*, 2000	Wall and Zeiss, 1995
1. Period of monitoring	1992-1995; 1996-1999	~ 8 months (230 days)	~ 8 months (250 days)
2. Cells	1 Test cell	1 Test cell 1 Control cell (no moisture)	3 Test cells (Enhanced) 3 Control cells (Inhibited)
3. Initial refuse height, m	3.00	1.00	Test cells - 1.01 Control cells - 1.44
4. Initial refuse density, kg/m^3	AG1-1640; DM3-880; PV1-590; DN1-~910	Test cell – 842 Control cell - 900	Test cells – 268 Control cells - 225
5. Surface area, m^2	3.14 (2.00m dia.)	0.28 (0.60m dia.)	0.26 (0.57m dia.)
6. Initial waste mass, kg	Variable: 5000-15000	~ 220-250	Test cells – 68; Control cells - 82
7. Type of waste	4 type of waste-fresh MSW, processed fresh MSW, partly sorted and tumbled MSW, aged MSW (Table 4.9)	Laboratory prepared-mainly food (66%) and paper (26%)	Shredded MSW
8. Enhancement techniques	Waste pretreatment and sorting, water addition.	Sea water addition (test cell)	Temperature 25°C (test cells); distilled water and sewage sludge addition (test cells), leachate recirculation.
9. Applied effective stress, kPa	25 - 600	Up to 10	10
10. Gas flow rates, l/kg/month	n/d *	n/d *	1.9
11. Cumulative gas production, litres/kg	n/d	n/d	12 (test cells)
12. Average methane content, %	n/d	n/d	25 (test cells)
13. Settlement, %	Mechanical properties of waste were determined under six different loadings.	Total: 28.3 (test cell), 25.8 (control cell)	Total - 45(test cells);31(control cells) Primary - 15 (test cells);12 (control cells) Secondary - 4(test cells), 2 (control cells)
References	Beaven & Powrie (1995); Powrie & Beaven (1999); Beaven (2000); Hudson *et al.* (2001).	Sadek *et al.* (2000); Khoury *et al.* 2000.	Wall and Zeiss (1995).

* n/d - not determined

tipping face can have a similar effect to the burial of the waste by several meters of overburden.

Table 4.9. Types of waste used in Pitsea cell.

Waste sample	Type of waste	Reference
DM3	Fresh, unprocessed MSW waste	Powrie & Beaven (1999)
PV1	Processed (pulverized) fresh waste with particles size > 150mm	Beaven (2000)
DN1	Partly sorted and tumbled fresh MSW waste	Hudson *et al.* (2001)
AG1	25year old partly degraded waste	Beaven (2000)

The results from Powrie & Beaven (1999) show that the hydraulic conductivity of fresh MSW (DM3) can fall by several orders of magnitude from greater than 10^{-5}m/s at shallow depths to less than 10^{-7}m/s at 50m depth (at ~ 500kPa), whereas the hydraulic conductivity of processed refuse (DN1) fell by five orders of magnitude to 10^{-9}m/s (Figure 4.28.[b]). Therefore, leachate movement may be restricted in deep landfills limiting leachate extraction and recirculation. The heavily compressed waste may have a hydraulic conductivity approaching that of "impermeable" liner materials.

However, absorption of fluid by waste material, flow through partially saturated material and the influence of gas generation on hydraulic conductivity all require further investigation. The stress dependency of waste hydraulic conductivity has major implications for the operation of leachate extraction and recirculation systems, and basal and side slope drainage design. These all influence the pore water pressure distributions within the waste body and hence the effective stresses. As an example, Hudson *et al.* (2004) presented experimental data to show how, in a gassing domestic waste, the degree of gas saturation and pore water pressure will affect the bulk density and drainable porosity. When gas was allowed to accumulate in the sample there was a reduction in drainable porosity and an increase in bulk density.

C. Sadek *et al.* (2000) and Khoury *et al.* (2000) study

A laboratory-scale experiment was conducted to correlate settlement rates with stabilization processes at a closed coastal landfill (Sadek *et al.*, 2000; Khoury *et al.*,

2000). Two cells (control and test cell) were designed and constructed to evaluate the effect of salt-water intrusion on biodegradation processes, settlement rates and leachate quality. They were filled with refuse composed mainly of food waste with an initial moisture content of approximately 80% (wet wt. basis). Both cells were operated under different conditions. While seawater was added to the test cell on a weekly basis in a quantity equal to the amount of leachate generated by the cell, no moisture was added to the control cell. A summary of the cells characteristics are given in Table 4.8.

In conclusion, Khoury *et al.* (2000) found that biodegradation and reduction of COD and TOC were limited both with and without seawater addition. Leachate quality varied considerably between the two cells. The control cell produced a stronger leachate due to the absence of dilution effects. In contrast, the test cell generated weaker leachate due to seawater addition with increased chloride and sulphate concentrations, which may have inhibited the biodegradation process in the test cell. As a result of their experiments the authors concluded that while the addition of moisture is commonly known to enhance biodegradation and stabilization processes in solid waste landfills (Noble *et al.*, 1988), its addition in the form of seawater does not appear to have similar effects, at least within the timeframe of the experiment.

Sadek *et al.* (2000) stated that the end of primary settlement and the beginning of secondary settlement was reached after 125 days, after which time the settlement rate in both cells decreased significantly. The results of this study indicate that the total magnitude of settlement after 230 days was 25.8% and 28.3% for the control and the test cell, respectively. The test column exhibited greater total settlement than the control column, with a difference amounting to about 9%, which can be attributed mainly to the increased moisture content in that column. Although the presence of seawater was associated with greater waste settlement, some of its mineral constituents could have inhibited the biodegradation process.

The major drawback in the Sadek *et al.* (2000) and Khoury *et al.* (2000) studies lie in the fact that the number of cells and the test duration were insufficient to assess in detail the effect of seawater on biodegradation processes in organic sea fills. To achieve this, long term experiments and field validation involving direct comparison of fresh water and seawater additions are needed.

The results of bioreactor landfill studies suggest that by optimising the right factors (moisture content, temperature, inoculation, recirculation), degradation can be

accelerated dramatically in the laboratory and to a certain extent in large-scale test cells (such as Brogborough and Landfill 2000) compared with conventional landfills. However, few, including Knox *et al.* (2005), have gone beyond 50 to 75% of the typical expectation of 200m^3 gas/wet tonne waste, especially at large scale. Two recent studies (Knox *et al.*, 2005; Augenstein *et al.*, 2005[a,b]) have shown that even when optimised leachate recirculation led to very high initial rates of gas formation (110m^3/t/annum and 60m^3/t/annum respectively) rates which then fell to approximately 5 to 7m^3/t/annum after 50% of the gas potential had been reached. This is similar to the rates in the Brogborough test cells at the end of that study. These observations suggest that perhaps 25 to 50% of the gas potential of MSW consists of slowly degradable matter whose anaerobic degradation can not be further accelerated by conventional techniques.

In laboratory studies, very high rates of degradation have been achieved under optimised conditions with a high percentage of readily degradable material, reaching as high as 800m^3 gas/t/annum (e.g. Beaven, 1996; Beaven & Walker, 1997) and approaching the full gas potential (200m^3/t/annum) in little more than 2 years.

4.7. Summary

The results of bioreactor landfill studies suggest that no large-scale study, either in the UK or abroad, has yet been continued long enough to achieve complete stabilisation of the waste. As an example, at Landfill 2000, solid samples in early 1995 still had biochemical methane potentials (BMP) of 76 (recirculation cell) and 161 (non-recirculation cell) m^3/dry tonne; at Brogborough, cumulative gas production until 1998 reached only 50% of the typical observed range for conventional landfills; at Yolo County, only 70% of the gas potential had been reached in 10 years.

The way in which gas generation rates decline, as the waste becomes depleted of degradable matter, has not been studied in detail. There are virtually no published data giving gas production curves for the last third, from full-scale landfills, while most large-scale test cells have either been discontinued at too early a stage or are still too young to have exhibited a significant decline. Some information is available from small-scale studies and useful observations can be made from some of the large-scale studies, such as Yolo County and Brogborough Cell 4, where the furthest progress along the gas production curve of any large scale test cells to date is represented. Their continued operation and monitoring are therefore of great importance.

In addition, all large-scale trials to date have been focused on degradation and there has been no large-scale trial or study of factors that influence landfill settlement. In most operating landfills the necessary data, such as accurate waste composition and waste placement history, were never recorded. Also the various parameters required for modelling work are not recorded at normal operating landfills and require significant effort and expense to measure. Often landfill operators are reluctant to allow researchers unhindered access to full-scale landfills as it interrupts their operation and can cause issues with methane energy recovery programs. Several full-scale data sets of surface settlement do exist but they are rare and well spread across the world. Settlements result from the waste self weight, and hence although the magnitude of the long-term settlements is modeled, the mechanism causing settlement is not. Of greater importance is the need for a waste model that can more closely represent both short-term and degradation controlled long-term behaviour inclusive of the heterogeneous properties of the waste. To achieve a comprehensive, interactive model, there is a need to run a project aimed specifically at understanding and quantifying the main factors affecting rates and magnitude of settlement in landfills to obtain a complete data set with respect to settlement, cumulative methane production, gas composition, waste composition and leachate characteristics at different stages of biodegradation.

Figures

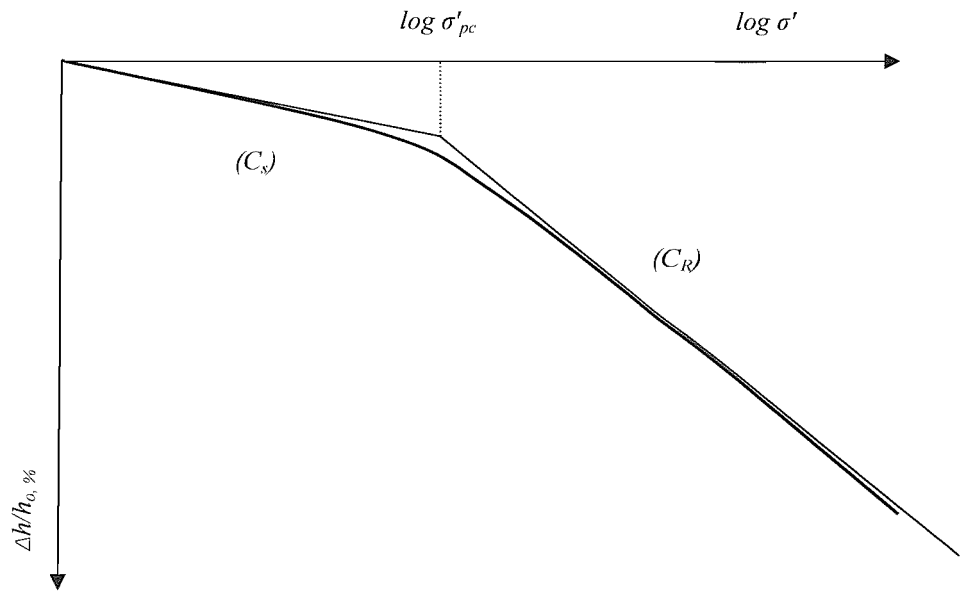

Figure 4.1. Illustration of primary consolidation according to Terzaghi theory (1943).

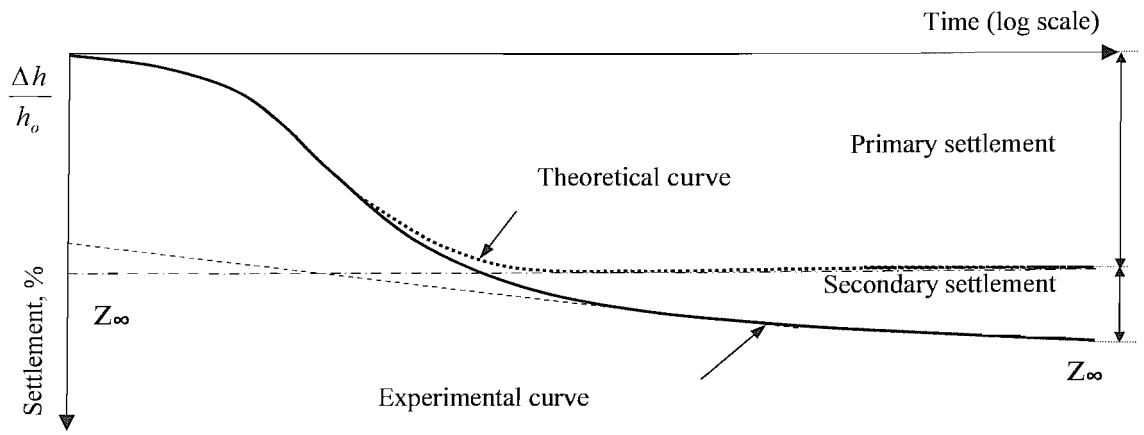

Figure 4.2. Illustration of theoretical and experimental settlement curves after Buisman (1936).

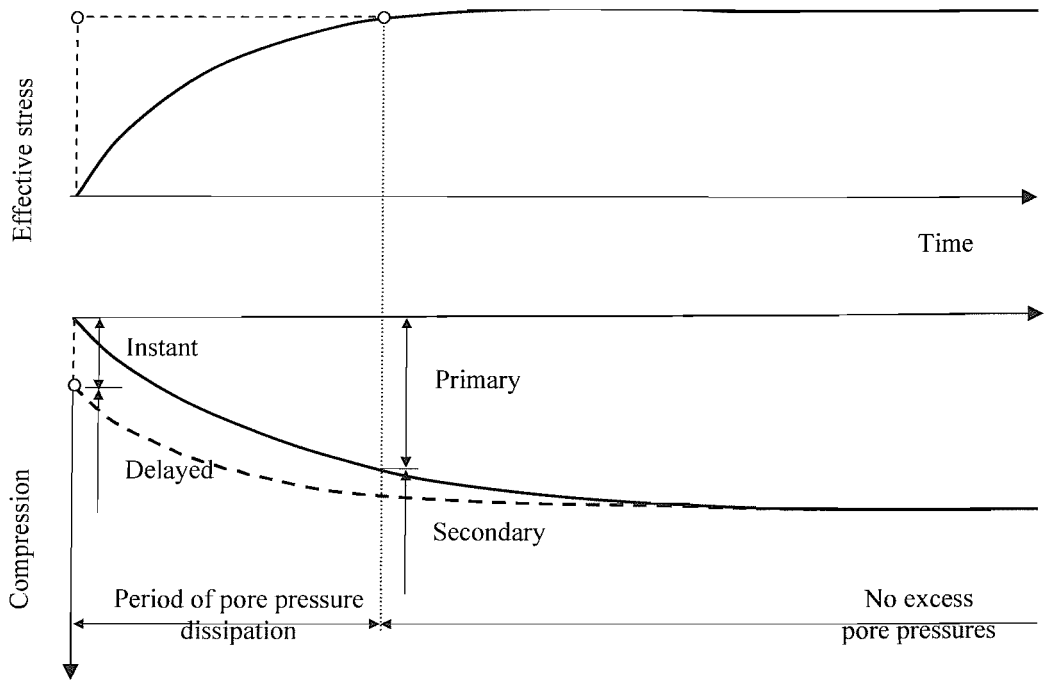

Figure 4.3. Definition of instant and delayed compression compared with primary and secondary compression, after Bjerrum (1967).

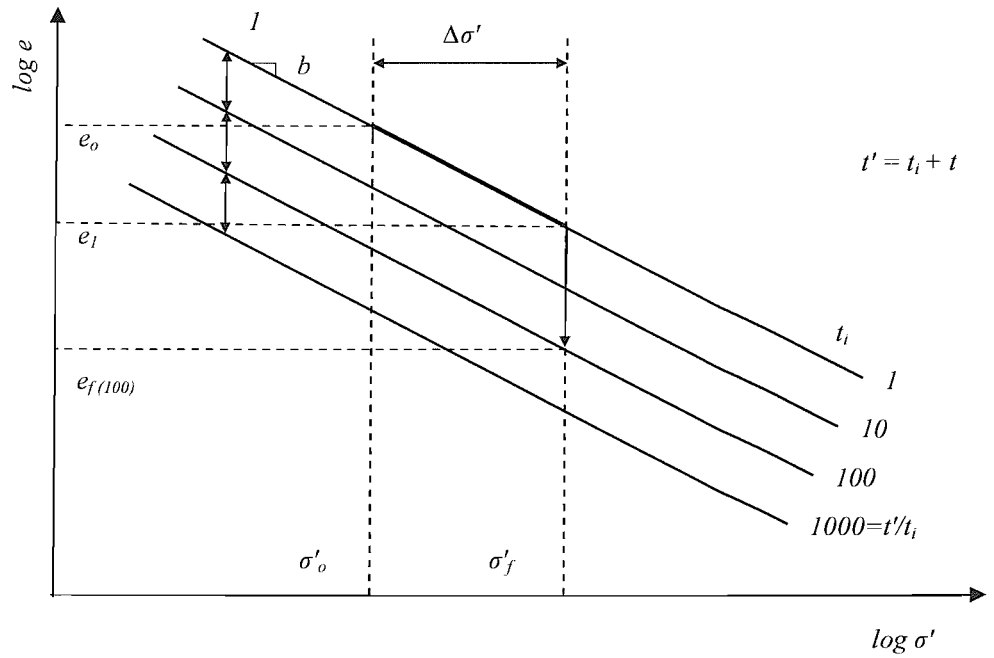

Figure 4.4. Illustration of Hansen (1969) model.

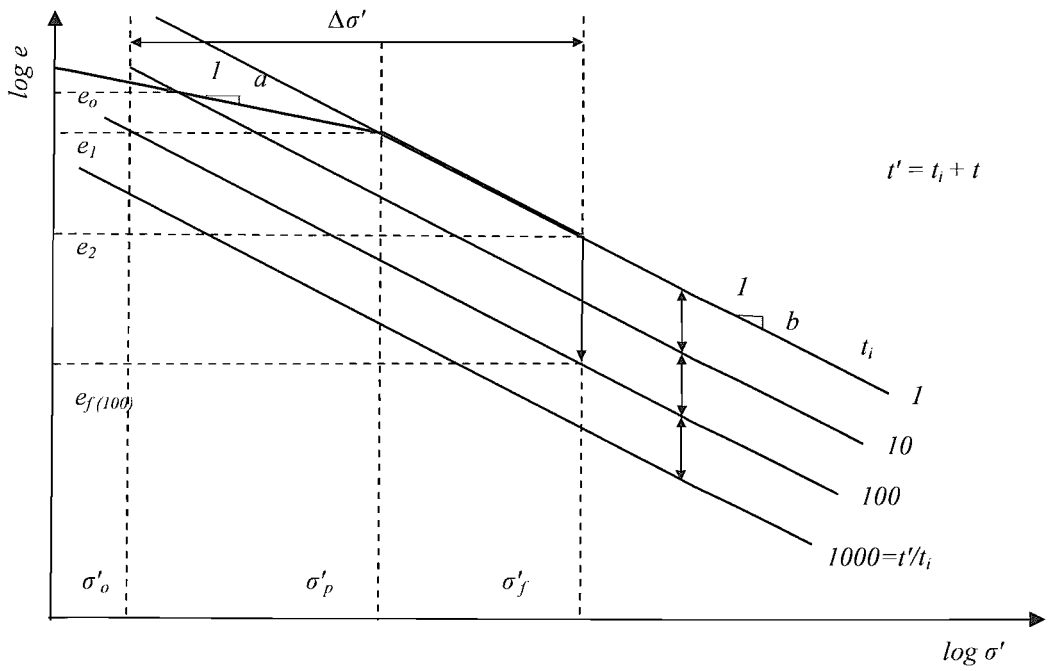

Figure 4.5. Illustration of Garlanger (1972) model.

a)

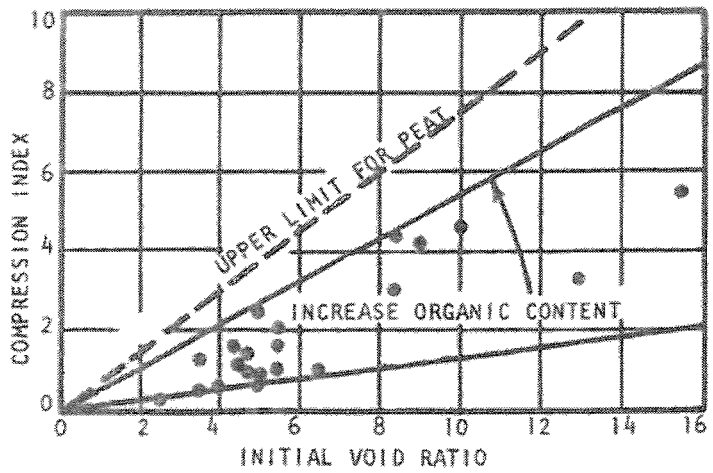

Figure 4.6. a) Primary compression index (C_c) and b) secondary compression index ($C_{a\varepsilon}$) against initial void ratio eo, Sowers (1973).

b)

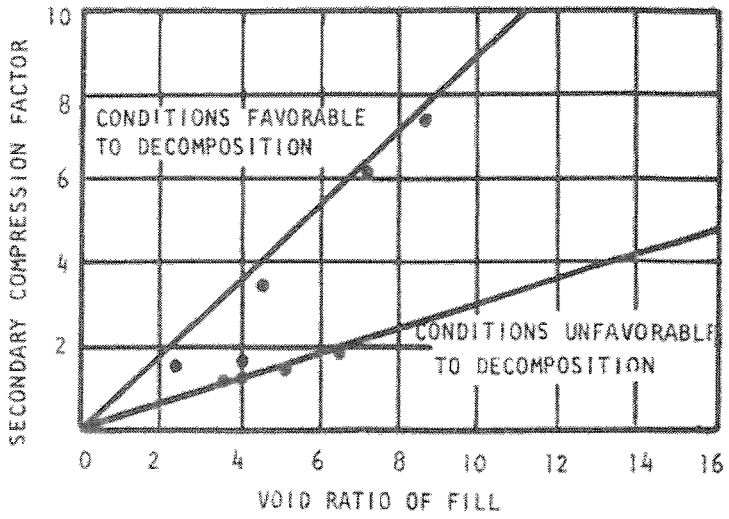

Figure 4.6. a) Primary compression index (C_c) and b) secondary compression index ($C_{a\varepsilon}$) against initial void ratio e_o, Sowers (1973).

a)

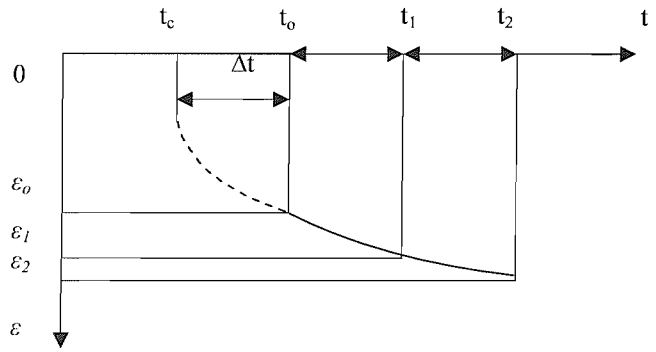

b)

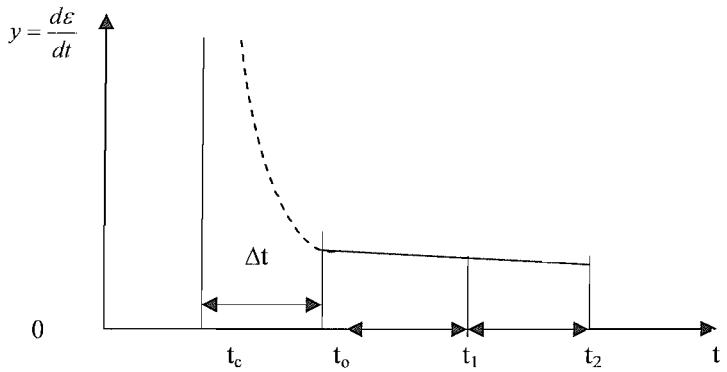

Figure 4.7. a) The Principle of Coumoulos and Koryalos (1997) method.

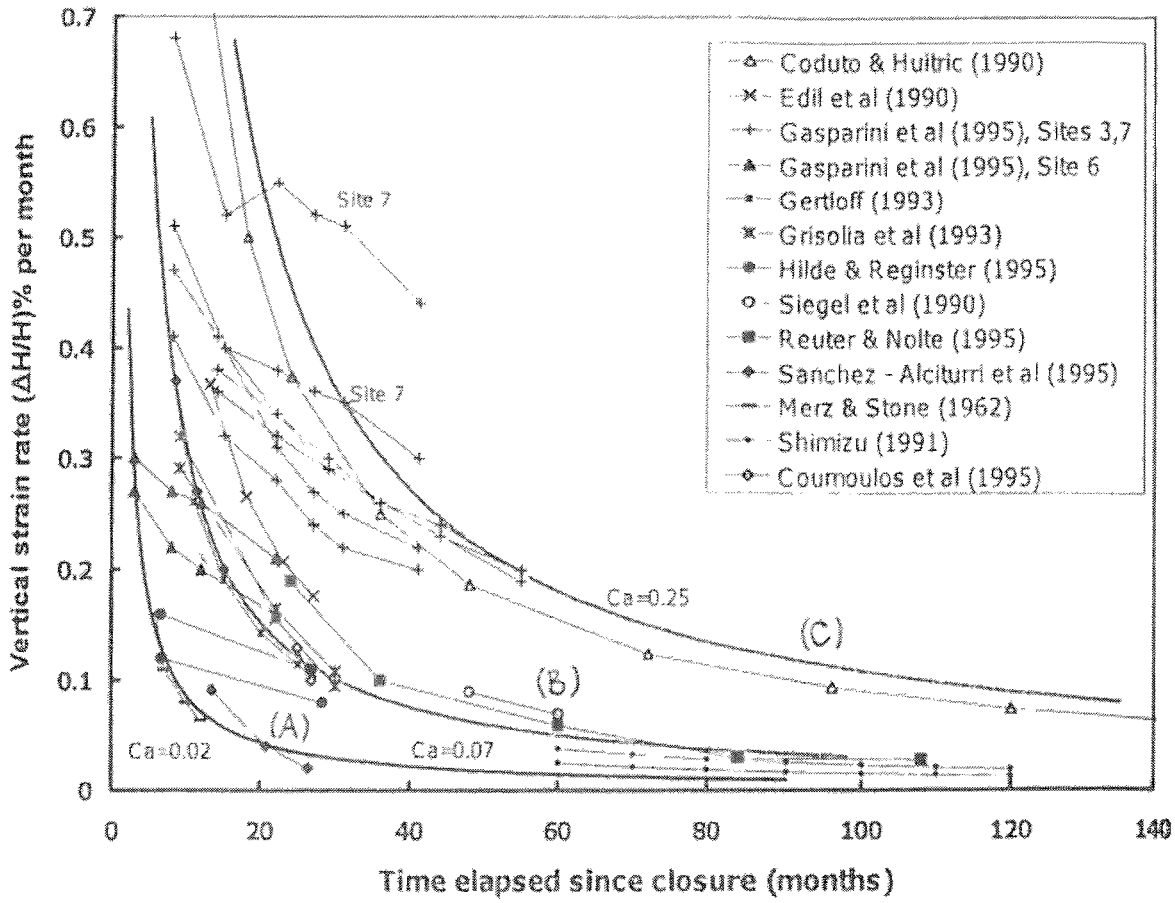

Figure 4.8. $C_{\alpha\varepsilon}$ **values (here** C_α**) determined by Coumoulos and Koryalos (1999).**

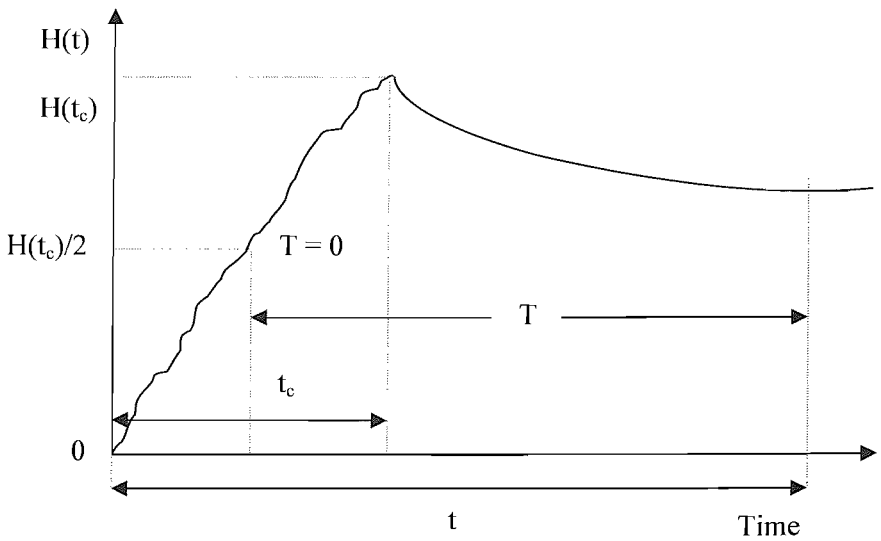

Figure 4.9. Definition of median fill age and its relationship with settlement rate.

a)

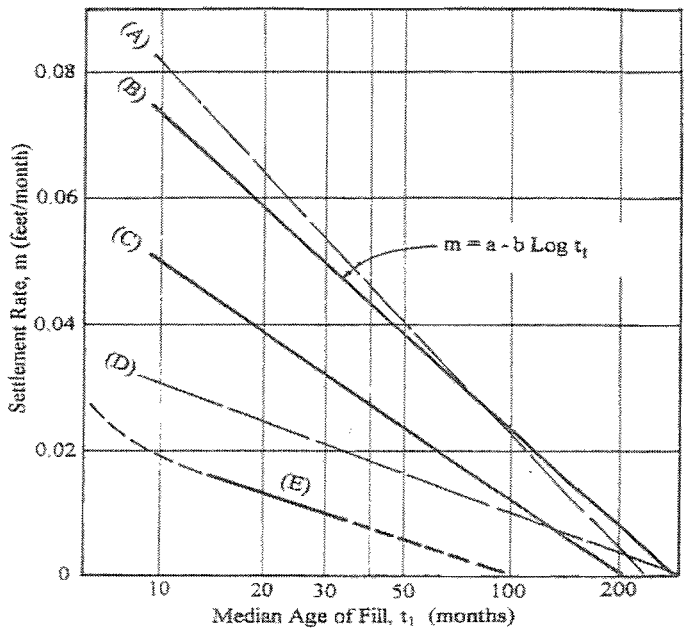

b)

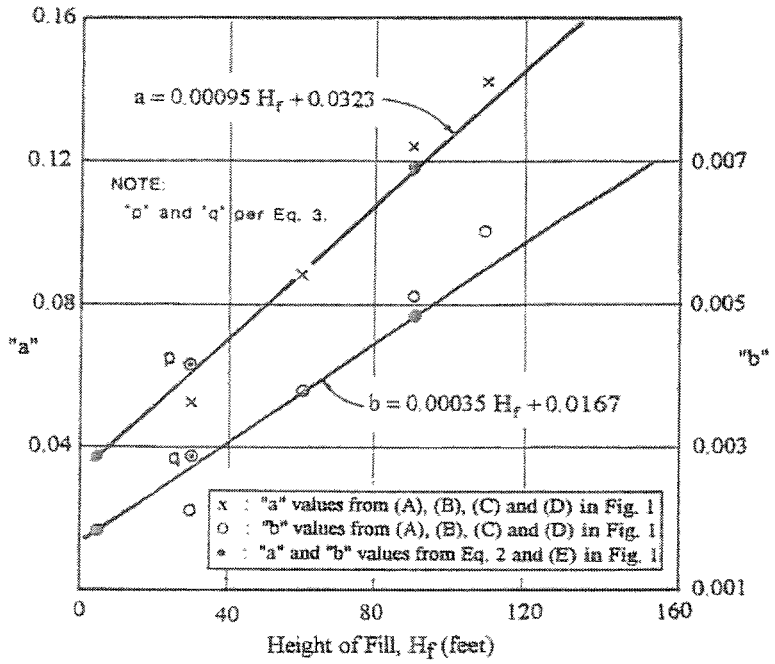

(Data from Yen and Scanlon, 1975)

(A) m = 0.142 – 0.060 LogT	$H(t_c) \geq 31$ m	$70 \leq t_c \leq 82$ months
(B) m = 0.124 – 0.051 LogT	$25 \leq H(t_c) \leq 31$ m	$70 \leq t_c \leq 82$ months
(C) m = 0.088 – 0.038 LogT	$12 \leq H(t_c) \leq 25$ m	$70 \leq t_c \leq 82$ months
(D) m = 0.052 – 0.021 LogT	$H(t_c) < 12$ m	$t_c < 12$ months

(Data from Rao *et al.*, 1977)

(E) m = 0.037 – 0.0185LogT	$H(t_c) = 1.5$ m	n/a

Figure 4.10. a) Linear relationship between settlement rate and fill age; b) Evaluation of settlement rate parameters *a* and *b* by Sohn and Lee (1994).

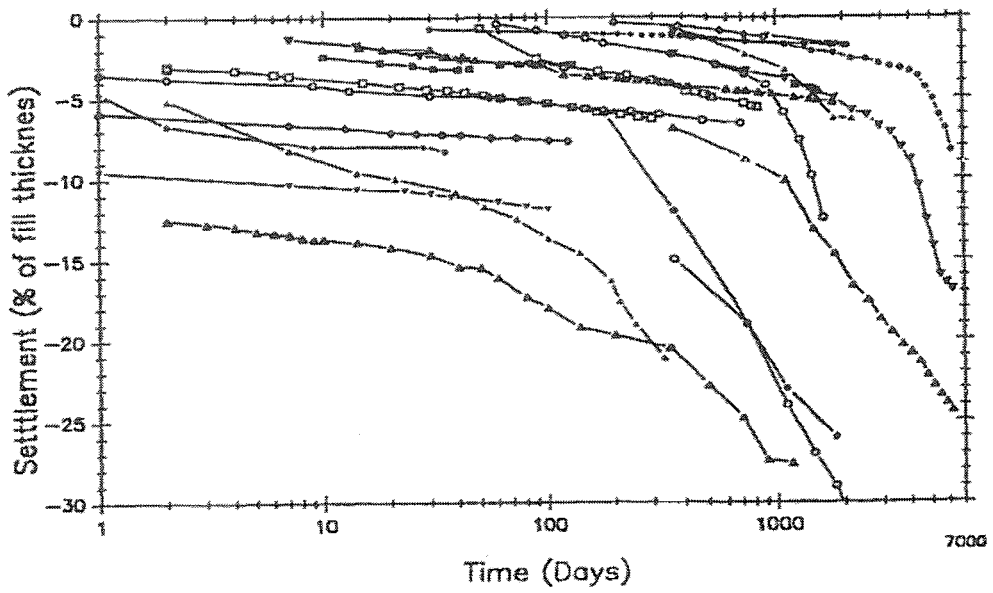

Figure 4.11. Landfill settlement vs. log-time relationships for 24 field case histories (Edgers *et al.*, 1992).

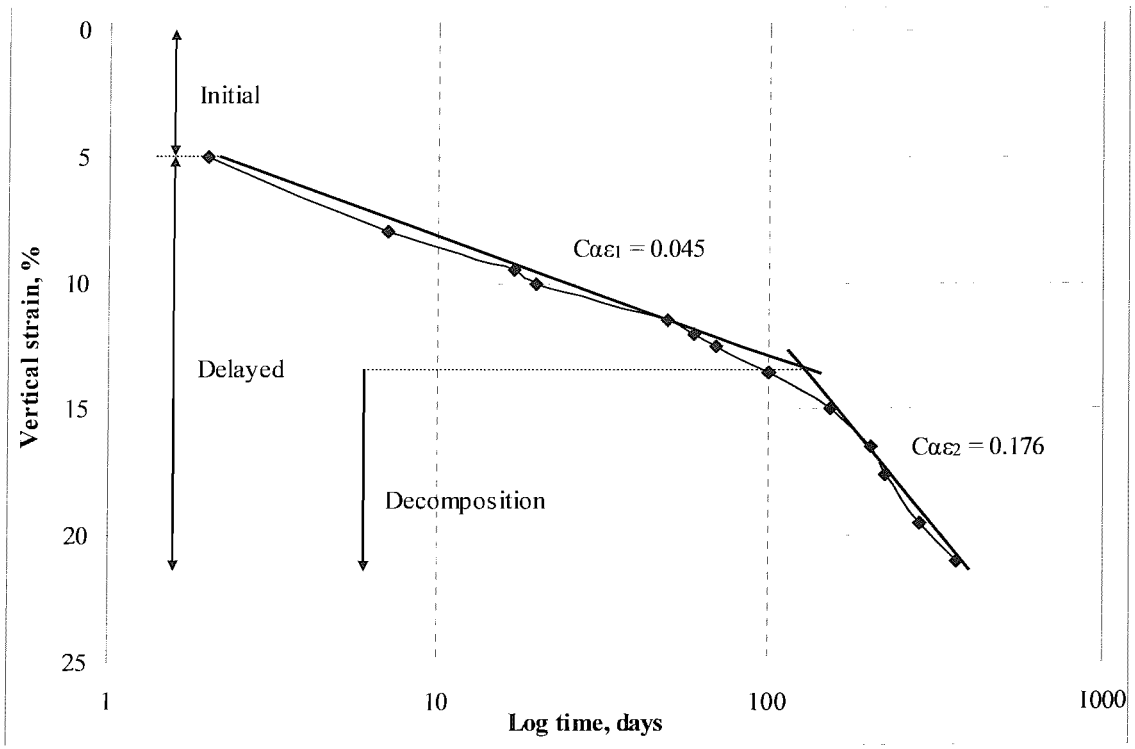

Figure 4.12. Idealized plot of landfill settlement vs. log-time (Bjarngard and Edgers, 1990).

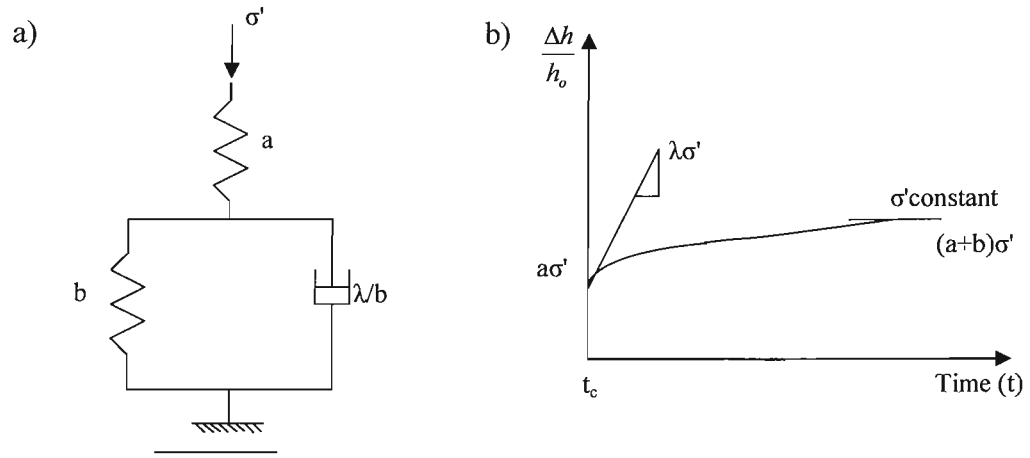

Figure 4.13. Gibson and Lo model (1961) representation.

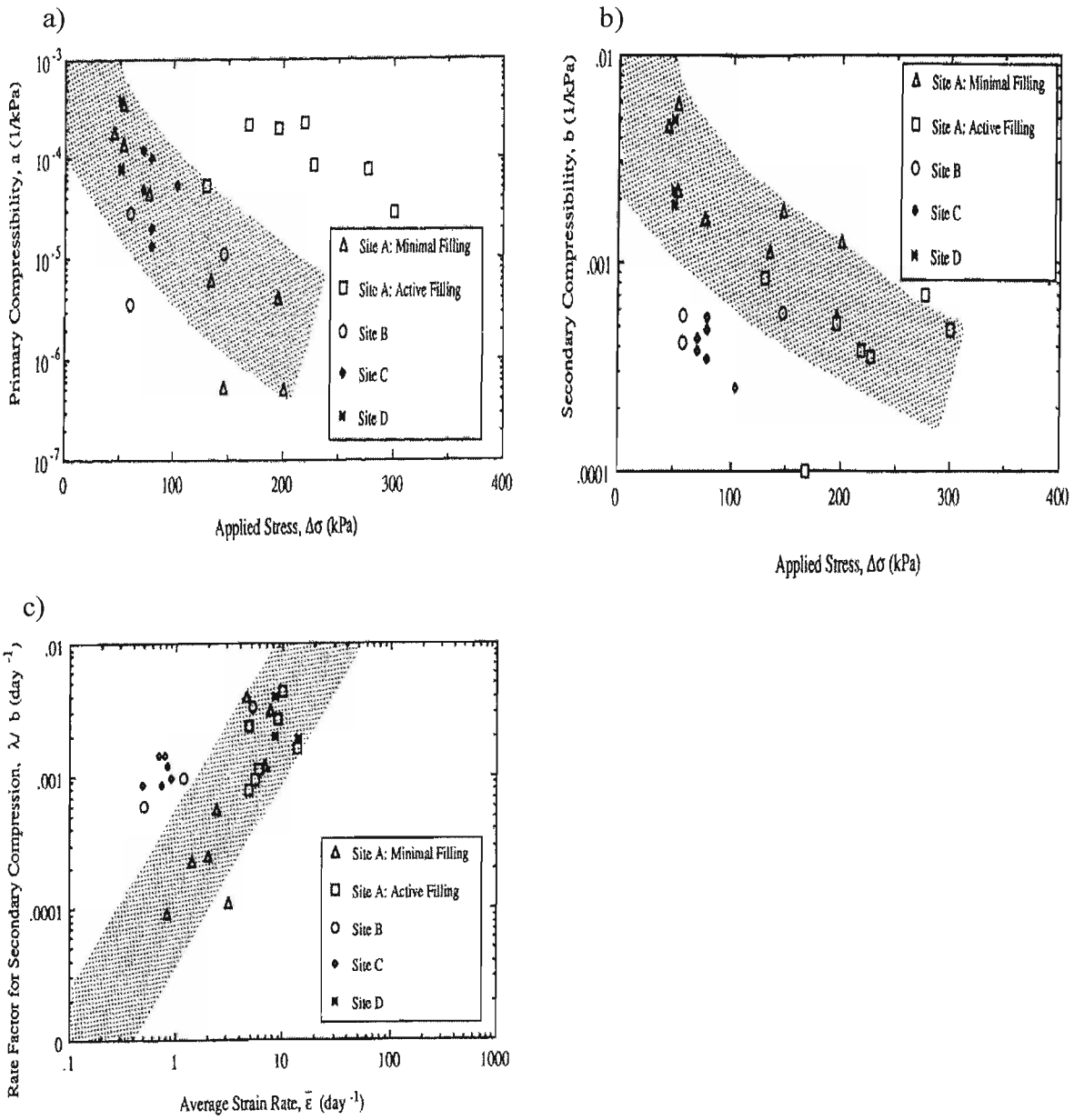

Figure 4.14. Empirical parameters *a, b* and *λ/b* of the Gibson and Lo model (1961) derived from the Edil *et al.* (1990) study.

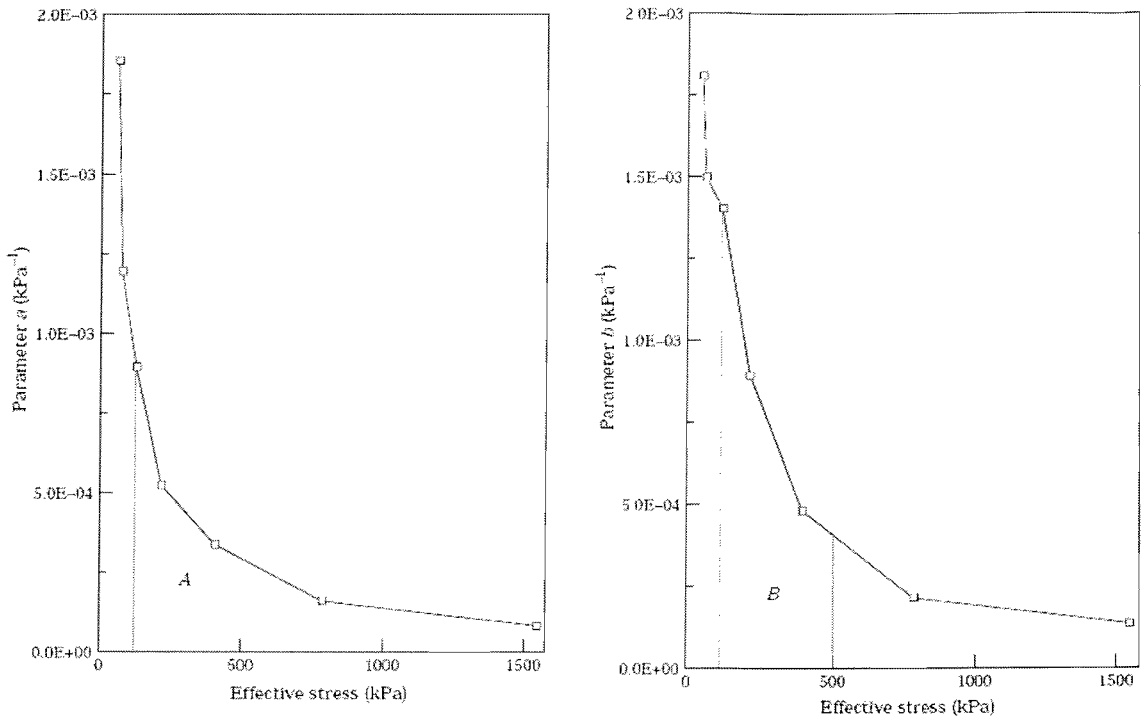

Figure 4.15. Values of *a* and *b* proposed by Rao *et al.* (1977).

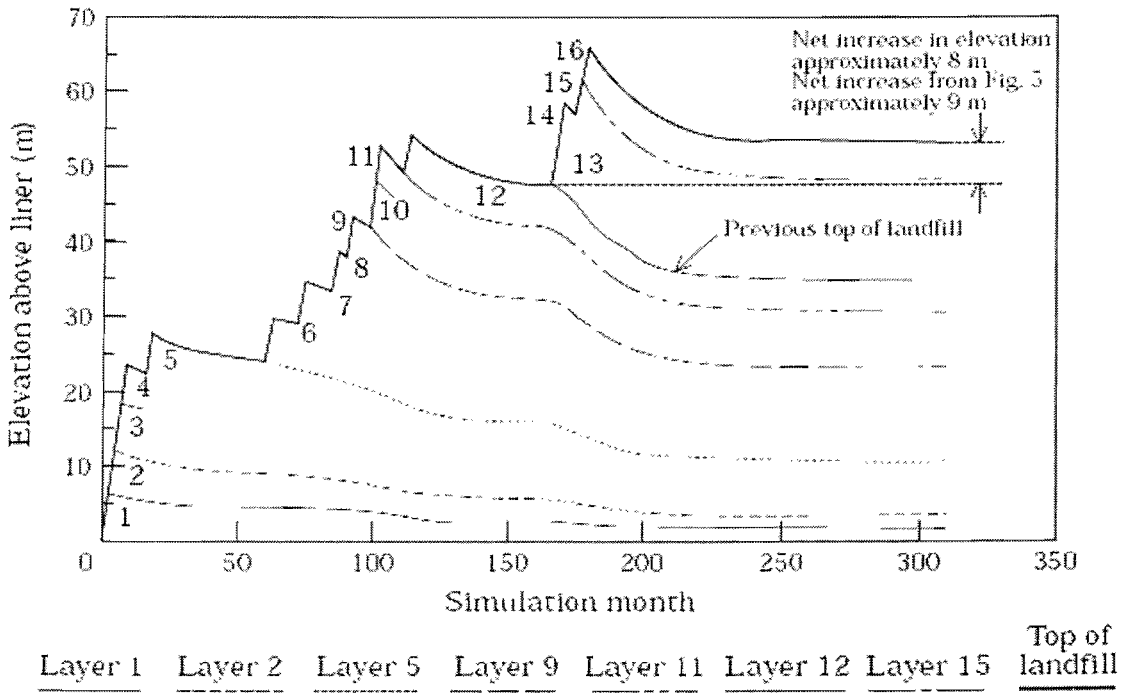

Figure 4.16. Bleiker *et al.* (1995) model results of the 25.8 m vertical expansion. Numbers indicate layers.

a)

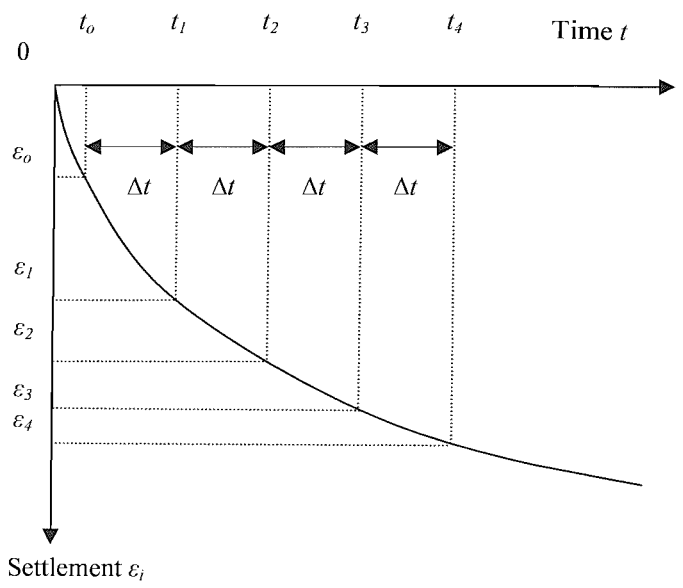

b)

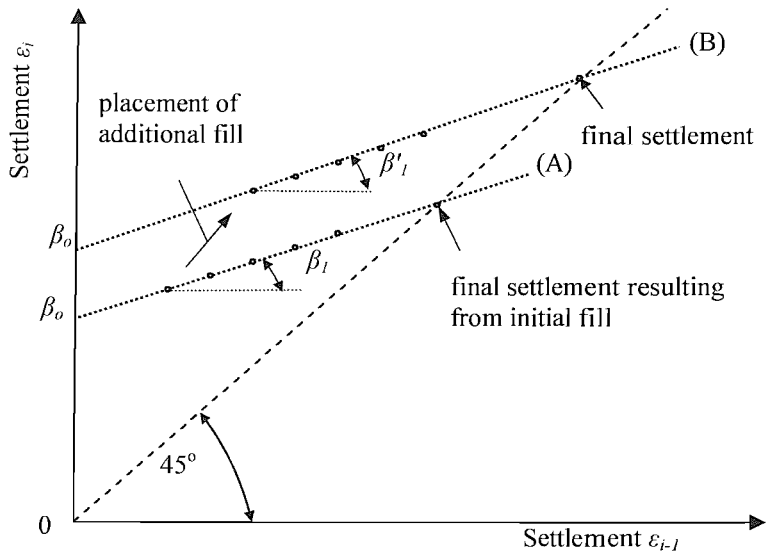

Figure 4.17. Asoaka (1978) construction and interpretation (lines of different loading stages).

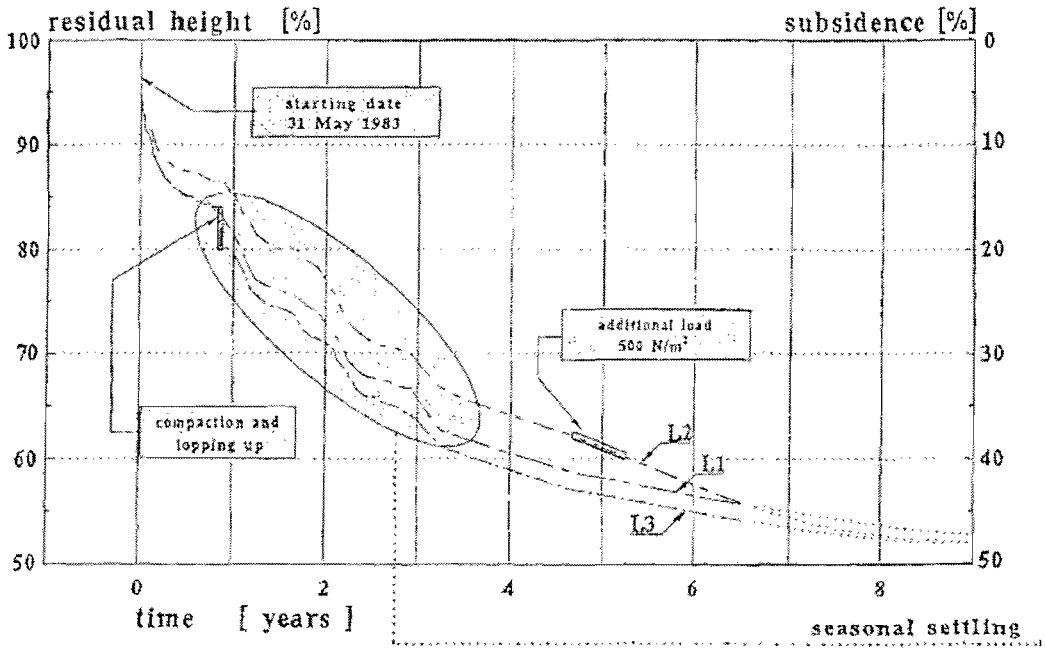

Figure 4.18. Settlement results from the compression tests carried out by Gandolla *et al.* (1992).

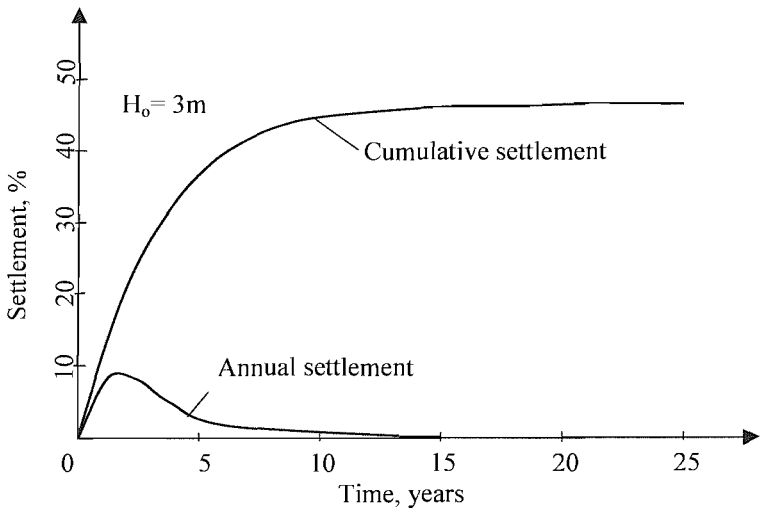

Figure 4.19. Evolution of settlement according to Gandolla *et al.* (1992).

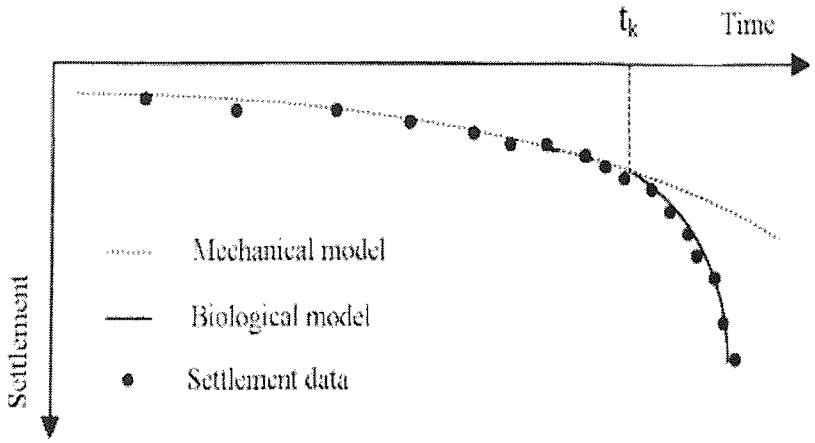

Figure 4.20. Comparison of settlements including effects of degradation with measured settlements (Edgers *et al.*, 1992).

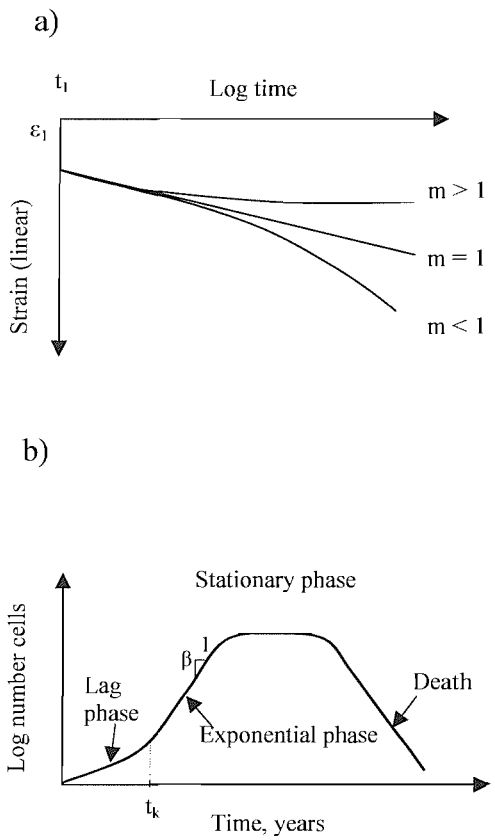

Figure 4.21. a) Creep curves predicted by Eq. 4.52 and Eq. 4.53 (Edgers *et al.*, 1992); b) Typical bacterial growth curve (after Mitchell, 1974).

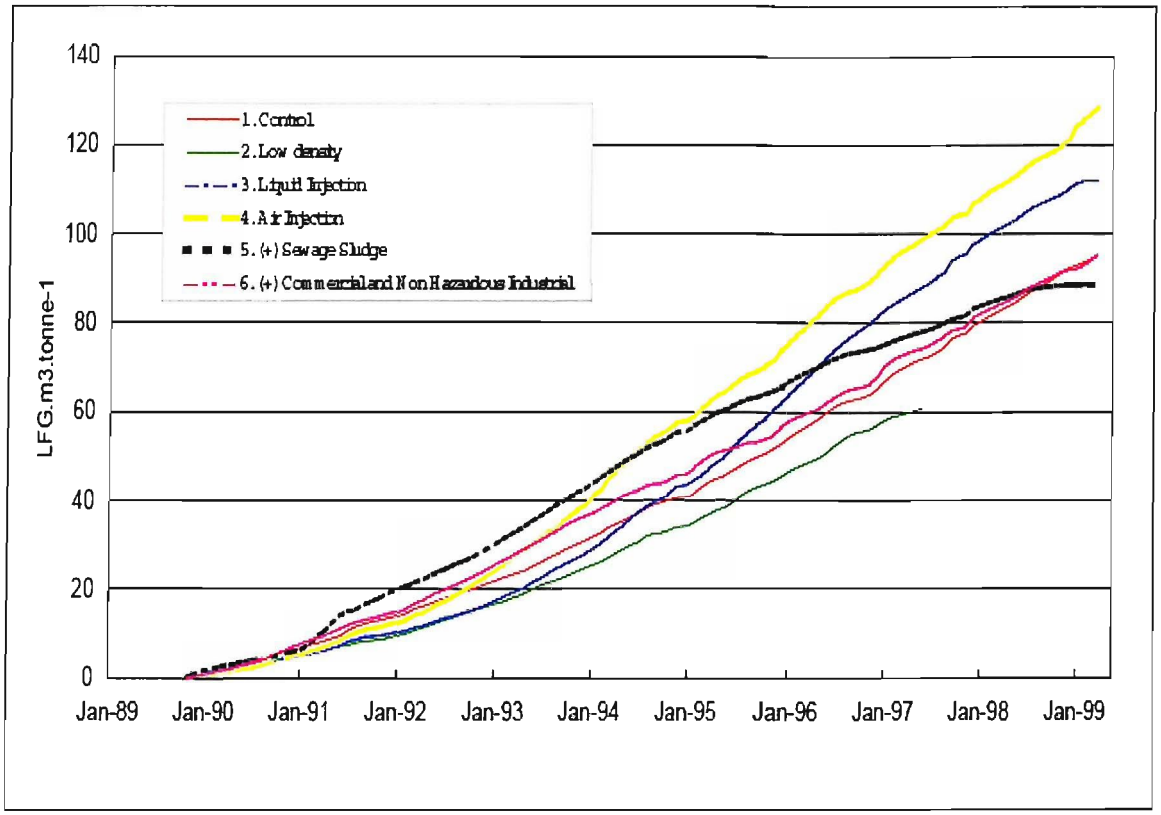

Figure 4.22. Cumulative gas generation at the Brogborough test cells (Knox *et al.*, 1999).

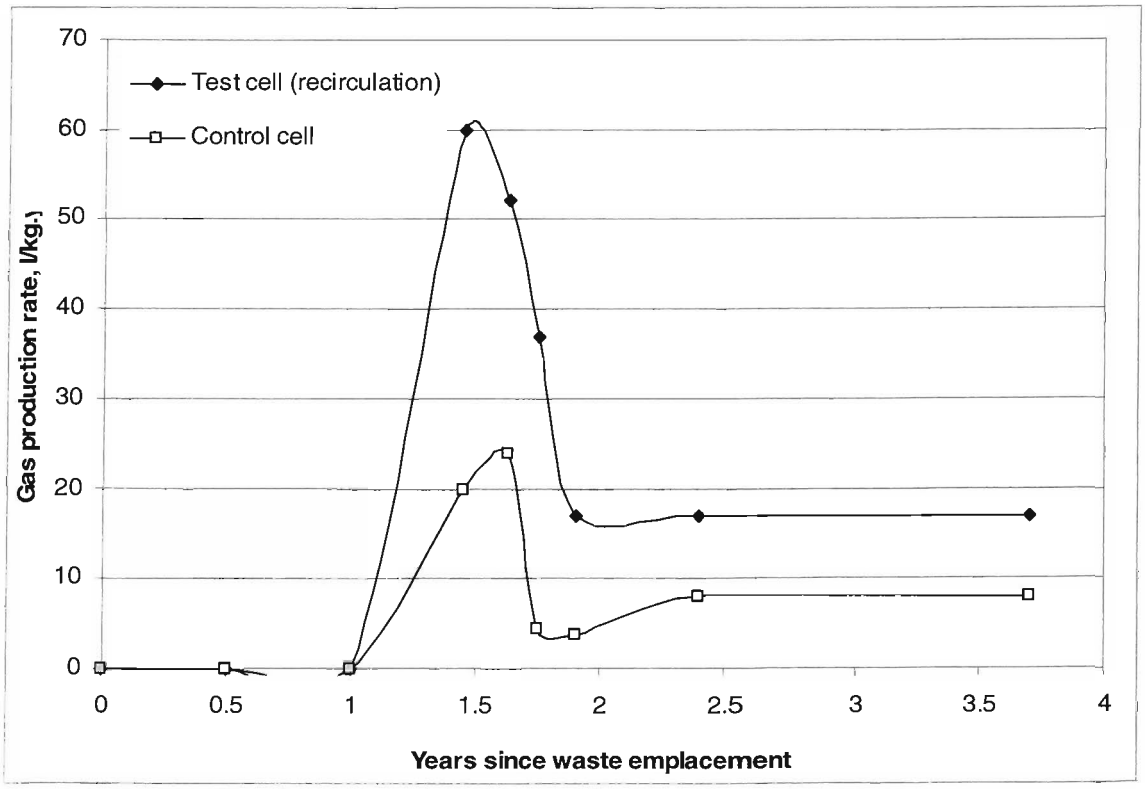

Figure 4.23. Cumulative gas flow at the Landfill 2000 test cells.

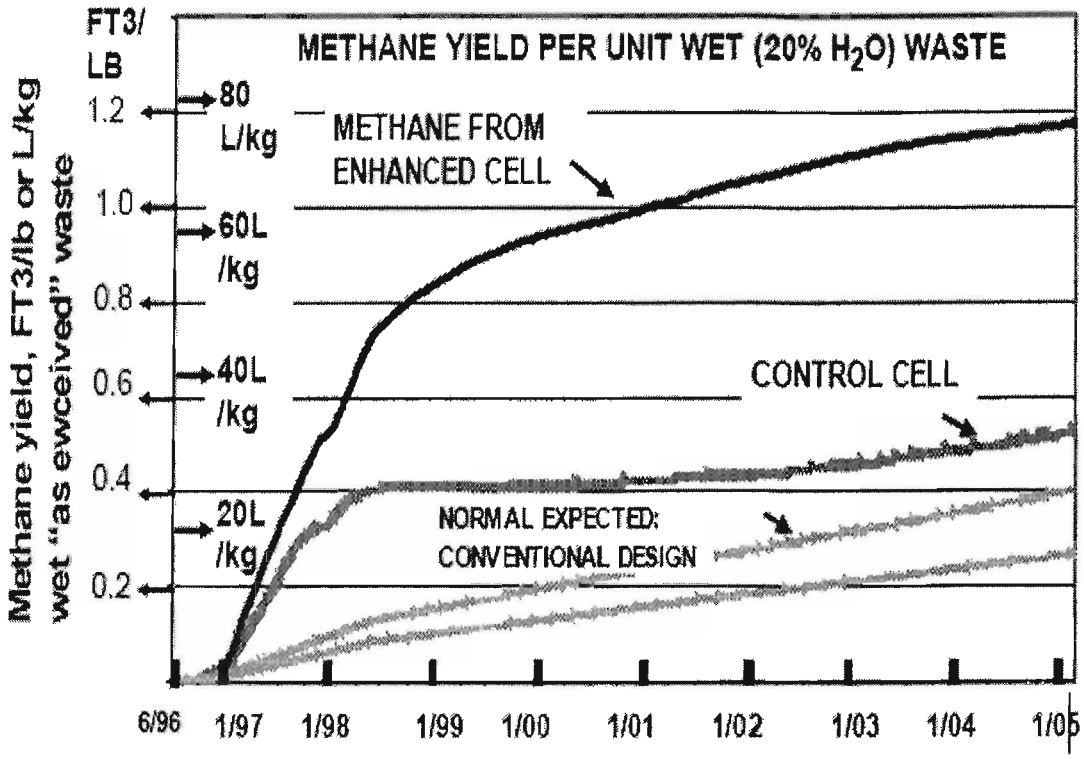

Figure 4.24. Methane production rate in enhanced and control cells. Shown for comparison are methane from control cell, and the "normal" generation expected from an un-enhanced conventional landfill (Augenstein *et al.*, 2005[a]).

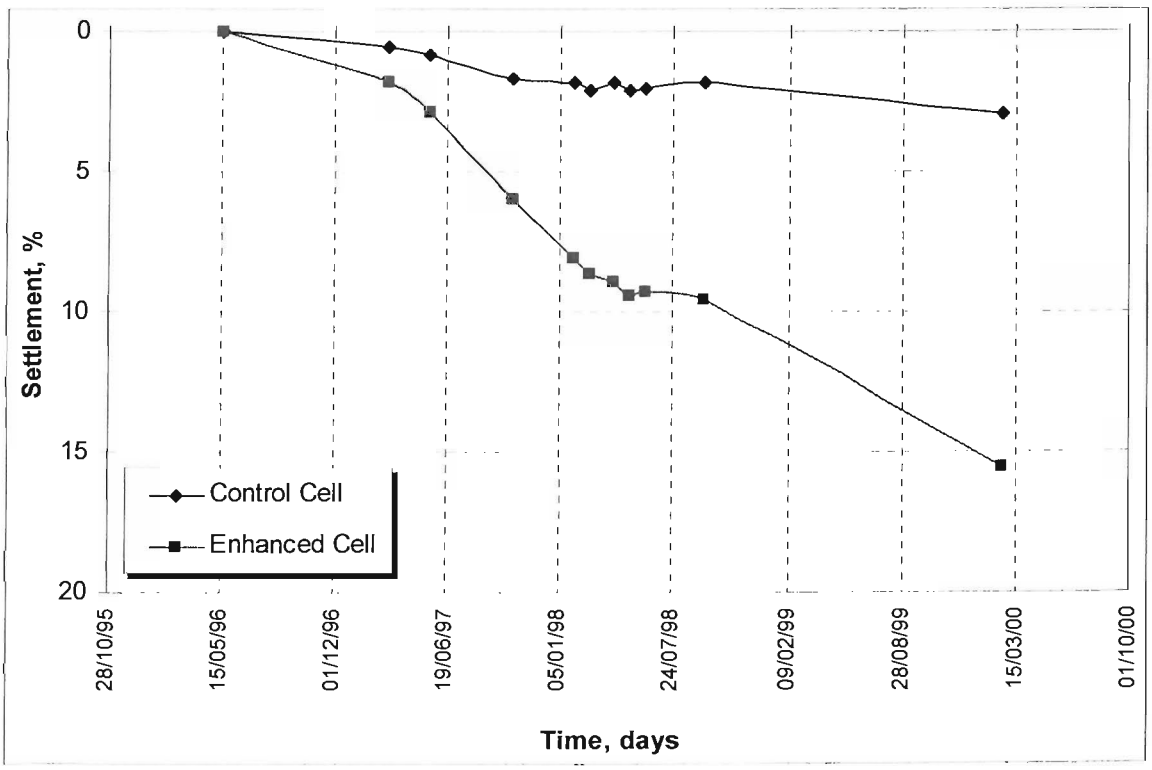

Figure 4.25. Waste settlement over time at Yolo County, California, USA (Mehta *et al.*, 2002).

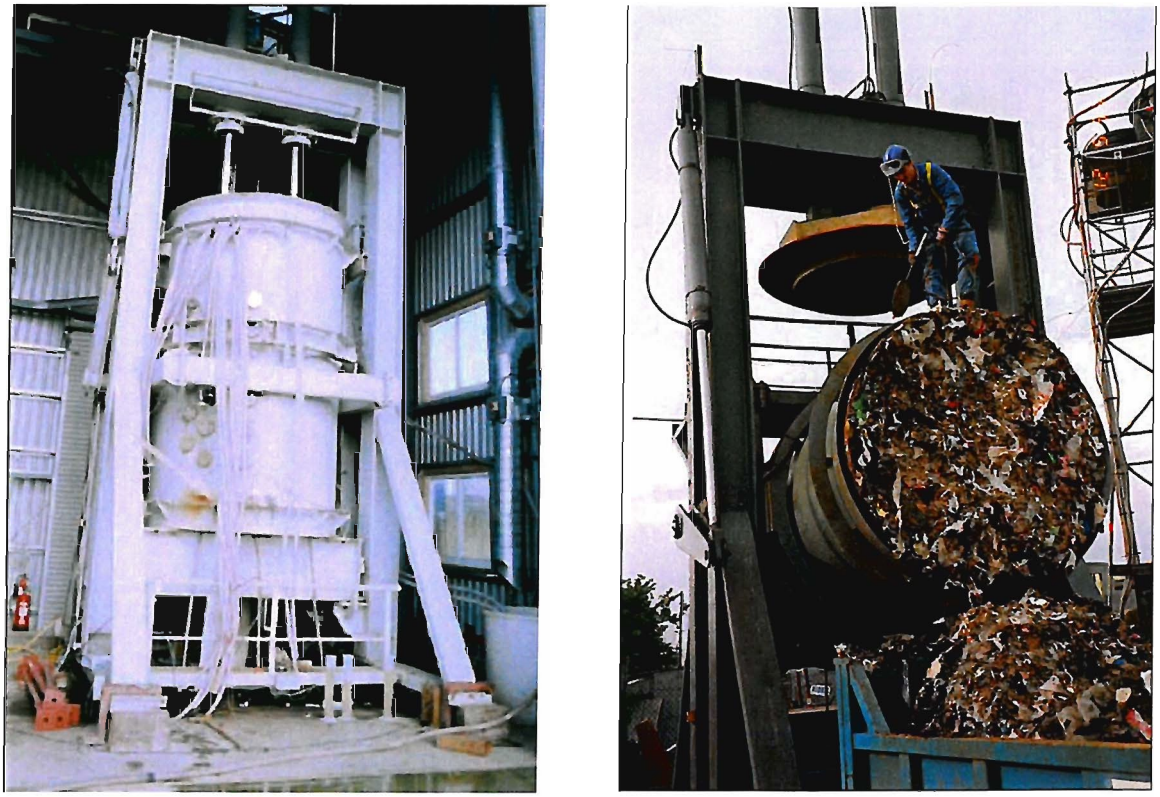

Figure 4.26. The Pitsea compression cell.

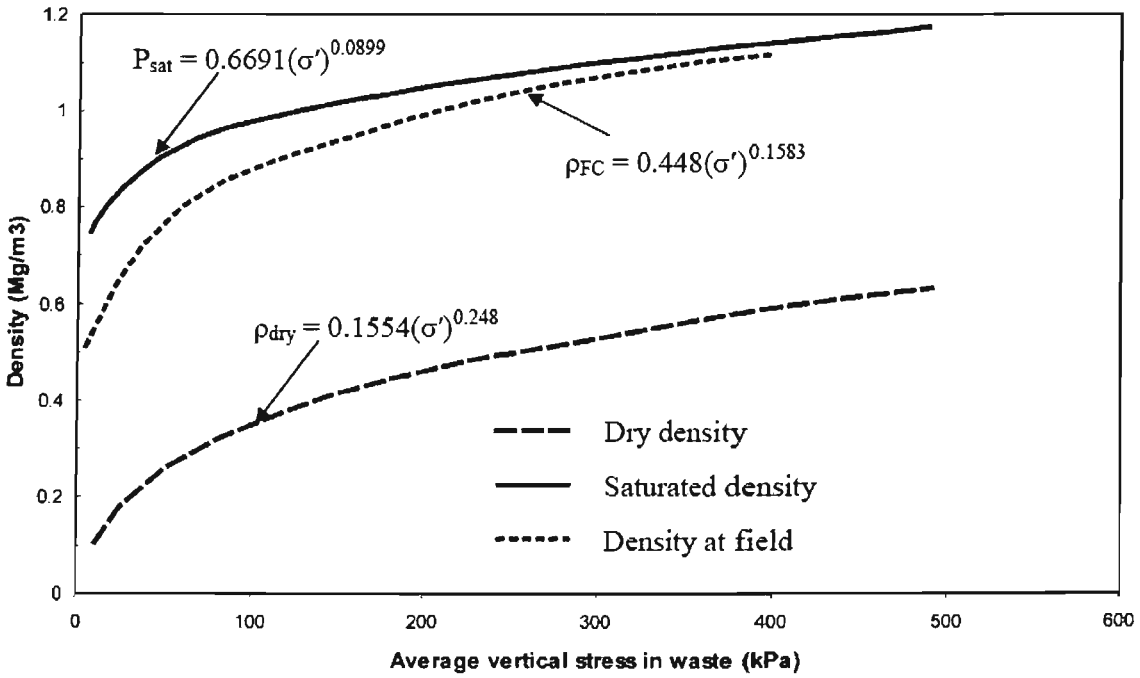

Figure 4.27. Relationships between density and average vertical stress. Trend lines shown are based on average measured values (after Powrie and Beaven, 1999).

a)

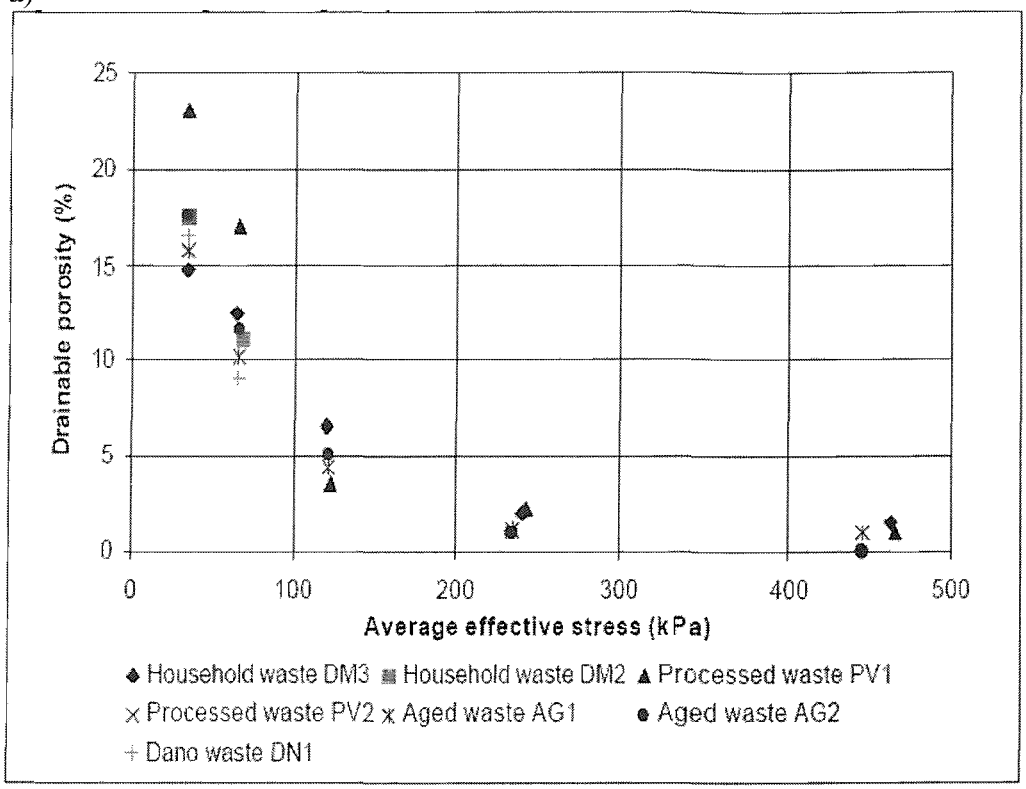

b)

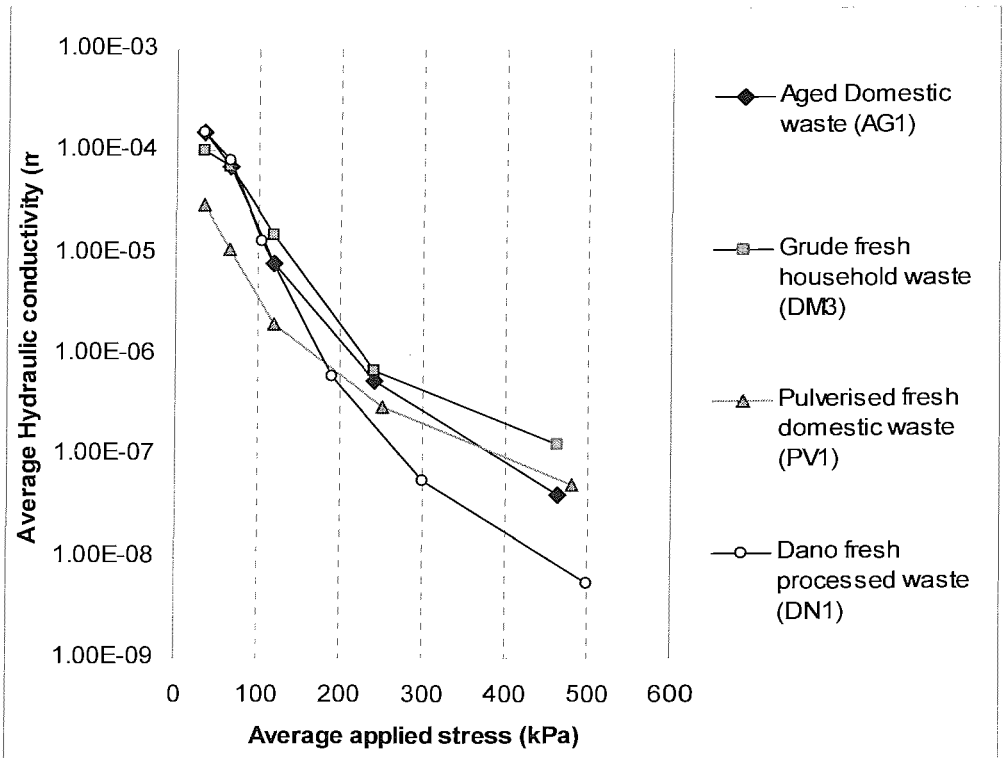

Figure 4.28. a) Relationship between average vertical effective stress and average drainable porosity (data from Powrie *et al.*, 2000); b) Vertical hydraulic conductivity against the logarithm of the vertical effective stress in first loading (data from Beaven, 2000 and Hudson *et al.*, 2001).

Chapter 5

Materials and methods

This chapter describes the characteristics of the waste samples used and its associated chemical and physical properties. The design and operation of the experimental reactors and the analytical techniques used are also reviewed.

5.1. Pre-test sample preparation procedure

In this study, a detailed characterization of two types of MSW was undertaken, waste AG – aged waste and waste FR – fresh waste. The wastes were obtained from different landfill sites as indicated in Table 5.1. Following the recovery of non-degraded newspapers and food packaging the approximate age of the AG waste was found to be approximately 15 years. Characterisation of the solid fraction of the AG sample indicated extensive degradation of the available organic matter. However, some components in the waste were substantially unaffected by degradation, possibly due to reduced moisture content.

The most common method for characterizing a waste is to separate the waste into a number of different components and determine the percentage of each component by dry weight. This process was done under cover at White's landfill facility and the results of the sorting analysis for the AG and FR samples are presented in Table 5.2. The large particles (> 40mm) of each sample were shredded using a commercial shredder and then sieved to carry out a particle size distribution (PSD) analysis, using the wet sieving method for fine equivalent soils, utilizing "standard set"of 13 sieves (BS 1377:1975) and the cone-and-quarter method for homogenization of the original sample (Table 5.3). A maximum shredded particle size of 40mm was adopted from Beaven & Powrie (1995). A representative test sample was then prepared by re-constituting the components together in their original proportions (Table 5.2). It was found that 90.6% of the shredded AG

waste sample and 96.6% of the shredded FR waste sample passed through the 37.5mm sieve (Figure 5.1 & Figure 5.2).

Table 5.1. Types of waste tested.

Waste reference	Waste Description
AG	Aged MSW sample obtained from the Rainham Landfill facility, Essex, UK (total dry weight of 128 kg).
FR	Fresh MSW sample obtained from the White's Pit Landfill facility, Dorset, UK (total dry weight of 190 kg).

Table 5.2. Breakdown of waste composition for AG and FR waste samples.

Component	AG sample		FR sample	
	Dry weight, kg	% by dry weight	Dry weight, kg	% by dry weight
Paper	12.31	9.60	52.00	27.34
Light plastic	12.59	9.82	19.32	10.16
Heavy plastic	8.78	6.85	18.78	9.87
Wood	4.85	3.78	6.06	3.19
Yard waste	n/a[1]	n/a[1]	35.00	18.40
Food	n/a[1]	n/a[1]	4.31	2.27
Textile	3.05	2.38	5.86	3.08
Combustible[2]	1.89	1.47	5.63	2.96
Metal	2.28	1.78	12.90	6.78
Glass	4.68	3.65	5.00	2.63
Others<10mm	77.75	60.66	25.33	13.32
Total	**128.17**	**100.00**	**190.19**	**100.00**

Note: [1] n/a = not applicable; [2] Combustible fraction of the waste includes leather, rubber, wipes, and disposable nappies.

A 100 g representative sample was prepared that contained the same proportions of the component composition as the original sample derived from the landfill site (Table 5.2). Plastics and non-grindable components (metal and glass) (AG sample - 22.10g, FR sample - 29.44g) were removed. The remaining components (AG sample - 77.90g, FR sample - 70.56g) were ground to a fine powder and analysed for lignin, cellulose, and hemicellulose (see details in section 5.5.10).

Table 5.3. Particle size distribution of processed waste.

Sieve size mm	AG sample			FR sample		
	Mass retained, g	Cumulative mass passing, g	% passing	Mass retained, g	Cumulative mass passing, g	% passing
75.000	0	705	100.0	0	0	0
63.000	9	696	98.7	0	880	100.0
37.500	58	638	90.5	30	850	96.6
20.000	105	533	75.6	272	578	65.7
10.000	132	401	56.9	215	363	41.2
6.300	81	320	45.4	71	292	33.2
3.350	73	247	35.0	66	226	25.7
2.000	40	207	29.4	42	184	20.9
1.180	37	170	24.1	36	148	16.8
0.600	42	128	18.2	38	110	12.5
0.300	46	82	11.6	38	72	8.2
0.150	36	46	6.5	32	40	4.5
0.063	41	5	0.7	33	7	0.8
pass	5	0	-	7	0	-

Table 5.4. Analysis of solid waste components.

Chemical analysis	AG sample		FR sample	
	Concentration (by dry mass analysed)	Concentration (by dry mass) in waste	Concentration (by dry mass analysed)	Concentration (by dry mass) in waste
Cellulose [1], %	6.34	4.94	35.25	24.87
Hemicellulose [1],%	0.97	0.76	9.45	6.67
Lignin [1], %	11.72	9.13	13.77	9.72
(C+H)/L ratio	0.62	0.62	3.24	3.24
TC [2], %	33.50	31.68	50.84	46.05
TN [2], %	0.63	0.59	1.05	0.95
LOI [2], %	54.02	51.09	85.89	77.80

Note: [1] Corrected for plastics and non-grindable components; [2] Corrected for non-grindable components.

For Total Carbon (TC), Total Nitrogen (TN) and Loss on Ignition (LOI) analyses, another representative sample was prepared in the same way as previously described. All non-grindables components (metal and glass) (AG sample 5.43g, FR sample - 9.41g) were removed from the sample, and then the remaining components (AG sample 94.57g, FR sample - 90.59g) were analysed for TC, TN, and LOI. Results are presented in Table 5.4.

5.2. BMP test assays

5.2.1. Introduction

To assess the gas potential of a solid waste it is necessary to determine the degradable fraction of the total carbon (TC) content. A Biochemical Methane Potential (BMP) test is often used for this purpose (Bogner, 1990; ASTM, 1992). The BMP assay is a procedure developed to determine the methane yield of an organic material during its anaerobic degradation by a mixed microbial flora in a defined medium. Several techniques exist for measuring the BMP of solid waste, although all generally involve the incubation of a small representative waste sample under controlled anaerobic conditions (usually mesophilic at 30°C). Methane generation is assessed by measurement of biogas production and biogas composition and this may continue for a long period of time. However, the precise procedures vary significantly among the published methods (Wang *et al.*, 1994; Eleazer *et al.*, 1997; Hansen *et al.*, 2004). The main differences in the methodologies relate to the pre-treatment procedures, gas measurement techniques and the duration of the test.

5.2.2. Waste samples tested

A subsample was taken from the original prepared sample and its individual components separated as previously described. The particle size of each of the constituents was further reduced to a maximum size of 10mm in diameter. The materials were then re-constituted to produce a waste sample that contained the same component composition (% w/w) as the original sample derived from the landfill site (Table 5.2).

A representative sample of the waste was then used to fill 1-litre reactors (HDPE, Nalgene Ltd) in order to simulate waste degradation under controlled anaerobic conditions (BMP test). The homogenization of the waste was important, given the scale of the test, to ensure representative sampling and reproducibility of the samples.

5.2.3. Mineral medium and inoculum

In order to accelerate the degradation of the waste by anaerobic bacteria, the addition of a laboratory prepared media containing mineral-nutrients (N, P, and S) and trace elements were used in these experiments. The inorganic macro-nutrients used in the medium are given in Table 5.5 and are the same as described by Florencio *et al.* (1995). The final pH

of the media was adjusted to pH 7.83 by adding a few drops (< 5ml/litre) of 2M NaOH. To ensure the presence of a viable methanogenic bacteria anaerobically digested sewage sludge, derived from an anaerobic digester at Millbrook Sewage Works (Southern Water, UK) was added to the medium. The waste samples were operated under fully saturated conditions to promote rapid stabilization.

Table 5.5. Recipe of a laboratory prepared media.

Reagent	Concentration, mg/l	Reagent	Concentration, mg/l
$K_2HPO_4.3H_2O$	330.000	NH_4Cl	280.000
$MgSO_4.7H_2O$	100.000	$CaCl_2.2H_2O$	10.000
$FeCl_2.4H_2O$	2.000	H_3BO_3	0.050
$ZnCl_2$	0.050	$MnCl_2.4H_2O$	0.500
$CuCl_2.2H_2O$	0.038	$(NH_4)6MoO_{24}.4H_2O$	0.050
$AlCl_3.6H_2O$	0.090	$NiCl_2.6H_2O$	0.142
$Na_2SeO_3.5H_2O$	0.164	$CoCl_2.6H_2O$	2.000
EDTA	1.000		

5.2.4. Experimental procedure

A series of three separate BMP test assays were carried out in this study. The first experiment was undertaken to determine the optimum sewage seed addition required to ensure rapid anaerobic degradation. In the second and third BMP experimental tests, successive BMP bottles were dismantled at various stages of the biodegradative process to allow the waste sample to be analysed for total carbon (TC) to facilitate the calculation of a C mass balance. The BMP apparatus is shown in Figure 5.3.

BMP test 1 was carried out in six plastic bottles (HDPE, Nalgene Ltd.) each with a capacity of 1000 ml. Four of the bottles were filled with AG waste, mineral media as previously described (section 5.2.3) and sewage sludge as outlined in Table 5.6, giving a total liquid volume of 500 ml. The mineral media had previously been sparged with N_2 to remove all traces of oxygen and had a pH value of 7.8. Two blanks were also prepared with medium and inoculum only to measure the biogas originating from the sewage sludge alone. The bottles were then sealed under a nitrogen atmosphere. No mechanical mixing of the waste took place during the test. The bottles were incubated in a water bath at 30°C to promote mesophilic methanogenic conditions. Biogas production was measured by collecting the gas produced from each bottle in an inverted glass burette containing water which was acidified with hydrochloric acid, to a pH value of 2.0, to prevent CO_2 dissolution. The measured volume of the biogas produced was corrected to

dry gas at standard temperature and pressure (STP) using the ambient temperature and pressure measurements and values of water *vapour pressure*. Standard temperature is defined as zero degrees Celsius (0°C), which translates to 273.2 degrees Kelvin (273.2°K). Standard pressure supports 760mm in a mercurial barometer (760 mmHg = 101.3kPa = 1013mBar = 1atm). The term *vapor pressure* was used to mean the partial pressure of water vapour in the atmosphere and it was calculated from the ambient temperature using Eq. 5.1 (Buck, 1981).

Eq. 5.1. $$p_w = 0.61121e^{[17.502T/(240.97+T)]}$$

where p_w is the water vapor pressure in kPa and T is the ambient temperature in °C.

Table 5.6. Nutrient addition for BMP test 1 (AG waste sample).

BMP test 1	Test duration, days	Mineral media, ml	Anaerobic digester sludge		Waste dry weight, g
			ml	% vol.	
B1	340	450	50	10	140
B2	340	450	50	10	140
B3	340	400	100	20	140
B4	340	400	100	20	140
B5-blank	340	400	100	20	-
B6-blank	340	450	50	10	-

Biogas is expected to be saturated with water vapor produced during the anaerobic decomposition of MSW. This produces about 22ml water per each litre of biogas when passing through a temperature differential of about 22°C (the average reference temperature measured in the laboratory during the operation of CAR1).

All biogas readings were standardised to dry gas at STP using the following equation:

Eq. 5.2. $$R = R_o \frac{p_a}{101.3} \times \frac{273.2}{273.2+T} \times \left(1 - \frac{p_w}{p_a}\right)$$

where R is the corrected reading, R_o is the uncorrected reading, 101.3 is the atmospheric pressure at sea level in kPa, p_a is the measured atmospheric pressure in the laboratory in kPa, 273.2 is the absolute zero temperature in Kelvin, T is the reference temperature in the laboratory in °C, and p_w is water vapor pressure in kPa (Eq. 5.1).

The procedure used to fill the reactors in the first BMP test assay was repeated in BMP tests 2 & 3. In BMP Test 2, three bottles were filled with AG waste, mineral media and

anaerobically digested sewage sludge and another bottle was used as a blank (Table 5.7). In the third BMB Test (Figure 5.4) twelve test bottles were filled with FR sample and a further two bottles were used as blank (Table 5.8).

Table 5.7. Nutrient addition for BMP test 2 (AG waste sample).

BMP test 2	Test duration, days	Mineral media, ml	Anaerobic digester sludge		Waste dry weight, g
			ml	% vol.	
B7	68	450	50	10	140
B8	196	450	50	10	140
B9	338	450	50	10	140
B10-blank	338	450	50	10	-

Table 5.8. Nutrient addition for BMP test 3 (FR waste sample).

BMP test 3	Test duration, days	Mineral media, ml	Anaerobic digester sludge		Waste dry weight, g
			ml	% vol.	
B11	8	630	70	10	100
B12	19	630	70	10	100
B13	51	630	70	10	100
B14	116	630	70	10	100
B15	135	630	70	10	100
B16	162	630	70	10	100
B17	217	630	70	10	100
B18	280	630	70	10	100
B19	348	630	70	10	100
B20	539	630	70	10	100
B21	720	630	70	10	100
B22	919	630	70	10	100
B23-blank	162	630	70	10	-
B24-blank	919	630	70	10	-

Based on the gas production rates, the BMP reactors of Test 2 & 3 were sequentially sacrificed at various times during the test to observe compositional changes at different stages of degradation with respect to time of incubation. Leachate samples were taken from each bottle at the end of the test and analysed for total organic carbon (TOC), inorganic carbon (IC), dissolved organic carbon (DOC), volatile fatty acids (VFAs) and various cations and anions. Samples of gas were taken from each BMP test bottle at various intervals and analysed for CH_4 and CO_2 using gas chromatography. The degree of biodegradation in each reactor was further assessed by comparing the cumulative

methane production with the data from TC, Neutral Detergent Fibre (NDF), Acid Detergent Fibre (ADF) and Acid Digestible Lignin (ADL) determinations for the waste remaining in the bioreactors (see details in section 5.5.10). The duration of each BMP test before sampling is outlined in Table 5.7 and Table 5.8.

5.2.5. BMP test 1

This test was undertaken in order to provide a guideline for the optimum sewage seed addition to be applied in all further CAR tests. Biogas production in the BMP tests 1 was observed for 340 days (Figure 5.5). The most active vessels in terms of gas production were bottles 1 and 2 where 4.30 and 3.61 litres gas/kg dry wt. waste, respectively were produced (Table 5.9). Gas production in the tests supplemented with a 10% digester sludge seed allowed anaerobic methanogenic conditions to become quickly established leading to waste degradation and gas production. Indeed it was able to do this faster than that observed with a 20% seed (bottles B3 and B4), although the reasons for this need to be further evaluated.

Table 5.9. Cumulative gas production at standard temperature and pressure (STP) for BMP1 bottles (litres / kg dry matter (DM)).

10% sludge addition			20% sludge addition		
B1	B2	B6 - blank	B3	B4	B5 - blank
4.30	3.61	0.11	0.51	1.42	0.40
Experiment duration - 340 days					

The results from BMP test 1 highlighted the fact that the development of a methanogenic biodegradation potential in the waste material could be hastened utilising a 10% inoculum of anaerobic digester sludge in the liquid medium applied to the waste. This finding was then applied to a subsequent experiment with Consolidating Anaerobic Reactor 1 (CAR1).

5.3. Compression tests

5.3.1. Design of Consolidating Anaerobic Reactors (CARs)

The main laboratory tests forming this study were carried out in four purpose built Consolidating Anaerobic Reactors (CARs) (Figure 5.6) designed and constructed to allow a representative overburden to be applied to an element of waste. The reactors

comprised two main elements: a Perspex cylinder to house the waste and a load delivery system that can apply a constant surcharge to the waste. The Perspex cylinder had a wall thickness of 6mm, and an internal diameter of 480mm, and was approximately 900mm in height. A load could be applied on the waste mass through a system comprising a hydraulic cylinder and a load platen. The hydraulic pressure supplied to the cylinder was controlled through a central controller and displayed the current applied stress. A constant load could be maintained by means of a feedback load cell placed between the cylinder and the platen and this relayed the applied stress data back to a signal amplifier on the control panel. A perforated steel (Grade 316) load platen rests on the top of the waste to allow leachate to pass through the waste column and through which a vertical constant load could be applied via a 65mm hydraulic cylinder. In this system a maximum vertical load of 27 kN was allowed to be applied to the surface of the waste sample. Assuming a uniform distribution of vertical load over the cross sectional area of the waste, this would be equivalent to an applied stress of 150kPa. Taking the bulk unit weight of a landfill as approximately $10kN/m^3$, the CARs were capable of simulating loads which correspond to a 15m waste overburden.

Leachate inlet and gas outlet ports were incorporated into each cell as shown in Figure 5.6. Two further inlets situated at the bottom of each cell were used to introduce liquid and nitrogen gas (N_2) into the cells at the beginning of the experiment. Leachate was periodically recirculated from the bottom to the top of each CAR using a peristaltic pump. During the recirculatory periods the leachate flow rate through the CARs was maintained at 17.2 l/h using a Watson Marlow pump (model 505S equipped with a 304MC pump head and 1.65mm bore marprene tube). The remainder of the tubing used for leachate recirculation and gas removal was polyvinyl chloride (PVC).

A viewing window along the entire height of the cell allowed visual observations of the refuse to be made throughout the settlement and degradation processes. The CARs were situated in a temperature-controlled room, at a temperature of 22-23°C. pH and redox potential measurements were taken by using pH and redox probes placed in a flow-through cell (Waterra, UK Ltd.) located adjacent to the loading frame. The temperature within the waste, pH and redox potential (Eh) were continuously monitored using a Campbell CR1OX data logging system.

A novel technique for measuring the volume of biogas produced was developed for use with the cells. Biogas is allowed to build up in the headspace of the cell to a small positive pressure above ambient (Δp) following which the biogas is then vented

automatically to the atmosphere via a solenoid valve. The solenoid valve is operated by the data logging system in response to the limiting pressure of Δp being measured and the data logging system records each time the valve is activated. The volume of gas that must be generated (V_g) to activate the pressure release valve is calculated using the Boyle-Marriott Law.

Eq. 5.3 $$p_1 V_1 = p_a V_a \quad \text{with} \quad p_1 = p_a + \Delta p$$

Eq. 5.4 $$V_g = V_a - V_1$$

Where p_a is the atmospheric pressure in kPa; V_a is the volume of the gas at atmospheric pressure; p_1 is the pressure build up (kPa); Δp is the limiting increase in the pressure, which has values of 0.1kPa (AG waste sample) and 1.0kPa (FR waste sample); V_1 is the volume of the gas at pressure p_1; and Vg is the volume of the biogas generated.

Since the total biogas produced in the CARs depends on the temperature, pressure and water vapour pressure variations, it was essential to normalize all readings of biogas production to dry gas at STP (see section 5.2.4). This was done using Eq. 5.1.

5.3.2. Operational procedure

The standard test methodology used to prepare the two waste samples (AG and FR waste) for the compression tests are presented below. In all cases the general procedure followed in setting up each CAR was as follows:

1. A gravel drainage layer (15 to 20mm) was placed in the base of each CAR to prevent clogging. Prior to loading, the gravel was washed with distilled water to remove fines and oven dried at 105°C to a constant weight.
2. A geotextile membrane (PP squared mesh 5mm/5mm) was placed on the top of the gravel layer to separate the waste from the gravel surface.
3. Representative samples of waste (section 5.1) were oven dried at 70°C to a constant weight and then loosely placed into each cell. Further layers of waste were loaded and compressed until a waste height of approximately 0.80m was achieved.
4. A geotextile membrane was placed on the top of waste.

5. A drainage layer of washed and dried gravel (15 to 20mm) was placed on top of the geotextile.
6. The CAR was placed within a compression rig and then completely sealed with appropriate valves for gas and leachate handling.
7. The waste in the cell was sparged with N_2 to remove any oxygen trapped within the cell during the filling period.
8. The waste in each CAR was fully saturated with the laboratory prepared mineral media previously described containing 10% v/v anaerobically digested sewage sludge (section 5.2.3) to accelerate the initiation of methanogenic waste degradation in each CAR. The media was introduced into each reactor from the inlet situated at the bottom of each cell using a Watson Marlow pump. The volume of the media within the waste was recorded.
9. The waste and the media were then sparged with N_2 from the bottom up, to remove any trace of oxygen.
10. The platen was lowered onto the gravel and then an initial load was applied through the hydraulic system.
11. After 24 hours measurements of waste depth and leachate depth were taken.
12. Leachate was intermittently recirculated through the column. During this time it is to be expected that a certain amount of mechanical mixing of leachate was occurring in the cells.

Four separate consolidating cells were constructed for the study to simulate varying depths within the waste. However, in the first stage of the experiment, only one reactor (CAR1) was initiated for use. This reactor was filled with 56 kg (dry weight) of shredded aged MSW (AG waste sample). A stress of approximately 50kPa was applied to the waste, which corresponds to a 4-5 m layer of refuse overlying the waste element. Waste settlement in the first CAR was measured using a scale fixed to the cell. The addition of 90 litres of mineral media/sewage sludge to the waste resulted in an *initial* settlement of approximately 2.9% under no applied load. 24 hours after loading, the waste settled 22.1% of the initial height, which is thought to be due to a lack of adequate initial compaction of the waste during the sample preparation stage (section 5.3.2) and was considered to be the end of *primary* compression phase. A picture of CAR1 is shown in Figure 5.7 and the start-up conditions of CAR1 are given in Table 5.10.

In the second stage of the experiment another three large scale consolidating anaerobic reactors (CAR2, CAR3 & CAR4) containing 27 kg of shredded fresh MSW (FR waste sample) were assembled. 3 x 90 litres of synthetic leachate prepared in the laboratory containing 10% v/v anaerobically digested sewage sludge were added to the waste sample to accelerate the initiation of methanogenic waste degradation in each cell. It was considered that the waste sample should be fully saturated to promote rapid stabilization. CAR2 and CAR3 were used as test cells. The third consolidating cell (CAR4) is an interesting and unique control reactor which is distinguished from a normal test reactor by the fact that the leachate was acidified initially, by adding a mixture of acetic and propionic acid at a concentration of 10 g/litre each with a final media pH = 3.8, and at day 289 by adding propionic acid only at a concentration of 9 g/litre, to inhibit and ultimately prevent the onset of methanogenesis. The toxic effects of the VFAs when they are present at these high concentrations towards methanogens has been well documented (Angelidaki *et al.,* 1993). This effect was used here to inhibit methane formation in the control cell.

In order to model landfill settlement, a constant load was applied to the reactors according to Table 5.10. CAR2 was subjected to a stress of 150kPa, which corresponds to a 14-15 m layer of refuse overlying the waste element. CAR3 and the control cell (CAR4) were subjected to an initial compression of 50kPa, which is representative of a burial depth of 4-5m. The compression of the waste was monitored as a function of time by measuring the downward movements of the loading platen. The *primary* compression was considered to occur immediately on application of the load due to a lack of adequate compaction of the waste and resulted in a settlement of 48.7% for CAR2, 33.4% for CAR3 and 37.4% for CAR4 (the control). The laboratory cells are shown in Figure 5.8 & Figure 5.9 and the process of FR sample initial preparation is shown in Figure 5.10.

It should be noted that in this study, the settlement observed in the CARs during filling and loading was considered to be caused by initial and primary compression of the waste due to a lack of adequate compaction during the sample preparation stage, and was not included into the total settlement determination.

Table 5.10. Test methodology and start-up conditions of CARs.

No	Description	CAR 1 AG sample	CAR 2 FR sample	CAR 3 FR sample	CAR 4 FR sample
1	A gravel drainage layer (15mm to 20mm) was placed in the base of each CAR to prevent clogging.				
	Depth	5.0 cm	5.0 cm	5.0 cm	5.0 cm
	Volume	9.0 litres	9.0 litres	9.0 litres	9.0 litres
	Drainable pore space (measured)	3.5 litres	3.5 litres	3.5 litres	3.5 litres
2	A geotextile membrane (PP squared mesh 5mm/5mm) was placed on the top of the gravel layer to separate the waste from the gravel surface.	Yes	Yes	Yes	Yes
3	Representative samples of waste (section 5.1) were then loosely placed into each cell. Further layers of waste were loaded and compressed until a waste height of approximately 0.80m was achieved.				
	Dry mass	56.2 kg	27.0 kg	27.0 kg	27.0 kg
4	A geotextile membrane was placed on the top of waste	Yes	Yes	Yes	Yes
5	A drainage layer of washed and dried gravel (15mm to 20mm) was placed on top of the geotextile.				
	Depth	9.8 cm	9.5 cm	9.0 cm	10.0 cm
	Volume	17.7 litres	17.2 litres	16.3 litres	18.1 litres
	Drainable pore space (measured)	8.8 litres	8.5 litres	8.0 litres	8.9 litres
6	The CAR was placed within a compression rig and then completely sealed with appropriate valves for gas and leachate handling.	Yes	Yes	Yes	Yes
7	The waste in the cell was sparged with N_2 to remove any oxygen trapped within the cell during the filling period.	Yes	Yes	Yes	Yes
8	The waste in each CAR was fully saturated with the laboratory prepared mineral media previously described containing 10% anaerobically digested sewage sludge (section 5.2.3).				

No	Description	CAR 1 AG sample	CAR 2 FR sample	CAR 3 FR sample	CAR 4 FR sample
	The media was introduced into each reactor from the inlet situated at the bottom of each cell using a Watson Marlow pump. The volume of the media within the waste was recorded.				
	Volume added	90.0 litres	90.0 litres	90.0 litres	90.0 litres
9	The waste and the media were then sparged with N_2 from the bottom up, to remove any trace of oxygen.	Yes	Yes	Yes	Yes
10	The platen was lowered onto the gravel and then an initial load was applied through the hydraulic system.				
	Applied stress	50 kPa	150 kPa	50 kPa	50 kPa
11	After 24 hours the following measurements were taken:				
	Waste depth	0.62 metres	0.34 metres	0.42 metres	0.40 metres
	Waste dry density (calculated)	0.497 t/m^3	0.437 t/m^3	0.357 t/m^3	0.343 t/m^3
	Depth of leachate pond (measured)	0.17 metres	0.29 metres	0.25 metres	0.27 metres
	Volume of leachate pond (calculated)	30.76 litres	52.48 litres	45.24 litres	48.86 litres
12	Leachate was intermittently recirculated through the column. During this time, it is to be expected that a certain amount of mechanical mixing of leachate was occurring in the cells.				
	Recirculation rate (when in use)	17.2 litres/hr	17.2 litres/hr	17.2 litres/hr	17.2 litres/hr
13	The CARs were operated and monitored for:	338 days	919 days	919 days	919 days

5.3.3. *Monitoring parameters*

In an attempt to establish a better understanding of the degradation process and its effect on waste settlement, it was necessary to determine a range of parameters in which to operate laboratory scale test cells to record data on the degradation process. In brief, the experimental system comprised control measurement process parameters that included:

1. The measurement of magnitude of vertical applied stress imposed by the load delivery system.
2. A gas vent system which controlled the maximum pressure increase allowed prior to venting to the atmosphere via a solenoid valve.
3. Recording the headspace gas pressure in the cell that was allowed to build up to a small positive pressure above ambient (Δp) following which the biogas is then vented automatically to the atmosphere via the gas vent system.
4. Monitoring of the settlement of the waste as a function of time by recording the downward movements of the loading platen under constant load in each CAR.
5. Manual measurements of the depth (and hence volume) of the leachate pond above the top platen to establish headspace volume.
6. Waste temperature.
7. Room temperature.
8. Atmospheric pressure.
9. pH and Redox potential (Eh) in the recirculated leachate.
10. Biogas composition - samples of gas were taken from the CARs and analysed of CH_4 and CO_2 in the biogas (using gas chromatography) at selected frequencies (Table 5.11).
11. Leachate composition - leachate samples were collected from the CARs at intervals given in Table 5.12 and analysed for

    - inorganic carbon (IC);
    - total organic carbon (TOC);
    - dissolved organic carbon (DOC);
    - volatile fatty acids (VFAs);
    - heavy metals; and

- major cations and anions.

Table 5.11. Frequency of gas analyses.

CAR Reference	Months into experiment	Gas sampling frequency
CAR1(AG waste sample)	0-3	every 3rd week
	4-9	every 2nd week
	9-11	every 3rd week
CAR2, CAR3 & CAR4 (FR waste sample)	0-3	every 2nd day
	4-6	every 2nd week
	7-16	every 4th week
	17-30	every 6th week

Table 5.12. Frequency of leachate analyses.

CAR Reference	Months into experiment	Leachate sampling frequency
CAR1(AG waste sample)	0-3	every day
	4-6	every 2nd day
	7-9	every 4th day
	9-11	every week
CAR2, CAR3 & CAR4 (FR waste sample)	0-3	every day
	4-6	every week
	7-16	every 2nd week
	17-30	every 5th week

There are a number of externally controlled factors that have an impact on the degradation (e.g., temperature within the waste, recirculation events) and settlement (applied stress) of waste within the CARs. Figure 5.11 & Figure 5.12 show the logged applied stress for each cell and demonstrates that the stress was maintained very consistently over the duration of the experiment for the CARs filled with FR waste sample and not very consistently for CAR1. Figure 5.13 & Figure 5.14 show the monitored temperature of each CAR.

In order to accelerate the initiation of methanogenic waste degradation the temperature in each CAR was increased using a heated blanket, with heat losses controlled by an insulation blanket. The temperature in CAR1 was increased from 21°C to approximately 35°C from day 65 of the experiment. CAR2 and CAR3 operated at an approximately constant temperature (between 28 and 32°C) over the whole duration of the experiment. The temperature in CAR4 (control) was maintained in the same range as in CAR2 & CAR3 for the first 284 days of the experiment and thereafter was decreased to approximately 21°C in order to inhibit waste degradation. The data points on the four graphs that fall outside the general trend lines were caused by data logger failures and do

not represent rapid changes in the operating conditions. Figure 5.15 & Figure 5.16 provide details on cumulative leachate recirculation volumes. The operational procedure for leachate recirculation is detailed in Table 5.13.

Table 5.13. Leachate recirculation events.

CAR Reference	Months into experiment	Recirculation event	Average rate, litres/day
CAR1 (AG waste sample)	0-3	every day	30.43
	4-6	every 2nd day	24.84
	7-9	every 4th day	9.38
	9-11	Every week	5.10
CAR2, CAR3 & CAR4 (FR waste sample)	0-3	every day	36.18
	4-6	Every week	5.02
	7-16	every 2nd week	2.31
	17-30	every 5th week	0.94

5.4. Post test sample preparation procedure

Prior to analysis, the waste samples were pre-treated according to the following procedure, summarised in Figure 5.17.

1. The degraded wet sample containing biomass was oven dried at 70°C to a constant weight.
2. The dried sample was then washed with distilled water through a 2mm sieve until the washings were clear so as to remove any attached biomass.
3. The washings were analysed for IC, TC, total solids (TS), volatile solids (VS) and loss on ignition (LOI)(section 5.5.8).
4. The washed samples were then oven dried at 70°C to a constant weight.
5. The dried samples were then divided into three further subsamples for subsequent analyses.
6. Metal and glass were separated from the subsamples which underwent TC and LOI analyses.
7. Metal, glass and plastics were separated from the subsamples which were subjected to fibre analyses (section 5.5.10).

5.5. Analytical measurements

5.5.1. Carbon analysis

A high-temperature total carbon analyser (Dohrman Rosemount DC-190, USA) was used to measure the leachate total carbon (TC). The equipment contains a vertical quartz combustion tube packed with cobalt catalyst. Air flows through it at a rate of 200 ml/min. The furnace was operated at 800°C. The boat sampling mode was utilised due to the high concentrations of suspended solids in the samples. The samples were analysed twice and the average value taken.

The rate of removal of the TOC in the leachate was determined by measuring concentration changes in 5 ml samples collected at different stages of the biodegradative process. The samples were immediately preserved by the addition of 50 µl of 100% hydrochloric acid and stored in plastic vials in refrigerator at 4°C for up to a month (Banfield *et al.*, 1978). The acid addition caused IC to be removed from the samples thus giving the TOC (TOC = TC - IC).

At the same time, another 5ml leachate samples were collected and filtered though a filter made of special glass microfibres (MF 200, Fisher Scientific), thus giving the total dissolved organic content of the samples (TDOC). These samples were immediately preserved and stored in the same way as the TOC samples. Again there was a removal of IC by the addition of the acid.

The equipment utilised a single point calibration which was carried out each time prior to an analysis. Only one standard was required which was prepared by using Glycine at a concentration level dependent on the concentration range of the samples.

5.5.2. VFA analysis

VFAs concentrations in the leachate were determined by measuring concentration changes in 1 ml leachate samples collected from each cell throughout the experiment. The samples were immediately preserved by the addition of 100 µl of 100% formic acid and stored in plastic vials in a refrigerator at 4°C for up to a month prior to analysis (Banfield *et al.*, 1978).

Concentrations of the leachate VFAs were determined by gas chromatography (GC) using a Varian 3400CX Gas Chromatograph with a flame ionisation detection (FID) in

conjunction with an SGE BP21 megabore analytical column (25m × 0.53mm i.d., film thickness 0.5mm, SGE Ltd.) according to standard procedures (Banfield *et al.*, 1978).

A calibration procedure was carried out prior to each analysis using a mixture of VFA (acetic, propionic, iso and n-butyric, iso- and n- valeric, n-caproic and caprylic acids, shown in order of elution) with concentration levels of 50mg/l, 100mg/l, 250mg/l and 500mg/l. The results showed a linear correlation for each of the standards in question. An example of calibration curves is shown in Figure 5.18.

5.5.3. *Anion analysis (Cl^-, NO_2^-, NO_3^-, PO_4^{3-}, SO_4^{2-})*

5 ml sample volumes were collected from each CAR, filtered though a filter made of special glass microfibres (MF 200, Fisher Scientific) and immediately frozen.

Anion analysis was carried out using a Dionex-500 ion chromatograph using an AS9 anion column in conjunction with an ASRS-1 anion suppressor (Dionex Ltd.). 25µl volume injections were applied to the column using a Dionex AS40 autosampler, incorporating a rheodyne injection valve. Detection was by a Dionex ED-40 electrochemical detector operating in conductivity mode. The eluent consisted of 8mM sodium carbonate and 1mM sodium bicarbonate pumped at a flow rate of 1.0 ml/min.

A calibration procedure was carried out prior to each analysis using a mixture of *NaCl*, $NaNO_2$, KNO_3, KH_2PO_4, and $MgSO_4.7H_2O$ with concentration levels of 100, 200, 400, 600, 800, 1000 µM. The results showed a linear correlation for each of the anions in question. An example of the calibration curves is shown in Figure 5.19.

5.5.4. *Cation analysis (Na^+, NH^{4+}, K^+, Mg^{2+}, Ca^{2+})*

5 ml sample volumes were collected from each CAR, preserved by the addition of 20 µl of 100% methanesulfonic acid (MSA) and then immediately frozen. Prior to analysis the samples were unfrozen and then filtered though filters made of special glass microfibres (MF 200, Fisher Scientific).

Cation analysis was carried out using a Dionex-500 ion chromatograph using a CS12A cation column in conjunction with a CSRS-II cation suppressor (Dionex Ltd.). The mobile phase was 20mM methanesulphonic acid pumped at a rate of 1.0 ml/min.

A calibration procedure was carried out using a mixture of $NaCl$, NH_4NO_3, KH_2PO_4, $MgSO_4.7H_2O$, and $CaCl_2.2H_2O$ with concentration levels of 100, 200, 400, 600, 800, 1000 μM. The results showed a linear correlation for each of the cations in question. An example of the calibration curves is shown in Figure 5.20.

5.5.5. *ICPMS analysis*

20 ml unfiltered leachate sample volumes were collected at different stages of the biodegradative process and acidified with 2% HNO_3 (Aristar, VWR). 10 ml of each sample was then filtered through a filter made of special glass microfibres (MF 200, Fisher Scientific) and analysed for Al^{3+}, Co^{2+}, Ni^{2+}, Cu^{2+}, Zn^{2+}, $Mo^{?}$, Cd^{2+} and Pb^{2+} at the National Oceanography Centre (NOC), University of Southampton on a VG Elemental PlasmaQuad PQ2+ ICP-MS. The ICP-MS analysis was also carried out on the remaining 10ml of each unfiltered leachate sample which had been previously digested using Microwave Accelerated Reaction System (MARS5) following method EPA 3051A (1998) developed by the Environmental Protection Agency, USA for a closed vessel (XP-1500 Plus).

5.5.6. *Iron analysis*

10 ml unfiltered leachate sample volumes were collected at different stages of the biodegradative process and acidified with 2% HNO_3 (Aristar, VWR). 5 ml of each sample was filtered through a filter made of special glass microfibres (MF 200, Fisher Scientific) and analysed for total iron (Fe^{2+} and Fe^{3+}) using an Atomic Absorption Spectrophotometer (Spectr AA-200, Varian, Australia). A hollow-cathode lamp for analysing Fe^{2+}/Fe^{3+} was used (S. & J. Juniper & Co, Essex, UK) at a wavelength of 248.3 and a slit width of 0.2mm. The lamp current was 5mA. The sample was burnt in an acetylene/air flame where the air flow rate was 13.50 litres/min and the acetylene 2.0 litres/min.

A calibration procedure was carried out using iron solution (1000 ppm in 1M nitric acid, Fisher Scientific) as a standard. A linear correlation was obtained for standard solutions containing 1, 2, 5 and 10 mg *Fe*/litre. The standard solutions were preserved by addition of nitric acid following the same procedure as for the leachate samples.

The AA analysis was also carried out on the remaining 5ml of each unfiltered leachate sample which had been previously digested using Microwave Accelerated Reaction System (MARS5) following method EPA 3051A (1998) developed by the Environmental Protection Agency, USA for a closed vessel (XP-1500 Plus).

5.5.7. Gas analysis

Gas samples were collected using hypodermic syringes which were inserted through the three way valves installed on the top of each CAR and BMP reactor. The samples were immediately analysed.

The composition of the biogas (methane and carbon dioxide) was determined by gas chromatography (GC Varian 3800 gas chromatograph) equipped with a thermal conductivity detector (TCD) and two columns (a Haysep C 80-100 mesh and a Molecular Sieve 13 X 60-80 mesh, Analytical Columns, UK) both columns were one meter long, 6mm od and operated isothermally at 50°C in a back-flush mode. TCD temperature was 200°C, injection temperature 100°C. The injection volume was 0.25 ml and the carrier gas was argon at a flow rate of 6 ml/min.

The equipment utilised a single point calibration. The calibration procedure was carried out prior to each analysis using a calibration mixture of methane and carbon dioxide with concentration levels of 65% and 35% respectively, similar to the concentration range of the gas samples analysed.

5.5.8. Physical tests

Gravimetric testing for waste dry matter (DM), loss on ignition (LOI) and ash content were carried out according to standards methods (ISO 11465, BS EN13039, BS EN12880 respectively). The DM contents were determined at 105°C and the LOI and ash content at 550°C. However, when a waste sample contained plastic matter the DM contents were determined at 70°C (to a constant weight) to prevent the plastic matter from melting/burning. LOI is the difference between dry matter and the ash content. Any change in LOI across the process should represent the loss attributable to biodegradation. It should be noted that this method also includes losses due to the combustion of elements other than carbon and materials, which are non-biodegradable (e.g. plastics). Furthermore, LOI is important as it allows to determine whether or not the sample tested had been diluted with inert materials during the biodegradative process. The physical

tests described above provide a relatively constant basis through the process and allow some biological tests to be expressed in terms of DM or LOI.

5.5.9. Elemental analysis

The Total Carbon (TC) and Total Nitrogen (TN) content of the initial solid waste samples (AG & FR waste samples) and the waste samples collected at different stages of biodegradation process were determined using a macro Leco CNS2000 Elemental analyser capable of analysing sample weights up to 2.0 g. Prior to analysis, waste samples were pre-treated according to a procedure shown in Figure 5.17, dried at 70°C and then milled to a fine powder using a Knifetec 1095 Sample Mill (Foss) in conjunction with a Cyclotec 1093 sample Mill (Foss). All non-grindable components (metal and glass) were removed and weighed. The CN of the sample was determined by dry combustion at 1450°C with a pure oxygen atmosphere in the furnace. The combustion products carbon dioxide and nitrogen oxides are detected by infrared (IR) and thermal conductivity (TCD) cells respectively.

5.5.10. Fibre analysis

Fibre analysis was performed using the Foss Technology system FibreCap 2021/2023 (Kitcherside *et al.,* 2000). Prior to analysis each sample was pre-treated according to the procedure shown in Figure 5.17, dried at 105°C and then ground to a fine powder using a Knifetec 1095 Sample mill (Foss) in conjunction with a Cyclotec 1093 sample Mill (Foss). Plastic materials and all non-grindables, such as metal and glass, were removed and weighed. Different fibre fractions were analyzed in triplicate. The Neutral Detergent Fibre (NDF) test was carried out using chemical procedures as described by Van Soest *et al.* (1991) except that the sample was retained in the FibreCap capsule (0.3-0.5g of milled sample was introduced in each capsule). This procedure uses α-amylase at two stages in the extraction process to improve the solubilisation of starch. The Acid Detergent Fibre (ADF) test was performed when waste samples were digested using a cationic detergent (*Cetyltrimethylammoniumbromide*, 20 g/l) in 0.5M sulphuric acid for 1 hour after reaching boiling point. ADL was assessed by further treating the non-dried and non-ashed residues from previously performed ADF tests (first-step digestion) with 72% sulphuric acid at room temperature for 4 hours to dissolve the cellulose, leaving lignin as the residue (Effland, 1977). A schematic of the fibre analysis system used in this study is

shown in Figure 5.21. The specific cell wall components (cellulose and hemicellulose) were estimated using Eq. 2.42 & Eq. 2.43.

5.6. Carbon mass balance analysis

5.6.1. Introduction

A carbon mass balance is an essential part of environmental engineering. An accurate and complete mass balance will confirm the validity of a process, making it possible to perform necessary analyses, including experimental design, test performance and cost analysis. The mass balance concept is based on the fundamental physical principle that within a closed system the total mass of individual elemental components remains constant. There may be movement of mass and transformation of mass to different forms but it is not created or destroyed. A general mass balance accounts for the overall mass entering, exiting and accumulating in a system. The balance is performed using the following equation:

Eq. 5.5 $$\Sigma m_{in} - \Sigma m_{out} - \Sigma m_{accumulated} \equiv 0$$

This equation states that the sum of the masses flowing into a system (inputs), minus the sum of the masses flowing out of the system (outputs), minus the sum of the mass being accumulated within the system must be equal to zero. The first step in performing a mass balance is defining the system and identifying its boundaries. Once the system is defined, all the mass terms should be identified. For the purposes of the mass balance analyses being considered here the closed system can be taken to be any anaerobic reactor used in this study. The carbon based biodegradative process in this study has two inlet terms: initial waste and seeded mineral media; two outlet terms: biogas and leachate TOC and IC; and two measured accumulation terms: degraded waste and carbonate precipitates (Figure 5.22).

Performing an accurate mass balance on a running system of the size of the CAR experiments requires a little more consideration than just addition and subtraction of the masses involved. For a complete mass balance, the uncertainty of the measurements must be determined and taken into account in the calculations. Performing a mass balance based on incorrect or inaccurate data can potentially be more problematic than not performing a mass balance at all.

A mass balance can be a valuable tool for trouble-shooting. All the mass that flows through and accumulates within a system must be accounted for. If the masses do not balance, it may be an indication of a problem or of a process accruing within the system not accounted for. Because it might be difficult to assess the situation if the errors are great or the error limits are unknown, it must be reiterated that the measurements must be evaluated and analyzed to determine these limits. Because all data will contain some degree of uncertainty, it should be determined what amounts of error are acceptable and possible solutions for reducing any errors that are unacceptable considered.

5.6.2. Carbon mass balance calculations

To summarise the key features of the methodology, there are several main elements in the carbon mass balance in the CAR reactors that should be considered:

- Initial waste TC content;
- Initial mineral media TC content;
- Carbon output as methane - *[C-CH_4]*;
- Carbon output as carbon dioxide - *[C-CO_2]*;
- Carbon output as leachate (TOC+IC) - *[C-Leachate]*;
- Carbon output as carbonates (precipitated and dissolved) ($CaCO_3$ and $MgCO_3$) - *[C-$CaCO_3$]* and *[C-$MgCO_3$]*; and
- Residual TC in waste - *[C-Waste]*.

In a closed system where the only carbon fates are methane, carbon dioxide, $CaCO_3$, $MgCO_3$ and residual waste carbon, the system can be defined by the following equation:

Eq. 5.6. $$Initial\ waste\ TC + Initial\ media\ TC = [C\text{-}CH_4] + [C\text{-}CO_2] + [C\text{-}CaCO_3] + [C\text{-}MgCO_3] + [C\text{-}Leachate] + [C\text{-}Waste]$$

As mentioned in section 5.6.1, it is virtually inposible to achieve closure of carbon mass balance. An estimation of an carbon bass balance error can be made with the following equation:

Eq. 5.7. $$Mass\ balance\ error = Expected\ value - Actual\ value,\ g/kg\ DM$$

Where,

Expected value = Initial waste TC + Initial media TC, g/kg DM; and

Actual value = [C-CH_4] + [C-CO_2] + [C-$CaCO_3$] + [C-$MgCO_3$] + [C-Leachate] +

[C-Waste].

The error can also be expressed as a percentage of the expected value:

Eq. 5.8. $$Mass\ balance\ error,\% = \frac{Expected\ value - Actual\ value}{Expected\ value} \times 100$$

A. Carbon output as biogas:

The carbon content under the methane form can be calculated as follows:

Eq. 5.9 $$[C-CH_4]^i = \frac{[CH_4]^i}{100} \frac{V^i\ M_C\ \rho_{CH_4}}{M_{CH_4}}$$

Where:

$[C-CH_4]^i$ = carbon content as methane in the biogas at time t = i, g/kg dry matter (DM);

$[CH_4]^i$ = concentration of methane in the biogas at time t = i, %;

V^i = cumulative volume of the biogas produced from the beginning of the test to time t=i, litres/kg DM;

ρ_{CH_4} = density of methane at STP, kg/m^3;

M_C = molar mass of carbon (12 g/mol);

M_{CH_4} = molar mass of methane (16 g/mol).

The carbon concentration in the biogas derived from the carbon dioxide was evaluated according to Eq. 5.10.

Eq. 5.10 $$[C-CO_2]^i = \frac{[CO_2]^i}{100} \frac{V^i\ M_C\ \rho_{CO_2}}{M_{CO_2}}$$

Where:

$[C-CO_2]^i$ = carbon content as carbon dioxide in the biogas at time t = i, g/kg DM;

V^i = cumulative volume of the biogas produced between the beginning of the test and the time t = i, litres/kg DM;

$[CO_2]^i$ = concentration of methane in the biogas at time t = i, %;

M_C = molar mass of carbon (12 g/mol);

ρ_{CO_2} = density of carbon dioxide at STP, kg/m^3;

M_{CO_2} = molar mass of carbon dioxide (44 g/mol).

Biogas production was measured at approximately 30°C. All biogas readings were standardised to dry gas at STP using Eq. 5.2:

B. Carbon output as leachate:

The TC concentration in the leachate was calculated as follows:

Eq. 5.11 $$[C-Leachate]^i = \frac{[TOC+IC]^i V_{leachate}}{M_{waste}}$$

Where:

$[C-Leachate]^i$ = Leachate TC content at t = i, g/kg DM;

$[TOC+IC]^i$ = Leachate TC content at t = i, mg/l;

$V_{leachate}$ = volume of leachate in the reactor, litres;

M_{waste} = initial waste dry mass, kg.

C. Carbon output as $CaCO_3$ and $MgCO_3$:

This represents both precipitated IC and dissolved IC in the leachate during the test period.

Eq. 5.12 $$[C-CaCO_3]^i = \frac{[Ca^{2+}]^i M_C V_{leachate}}{M_{Ca} M_{waste}}$$

Eq. 5.13 $$[C-MgCO_3]^i = \frac{[Mg^{2+}]^i M_C V_{leachate}}{M_{Mg} M_{waste}}$$

Where:

$[C-CaCO_3]^i$, g/kg DM;

$[C-MgCO_3]^i$, g/kg DM;

$[Ca^{2+}]^i$ = calcium concentration in the leachate at time t = i, g/l;

$[Mg^{2+}]^i$, g/l;

M_C = molar mass of carbon (12 g/mol);

M_{Ca} = molar mass of calcium (40.1 g/mol);

M_{Mg} = molar mass of magnesium (24.3 g/mol).

Figures

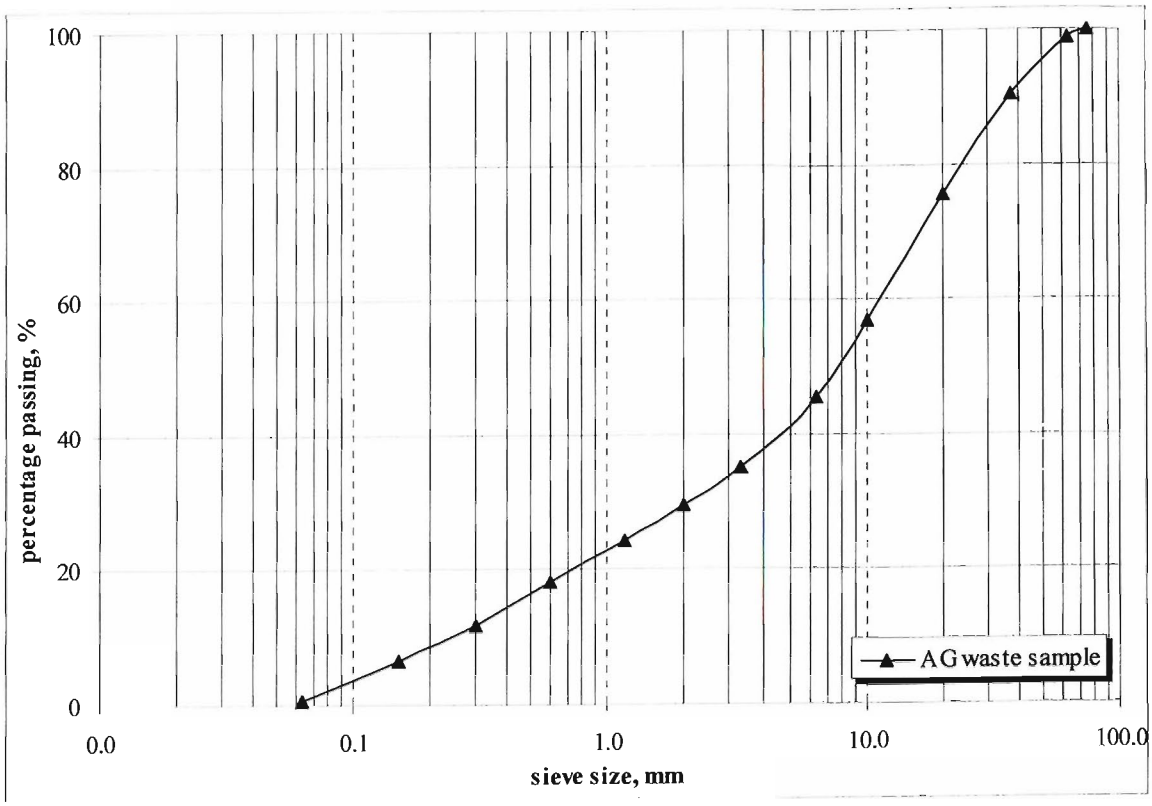

Figure 5.1. Grading curve for AG waste sample.

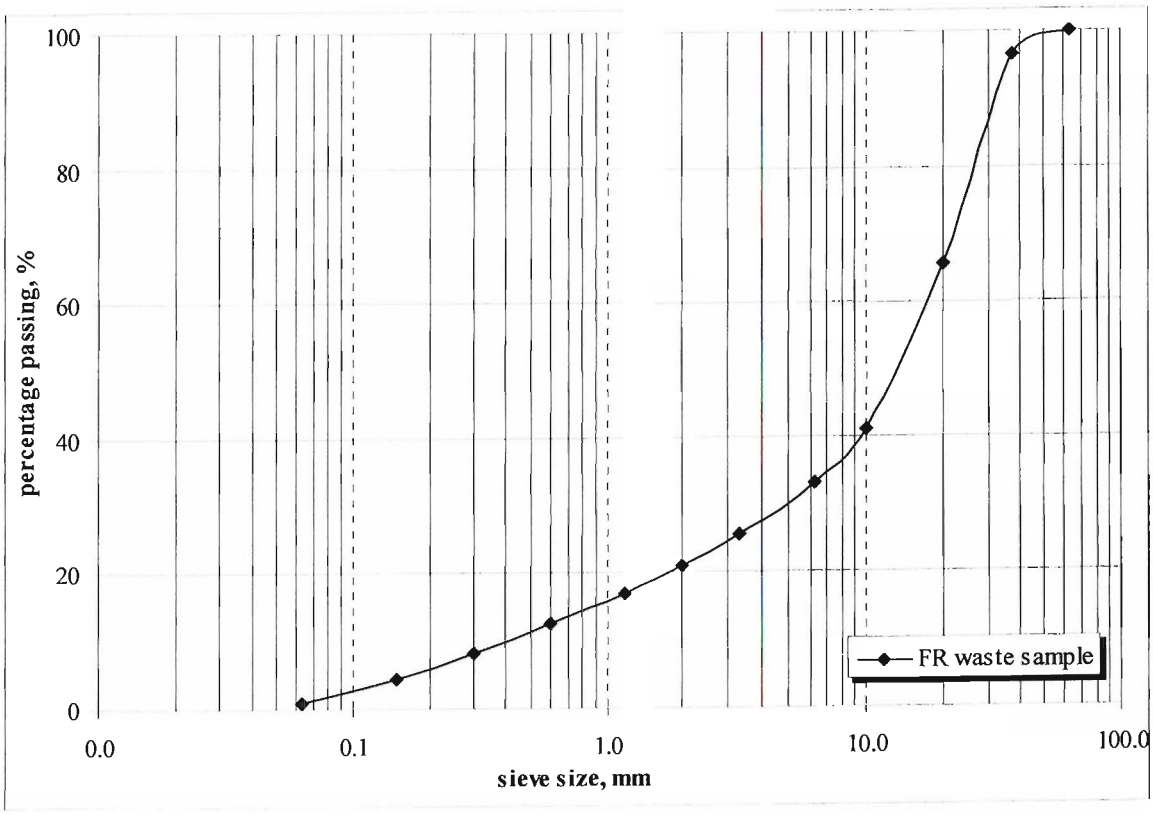

Figure 5.2. Grading curve for FR waste sample.

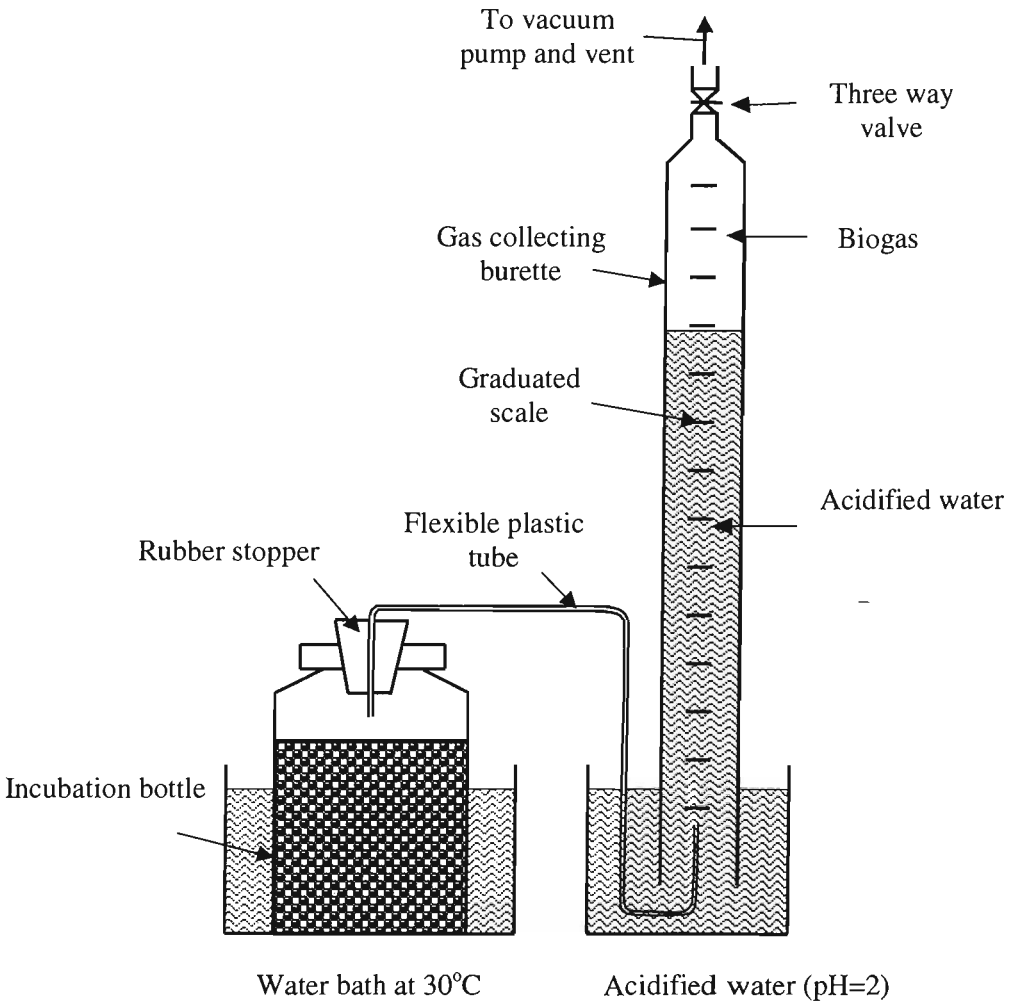

Figure 5.3. Schematic view of BMP apparatus (not to scale).

Figure 5.4. BMP test assay apparatus.

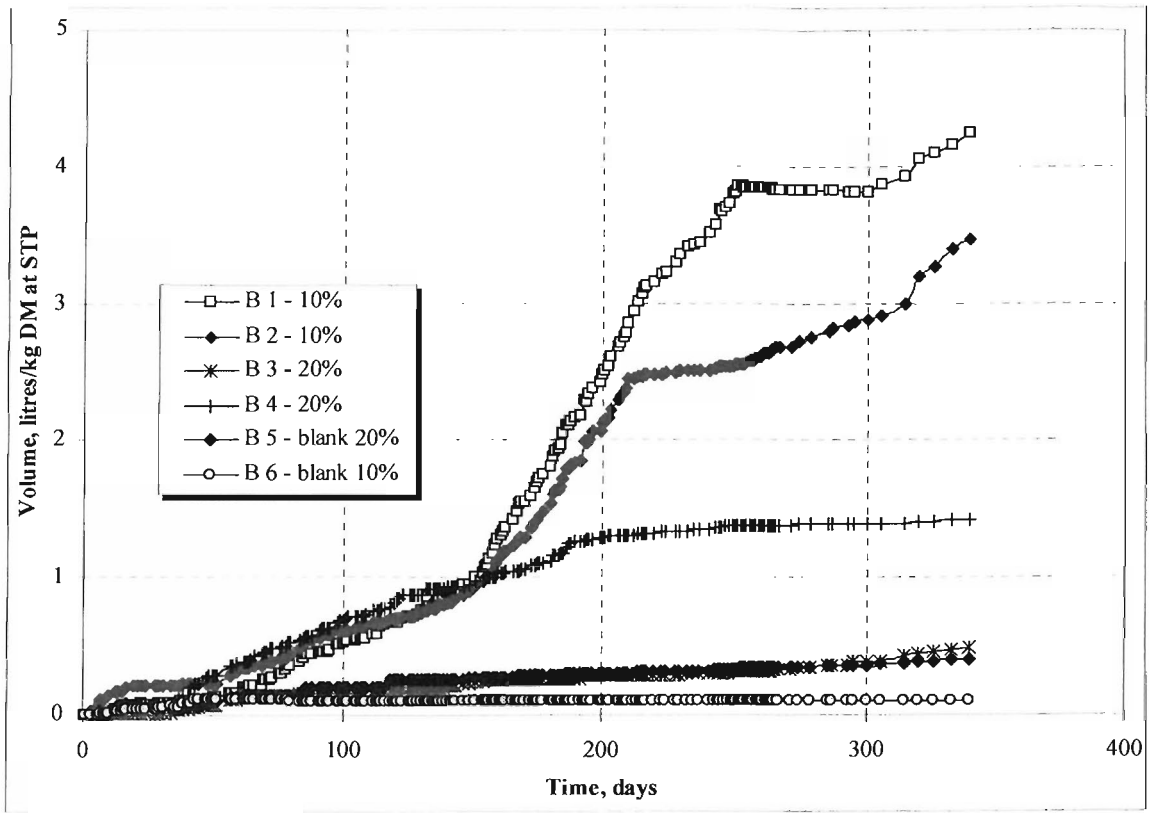

Figure 5.5. Cumulative biogas production in litres/kg dry matter (DM) at standard temperature and pressure (SPT) for BMP1 bottles.

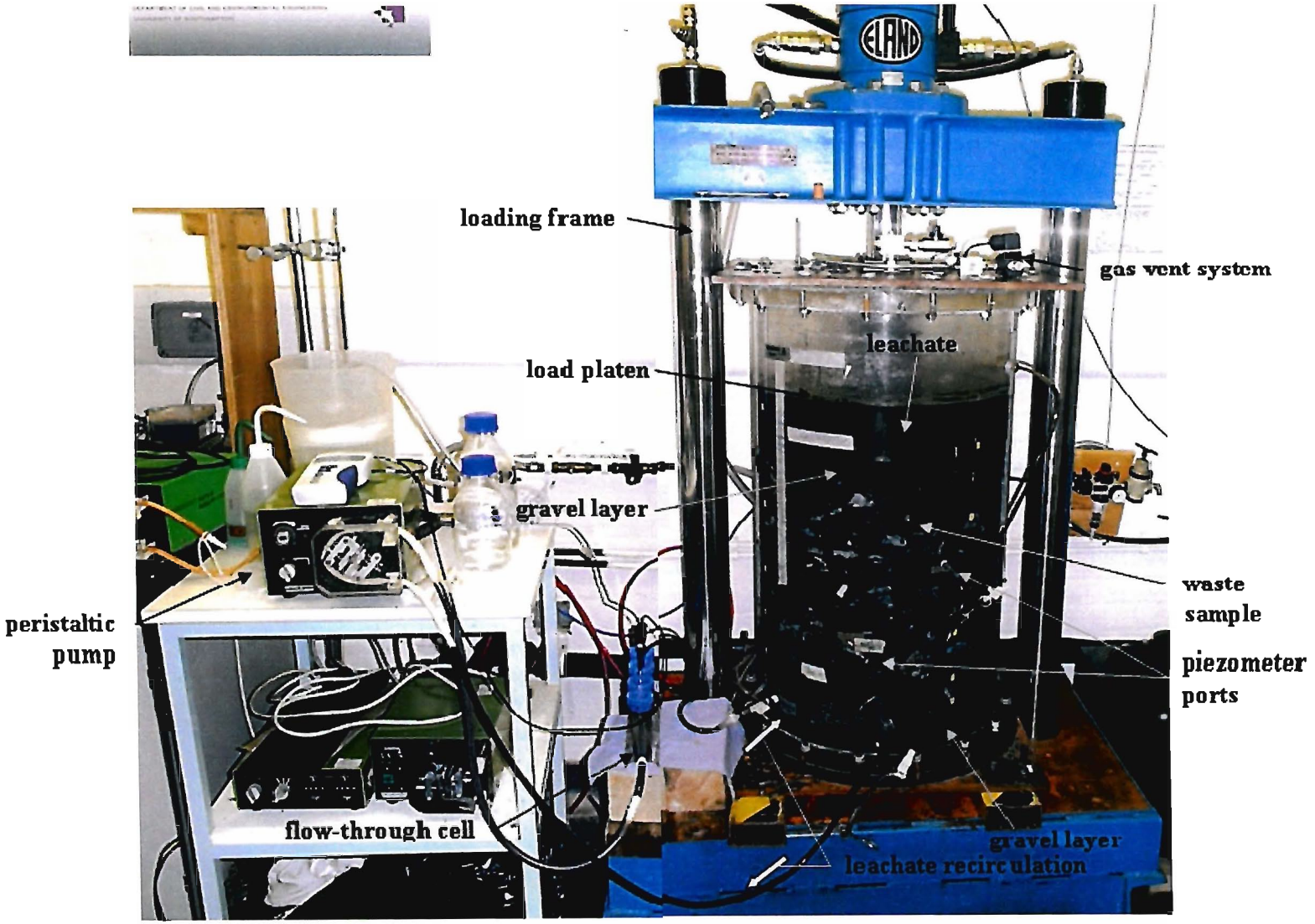

Figure 5.6. Experimental set-up of the CAR.

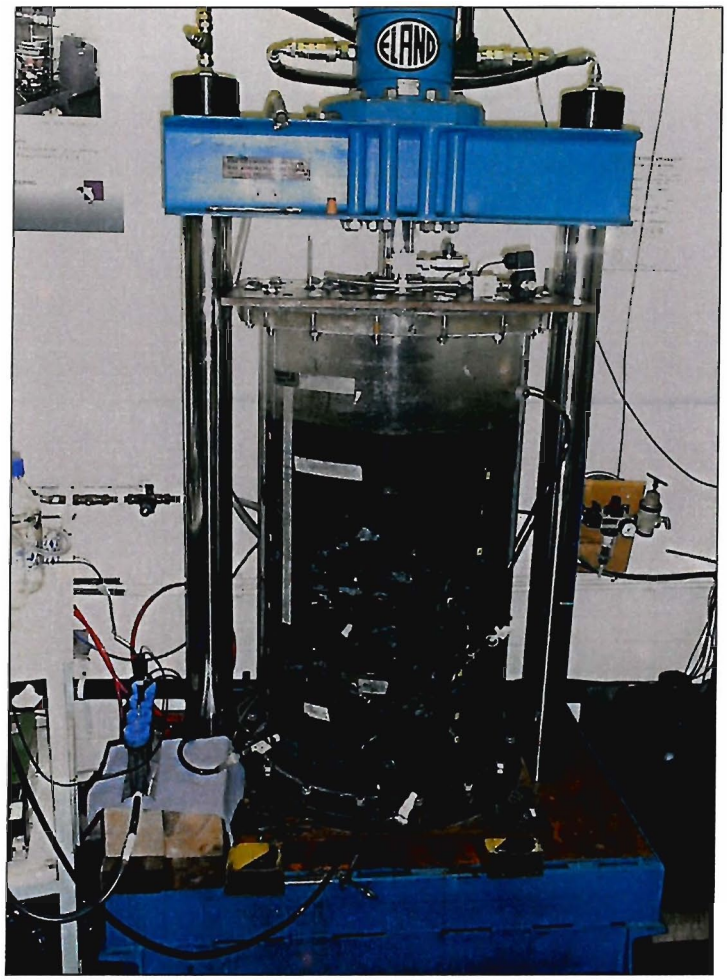

Figure 5.7. Consolidating Anaerobic Reactor 1.

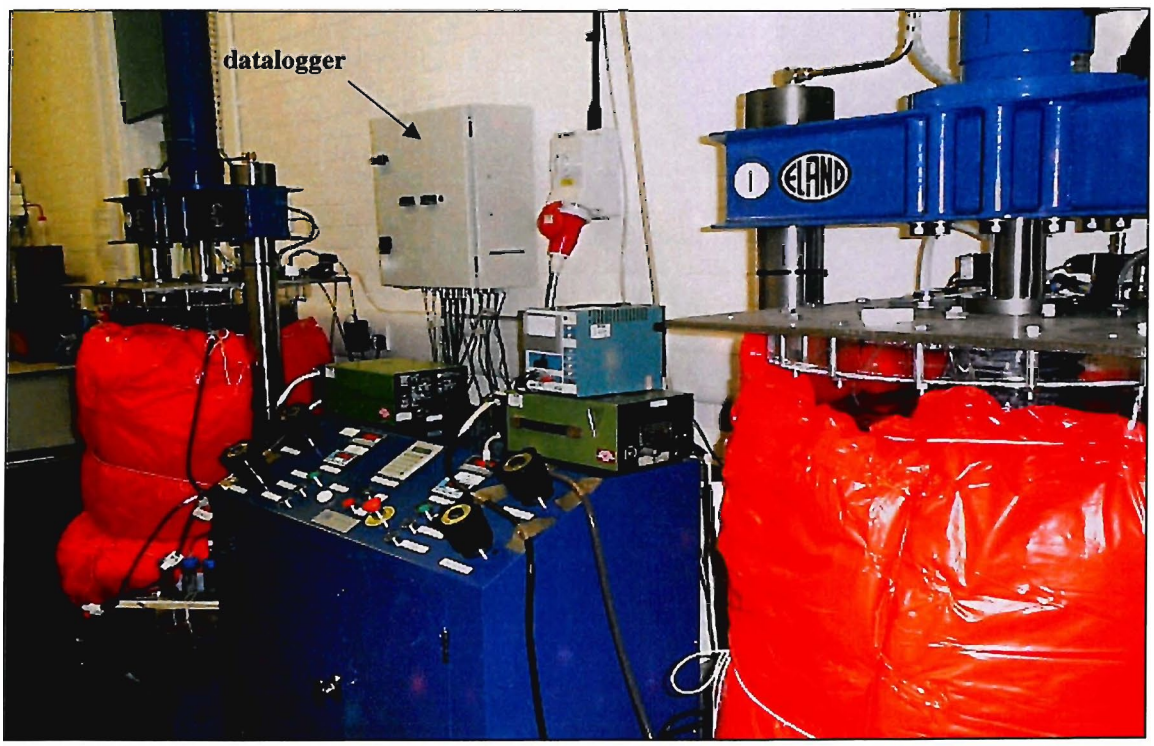

Figure 5.8. Consolidating Anaerobic Reactors 2 and 3.

Figure 5.9. Consolidating Anaerobic Reactor 4 - Control Cell.

Figure 5.10. Initial preparation of the FR waste sample.

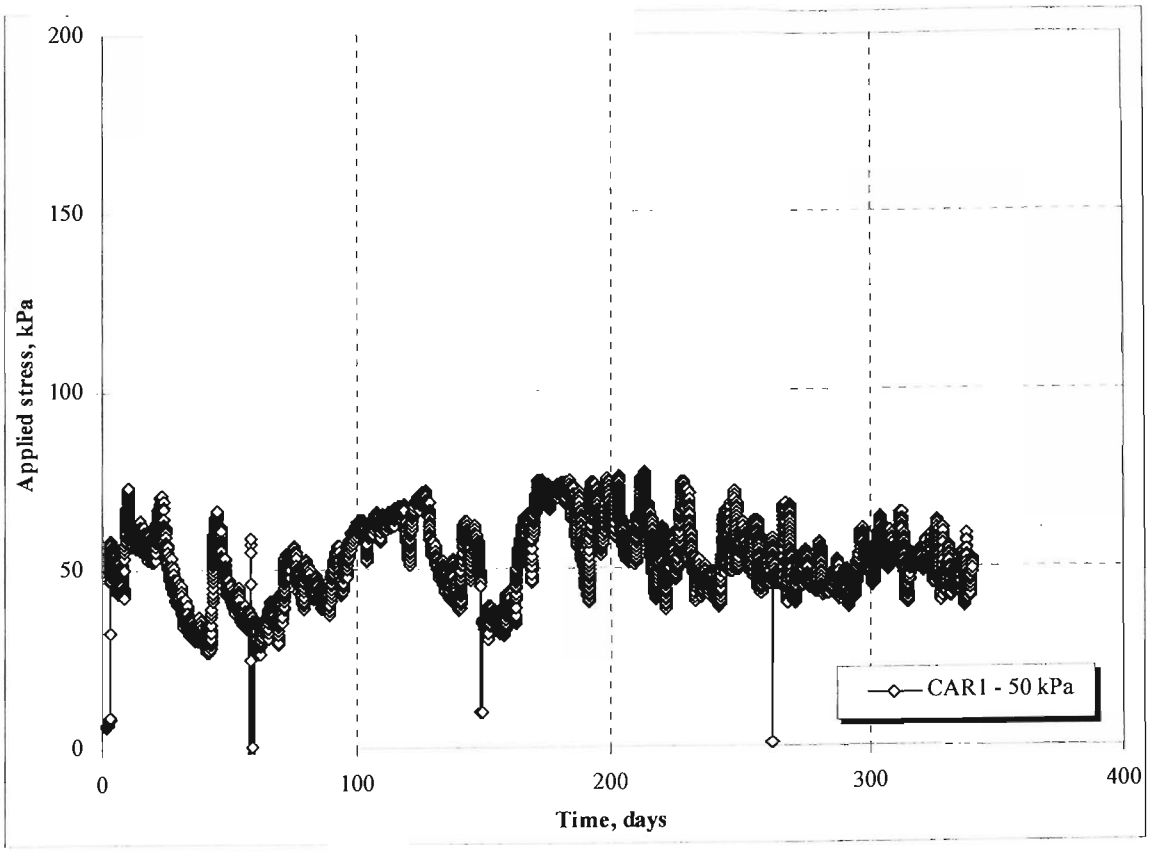

Figure 5.11. Monitored applied stress to CAR1.

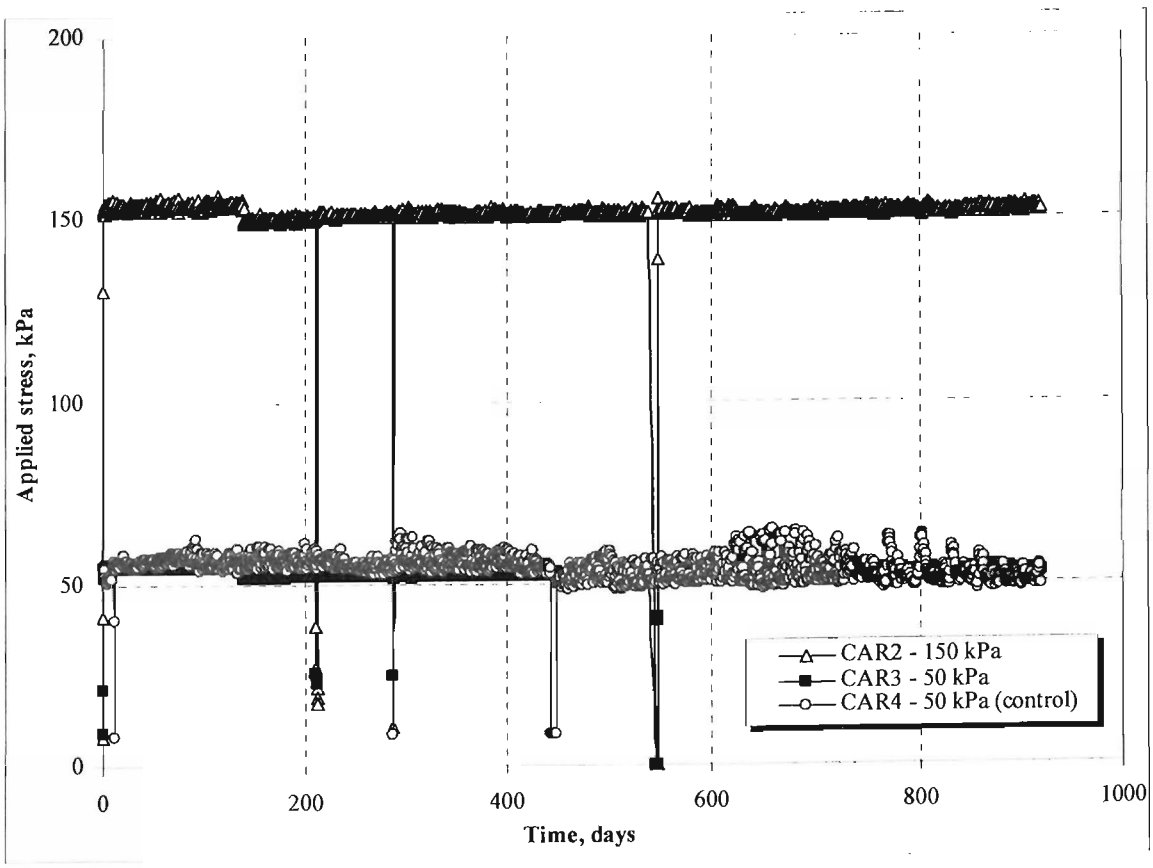

Figure 5.12. Monitored applied stress to CARs 2, 3 & 4.

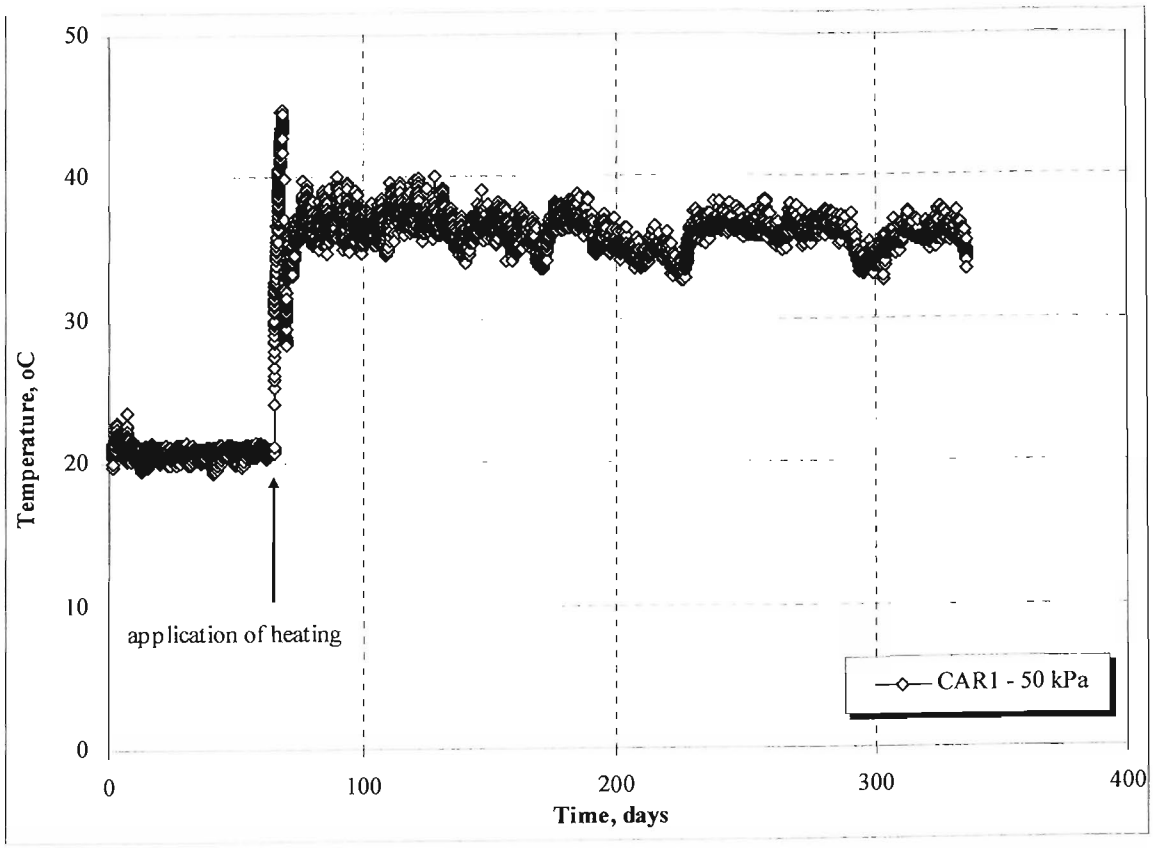

Figure 5.13. Monitored temperature to CAR1.

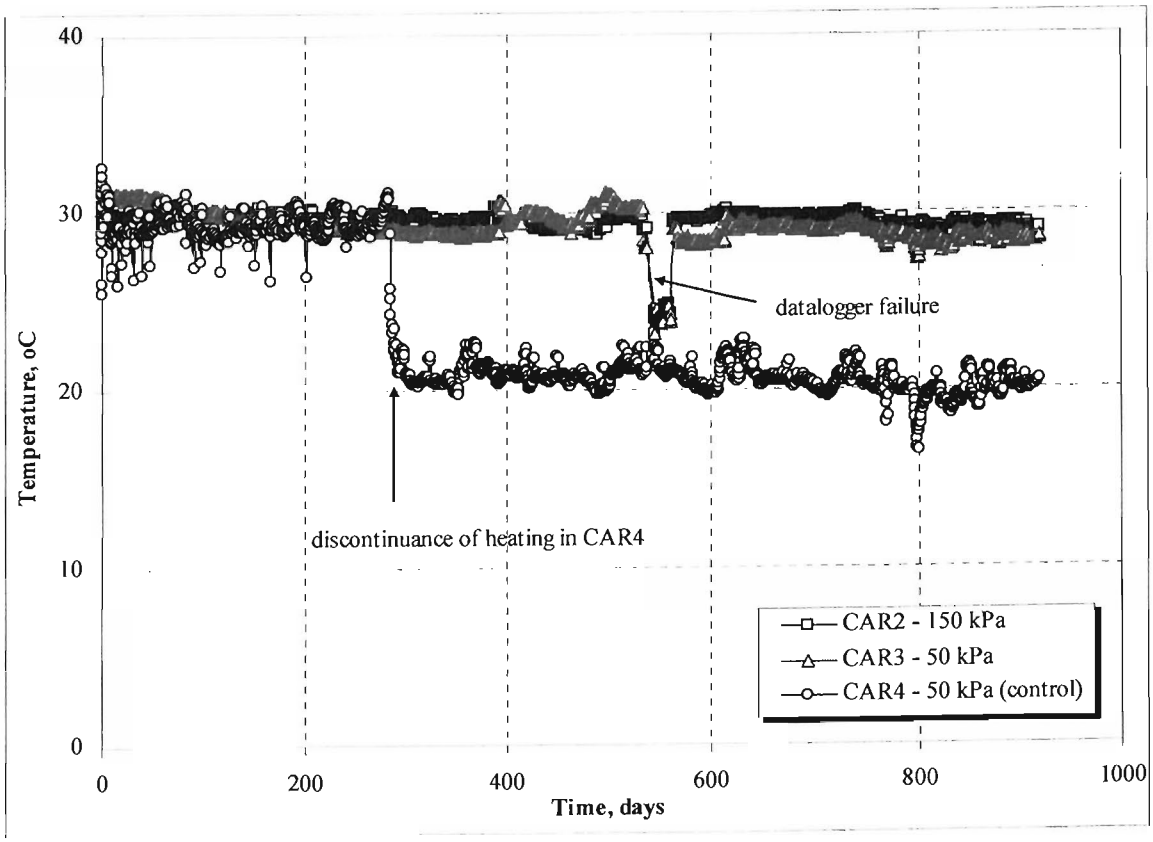

Figure 5.14. Monitored temperature to CAR2, CAR3 & CAR4.

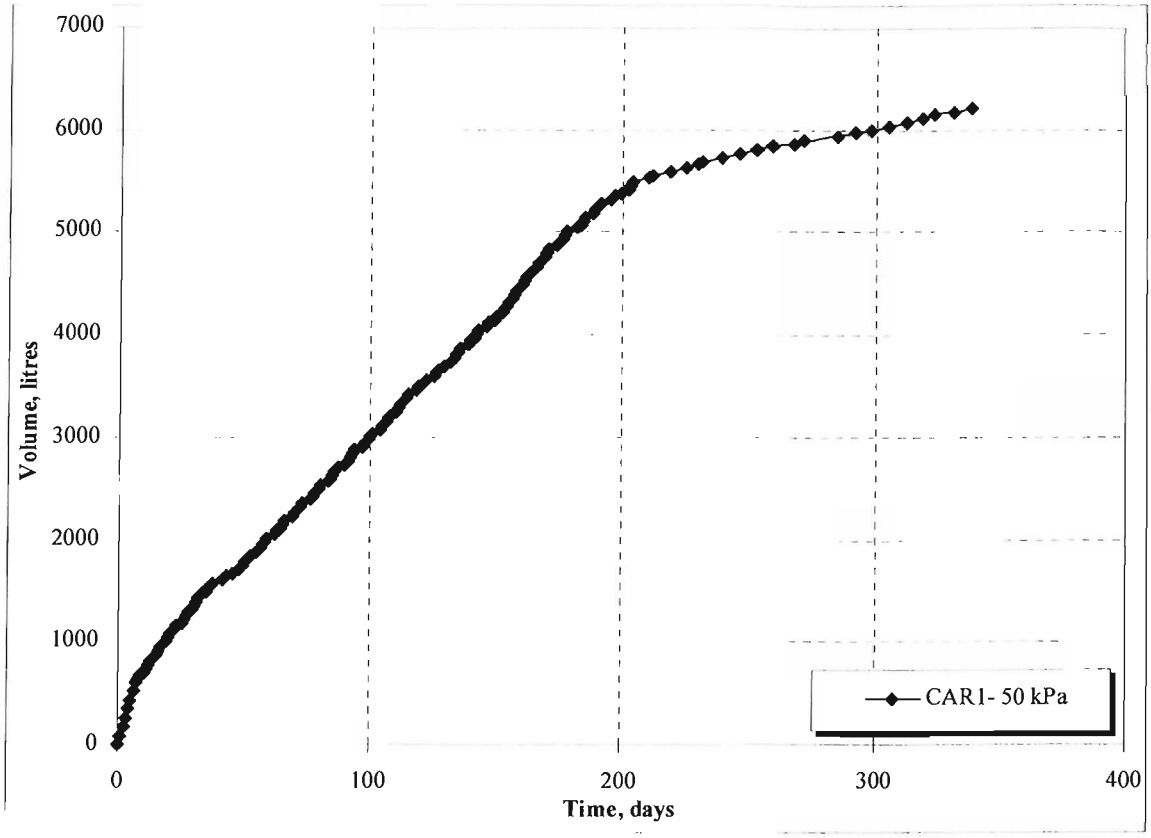

Figure 5.15. Cumulative recirculated leachate volume in CAR1.

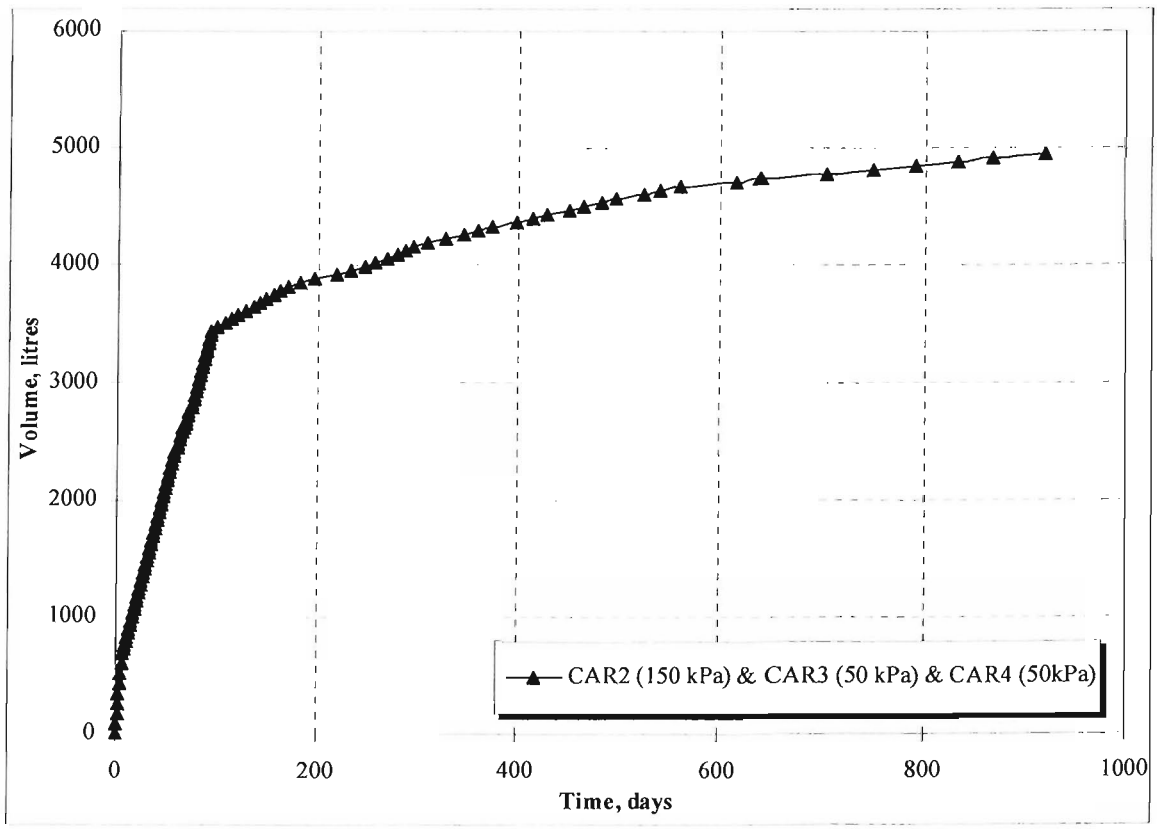

Figure 5.16. Cumulative recirculated leachate volume in CAR2, CAR3 & CAR4.

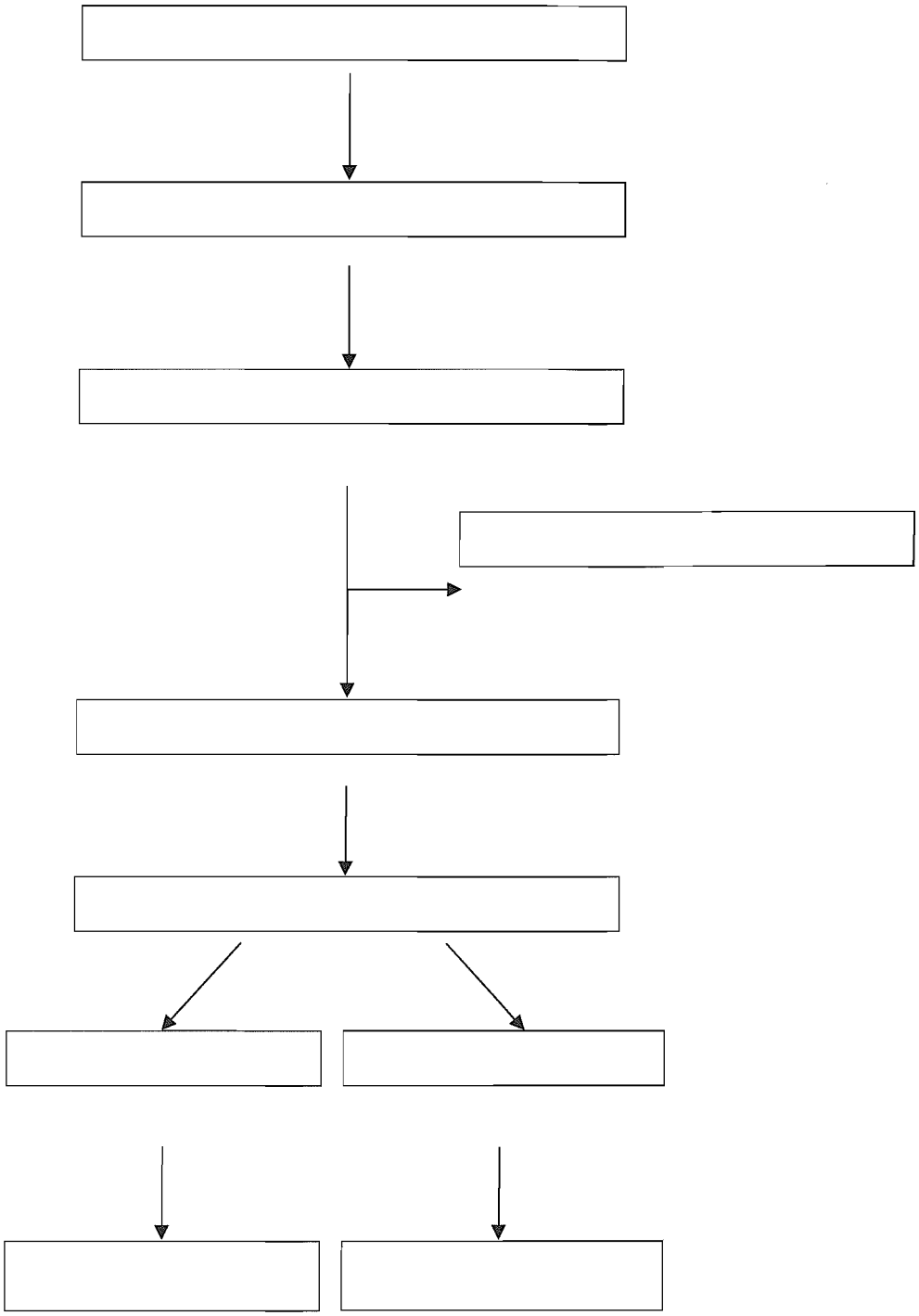

Figure 5.17. Post test sample preparation procedure.

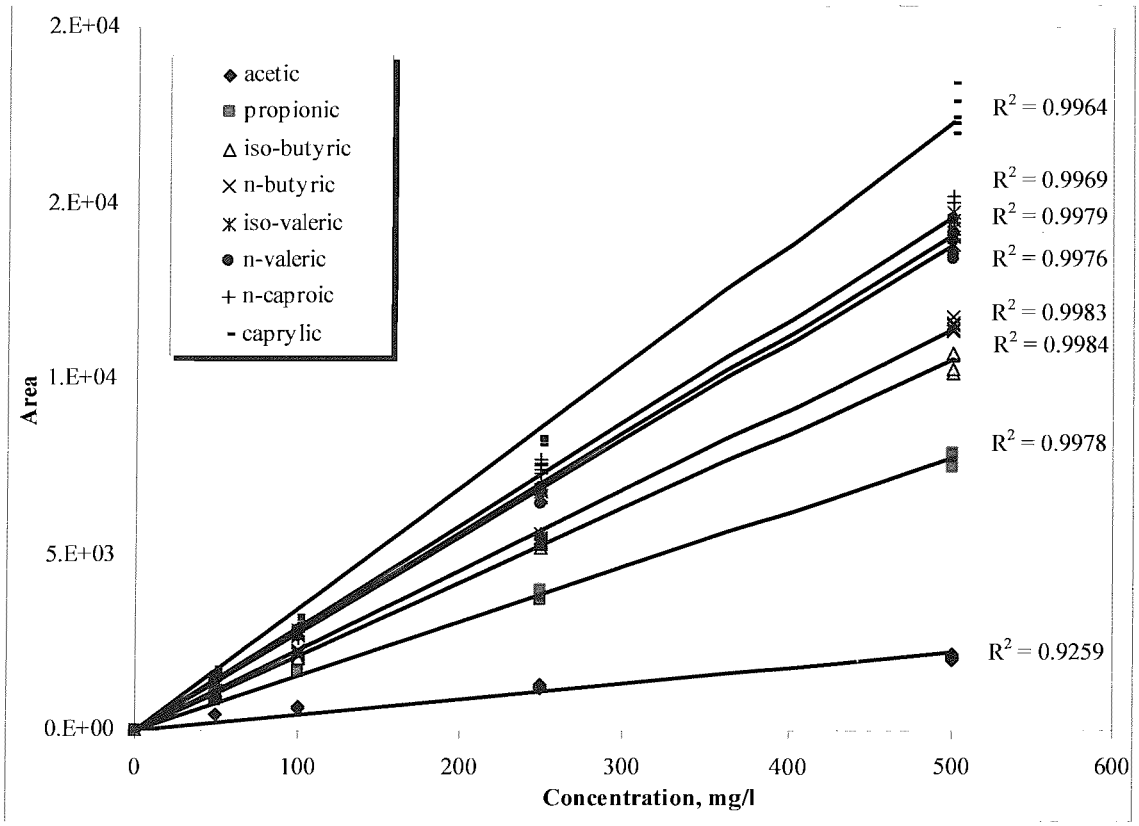

Figure 5.18. VFAs calibration curves using five different standard concentrations.

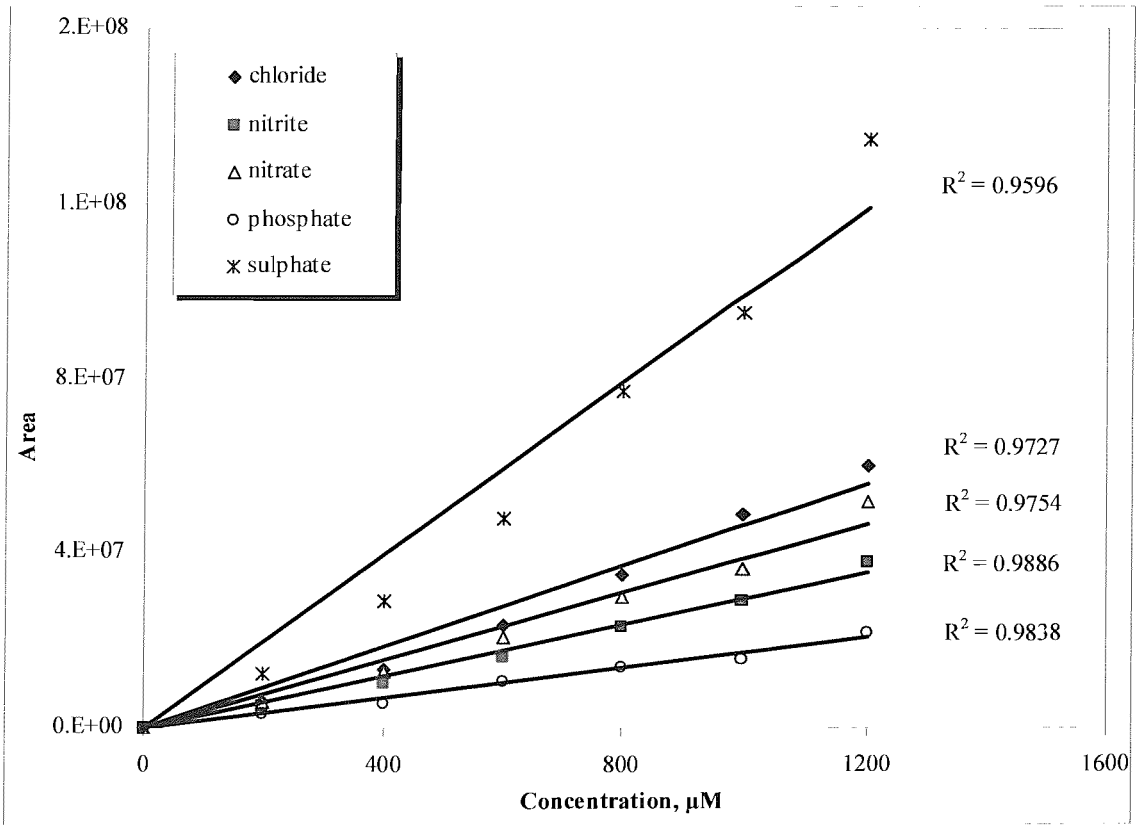

Figure 5.19. Anions calibration curves using six different standard concentrations.

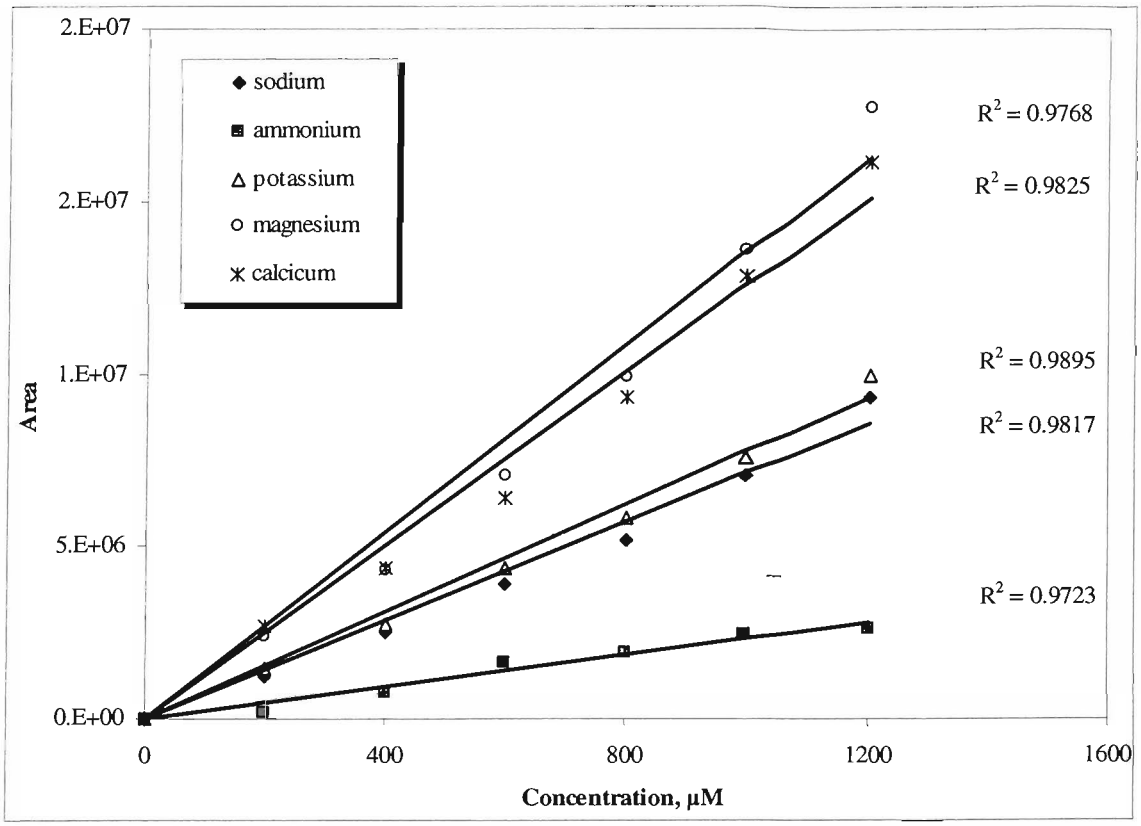

Figure 5.20. Cations calibration curves using six different standard concentrations.

Figure 5.21. Fibre analysis system.

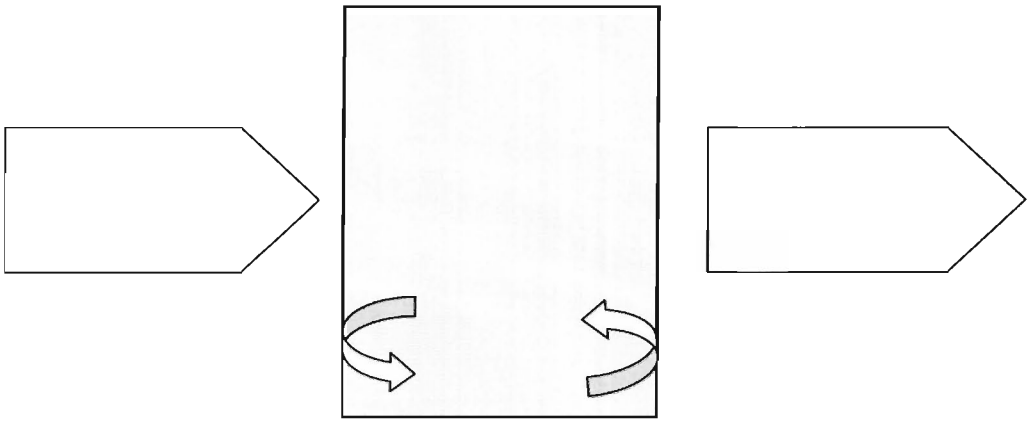

Figure 5.22. Schematic representation of the mass balance model in an anaerobic reactor.

Chapter 6

Results and discussion:

Laboratory experiments involving aged MSW (sample AG)

In the following chapter, the degradability of the waste selected for this study is quantified by means of a series Biochemical Methane Potential (BMP) tests. The volumes of the gas produced (section 6.1.1) and the settlement observed in CAR1 which was filled with aged MSW sample (sample AG) (section 6.1.2) are reported and compared with theoretical rates. Inter-relationships between the onset of biodegradation of the waste and associated leachate chemical parameters are discussed in sections 6.1.3 to 6.1.9 . In addition, the changes in the composition of the leachate during waste biodegradation are presented to allow the inter-relationship between secondary settlement and biodegradation to be established. The anaerobic biodegradation potential of the waste (AG sample) is characterized in section 6.2.

6.1. CAR filled with AG waste sample

6.1.1. pH and gas production rate

Initially the pH of the recirculated leachate was between pH 7.14-7.16 (Figure 6.1). This value rose to pH 7.24, and then decreased to within a range of pH 6.85-6.89 for 25 days. There was a significant increase in the pH after day 122 (pH 7.56) followed by a gradual decrease in pH to a level of around pH 6.93 by the end of the test (919 days).

The total gas production from the CAR was 79.43 litres at STP (1.41 litres/kg dry wt.) by day 338, at which time over 64.8% of the biogas was methane and 25.9% CO_2 (Figure 6.2 & Figure 6.3). Typical values for both methane and carbon dioxide are between 45% and 65% by volume (Tchobanoglous *et al.*, 1993).

The daily volume of gas produced varied between 0.0 and 6.1 litres. The reason for this variation is that gas was released into the CAR headspace by ebullition of trapped gas in the void space of the waste sample. The maximum daily gas production rate was 0.109 litres/ kg dry wt. waste /day on day 69 (Figure 6.4).

6.1.2. Settlement in CAR1 - AG waste sample

The settlement in CAR1 was measured for a period of 338 days. The observed data are presented as a percentage of the settlement of the initial refuse height which was recorded 24 hours following load application. As discussed previously in section 5.3.2, the settlement observed in the CARs during filling and loading was considered to be caused by initial and primary compression of the waste due to a lack of adequate compaction during the sample preparation stage, and was not taken into consideration. A settlement classification described in section 1.1 was adopted in this study.

Based on the settlement readings and the change in the slope of strain-log time curve for CAR1 (Figure 6.5), the time for intermediate settlement to occur was determined to be 56 days. At the end of this phase, the waste settled by 3.9%, which is most likely to have been caused by delayed mechanical interactions between the waste constituents due to crushing, bending and reorientation as a result of loading.

Results highlight the importance of temperature in promoting stabilisation of the waste. Upon heating the reactor to a temperature of approximately 35°C at day 65, a noticeable increase in the rate of gas production was immediately observed (Figure 6.2). A concurrent increase in settlement rate was also recorded. The highest degree of settlement recorded was between day 65 and day 193 which was considered to be due to both physical compression and biodegradation. After 193 days the rate of settlement in CAR1 decreased, indicating that most of the biodegradation was to have taken place and that, the cause of settlement was likely to be due to physical creep compression.

The total magnitude of settlement after 338 days was approximately 9.0% (Table 6.1). If 3.9% is assumed to be due to mechanical compression then the remaining 5.1% may be as a result of waste biodegradation leading to long-term secondary settlement. This observation was further verified using a cell (CAR4 - see section 5.3.2) in which biologically mediated reactions were inhibited, thereby allowing microbial and physicochemically mediated compression phenomena to be more easily distinguished.

The total secondary settlement and the settlement due to biodegradation observed in CAR1 are depicted as a log-time scale in Figure 6.5 and Figure 6.6, respectively. The data are presented as a percentage of the settlement of the initial refuse height.

Table 6.1. Settlement results in CAR1.

Reactor	Bulk density [1], kg/m^3	Time period, days	Waste height before loading, m	Actual settlement, m (%)[2]	h_p[3], m	h_s[4], m	h_b[5], m	h_r[6], m
Intermediate secondary settlement								
CAR1 (50kPa)	516.64	2 - 56	n/a	0.024 (3.9)	n/a	0.599	n/a	n/a
Long-term biodegradative secondary settlement								
CAR1 (50kPa)	541.97	56 - 192	n/a	0.028 (4.5)	n/a	n/a	0.571	n/a
Residual secondary settlement								
CAR1 (50kPa)	545.80	193 - 338	n/a	0.004 (0.6)	n/a	n/a	n/a	0.567

Note: [1] Calculated at the end of each phase; [2] Measured at the end of each phase; [3] h_p is height of waste at the end of primary compression phase; [4] h_s is height of waste at the end of intermediate secondary compression phase; [5] h_b is height of waste at the end of long-term secondary compression phase; [6] h_r is height of waste at the end of the test; and [7] n/a - not applicable.

6.1.3. Degradation

The TOC content of the leachate samples from the cells decreased from initial values of 884.2mg/l to 266.1mg/l after 338 days of the experiment. At the same time, the total dissolved organic carbon content (TDOC) of the leachate samples, which had been previously been filtered though Whatman GF/C filters (section 5.5.1), increased from 101.8mg/l to 242.2mg/l (Figure 6.7). This increase was most likely due to the degradation of solid organic matter resulting in the formation of a range of soluble organic compounds as yet unidentified. During the test period, a gradual increase in the inorganic carbon content to a level of 151.4mg/l was also observed (Figure 6.7).

6.1.4. VFA concentration

Eight VFAs were analyzed in the leachate – acetic, propionic, n- and iso-butyric , n- and iso-valeric, caproic and caprylic acids. The concentrations of the VFAs in the leachate are shown in Figure 6.8. The VFAs were generally present in small concentrations (below 20mg/l), this being most likely due to their rapid turnover and utilisation by initially the sulphate reducing bacteria (SRB) (day 0-65) and latterly by the methanogenic bacterial population (day 65-338). Noticeably, the concentrations of n-valeric, caproic and caprylic acids were higher during the early stages of the experiment

(day 0-20) presumably as a result of hydrolysis of the more easily biodegradable material in the waste.

6.1.5. Sulphate

In the presence of sulphate, the growth of methanogenic bacteria may be restricted due to the presence of sulphate reducing bacteria, which use acetate as a carbon source and sulphate as an electron acceptor. The growth of the sulphate reducing bacteria on acetate is energetically more favourable compared to the growth of methanogenic bacteria. Based on the kinetics of VFA (acetic, propionic and butyric acids) and hydrogen utilisation by SRB, acetogenic and methanogenic bacteria, the SRB will be able to out-compete the acetogenic and methanogenic bacteria (Oude Elferink *et al.*, 1994) (section 2.3.3). A comparison between Figure 6.2 and Figure 6.9 reveals the influence of sulphate on methane formation. At day 65 of the experiment all the sulphate in the leachate was removed and this resulted in a simultaneous increase in the rate of biogas production (Figure 6.4).

6.1.6. Redox potential

The oxidation-reduction state of an aqueous environment can be stated in terms of its redox potential. In the literature this is generally expressed in volts (Eh), or as the negative logarithm of the electron activity (pE). These terms are also directly related to the free energy of the system. Many reactions in leachate are governed by the redox potential and pH. Among these are the solubilization or precipitation of iron, manganese and other metals; sulphur and phosphorus transformation; conversion of nitrogen forms; and other reactions (Qasim and Chiang, 1994).

The redox potential, Eh, was measured continuously in CAR1 to monitor the general condition of the methanogenic culture. In general, after nutrient media and activated sludge addition, the redox was -236mV, then decreased slowly, with some fluctuations, and settled around at -440mV by the 140 day of the experiment followed by a further gradual change in Eh value to a level of approximately -100mV by the end of the test (Figure 6.10).

6.1.7. Ammonium concentration

Most of the organic nitrogen that occurs in domestic wastes is in the form of proteins or their degradation products: polypeptides and amino acids. Because of the anaerobic condition in the CAR, there is no conversion of ammonium ions into nitrites and nitrates (through nitrification) (section 2.3.2). This would explain the observed gradual increase in the ammonium concentration to a level of 302.3mg/l during the test period (Figure 6.11).

6.1.8. Calcium and magnesium precipitation

A gradual decrease of Ca^{2+} and Mg^{2+} ions from the leachate was observed during the waste biodegradation process (Figure 6.12). At the beginning of the experiment, the concentrations of calcium and magnesium ions initially increased to 530.9mg/l and 112.9mg/l respectively from 204.8mg/l and 26.3mg/l possibly due to both pH decease and waste biodegradation processes. Thereafter a significant decrease in both their concentrations was observed (to 146.0 and 49.7mg/l respectively) when CAR1 was heated and its temperature maintained at approximately 35°C. This was almost certainly due to the precipitation of the elements and this may have been triggered by the onset of microbial activity observed with heating. Rates of gas production, removal of sulphate and enhanced ammonia production were all immediately increased by the increase in the temperature. Additionally, there was also a dip in the pH from neutrality to about 6.8.

6.1.9. Heavy metals

Nine metals were analyzed in the leachate: *Fe*, *Al*, *Zn*, *Cu*, *Co*, *Pb*, *Ni*, *Mo* and *Cd*. The concentrations of the metals in the leachate are shown in Table 6.2. Generally the concentration of all metals progressively decreased with time. The results indicate that about 97% of *Al*, *Zn*, *Cu* and *Co*, about 83% of *Pb* and *Ni*, about 75% of *Mo* and *Cd*, and 27% of *Fe* were removed from the liquid phase via form of metabolic uptake within the first 66 days of the experiment (Figure 6.13 to Figure 6.15) due to the establishment of a highly reducing environment and the formation of sulphide from sulphate reduction which promotes metal precipitation in the form of metal uptake (section 2.4). During the methanogenic phase (66-338 day) heavy metal concentrations continued to decrease gradually and the metal removal was not considered to have inhibitory effects on methane formation. The results are very similar to the ranges of leachate heavy metal concentrations reported by Robinson (1995) for six old landfills in the UK.

Table 6.2. Concentration of heavy metals in leachate samples in CAR1.

Day	Dissolved concentration, µg/litre								
	Fe	Al	Zn	Cu	Co	Pb	Ni	Mo	Cd
1	92800.0	39659.39	5035.38	4217.49	732.57	392.72	275.38	47.36	7.05
13	52080.0	231.61	1508.84	986.51	46.58	591.90	165.02	177.42	16.68
37	38780.0	80.30	493.52	131.04	24.78	61.67	71.50	31.26	3.34
66	67400.0	118.62	368.62	85.39	8.28	69.09	44.41	10.75	1.89
80	16900.0	84.85	743.54	40.91	5.60	25.91	32.32	7.52	1.12
94	18000.0	44.56	300.06	24.40	5.23	1.36	27.08	6.57	0.41
111	26950.0	131.17	666.11	35.39	7.92	21.35	43.80	7.19	0.83
129	24890.0	446.95	857.56	40.03	7.52	24.34	43.23	6.41	1.04
148	24780.0	170.15	657.62	22.37	7.49	11.42	36.42	6.32	0.58
190	16540.0	95.02	110.68	17.12	8.33	7.33	35.46	6.22	0.24
225	19750.0	164.05	403.05	26.39	18.85	7.97	35.94	7.48	0.63
259	12252.0	219.74	567.47	19.45	8.62	4.39	42.25	8.53	0.43
298	7512.0	182.56	561.85	20.02	10.08	4.15	48.28	10.03	0.40
338	1095.0	114.58	541.35	17.04	6.42	2.32	32.59	6.36	0.36
Day	**Total concentration, µg/litre**								
	Fe	**Al**	**Zn**	**Cu**	**Co**	**Pb**	**Ni**	**Mo**	**Cd**
1	190300.0	415127.00	5521.30	5018.82	857.10	852.19	757.29	49.73	13.74
13	142100.0	3990.00	1819.67	1292.33	75.47	1550.78	486.82	239.52	32.52
37	91700.0	1583.82	555.04	207.51	29.67	192.47	218.78	41.59	8.68
66	104100.0	1530.61	747.40	89.98	24.27	108.65	108.88	30.97	5.87
80	74200.0	1835.39	2451.24	131.56	5.81	130.68	41.77	30.93	6.94
94	57900.0	7405.25	389.92	78.64	7.45	315.19	52.40	10.38	5.14
111	68200.0	7635.53	1483.75	625.95	9.38	299.02	71.30	11.11	20.04
129	69000.0	3993.20	2189.83	1376.13	8.50	105.92	44.57	6.97	30.21
148	61500.0	506.54	711.03	105.95	8.44	52.31	43.59	5.89	4.67
190	54100.0	4638.72	200.79	146.80	11.90	35.41	64.89	10.99	4.17
225	33900.0	3897.88	529.92	135.25	40.54	37.03	62.89	12.93	3.90
259	33600.0	1687.98	689.10	119.72	22.28	71.13	43.72	15.32	6.45
298	36600.0	3950.13	582.42	80.36	14.30	39.54	51.65	9.56	3.72
338	3590.0	2727.94	591.57	67.66	11.53	48.85	42.60	7.76	5.18

The final total metals concentrations in CAR1 were found to be less than or comparable to the European Drinking Water Standards (EDWS) (Council Directive 98/83/EC) which is an extremely strict standard for leachate. For example, *Zn*, *Cu*, *Co* and *Mo* concentrations (and their EDWS concentrations listed in parentheses) were 591.6(5000), 67.7(2000), 11.5(no EDWS) and 7.8(no EDWS) µg/litre and were found to be below the

standards. *Fe, Al, Pb, Ni* and *Cd* concentrations (and their EDWS) were 3590.0(200), 2727.9(200), 48.8(25), 42.6(20), 5.2(5) µg/litre and were found to exceed the standards. While these data suggest that metal concentrations will not be problematic for the environment in a short-term, their long-term effect remains to be established due to the possibility of remobilization of metals if the landfill becomes aerobic (section 2.3.4).

It should be noted that the heavy metal concentrations were elevated in the CAR1 with the anaerobic sludge addition at the beginning of the experiment. The actual contribution of the sludge to leachate heavy metals is shown in Table 6.3.

Table 6.3. Sludge contribution to leachate heavy metal concentrations.

Fe	Al	Zn	Cu	Co	Pb	Ni	Mo	Cd
Dissolved concentration, µg/litre								
347.8	394.40	872.23	35.69	2.13	5.73	7.14	0.07	0.42
Total concentration, µg/litre								
15963.0	11968.47	2541.66	1298.63	9.56	352.92	125.96	16.85	6.54

6.1.10. Summary

- The total magnitude of settlement in CAR1 after 338 days was approximately 9.0%. During the test in CAR1, it was determined that 43% of the total settlement took place within 65 days after loading and a further 57% settlement occurred over a longer period of time due to degradation effects;
- The total gas production from the CAR was 79.43 litres at STP (1.41 litres/kg dry wt.) by day 338, at which time over 64.8% of the biogas was methane and 25.9% CO_2;
- At day 65 of the experiment all the sulphate in the leachate was removed and this resulted in a simultaneous increase in the rate of biogas production;
- A gradual increase in the ammonium concentration to a level of 302.3mg/l during the test period was observed;
- Results highlight the importance of temperature in promoting stabilisation of the waste. Upon heating the reactor to a temperature of approximately 35°C at day 65, a noticeable increase in the rate of gas production was immediately observed. Rates of gas production, removal of sulphate and enhanced ammonia production were all immediately increased by the increase in the temperature. Additionally, there was also a dip in the pH from neutrality to about 6.8;

- A gradual removal of Ca^{2+} and Mg^{2+} ions from the leachate was observed during the waste biodegradation process. This was almost certainly due to the precipitation of the elements and this may have been triggered by the onset of microbial activity observed with heating; and
- The test results indicate that about 97% of *Al*, *Zn*, *Cu* and *Co*, about 83% of *Pb* and *Ni*, about 75% of *Mo* and *Cd*, and 27% of *Fe* were removed from the liquid phase via form of metabolic uptake within the first 66 days of the experiment due to the establishment of a highly reducing environment and the formation of sulphide from the sulphate reduction. The final total metals concentrations in CAR1 were found to be less than or comparable to the European Drinking Water Standards (EDWS) (Council Directive 98/83/EC) which is an extremely strict standard for leachate.

6.2. Prediction the rate and potential of MSW biodegradation in CAR1 filled with AG waste sample (BMP test 2)

A second BMP test (BMP2) (described in section 5.2) was performed to characterize the anaerobic biodegradation potential of an aged MSW (AG waste sample). This characterization included the measurement of the component quality and quantity of the biogas produced, determination of the loss of cellulose and hemicellulose as indicated by measurements of Neutral Detergent Fibre (NDF) and Acid Detergent Fibre (ADF), and the assessment of various leachate chemical characteristics at key phases during the biodegradation process. The biodegradable processes in the bioreactors were studied over a period of 338 days at approximately 30°C. The reactors were sequentially sacrificed at different stages of the biodegradative process, as dictated by the gas production rate, and samples from the waste, leachate and gas fraction taken for chemical analyses. The various stages of the degradation process were identified and characterised according to changes in the methane yield of the waste remaining with respect to the remaining levels of NDF and ADF and the cellulose plus hemicellulose to lignin ratio ((C+H)/L).

6.2.1. Biogas production and pH (BMP test 2)

Cumulative gas production data for the various BMP test reactors are presented in Figure 6.16, and the cumulative volume of methane produced from each BMP test reactor is given in Table 6.4. This data has been corrected for gas production due to the anaerobic sludge seed observed in the control bottle which was found to be 19.3% (B7), 47.8% (B8) and 45.8% (B9) of the total biogas produced in the reactors. The pH values of the

leachate samples taken when the BMP test reactors were destructively sampled on days 68, 196 and 338 days respectively are shown in Figure 6.17. Initially, the pH of the leachate was 7.1, although this value dropped to 6.8 after 68 days then increased gradually to a level of 7.1 by the end of the test.

Table 6.4. Methane production and fibre analysis data for sampled BMP2 reactors.

Waste sample	Initial waste	B7	B8	B9	Final waste in CAR1
Days into test	0	68	196	338	338
Dry mass, kg	0.140	0.137	0.131	0.124	50.00[1]
Cumulative biogas production (STP)[2], l/kg DM	0.00	0.46	0.85	1.24	0.93
Cumulative methane production (STP), litres /kg DM	0.00	0.23	0.49	0.76	0.60
NDF, g/kg DM	148.26	148.55	136.18	123.95	126.59
NDF[3], %	14.83	14.86	13.62	12.40	12.66
ADF, g/kg DM	140.66	142.33	126.18	118.81	119.87
ADF[3], %	14.07	14.23	12.62	11.88	11.99
ADL(Lignin), g/kg DM	91.28	90.39	75.18	84.10	89.20
ADL(Lignin)[3],%	9.13	9.04	7.52	8.41	8.92
Cellulose, g/kg DM	49.38	51.93	51.00	34.71	30.67
Cellulose[3], %	4.94	5.19	5.10	3.47	3.07
Hemicellulose, g/kg DM	7.59	6.22	10.00	5.14	4.74
Hemicellulose[3],%	0.76	0.62	1.00	0.51	0.47
(C+H)/L ratio[3]	0.62	0.64	0.81	0.47	0.42
TC, g/kg DM	316.82	300.51	294.93	293.12	288.87
TC[3], %	31.68	30.05	29.49	29.31	28.89
TN, g/kg DM	5.93	7.34	6.61	6.30	7.42
TN[3], %	0.59	0.73	0.66	0.63	0.74
LOI, g/kg DM	510.89	497.66	499.04	488.85	492.55
LOI[3], %	51.09	49.77	49.90	48.89	49.26
TC utilised, g/kg DM	0.00	16.31	21.89	23.70	27.95
Methane recovery (STP)[4], %	0.00	0.97	2.08	3.21	2.55

Note: [1] Estimated value calculated by assuming loss of dry mass similar to that observed in the BMP2 test; [2] Corrected for sludge contribution to biogas production; [3] The data are presented as a percentage of the final waste dry mass ; and [4] The measured cumulative methane production at STP divided by the theoretical production calculated by assuming conversion of 100% of the cellulose and hemicellulose to methane and carbon dioxide (Eq. 6.3).

The total biogas production (carbon dioxide + methane) from the waste sample in the BMP2 reactors per kg dry matter was 1.24 litres at STP, at which time over 61.5% vol. of the biogas produced was methane and 28.40% carbon dioxide (Figure 6.16 & Figure 6.18). The maximum daily gas production rate was recorded for test reactor B9 on day 110 (0.09 litres/kg dry wt. waste/day) (Figure 6.19).

The initial cellulose, hemicellulose, lignin and LOI content for the waste used in this study were 4.94%, 0.76%, 9.13% and 51.09% respectively (Table 6.4). The theoretical methane potential, based on complete cellulose and hemicellulose conversion to methane, was calculated using the stoichiometric relationships given in Eq. 6.1 & Eq. 6.2 respectively (Barlaz, 2006). In each equation, the same molar quantities of CH_4 and CO_2 are produced. Biogas typically contains more CH_4 than CO_2 because CO_2 is partially soluble in water and therefore it can be expected that some would dissolve in the leachate.

Eq. 6.1. $$(C_6H_{10}O_5)_n + nH_2O \rightarrow 3nCH_4 + 3nCO_2$$

Eq. 6.2. $$(C_5H_8O_4)_n + nH_2O \rightarrow 2.5nCH_4 + 2.5nCO_2$$

The theoretical methane potential of cellulose ($C_6H_{10}O_5$) and hemicellulose ($C_5H_8O_4$) was then calculated to be 414.8 and 424.2 litres methane per kg dry weight of cellulose and hemicellulose respectively at STP (Eq. 6.1 & Eq. 6.2, Barlaz, 2006). Using data for cellulose and hemicellulose content of the waste presented in Table 6.4 it can be calculated that the theoretical methane production per kg dry weight of waste is 414.8 x 0.0494 = 20.49 litres and 424.2 x 0.0076 = 3.22 litres respectively. The total loss of cellulose and hemicellulose in the reactors was found to be 14.67g/kg dry wt. and 2.45g/kg dry wt. respectively, which should lead to a production of 414.8 x 0.01467 = 6.09 litres of methane/kg of dry waste as a result of cellulose degradation and 424.2 x 0.00245 = 1.04 litres methane/kg of dry waste due to hemicellulose degradation at STP. The methane potential of lignin was considered to be zero because of its inability to decompose under anaerobic conditions (Young & Frazer, 1987). In this study, the total measured methane production from the reactors at STP was found to be only 1.24 l/kg dry weight which gives a methane recovery of 3.21% calculated using the following equation:

Eq. 6.3. $$[CH_4]_{rec},\% = \frac{[CH_4]_m}{[CH_4]_t} \times 100$$

where $[CH_4]_{rec}$ is the methane recovery in %; $[CH_4]_m$ is the measured cumulative methane production at STP in l/kg wt.; and $[CH_4]_t$ is the theoretical methane production per kg dry wt. calculated by assuming conversion of 100% of the cellulose and hemicellulose to methane and carbon dioxide.

The total measured methane production in the BMP3 bottles (1.24 l/kg dry weight) is much less than the expected methane production which was calculated based only on the total dry mass of cellulose and hemicellulose removed during the test (6.09 + 1.04 = 7.11 l/kg dry wt.). This discrepancy between the calculated methane production (7.11 litres CH_4) and the measured methane production (1.24 l/kg dry wt.) is probably due to the fact that some carbon is utilised by the bacteria for cell growth rather than gas generation, and that some is dissolved in the leachate, or could be attributed to the waste age which was found to be 15 years (section 5.1), or to the following sources of errors: unaccounted gas production due to leakage of gas, sampling errors and analytical errors related to gas composition analysis. Non-availability of the cellulose of the aged waste was also suggested by Barlaz *et al.* (1989[b]) in optimized laboratory studies of anaerobic degradation.

6.2.2. Leachate characteristics (BMP test 2)

Eight VFAs were analyzed in the leachate – acetic, propionic, n- and iso-butyric , n- and iso-valeric, caproic and caprylic acids. Only the concentrations of acetic, propionic, n-butyric and caprylic acids are shown (Figure 6.17). The highest total volatile fatty acid concentration was observed to be 503.53mg/l at the beginning of the biodegradation period. Thereafter, the accumulation of carboxylic acids decreased rapidly as they were utilised faster than they were being produced. At the same time the methane production rates were observed to decrease gradually after day 35 (Figure 6.17 & Figure 6.19).

The total organic carbon (TOC) content of the leachate samples taken from the reactors was found to decrease gradually from an initial value of 895.4mg/l to a level of 259.3mg/l by the end of the test (day 338) (Figure 6.20). The dissolved organic content of the samples (TDOC) however, determined after filtering through Whatman GF/C filters, increased from 108.3mg/l (day 1) to 240.8mg/l (day 338). This increase was most likely due to the degradation of solid organic matter resulting in the formation of a range of soluble organic compounds as yet unidentified.

6.2.3. Chemical composition of solid waste samples (BMP test 2)

To monitor the progression of carbon speciation from the solid waste samples to the liquid and gas phases a carbon mass balance was undertaken. After 338 days the BMP2 bottle tests were emptied and samples from the waste, leachate and gas fractions taken for total carbon analyses. The results were compared with those obtained from similar samples taken from CAR1. The duration of the tests and the initial waste characteristics for both experiments were the same. A comparison of the mass balance for CAR1 and all the BMP2 bottles containing the waste sample is shown in Table 6.5. The data on the carbon balance in BMP2 test and CAR1 indicate that the carbon which was utilised during the biodegradation period was 23.70g/kg dry wt. and 27.95g/kg dry wt. respectively. Additionally, the carbon mass balance calculations provide a good relationship between the waste TC and the cumulative biogas production in BMP2 test with $R^2 = 0.87$ (Figure 6.21). As shown in Table 6.5 the utilised during the biodegradation period total carbon that was transferred into biogas was only 2.52% for BMP2 bottle test and 1.62% for the CAR by the end of the test. Data also shows that the mass of the initial carbon which was transferred into leachate after 338 days was relatively low (5.63% for BMP2 test and 2.39% for the CAR). Although this can almost certainly be attributed to the age of the waste (15 years) where it can be expected that the most readily biodegradable fraction of the original waste would have been already remineralised. In this instance, the majority of the total carbon released from the solid fraction of the waste during biodegradation was thought to be either precipitated as $CaCO_3$ and/or utilised for bacterial biomass. The loss of carbon to deposition of carbonate precipitates was estimated using the drop in calcium concentrations between the beginning and the end of the test (Figure 6.22), although other carbonate species could have been formed. It was found that only 0.66% of the TC loss was fixed within the consolidating reactor at the end of the test period as $CaCO_3$ precipitates, whereas this amount was 2.04% for the BMP2 test. Mg^{2+} did not precipitate as $MgCO_3$ over the test period due to insufficient anions to form $MgCO_3$. Precipitation of $CaCO_3$ and $MgCO_3$ is discussed in great details in section 7.1.8.

The results of the carbon mass balance carried out for BMP2 bottles and CAR1 indicate that carbon inputs exceeded carbon outputs by 7.55% and 8.82%, respectively (calculated by Eq. 5.8) (Table 6.5). This difference is probably due to the fact that some carbon is utilised by the bacteria for cell growth rather than gas generation, and that some is

dissolved in the leachate, or could be due to the waste age (15 years, see section 5.1), or to the sources of errors similar to those listed in section 6.2.1.

Table 6.5. Summary of carbon mass balance for AG waste sample.

Parameter	BMP2	CAR1
$TC_{t=o,\ waste}$, g/kg DM.	316.82	316.82
$TC_{t=o,\ leachate}$, g/kg DM.	2.97	1.47
$TC_{t=ti,\ waste}$, g/kg DM.	293.12	288.87
$TC_{t=ti,\ leachate}$, g/kg DM.	1.33	0.67
$TC_{t=ti,\ CaCO_3}$, g/kg DM.	0.48	0.18
$TC_{t=ti,\ MgCO_3}$, g/kg DM.	0.09	0.02
$TC_{t=ti,\ CH_4}$, g/kg DM.	0.41	0.32
$TC_{t=ti,\ CO_2}$, g/kg DM.	0.19	0.13
Unaccounted C[1], g/kg DM.	24.16	28.09
Mass balance error[2], %	7.55	8.82

Note: $TC_{t=o,\ waste}$ indicates the total carbon in the wastes before the beginning of the test; $TC_{t=ti,\ waste}$ indicates the total carbon in the waste samples after 340 days of test; $TC_{t=o,\ leachate}$ and $TC_{t=ti,\ leachate}$ are the TC content (TOC+IC) of leachate samples taken at time t = 0 and t = i respectively; $TC_{t=ti,\ CaCO_3}$ is the carbon content as $CaCO_3$ (precipitated and dissolved) in the leachate at time t = i; $TC_{t=ti,\ MgCO_3}$ is the carbon content as $MgCO_3$ (dissolved only) in the leachate at time t = i; $TC_{t=ti,\ CH_4}$; $TC_{t=ti,\ CO_2}$ are the carbon in the biogas as methane and carbon dioxide respectively, at the end of the test; [1] calculated by Eq. 5.7; and [2] calculated by Eq. 5.8.

A compilation of data from the literature on carbon conversion during degradation of waste suggests that landfill leachates are characteristically saturated with respect to calcite ($CaCO_3$), for a range in pH (5.9-8.1) (Manning and Robinson, 1999). Mineralogical analysis of suspended solids from the leachate identified the presence of calcite, which also occurs as scale form which has been observed to form in drainage systems (Fleming *et al.*, 1999). Niemann and Hatheway (1997) carried out experiments to determine the stability of carbonate aggregate in the presence of model leachates. Their results showed negligible carbonate dissolution at pH 6-6.5. In these circumstances, using mass balance considerations (Table 6.5), it can be shown that between 87.08 and 96.58% of the total carbon loss may be fixed within the reactors as calcium carbonate or biomass.

Average values of NDF, ADF, hemicellulose, cellulose and lignin contents of the waste samples taken at different stages of the biodegradation process are shown in Table 6.4. All the data are presented as a percentage of the waste dry mass.

The NDF content, which is indicative of the entire fibre fraction of the waste, showed a decreasing trend over the test period (Figure 6.23). The NDF degradation rate shows gradually increasing trend over the testing period with indicating cellulose and hemicellulose degradation. A similar trend was showed for the ADF data which represents a portion of the waste that contains only cellulose and lignin (Figure 6.24). The NDF and ADF average biodegradation rates were observed to be approximately 0.07g/kg dry wt./day for both.

The cellulose content was estimated using Eq. 2.42. The percentage of cellulose in the waste decreased with sample age at an average rate of 0.043g/kg dry wt./day over a period of 338 days. Thus, 30% of the cellulose degraded over the period of 338 days (Table 6.4). As discussed in section 2.5, cellulose content should decrease in proportion to waste TC content. However, the TC content of solid waste samples tested showed a decreasing trend over the test period which was found not to be consistent with the depletion of cellulose (Figure 6.25). To better understand this relationship, the cellulose concentration was plotted against TC in Figure 6.26. As can be seen, the correlation between these two parameters was found to be very poor (R^2=0.17). This could be attributed to the age of the waste (15 years) where it can be expected that the most readily biodegradable cellulose of the original waste would have been already degraded. Based on a number of excavation studies Ham and Bookter (1982) observed that the extent of cellulose decomposition varied with landfill conditions and did not appear to completely degrade. Various researchers have also found that at least 18% of the cellulose and hemicellulose in waste is not available for degradation due to variations in its degree of crystallinity and its association with lignin (Bingemer & Crutzen, 1987; Bogner, 1992; Bogner & Spokas, 1995) (section 2.5).

Hemicellulose was assessed as the NDF value minus the ADF values (Eq. 2.43). Even though the data for hemicellulose content was inconsistent, there was a 33% decrease in the hemicellulose content by weight during the period of the BMP test.

The test results show that (C+H)/L ratio in the analysed samples decreased with increasing volume of biogas (Figure 6.27). It was determined that the (C+H)/L ratio decreased inconsistently (only by 33% over the biodegradation period of 338 days) and this can almost certainly be attributed to the age of the waste (15 years) where it can be expected that the waste would contain very little readily biodegradable organic components and any polymers remaining would also be very resistant to degradation.

6.2.4. Correlation between fibre analysis data and BMP test 2 data

NDF, ADF, cellulose, (C+H)/L ratio, waste TC, and waste biochemical methane potential are all parameters that have been used to assess the biodegradation potential of both fresh and aged MSW. Correlations between these parameters were shown to exist for the BMP test reactors used in this study (Figure 6.25 to Figure 6.28). Results show that these parameters were all decreased by degradation. There was not a good statistical correlation between cellulose content and the cumulative methane production rate with R^2 value of 0.54 (Figure 6.28). Comparison between the methane production and LOI indicates that there was a good correlation between these two parameters (R^2 value of 0.62) (Figure 6.29). The data presented in Figure 6.30 also shows a very good correlation between the ADF degradation rate and methane recovery of the waste (Eq. 6.3) (R^2 value of 0.74). The best correlation found was between the NDF biodegradation rate and the methane recovery of the waste with a R^2 value of 0.87 (Figure 6.31). There was not a good statistical correlation between the (C+H)/L ratio and the cumulative methane production for the BMP2 bottles (R^2=0.08, graph is not shown) possibly due to the age of the waste where it can be expected that all the biologically available carbon had already been degraded. This led to the conclusion that measured cellulose and hemicellulose content in well degraded samples did not represent all the potentially bioavailable carbon in the aged samples.

6.2.5. Summary

The data from this test indicates that well degraded MSW still contain a significant percentage of slowly degradable organic matter which remains in the waste for a long period of time. It was also found that the parameters NDF, ADF, cellulose and methane potential for the BMP2 test samples were interrelated. The (C+H)/L ratio, in this instance, was found not to be correlated with the methane produced, which led to the conclusion that the measured cellulose and hemicellulose content in well degraded samples did not represent total bioavailable carbon. To provide an accurate prediction of the degree of biodegradation and BMP of a test sample, the test findings were further explored however using a greater number of BMP test bottles filled with a fresh readily degradable MSW (section 7.4).

Figures

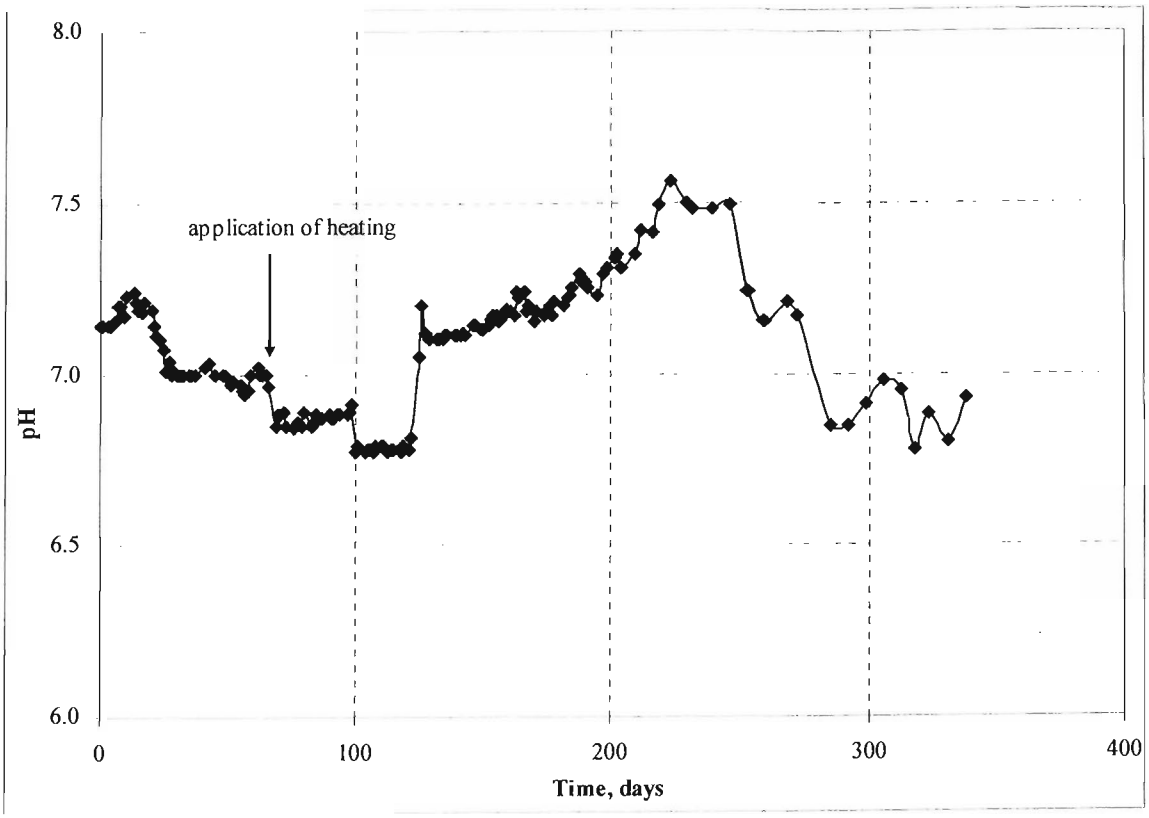

Figure 6.1. pH in CAR1.

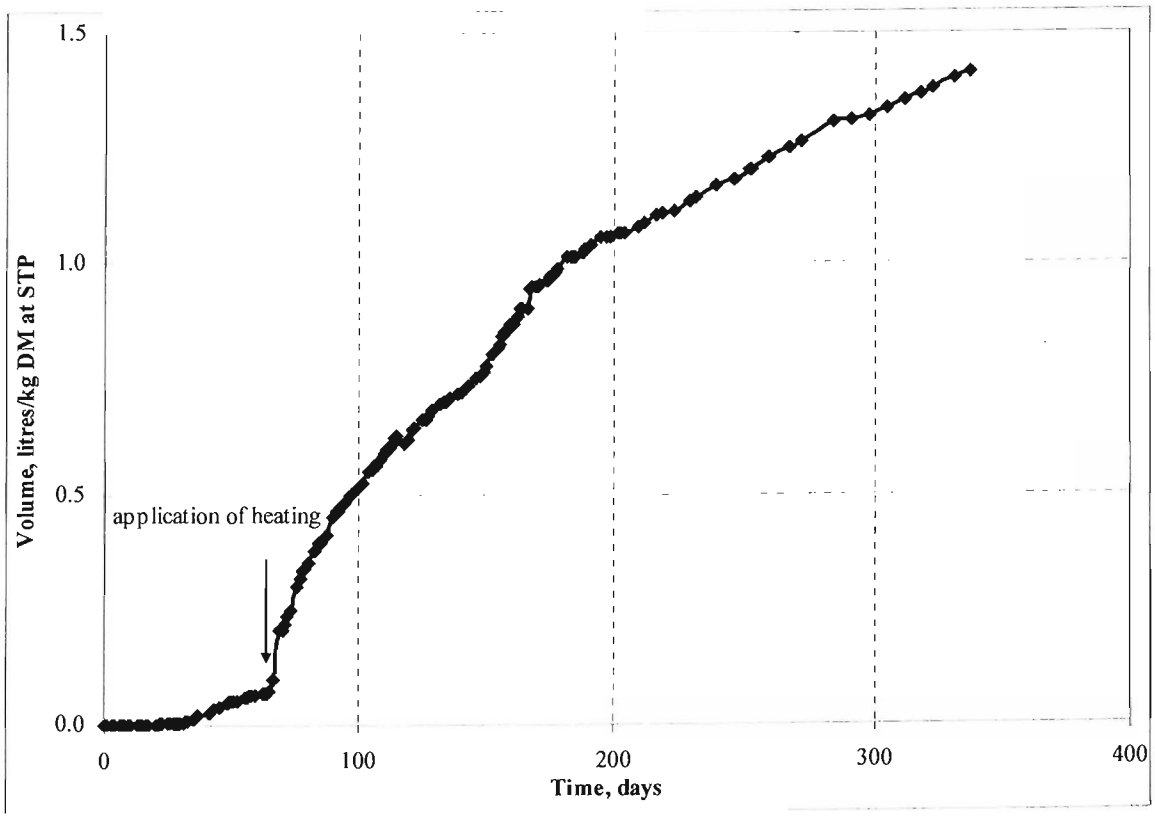

Figure 6.2. Cumulative gas production for CAR1 (AG waste sample).

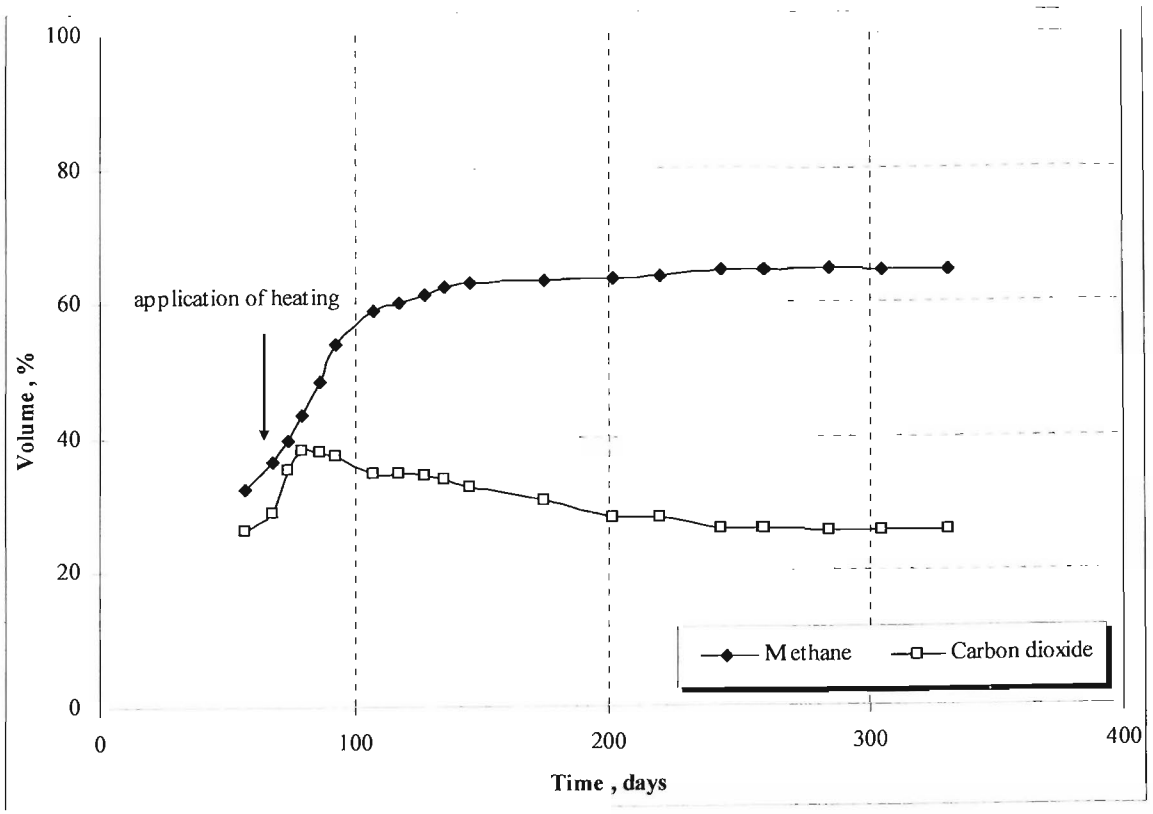

Figure 6.3. Gas composition for CAR1.

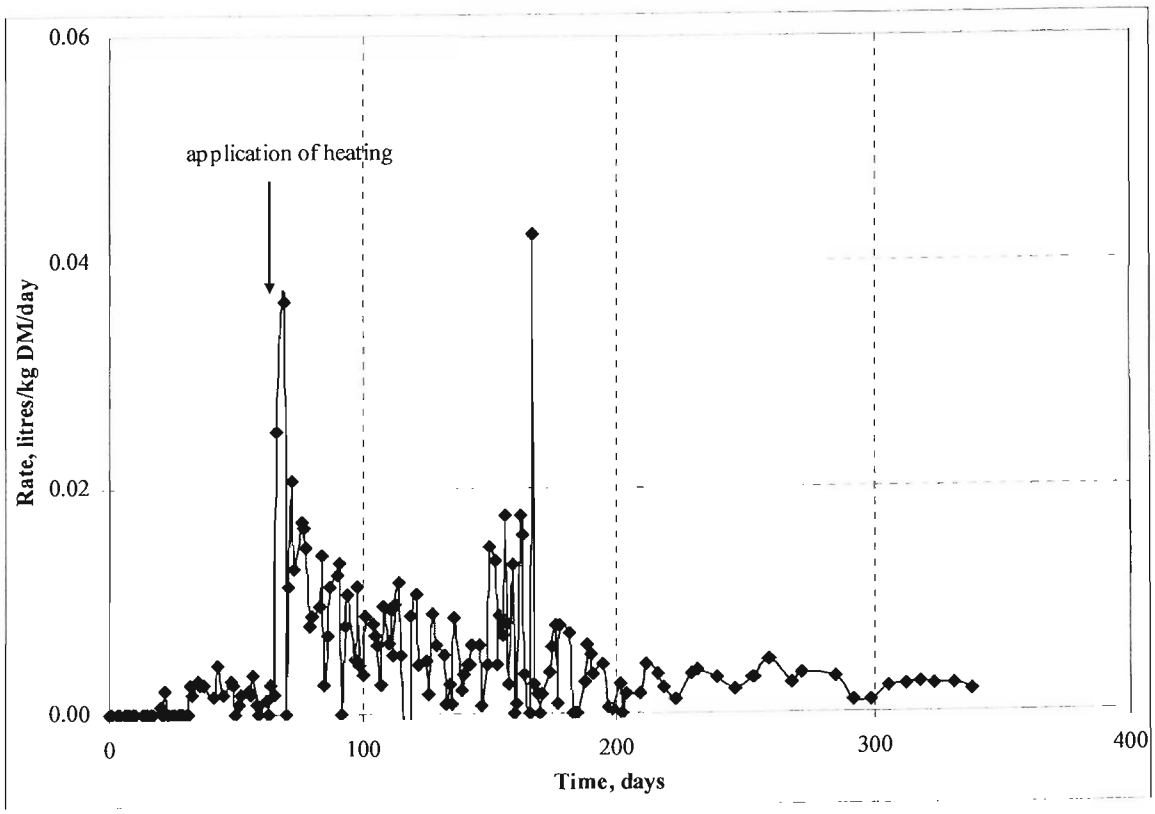

Figure 6.4. Daily gas production in CAR1.

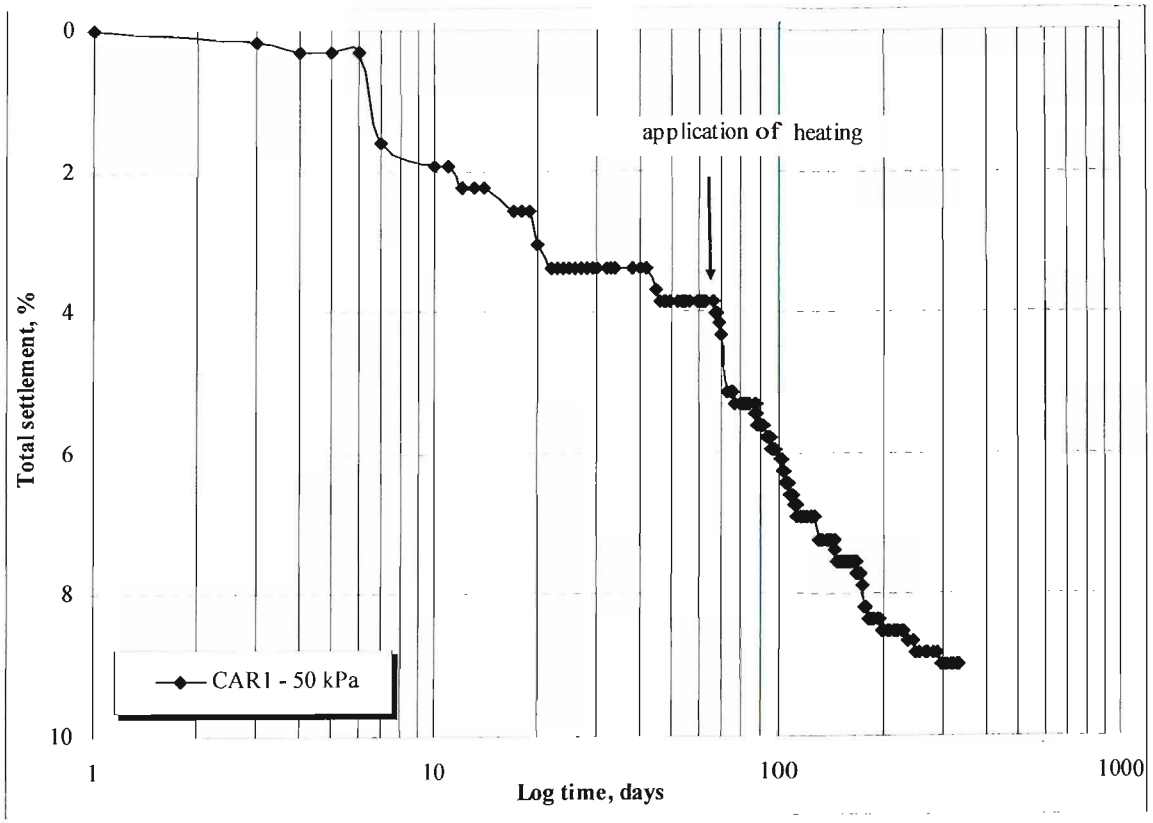

Figure 6.5. Observed total settlement in CAR1.

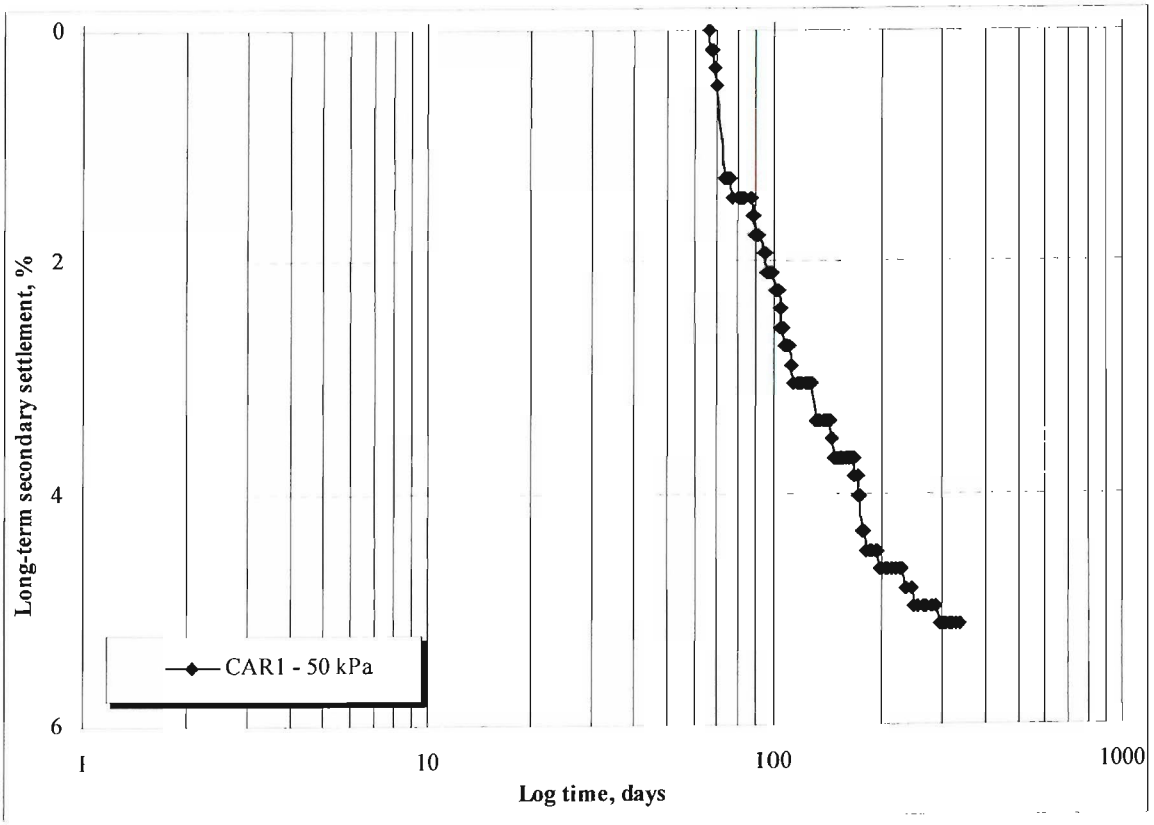

Figure 6.6. Observed long-term secondary settlement in CAR1.

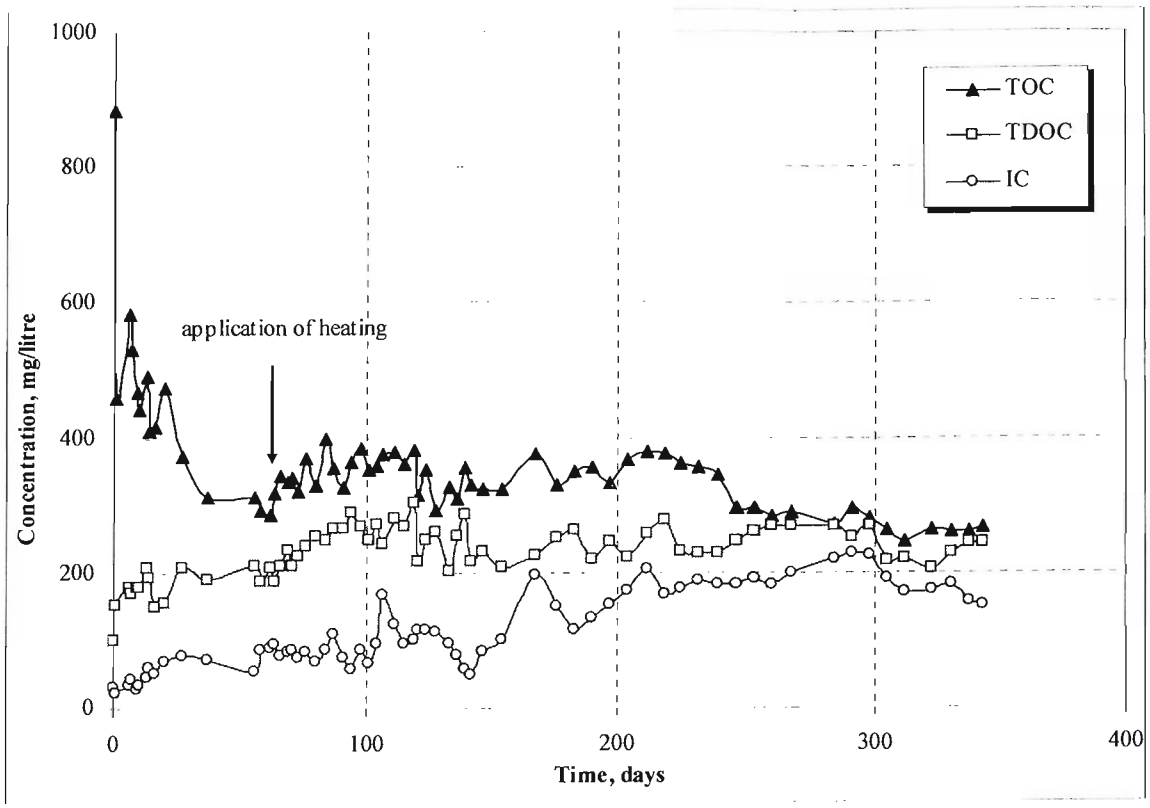

Figure 6.7. Leachate carbon in CAR1.

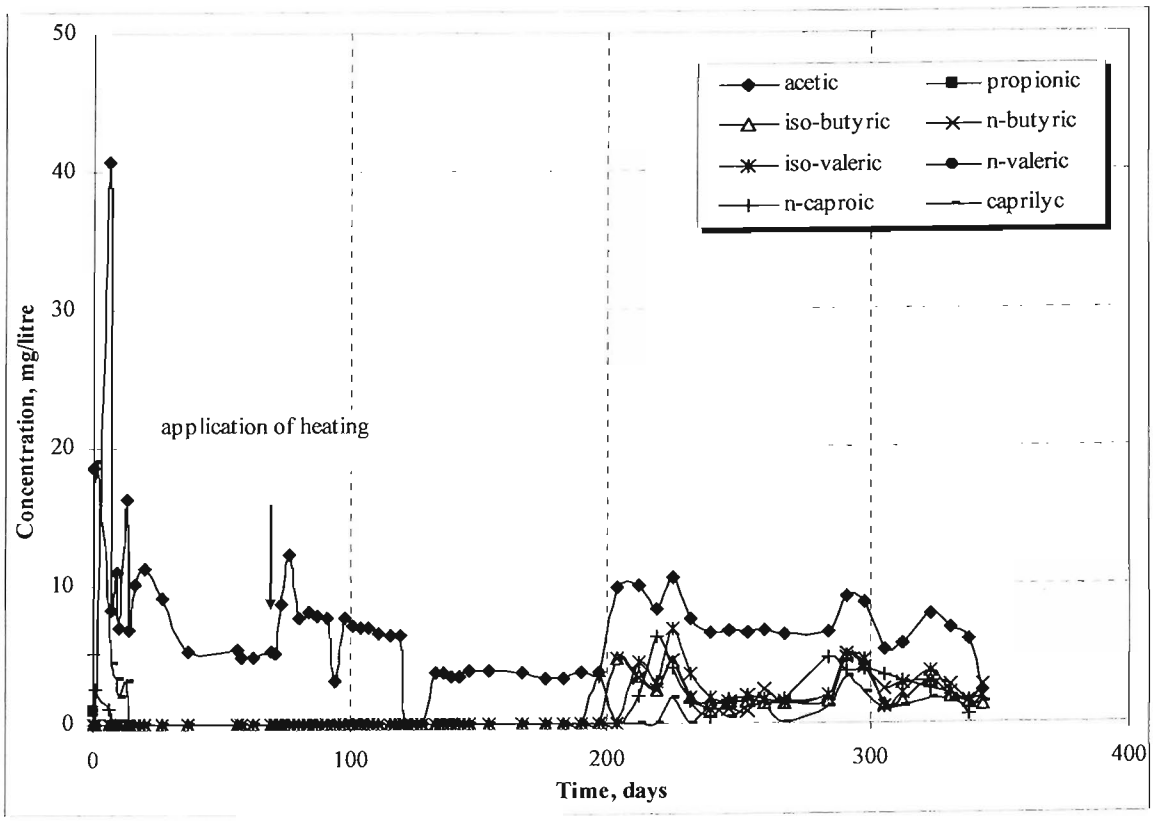

Figure 6.8. Leachate VFAs in CAR1.

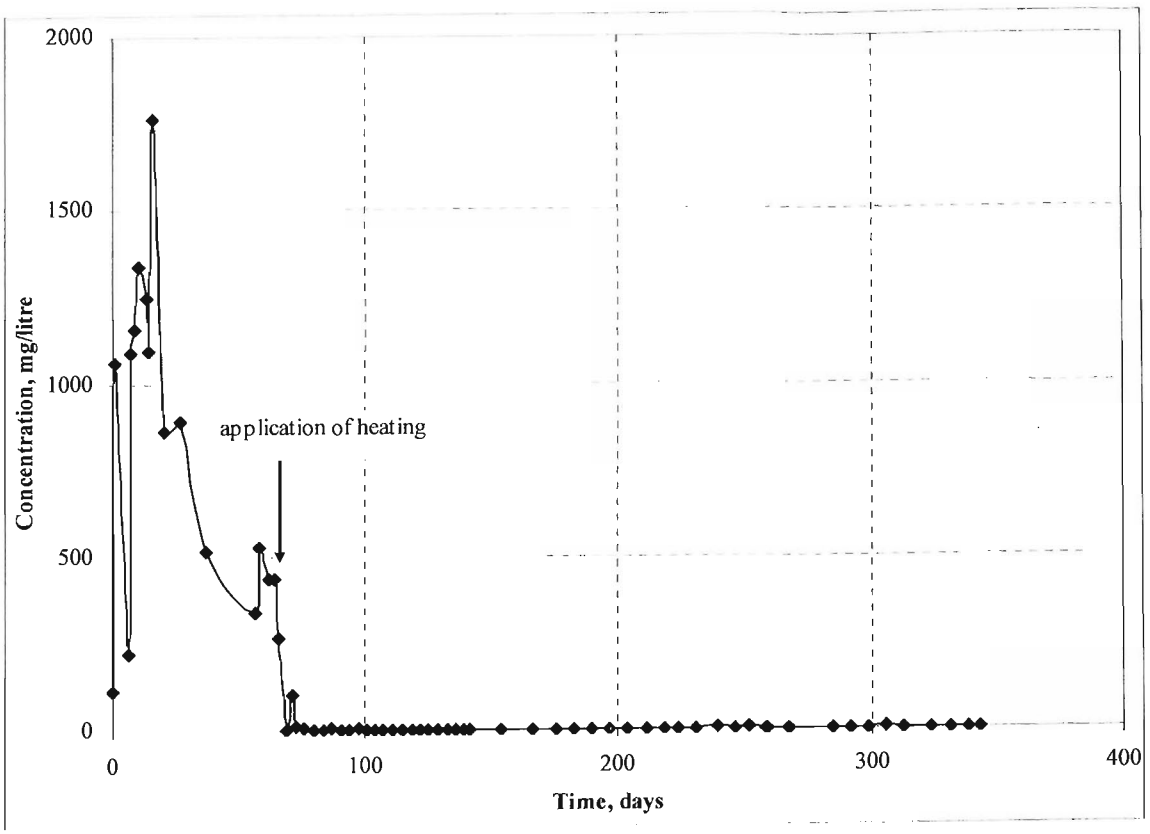

Figure 6.9. Sulphate concentration in CAR1.

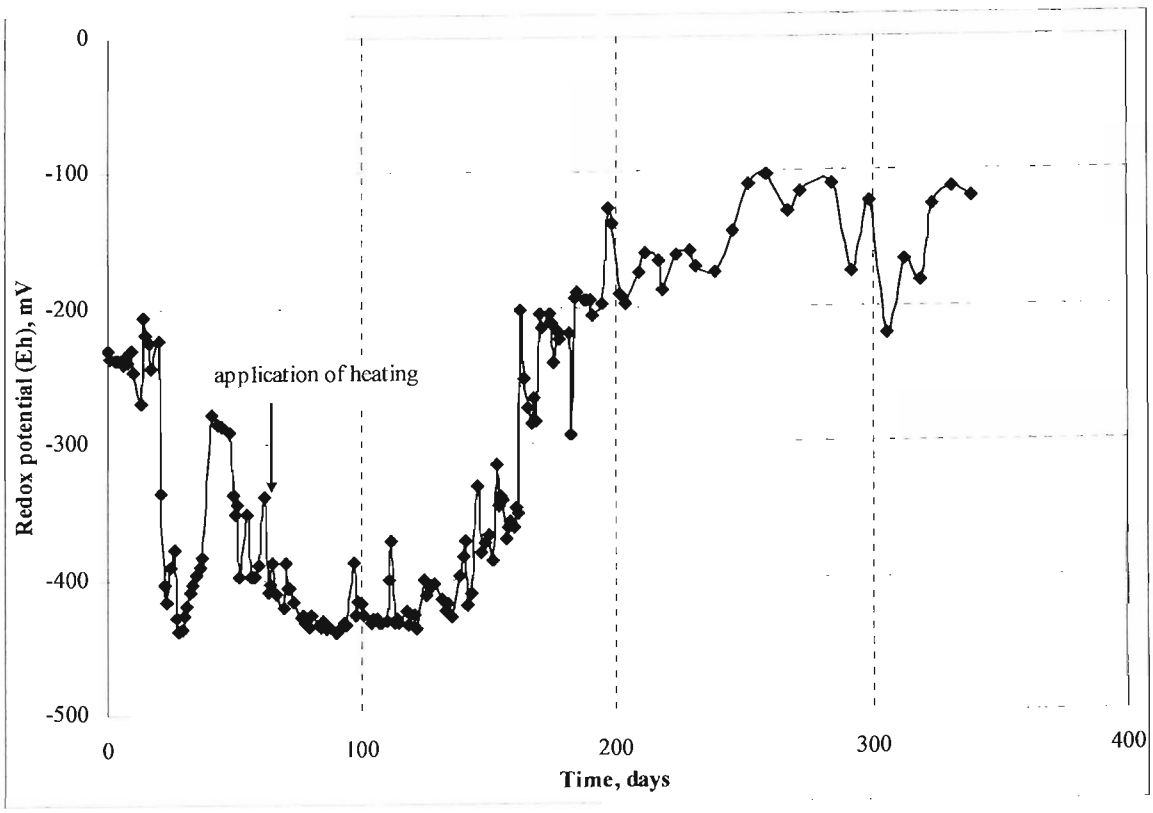

Figure 6.10. Redox potential in CAR1.

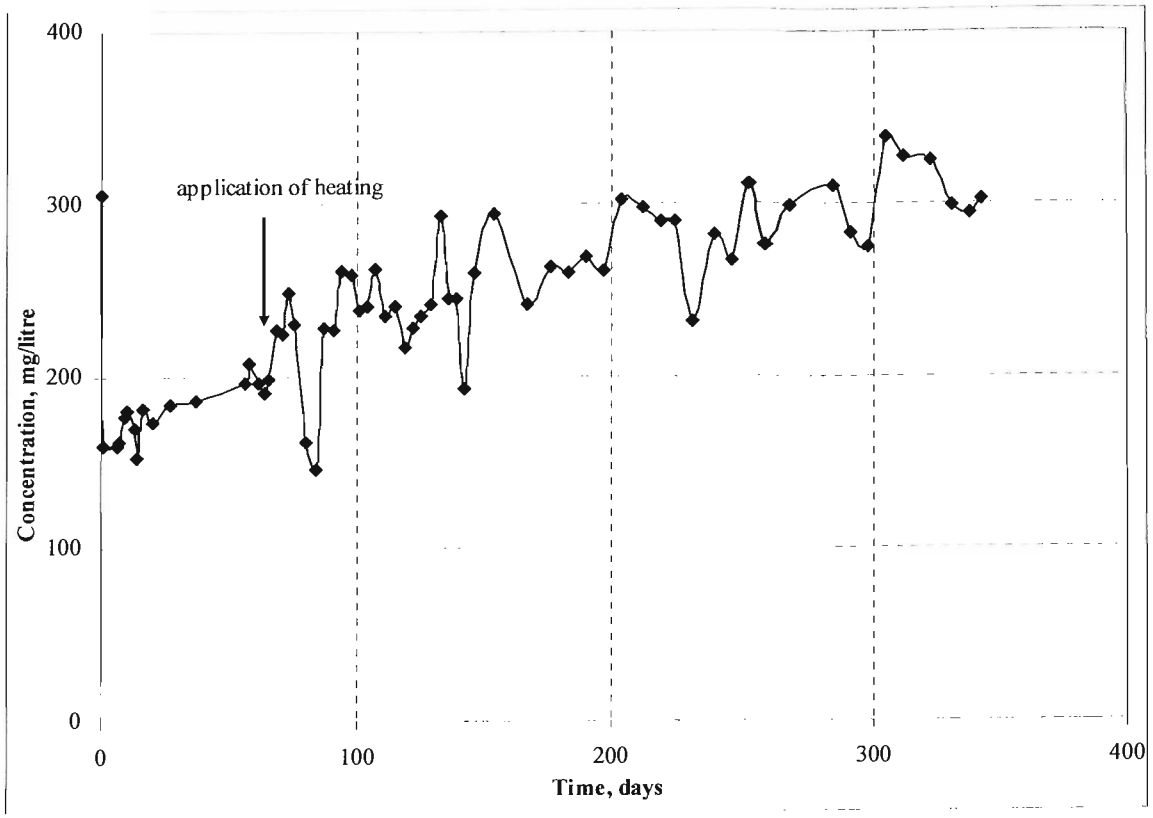

Figure 6.11. Ammonium concentration in leachate in CAR1.

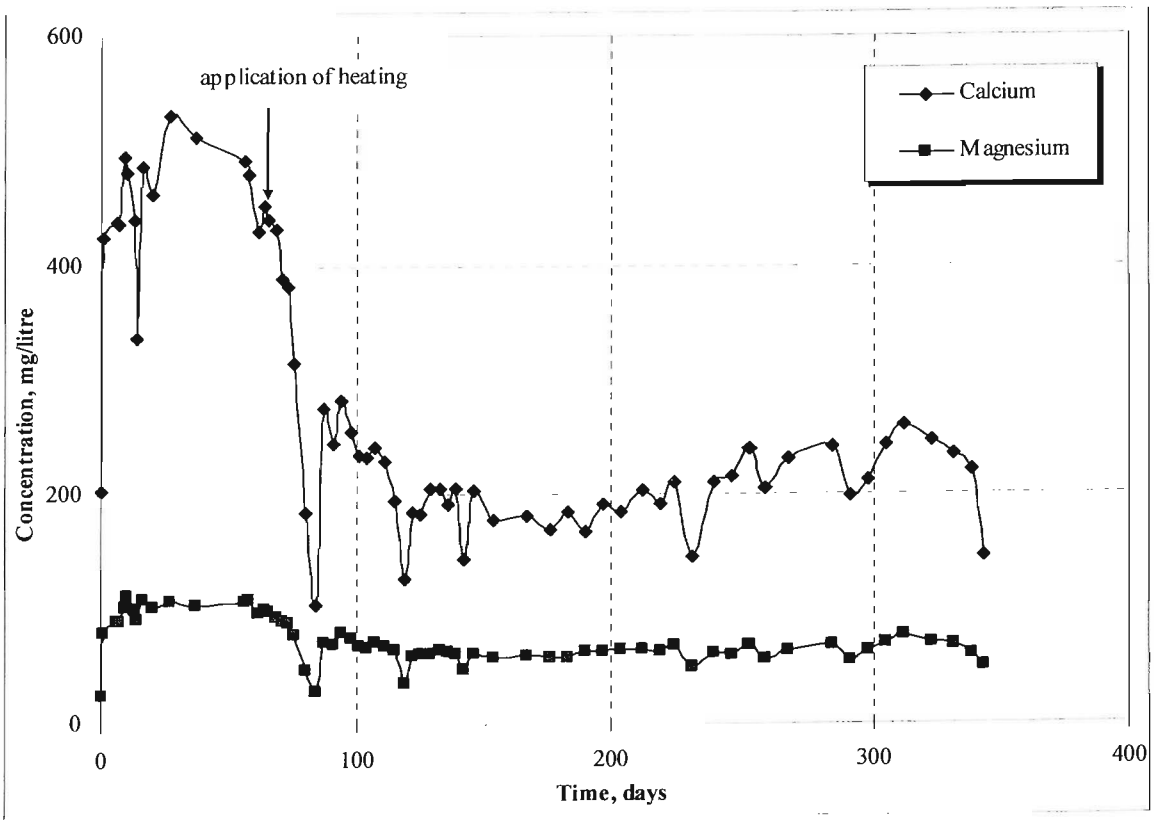

Figure 6.12. Calcium and magnesium concentrations in leachate in CAR1.

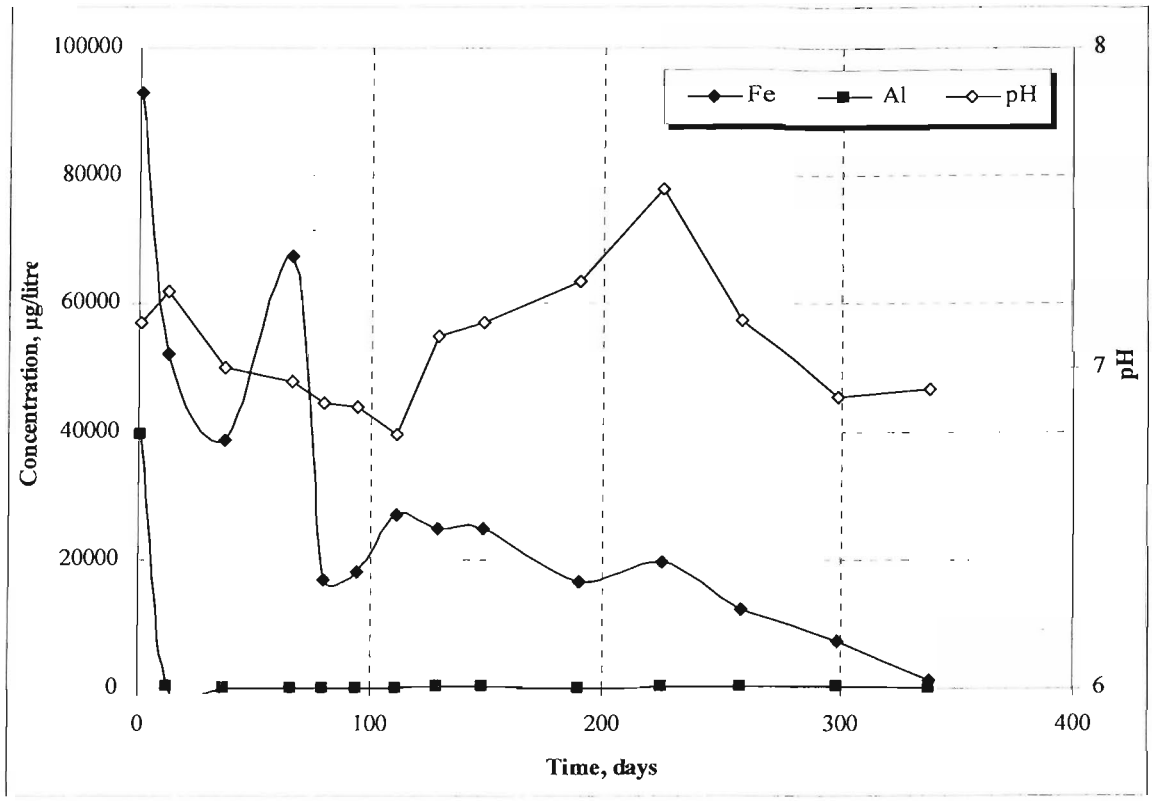

Figure 6.13. Fe and Al concentrations in leachate in CAR1.

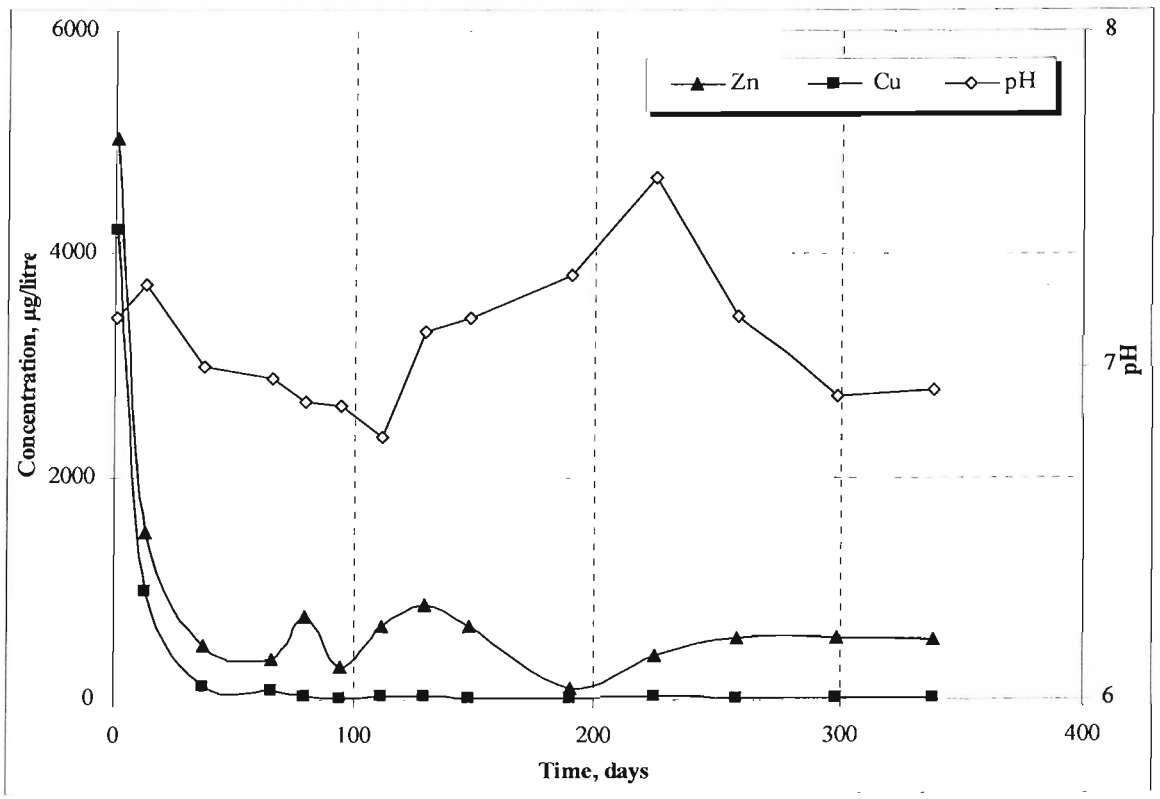

Figure 6.14. Zn and Cu concentrations in leachate in CAR1.

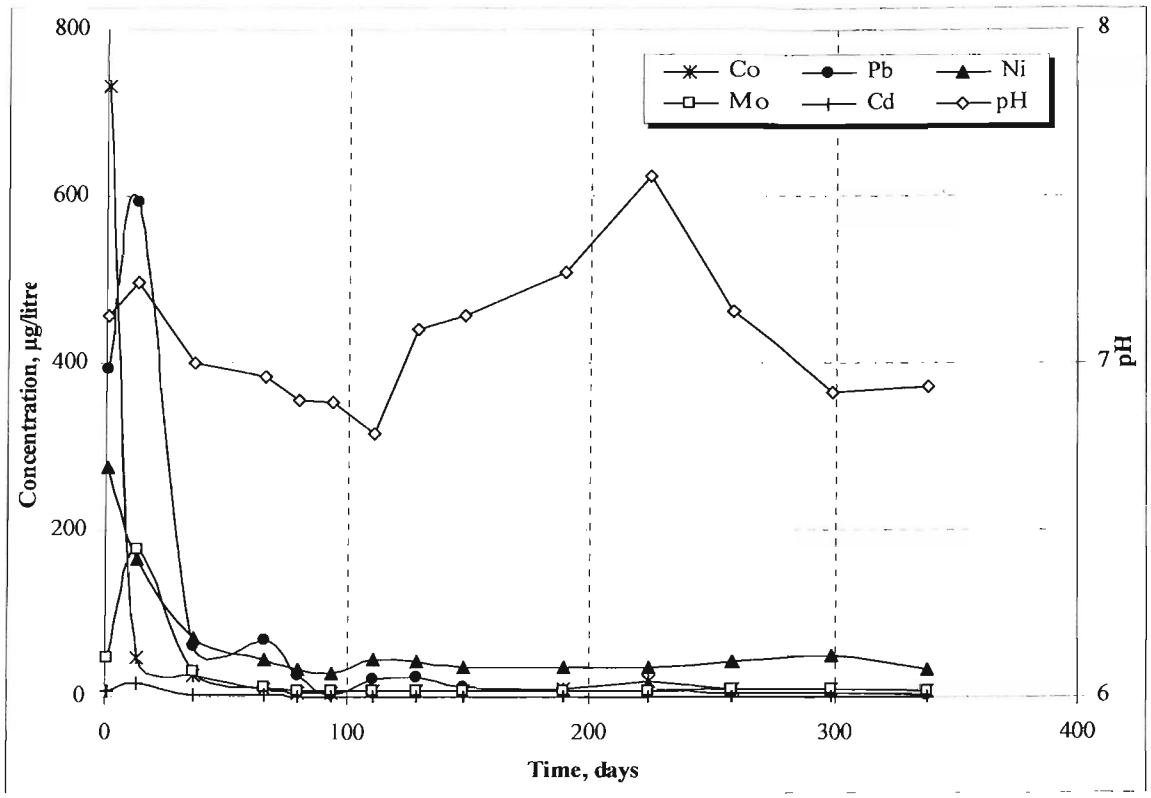

Figure 6.15. Co, Pb, Ni, Mo and Cd concentrations in leachate in CAR1.

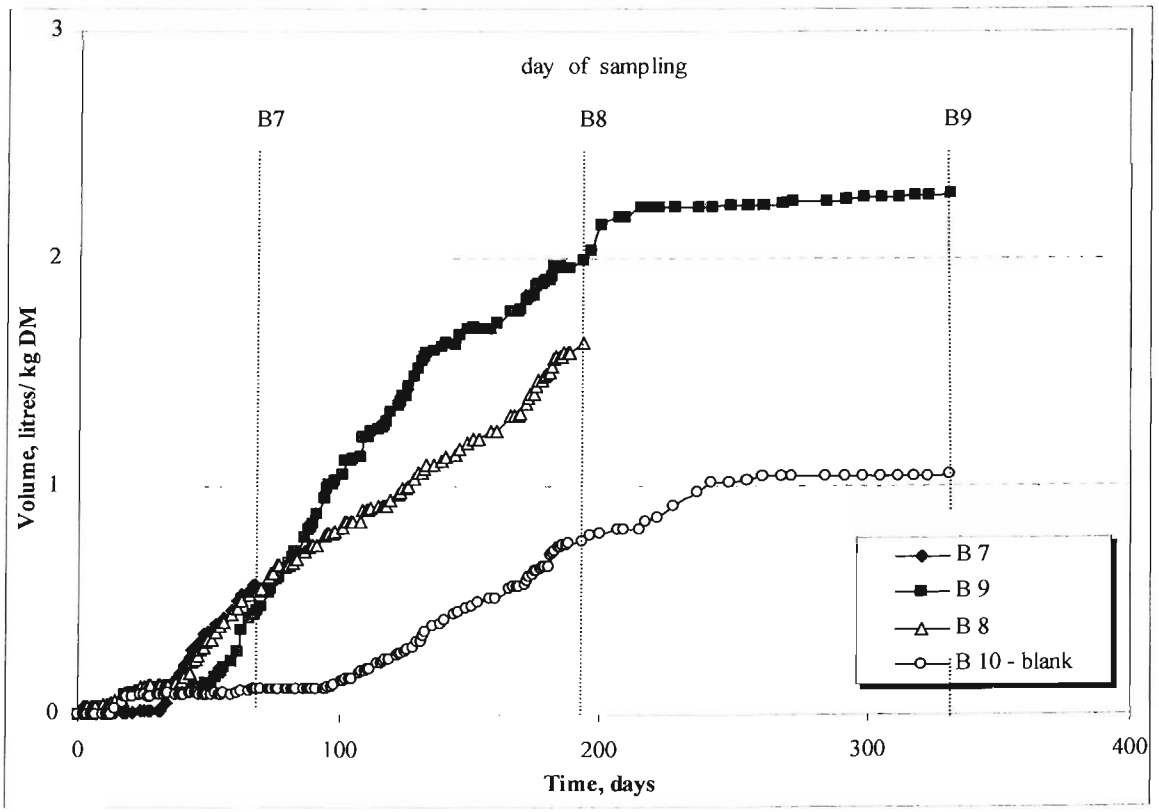

Figure 6.16. Cumulative biogas production at STP for the BMP2 bottles.

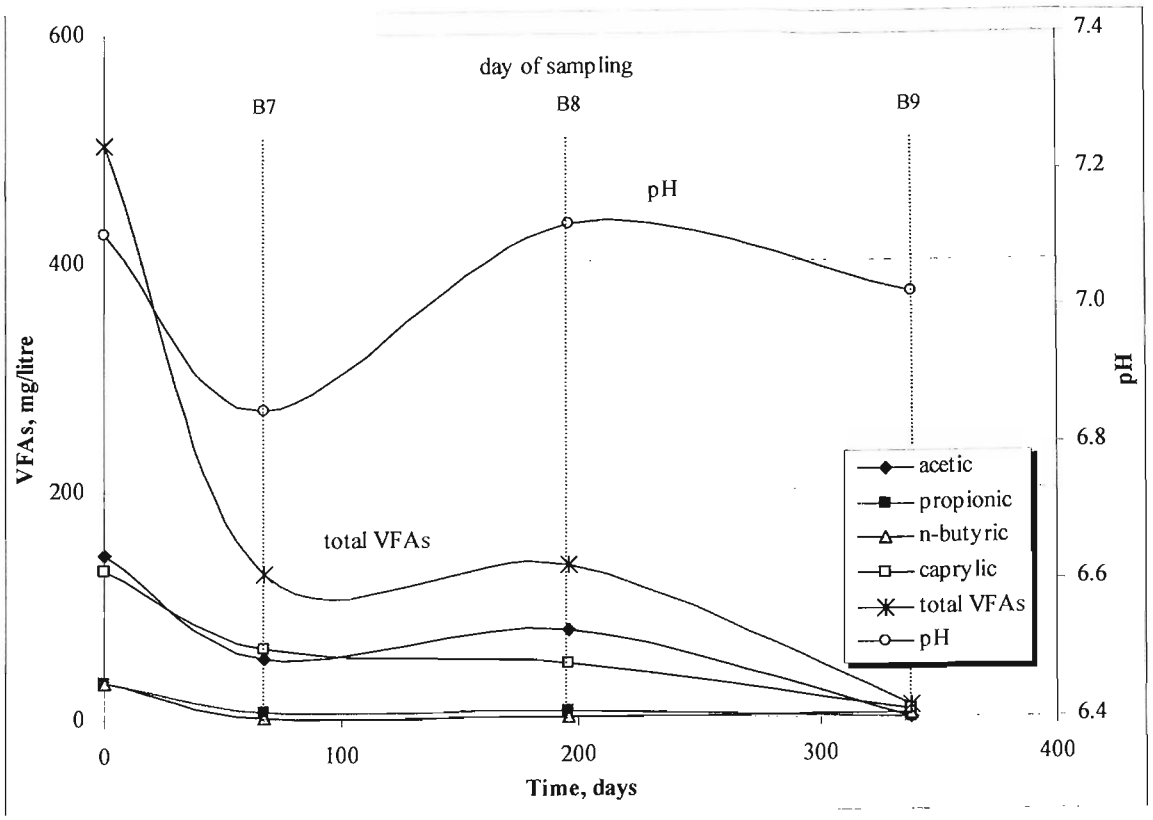

Figure 6.17. Leachate VFAs and pH in the BMP2 bottles.

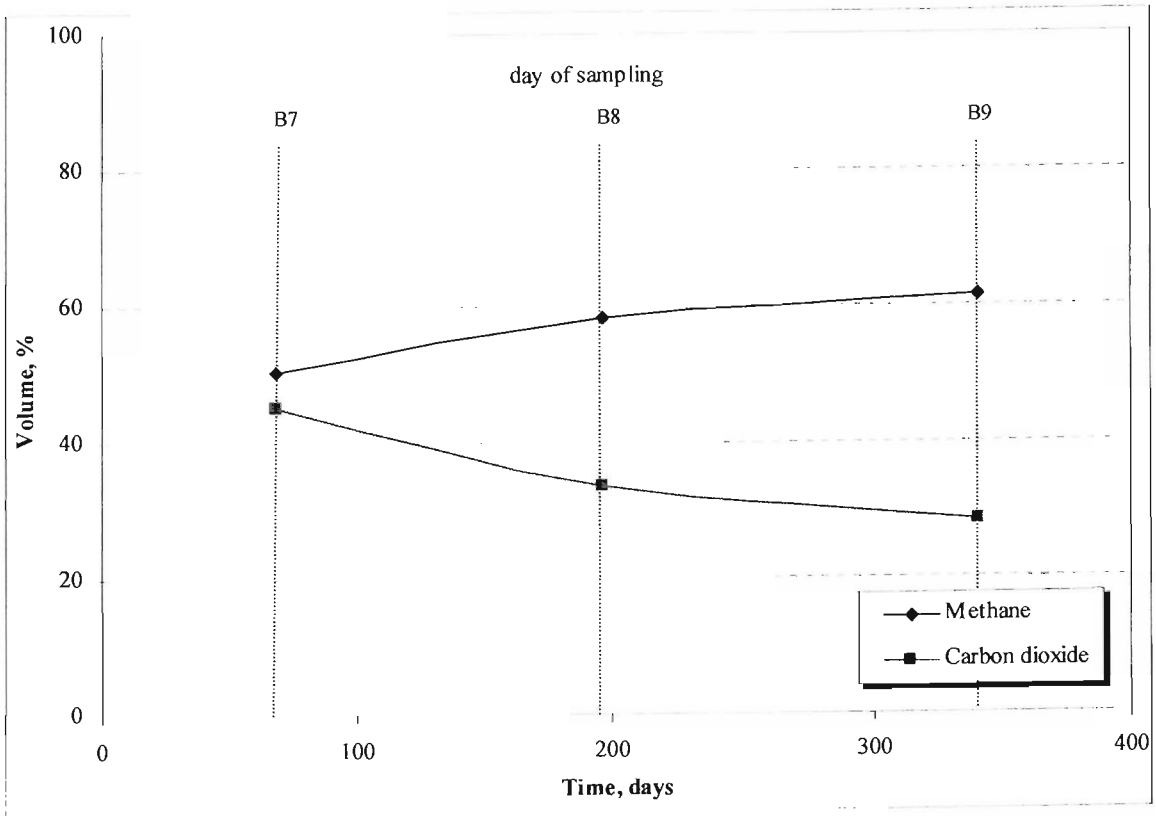

Figure 6.18. Gas composition for the BMP2 bottles.

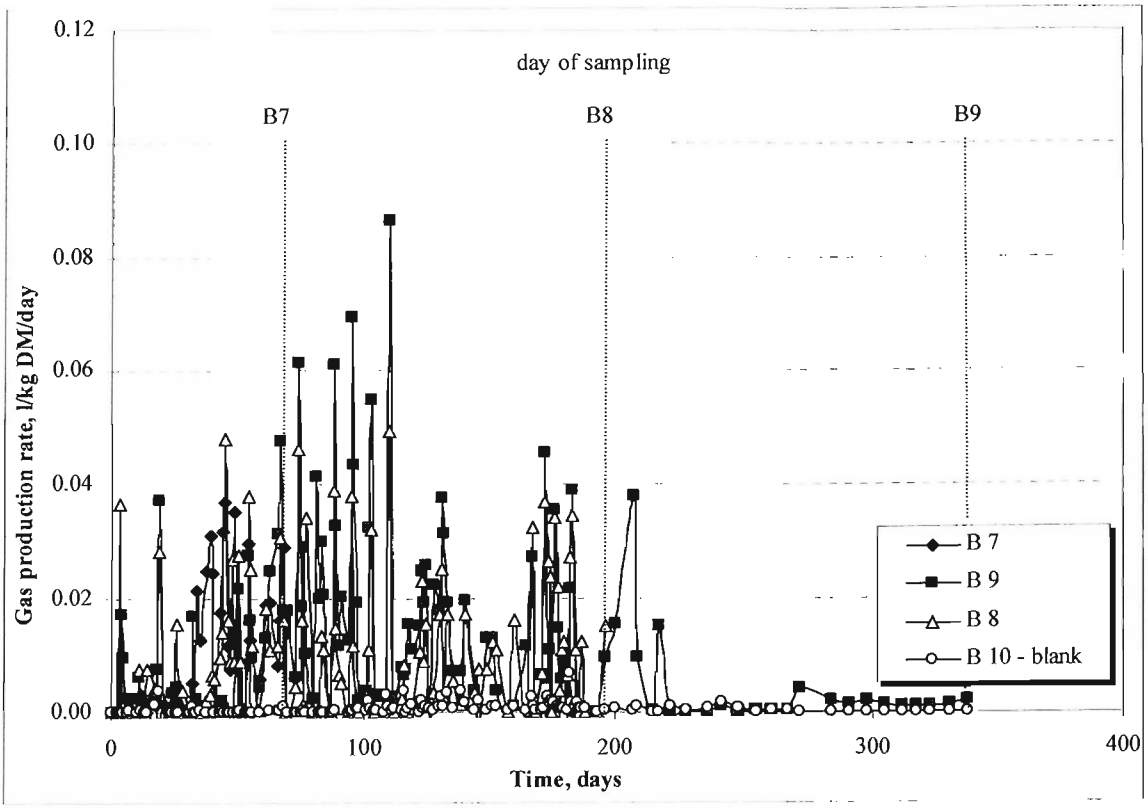

Figure 6.19. Gas production rate for the BMP2 bottles.

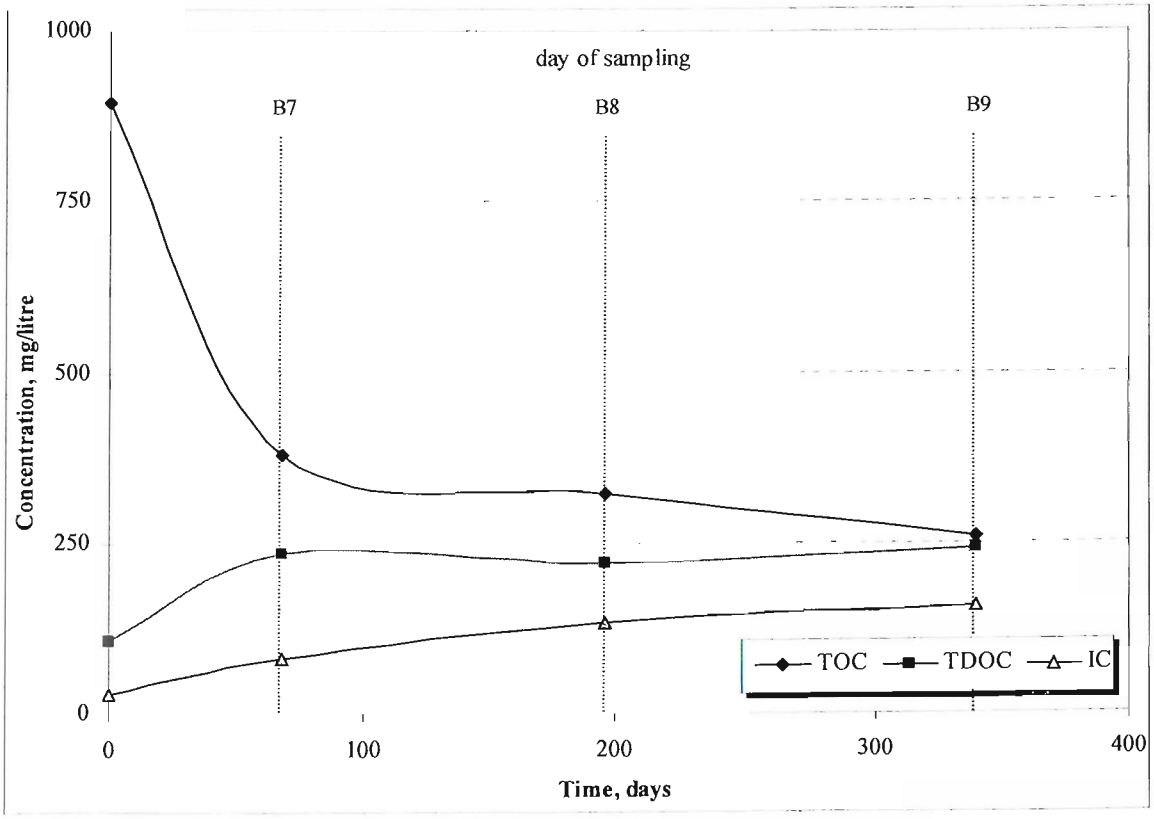

Figure 6.20. Leachate carbon for the BMP2 bottles.

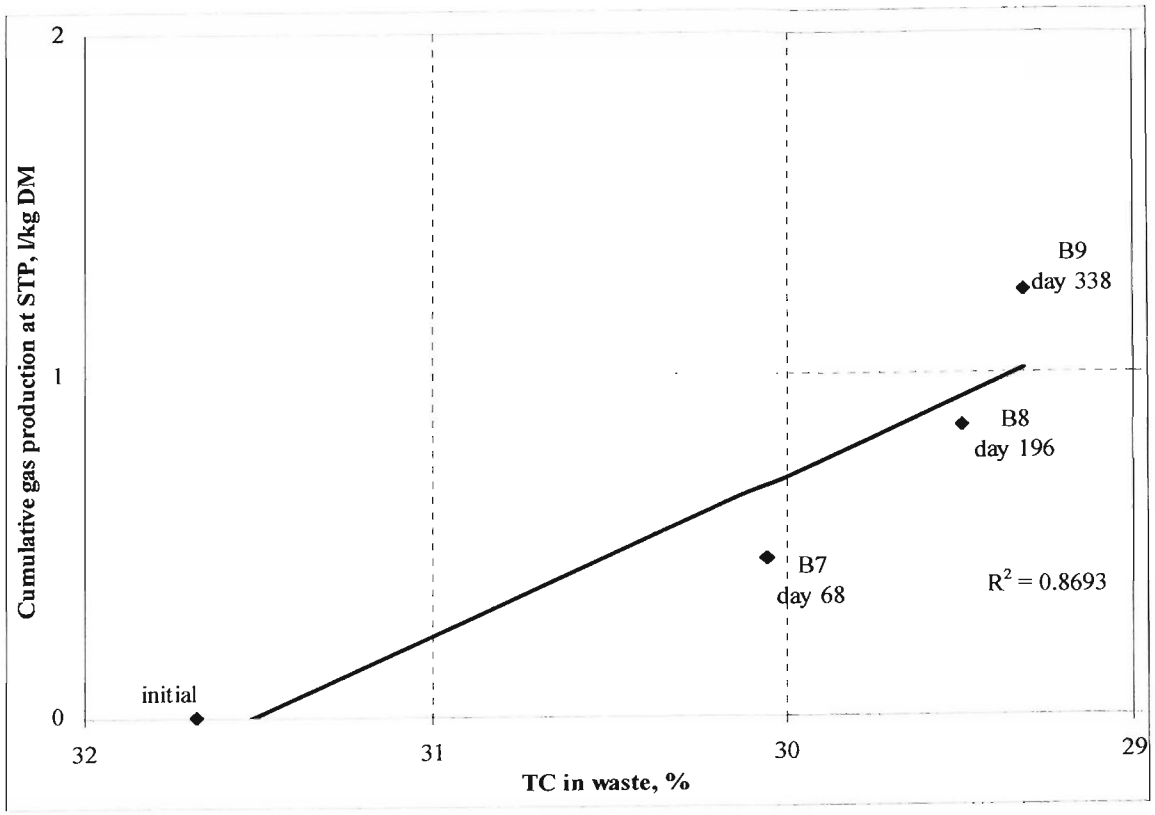

Figure 6.21. Waste TC vs. cumulative gas production in the BMP2 test bottles.

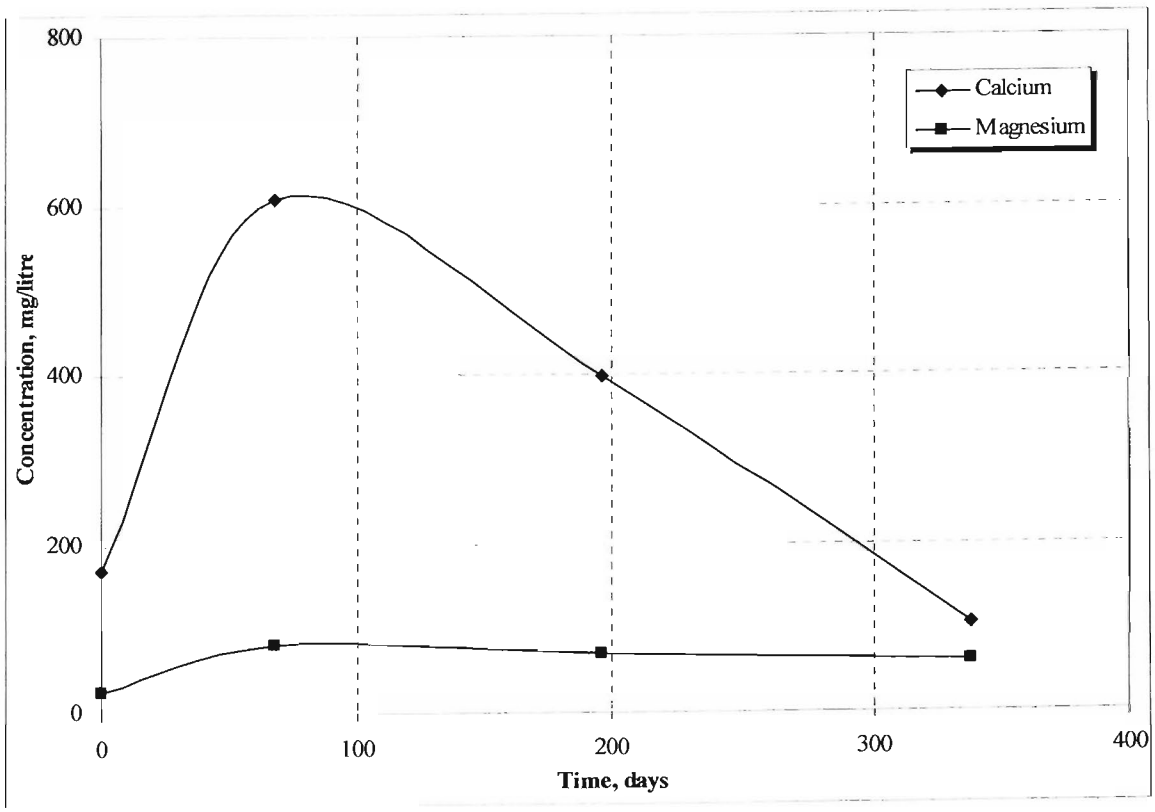

Figure 6.22. Calcium and magnesium concentrations in leachate in the BMP2 test bottles.

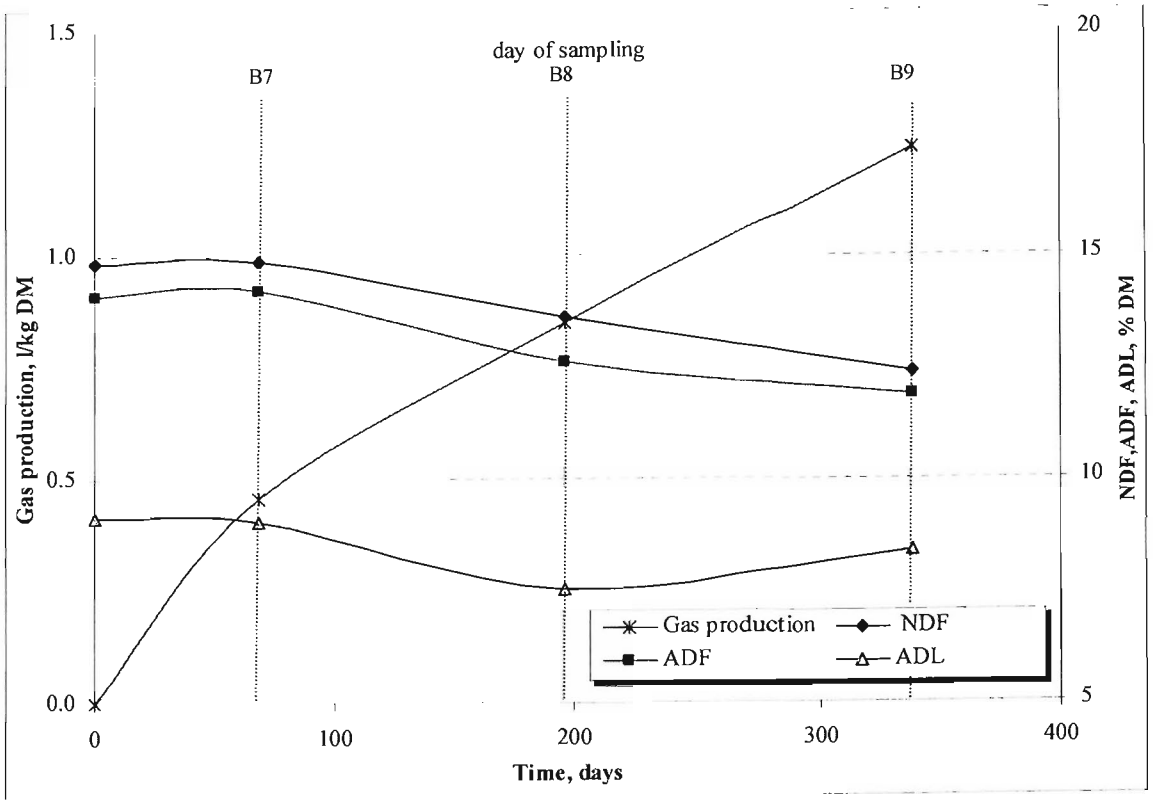

Figure 6.23. Cumulative gas production, NDF, ADF and ADL vs. time for the BMP2 bottles.

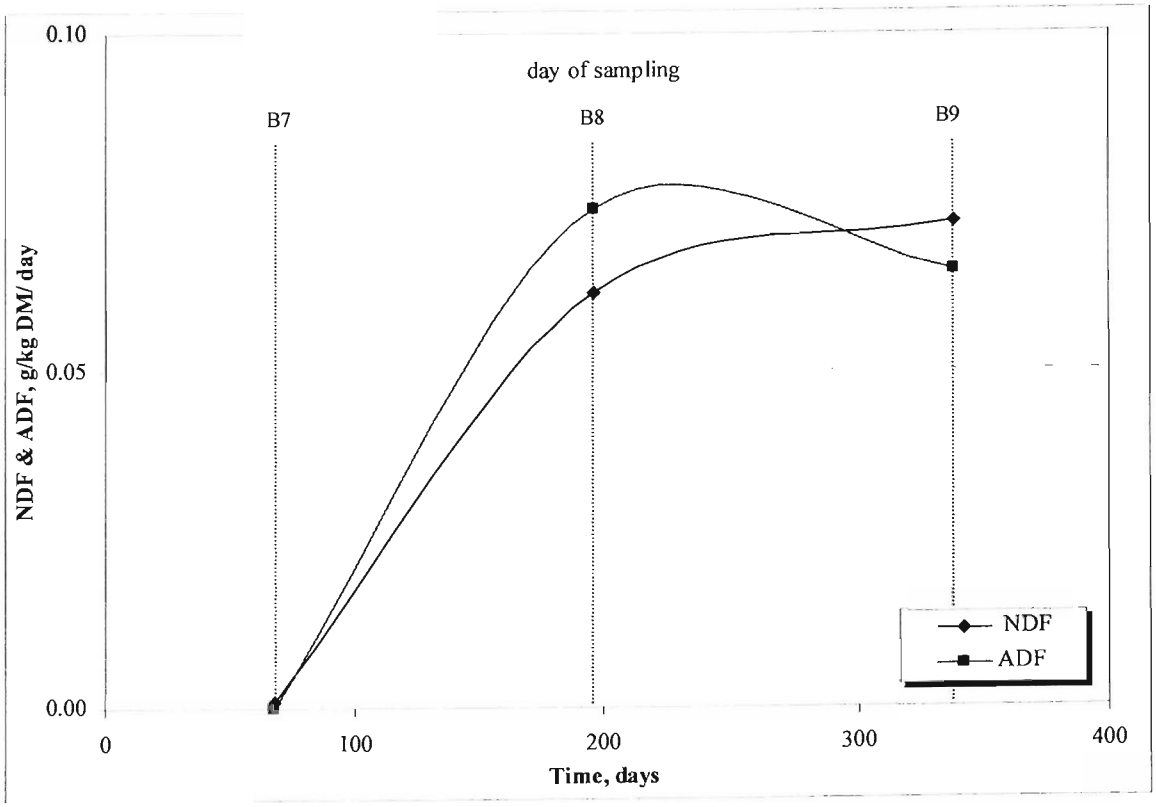

Figure 6.24. NDF & ADF rates vs. time in the BMP2 bottles.

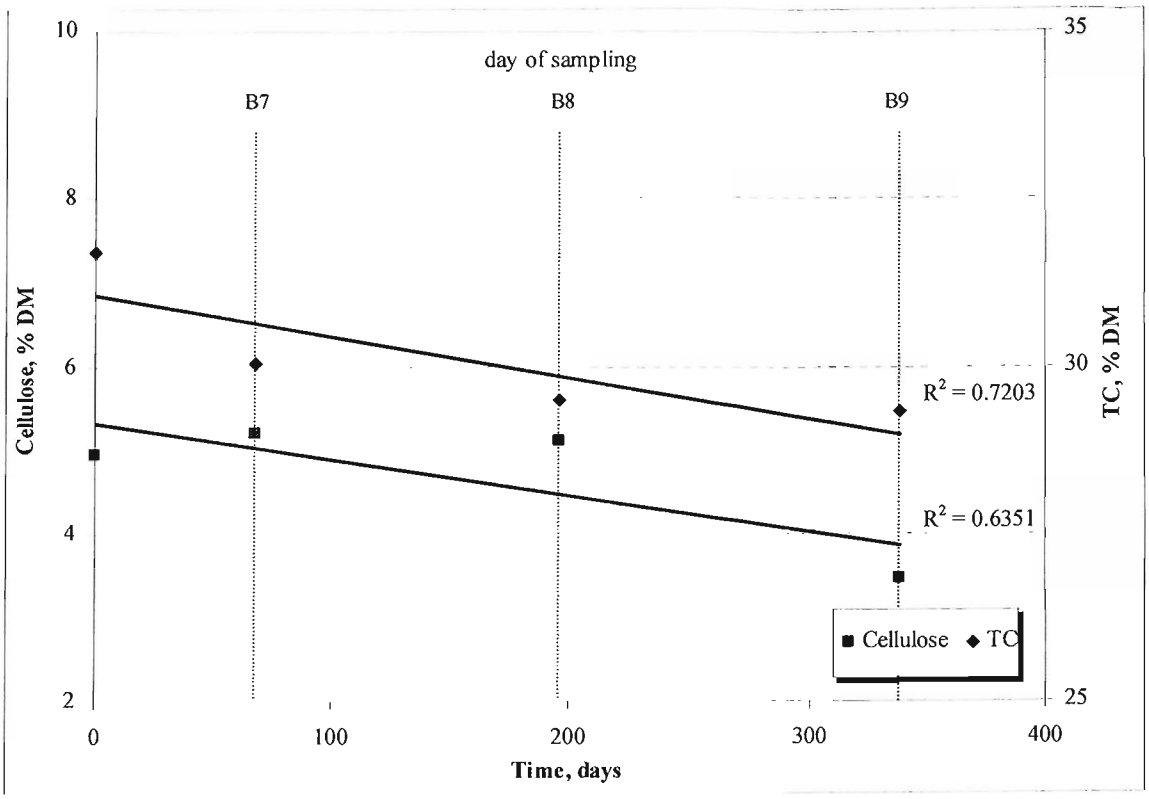

Figure 6.25. Waste TC & Cellulose vs. time for the BMP2 bottles.

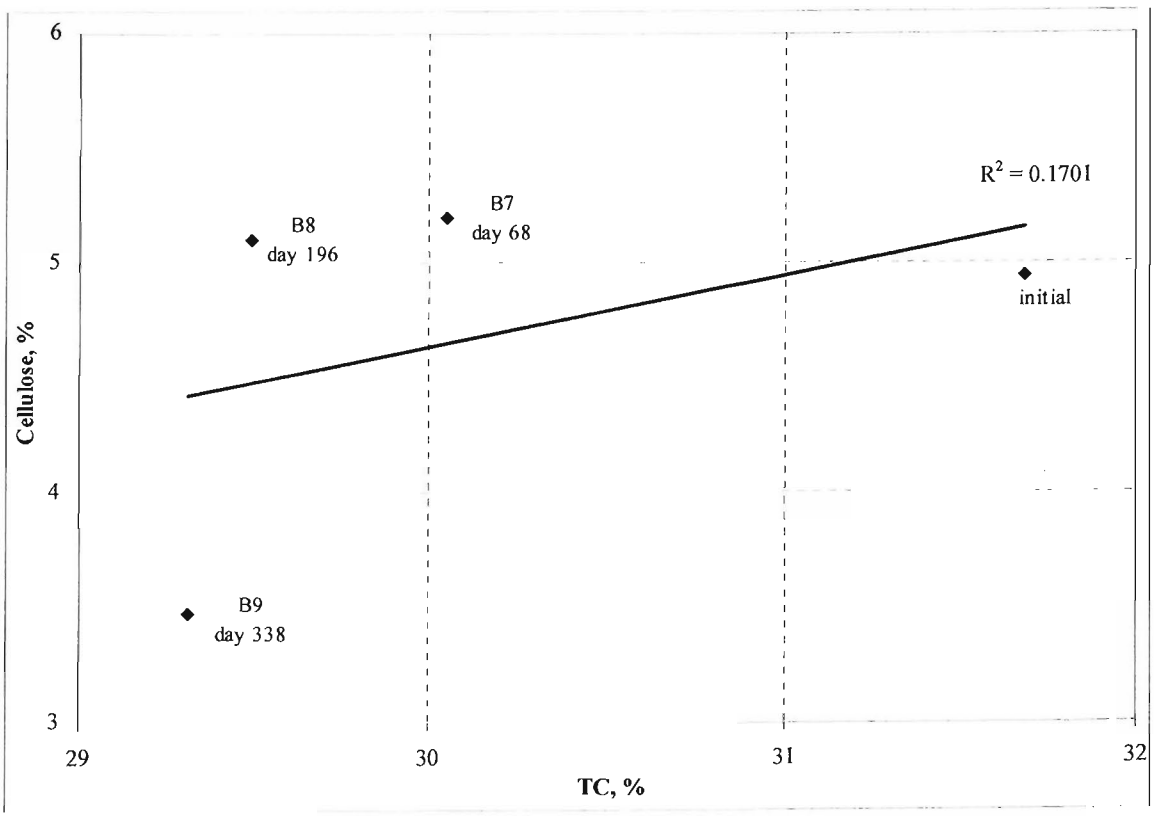

Figure 6.26. Correlation between cellulose content and waste TC for the BMP2 bottles.

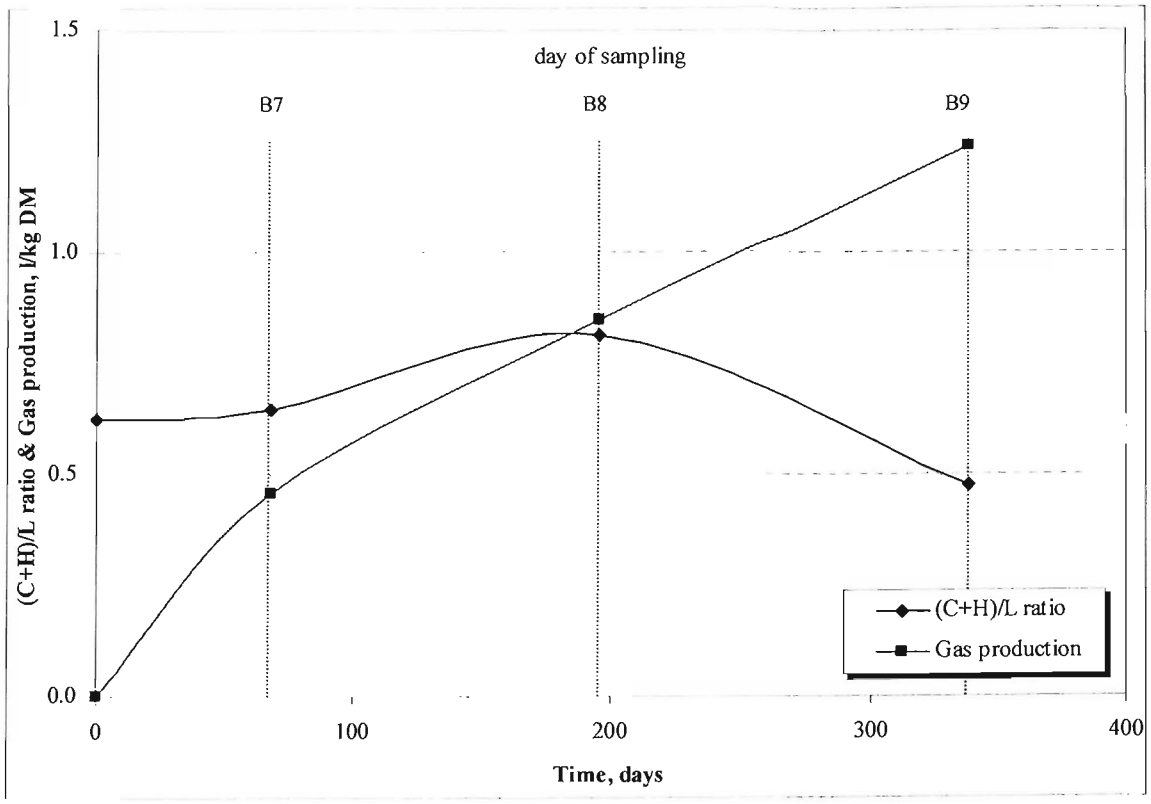

Figure 6.27. (C+H)/L & Cumulative gas production vs. time for the BMP2 bottles.

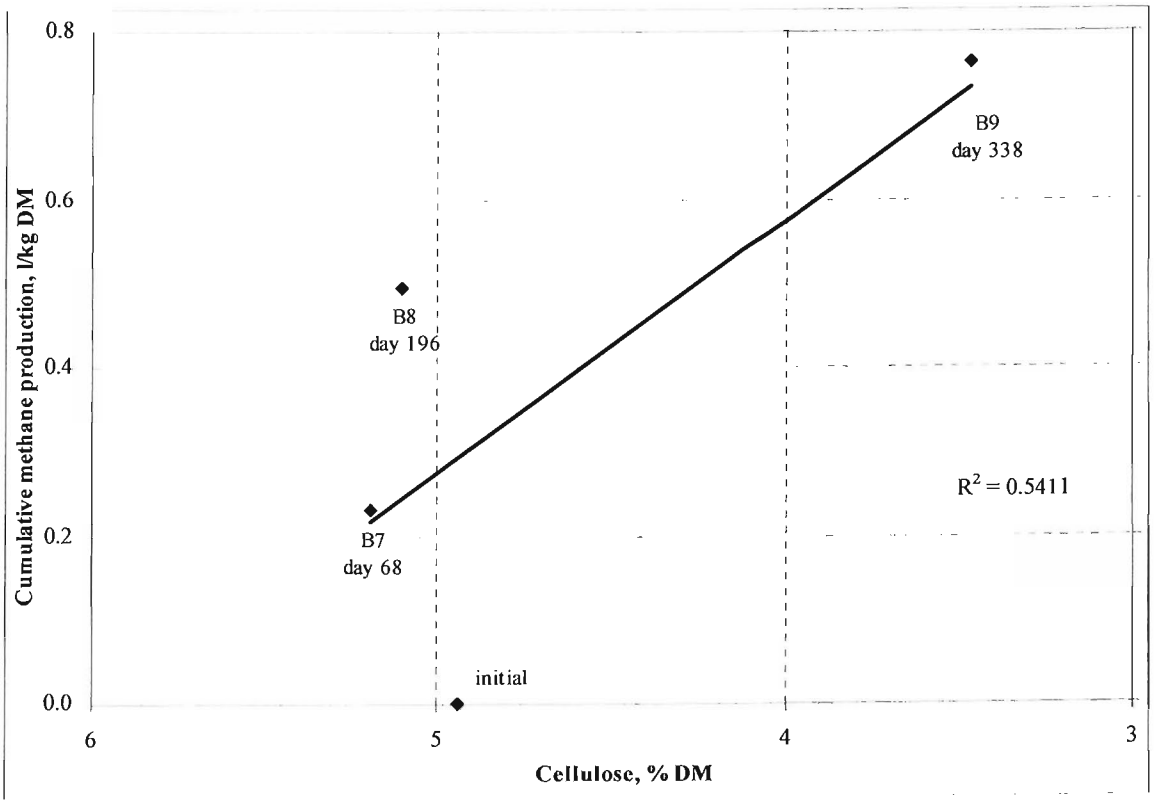

Figure 6.28. Correlation between cellulose content and cumulative methane production for the BMP2 bottles.

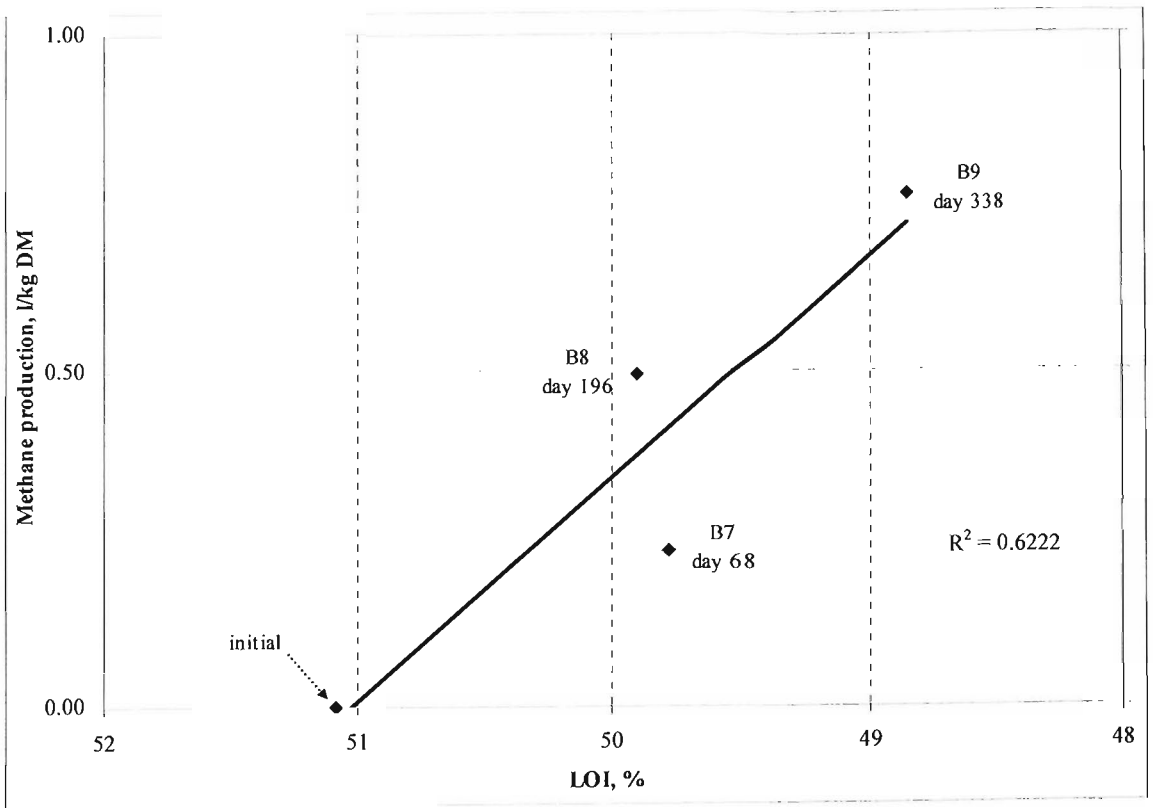

Figure 6.29. Correlation between methane production and LOI for the BMP2 bottles.

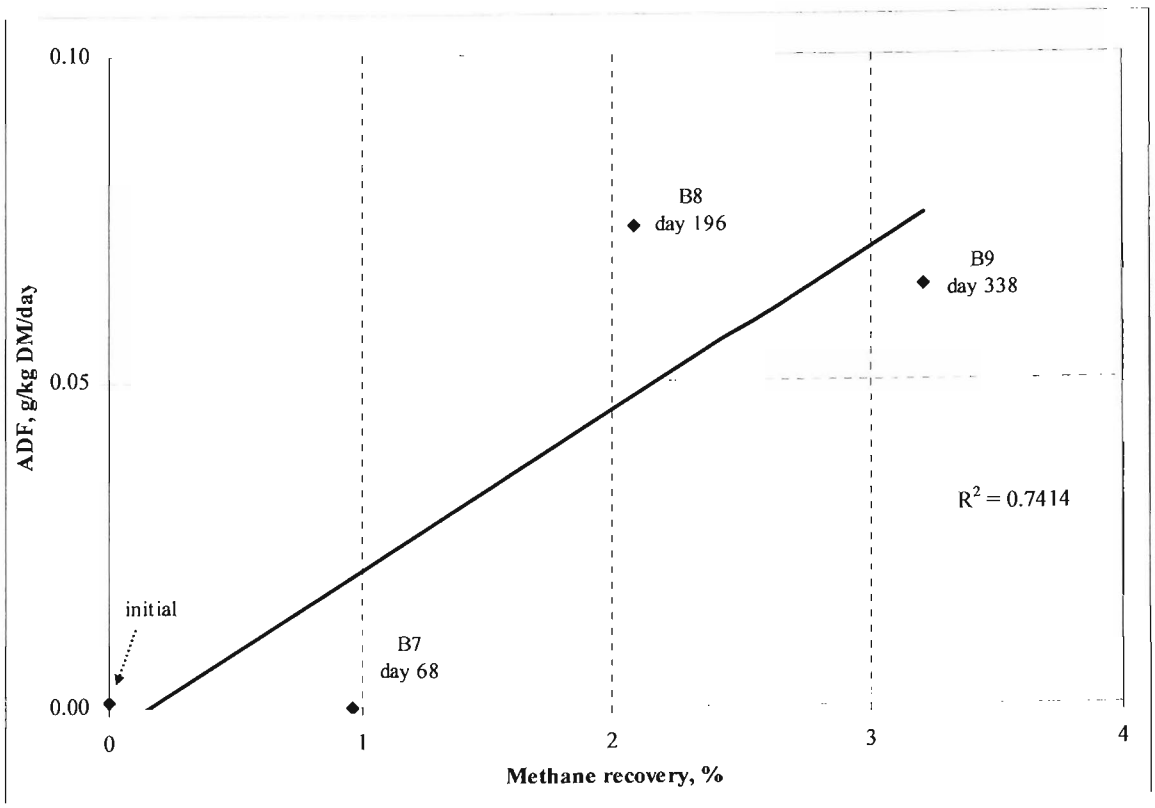

Figure 6.30 Correlation between methane recovery and ADF biodegradation rate for the BMP2 bottles.

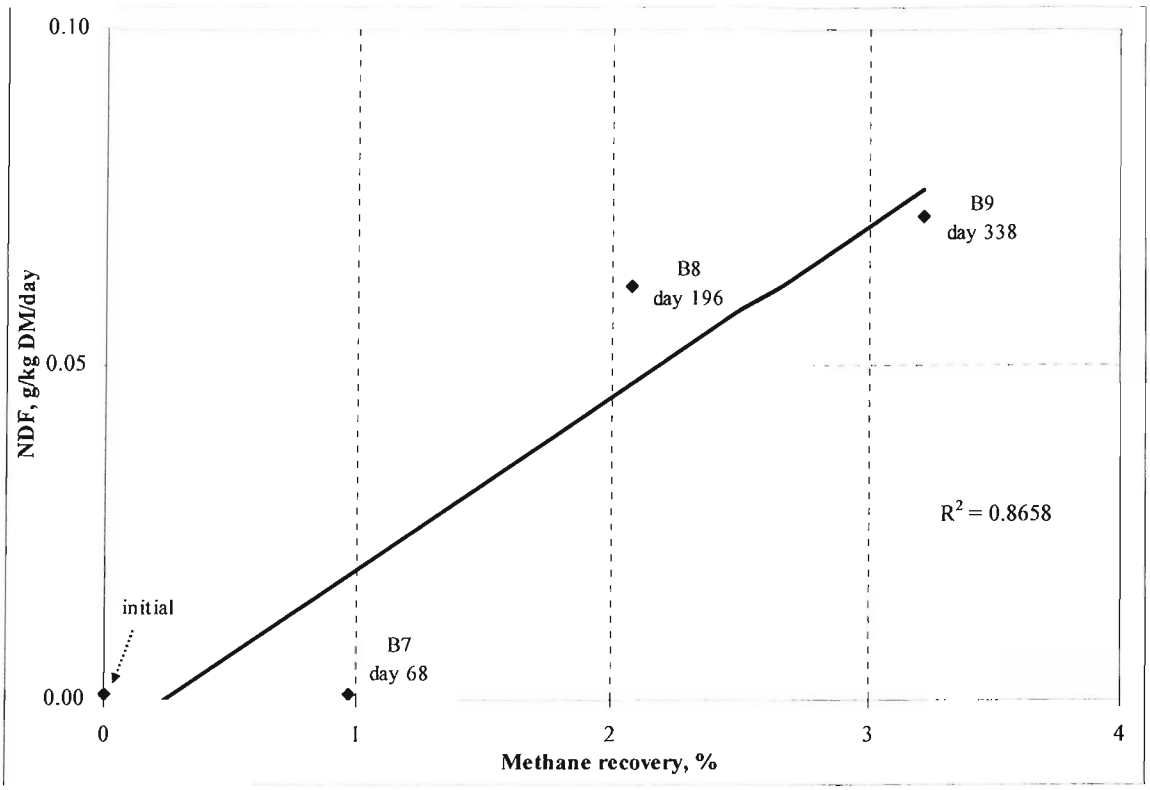

Figure 6.31. Correlation between methane recovery and NDF biodegradation rate for the BMP2 bottles.

Chapter 7

Results and discussion:

Laboratory experiments involving fresh MSW (sample FR)

Three purpose-designed test cells (section 5.3) were constructed to observe both degradation and settlement of a fresh MSW sample over an extended period of time (919 days). The volumes of the gas produced during the test are reported in section 7.1.1. Waste settlement rates exhibited in the CARs are estimated in section 7.1.2. Inter-relationships between the onset of biodegradation and associated leachate chemical parameters are discussed in the context of their influences on the degree and rate of settlement of the waste material. In addition, the changes in the composition of the leachate during waste biodegradation with regard to the removal of the organic substrate and the reduction of TOC, IC, DOC, VFA, various cations and anions and metals are presented (sections 7.1.3 to 7.1.9) to allow the inter-relationships between settlement and biodegradation to be established. Results are compared with those obtained by other researchers and the mechanisms of settlement further discussed. The results of drainable porosity tests carried out on the test reactors (CAR2 & 3) are discussed in section 7.2. Data on the chemical composition of the waste material retrieved from the test reactors filled with fresh MSW on their dismantling is provided in section 7.3. The degradability of the FR waste sample selected for the study is quantified by means of a BMP test (BMP3) and a prediction of the rate and potential of MSW degradation is made in section 7.4 .

7.1. CARs filled with FR waste sample (CARs 2, 3 & 4)

7.1.1. pH and gas production rate

The pH of the leachate was measured at different stages of the experiment and is given in Figure 7.1. Initially the pH of the leachate in CARs 2 & 3 was 5.87 and 5.55 respectively. These values increased to a maximum pH of 7.50 (cell 2) and 7.21 (cell 3), and then decreased gradually to a level of 6.60 and 6.78 respectively. There was an increase in the pH value in both test cells after day 308, followed by a slight increase in the pH value to a level of 7.06 (cell 2) and 7.25 (cell 3) by the end of the test.

Figure 7.1 also shows the pH in the control cell (CAR4) was considerably lower than for the test cells 2 & 3. This was due to the acidification of the cell with a mixture of carboxylic acids (see section 5.3.2) to prevent the establishment of methanogenic conditions. The initial pH was 4.78. This value then settled within a constant range of between 4.8 - 5.3 for 428 days, and then rapidly increased to a level of around 6.8 and remained constant until the end of the test. This rapid increase in the pH value was considered to be due to the establishment of a methanogenic bacterial consortium in the control test that led to the observed increase in biogas production and methane concentration in the cell.

Cumulative gas production for the reactors is presented in Figure 7.2, and the composition of biogas produced from each reactor is given in Figure 7.3. As shown by the biogas production data in Figure 7.2 and the pH data in Figure 7.1, the results can be distinctly divided in four phases: Phase I, *the acidogenic phase* (0 - 9 days), where the long-chain fatty acids (propionic, butyric, valeric and caproic acids) were the main product, the pH was low (5.5 - 5.8) (Figure 7.1, Figure 7.4 & Figure 7.5); and the biogas production was negligible; Phase II, *the acetogenic phase* (10 - 40 days), when the long-chain VFAs were converted to acetate, carbon dioxide and hydrogen and the biogas production was still negligible (Figure 7.4), Phase III, *the accelerated methanogenic phase* (41 - 140 days), where the maximum biogas production rate was recorded (Figure 7.7); and Phase IV, *the decelerated methanogenic phase* (141 - 919 days), where the rate of gas production decreased even though the methane and carbon dioxide concentrations remained constant (Figure 7.3). During this last phase, the cumulative curve of biogas production showed the characteristic plateau (Figure 7.2).

The total biogas production (carbon dioxide + methane) at STP from the waste sample was 314.76 litres/kg dry wt. and 256.03 litres/kg dry wt. for cell 2 and cell 3 respectively.

At the same time, methane concentration in the test cells reached 61.73% vol. (CAR2) and 62.06% vol. (CAR3) (Figure 7.3). The gradually increasing methane concentration in the biogas produced was consistent with the gradual adaptation of the methanogenic bacteria that occurs during the transition to the methanogenic phase. Due to the degradation of the organic matter, oxygen was consumed within a short time, which resulted in rapid carbon dioxide production in both test cells (Figure 7.8). The carbon dioxide concentration in the test cells increased up to 85% (day 5) and then rapidly decreased and settled in the range between 26% and 20% by the end of the experiment. The maximum daily gas production rates for the test cells were recorded at day 53 – 9.73 litres/ kg dry wt./day at STP (CAR2) and at day 119 - 8.56 litres/ kg dry wt. at STP (CAR3). The most likely reason for this variation is that gas was released into the column headspace periodically through ebullition of trapped gas within the waste body. A similar observation for gassing waste was made by Hudson *et al.* (2001).

Figure 7.2 also shows the cumulative gas production in the control cell (CAR4), where it can be seen that at day 280 the control cell started to produce biogas. 9 days later (day 289) the control was acidified again by adding propionic acid only at a concentration of 9 g/litre, to further inhibit the onset of methanogenesis. This attempt proved to be unsuccessful and by day 314 stable methanogenic conditions were observed in the control. This can almost certainly be attributed to the adaptation of the microbial population to methanogenic conditions and the pH. The changes in the biogas composition in the control cell in time are shown in Figure 7.3. The four stages of degradation as previously described in section 2.1 were also observed in CAR4: *the acidogenic phase* between day 0 and day 90th, during which CO_2 and long chain VFAs were produced (Figure 7.1 & Figure 7.6); *the acetogenic phase* from day 91st to day 314th, when the VFAs were the main product of biodegradation and the biogas production rate was still low (Figure 7.6 & Figure 7.7), *the accelerated methanogenic phase* (315 - 750 day), where the maximum biogas production rate was observed (day 534 - 5.79 l/kg dry wt. at STP) (Figure 7.7) and *the decelerated methanogenic phase* (750 - 919 day), where the rate of methane production decreased (Figure 7.2 & Figure 7.7). The methane production seemed to be linked to VFAs consumption suggesting the establishment of acetoclastic methanogens. The overall production of carbon dioxide and methane at STP from the control reactor was 71.23 litres/kg dry weight. Simultaneously, methane and carbon dioxide concentrations reached values of 61.7% vol. and 25.5% vol., respectively by the end of the test period.

7.1.2. Settlement in CARs 2, 3 & 4 - FR waste sample

The focus of the present research was the development of a comprehensive data set on waste settlement rates over an extended time period that would help to identify and quantify the factors affecting settlement in landfills and the calibration of a mathematical model of landfill degradation and transportation processes. The settlement in the CARs was measured for a period of 919 days. The observed data are presented as a percentage of the settlement of the initial refuse height recorded 24 hours after load application to facilitate their graphical representation. As discussed previously in section 5.3.2, the settlement observed in the CARs during filling and loading was considered to be caused by initial and primary compression of the waste due to a lack of adequate compaction during the sample preparation stage, and was not taken into consideration. A settlement classification described in section 1.1 was adopted in this study.

The monitored total settlements in the CARs are plotted against log-time in Figure 7.9. An examination of these plots suggests that three stages of settlement behaviour occurred: intermediate secondary settlement, long-term secondary settlement and residual settlement. Selected parameters of recorded settlement data for the cells are summarized in Table 7.1.

Intermediate secondary settlement

Based on the change in the slope of the strain-log time curve for the CARs (Figure 7.9), the times for intermediate settlement to occur were determined (Table 7.1). At the end of this phase, the cells settled as shown in Table 7.1, which was most likely to be mainly attributable to physical compression due to a lack of adequate compaction of the waste. A concurrent increase in the gas production rate was also recorded during this stage (Figure 7.3). As can be seen in Table 7.1, test cells 2 & 3 developed an almost similar rate of intermediate secondary compression characteristics to that observed in the control cell (CAR4) (values between 7.3 and 8.3%), where biodegradation processes were inhibited. This led to the conclusion that the settlement behaviour in this stage was dominated by mechanical interactions due to delayed compression of the wastes.

Long - term biodegradative secondary settlement

The long-term secondary settlement observed in the CARs are depicted in log-time scale in Figure 7.10. The test results demonstrate that settlement at this stage was linear with

the logarithm of time. As can be seen in Table 7.1 the test cells exhibited a similar rates of long-term secondary compression (16.9% in CAR2 and 13.4% in CAR3), that were higher than the intermediate secondary compression rates which were possibly due to the combined effects of mass loss and biodegradation. The only difference between CAR2 and 3 was in the stress applied to the cells at the beginning of the test. Conversely, the increased load in CAR2 appeared to lead to increased rates of long-term secondary compression (Table 7.1).

Table 7.1. Settlement results in CARs 2, 3 & 4.

Reactor	Bulk density [1], kg/m^3	Time period, days	Waste height before loading, m	Actual settlement, m (%) [2]	h_p [3], m	h_s [4], m	h_b [5], m	h_r [6], m
Intermediate secondary settlement								
CAR2 (150kPa)	476.2	2 - 54	n/a	0.028 (8.3)	n/a	0.313	n/a	n/a
CAR3 (50kPa)	385.2	2 - 31	n/a	0.029 (7.3)	n/a	0.388	n/a	n/a
CAR4 (50kPa)-control	396.8	2 - 31	n/a	0.026 (6.5)	n/a	0.377	n/a	n/a
	400.0	2 - 54	n/a	0.030 (7.4)	n/a	0.373	n/a	n/a
	421.5	2 - 345 [8]	n/a	0.049 (12.4)	n/a	0.354	n/a	n/a
Long-term biodegradative secondary settlement								
CAR2 (150kPa)	584.9	55 - 596	n/a	0.058 (16.9)	n/a	n/a	0.255	n/a
CAR3 (50kPa)	449.3	32 - 238	n/a	0.056 (13.4)	n/a	n/a	0.332	n/a
CAR4 (50kPa)-control	421.5	32 - 345	n/a	0.023 (5.6)	n/a	n/a	0.354	n/a
	421.5	55 - 345	n/a	0.019 (4.8)	n/a	n/a	0.354	n/a
	454.9	346 - 919 [9]	n/a	0.026 (6.2)	n/a	n/a	0.328	n/a
Residual secondary settlement								
CAR2 (150kPa)	604.2	597 - 919	n/a	0.008 (2.4)	n/a	n/a	n/a	0.247
CAR3 (50kPa)	474.8	239 - 919	n/a	0.018 (4.3)	n/a	n/a	n/a	0.314
CAR4 (50kPa)-control	n/r [10]	n/r	n/a	n/r	n/a	n/a	n/a	n/r

Note: [1] Calculated at the end of each phase; [2] Measured at the end of each phase; [3] h_p is height of waste at the end of primary compression phase; [4] h_s is height of waste at the end of intermediate secondary compression phase; [5] h_b is height of waste at the end of long-term secondary compression phase; [6] h_r is height of waste at the end of the test; [7] n/a - not applicable; [8] actual duration of intermediate secondary settlement phase in CAR4; [9] actual duration of long-term secondary settlement phase in CAR4; and [10] residual settlement stage in CAR4 has not been reached yet.

Residual secondary settlement

As can be seen in Figure 7.9 periods of accelerated settlement rates were followed by periods of relatively small compression rates. Residual settlements were found to be

2.4% in CAR2 and 4.3% in CAR3, i.e. approximately two times less than the intermediate secondary settlements. The slowly decreasing rates of settlement in this stage were indicative of the exhaustion of the readily biodegradable matter in these CARs.

As previously discussed, CAR4 may be considered to be a control only until day 314, where degradation was initiated. With this assumption, it can be concluded that prior to this the amount of settlement was likely to be caused by physical compression processes such as crushing, reorientation and ravelling of the waste particles following load application.

If the shapes of the settlement curves observed in the test cells (CAR2 & 3) are compared to the shapes of the curves obtained in full-scale landfill (Figure 4.11 & Figure 7.9) it can be concluded that the same mechanisms are likely to be responsible for the settlement.

7.1.3. Degradation

The total organic carbon (TOC) content of the leachate samples taken from the reactors at different stages of biodegradative process increased from initial values of 907mg/l to approximately 6000mg/l after 15 days and then decreased gradually to a level of 584mg/l for CAR2 and 537mg/l for CAR3 by the end of the test (Figure 7.11 & Figure 7.12). At the same time the TDOC content of the leachate samples (these had previously been filtered though Whatman GF/C filters) increased from 69mg/l to 4879mg/l (day 8) and 5188mg/l (day 8) for CAR2 and CAR3 respectively and then decreased, showing the same pattern as TOC to approximately 504mg/l for cell 2 and 490mg/l for cell 3 (day 919). The initial increase was most likely to be due to the degradation of solid organic matter resulting in the formation of a range of soluble organic matter. Results also show that carbon in the leachate is mostly in the dissolved form as the TOC values are only slightly larger than the TDOC values.

TOC and TDOC contents of the control cell (CAR4) increased from initial values of 853mg/l to 11853mg/l due to the addition of acetic and propionic acids at the beginning of the experiment and thereafter remained constant until day 280 whereafter degradation processes were initiated (Figure 7.13). 9 days later (day 289) the control was acidified again by adding propionic acid only at a concentration of 9g/litre, to further inhibit the onset of methanogenesis. As a consequence of waste biodegradation and the second acid

addition (section 5.3.2), the TOC and TDOC contents increased by day 463 where maximum values of 18790mg/ l and 16520mg/l were achieved, respectively. The TOC and TDOC contents then decreased sharply and subsequently settled to a level of around 603mg/l and 560mg/l, respectively by the end of the test (day 919).

7.1.4. VFA concentration

Eight VFAs were analyzed in the leachate – acetic, propionic, n- and iso-butyric , n- and iso-valeric, caproic and caprylic acids. As can be seen in Figure 7.4 and Figure 7.5 VFAs concentrations in the leachate for CARs 2 & 3 increased throughout the acetogenic phase (10 - 40 day) which explains the lag period between the beginning of the test and the onset of methane production. After day 40, the accumulation of the carboxylic acids decreased rapidly as they were consumed faster than they were produced which resulted in a simultaneous increase in the rates of biogas production (Figure 7.7).

The initial concentration of the total VFAs in CAR4 was very high (18777mg/litre) due to the addition of acetic and propionic acids at the beginning of the experiment (section 5.3.2). This value decreased gradually to 12615mg/l by day 148 and after that increased with some fluctuations to a level of 29105mg/l (278 day) possibly due to waste biodegradation processes. The increased levels of VFAs could be due to the interrelation between the different groups of microorganisms at this stage that enables them to tolerate the increased levels of VFAs, by providing a thermodynamically admissible reactions resulting in an increase in the methane production rate on day 287 (Figure 7.7). The VFAs of the control cell increased further after day 289 posibly due to the combined effects of the second addition of propionic acid (section 5.3.2) and waste biodegradqation. This resulted in peak measurement of total VFAs by day 372 where a maximum value of 46572mg/l was recorded. Then the total VFAs decreased sharply to 3086mg/l (449 day) and by the end of the test (919 day) reached a value of 46mg/l. As a consequence, the pH increased up to 6.6 (463 day) which indicated the irreversible state of the control overcoming the inhibitory effect of the VFAs and becoming methanogenic.

It is interesting to examine how the concentrations of the individual VFAs in CAR4 were built up. As mentioned before, at the beginning of the test (due to additions) acetate and propionate were the only VFAs in significant concentrations. During the first 148 days of the experiment in the control cell, both acids decreased but the propionate concentration was still higher than acetate (Figure 7.6). Simultaneously, after day 148, n-butyrate and n-valerate started to build up and prevailed over the other measured acids (except acetate

and propionate), showing a tendency for accumulation (above 1500mg/l each). A reasonable explanation may be that the anaerobic microorganisms producing acidic fermentation products, under stressing conditions (such as high VFAs levels and low pH), prefer forming acids with a lower dissociation constant (such as butyrate and valerate) over acetate and propionate, as an attempt to prevent further acidification. When organisms with a mixed-acid fermentation pattern are present, a decrease in their environmental pH often results in a shift from acid to alcohol production. This was, however, not investigated here. In previous studies (Ahring *et al.*, 1995; Hill and Botle, 1989) it was noted that butyrate, valerate and their isomers were highly sensitive to disturbances and it was proposed they be used as process indicators so as to provide an early warning of an impending process imbalance. The sensitivity of these parameters needs to be further verified in a separate experiment looking into the possibility of using these VFAs as an indicator of reactor stressing, even at an early stage, when the other indicators (such as TOC concentration and pH) are still within a normal range of values.

7.1.5. Sulphate reduction

As can be seen in Figure 7.14 the leachate samples collected from CARs 2 & 3 at day 1 of the experiment were found to have a high sulphate level (over 400mg/l). The sulphate concentration then started to decrease in both cells and eventually reached zero by day 29. The high level of sulphate at the beginning of the test was observed to inhibit the methane production in both cells as the SRB can outcompete the methanogens if sulfate remains available as an electron acceptor. As shown in Figure 7.3 the methane concentration reached a value of around 60% by day 12 in the test cells when the SO_4^{2-} in both test cells dropped below 111mg/litre. Due to this, it can be assumed that after removing all the sulphate in the leachate enough acetate was available for the methanogenic bacteria to increase activity. By day 22 of the experiment all the sulphate was removed from the leachate, resulting in a simultaneous increase in the rate of methane production (Figure 7.7).

Figure 7.14 shows that the sulphate concentration in the leachate in CAR4 also decreased gradually from initial values of 751.8mg/litres (day 19) to a value of 190.3 mg/litre (day 135). At the same time, a gradual decrease in the acetate concentration was also observed (Figure 7.6) possibly due to the action of acetate utilising SRB. As previously discussed, there was uncertainty regarding the kinetics of competition between SRB and methanogenic bacteria when acetate was utilised (see section 2.3.3). Between day 135

and day 257, the sulphate concentration in the control cell increased significantly reaching a value of 627.5mg/litre which corresponded very well with the increase in the acetate concentration possibly due to the onset of biodegradation of the waste organic matter in the control cell. Then the SO_4^{2-} concentration in CAR4 dropped significantly to a value of 72.4mg/litre (day 523) where the biogas production rate increased simultaneously and reached a maximum value of 5.97 l/kg dry wt./day (day 534) (Figure 7.7).

7.1.6. Redox potential

As can be seen in Figure 7.15, the redox potential appeared to be good indicator of the biodegradation phase changes. The redox potential in CAR2 and CAR3 dropped below zero simultaneously, after starting the test, to a level of -291mV and -414mV, respectively which was considered to be connected with the end of the acetogenic phase in both cells. Then it started to rise gradually and with some fluctuations settled around -120mV (CAR2) and -160mV (CAR3) towards the end of the test. This increase corresponded very well with the progression of the methanogenic phase together with the decrease of readily biodegradable organic carbon compounds in the leachate.

In the control cell (CAR4) the redox potential was in the range between -85mV and -150mV for the first 135 days of the experiment. Then it started to increase, reaching a maximum value of -25mV (day 169), followed by a gradual decrease to a level of -145mV by the end of the test (Figure 7.15).

7.1.7. Ammonium concentration

Ammonia is a product of protein degradation and is also the form in which nitrogen is assimilated by microbes for growth. Under anaerobic conditions nitrogen exists as undissociated ammonia gas, NH_3 and dissociated ammonia, NH_4^+ (Baird, 1995) and nitrogen within the landfill will thus be converted to these compounds as oxygen levels decline (section 2.3.2).

High rates of protein biomass degradation during hydrolysis simultaneously increased the concentration of ammonium in CARs 2 & 3 from initial values of 188.6mg/l, 188.6mg/l and 106.5mg/l to a level of 604.5mg/l and 621.0mg/l by day 51, respectively (Figure 7.16). There was a slight upward trend in concentration between day 51 and day 617 in

CAR3, whilst there was a slight decrease in CAR2. After day 617 a sharp increase in the NH_4^+ concentrations was observed. This could be due to a high experimental error or death/lysis of bacterial biomass. However, over the full duration of the experiment there was an increase in NH_4^+ concentrations to 778.3 mg/l in CAR2 and 967.8mg/l in CAR3. The accumulation effect of the ammonium ion in both cells indicates that nitrogen was present in quantities in excess of those which could be bound in the cell biomass during the growth of microbial populations in the CARs and that the buffering capacity of the leachate in the CARs was sufficient to keep ammonia in the form of ammonium ion.

In the literature, ammonium levels have been shown to be independent of the changing landfill processes and various authors have noted a gradual increase followed by fairly constant concentrations of ammonium in leachate (Ehrig and Scheelhase, 1993).

Figure 7.16 shows the evolution of ammonium in the leachate over the experiment in CAR4. An initial concentration of 106.5mg/l ammonium gradually increased to 849.8mg/l by day 397. After the beginning of methanogenic phase in CAR4 (day 314), the ammonium concentration reached its maximum (849.8mg/l)(Figure 7.16) and then decreased to 406.3mg/l by the end of the test period, This decrease is probably due to fact that some *N* is utilised by the bacteria as a *N*-source for microbial growth rather than being accumulated in the leachate.

7.1.8. Calcium and magnesium precipitation

Chemical analysis of leachate samples taken from the CARs showed a gradual decrease in calcium and magnesium ions which is almost certainly due to the precipitation of the elements during biodegradation. (Figure 7.17 & Figure 7.18). Noticeably, the concentrations of Ca^{2+} and Mg^{2+} ions in the CARs were higher during the early stages of the experiment (day 0-26) presumably as a result of low pH values (below 6.7 in all cells).

Initially, the concentrations of Ca^{2+} ions in the CARs 2, 3 & 4 increased to 1092.4mg/l (day 26), 1264.8mg/l (day 15) and 9847.9mg/l (day 51) respectively (Figure 7.17). Then there was a gradual removal of Ca^{2+} ions (to 391.3, 207.63 and 296.8mg/l respectively) from the leachate during the waste biodegradation process.

The solubility of $CaCO_3$ depends on the pH, which in turn governs the distribution of dissolved carbonate species (CO_3^{2-}, HCO_3^-) in the system. At lower pH the dissolved

carbonate species will be predominantly in the form of the bicarbonate ion (HCO_3^-). Without the availability of carbonates (CO_3^{2-}), calcium carbonate cannot be formed and calcium will stay in solution in the form of soluble calcium bicarbonate [$Ca(HCO_3)_2$]. At higher pH, CO_3^{2-} species will predominate leading to the formation and precipitation of $CaCO_3$. This explains why the molar solubility of $CaCO_3$ ranges from 1.7 at pH 4.0 to only 0.0011 at pH 8.0 which corresponds to $1.7x10^5$ mg$CaCO_3$/l or $6.8x10^4$ mgCa^{2+}/l at pH 4.0, 2002 mg$CaCO_3$/l or 802 mgCa^{2+}/l at pH6.0 and 110 mg$CaCO_3$/l or 44 mgCa^{2+}/l at pH 8.0 (Bialkowski, 2000). At a pH range between 4.6 and 7.5, as measured in the CARs during the test period, and assuming a power law relationship fit-curve at different pH values (4.0, 6.0 and 8.0), the solubility for Ca^{2+} was calculated. The Ca^{2+} concentrations in the leachate in CARs 2 & 3 were greater than the solubility product between day 5 and day 160, which is why precipitation mostly occurred in this period of time. In CAR4, the Ca^{2+} concentrations in the leachate did not exceed the solubility product until day 449, which leads to the conclusion that precipitation did not occur until than day.

The concentration of Mg^{2+} ions in the CARs 2 & 3 & 4 increased to 137.6mg/l (day 86), 128.9mg/l (day 93) and 226.0mg/l (day 397) respectively followed by a gradual decrease to a level of 71.1mg/l, 69.4mg/l and 135.9mg/l by the end of the biodegradation period (Figure 7.18).

Molar solubility of $MgCO_3$ ranges from 9.8 at pH 4.0 to only 0.0066 at pH 8.0 which corresponds to $8.3x10^5$ mg$MgCO_3$/l or $2.4x10^5$ mgMg^{2+}/l at pH 4.0, 9925 mg $MgCO_3$/l or 2861 mgMg^{2+}/l at pH6.0 and 558 mg $MgCO_3$/l or 161 mgMg^{2+}/l at pH 8.0 (Pankow, 1991; Bialkowski, 2000). At a pH range between 4.6 and 7.5, as measured in the CARs during the test period, and assuming a power law relationship fit-curve at different pH values (4.0, 6.0 and 8.0), the solubility for Mg^{2+} was calculated. The Mg^{2+} concentrations in the leachate in CARs 2, 3 & 4 did not exceed the solubility product during the test, which leads to the conclusion that Mg^{2+} remained mostly in the dissolved form over the test period and did not precipitate as $MgCO_3$ due to insufficient anions to form $MgCO_3$, although other precipitates of Mg^{2+}could have been formed. The gradual decrease in Mg^{2+} concentrations observed in leachate samples taken form the CARs, indicates that Mg^{2+} could have been precipitated via other than $MgCO_3$ form (e.g., $MgNH_4PO_4$, $Mg(OH)_2$, $Mg_3(PO_4)_2$) or adsorbed in the cell biomass during the growth of microbial populations.

7.1.9. Heavy metals

Nine metals were analyzed in the leachate: *Fe*, *Al*, *Zn*, *Cu*, *Co*, *Pb*, *Ni*, *Mo* and *Cd*. The heavy metal concentrations in the leachate are shown in Table 7.2, Table 7.3 and Table 7.4. The dissolved heavy metal concentrations of the leachate samples (which had previously been filtered though Whatman GF/C filters) from the CARs were observed to gradually decrease during the experiment. The heavy metal concentrations of the leachate samples which had been previously digested using Microwave Accelerated Reaction System (thus giving the total heavy metal concentrations) decreased, showing the same pattern as the dissolved heavy metal concentrations.

It should to be noted that the heavy metal concentrations were elevated in CARs 2 & 3 due to the addition of anaerobic sludge compared to that of the control reactor (CAR4). The sludge contribution to leachate metal concentrations in CARs 2 & 3 is shown in Table 7.5.

Possible metal depletion processes in CARs 2 & 3 were likely to be dominated by precipitation as metal sulphides, metal carbonates or metal hydroxides (for *Cu*, *Zn* and *Cd* only) considering the pH range in these cells (between 5.48 and 7.53). Other potential removal processes include metal precipitation as phosphate and sorption to bacterial cell and other surfaces. The importance of these secondary mechanisms need to be further evaluated.

Immobilisation of *Al*, *Cu*, *Pb*, *Cd*, *Zn*, *Co*, *Ni* and *Fe* from the soluble phase was completed in CARs 2 & 3 in 15 to 30 days and in CAR4 in 428 days (exept for *Al* and *Fe*) (Figure 7.19 to Figure 7.27). Some soluble metals remained in the CARs, even after 919 days into the test. For example, *Zn*, *Cu*, *Co* and *Mo* concentrations were found to be less than the European Drinking Water Standards (EDWS) (Council Directive 98/83/EC) which is an extremely strict standard for leachate. *Fe*, *Al*, *Pb*, *Ni* and *Cd* concentrations were found to exceed the standards.

The rate of metal precipitation in the CARs in order from the fastest to the slowest was determined from the test results given in Table 7.2, Table 7.3 & Table 7.4 as *Al*>*Cu*>*Pb*>*Cd*>*Zn*>*Co*>*Ni*>*Fe*. The order is similar to the solubility product values for S^-, CO_3^- or the OH^- if arranged from the smallest to the highest (Stumm and Morgan, 1981). Sulphate reduction (Figure 7.14) and metal precipitation for *Cu*, *Pb*, *Cd*, *Zn*, *Co*, *Ni* and *Fe* both occurred before day 29 when SRB were most active. When the pH in CARs 2 & 3 rose, depletion of *Ca* and *Mg* was observed. This suggest that *Cu*, *Pb*, *Cd*,

Zn, *Co*, *Ni* and *Fe* (Figure 7.19 to Figure 7.27) precipitate as sulphides while *Ca* and *Mg* form carbonates (Figure 7.17 & Figure 7.18). Because of the ability of *Al* and *Cu* to precipitate as oxides or hydroxides when leachate pH is below 5.6 (Stumm and Morgan, 1981) their precipitation occurred faster than the other metals during the duration of the acidogenic phase in the CARs (Figure 7.19, Figure 7.20, Figure 7.22, Figure 7.23, Figure 7.26 and Figure 7.27, p. 239). This type of precipitation is known also as acidic.

It was observed that in CARs 2 & 3 the smallest concentration of sulphate (i.e., 0.8mg/litre at day 29) is the most favorable condition for all the metals to precipitate as sulphides, except for Al. In the control cell (CAR4), a reduced amount of sulphate (153.4mg/litres at day 428) was sufficient for all the metals to precipitate as metal sulphides (except *Al*), if factors as pH and Redox in the reactor were favorable to form more dissolved sulphide.

Based on the heavy metals data it can be concluded that most of the heavy metals were precipitated during the SRB active phase. Therefore, it can be assumed that metals were precipitated as metal sulphide at the same time when the sulphide was produced. However, the results show that precipitation processes for metals are slow and directly related to bacterial activity and the order of precipitation is controlled by the solubility product values.

Once waste is completely stabilized under anaerobic conditions, it is theoretically possible that a new population of aerobic micro-organisms slowly replaces the anaerobic forms and aerobic conditions are re-established where oxygen diffusion into the system is suspected. Thus, over time the anaerobic environment is hypothesized to become an aerobic. The mechanisms by which heavy metals concentrations could increase if aerobic conditions are re-established are oxidation of metal sulphides to metal sulphates which are generally more soluble, increased complexation capacity of oxidized humic acids and increased metals mobilization due to a pH decrease (Flyhammar *et al.*, 1998; Martensson, *et al.*, 1999). A pH decrease could occur due to the increased CO_2 partial pressure associated with aerobic conditions and the oxidation and re-solubilisation of sulphides to sulphate. Re-solubilisation of sulphides and carbonates will occur only if the pH of the leachate drops below 6.0 (Stumm & Morgan, 1981). Because of the large number of processes that affect metals mobility in landfills including re-solubilisation of carbonate or hydroxide precipitates, Redox potential and its effect on sulphides, complexation, ion exchange, and sorption, additional experiments that are designed to facilitate predictions of heavy metals release in a long-term are required.

Table 7.2. Concentration of heavy metals in leachate samples in CAR2.

Day	Dissolved concentration, µg/litre								
	Fe	Al	Zn	Cu	Co	Pb	Ni	Mo	Cd
0	25210.0	37514.43	2691.26	1577.29	320.79	248.73	109.47	44.77	4.09
12	8310.0	1633.98	576.12	40.71	16.78	29.78	56.04	2.22	0.61
29	11810.0	940.06	574.74	35.42	16.64	30.42	59.50	2.13	0.67
50	2230.0	412.27	319.79	23.77	30.39	9.35	53.77	1.72	0.43
98	1660.0	451.59	248.17	35.49	42.68	4.07	56.82	1.81	0.33
135	1490.0	312.43	202.85	14.55	32.55	3.01	67.82	1.89	0.25
181	3420.0	171.91	280.03	76.41	28.74	4.32	59.25	2.45	0.51
245	1560.0	255.61	1046.43	48.25	29.09	1.45	45.65	1.08	0.12
278	3610.0	505.88	228.52	88.58	34.33	1.47	81.76	0.86	0.22
345	14860.0	4528.37	412.82	193.66	44.14	41.39	228.84	2.81	0.69
397	5600.0	47.43	675.37	76.39	22.68	3.19	105.51	0.42	0.06
428	15300.0	2876.88	682.36	155.58	25.39	48.69	68.96	2.41	0.68
463	21680.0	8727.59	551.99	294.05	42.18	56.36	117.12	1.61	0.94
496	6200.0	744.86	298.22	70.93	24.78	5.02	122.60	0.97	0.26
560	5840.0	1417.78	290.70	63.25	24.47	3.21	99.07	0.49	0.18
639	5680.0	217.01	285.57	61.53	26.77	1.38	113.73	1.11	0.11
700	5270.0	153.59	326.01	73.32	26.98	4.51	116.97	0.84	0.20
791	6210.0	289.87	324.02	86.26	29.79	4.61	121.57	0.25	0.31
919	5950.0	339.86	535.85	62.66	25.20	5.73	110.43	0.67	0.25
Day	**Total concentration, µg/litre**								
	Fe	**Al**	**Zn**	**Cu**	**Co**	**Pb**	**Ni**	**Mo**	**Cd**
0	156900.0	100520.19	2779.43	2445.25	1510.32	2721.60	636.51	430.56	23.94
12	18200.0	13801.97	1830.38	96.79	27.15	65.89	103.52	4.52	9.30
29	25200.0	1737.93	1246.07	80.45	21.70	80.96	81.84	5.27	4.42
50	13000.0	12502.32	459.05	96.36	44.98	49.52	75.01	5.69	4.38
98	7700.0	602.78	413.35	82.84	52.46	21.23	65.98	2.37	4.13
135	8600.0	13575.29	351.85	110.13	34.13	54.69	71.33	3.56	3.75
181	7800.0	1192.67	705.05	86.78	37.52	29.90	85.57	4.08	3.85
245	4200.0	894.05	1745.24	51.80	40.03	59.72	67.00	4.90	3.88
278	9400.0	1067.40	306.00	141.72	37.78	58.87	111.64	4.11	3.98
345	20300.0	4561.46	954.74	233.27	45.69	75.26	315.47	13.51	4.49
397	9500.0	1578.40	722.21	246.41	24.29	59.42	135.94	4.19	5.99
428	18500.0	2876.88	958.74	285.32	44.24	56.75	138.28	4.61	4.44
463	28300.0	12371.05	707.33	316.31	50.57	134.93	133.22	9.06	5.51
496	8100.0	916.92	659.10	135.92	27.61	30.95	260.53	5.97	3.76
560	9800.0	2046.43	511.09	142.97	24.82	21.39	106.94	4.70	4.10
639	7200.0	1351.97	578.72	95.09	27.72	23.45	121.39	4.57	3.29
700	6600.0	653.43	491.74	105.97	28.93	23.93	124.20	4.26	3.83
791	8000.0	481.06	816.18	115.28	31.26	27.75	131.29	4.49	3.66
919	6200.0	2089.58	1203.46	447.46	36.63	147.41	184.59	3.82	3.34

Table 7.3. Concentration of heavy metals in leachate samples in CAR3.

Day	Dissolved concentration, µg/litre								
	Fe	Al	Zn	Cu	Co	Pb	Ni	Mo	Cd
0	37210.0	39369.48	3261.79	1431.81	505.08	273.67	181.98	65.94	14.27
12	98500.0	5266.74	455.93	78.14	48.50	71.13	165.80	4.08	0.64
29	13230.0	865.97	339.86	28.85	10.16	16.94	53.19	1.31	0.21
50	12380.0	1273.14	375.87	39.69	18.95	18.09	73.40	2.17	0.25
98	6090.0	349.66	363.60	16.02	18.84	3.75	70.55	2.26	0.16
135	12350.0	685.68	224.82	19.81	34.10	6.15	149.71	5.63	0.13
181	9420.0	464.20	152.04	56.72	23.32	4.77	84.30	0.48	0.27
245	4170.0	296.22	519.43	44.23	20.05	3.01	52.73	0.42	0.16
278	9020.0	529.22	561.54	69.62	28.92	2.45	78.70	0.41	0.15
345	5640.0	395.25	508.41	68.46	31.10	1.79	111.19	0.57	0.22
397	14650.0	2061.70	604.23	115.57	33.22	25.92	142.62	0.81	0.45
428	13420.0	1516.30	1260.61	92.60	25.02	12.88	101.73	2.11	0.32
463	9000.0	542.08	802.75	187.50	32.03	5.35	142.78	1.89	0.62
496	13840.0	2274.63	713.74	143.22	40.37	19.80	148.38	2.56	1.43
560	11800.0	1755.62	766.00	133.31	34.20	12.41	128.67	0.65	0.47
639	8750.0	661.90	432.58	80.55	39.53	12.72	140.85	0.48	0.28
700	19470.0	3711.68	670.81	176.21	46.77	30.43	131.09	0.50	1.85
791	9300.0	228.78	278.20	148.70	36.34	30.94	127.21	0.25	4.15
919	9490.0	455.43	375.89	64.53	33.37	13.00	125.77	0.14	2.74
Day	**Total concentration, µg/litre**								
	Fe	**Al**	**Zn**	**Cu**	**Co**	**Pb**	**Ni**	**Mo**	**Cd**
0	169600.0	134857.39	3686.88	2508.86	2115.54	2578.95	606.98	520.85	84.61
12	113200.0	10368.32	1110.09	314.37	77.32	183.03	251.61	18.51	13.74
29	22300.0	1195.66	565.63	180.13	17.82	81.54	79.60	8.03	5.62
50	20800.0	1875.58	520.74	256.70	36.07	65.39	120.88	9.93	5.30
98	15500.0	401.40	395.12	78.91	25.68	150.07	100.87	11.91	4.35
135	15200.0	870.38	462.21	79.22	52.10	24.42	148.50	7.31	3.37
181	13100.0	885.99	624.49	59.61	23.38	19.22	100.24	5.18	3.62
245	9500.0	952.23	650.75	43.40	21.79	118.06	52.27	4.62	11.56
278	14700.0	1441.08	583.01	78.77	39.98	173.22	118.31	6.00	18.84
345	14400.0	980.23	754.20	70.36	32.59	141.65	124.27	6.87	15.21
397	20800.0	2328.45	893.84	126.64	36.22	166.42	155.64	7.66	15.42
428	19800.0	1900.79	1383.23	142.14	41.04	140.21	164.46	7.67	14.16
463	26600.0	5262.16	2602.31	473.46	44.00	152.29	139.18	7.45	12.70
496	30700.0	8620.64	767.97	213.97	56.03	165.80	154.39	10.77	13.35
560	18200.0	2049.18	803.39	160.09	39.30	107.46	146.78	5.82	9.29
639	15700.0	2137.95	566.29	94.01	37.64	110.66	162.47	4.95	11.65
700	27800.0	4949.10	905.93	180.39	47.13	163.90	161.68	6.29	11.98
791	17200.0	333.22	499.05	166.70	43.85	165.34	151.99	6.31	15.65
919	12000.0	2926.77	876.94	298.40	39.92	120.71	135.63	3.20	24.82

Table 7.4. Concentration of heavy metals in leachate samples in CAR4.

Day	Dissolved concentration, µg/litre								
	Fe	Al	Zn	Cu	Co	Pb	Ni	Mo	Cd
0	880.0	111.49	51.15	23.83	538.14	3.02	47.18	34.62	0.14
12	83990.0	3244.17	8461.89	149.82	263.39	46.13	345.10	13.07	2.13
29	79760.0	2167.67	8969.30	109.80	315.35	14.18	403.16	10.17	0.69
50	191120.0	1981.32	342.49	61.48	19.38	10.87	457.49	8.49	0.92
98	384040.0	719.38	6114.31	83.77	363.36	10.44	440.39	9.67	0.34
135	297120.0	887.55	6498.82	78.19	402.07	10.40	480.41	8.34	0.20
181	480960.0	589.79	6417.89	85.66	453.14	11.51	509.60	11.69	1.65
245	332520.0	605.20	3241.64	71.50	321.11	9.81	393.97	6.74	1.17
278	472160.0	393.62	869.70	97.07	319.11	8.53	440.97	6.87	0.70
345	895520.0	509.08	228.06	63.58	146.24	10.85	313.61	4.02	0.31
397	756960.0	848.50	467.23	80.19	136.15	1.96	349.05	3.07	1.11
428	4614400.0	86.89	212.71	59.11	18.14	5.33	240.98	7.04	0.11
463	3914240.0	42.14	216.77	69.00	9.79	1.03	177.89	3.41	0.25
496	3028480.0	12.75	186.11	47.65	6.99	6.02	145.15	3.45	0.32
560	2544640.0	37.20	171.91	50.12	5.55	0.12	121.00	1.29	0.05
639	211840.0	62.32	209.72	75.44	13.90	13.61	192.80	1.53	0.02
700	51800.0	82.00	198.63	65.46	14.97	7.96	221.18	4.16	0.41
791	50400.0	22.41	203.90	77.89	15.55	9.46	230.38	2.23	0.08
919	55200.0	19.26	196.94	61.22	12.43	7.37	196.25	2.02	0.12
Day	**Total concentration, µg/litre**								
	Fe	**Al**	**Zn**	**Cu**	**Co**	**Pb**	**Ni**	**Mo**	**Cd**
0	3800.0	110690.86	3160.86	2803.56	608.50	706.38	219.48	143.73	15.41
12	131300.0	3649.97	15887.34	246.52	749.94	285.99	883.72	20.70	6.64
29	198200.0	3594.35	9148.46	125.98	448.05	138.19	544.51	13.90	5.01
50	323200.0	3378.70	9087.15	121.86	697.09	43.73	819.87	8.43	3.73
98	464800.0	4537.98	8157.86	101.73	737.37	110.23	860.93	9.84	4.25
135	586400.0	4338.27	7058.08	87.25	664.05	90.99	764.55	9.12	4.10
181	798200.0	594.71	21856.01	274.10	1509.94	85.72	1509.73	12.60	4.61
245	912200.0	972.45	10536.99	198.90	867.78	84.12	1006.56	10.88	4.45
278	1202000.0	860.96	2710.88	141.53	642.33	102.05	906.18	12.28	4.88
345	1631000.0	1264.23	733.18	85.73	225.41	43.29	476.52	18.17	3.49
397	1093000.0	1632.71	696.79	84.30	155.89	21.76	434.32	6.37	4.41
428	5210000.0	373.16	558.15	64.26	20.83	24.62	284.25	10.02	3.30
463	5239000.0	304.68	2359.24	69.08	9.96	21.90	200.23	9.72	3.78
496	5188000.0	131.18	612.73	76.75	7.25	26.55	185.09	12.09	3.16
560	4596000.0	417.81	450.58	56.37	5.90	21.80	150.21	7.39	2.96
639	393000.0	810.32	706.32	86.20	15.56	34.61	235.90	8.34	3.74
700	75600.0	274.99	668.26	83.07	19.86	30.95	307.69	9.97	3.81
791	87400.0	282.80	579.32	64.71	16.60	31.44	272.57	11.55	3.62
919	73800.0	834.75	886.22	79.57	15.07	30.22	268.65	5.41	3.31

Table 7.5. Sludge contribution to leachate heavy metal concentrations.

Fe^{2+}/Fe^{3+}	Fe	Al	Zn	Cu	Co	Pb	Ni	Mo
Dissolved concentration, µg/litre								
304.00	461.05	737.36	23.81	1.49	4.42	6.40	0.05	0.38
Total concentration, µg/litre								
12400.00	12760.48	2426.72	1342.68	8.89	303.80	105.39	13.84	5.02

7.1.10. Summary

- The primary compression in the CARs 2 & 3 resulted in 48.7 and 33.4%, respectively which was thought to be due to a lack of adequate compaction of the waste and was not included in the total settlement calculations;
- Test cells 2 & 3 exhibited almost identical intermediate secondary compression rates compared to that in the control cell (CAR4) (values between 7.3 and 8.3%), which is thought to be dominated by mechanical interactions due to delayed compression of the wastes and was not linked to biodegradation;
- An applied stress of 50kPa (5m depth in a landfill) resulted in 17.7% long-term secondary compression in test cell 3 whereas 150kPa (15m depth) caused a 19.3% long-term secondary compression in test cell 2, which was thought to be due to the combined effects of mechanical compression and biodegradation;
- The long-term secondary settlement exhibited in both test cells was found to be dependent on waste depth; The increased stress in CAR2 appeared to lead to 20% increased rates of long-term secondary compression in comparison to CAR3;
- The dominant cause of long-term settlement in CARs 2 & 3 was likely to be due to a major reduction in volume as a result of waste biodegradation;
- The close similarity of the CARs settlement behaviour to full-scale observations suggests that the test cells can effectively simulate actual landfill settlement;
- The total biogas production (carbon dioxide + methane) at STP from the waste sample per kg dry matter was 314.31 litres/ kg and 256.03 litres/ kg for cell 2 and cell 3 respectively. At the same time, methane concentration in the test cells reached 62.7% vol. (CAR2) and 68.1% vol. (CAR3);
- The results obtained of leachate samples taken from CAR2 & CAR3 can be divided in distinct four phases:

Phase I: *the acidogenic phase* (0 - 9 days), when the long-chain fatty acids (propionic, butyric, valeric and caproic acids) were the main product and the pH was low (5.5 - 5.8);

Phase II: *the acetogenic phase* (10 - 40 days), when the long-chain VFAs were converted to acetate, carbon dioxide and hydrogen, and the biogas production was negligible;

Phase III: *the accelerated methanogenic phase* (40 - 140 days), where the maximum biogas production rate was recorded; and

Phase IV: *the decelerated methanogenic phase* (140 - 919 days), where the rate of methane production decreased, even though the methane and carbon dioxide concentrations remained constant;

- At day 22 of the experiment all the sulphate in the leachate was depleted resulting in a simultaneous increase in the rate of methane production;
- A gradual increase in the ammonium ion concentration was observed in leachate samples taken form the CARs, indicating that nitrogen was in quantities in excess of those which could be bound in the cell biomass during the growth of microbial populations in the CARs;
- Chemical analysis of leachate samples taken from the CARs showed a gradual decrease in calcium and magnesium ions which is almost certainly due to the precipitation of these elements during biodegradation;
- CAR4 is an interesting and unique control reactor because despite all the efforts to prevent the onset of biodegradation and methane formation, the control overcame the inhibitory effect of the VFAs and became methanogenic. After day 314 the control cell started to produce biogas. This was considered to be due to the establishment of a methanogenic bacterial consortium in the control test that led to an increase in biogas production and methane concentration in the cell;
- CAR4 can be accepted as a control until day 314 where the onset of degradation processes occurred. With this assumption it can be concluded that the amount of settlement which was likely to be caused by compression processes was only 12.0% (until 314); and
- Solubility product controls the heavy metals precipitation order as well as the type of solid formation. However, bacterial activities are responsible for producing sulphides and carbonates, which control, in general, precipitation rates.

Immobilisation of *Al*, *Cu*, *Pb*, *Cd*, *Zn*, *Co*, *Ni* and *Fe* from the soluble phase was completed in CARs 2 & 3 in 15 to 30 days and in CAR4 in 428 days (except for *Al* and *Fe*). Some soluble metals remained in the CARs, even after 919 days into the test.

7.2. Total porosity

To investigate the reduction in total porosity due to compression and biodegradation, drainable porosity and moisture content were measured for CAR2 & CAR3 at the end of the experiment. Voids formed in waste sample can lead to a high source of error when determining drainable porosity. It was therefore decided to drain the leachate from each cell and then pump it back again from the bottom up to remove any trapped gas bubbles and then to perform the porosity test.

The waste was first allowed to drain to completely remove any water that could be released under gravity. The data was obtained by draining the sample in stages and measuring the volume drained and the water level in a piezometer pipe connected to the cell wall after each stage. The drainable porosity (n_e) was calculated as the volume of drainable voids per unit total volume (Eq. 3.5).

No data is available for the initial drainable porosity in the cells. To avoid any oxygen to re-enter the cells and disturb the anaerobic conditions in the CARs the drainable porosity test was not carried out at the beginning of the experiment. However, the volume of the leachate introduced in each cell from the bottom up, before load was applied, was measured and the movement of the load platen recorded. These values allowed the calculation of the volume of the leachate in the waste sample immediately after loading and allowed the estimation of the initial waste total porosity in each test cell. This was achieved by relating the volume of the leachate in the waste sample after loading to the volume of total voids in the waste. The total porosity was determined as the volume of total voids per unit total volume (Eq. 3.1).

After completing the drainable porosity test two core samples were obtained from each cell by drilling into the waste sample with a hollow steel tube (details in 7.3). The samples where then removed from the tube, divided into 6 subsamples and then oven dried at 70°C to a constant weight. Moisture content (ω_{wet}) was determined using Eq. 3.3. The results are given in Table 7.6. The range of variation in moisture content of the waste was found to be between 34.12% and 56.57%, with lower levels seen in CAR2

where the higher stress was applied. The total porosity was then calculated by summing the drainable porosity and moisture content (thus giving the volume of total voids in the waste) and dividing by the waste total volume. The results are presented in Table 7.7.

The total porosity data revealed that the two cells developed different porosities with respect to time. As can be seen in Table 7.7, a reduction in the total porosity of 24.2% and 39.3% occurred in CARs 2 & 3 respectively, after a period of 919 days. CAR2 experienced less reduction in total porosity over the test period, which was attributed mainly to the higher stress applied in this reactor. As summarised in section 7.1.10 CAR2 was also found to have a 20% increase in the rate of long-term secondary settlement when compared to CAR3.

Table 7.6. Moisture content for the core samples.

CAR2 (150kPa) moisture content (ω_{wet}), %			**CAR3 (50kPa) moisture content (ω_{wet}), %**		
depth, cm	core 1	core 2	depth, cm	core 1	core 2
4	49.57	40.76	5	48.06	48.06
8	46.36	34.12	10	34.79	35.62
12	40.78	39.30	15	43.42	45.96
16	37.96	43.10	20	41.24	47.22
20	40.91	44.43	25	46.34	52.03
24	39.58	38.22	30	56.57	49.65
average core ω_{wet}	42.53	39.99	average core ω_{wet}	45.07	46.42
average ω_{wet} in CAR2		41.29	average ω_{wet} in CAR3		45.75

Table 7.7. Comparison between initial and final parameters.

Parameter	**CAR2 - 150kPa**	**CAR3 - 50kPa**
Initial waste		
Drainable porosity, %	n/d [3]	n/d
Moisture content (wet), %	n/d	n/d
Total porosity, % [1]	40.80	51.72
Final waste		
Drainable porosity, %	5.97	9.67
Moisture content (wet), % [2]	41.29	45.75
Total porosity, %	30.92	31.39

Note: [1]estimated; [2] average values for the whole reactor as in Table 7.6; and [3] n/d - not determined.

7.3. Dismantling of CARs 2 & 3

7.3.1. Dismantling procedure

The aims of the dismantling process was to obtain core samples from the experimental reactors and gain further information on the chemical composition of the waste material at the end of the experiment in order to be able to assess variability in the degradation of the waste body.

The method for reactor dismantling involved draining out the leachate, lifting the load platen, unbolting the top section, and removing each cell from the loading frame with the aid of a manual forklift. Two core samples (100mm ID) were then taken from each reactor by drilling into the waste sample with a hollow steel tube (Figure 7.28). The tube was positioned upright into the cell using two straps that were attached to the tube. The waste sample was pushed intact into the tube by using a load applied through the cell platen. The cell was then removed from the loading frame again and the tube extracted from the waste with the aid of two metal chains and a portable crane (Figure 7.29). The waste sample was extruded from the sample tube using a hand operated extruder with a hydraulic jack. Each extruded sample was divided into 6 subsamples of approximately 4cm- and 5cm-length each, respectively. The six subsamples from the first core was pre-treated according to the procedure described in section 5.4 and Figure 5.17 and analysed for TC, TN, LOI, cellulose, hemicellulose, lignin, NDF and ADF. The waste material tested was stored in air-tight plastic bags prior each analysis. The six subsamples from the second core was dried at 70°C to a constant weight and placed in air-tight plastic bags for archive.

7.3.2. Chemical analysis of the waste subsamples

A. Total carbon, total nitrogen and LOI data

The total carbon content (TC) is the sum of both inorganic (IC) and organic carbon (TOC) in the sample. IC of the core samples was not determined in this study. LOI (loss-on-ignition) represent volatile and readily oxidised organic carbon forms (i.e. total organic matter) (section 5.5.8). Note that the TC is not the same as total organic matter as determined by LOI. While the TC includes both organic and inorganic carbon matter, LOI determinations represents all organic matter, including some non-carbon matter (Godley *et al.*, 2004).

The total carbon content (TC) and LOI of the core samples are given in Table 7.8. As seen in the table, the average TC content for CAR3 was 9.7% higher than that obtained for the other cell. The increased value of TC utilization in CAR2 (Table 7.8) suggests that carbon removal from CAR2 was greater than that for the other test cell.

Figure 7.30 shows the TC content of the core samples taken from CARs 2 & 3 as a function of depth below waste surface (values from Table 7.8). The TC content in the two test cells was found to vary between 26.43% and 39.00% (Table 7.8). As can be seen, both TC curves follow similar trends with lower TC values in the 2nd, 3rd, and 5th layers and higher values for the 1st, 4rd, and 6th layers. The lowest TC values was obtained for subsamples taken from 8 to 10 cm below the surface (26.43% in CAR2 and 31.70% in CAR3) which suggest that the rate of biodegradation varies with depth. Table 7.8 also gives the LOI data obtained from the core samples. It was found that LOI curves for both cells corresponded very well to the TC curves. There was a good statistical correlation between TC content and LOI data with R^2 value of 0.8856 (CAR2) and 0.8087 (CAR3) assuming a linear relationship (Figure 7.31, p. 245). The relationship between the two values was found to be TC*a = LOI, with values for a between 1.64 and 1.83 for CAR2 and between 1.49 and 1.72 for CAR3.

B. Fibre analysis data

Variations in NDF, ADF & ADL content in depth are given in Figure 7.32 and variations in cellulose, hemicellulose and TC content along the height of the reactors are presented in Figure 7.33. As can be seen the cellulose content decreased in proportion to the waste TC content, which is because cellulose constitutes a significant fraction of the initial TC in the waste (in this study 58.07%, see Table 5.4). While there were some variations in the cellulose, hemicellulose and TC content of the core subsamples, with some having high concentrations (1st, 4rd, and 6th subsample in both cells), values were interrelated. There was a good statistical correlation between cellulose content and TC content in CARs 2 & 3 with R^2 value of 0.82 and 0.81, respectively (Figure 7.34).

It was also found that even at different applied loads, similar fluctuations in waste TC, LOI, NDF, ADF and cellulose contents were observed. TC, LOI, NDF and ADF analyses of the waste samples taken the test cells showed significant differences in the extent of biodegradation at different depths within the cells. The variation in all these parameters was probably caused by different bacterial activities or random local variations in material composition within each layer of the waste sample, with elevated parameter

values in the 1st, 4rd, and 6th layers and lowered values in the 2st, 3rd, and 5th layers. The reason for this variation has not yet been identified.

The inconsistencies in TN, ADL and hemicellulose contents made it difficult to draw any definite conclusions from these analyses.

7.3.3. Summary

- The TC utilised in CAR2 as a result of biodegradation was approximately 30% higher that that observed in CAR3;
- Good statistical correlations were found between TC content and LOI data with R^2 value of 0.887 (CAR2) and 0.783 (CAR3); In addition, the cellulose content and TC content in CAR 2 & 3 had R^2 values of 0.82 and 0.81, respectively; and
- The data shows a very clear variation in waste TC, LOI, NDF, ADF and cellulose with depth in the reactors. As a result, all these parameters were found to be depth dependant variables.

Table 7.8. Elemental and fibre analysis data for the core samples.

Subsample		Depth, cm	Dry mass, g	NDF, %	ADF, %	ADL (lignin), %	Cellulose, %	Hemi-cellulose, %	TC, %	TN, %	LOI, %	TC utilised[1], g/kg DM
CAR2 - 150kPa	1	4	86.50	28.39	26.00	16.84	9.16	2.39	33.34	1.17	64.51	127.12
	2	8	140.36	17.99	17.60	10.27	7.32	0.39	24.40	0.93	47.97	216.55
	3	12	148.81	26.28	24.87	17.03	7.83	1.42	25.86	1.00	48.52	201.88
	4	16	114.71	26.22	24.95	15.42	9.53	1.27	30.33	1.08	59.99	157.24
	5	20	99.08	19.04	15.99	7.63	8.36	3.05	28.49	1.00	54.13	175.60
	6	24	106.51	22.49	18.94	9.83	9.11	3.56	30.66	1.09	54.51	153.86
	Average for CAR2			**23.40**	**21.39**	**12.84**	**8.55**	**2.01**	**28.85**	**1.05**	**54.94**	**172.04**
CAR3 - 50kPa	1	5	135.39	31.93	28.10	18.01	10.09	3.83	34.41	1.26	64.23	116.42
	2	10	166.48	20.84	18.65	10.86	7.79	2.19	29.23	1.01	50.57	168.24
	3	15	161.09	19.63	17.80	9.45	8.34	1.83	29.67	0.91	52.92	163.80
	4	20	124.98	26.44	22.76	11.15	11.61	3.67	35.96	1.48	62.38	100.94
	5	25	151.05	23.36	20.70	10.87	9.83	2.66	30.49	0.98	50.43	155.63
	6	30	226.12	24.18	21.07	12.14	8.93	3.11	31.61	1.01	51.11	144.35
	Average for CAR3			**24.40**	**21.51**	**12.08**	**9.43**	**2.88**	**31.89**	**1.11**	**55.27**	**141.56**

Note: [1]This value was calculated assuming that the initial TC in each subsample was equal to the initial TC for the whole reactor (data given in Table 5.4); concentrations given are by dry mass in waste.

7.4. Prediction the rate and potential of MSW biodegradation in CAR2 & CAR3 filled with FR waste sample

BMP3 test was performed to characterize the anaerobic biodegradation potential of a fresh, well characterised MSW (FR waste sample). The experiment was carried out as outlined in section 5.2. To achieve this measurement of the components and quantity of the biogas produced, determination of the loss of cellulose and hemicellulose as indicated by measurements of Neutral Detergent Fibre (NDF), Acid Detergent Fibre (ADF) and Acid Digestible Lignin (ADL), and the assessment of various leachate chemical characteristics at key phases during the biodegradation process was carried out. Biodegradable processes in the bioreactors were studied over the same period of time as in the CARs (919 days) at approximately 30°C. The reactors were sequentially sacrificed at different stages of the biodegradative process, as dictated by the gas production rate, and samples from the waste, leachate and gas fraction were chemically analysed. Relationships between the chemical composition of the waste and the capacity for predicting the BMP of fresh waste and waste which undergone various degrees of biodegradation are discussed.

7.4.1. Biogas production and pH

The pH values of the leachate samples taken when the BMP test reactors were destructively sampled on days 8, 19, 51, 116, 135, 162, 217, 280, and 919 days respectively are shown in Figure 7.35. Initially, the pH of the leachate was 7.80. This value dropped to 5.35 due to carboxylic acid accumulation, and then gradually increased to a level of 7.77 during the transition from acetogenic phase to the methanogenic phase. There was a significant increase in the pH after day 19 followed by a simultaneous increase in the rate of methane production.

Cumulative gas production measured from the BMP test reactors is shown in Figure 7.36 & Figure 7.37, and the cumulative volume of methane produced from each BMP test reactor is given in Table 7.9. Gas production data were corrected for the gas produced from the addition of an anaerobic sludge seed observed in a number of control cells operated under the same conditions as the BMP reactors. The gas production correction based on the control cells was found to be between 0.5%(B22) and 7%(B11) of the total amount of biogas produced in the reactors. Details of the waste composition and

cumulative gas production for the two large scale long term waste settlement studies (CAR2 and CAR3) are also presented in Table 7.9.

Similar to observations made by other researchers (Christensen *et al.,* 1996; Barlaz *et al.,* 2002), the results can be distinctly divided in three phases:

- Phase I, *the acidogenic phase* (0-8 days), during which the long-chain fatty acids were the main product, and the pH was low (5.45) (Figure 7.35),
- Phase II, *the acetogenic phase* (9-51 days), when VFAs were the main product (Figure 7.35),
- Phase III, *the accelerated methanogenic phase* (52-135 days), where methane was the main product of waste degradation and
- Phase IV, *the decelerated methanogenic phase* (136-919 days), where the rate of methane production decreased even though the methane and carbon dioxide concentrations remained constant (Figure 7.38).

The duration of the observed four phases of biodegradation in the BMP3 reactors was found to be very close to the duration of the same phases observed in CARs 2 & 3.

The cumulative biogas production (carbon dioxide + methane) from the FR waste sample was 224.25 litres/kg dry wt. at STP, at which time over 50.2% vol. of the biogas produced was methane (Figure 7.37 & Figure 7.38). The gradually increasing proportion of methane in the gas generated is consistent with the gradual adaptation of the microbial population to methanogenic growth conditions. The acid-consuming methanogenic bacteria are more seriously inhibited by the low pH than the acid-producing acetogenic bacteria, resulting in methane production inhibition, as observed out by Wang *et al.* (1997). The maximum daily gas production rate was recorded for B15 and B16 at day 41 (9.50 litres/ kg dry wt./day) (Figure 7.39 & Figure 7.40). The daily gas production curves for BMP test reactors were almost identical, indicating that these reactors behaved similarly.

The initial cellulose, hemicellulose, lignin and LOI content for the FR waste sample was 24.87%, 6.67%, 9.72% and 77.80% respectively (Table 7.9). Thus cellulose, hemicellulose and lignin concentration accounted for 53.03% of the LOI. The theoretical methane potential, assuming conversion of 100% of the cellulose and hemicellulose to methane and carbon dioxide was found to be 414.8 and 424.2 litres CH_4/kg dry wt. of

Table 7.9. Biogas production and fibre analysis data for sampled reactors.

Waste sample	Initial waste	B11	B12	B13	B14	B15	B16	B17	B18	B19	B20	B21	B22	Final waste	
														CAR2	CAR3
Days into test	0	8	19	51	116	135	162	217	280	348	539	720	919	919	919
Dry mass, kg	0.1000	0.0972	0.0965	0.0852	0.0881	0.0866	0.0869	0.0877	0.0853	0.0867	0.0799	0.0784	0.0755	20.385[1]	20.385[1]
Cumulative biogas production (STP)[2], l/kg DM	0.00	4.82	10.78	90.35	153.04	160.44	177.88	188.06	204.95	215.04	222.48	224.25	243.55	313.76	255.45
Cumulative methane production (STP), litres /kg DM	0.00	1.11	6.38	61.19	100.99	108.21	120.14	118.95	126.87	128.59	128.88	139.40	146.48	193.68	158.53
NDF, g/kg DM	412.54	407.86	407.88	322.19	361.99	370.19	359.83	341.03	336.86	324.13	351.54	306.84	292.51	234.03	243.97
NDF[3], %	41.25	40.79	40.79	32.22	36.20	37.02	35.98	34.10	33.69	32.41	35.15	30.68	29.25	23.40	24.40
ADF, g/kg DM	345.86	343.89	333.66	261.50	308.33	286.26	318.58	312.76	323.29	280.26	269.49	259.89	242.03	213.89	215.14
ADF[3], %	34.59	34.39	33.37	26.15	30.83	28.63	31.86	31.28	32.33	28.03	26.95	25.99	24.20	21.39	21.51
ADL(Lignin), g/kg DM	97.19	82.86	80.26	97.41	141.88	104.26	117.15	124.56	122.82	129.37	138.03	169.59	204.22	128.40	120.81
ADL(Lignin)[3, 4],%	9.72	8.29	8.03	9.74	14.19	10.43	11.72	12.46	12.28	12.94	13.80	16.96	20.42	12.84	12.08
Cellulose, g/kg DM	248.67	261.03	253.40	164.09	166.45	182.00	201.43	188.19	200.47	150.89	131.46	90.30	37.81	85.50	94.33
Cellulose[3], %	24.87	26.10	25.34	16.41	16.64	18.20	20.14	18.82	20.05	15.09	13.15	9.03	3.78	8.55	9.43
Hemicellulose, g/kg DM	66.68	63.97	74.22	60.68	53.66	83.93	41.25	28.27	13.57	43.87	82.05	46.96	50.48	20.14	28.83
Hemicellulose[3],%	6.67	6.40	7.42	6.07	5.37	8.39	4.12	2.83	1.36	4.39	8.21	4.70	5.05	2.01	2.88

Waste sample	Initial waste	B11	B12	B13	B14	B15	B16	B17	B18	B19	B20	B21	B22	Final waste	
														CAR2	CAR3
(C+H)/L ratio[3]	3.24	3.92	4.08	2.31	1.55	2.55	2.07	1.74	1.74	1.51	1.55	0.81	0.43	0.91	1.17
TC, g/kg DM	460.53	460.39	439.74	408.56	450.17	431.02	429.59	440.79	401.53	426.60	345.92	373.84	302.44	288.46	318.94
TC[3], %	46.05	46.04	43.97	40.86	45.02	43.10	42.96	44.08	40.15	42.66	34.59	37.38	30.24	28.85	31.89
TN, g/kg DM	9.48	8.45	14.67	11.58	11.47	8.30	12.50	10.80	12.88	17.01	11.13	11.03	12.98	10.45	11.07
TN[3], %	0.95	0.85	1.47	1.16	1.15	0.83	1.25	1.08	1.29	1.70	1.11	1.10	1.30	1.05	1.11
LOI, g/kg DM	778.04	752.94	734.00	733.15	717.58	733.12	721.16	715.02	707.42	698.06	701.38	670.44	645.76	549.40	552.70
LOI[3], %	77.80	75.29	73.40	73.31	71.76	73.31	72.12	71.50	70.74	69.81	70.14	67.04	64.58	54.94	55.27
TC utilised, g/kg DM	0.00	0.14	20.65	51.97	10.36	29.51	30.94	19.74	58.99	33.93	114.61	86.68	158.09	172.07	141.59
Methane recovery (STP)[5], %	0.00	0.85	4.86	46.55	76.83	82.32	91.40	90.49	96.51	97.83	98.05	106.05	111.44	147.34	120.60

Note: [1] Estimated value calculated by assuming loss of dry mass similar to that observed in the BMP3 test; [2] Corrected for sludge contribution to biogas production; [3] The data are presented as a percentage of the final waste dry mass; the data given for CAR2 & CAR3 are the average data as in Table 7.8; [4] The percentage of lignin in the waste dry mass is expected to increase with sample age as the cellulose and hemicellulose (C+H) fraction of the waste decreases with time, lignin thereby becoming a greater proportion of the remaining waste; and [5] The measured cumulative methane production at STP divided by the theoretical production calculated by assuming conversion of 100% of the cellulose and hemicellulose to methane and carbon dioxide (Eq. 6.3).

cellulose and hemicellulose respectively at STP (Eq. 6.1 & Eq. 6.2). Using the measured cellulose and hemicellulose content from the BMP reactors presented in Table 7.9, it can be calculated that the theoretical methane production per kg dry weight of waste will be 414.8 x 0.2487 = 103.16 litres CH_4/kg dry wt. and 424.2 x 0.0667 = 28.29 litres CH_4/kg dry wt. respectively. The total loss of cellulose and hemicellulose in the reactors was found to be 210.9g/kg dry wt. and 16.2g/kg dry wt. respectively, which should lead to a production of 414.8 x 0.2109 = 87.48 litres of methane/kg of dry waste as a result of cellulose degradation and 424.2 x 0.0162 = 6.87 litres methane/kg of dry waste due to hemicellulose degradation at STP. The methane potential of lignin was considered to be zero because of its inability to decompose under anaerobic conditions (Young & Frazer, 1987). In this study, the total measured methane production from the reactors at STP was found to be 146.48 litres CH_4/kg dry wt. This gives 111.44% methane recovery calculated on the basis of the total measured cumulative methane production divided by the theoretical production assuming conversion of 100% of the cellulose and hemicellulose to methane (section 6.2.2, Eq. 6.3). This discrepancy between the calculated methane production (103.16 + 28.29 = 131.45 litres CH_4/kg dry wt.) and the measured methane volume (146.48 litres CH_4/kg dry wt.) is probably due to the fact that some methane was generated during the degradation of other waste constituents (such as proteins and fats) that had not been accounted for in the original compositional analysis. Similar observations were made for CAR2 and CAR3, where the discrepancy was found to be even higher Table 7.8.

7.4.2. Leachate characteristics

Eight VFAs were analyzed in the leachate – acetic, propionic, n- and iso-butyric , n- and iso-valeric, caproic and caprylic acids. Only the concentrations of acetic, propionic, n-butyric and n-valeric acids are shown (Figure 7.35). VFA concentrations in the leachate increased with a corresponding decrease in the pH and increase in the biogas production rates, which is indicative of unbalanced digestion conditions. The imbalance is due to the difference in activities between the hydrolytic/fermentative bacteria (section 2.3) and the acetogenic and methanogenic bacteria that work together to convert these by-products to CH_4 and CO_2 and water. The highest total volatile fatty acid concentration observed was 20367mg/l on the 19th day of the biodegradation period. Thereafter, the accumulation of carboxylic acids decreased rapidly as they were utilised faster than they were produced (Figure 7.35).

The TOC content of the leachate samples taken from the reactors upon sampling was observed to increase from an initial value of 907.4mg/l to 6264.0mg/l after 19 days and then decreased gradually to a level of 635.4mg/l by the end of the test (day 919) (Figure 7.41). The DOC of the leachate samples (DOC) increased from 68.8mg/l to 5890.0mg/l (day 19) and then decreased with the same pattern as TOC to 371.6mg/l. Results show that carbon in the leachate is mostly in the dissolved form as the TOC values are only slightly larger than the TDOC values.

7.4.3. Chemical composition of solid waste samples

A detailed mass balance for TC was undertaken to monitor the evolution of the carbon transfer from the solid to the liquid and gas phases. After 919 days all of the BMP3 bottles were emptied and samples from the waste, leachate and gas fractions taken for total carbon analyses. The results were compared with those obtained from similar samples taken from CARs 2 & 3 (Table 7.10). The duration of the tests and the initial waste characteristics for all BMP3 bottles, CARs 2 & 3 were the same.
The data on the carbon balance carried out on BMP3, CAR2 & CAR3 test reactors indicates that 158.09g, 172.07g and 141.59g of carbon per kg dry wt., respectively was utilised during the period of biodegradation. The total loss in dry weight of the initial waste sample in BMP3 test bottles was found to be 24.50g. It was observed that the majority of the utilised TC was transferred into biogas (74.22% for the BMP3 test, 88.50% for CAR2 and 87.14% for CAR3) by the end of the 919-day monitoring period, and only 4.43% (BMP3 bottles), 2.49% (CAR2) and 3.11% (CAR3) into the leachate (Table 7.10) (although this is maybe an underestimate). The loss of carbon to deposition of carbonate precipitates was estimated using the drop in calcium concentrations between the beginning and the end of the test (Figure 7.42), although other carbonate species could have been formed. Mg^{2+} did not precipitate as $MgCO_3$ over the test period due to insufficient anions to form $MgCO_3$. Precipitation of $CaCO_3$ and $MgCO_3$ is discussed in greater details in section 7.1.8. It was calculated that only 0.41% and 0.75% of the TC loss was fixed within CAR2 and CAR3 reactors, respectively at the end of the test period presumably as $CaCO_3$ precipitate, whereas this amount was 1.00% for the BMP3 test bottles.

The carbon mass balance calculations made for BMP3 bottles and the consolidating reactors indicate that carbon inputs exceeded carbon outputs by 8.15%, 3.77% and 3.37%, respectively (Table 7.10). However, there are number of potential sources of error

in the carbon mass balance, that have not been quantified including: carbon utilised for bacterial biomass; carbon precipitated as insoluble products other than $CaCO_3$ (carbonates of other metals which were found to be present in the leachate such as *Pb, Co, Cd, Zn, Fe, Cu* and *Ni*, section 7.1.9); and random errors due to the precision limitations of the measurement devices used in the experiment.

Table 7.10. Summary of carbon mass balance for FR waste sample.

Parameter	BMP3	CAR2	CAR3
$TC_{t=o,\ waste}$, g/kg DM.	460.53	460.53	460.53
$TC_{t=o,\ leachate}$, g/kg DM.	6.60	3.14	3.14
$TC_{t=ti,\ waste}$, g/kg DM.	302.44	288.46	318.94
$TC_{t=ti,\ leachate}$, g/kg DM.	7.00	4.28	4.40
$TC_{t=ti,\ CaCO_3}$, g/kg DM.	1.58	0.70	1.06
$TC_{t=ti,\ MgCO_3}$, g/kg DM.	0.10	0.10	0.10
$TC_{t=ti,\ CH_4}$, g/kg DM.	78.64	103.96	85.10
$TC_{t=ti,\ CO_2}$, g/kg DM.	38.70	48.32	38.29
Unaccounted C[1], g/kg DM.	38.08	17.48	15.62
Mass balance error[2], %	8.15	3.77	3.37

Note: $TC_{t=o,\ waste}$ indicates the total carbon in the wastes before the beginning of the test; $TC_{t=ti,\ waste}$ indicates the total carbon in the waste samples after 919 days of test; $TC_{t=o,\ leachate}$ and $TC_{t=ti,\ leachate}$ are the TC content (TOC+IC) of leachate samples taken at time t = 0 and t = i respectively; $TC_{t=ti,\ CaCO3}$ is the carbon content as $CaCO_3$ (precipitated and dissolved) in the leachate at time t = i; $TC_{t=ti,\ MgCO3}$ is the carbon content as $MgCO_3$ (dissolved only) in the leachate at time t = i; $TC_{t=ti,\ CH4}$, and $TC_{t=ti,\ CO2}$ are the carbon in the biogas as methane and carbon dioxide, respectively at the end of the test; [1] calculated by Eq. 5.7; and [2] calculated by Eq. 5.8.

NDF, ADF and ADL analysis was performed as outlined in section 5.5.10. Average values of NDF, ADF, hemicellulose, cellulose and lignin contents of the waste samples taken at different stages of the biodegradation process are shown in Table 7.9. All the data are presented as a percentage of the initial waste dry mass. The NDF content of the waste samples taken from BMP3 test bottles, which is indicative of the entire fibre fraction of the waste, showed a decreasing trend over the test period (Figure 7.43). Initially, the NDF biodegradation rate increased to a level of 1.77gNDF/kgDM/day after 51 days indicating the beginning of cellulose and hemicellulose degradation when the bacterial growth is the highest. This value dropped to 0.31gNDF/kgDM/day during the accelerated methanogenic phase (52-135 days) which corresponds to a decrease in carboxylic acid concentrations and an increase in pH (Figure 7.35) and after that decreased further to a level of 0.13gNDF/kgDM/day by the end of the test (Figure 7.44).

A similar trend was showed for the ADF data which represents a portion of the waste that contains only cellulose and lignin (Figure 7.44). The NDF and ADF average biodegradation rates were observed to be (412.54-292.51)/919=0.38 and (345.86-242.03)/919=0.33g/kgDM/day respectively over the whole period of test.

The cellulose content was estimated using Eq. 2.42. The percentage of cellulose (section 2.5, Eq. 2.42) in the waste in the BMP3 bottles decreased with sample age at an average rate of (248.67-37.81)/919=0.299g/kgDM/day over a period of 919 days. Thus, 84.8% of the cellulose degraded over the period of 919 days (Table 7.9). Hemicellulose was assessed as the NDF values minus the ADF values (section 2.5, Eq. 2.43). However, the data for hemicellulose content was the most variable of all the parameters measured and cannot be conclusive. Therefore, it can be concluded that cellulose alone is more indicative of the degradation that is occurring under anaerobic conditions than hemicellulose.

However, the rate of hydrolysis is relatively slow and can be limiting in anaerobic biodegradation of waste which contains lignin. Furthermore, the rate of methane production is often limited by the rate of biopolymer destruction and/or effective metabolic interaction between hydrolytic bacteria and the methanogens (Zeikus 1980[a,b,c]). In contrast, it is interesting to note that the waste sample used to fill BMP3 bottles, CARs 2 & 3 underwent nearly complete degradation as measured by either cellulose content or the extent of degradation expressed as methane recovery (Table 7.9). This suggests that the lignin concentration does not always reflect the degree to which lignin inhibits cellulose bioavailability (Eleazer *et al.*, 1997, section 2.5).

A common way to demonstrate the extent of biodegradation or the biodegradation potential is to use the cellulose + hemicellulose to lignin ratio (C+H)/L (Wang *et al.*, 1994; Hossain *et al.*, 2003). Values between 2 and 4 have been reported in the literature for fresh MSW (Bookter *et al.*, 1982; Hossain *et al.*, 2003), and lower values are associated with decomposed waste (Mehta *et al.*, 2002; Suflita *et al.*, 1992; Ham *et al.*, 1993[a]). As the waste degrades, the percentage of cellulose and hemicellulose (C+H) into the waste sample has been shown by other researchers to decrease with time (Ham *et al.*, 1993[b]; Suflita *et al.*, 1992; Wang *et al.*, 1994). Consequently, it can be expected that the percentage of lignin in the waste dry mass would increase with sample age as the C+H fraction of the waste biodegrades, lignin thereby becoming a greater proportion of the remaining waste. The ADL data in this study indicate that the percentage of lignin in the waste sample tested increased from initial value of 9.72% to a value of 20.42% by the

end of the test period (Table 7.9). In this test the (C+H)/L ratio in the analysed samples decreased concurrent with the increasing volume of methane produced (Figure 7.45). It was determined that the (C+H)/L ratio decreased at an average rate of (3.24-0.43)/919 = 0.0031 per day and approximately 116 days were required for this parameter of biodegradation to decrease from an initial value of 3.24 to a value of 1.55 (about 50% reduction). In a laboratory scale simulation carried out by Hossian *et al.* (2003) 50% of the initial (C+H)/L ratio was reported to be degraded over a period of 24 days. This enhanced biodegradation was probably due to the leachate recirculation applied to the bioreactors during the test.

7.4.4. Correlations between fibre analysis data and BMP test data

NDF, ADF, cellulose, (C+H)/L ratio, waste TC, and waste biochemical methane potential are all parameters that were used to assess the biodegradation potential of fresh MSW. Correlations between these parameters were shown to exist for the BMP test reactors used in this study (Figure 7.46 to Figure 7.56). There was a good statistical correlation between cellulose content and cumulative gas production rate with R^2 value of 0.64 (Figure 7.46). Other studies have often found a positive relationship between the cellulose content and waste biodegradability assessed by BMP tests (Barlaz *et al.* 1997).

The comparison between the NDF biodegradation rate and biogas production rate indicates that there was a relatively good correlation between these two parameters with $R^2 = 0.59$ (Figure 7.47). While the data in Figure 7.48 shows a relationship, the relatively low correlation coefficient ($R^2 = 0.51$) suggest that factors in addition to ADF biodegradation rates influence the gas production rates.

To the extent that cellulose constitutes a significant fraction of the initial TC presented in the waste (in this study 54.0%) and is degradable, cellulose content should decrease in proportion to the waste TC content. As can be seen in Figure 7.49 the TC content of solid waste samples showed a decreasing trend over the test period which is consistent with the depletion of cellulose. To better illustrate this relationship, cellulose content was plotted against total carbon content in Figure 7.50 where it can be seen that there was a good statistical correlation, with a R^2 value of 0.74.

TC represents a fraction of the waste organic matter determined by LOI, with the TC being between 46.8 and 62.7% of the LOI measured in the BMP3 bottles. While the TC includes both organic and inorganic carbon matter, LOI determinations represents all

organic matter, including some non-carbon matter (Godley *et al.*, 2004). Therefore, the TC and LOI would be expected to correlate well. As can be seen in Figure 7.51 a statistically significant correlation was found for these two parameter (R^2=0.69).

It is interesting to examine if there is a correlation between a non-biological test (such as LOI) and a biological test (such as BMP). When comparing LOI data with BMP data, a reasonable correlation between these two tests was found (R^2=0.67, Figure 7.52) indicating that LOI test may provide in some cases a reasonable replacement for biological tests at a low cost.

There was a strong statistically valid correlation between the LOI measured in the BMP3 reactors and the (C+H)/L ratio (R^2 = 0.73, Figure 7.53). Despite the fact that LOI analysis is less expensive, its use as a substitute for (C+H)/L ratios would results in less accuracy, because the (C+H)/L ratio eliminates the effect of sample dilution with soil, which is not possible with LOI analysis.

There was a statistically significant correlation between the pH observed in the BMP3 bottles and the corresponding (C+H)/L ratio (R^2 = 0.84). As can be seen in Figure 7.54 a higher pH is correlated with a lower (C+H)/L ratio, i.e. more degraded waste. This can be attributed to the activity of the methanogenic bacteria which is more active at neutral pH. This relationship is consistent with data reported by Ham *et al.* (1993[b]) in which eight of nine samples excavated from a New York landfill that were actively producing methane and had a pH of between 6.98 and 7.91. The optimal pH for refuse methanogenesis is 6.8–7.4 (Zehnder, 1978).

The best correlations found were between (C+H)/L ratio and cumulative methane production (Figure 7.55) and between the (C+H)/L ratio and methane recovery (Figure 7.56) with R^2 value of 0.84 for each curve, which indicates that measured cellulose and hemicellulose contents in fresh MSW represent readily biodegradable carbon.

7.4.5. Summary

- Although BMP tests provide a more realistic basis for comparing the relative biodegradability of MSW, it is more prone to error and variability than physical and chemical tests. Therefore it is good to have a simple, less costly and rapid physical and chemical method that may provide an indication of the waste biodegradability and a useful alternative to BMP tests;

- The study concludes that the TC analysis has advantages for accuracy and reproducibility and it is a useful measurement as it provides an expression of the amount of waste mineralised by biodegradation process but is not a completely reliable indicator for prediction the rate and potential of MSW biodegradation;
- TN, ADL and hemicellulose contents in all BMP3 test reactors proved to be very variable indicators, where only relatively small changes in their concentration were observed with sample age;
- The BMP3 test results indicate that changes in values for NDF, ADF, cellulose, (C+H)/L ratio and methane potential for the BMP test samples that have been found are interrelated. Additionally, the best correlation found was between the (C+H)/L ratio and BMP (R^2=0.84), which indicates that measured cellulose and hemicellulose contents in fresh MSW give a realistic assessment of the readily biodegradable carbon; and
- The correlation between all the chemical parameters mentioned above suggest that monitoring only one of these parameters may be sufficient to provide an accurate prediction of the degree of biodegradation and BMP of a fresh MSW sample without extensive monitoring methods.

Figures

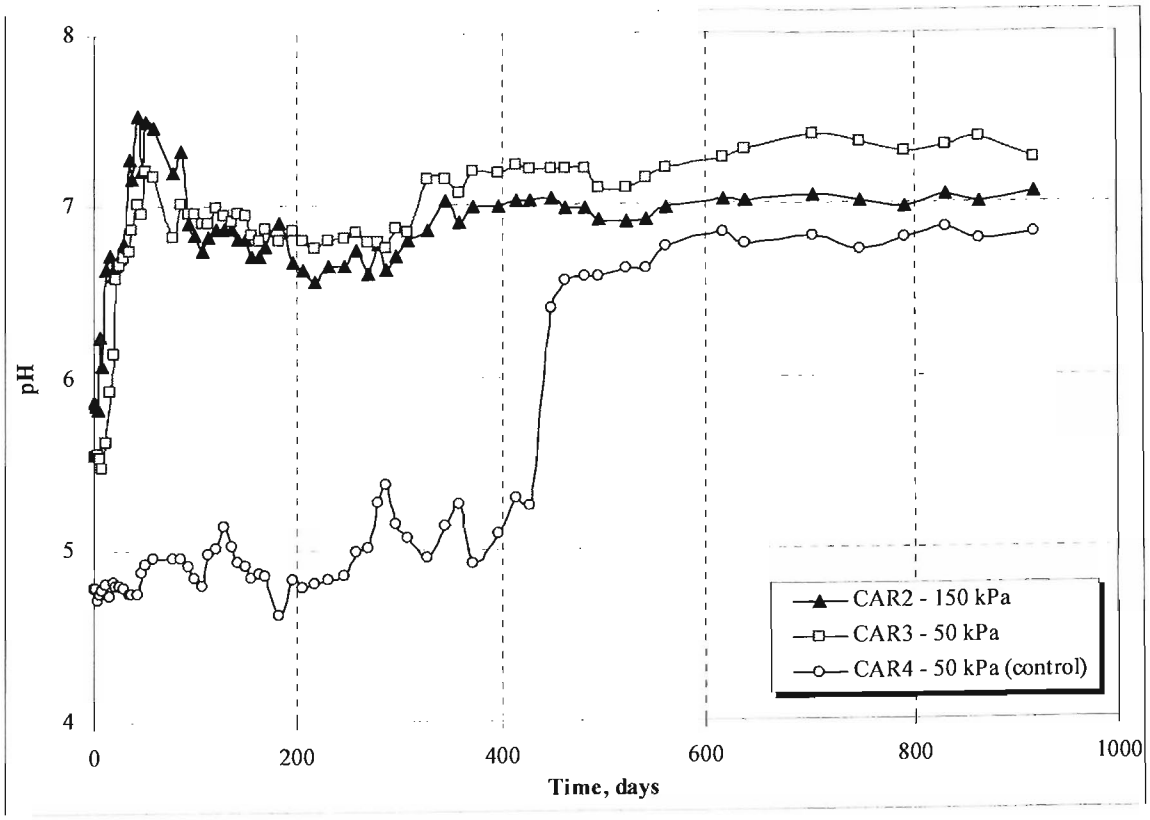

Figure 7.1. pH in CARs 2, 3 & 4.

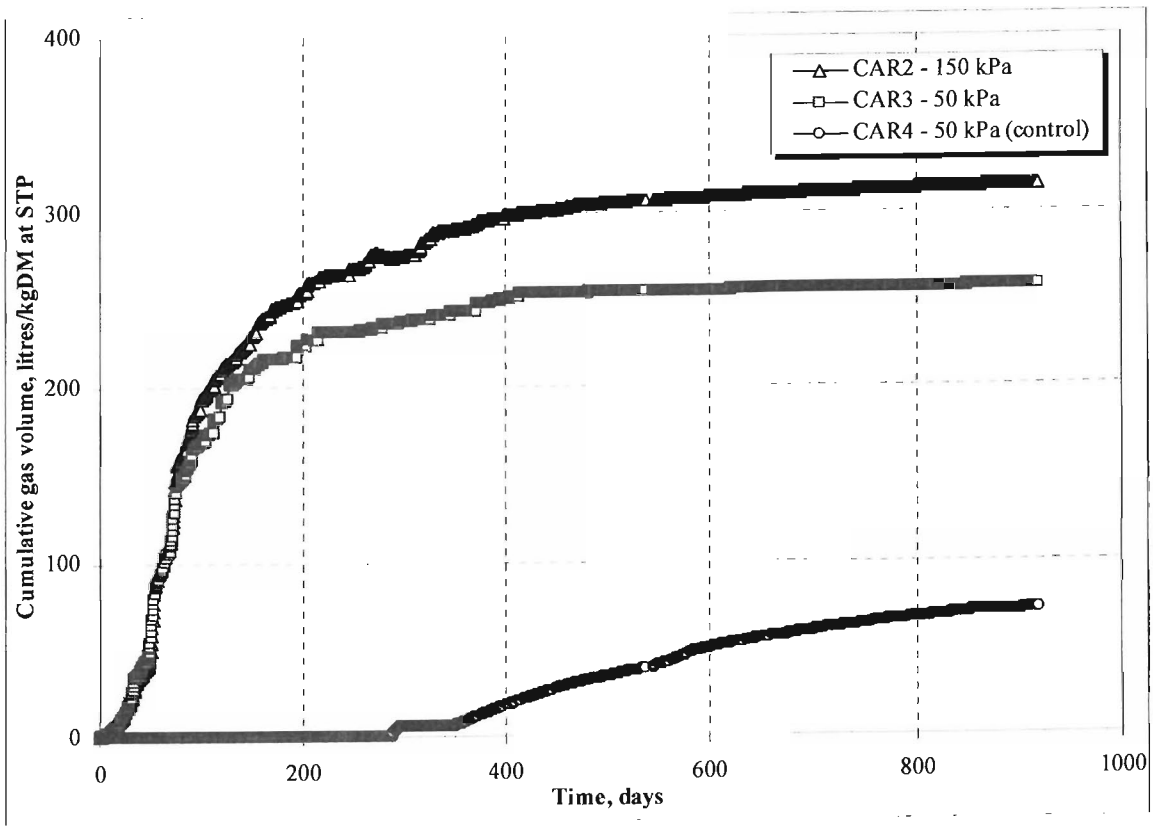

Figure 7.2. Cumulative gas production at STP in CARs 2, 3 & 4.

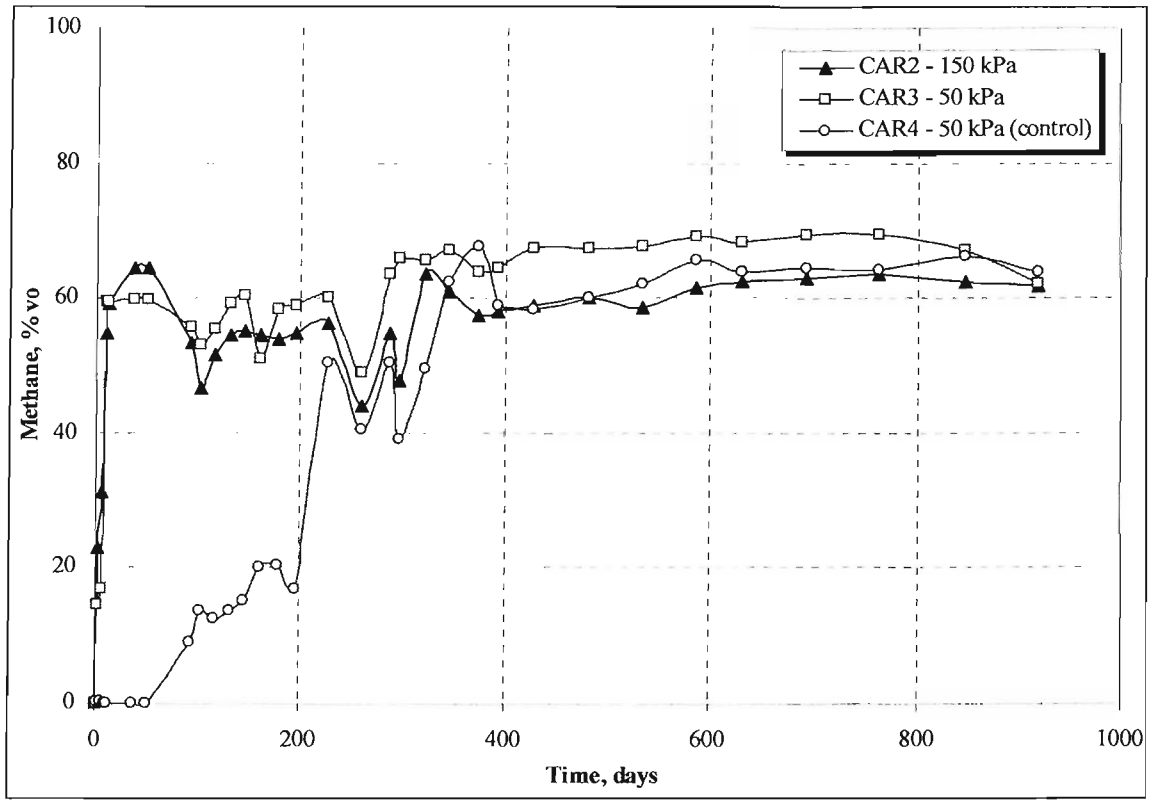

Figure 7.3. Methane in CARs 2, 3 & 4.

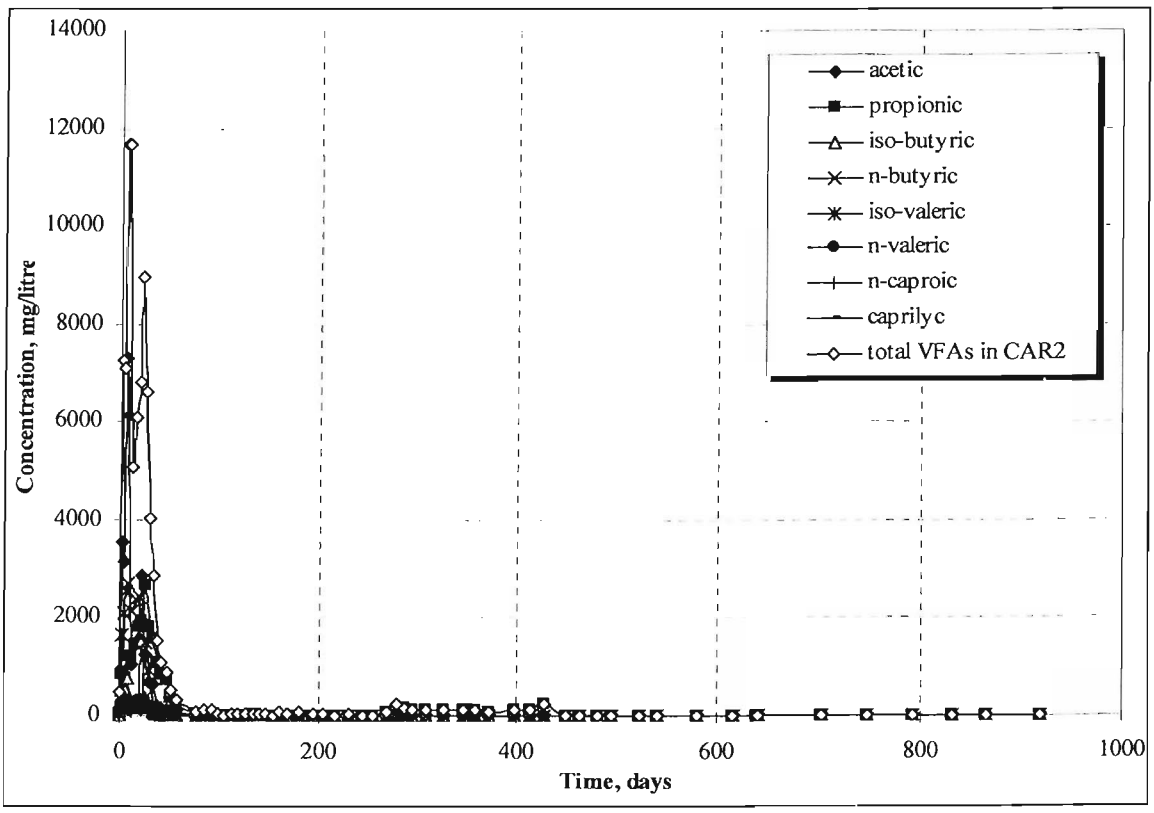

Figure 7.4. Leachate VFAs in CAR2 (150kPa).

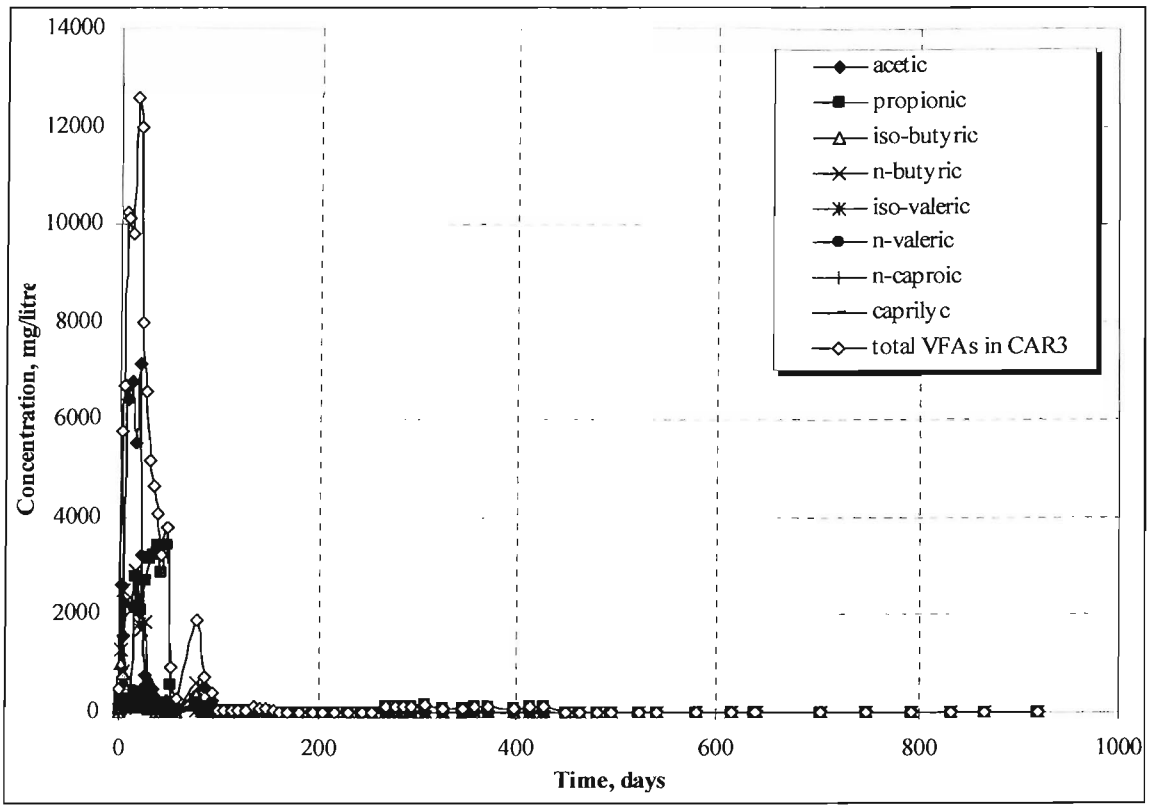

Figure 7.5. Leachate VFAs in CAR3 (50kPa).

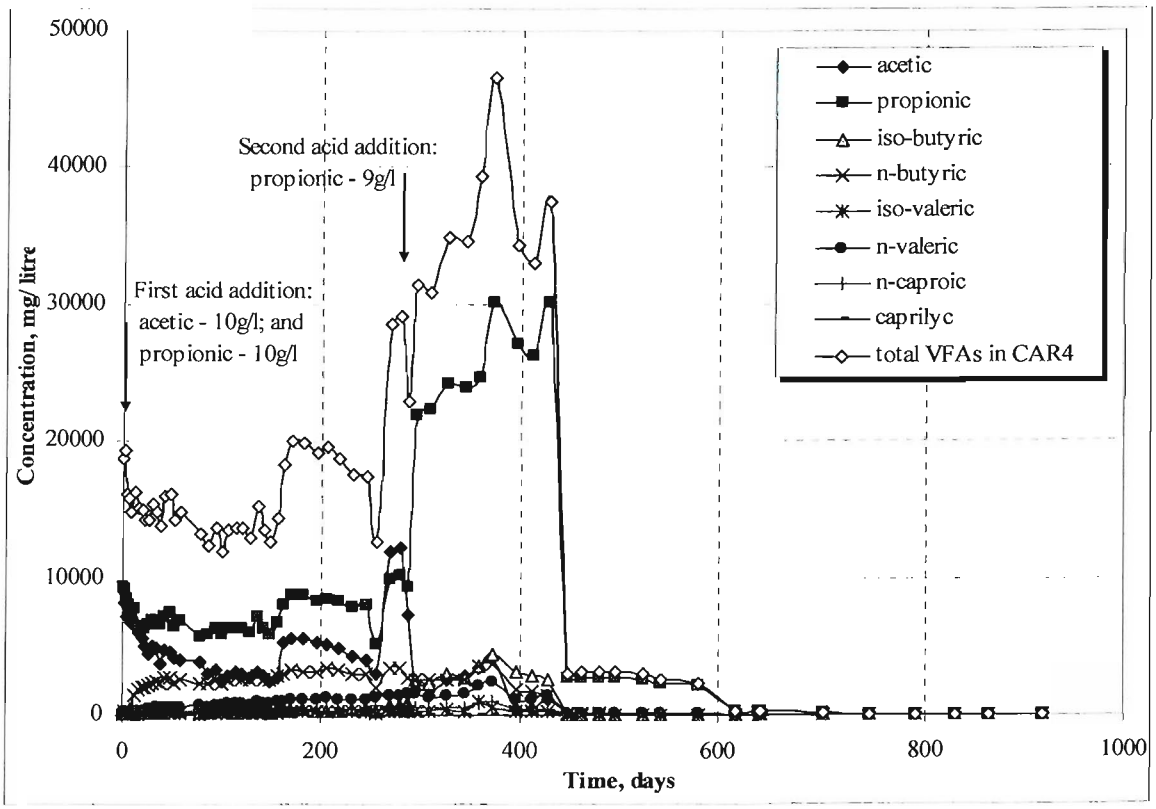

Figure 7.6. Leachate VFAs in CAR4 (50kPa)

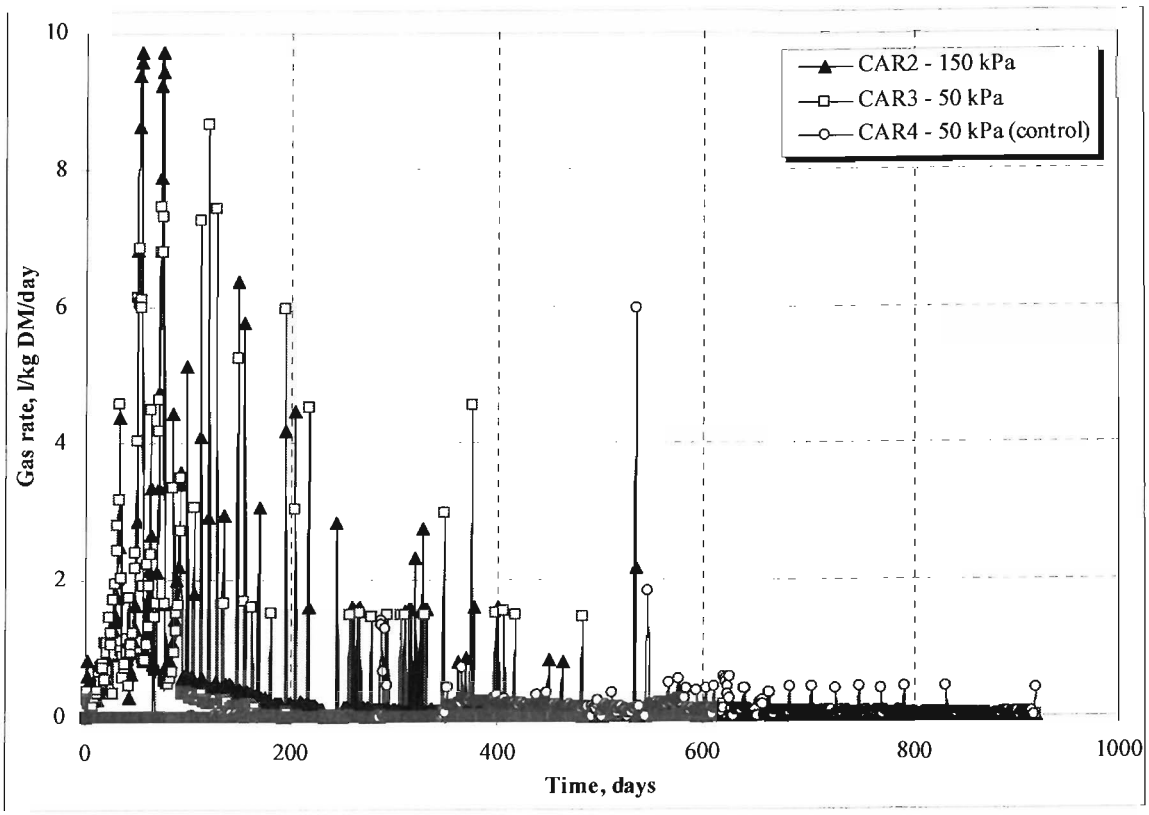

Figure 7.7. Daily gas production in CARs 2, 3 & 4.

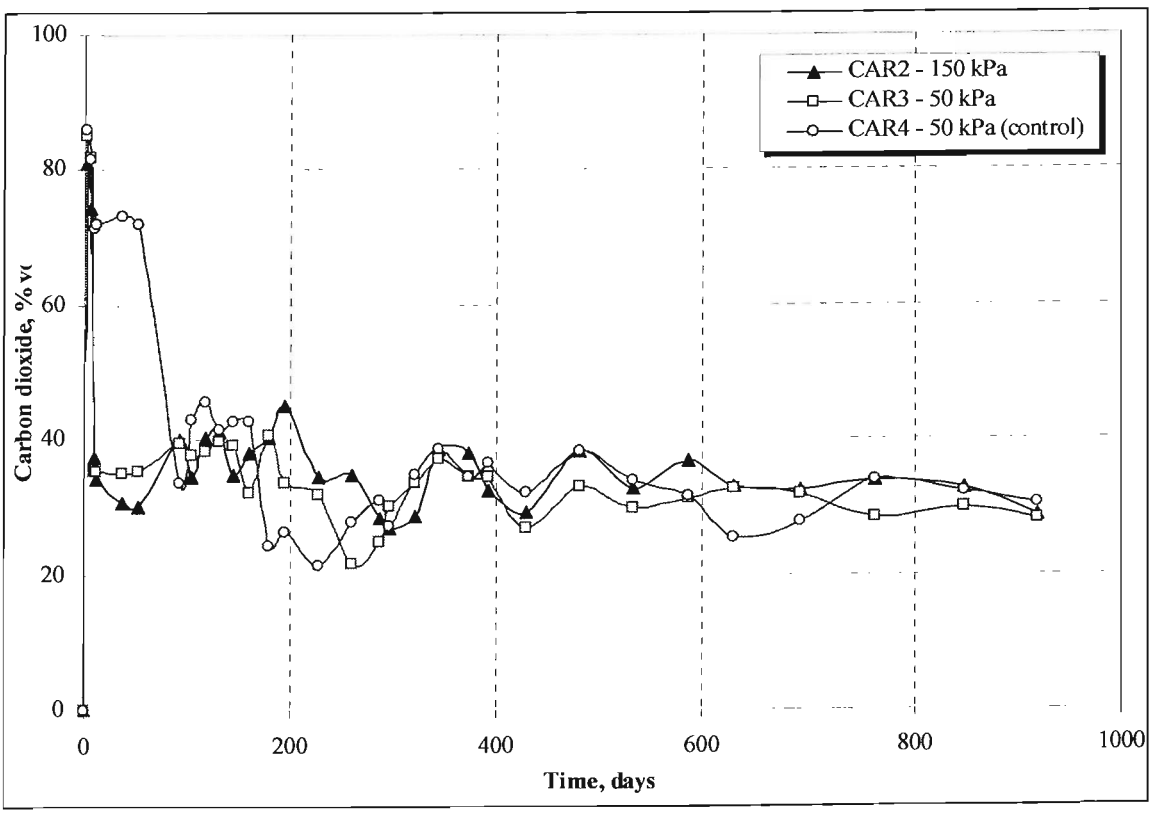

Figure 7.8. Carbon dioxide in CARs 2, 3 & 4.

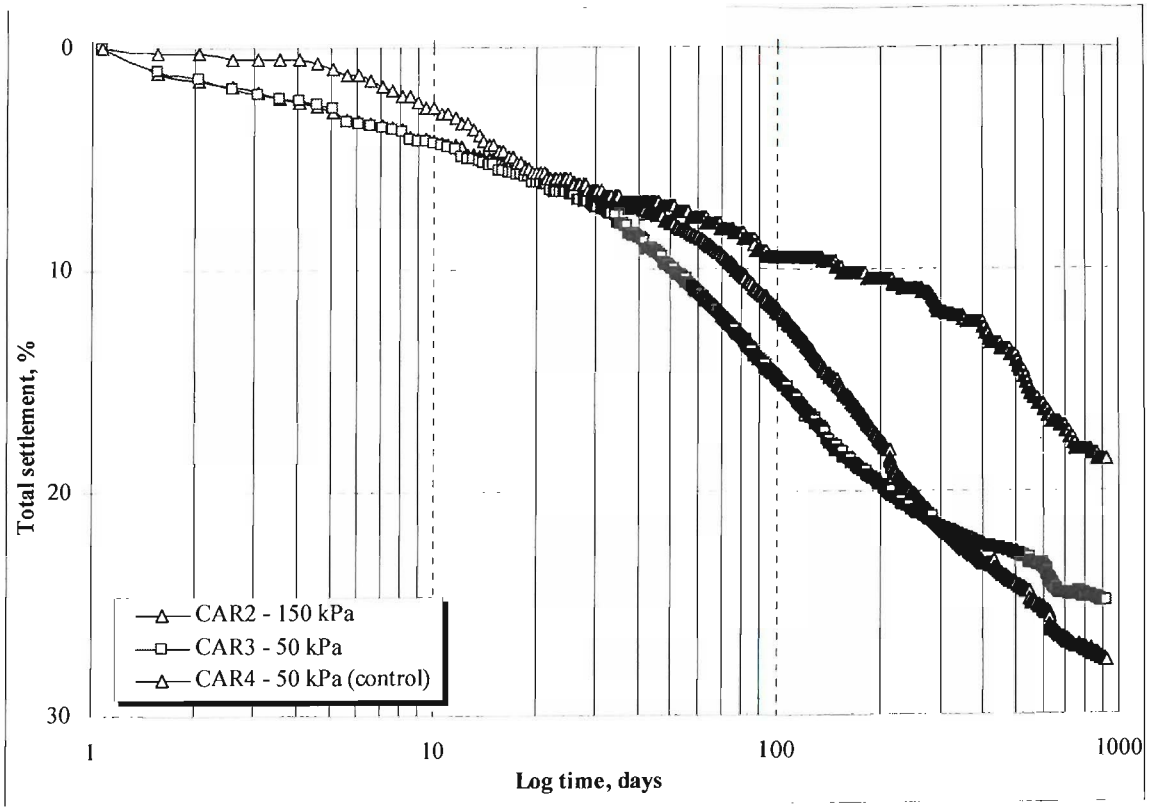

Figure 7.9. Observed total settlement in CARs 2, 3 & 4.

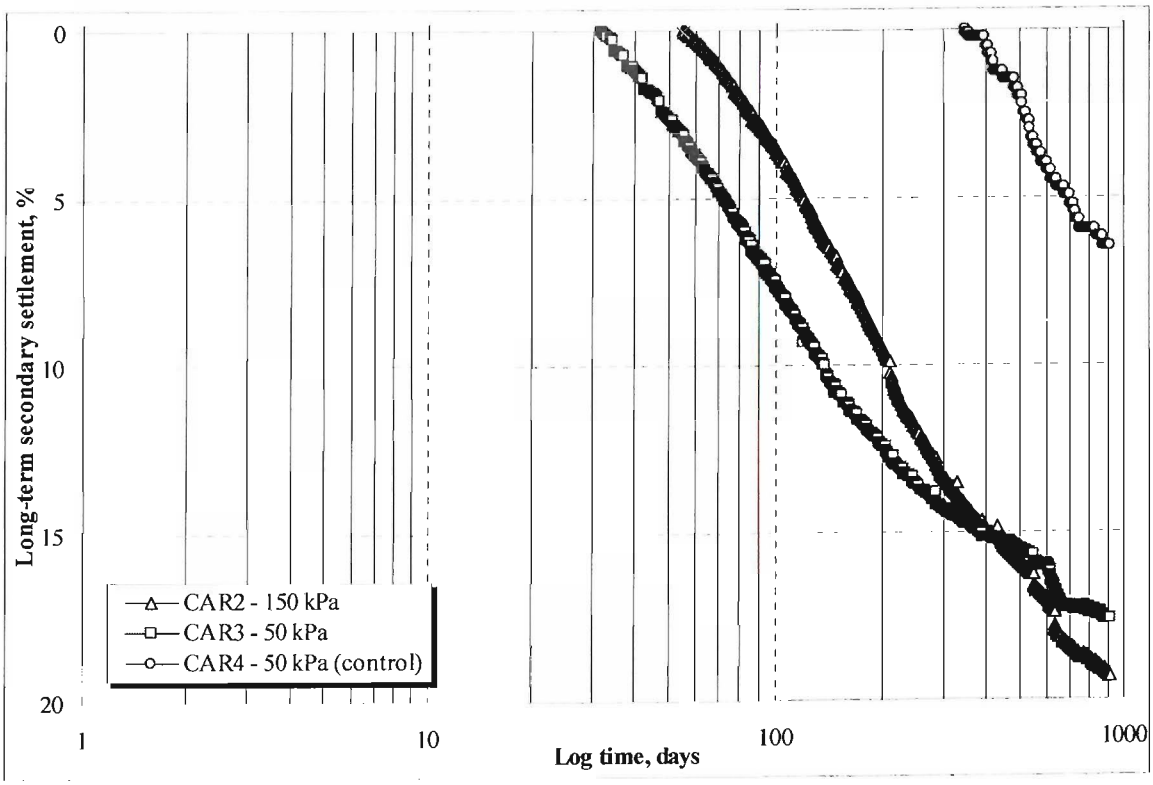

Figure 7.10. Observed long-term secondary settlement in CARs 2, 3 & 4.

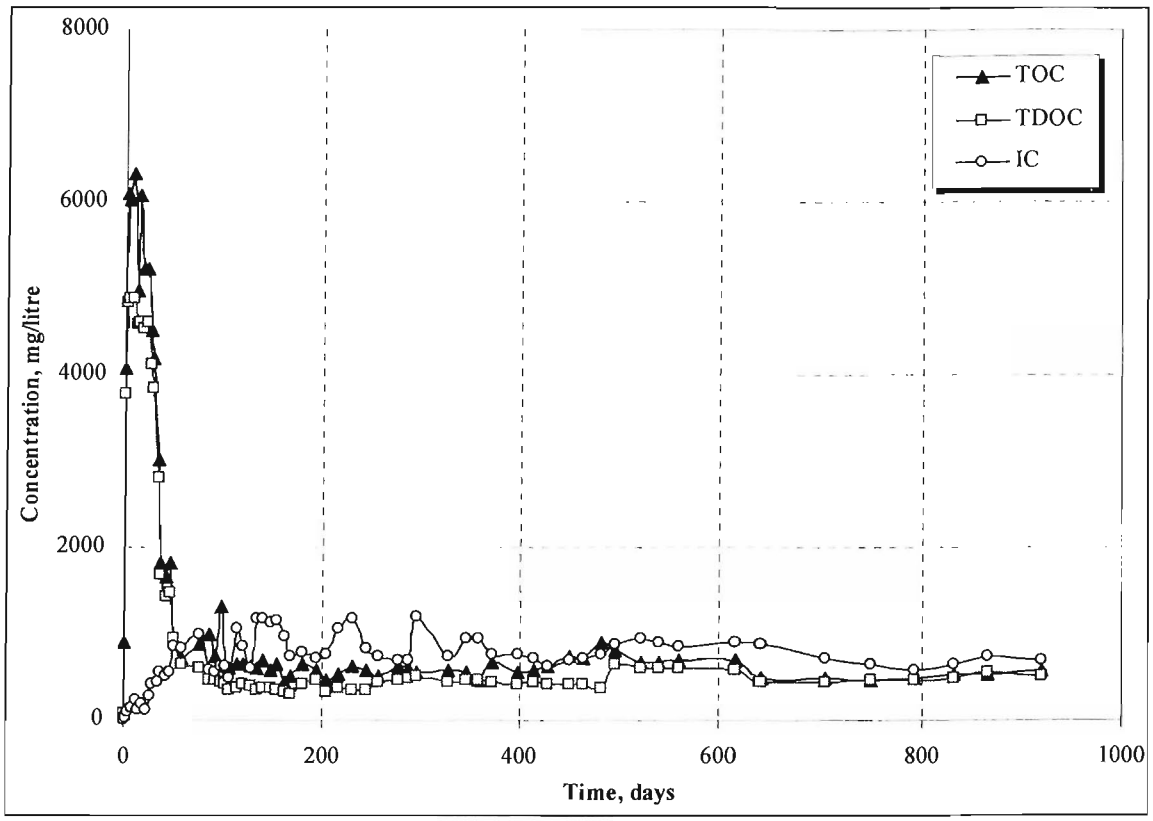

Figure 7.11. Leachate carbon in CAR2 (150kPa).

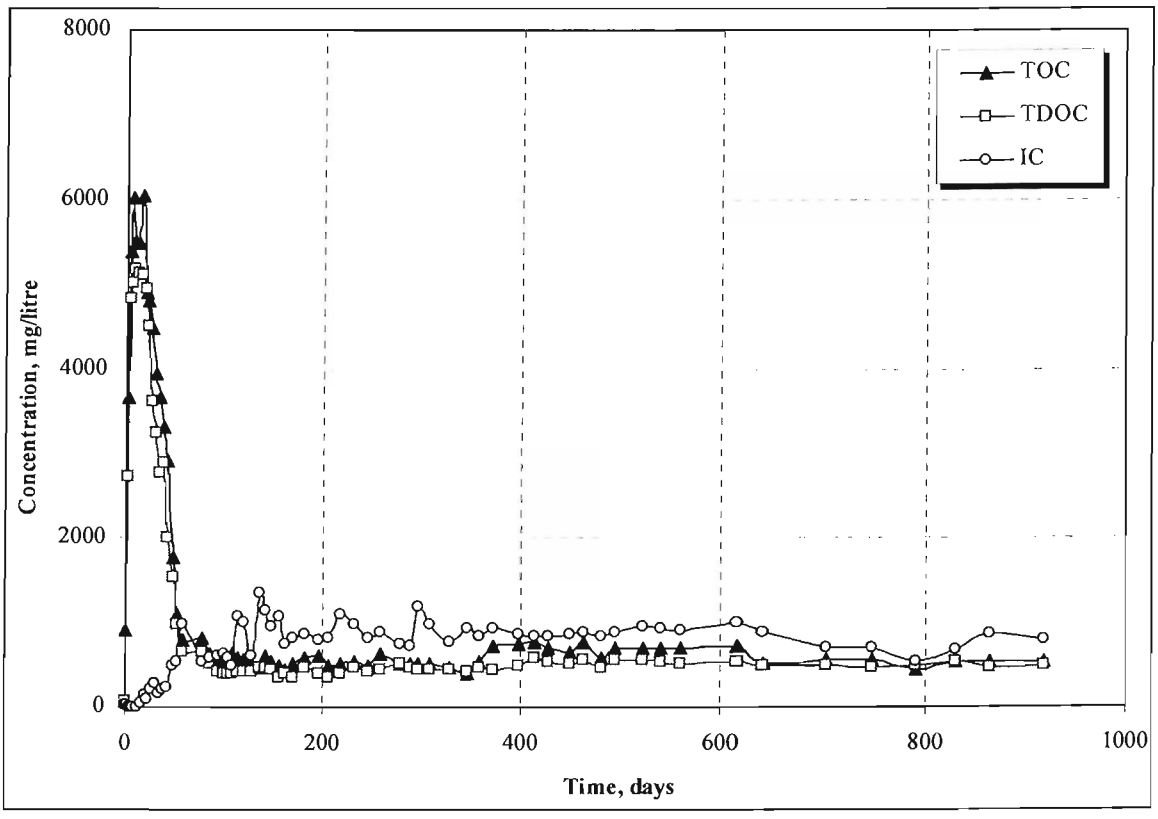

Figure 7.12. Leachate carbon in CAR3 (50kPa).

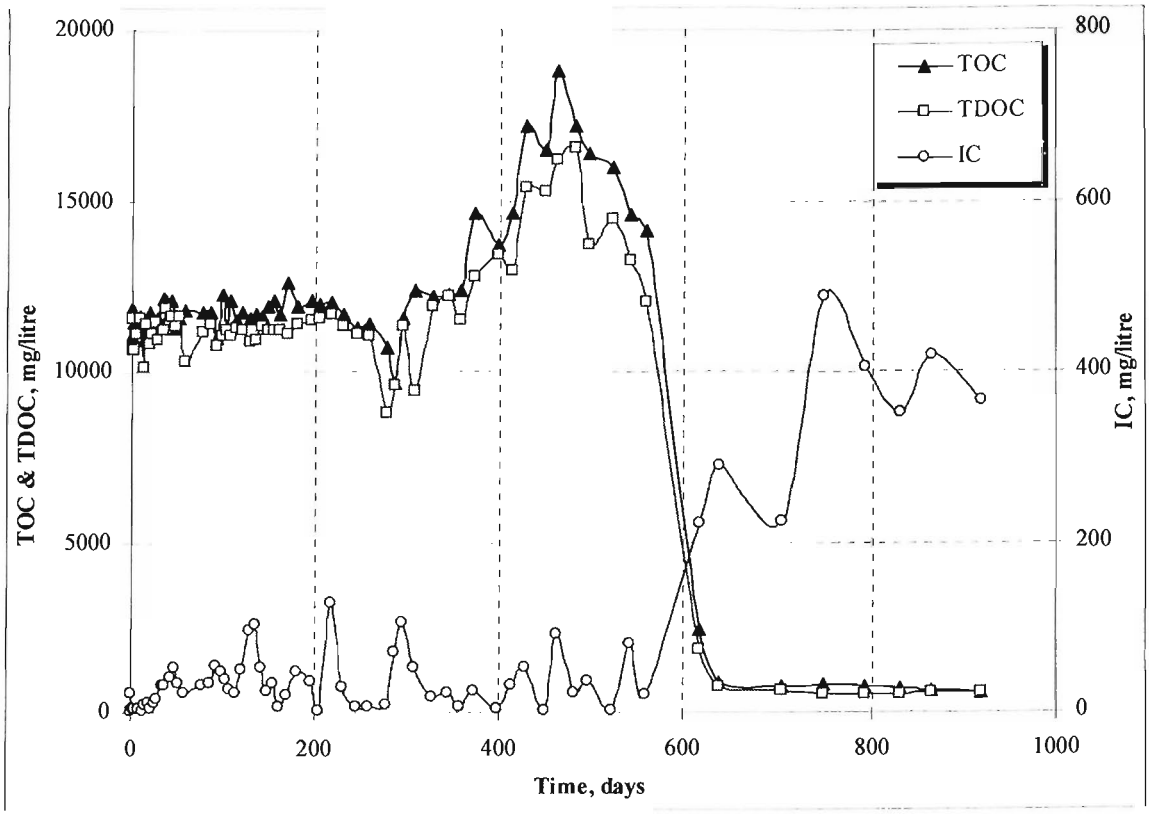

Figure 7.13. Leachate carbon in CAR4 (50kPa - control).

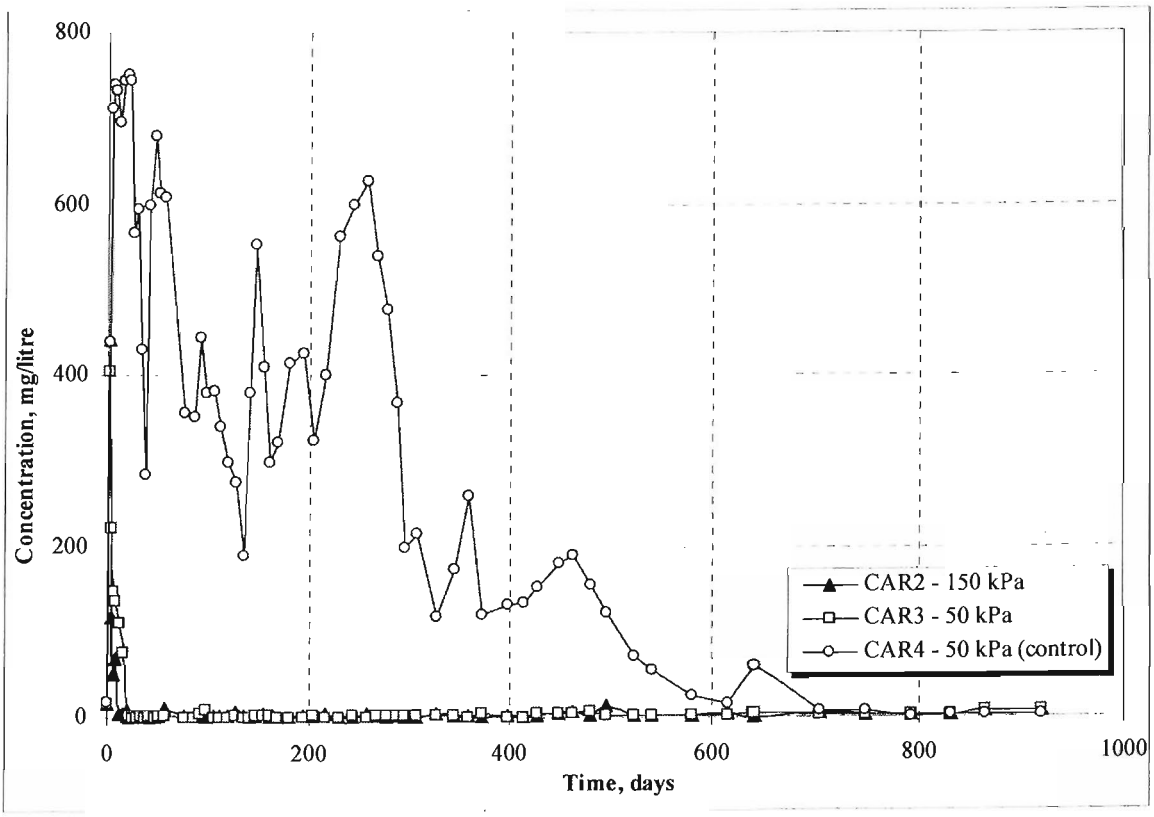

Figure 7.14. Sulphate concentration in CARs 2, 3 & 4.

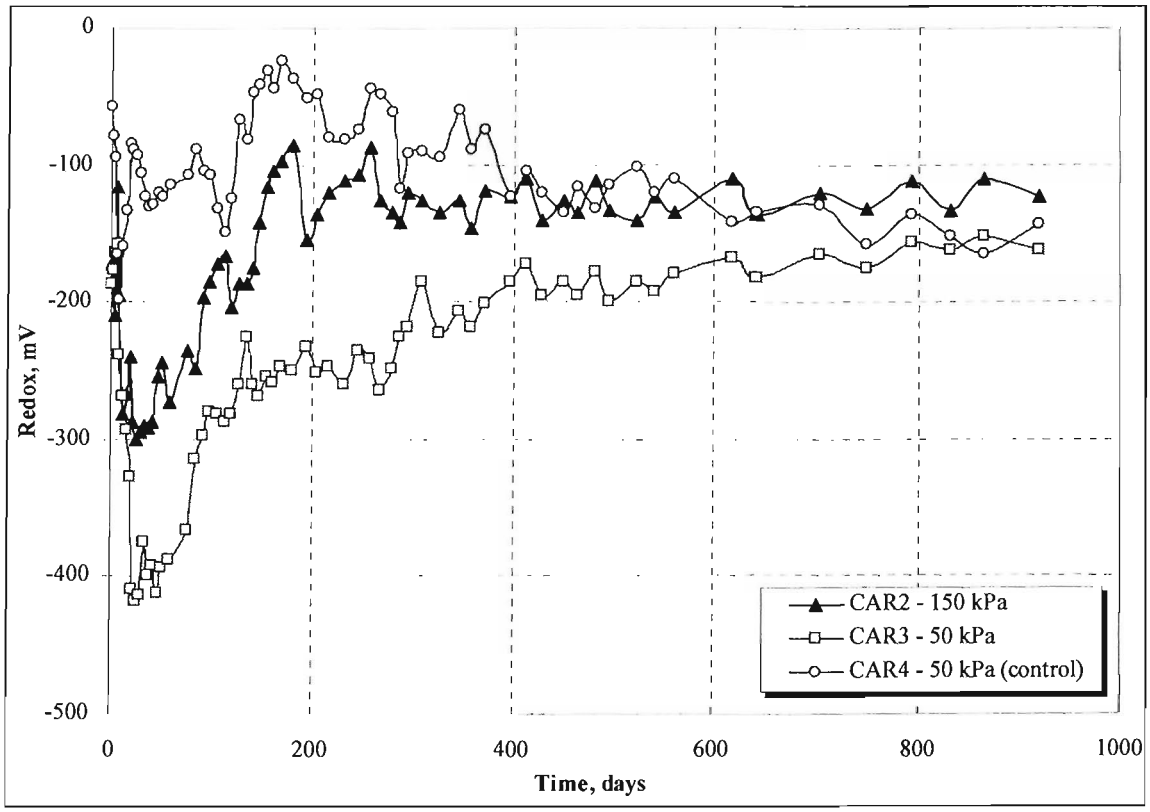

Figure 7.15. Redox potential in CARs 2, 3 & 4.

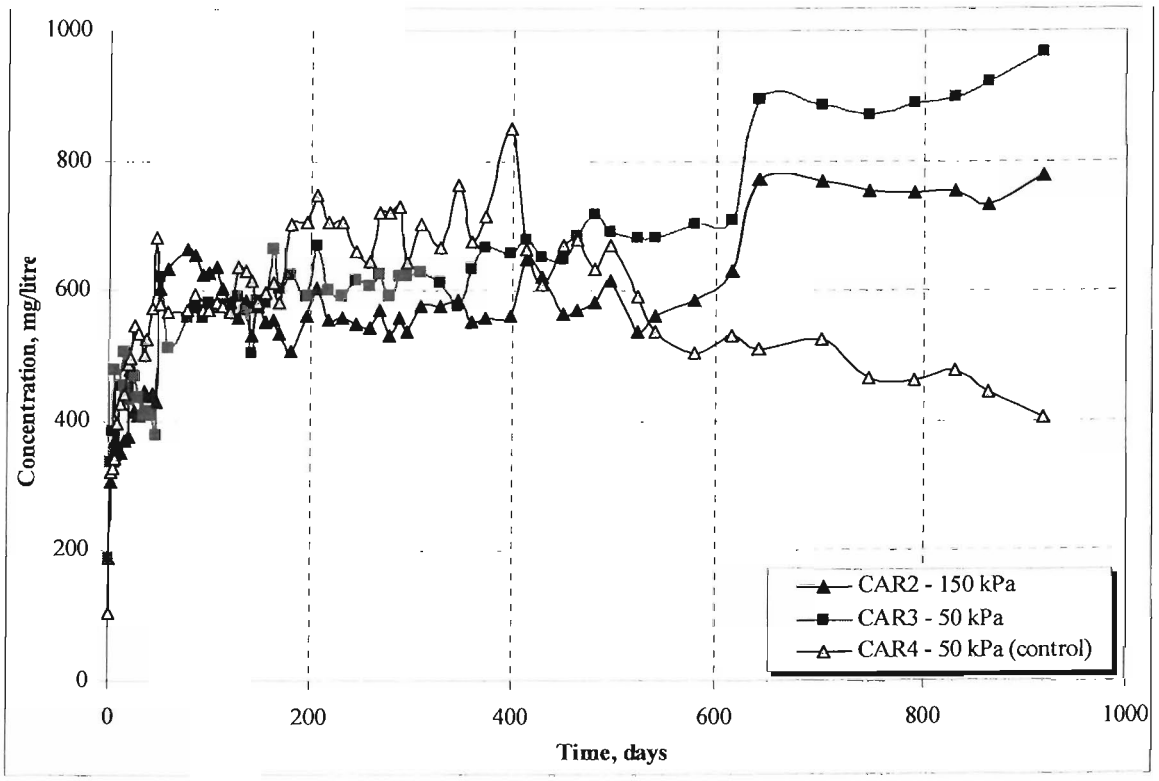

Figure 7.16. Ammonium concentration in CARs 2, 3 & 4.

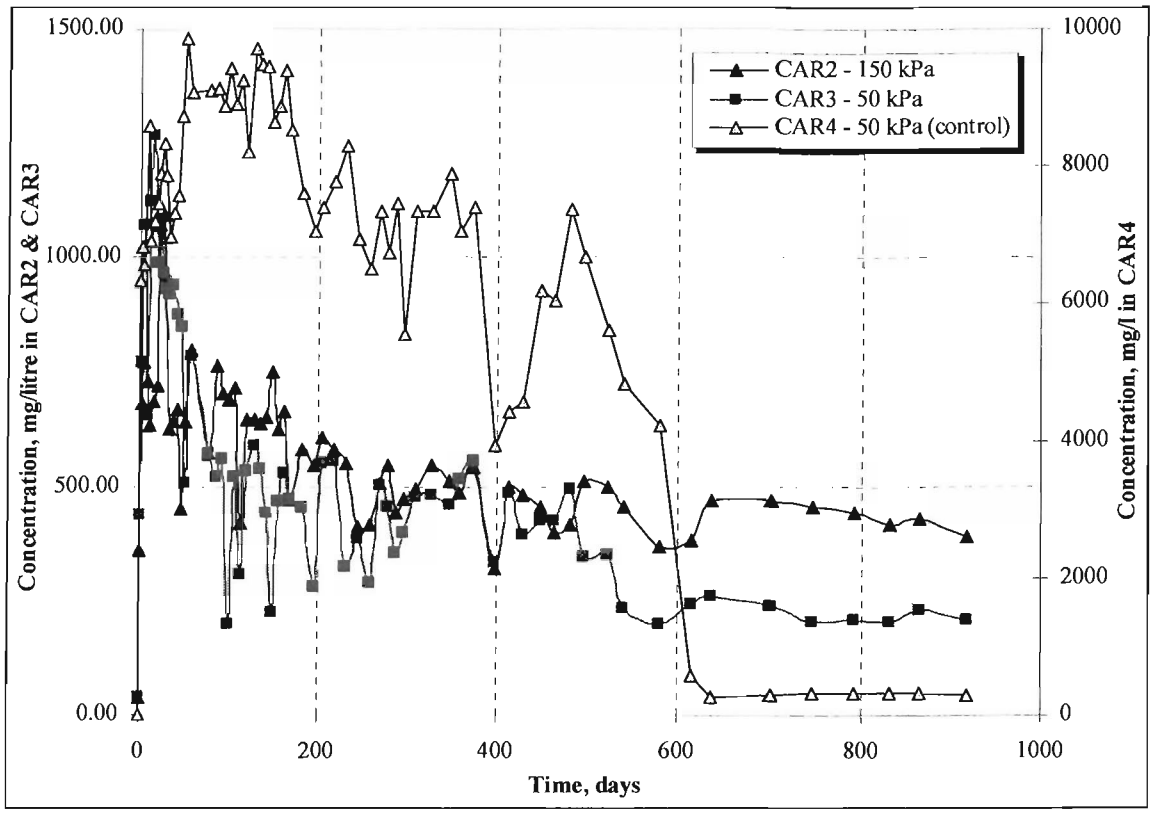

Figure 7.17. Calcium concentration in CARs 2, 3 & 4.

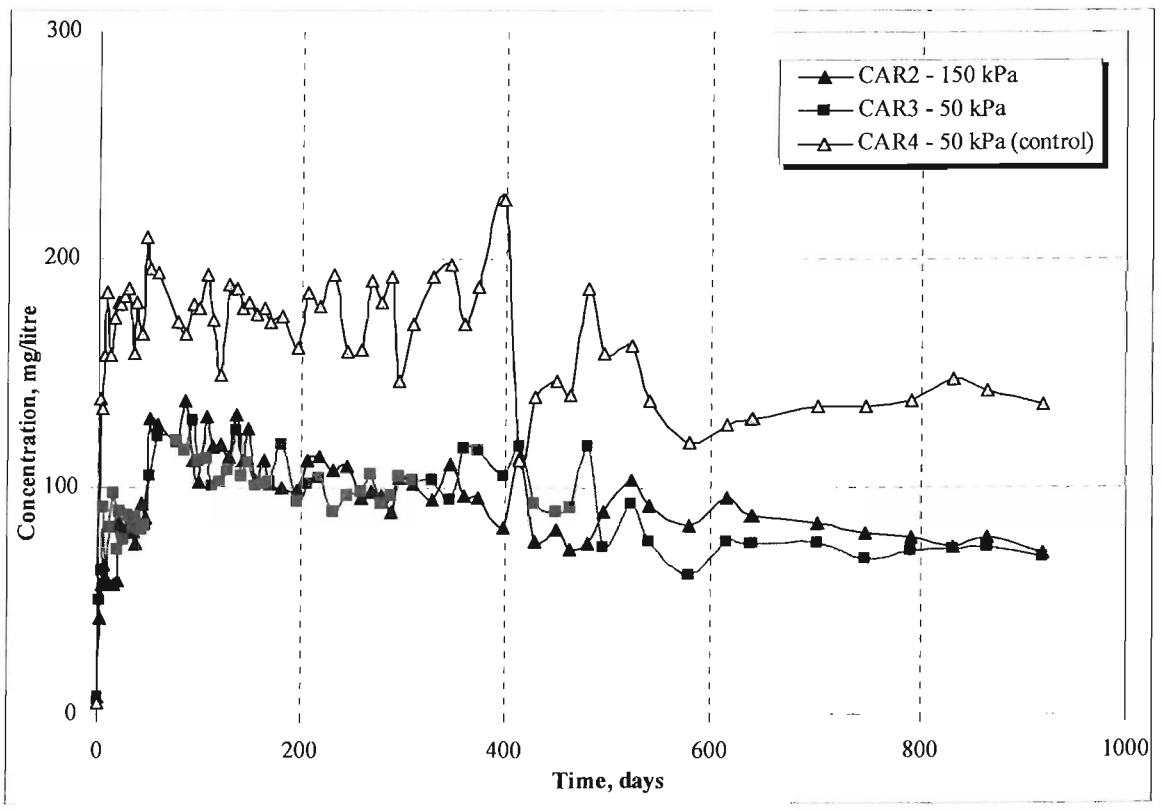

Figure 7.18. Magnesium concentration in CARs 2, 3 & 4.

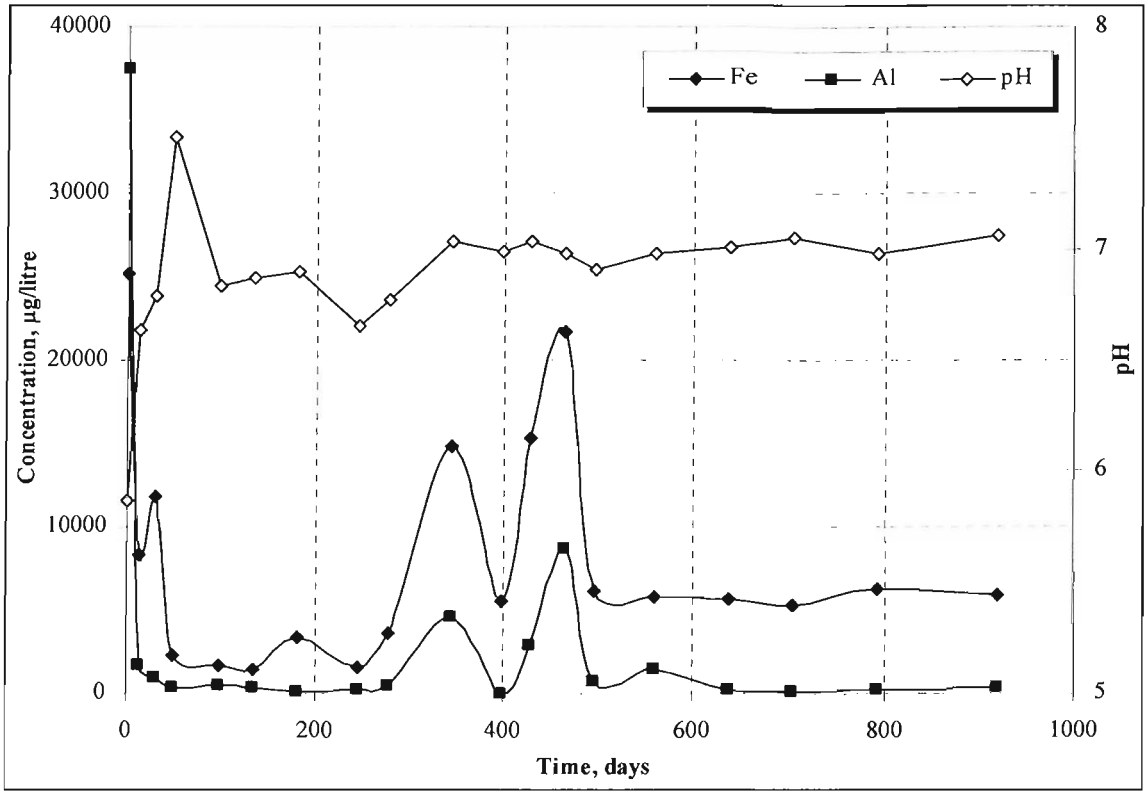

Figure 7.19. Fe and Al concentrations in leachate in CAR2.

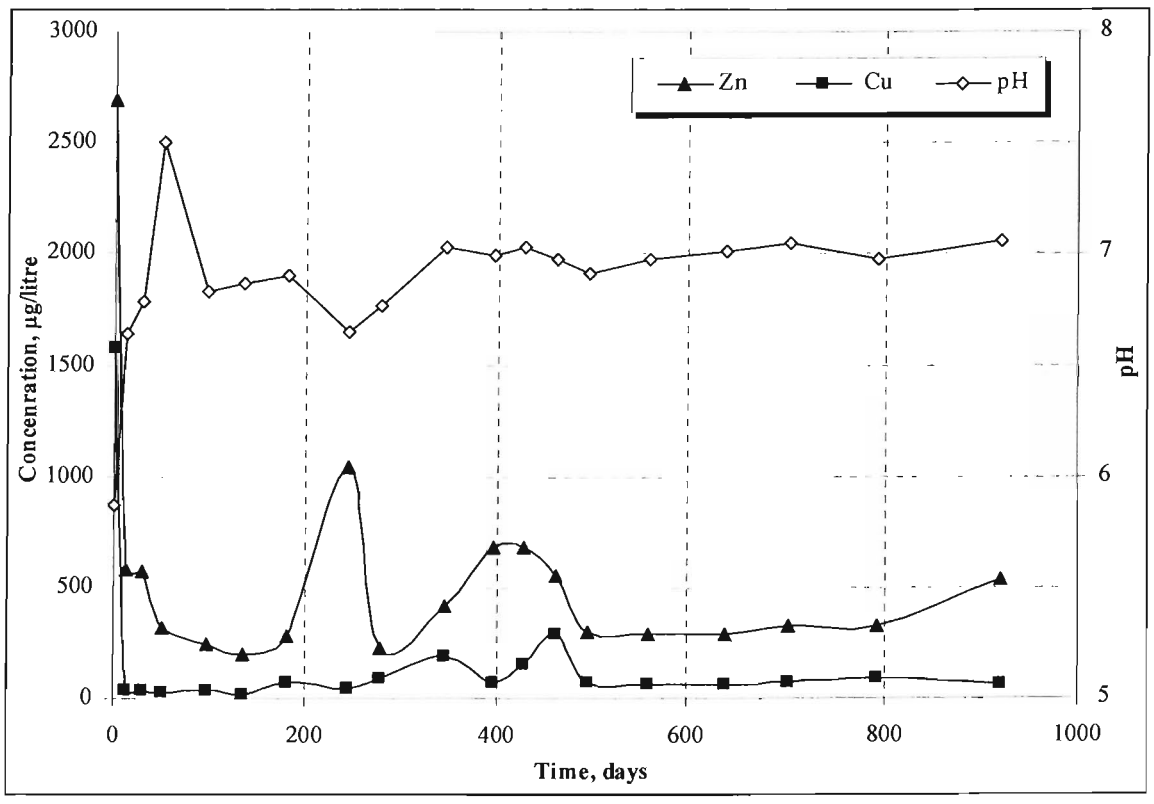

Figure 7.20. Zn and Cu concentrations in leachate in CAR2.

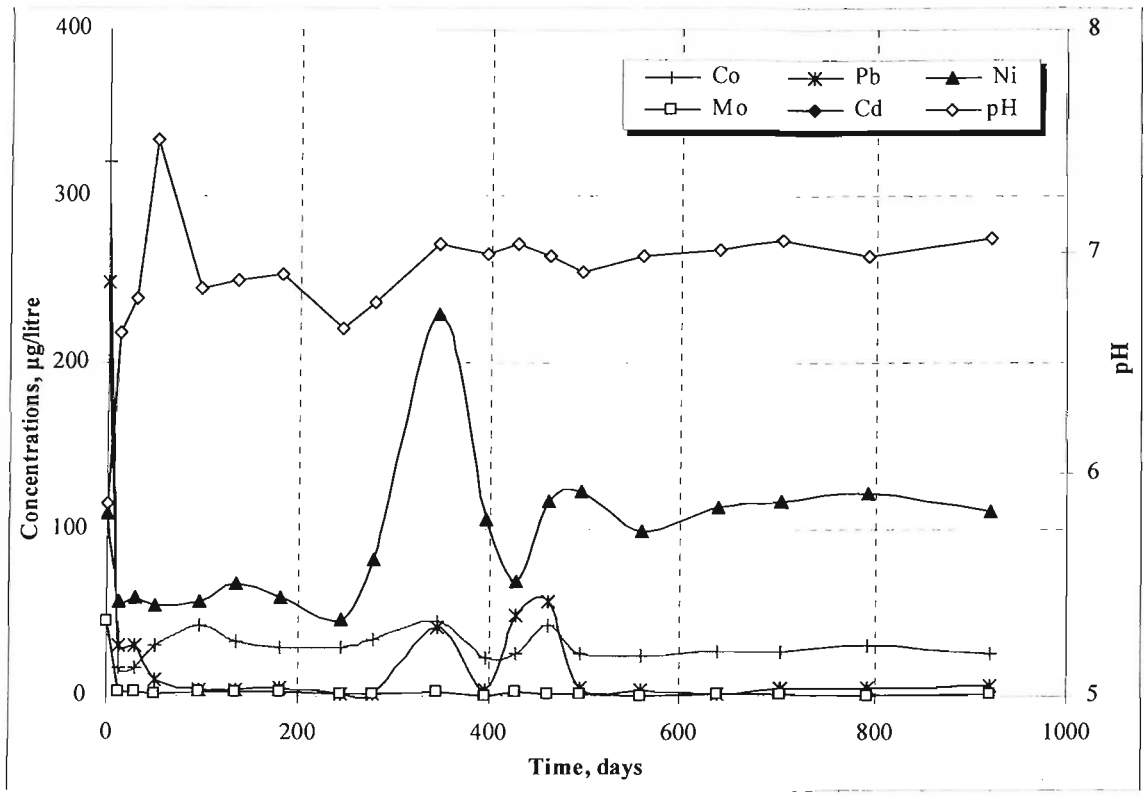

Figure 7.21. Co, Pb, Ni, Mo and Cd concentrations in leachate in CAR2.

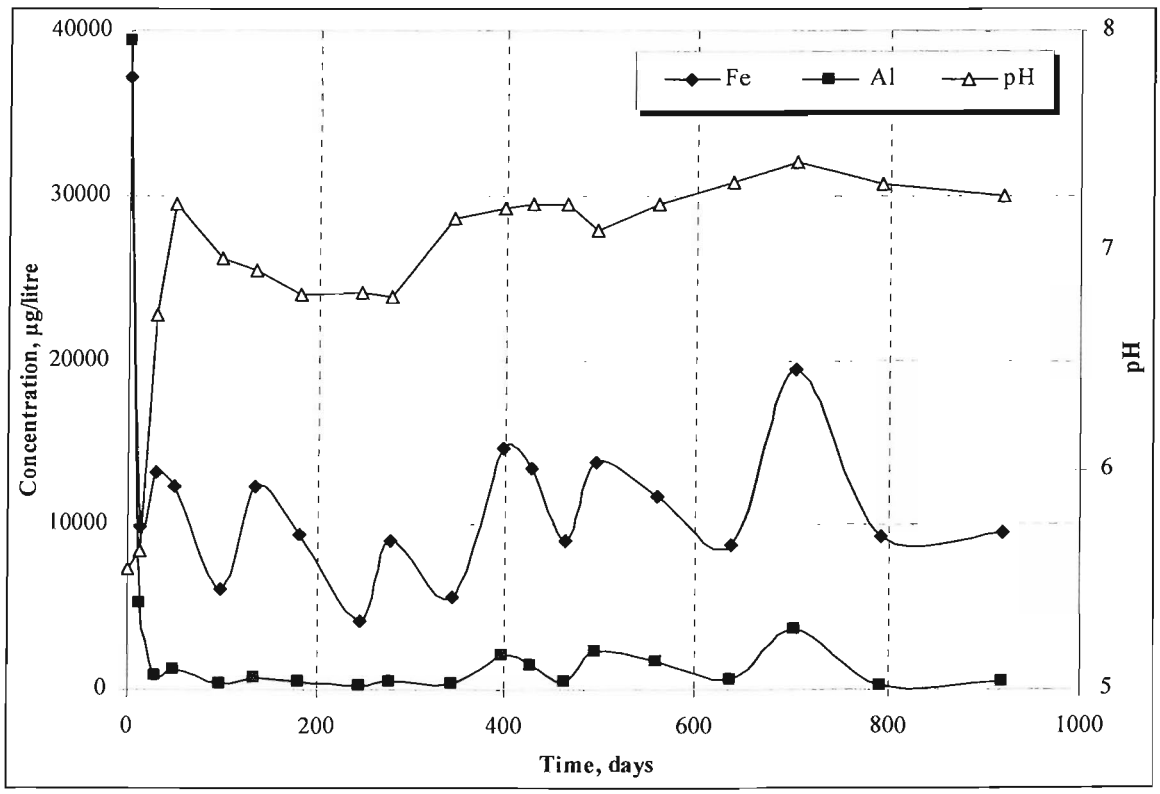

Figure 7.22. Fe and Al concentrations in leachate in CAR3.

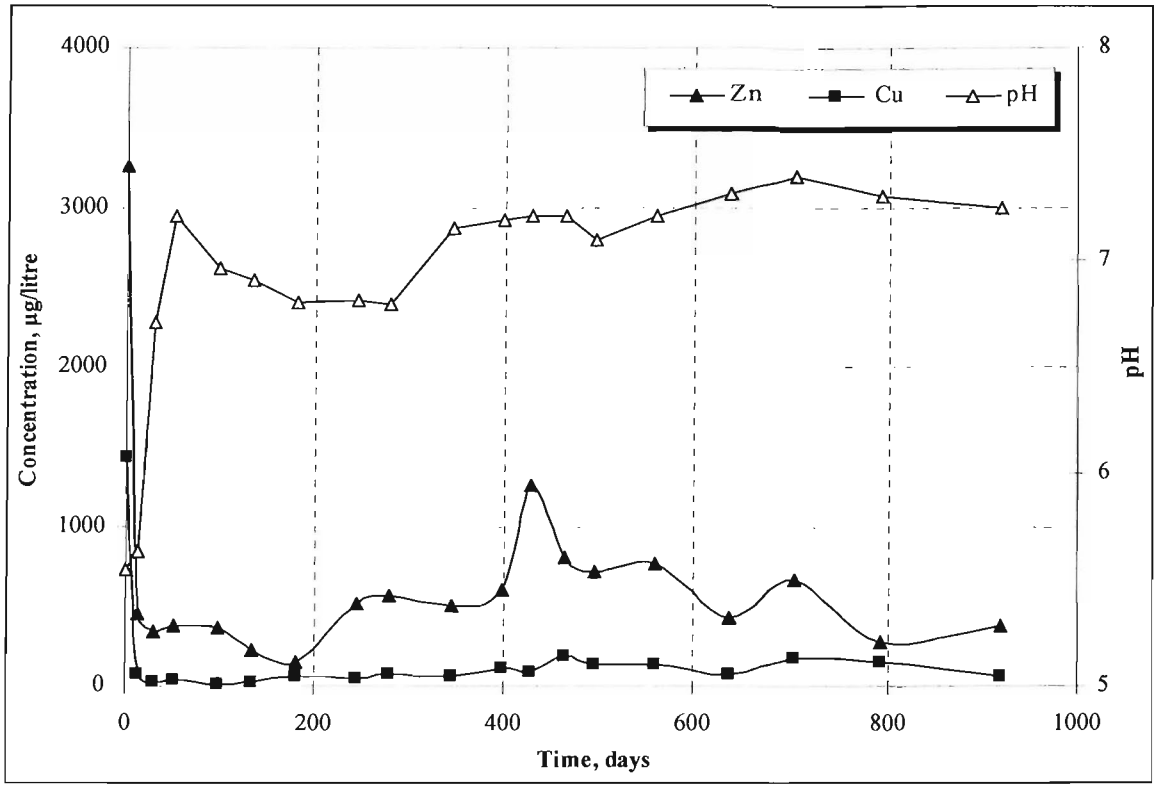

Figure 7.23. Zn and Cu concentrations in leachate in CAR3.

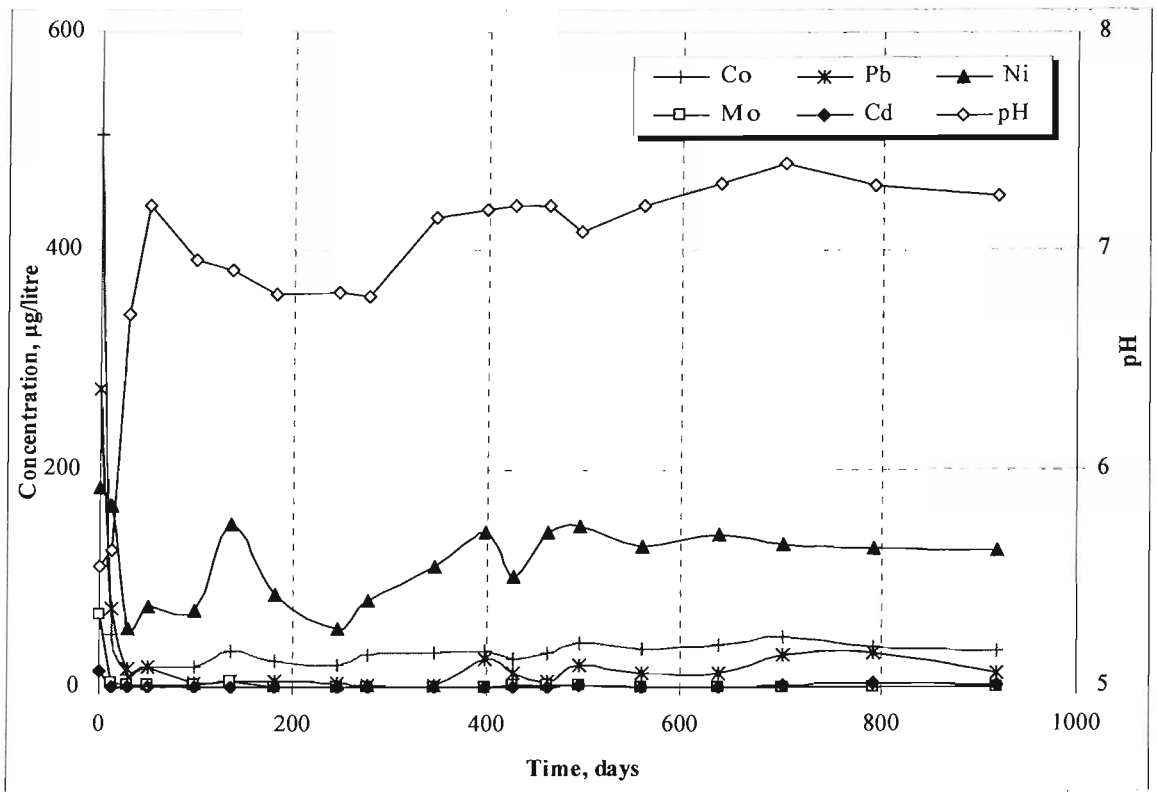

Figure 7.24. Co, Pb, Ni, Mo and Cd concentrations in leachate in CAR3.

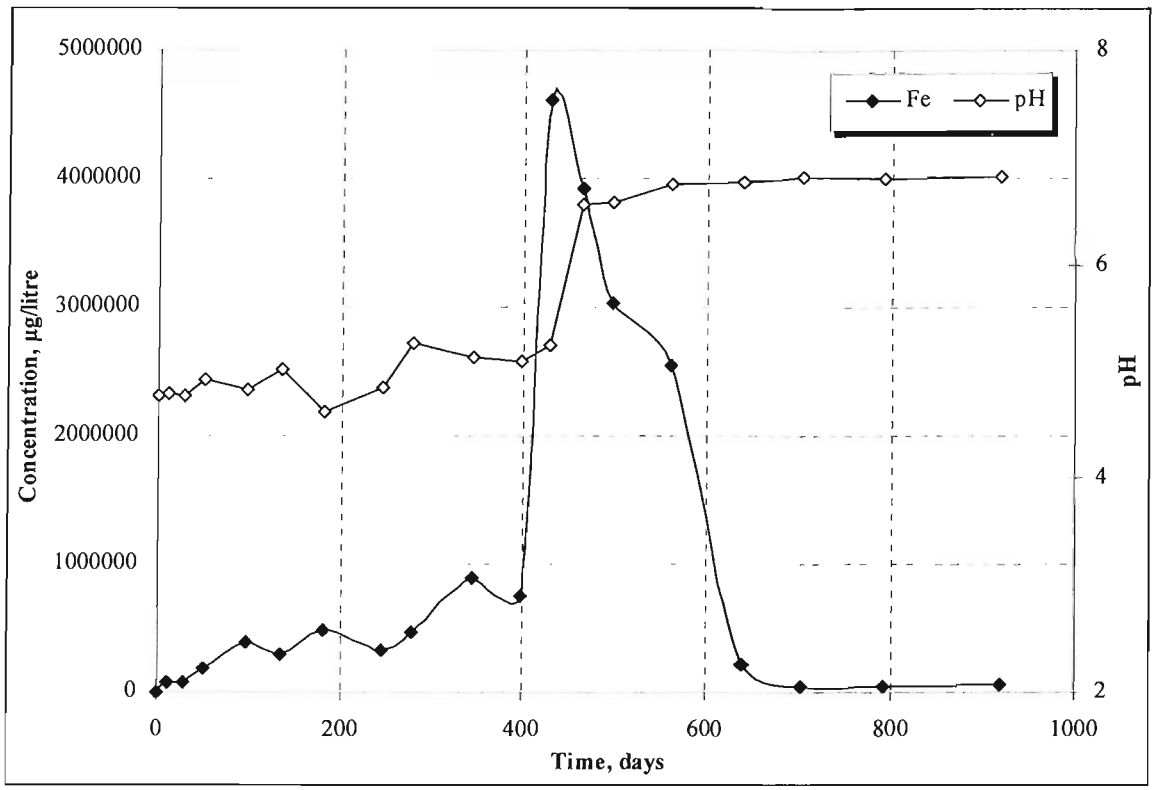

Figure 7.25. Fe concentrations in leachate in CAR4.

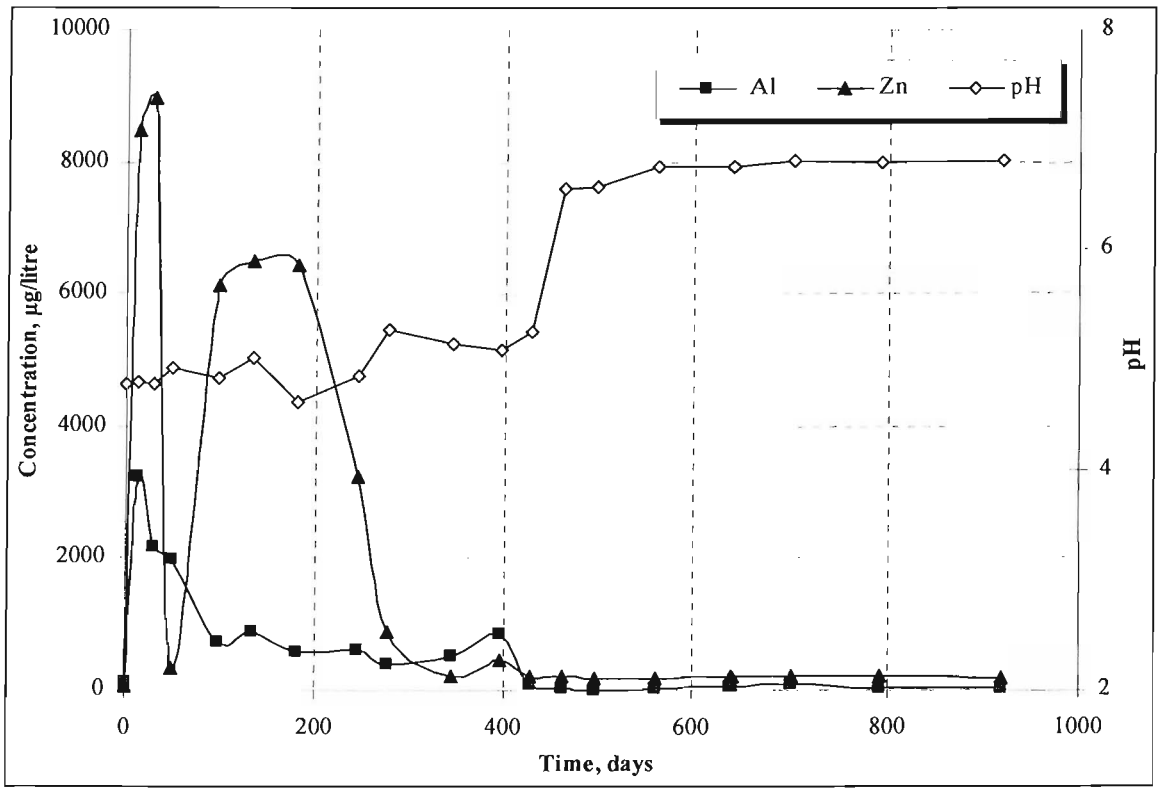

Figure 7.26. Al and Zn concentrations in leachate in CAR4.

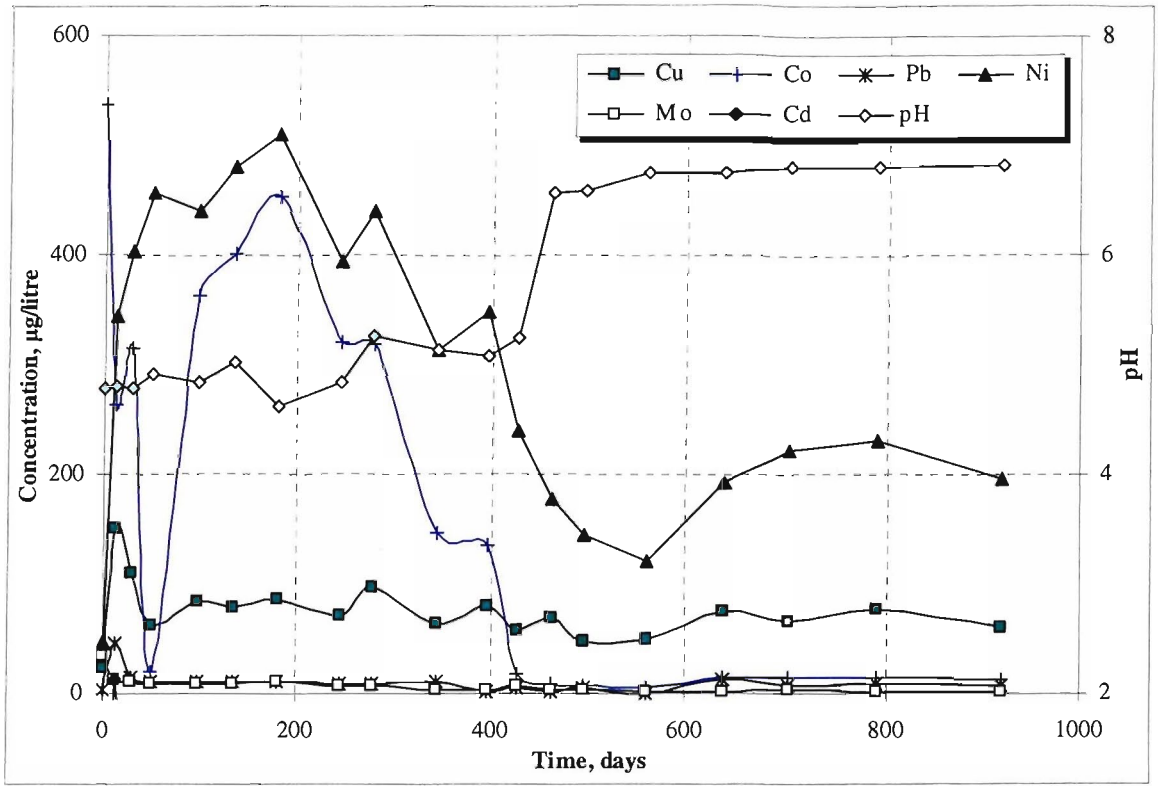

Figure 7.27. Cu, Co, Pb, Ni, Mo and Cd concentrations in leachate in CAR4.

a) b)

Figure 7.28. Reactor dismantling: a) an empty sample tube with attached chains; b) returning the reactor into the loading frame by using a manual forklift.

a) b)

Figure 7.29. Extracting a core sample with the aid of metal chains using a portable crane.

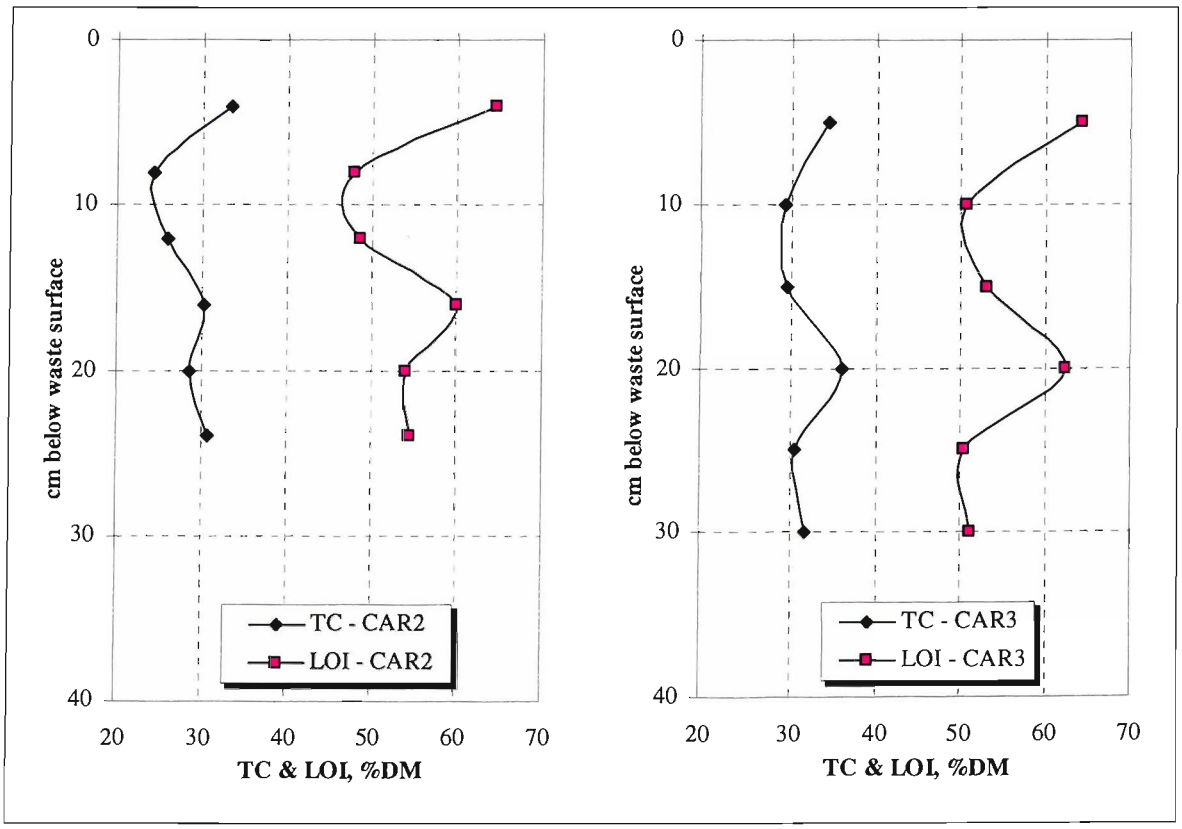

Figure 7.30. TC content and LOI of the core samples taken from CARs 2 & 3 at the end of the experiment as a function of depth below waste surface (values from Table 7.8).

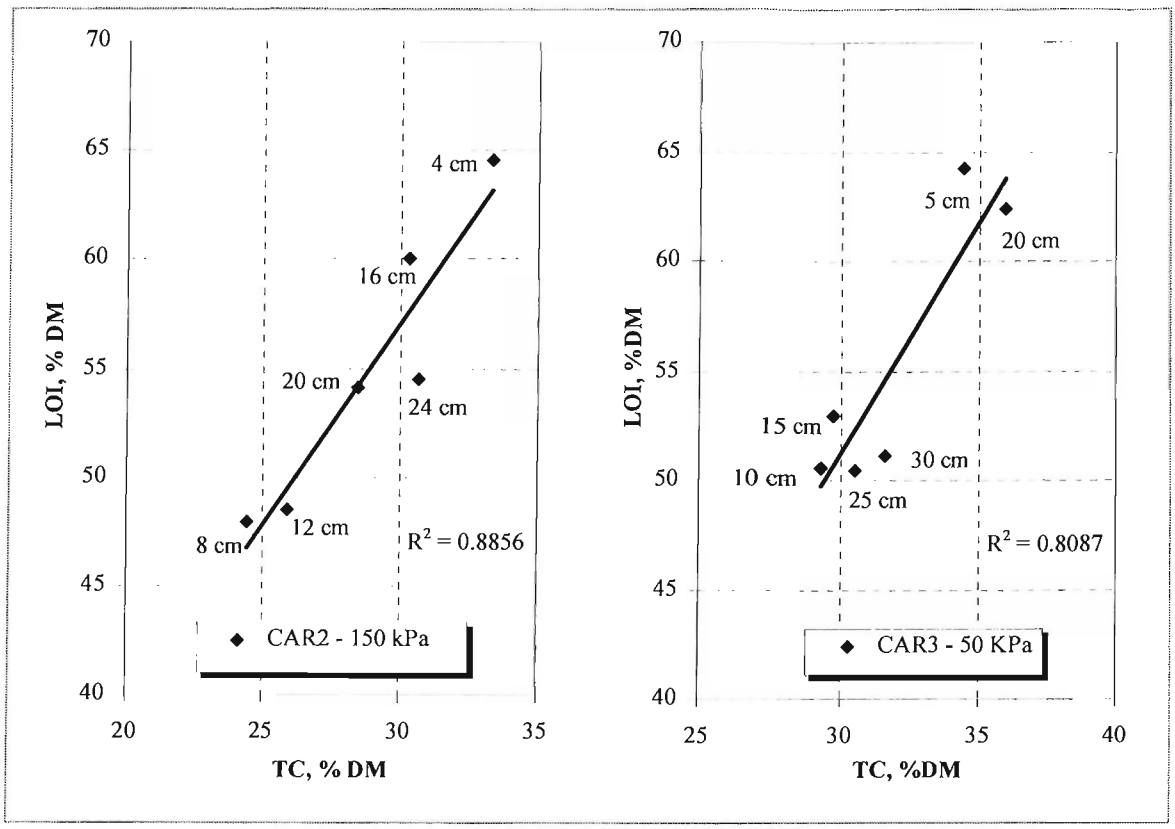

Figure 7.31. Correlation between TC content and LOI of the core samples taken from CARs 2 & 3 at the end of the experiment.

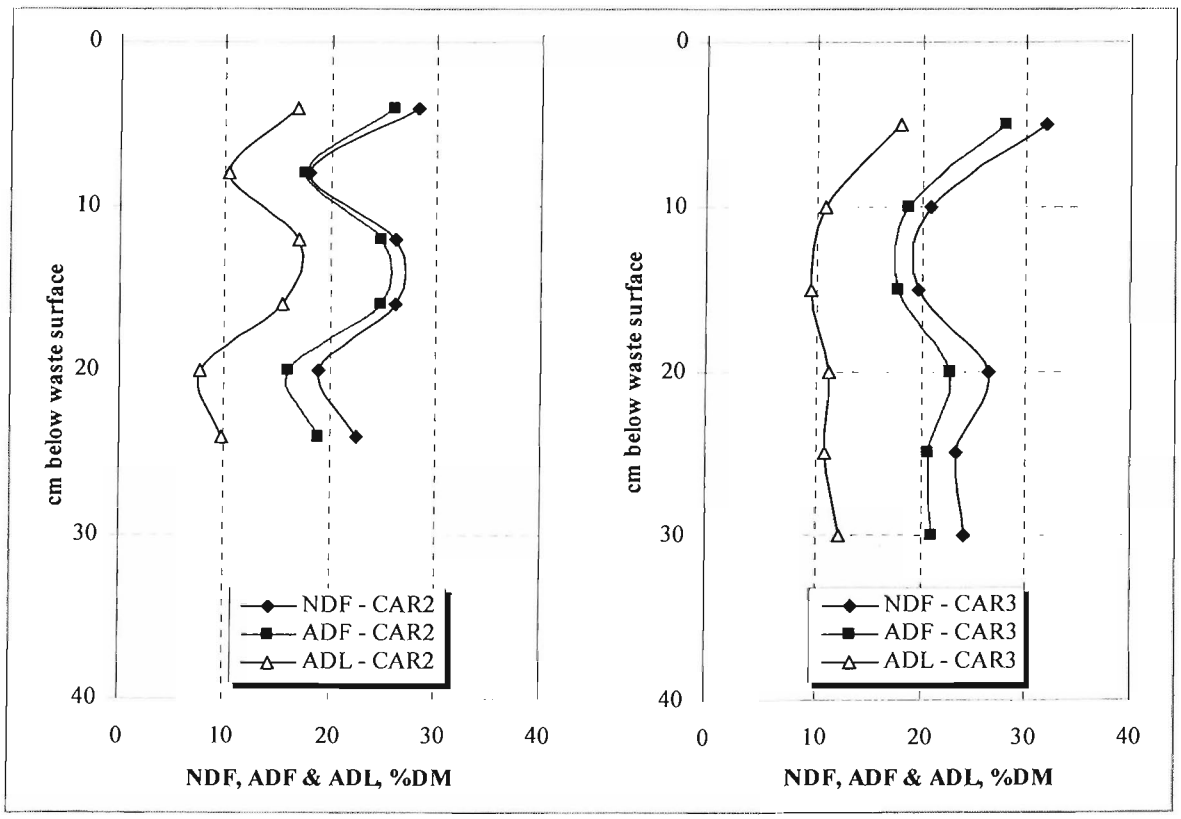

Figure 7.32. Variations in NDF, AFD and ADL along the height of the reactors.

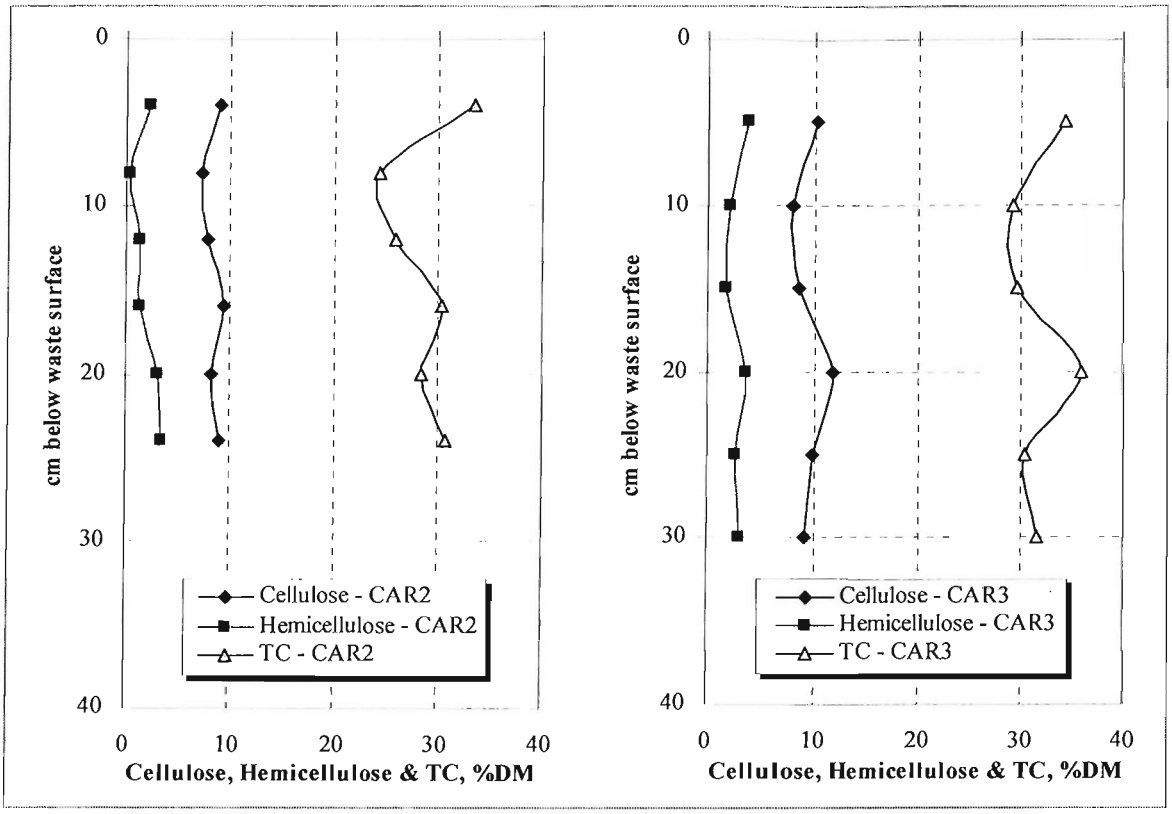

Figure 7.33. Variations in cellulose, hemicellulose and TC content along the height of the reactors.

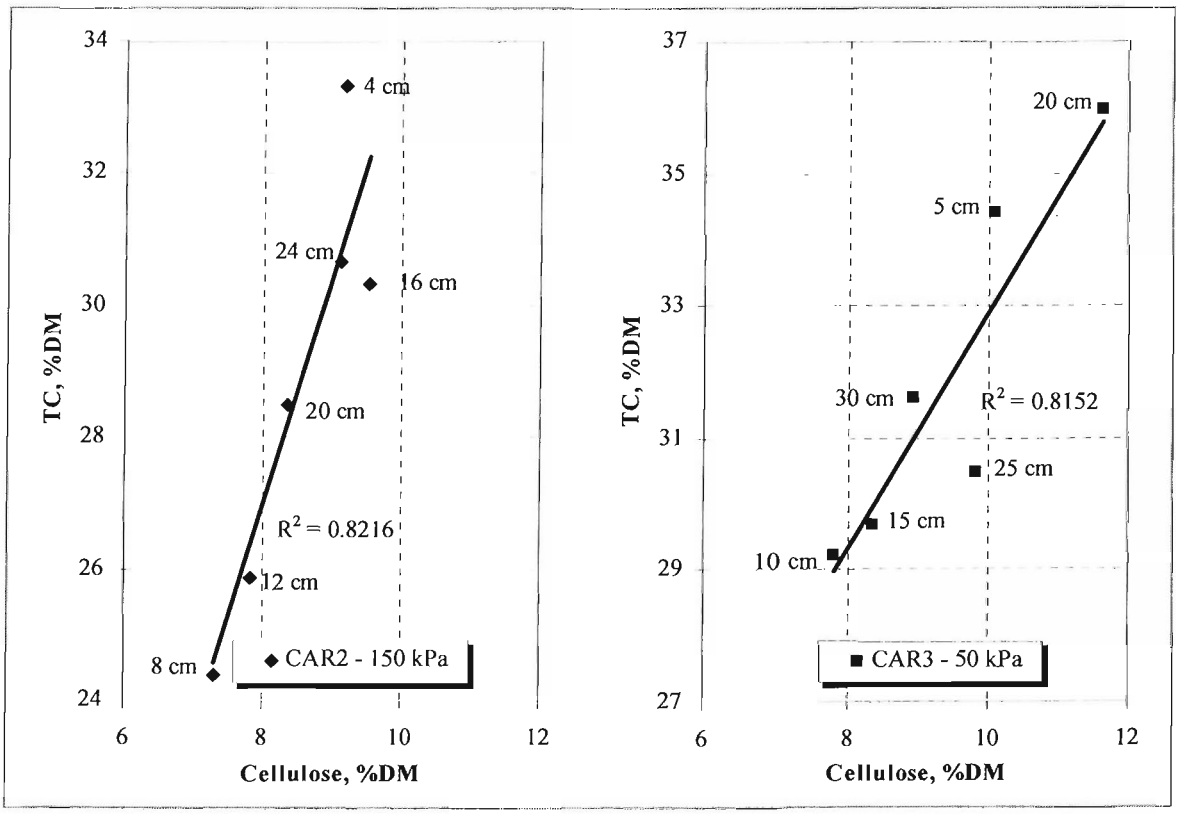

Figure 7.34. Correlation between cellulose content and TC content.

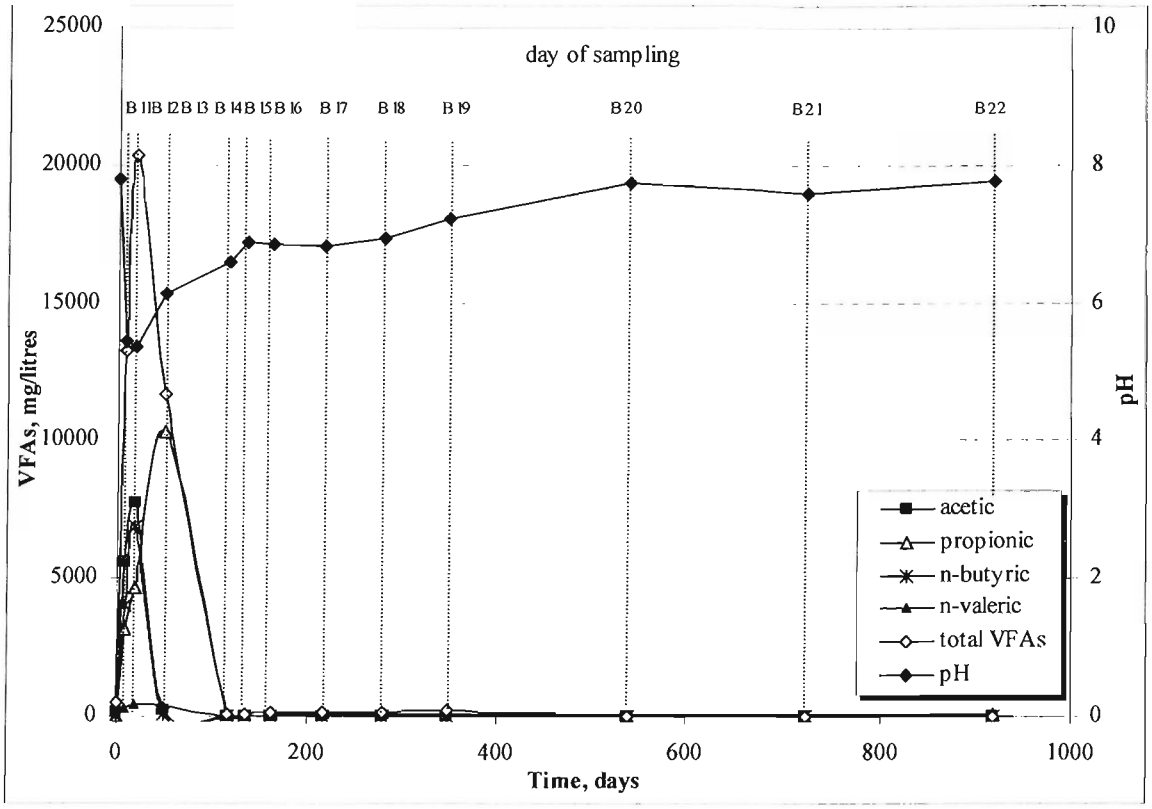

Figure 7.35. Leachate VFAs and pH in BMP3 bottles.

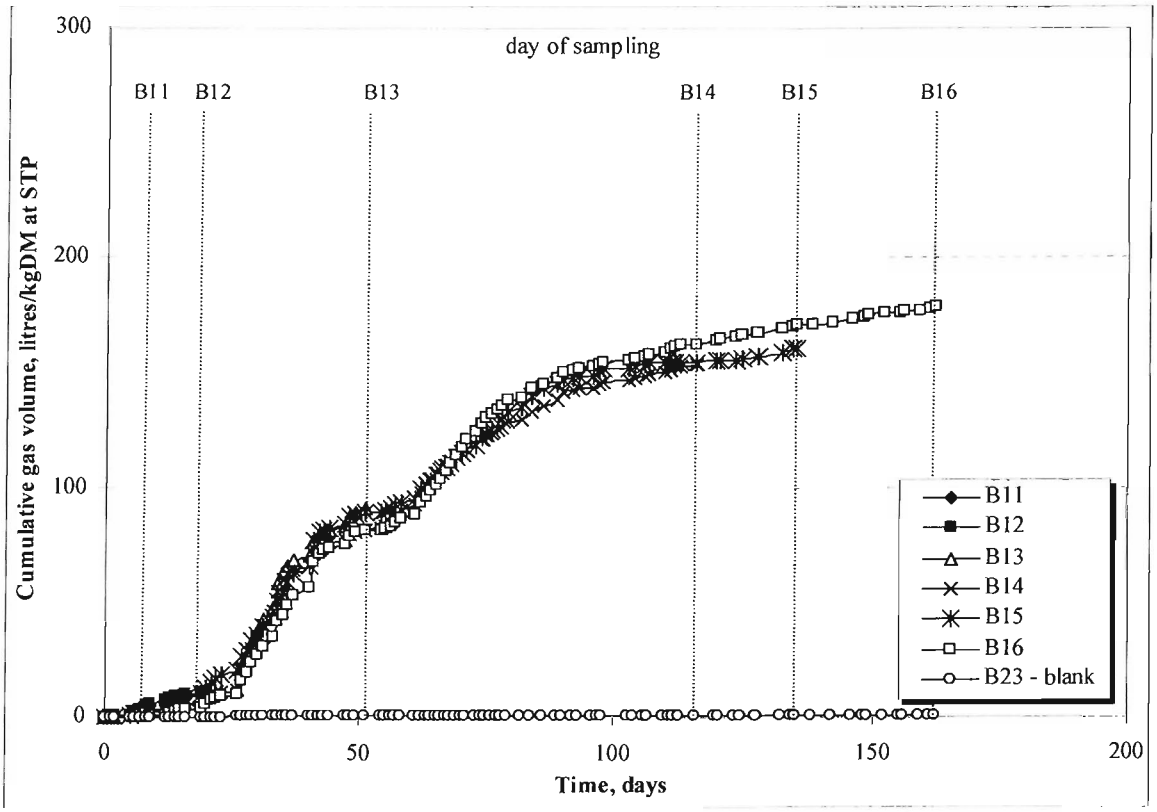

Figure 7.36. Cumulative gas production in BMP3 bottles (from B11 to B16 and B23).

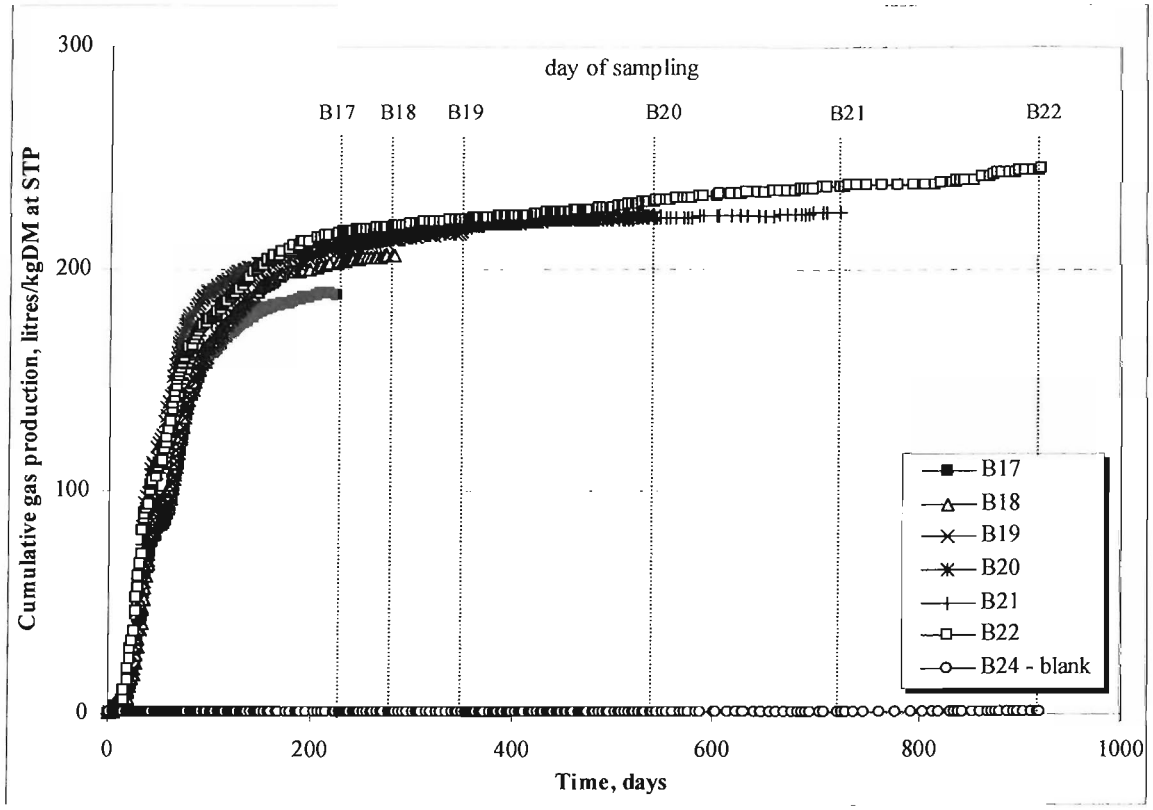

Figure 7.37. Cumulative gas production in BMP3 bottles (from B17 to B22 and B24).

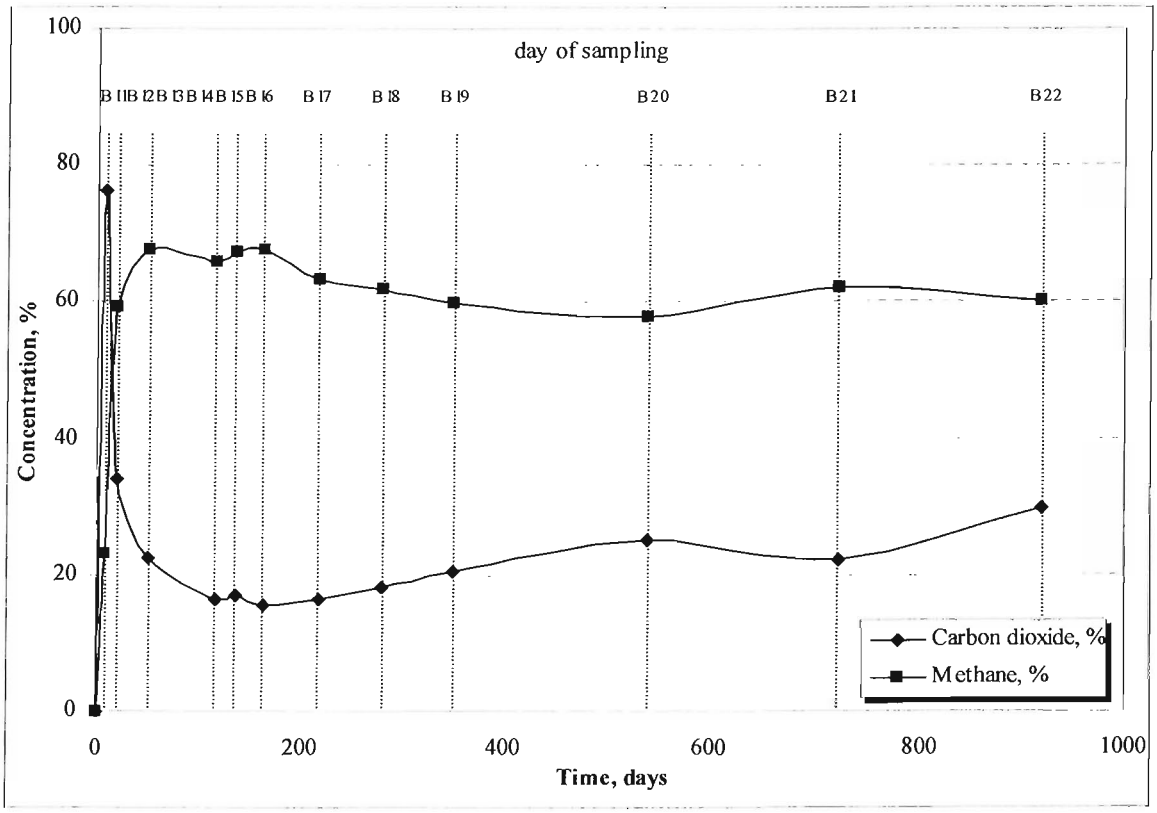

Figure 7.38. Biogas composition in BMP3 bottles.

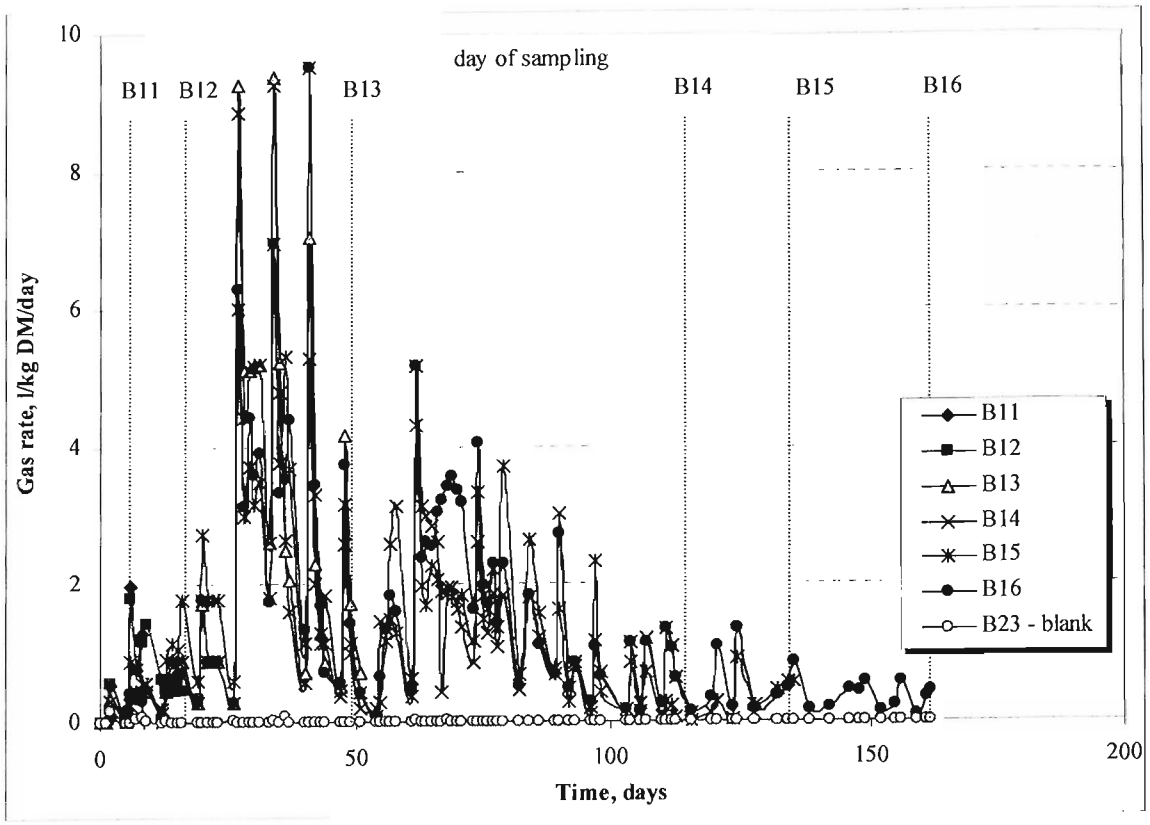

Figure 7.39. Gas production rate for BMP3 bottles.

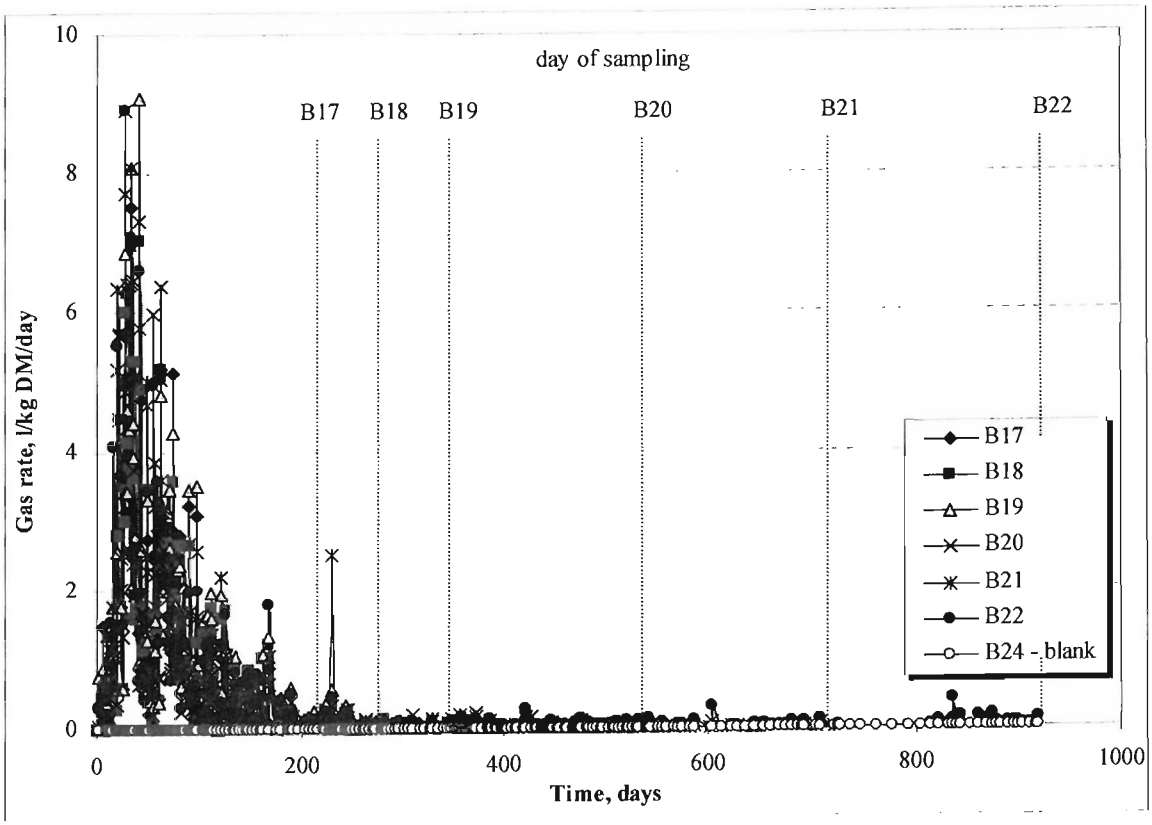

Figure 7.40. Gas production rate for BMP3 bottles.

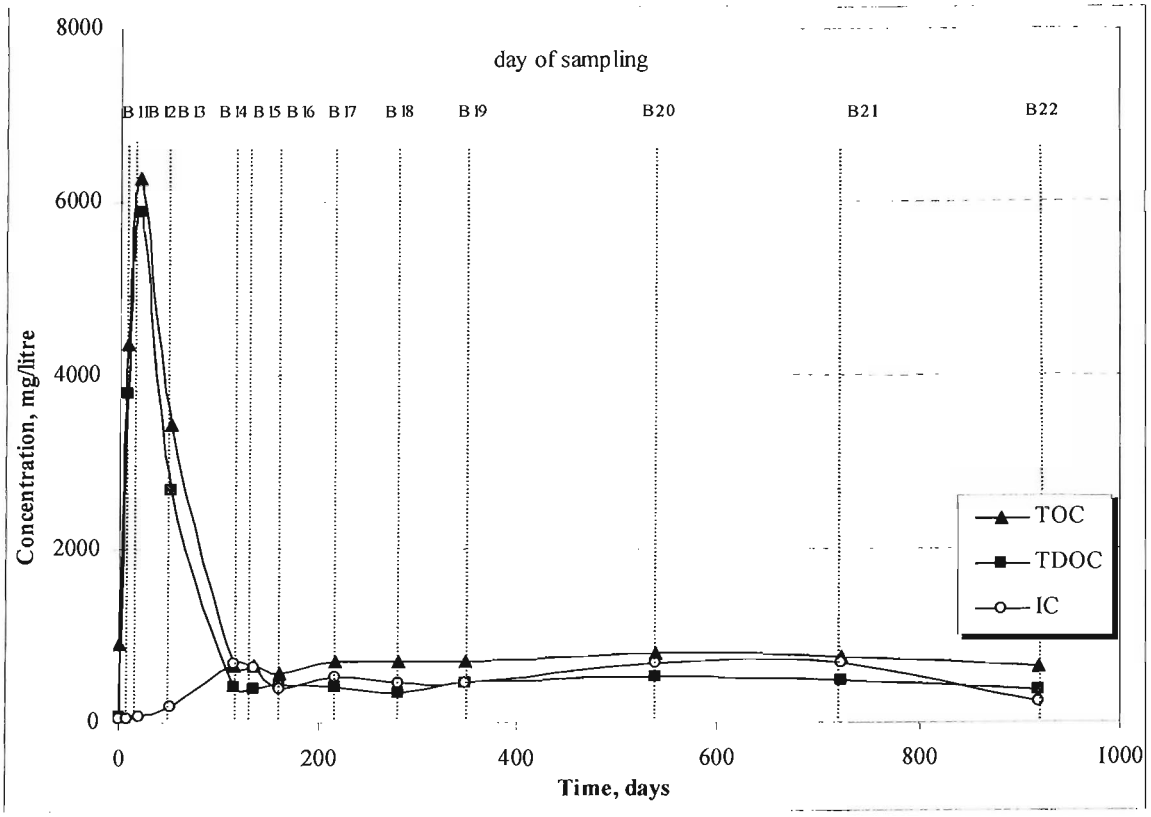

Figure 7.41. Leachate carbon in BMP3 bottles.

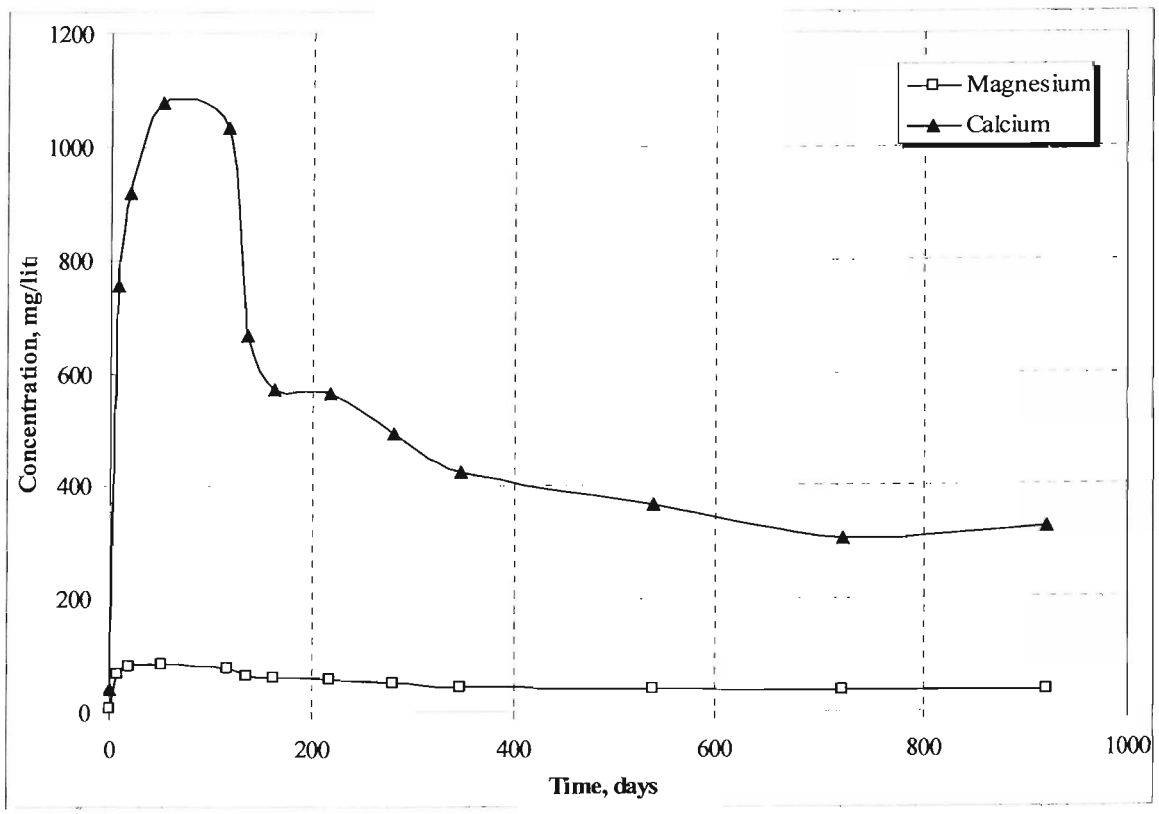

Figure 7.42. Calcium and magnesium concentrations in the BMB3 reactors.

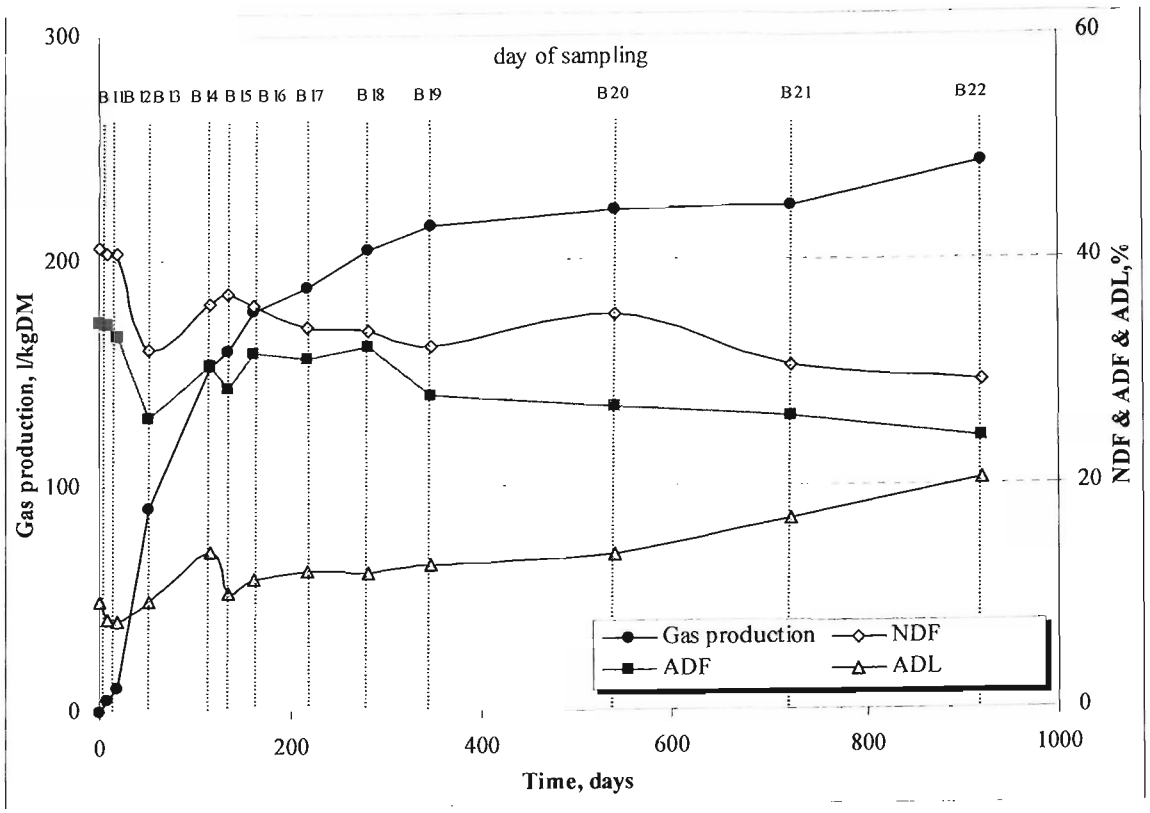

Figure 7.43. Cumulative gas production, NDF, ADF and ADL vs. time for BMP3 bottles.

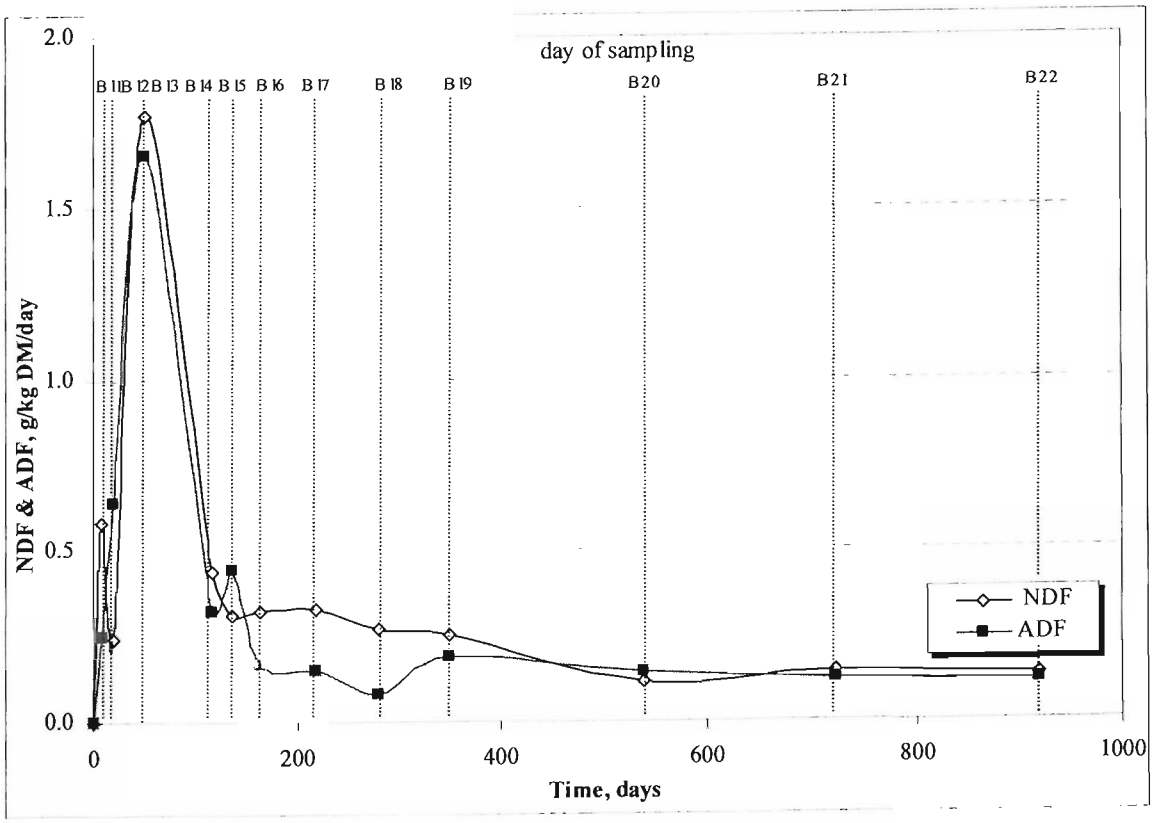

Figure 7.44. NDF and ADF vs. time for BMP3 reactors.

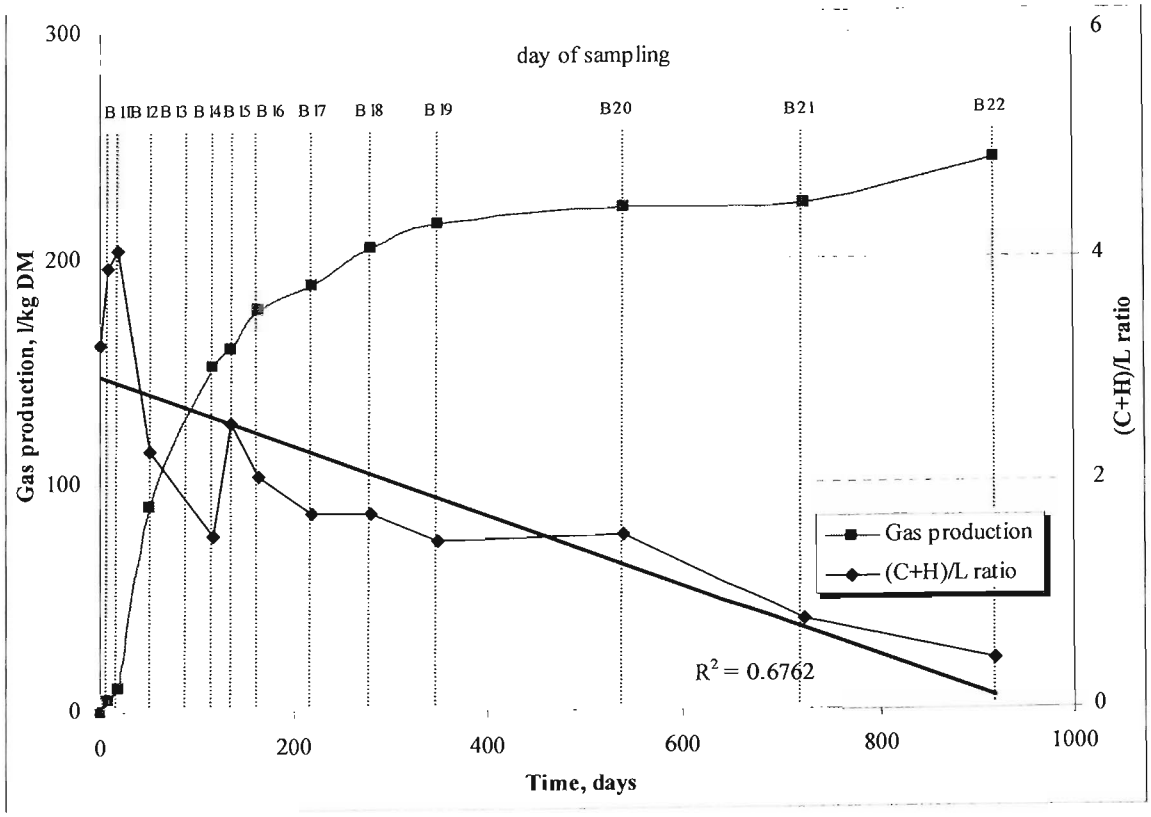

Figure 7.45. (C+H)/L and Cumulative gas production vs. time for BMP3 reactors.

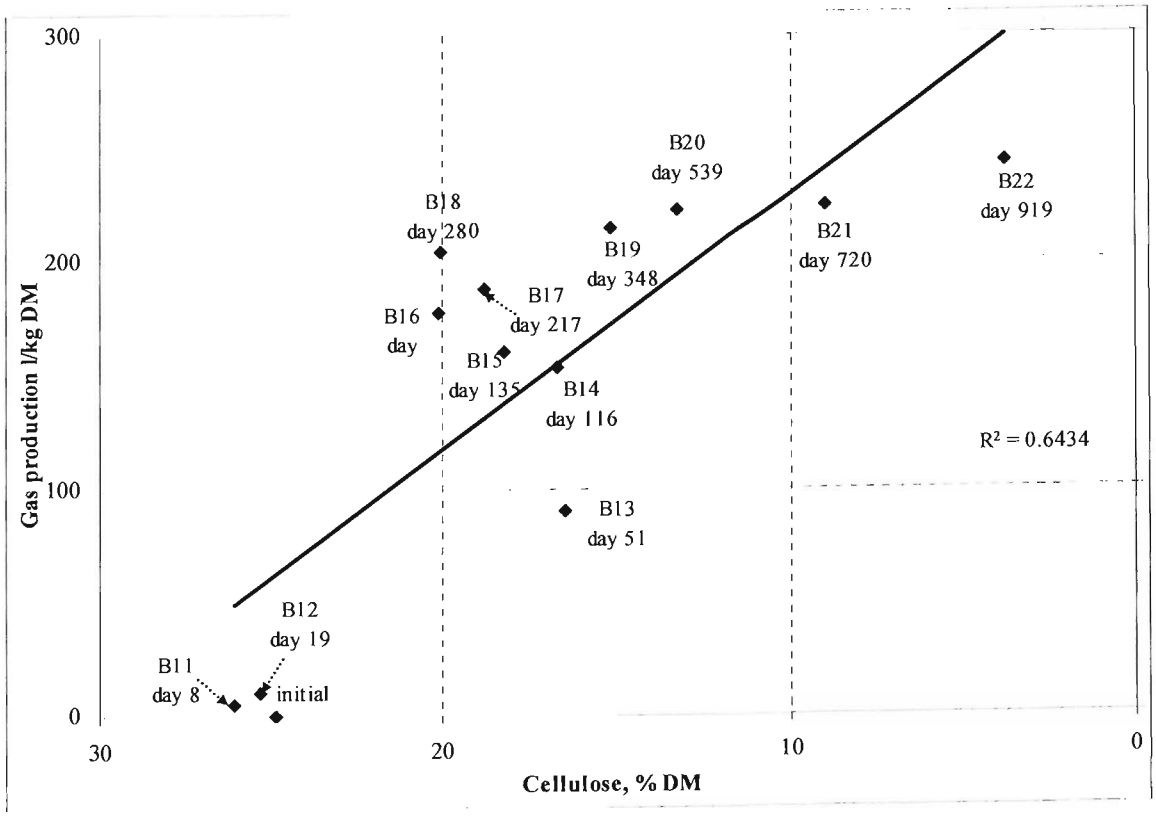

Figure 7.46. Correlation between cellulose content and cumulative gas production.

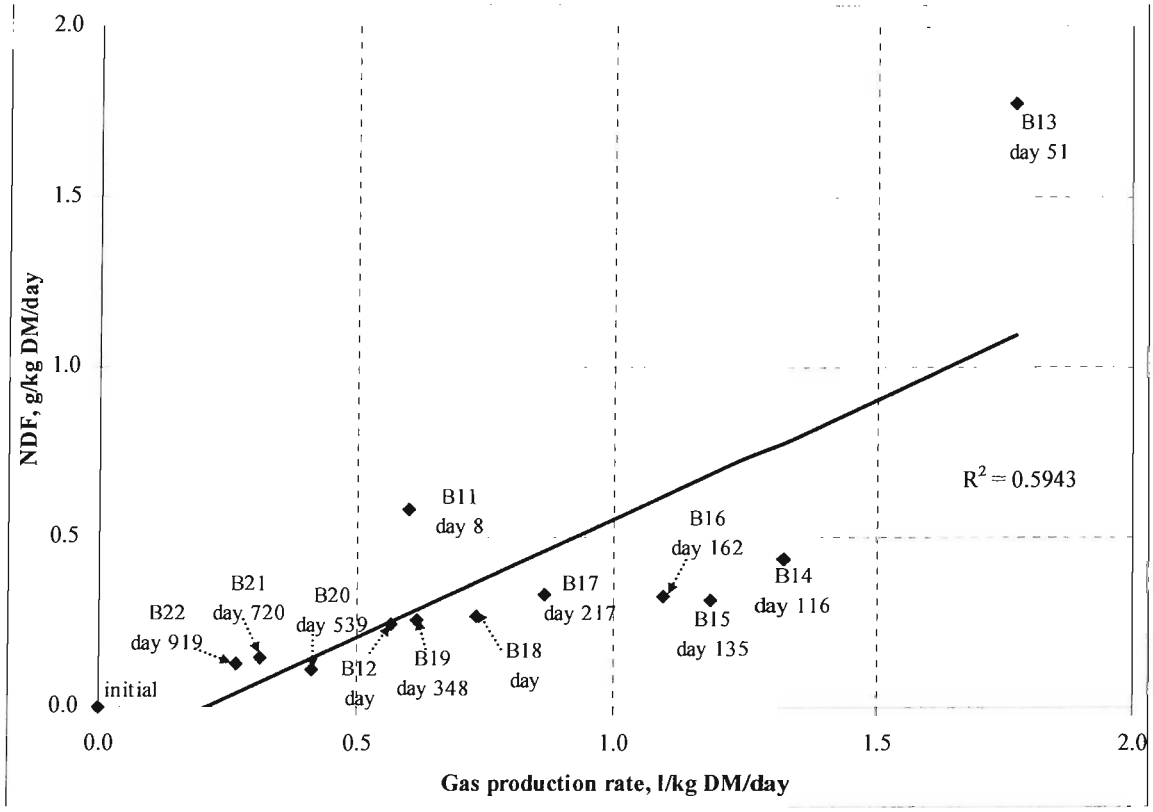

Figure 7.47. Correlation between gas production rate and NDF biodegradation rate.

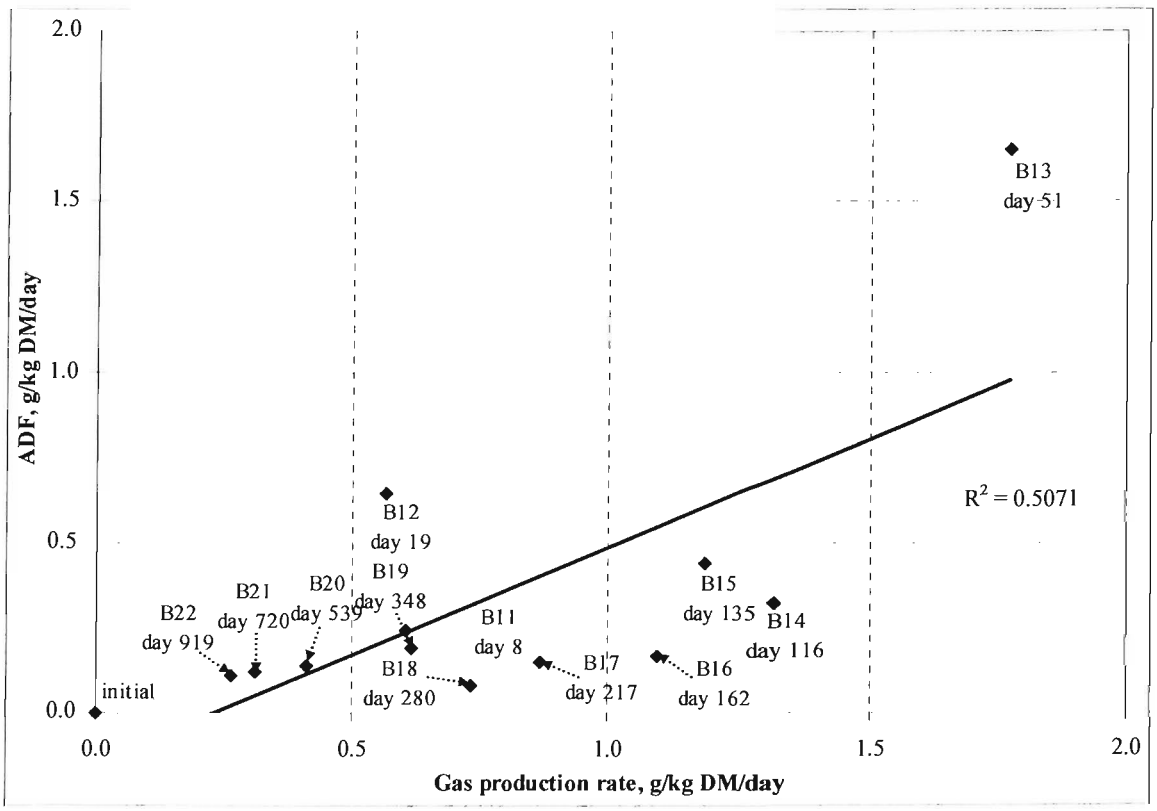

Figure 7.48. Correlation between gas production rate and ADF biodegradation rate.

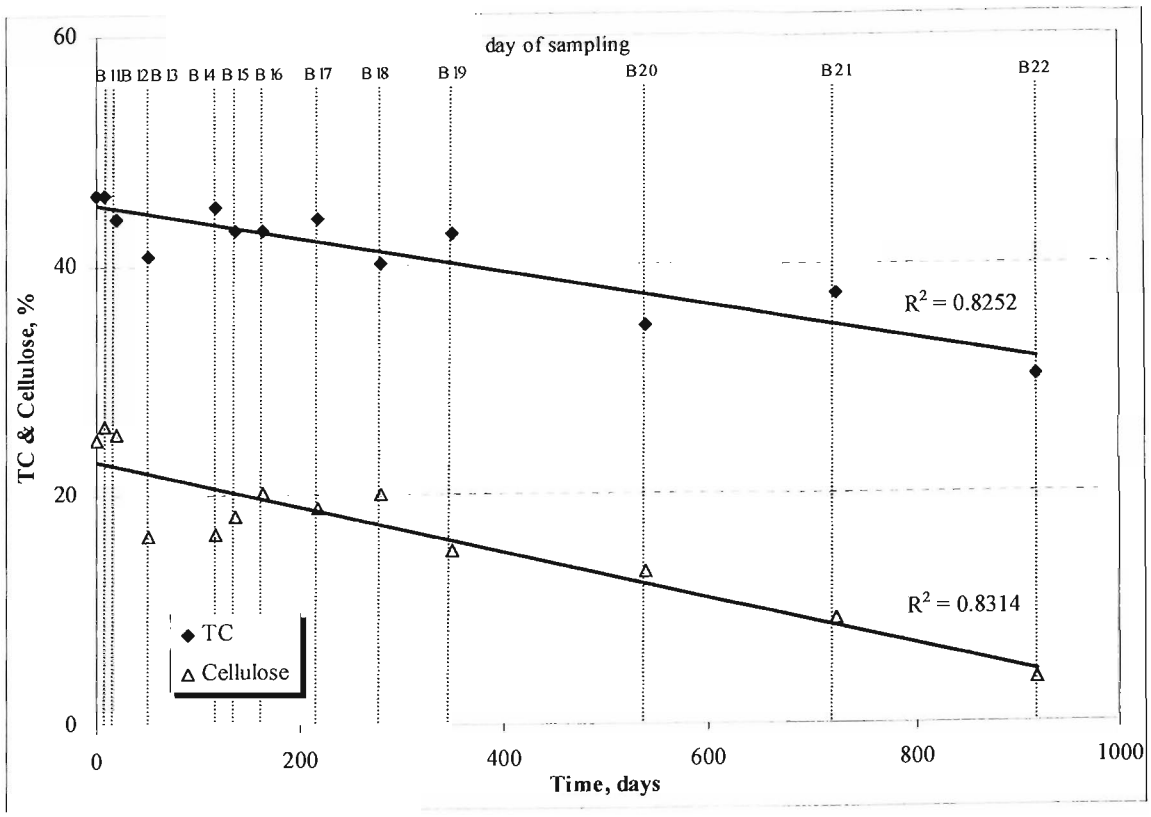

Figure 7.49. TC and cellulose vs. time for BMP3 reactors.

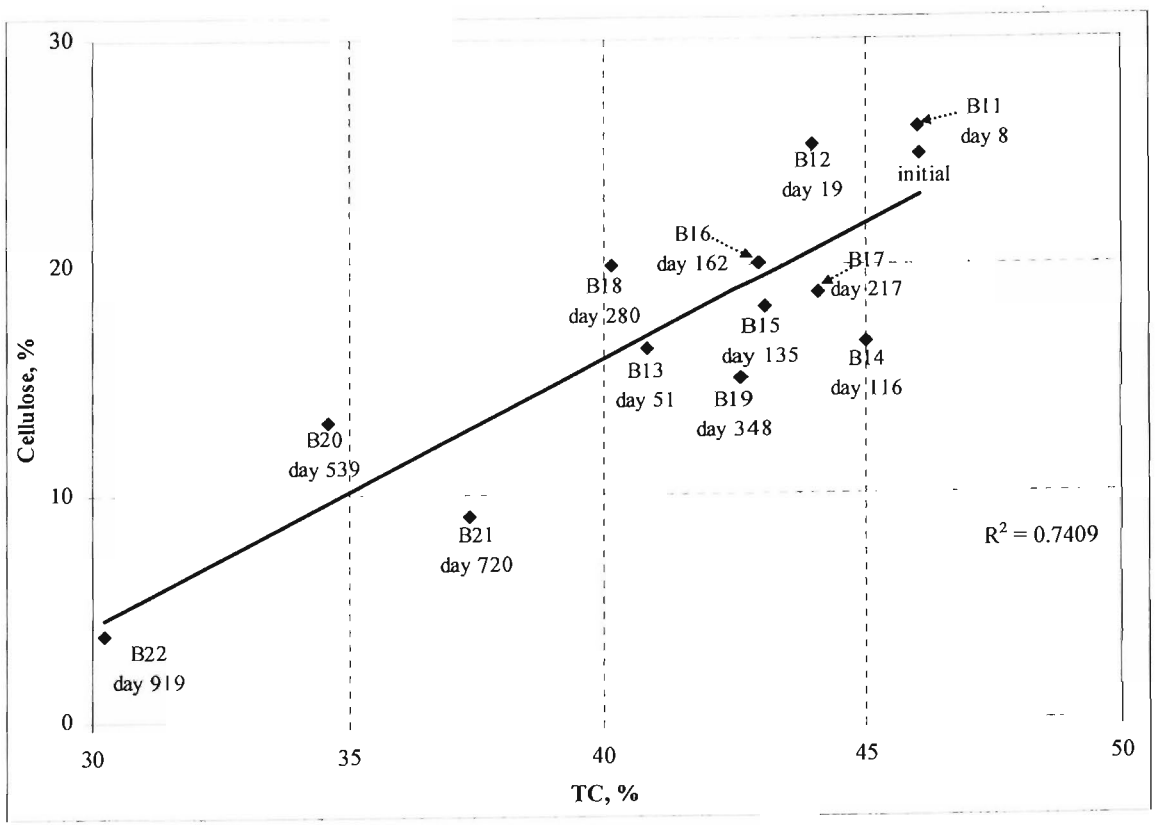

Figure 7.50. Correlation between waste TC and cellulose content.

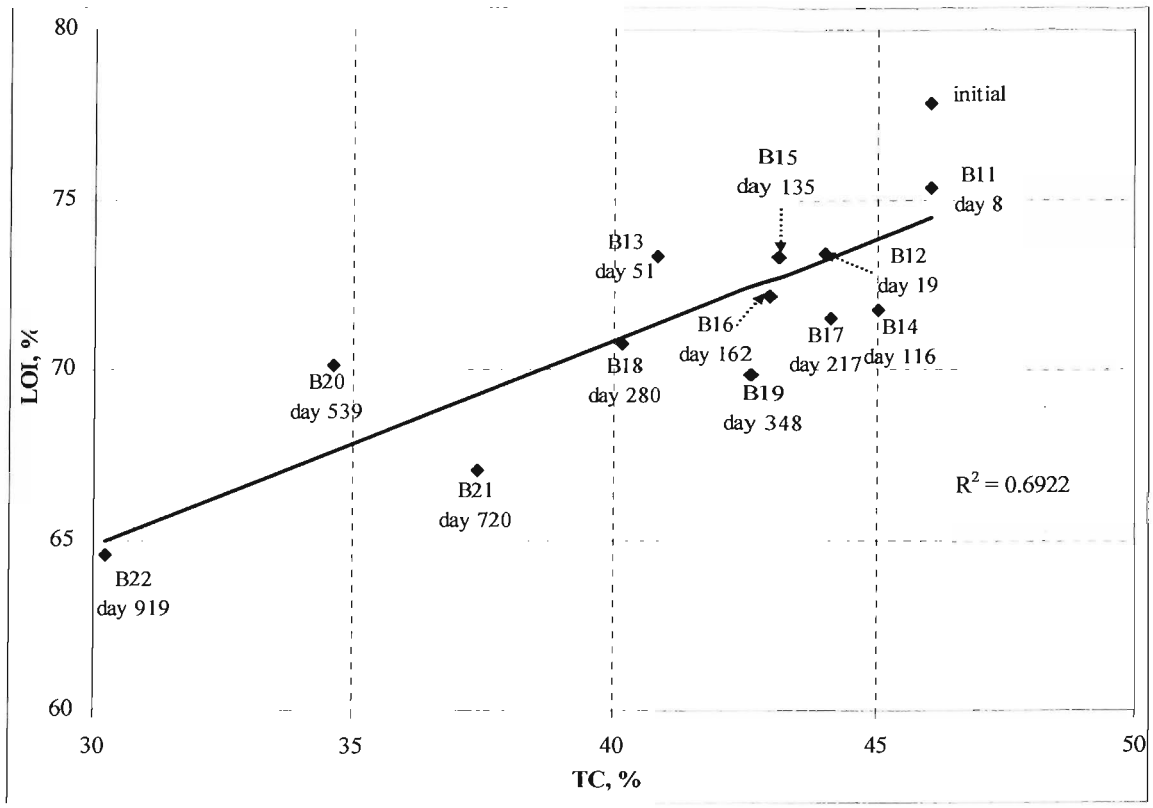

Figure 7.51. Correlation between LOI and waste TC for BMP3 bottles.

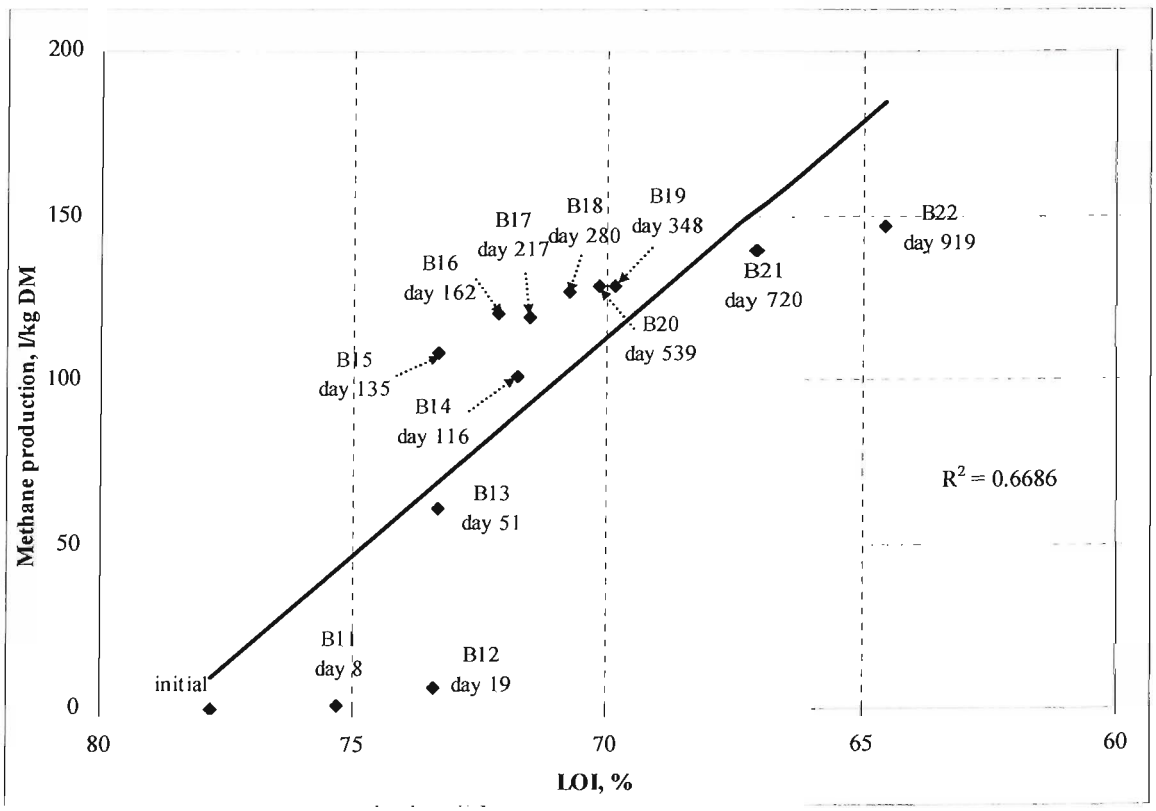

Figure 7.52. Correlation between LOI and methane production for BMP3 bottles.

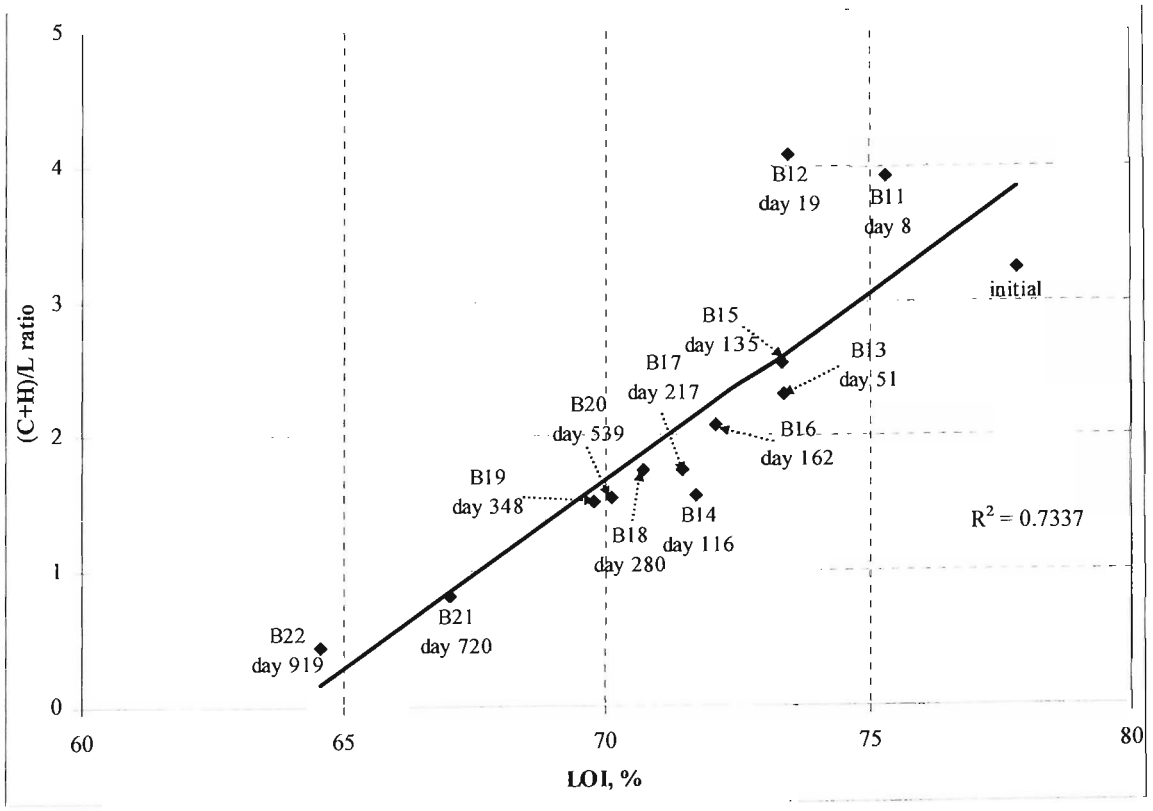

Figure 7.53. Correlation between LOI and (C+H)/L ratio for BMP3 reactors.

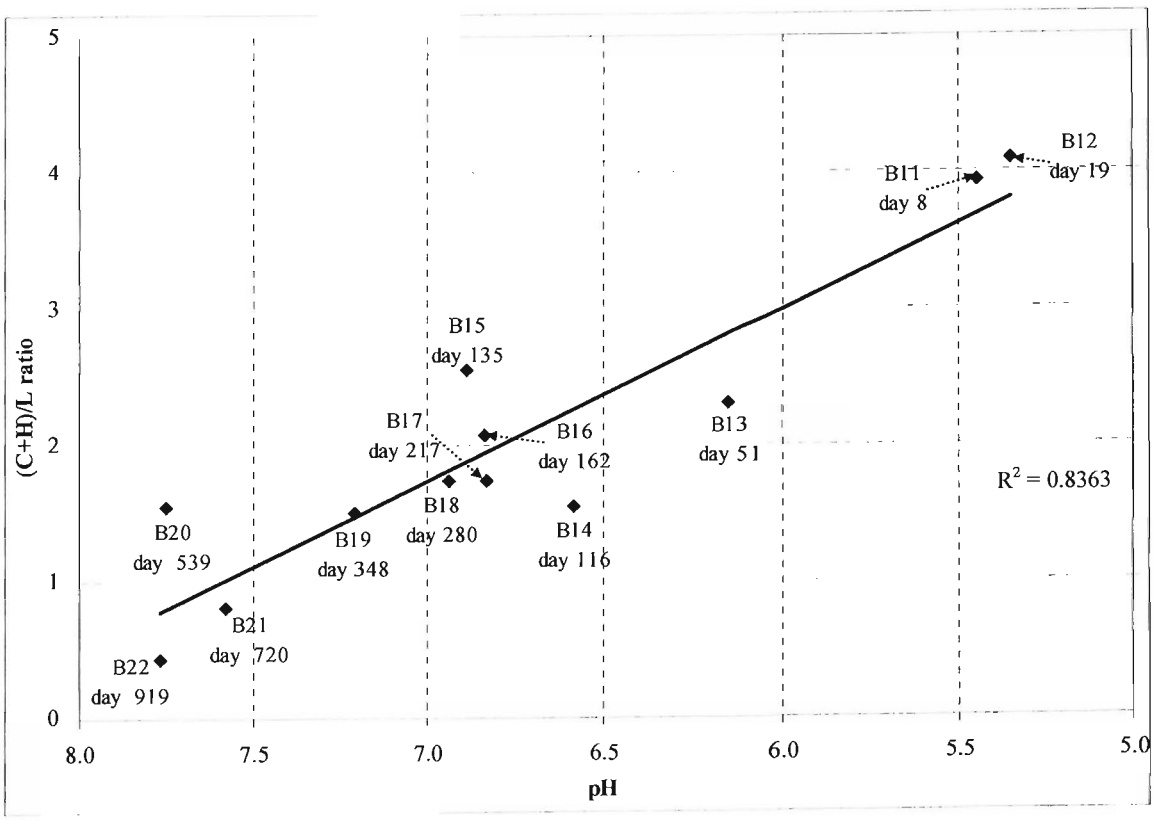

Figure 7.54. Correlation between pH and (C+H)/L ratio for BMP3 reactors.

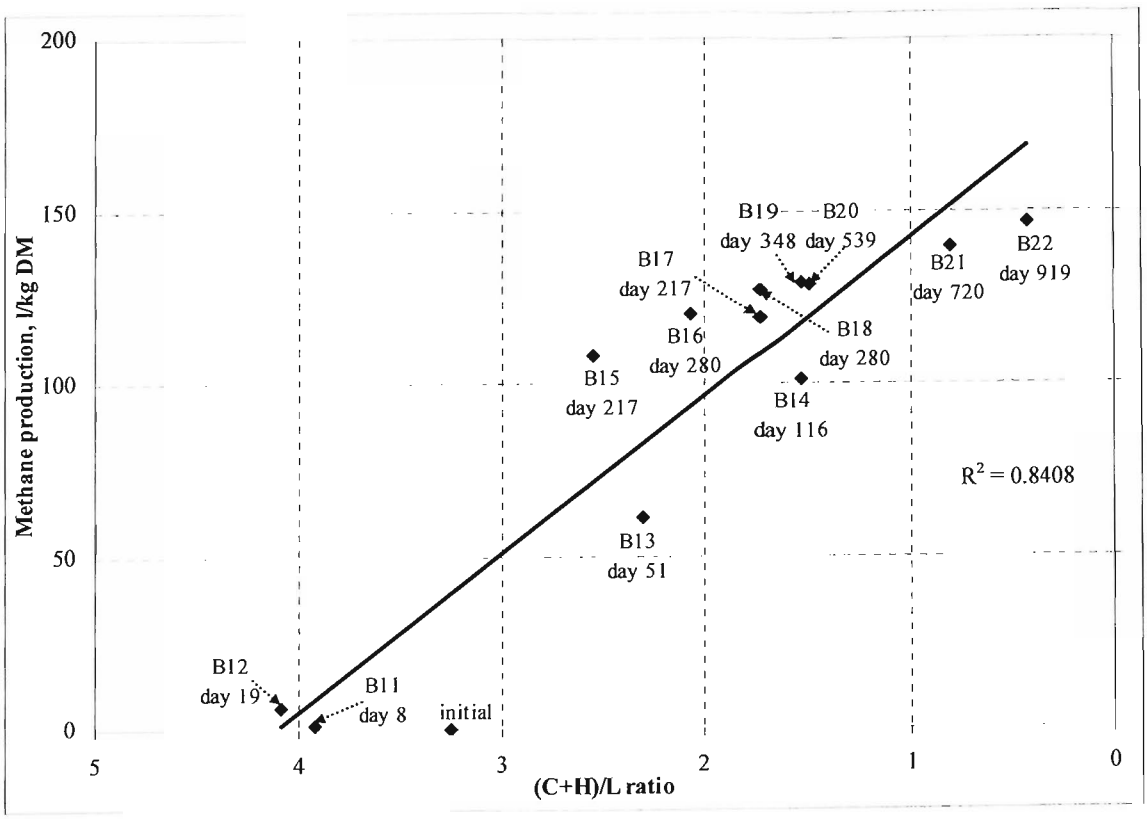

Figure 7.55. Correlation between cumulative methane production and (C+H)/L ratio.

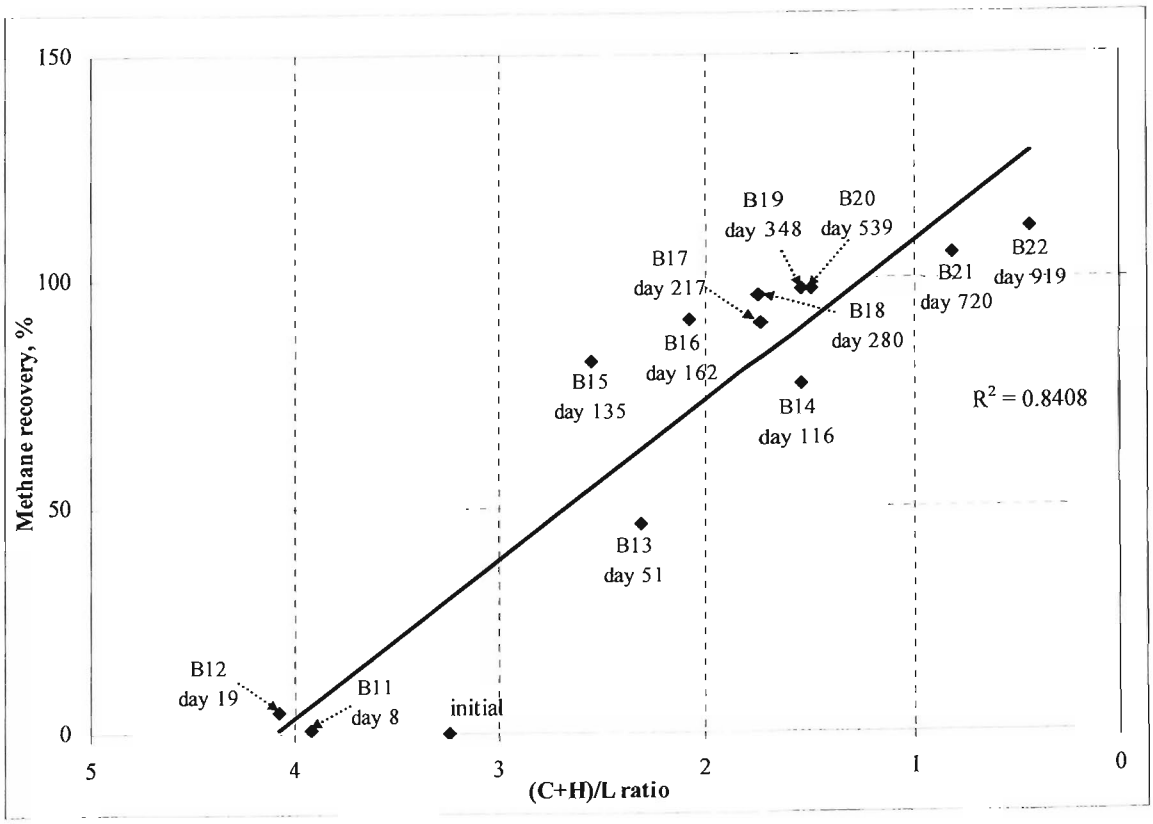

Figure 7.56. Correlation between (C+H)/L ratio and methane recovery.

Chapter 8

Results and discussion:

Comparative assessment of settlement models.

Correlation between settlement and biodegradation.

In this study, landfill settlement was characterised with the following classification: *load-induced settlement* associated with initial and primary settlement processes (such as filling and loading of CARs), which were not included in settlement simulations, and *creep and biodegradation-induced settlement* associated with the secondary settlement process, which was simulated using four CARs and predicted by time-dependent settlement models. Secondary settlement was further divided into three sub-stages as outlined in section 1.1: *intermediate settlement*, where the settlement is dominated by mechanical interactions due to creep of the waste skeleton; *long-term settlement* which is due to both creep of the waste structure and biodegradation of bioavailable organic matter; and *residual settlement* due mainly to mechanical creep and delayed degradation of those organic waste components that are resistant to biodegradation over the previous stages. In this chapter, five commonly used settlement models were used to simulate the experimental results and to predict the long-term settlement characteristics of the waste. The model proposed by Sowers (1973) was used in section 8.1.1 to represent the different stages of the secondary settlement independently, and the Gibson and Lo model (1961), the Power Creep Law model (Edil *et al.*, 1990) and the Hyperbolic Law model (Ling *et al.*, 1998) were used in section 8.1.2, 8.1.3 and 8.1.4, respectively to represent secondary settlement as a single process. However, the last three models require the use of curve fitting coefficients to illustrate compressive properties, and there is very limited information available in the literature to determine these parameters. Finally, the Park and Lee (1997) model (section 8.1.5) was used to estimate the long-term settlement due to degradation of waste organic matter using first-order kinetics. A summary of the key

findings on the settlement interpretations in comparison to the experimental results is presented in section 8.1.6. The relationship between settlement and biodegradation is discussed in section 8.2.

8.1. Interpretation of settlement results using existing settlement models

8.1.1. The one-dimensional consolidation model (Sowers, 1973)

The Sowers model (1973) assumes that the secondary settlement curve is linear with respect to the logarithm of time. According to this model (section 4.2.2), settlement can be determined by the following equations:

Eq. 8.1
$$\frac{\Delta h(t)}{h} = C_R \log\left[\frac{\sigma_o^{'} - \Delta\sigma^{'}}{\sigma_o^{'}}\right] + C_{\alpha\varepsilon} \log\frac{t}{t_{ref}}$$

where, $\Delta h(t)$= settlement, m;

h = height of waste, m;

C_R = compression ratio;

$\sigma_o^{'}$ = effective stress, kPa;

$\Delta\sigma^{'}$ = increase in vertical stress due to the fill placement, kPa;

$C_{\alpha\varepsilon}$ = secondary compression index;

t = time for which settlement is completed, days; and

t_{ref} = time for secondary compression to start, days.

As stated previously in section 1.1, the settlement observed during filling and loading was considered to be caused by initial and primary compression of the waste due to a lack of adequate compaction during the sample preparation stage, and was not included in the total settlement determination. In this study, the wastes were assumed to be in secondary settlement stage when the filling was complete and the effects of the surcharge resulting from the self-weight of upper layers of waste on the settlement observed in the CARs was considered to be negligible. Therefore, the increase in the vertical stress due to an externally applied stress $\Delta\sigma'$, is equal to zero. As a result, Eq. 8.1 can be transformed to:

Eq. 8.2
$$\frac{\Delta h_s(t)}{h_{ref}} = C_{\alpha\varepsilon}.\log\frac{t}{t_{ref}}$$

In order to estimate intermediate secondary, long-term secondary and residual settlements independently, the above equation was divided into three similar equations as follows:

Eq. 8.3 $$\frac{\Delta h_s(t)}{h_{ref}} = C_{\alpha\varepsilon 1} \log \frac{t}{t_{initial}} \qquad t_{initial} < t < t_1$$

Eq. 8.4 $$\frac{\Delta h_s(t)}{h_{ref}} = C_{\alpha\varepsilon 2} \log \frac{t}{t_1} \qquad t_1 < t < t_2$$

Eq. 8.5 $$\frac{\Delta h_s(t)}{h_{ref}} = C_{\alpha\varepsilon 3} \log \frac{t}{t_2} \qquad t_2 < t < t_{final}$$

where, $\Delta h_s(t)$= secondary settlement at time t_{ref}, m;

h_{ref} = height of waste upon completion of primary settlement, m;

$t_{initial}$ = time of primary compression to occur, days;

t_1 = time for completion of *intermediate* secondary settlement, days;

t_2 = time for completion of *long-term* secondary settlement, days;

t_{final} = end of experimental observations period, days;

$C_{\alpha\varepsilon 1}$ = *intermediate* secondary compression index or the slope of the strain versus log-time curve for $t_{initial} < t < t_1$;

$C_{\alpha\varepsilon 2}$ = *long-term secondary* compression index or the slope of the strain versus log-time curve for $t_1 < t < t_2$; and

$C_{\alpha\varepsilon 3}$ = *residual* secondary compression index or the slope of the strain versus log-time curve for $t_2 < t < t_{final}$.

In this study $t_{initial}$ = 1 day, t_{final} = 338 days (CAR1) and 919 days (CARs 2, 3 & 4).

Eq. 8.3 to Eq. 8.5 give a linear relationship between settlement and log t.

As shown in Figure 7.9 and Figure 8.1, a corresponding similarity between the gas production rate and settlement rate were found to exist which led to the conclusion that settlement due to the biodegradation of waste was related to gas production. This similarity was then used to determine the time factors t_1 and t_2 from the gas production curves and the corresponding settlement data in the CARs. While there is a similarity between the values of t_1 for CAR2 and CAR3, respectively, the values of t_2 are very different. This difference can be attributed to the fact that CAR2 produced gas for longer compared to CAR3 (Figure 8.1).

The settlement data acquired from the CARs were then used to back-calculate secondary compression indices for each secondary settlement stage in each cell. The one-dimensional consolidation model parameters derived from the settlement data for the four consolidating cells are given in Table 8.1.

The estimated intermediate secondary compression index ($C_{\alpha\varepsilon 1}$), ranged in value from 0.0295 (AG waste) to 0.0509 (FR waste). The values of $C_{\alpha\varepsilon 1}$ for the reactors filled with FR waste sample were found to be approximately two times higher than that calculated for the reactor filled with AG waste sample, although the reasons for this need to be further evaluated. Similar findings were reported by Park and Lee (2002) when comparing various mechanical secondary compression indexes found in the literature.

The $C_{\alpha\varepsilon 2}$ values estimated in this study varied from 0.0819 (AG waste) to 0.1760 (FR waste) (Table 8.1). The lowest rate of $C_{\alpha\varepsilon 2}$ estimated in CAR1 was considered to be due to the age of the waste where it can be expected that most biodegradable components had already been degraded. Therefore, the long-term secondary settlement CAR1 was most likely to be caused by the mechanical compression of the non-biodegradable matter. It was also found that CAR2 exhibited a greater long-term secondary compression coefficient than that observed in CAR3 which is indicative of enhanced biodegradation in CAR2.

Table 8.1. Best-fit parameters for the one-dimensional consolidation model (Sowers, 1973).

Parameter	CAR1 - 50kPa (AG waste)	CAR2 - 150 kPa (FR waste)	CAR3 - 50kPa (FR waste)	CAR4 - 50kPa (FR waste - control)
$C_{\alpha\varepsilon 1}$	0.0295	0.0416	0.0509	0.0503
$C_{\alpha\varepsilon 2}$	0.0819	0.1760	0.1537	0.1754
$C_{\alpha\varepsilon 3}$	0.0277	0.0748	0.0756	n/r [1]
t_1, days	56	54	31	345
t_2, days	192	596	238	n/r
R^2	0.9952	0.9976	0.9987	0.9967

Note: [1]residual settlement stage in CAR4 not reached yet; R^2 is the correlation coefficient.

The values for $C_{\alpha\varepsilon 1}$ and $C_{\alpha\varepsilon 2}$ evaluated in this study were comparable to those reported in the literature (Bjarngard and Edgers, 1990; Gandolla *et al.*, 1992; Lee *et al.*, 1995; El-Fadel *et al.*, 1999) (Table 4.3). However, the authors did not report values for the residual secondary compression index ($C_{\alpha\varepsilon 3}$) possibly due to the fact that all these experiments

was conducted either on a small scale and/or over an insufficient timescale for the residual settlement to occur.

Figure 8.2 to Figure 8.5 show the one-dimensional consolidation model interpretations and the observed CARs settlement profiles. The Sowers model (1973) provided a good interpretation of the settlement results at all stages of compression. Furthermore, the settlement curves of CARs 1, 2 & 3 (Figure 8.2 to Figure 8.4) developed smaller slopes at greater times (values between 0.0277 and 0.0756) which can be attributed to both delayed mechanical compression and delayed degradation of the organic matter. It should be noted that in the literature the number of papers on MSW settlement studies observing a residual secondary settlement stage are very limited.

8.1.2. The Gibson & Lo (1961) model

The three empirical parameters (*a, b* and λ/b) were determined by using a logarithmic plot of strain rate ($\log\frac{\varepsilon(\infty)-\varepsilon(t)}{\sigma'}$) against time. From the slope ($-0.434\frac{\lambda}{b}$) and intercept ($\log b$) of the best-fit straight line, values of b and λ/b were determined. The primary compressibility parameter a was obtained by substituting the value of t_k and the corresponding strain $\varepsilon(t_k)$ in Eq. 4.40, where t_k is the time when the intermediate secondary settlement is complete.

In this study, the primary (*a*) and secondary compressibility (*b*) parameters varied between 3.07E-03 and 6.16E-02, and between 1.68E-01 and 4.29E-01, respectively, whereas the rate of secondary compression λ/b ranged from 2.21E-03 to 8.93E-03 (Table 8.2). While the values of λ/b fall within reported ranges, the values for a and b were greater by one or two orders of magnitude (Edil *et al.*, 1990; Park *et al.*, 2002), which can be attributed to the fact that CARs experiments were carried out under enhanced biodegradative conditions achieved by the various techniques described in section 5.2.3, which will have accelerated the waste biodegradation processes in the CARs and hence the settlement rates.

Variations in the Gibson and Lo model parameters with applied stress are shown in Figure 8.6. The amount of primary compressibility (*a*) decreases with an increase in applied stress and waste age. The secondary compressibility (*b*) is also shown to decrease with increasing stress applied and age of the waste. As the stress applied and the age of waste increases, the secondary compressibility (*b*) decreases. However, the rate of

secondary compression (λ/b) (Figure 8.6) increases with greater waste age, but does not show any significant trend with respect to the applied stress. Similar observations were made by Edil *et al.* (1990) and Lee *et al.* (1994), except for the variation of secondary compression (λ/b) which was found either to increase (Edil *et al.*,1990) or to vary (Lee *et al.*, 1994) with the increasing stress.

Table 8.2. Best-fit parameters for the Gibson and Lo model (1961).

Parameter	CAR1 - 50kPa (AG waste)	CAR2 - 150 kPa (FR waste)	CAR3 - 50kPa (FR waste)	CAR4 - 50kPa (FR waste - control)
$a \times 10^2$, 1/kPa	1.6455	1.9493	6.1597	0.3074
$b \times 10^1$, 1/kPa	1.7897	1.6750	4.2859	4.2537
$\lambda/b \times 10^3$, 1/day	8.9278	4.4060	7.4902	2.2054
R^2	0.9873	0.9976	0.9920	0.9770

Note: a is the amount of primary compressibility; b is the secondary compressibility; λ/b is the rate of secondary compression; R^2 is the correlation coefficient.

Figure 8.7 to Figure 8.10 shows the model interpretations for all CARs. The Gibson and Lo (1961) interpretations of the CARs settlement data resulted in an acceptable fit for all stages of settlement.

8.1.3. The Power Creep Law (Edil et al., 1990)

The settlement results obtained in this study were also analysed to determine Power Creep Law model parameters values (section 4.4.1). From the settlement curves plotted in log (ε) versus log (t), the long-term secondary settlement part was approximated as a straight line. Table 8.3 shows values of the model parameters and regression indexes obtained for each settlement dataset.

The values of the rate of compression n were found to be within reported ranges in previous studies, while values of the reference compressibility m were 10 to 10^3 times greater (Edil *et al.*, 1990; Ling *et al.*, 1998; El-Fadel *et al.*, 1999[b]; Kumar, 2000; Park *et al.*, 2002). This discrepancy can be explained in the same way as in the Gibson and Lo model (1961) and can also be attributed to the difference between the composition of the

waste tested in this study and the waste material in the other studies. However, values of *m* were found to be close to those reported in a study conducted by Sanchez-Alciturri *et al.* (1995), which covered the monitoring of a MSW landfill site, from the beginning of the construction period until closure, over a similar time period.

Table 8.3. Best-fit parameters for the Power Creep Law (Edil *et al.*, 1990).

Parameter	CAR1 - 50kPa (AG waste)	CAR2 - 150 kPa (FR waste)	CAR3 - 50kPa (FR waste)	CAR4 - 50kPa (FR waste - control)
m x 10^2, 1/kPa	1.3814	1.5743	8.0236	3.1386
n x 10^1, (t_r=1day)	4.6611	3.6967	2.7771	3.6274
R^2	0.9777	0.9793	0.9531	0.9853

Note: m is the reference compressibility; n is the rate of compression; t_r is the reference time introduced to make the time dimensionless; and R^2 is the correlation coefficient.

In order to develop a relationship between the applied stress, waste age and model parameters, the parameters were plotted with respect to σ' (Figure 8.11 & Figure 8.12). The reference compressibility parameter m has a definition similar to the primary compressibility parameter a from the Gibson and Lo model (1961). As expected, the reference compressibility m decreases with an increase in applied stress, but increase with waste age. The rate of compression, n, was found to increase as the stress applied and age of waste increased, but did not show any correlation with the applied stress. (Figure 8.12).

Data found in the literature concerning the correlation between the Power Creep Law parameters, applied stress and waste age are controversial. For example, data reported by Lee *et al.* (1994) about parameter m correlations with stress and material age compare very well with the data presented in this study, while data for n were found by the same authors, to be variable when plotted against applied stress and sample age. Edil *et al.* (1990) on the other hand reported that as the waste age increases, so does the parameter m, but no significant trends for m with respect to the applied stress were found. In the same study, the parameter n was found to vary with the applied stress and waste age.

A plot between parameters m and n (values as in Table 8.3) is shown in Figure 8.13. In general, n gradually decreased as the reference compressibility m increased. A relatively

good straight-line correlation was found to exist between the Power Creep Law parameters, with a correlation coefficient equal to 0.74.

Settlement interpretations using Power Creep Law are shown in Figure 8.14 to Figure 8.17 for Cells 1, 2, 3 & 4 respectively. The R^2 values for the reactors ranged from 0.95 to 0.98 showing a good agreement between actual and simulated settlement. The Power Creep Law predicted the intermediate settlement relatively well, but it overestimated the last stage of the observed settlement with up to 7%.

8.1.4. The Hyperbolic Law (Ling et al., 1998)

The settlement results obtained were also analyzed to determine the Hyperbolic Law parameters, ρ_o and S_{ult} according to Eq. 4.51. A linear regression analysis of the plot of $t/\varepsilon(t)$ versus t, the intercept and the slope of the best-fit line gave values of H_o/S_{ult} and H_o/ρ_o, respectively. Knowing the initial waste height in each reactor (H_o) the parameters ρ_o and S_{ult} ,were then calculated. The results are presented in Table 8.4.

Table 8.4. Best-fit parameters for the Hyperbolic Law (Ling *et al.*, 1998).

Parameter	CAR1 - 50kPa (AG waste)	CAR2 - 150 kPa (FR waste)	CAR3 - 50kPa (FR waste)	CAR4 - 50kPa (FR waste - control)
ρ_o x 10^4, m/day	7.8095	6.8513	1.3845	2.2394
S_{ult} x 10^1, m	0.7589	1.1095	1.1326	1.2330
H_o, m	0.623	0.341	0.417	0.403
R^2	0.9845	0.9973	0.9972	0.9785

Note: ρ_o is the initial rate of compression; S_{ult} is the ultimate settlement of the waste fill when $t \rightarrow \infty$; R^2 is the correlation coefficient; and H_o is the initial waste height.

The ranges of ρ_o and S_{ult} are also shown in Figure 8.18 and Figure 8.19 so that any trend of Hyperbolic Law parameters with the applied stress and waste age can be easily observed. A clear relationship between both parameters and waste age is shown. As the sample age increases, the initial rate of compression (ρ_o) was found to increase, while the ultimate settlement (S_{ult}), was observed to decrease. No relationship was discernible between the Hyperbolic Law parameters and the applied stress.

The results obtained from Hyperbolic Law interpretations were compared with values from the literature. It should be noted that those values from the literature cover a wide range of waste composition, waste age, operational-management practices and also present data obtained using *in situ* and laboratory test techniques. Park *et al.* (2002) investigated the long-term settlement characteristics by applying a number of prediction methods to fresh MSW and simulated the actual settlement curves obtained from seven different studies. The values reported by Park *et al.* (2002) for large-scale tests ranged from 0.0003 (Gandolla *et al.*, 1992) to 0.0066 (Lee *et al.*, 1995) for parameter ρ_o and from 0.228 (Rao *et al.*, 1977) to 1.695 (Gandolla *et al.*, 1992) for parameter S_{ult}. In other studies, the Hyperbolic Law parameters, ρ_o and S_{ult}, obtained for four different landfill sites, varied between 0.001 (Edil *et al.*, 1990) and 0.102 (Merz and Stone, 1962), and between 0.489 (Merz and Stone, 1962) and 1.14 (Edil *et al.*, 1990), respectively. The ρ_o and S_{ult} values estimated in this study varied from 0.0001 (FR waste) to 0.0008 (AG waste), and from 0.0759 (AG waste) to 0.1233(FR waste), respectively (Table 8.4). These values were found to be in the same order of magnitude as those reported by Park *et al.* (2002) for large-scale tests.

Figure 8.20 to Figure 8.23 show settlement interpretations using the Hyperbolic Law (Ling *et al.*, 1998). Here, the hyperbolic function simulated the settlement results in each test cells well, especially the long-term compression stage, where the settlement due to biodegradation dominates.

8.1.5. The biomechanical model (Park and Lee, 1997 & 2002[a])

The Park and Lee (1997, 2002) model (described in section 4.5.4) was applied to the settlement data observed in this study. To determine the model parameters, first the time lapse (given as t_{bio} in Eq. 4.64) from the starting point (t_c) at which the settlement due to biodegradation started was considered. For fresh MSW waste, t_c is assumed to be the time when the slope of the log-time-settlement curve becomes much greater than in the early stages of secondary settlement (Sowers, 1973; Bjarngard and Edgers, 1990). Therefore, the starting time (t_c), at which the settlement due to biodegradation occurs, was determined to be the same as time t_1 shown in Table 8.1. As previously discussed in section 4.5.4, the settlement due to mechanical compression can be represented using classical mechanical theory (Eq. 4.62), with values for $C_{\alpha\varepsilon 1}$ taken from Table 8.1. In order to determine the parameters used in the model proposed by Park and Lee (1997,

2002), a plot of the log strain rate ($\log\left(\frac{\Delta\varepsilon_{dec}}{\Delta t_{bio}}\right)$) vs. time t_{bio} was used. From the slope ($0.434k_{bio}$) of the best-fit straight line, a value of k_{bio} was determined. The ranges of k_{bio} and $\varepsilon_{tot\text{-}dec}$ observed in this study are given in Table 8.5.

The parameter values of the biochemical model derived from the CARs settlement data are presented in Figure 8.24. The reactor filled with the AG waste sample (CAR1), exhibited a total settlement due to degradation had a value of 4.54%, which was significantly lower than the reactors filled with FR waste sample (16.92% and13.39% in CARs 2 & 3, respectively). The value of the settlement rate due to degradation (k_{bio}) was in the range $7.30\text{x}10^{-3}$ - $2.81\text{x}10^{-3}$ $year^{-1}$ and increased with the age of the waste. Similar findings was reported by Park and Lee (2002) when the model was applied to settlement data of MSW landfills which had various fill ages.

Table 8.5. Best-fit parameters for the biomechanical model (Park and Lee, 1997, 2002).

Parameter	CAR1 - 50kPa (AG waste)	CAR2 - 150 kPa (FR waste)	CAR3 - 50kPa (FR waste)	CAR4 - 50kPa (FR waste - control)
t_c ,days	56	54	31	345
$\varepsilon_{tot\text{-}dec}$, %	4.54	16.92	13.39	6.20
k_{bio} x 10^3, 1/year	7.2972	3.7011	6.0972	2.8077
R^2	0.9900	0.9957	0.9897	0.9970

Note: t_c is the starting point of degradation based settlement; $\varepsilon_{tot\text{-}dec}$ is the total settlement due to degradation; k_{bio} is the settlement rate due to degradation; and R^2 is the correlation coefficient.

To better illustrate the relationship between model parameters, a linear regression analysis was conducted of the plot of k_{bio} versus $\varepsilon_{tot\text{-}dec}$ (Figure 8.24), which gave a good correlation with a R^2 value of 0.8173. It should be noted that data of k_{bio} and $\varepsilon_{tot\text{-}dec}$ obtained for the control reactor (CAR4) was excluded from the regression analyses because it was assumed that CAR4 did not represent real settlement conditions as degradation had been inhibited in the early stages.

As can be seen in Figure 8.25 to Figure 8.28, the biochemical model proposed by (Park and Lee, 1997, 2002) predicted settlement that matched reasonably closely that observed in the CARs at each settlement stage, with R^2 values between 0.9897 and 0.9970.

8.1.6. Assessment of the achieved modelling results

The performance of each model used in this study is assessed by:

- Its ability to simulate settlement results; and
- The accuracy of the interpretation with specific type of wastes.

In this regards, individual settlement data of all cells were combined as shown in Figure 8.29 to Figure 8.32. In these projections, the estimate of likely future settlement predicted by each model has been extended to 25 years. Table 8.6 gives the actual settlement data and the corresponding predicted data for the experiment duration and after 25 years (given in brackets). Even very well managed landfill cells, with enhanced biodegradation, may need to be monitored for periods of up to 50 years or more after completion of landfilling.

From the predicted test results and the data presented in Table 8.6, the following observations can be made:

Table 8.6. Comparative assessment of modelling results.

Model	CAR1 - 50kPa (AG waste)	CAR2 - 150kPa (FR waste)	CAR3 - 50kPa (FR waste)	CAR4 - 50kPa (FR waste - control)
Actual settlement, %	8.99	27.59	24.95	18.61
1D consolidation (Sowers, 1973), %	9.06 [1] (13.02) [2]	27.56 (34.76)	25.13 (32.62)	19.21 (36.66)
Gibson & Lo model (1962), %	9.32 (9.77)	27.61 (28.05)	24.49 (24.51)	18.62 (21.42)
Power Creep Law (Edil *et al.*, 1990), %	9.38 (48.13)	29.42 (68.38)	26.69 (50.29)	18.65 (42.66)
Hyperbolic Law (Ling *et al.*, 1998), %	9.44 (12.05)	27.66 (31.96)	24.94 (26.91)	19.13 (28.83)
Biomechanical model (Park and Lee, 1997), %	10.25 (15.05)	29.58 (34.81)	27.78 (32.84)	18.82 (25.04)

Note: [1] simulated settlement for the experiment duration; and [2] values in brackets is the predicted settlement for 25 years.

- The Sowers model (1973) gave a good interpretation of the settlement results at all stages of compression and for both types of waste;
- The Gibson and Lo (1961) model evaluated all stages of settlement in each reactor well, except for the control cell, but predicted up to 4% higher settlement values by the end of the CAR1 curve;
- The Power Creep Law provided a good interpretation of settlement only for the intermediate part of the settlement curve, where the settlement was thought to be due mainly to the delayed settlement of some of the waste components, but failed to simulate the shape of the curve of all the CARs over extended time scales, thus overestimating values of the total settlement by 4% to 7%;
- The hyperbolic function gave a good interpretation of settlement results in CARs 1, 2 & 3, especially in the long-term settlement stage, when biodegradation was the main factor affecting the amount of settlement recorded;
- The biochemical model (Park and Lee, 1997 & 2002) estimated the effect of biodegradation observed in the long-term settlement stages well, but overestimated the measured settlement in the CARs 1, 2 & 3 at the end of the test period by up to 7%;
- All model interpretations closely simulated the observed settlement in the CARs for the test duration with values of the correlation coefficient between 0.9531(Power Creep Law) and 0.9987(1D consolidation model) depending on the model used and the reactor simulated;
- In general, the Power Creep Law and the biochemical model predicted the first stage of secondary settlement well but it overestimated the long-term settlement for all cells by up to 7% and 14%, respectively. The magnitude of this discrepancy was observed to increase as the simulated time period increased;
- In terms of waste type, all the models used provided a good representation of the settlement data observed for the CAR filled with AG waste sample. However, the settlement behaviour of the FR waste sample (CARs 2, 3 & 4) was better predicted by the Sowers model (1973), Gibson and Lo model (1961) and Hyperbolic Law (Ling *et al.,* 1998) than the Power Creep Law and biochemical model (Park & Lee, 1997, 2002); and
- The estimated settlements over a 25 year period predicted by the Power Creep Law (Edil *et al.*, 1990) was 2 and 5 times greater than that predicted by the Gibson and

Lo (1961) model as the power function used caused a divergence at greater timescales.

8.2. Correlation between settlement and biodegradation

In the first stage of secondary settlement (intermediate stage), the low rate of biodegradation appears to lead to low secondary settlement rates. As discussed in section 1.1, biodegradation of readily biodegradable fraction of the waste leads to higher settlement rates. To establish the contribution of biodegradation to settlement in this study, the settlement data from CAR4 were interpreted as shown in Figure 8.33. The interpretation was done assuming that the control cell (CAR4) remained inhibited over the whole duration of the test and as a result of that the related settlement would have been linear with respect to the logarithm of time (i.e., associated with creep processes only). From the settlement curve plotted in Figure 8.33, the creep-induced settlement was approximated as a straight line and then its values were subtracted from the settlement values observed in CARs 2 & 3 (Table 8.7). It should be noted that, the value of the creep parameter associated with 50kPa applied stress (CARs 3 & 4) was assumed to be applicabale to the reactor subjected to an applied load of 150kPa (CAR2). This assumption was made because of the absence of any suitable creep correction factor, but in a reality it is recognized that the value might be slightly different (i.e., the creep parameter might be related to applied stress).

Table 8.7. Correlation between settlement and biodegradation in CARs 2, 3 & 4.

Parameter	CAR2 150kPa (FR waste)	CAR3 50kPa (FR waste)	CAR4 50kPa (FR waste - control)
Total settlement as measured, %	27.59	24.95	18.61
Settlement due to creep, %[1]	13.86	13.86	13.86
Settlement due to biodegradation, %	13.73	11.09	4.75

Note: [1] This value was calculated assuming that the control cell (CAR4) remained inhibited over the whole duration of the test and as a result of that the related settlement would have been linear with respect to the logarithm of time (Figure 8.2) (i.e., associated with creep processes only).

As can be seen in Table 8.7, the percentage of settlement observed in CARs 2, 3 & 4 that can be attributed to biodegradation was found to be 13.73%, 11.09% and 4.75%, respectively. These values were found to be lower than values obtained by Coduto and

Huitric (1990) (18 - 24%), possibly due to the fact that Coduto and Huitric (1990) determined the ultimate settlement due to biodegradation based on composition of waste typically received from 1964 to 1981.

Since biodegradation was determined to occur mainly during the long-term settlement stage, it was interesting to determine whether the settlement in each test cell correlated to the actual amount of biogas produced. Indeed, a very good linear statistical correlation between biogas generation and long-term secondary settlement was found to exist for CAR1 and CAR4, although the biodegradation rates were observed to be lower than the other cells (Figure 8.34 & Figure 8.35). However, to obtain a linear correlation between biogas production and long-term secondary settlement for the most bioactive test cells (CARs 2 & 3) the creep-induced settlement values (data given in Table 8.7) were subtracted from the long-term secondary settlement values observed in CARs 2 & 3 (thus giving the settlement associated with biodegradation only). A comparison between biodegradation-induced settlement and cumulative biogas production for CARs 2 & 3 indicates that there was a significant correlation between these two parameters with R^2 values of 0.93 and 0.96, respectively (Figure 8.36).

Figures

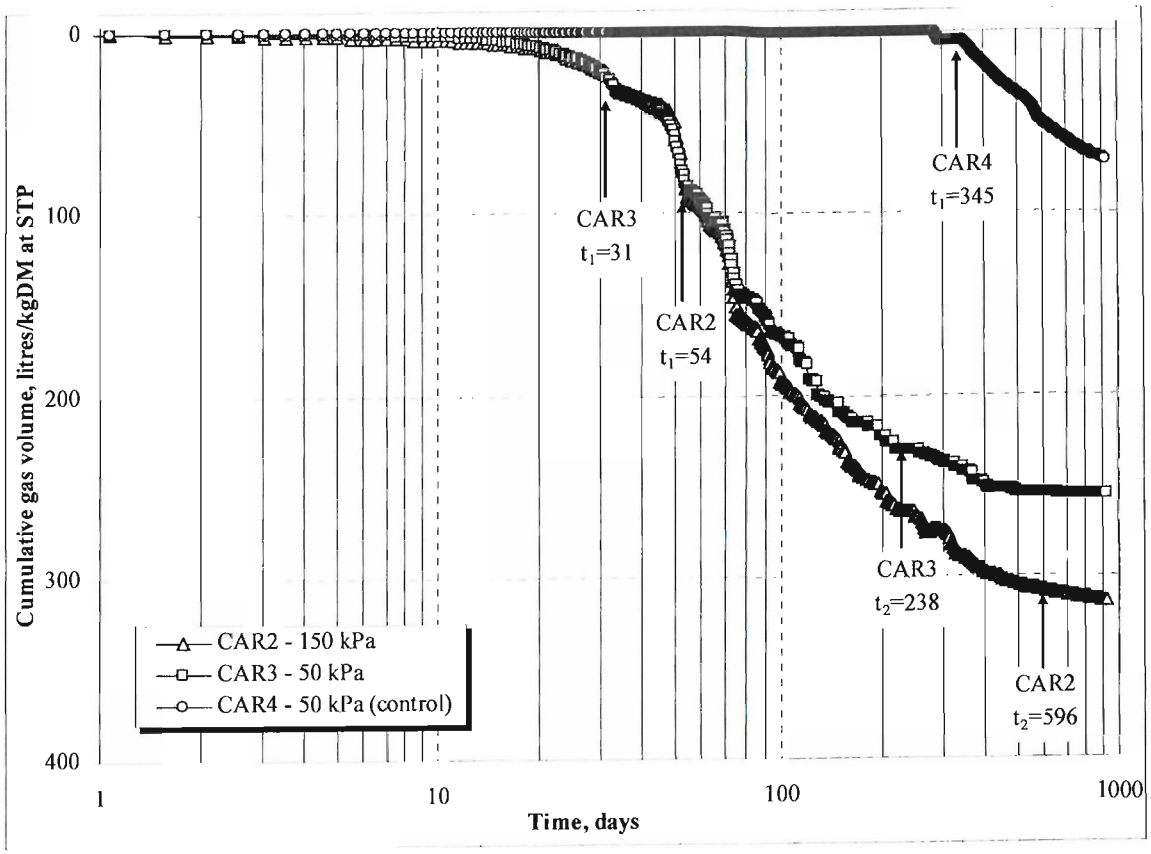

Figure 8.1. Cumulative gas production at STP in CARs 2, 3 & 4 plotted against log-time.

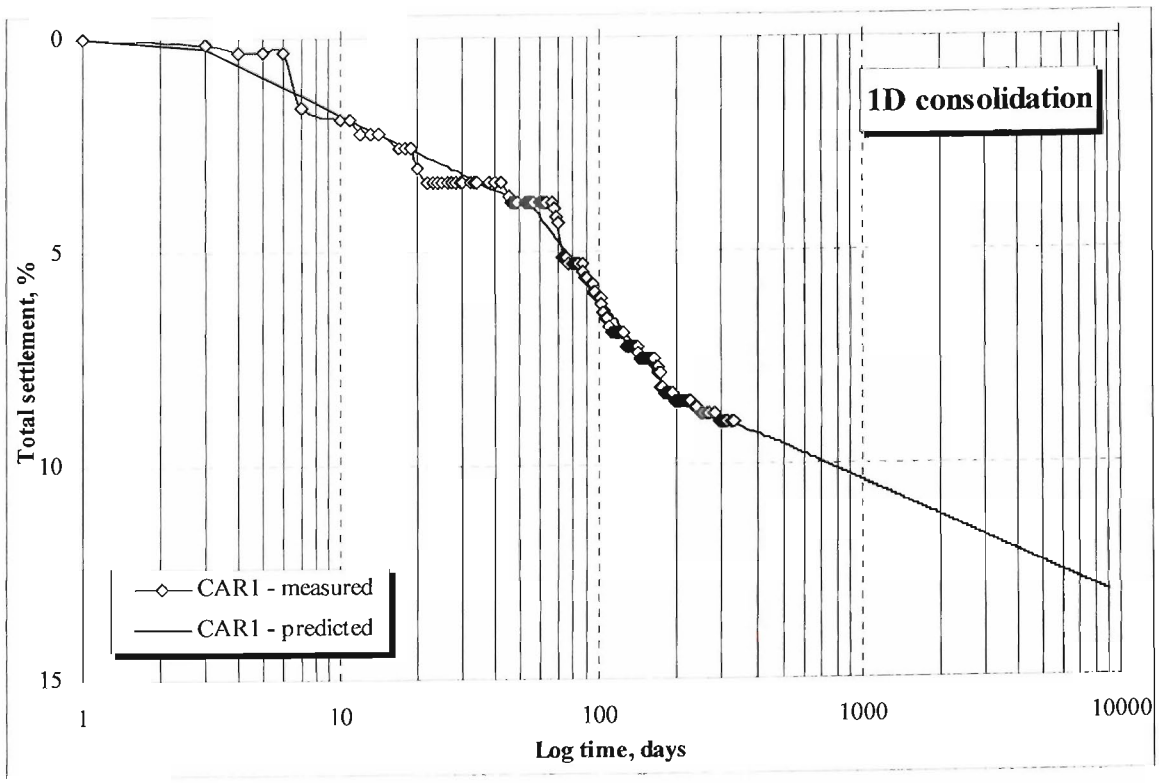

Figure 8.2. Estimated settlement by Sowers model (1973) for CAR1 - 50kPa (AG waste sample).

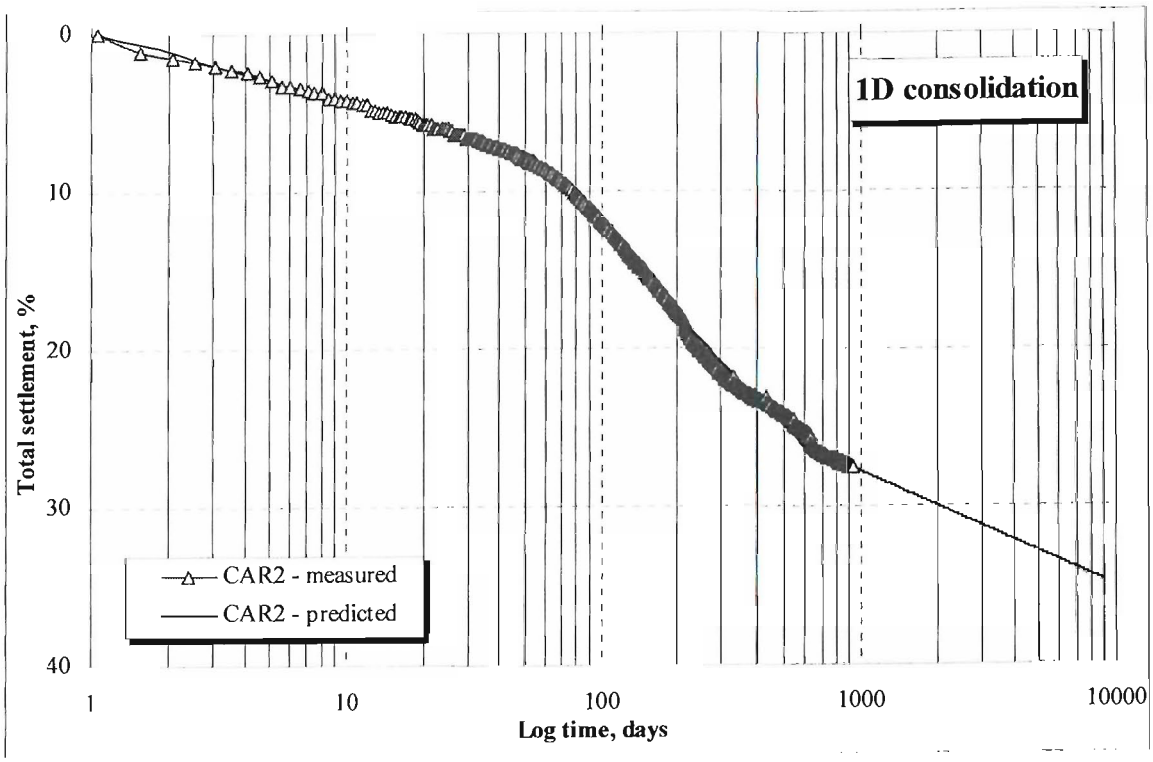

Figure 8.3. Estimated settlement by Sowers model (1973) for CAR2 - 150kPa (FR waste sample).

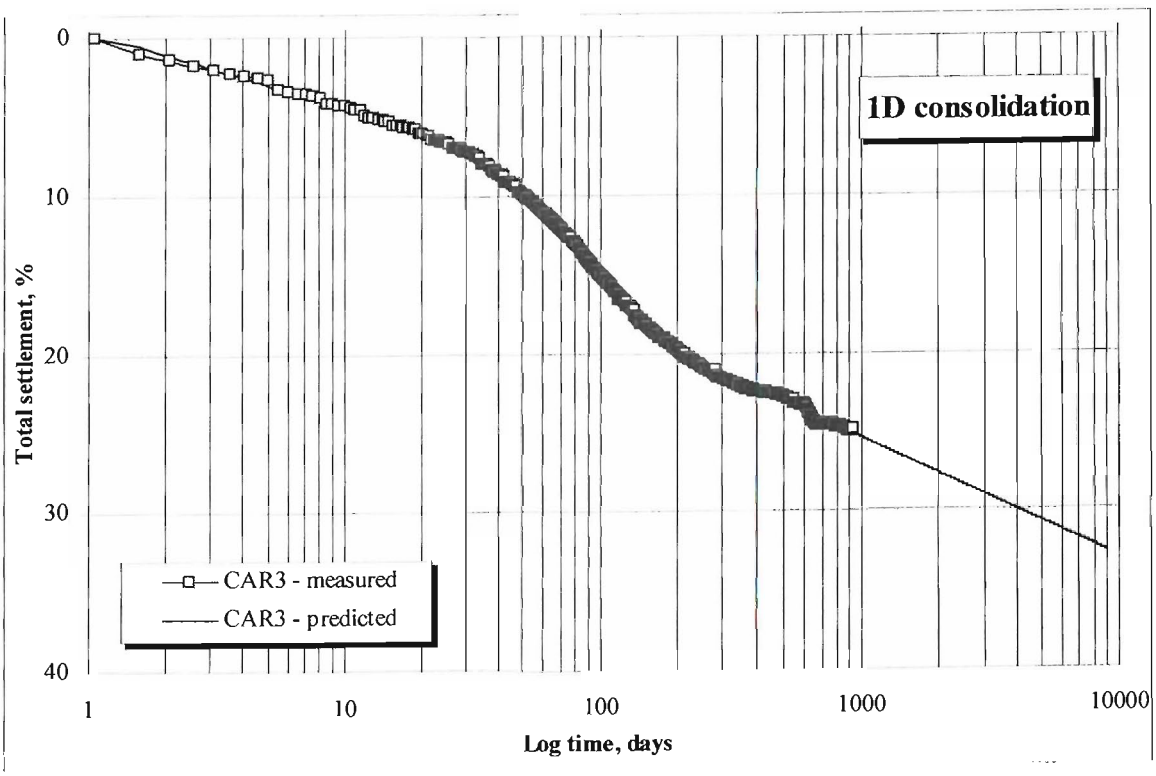

Figure 8.4. Estimated settlement by Sowers model (1973) for CAR3 - 50kPa (FR waste sample).

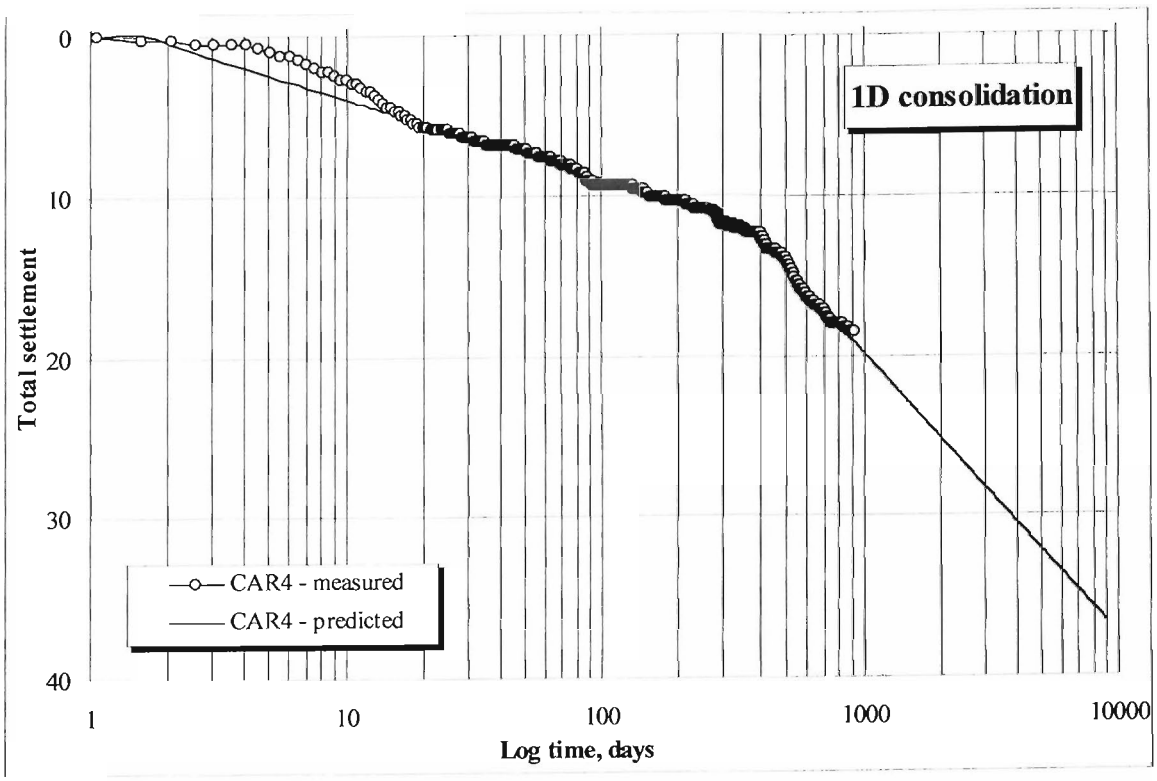

Figure 8.5. Estimated settlement by Sowers model (1973) for CAR4 - 50kPa (FR waste sample - control).

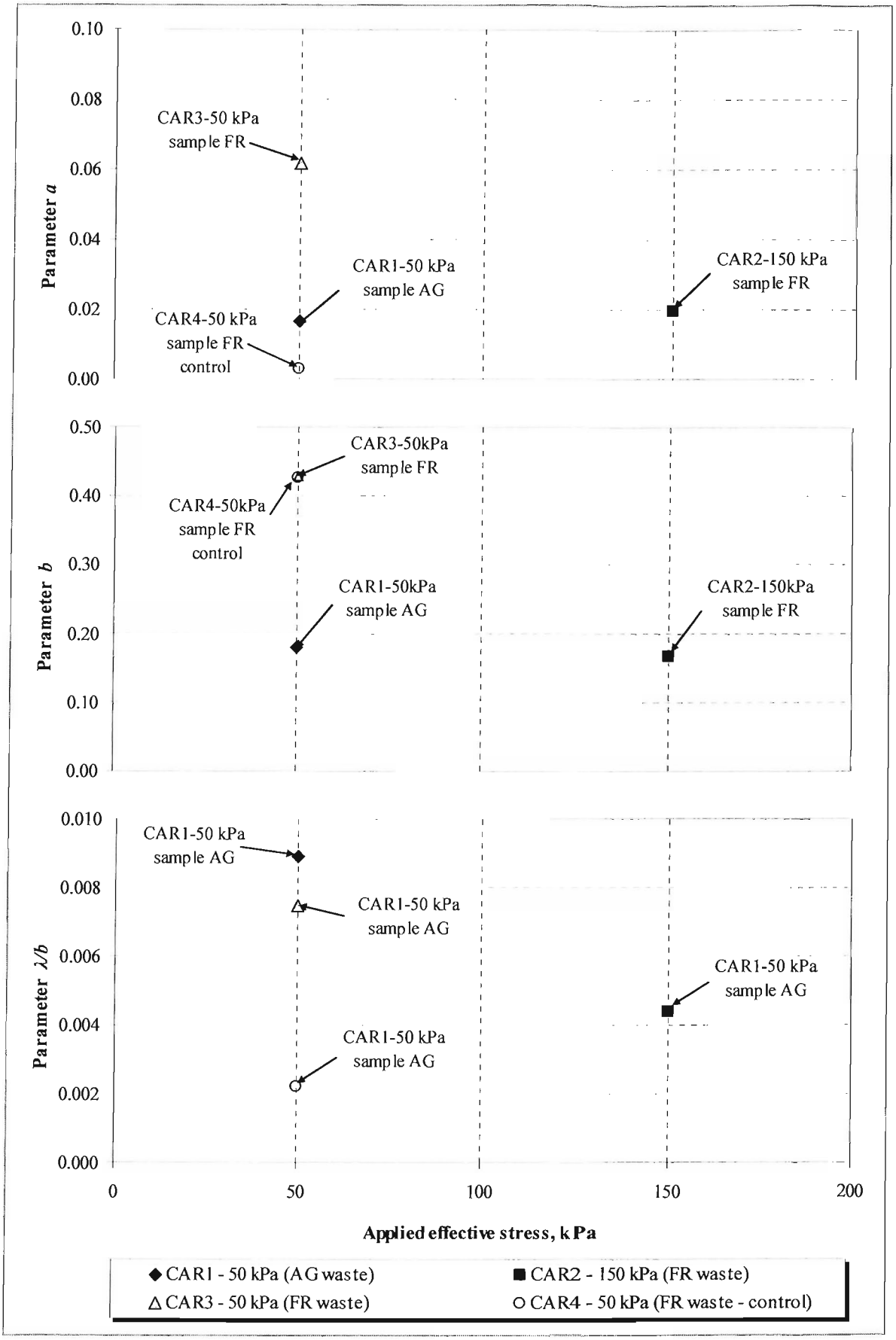

Figure 8.6. Relationship between applied stress and Gibson and Lo model (1961) parameters.

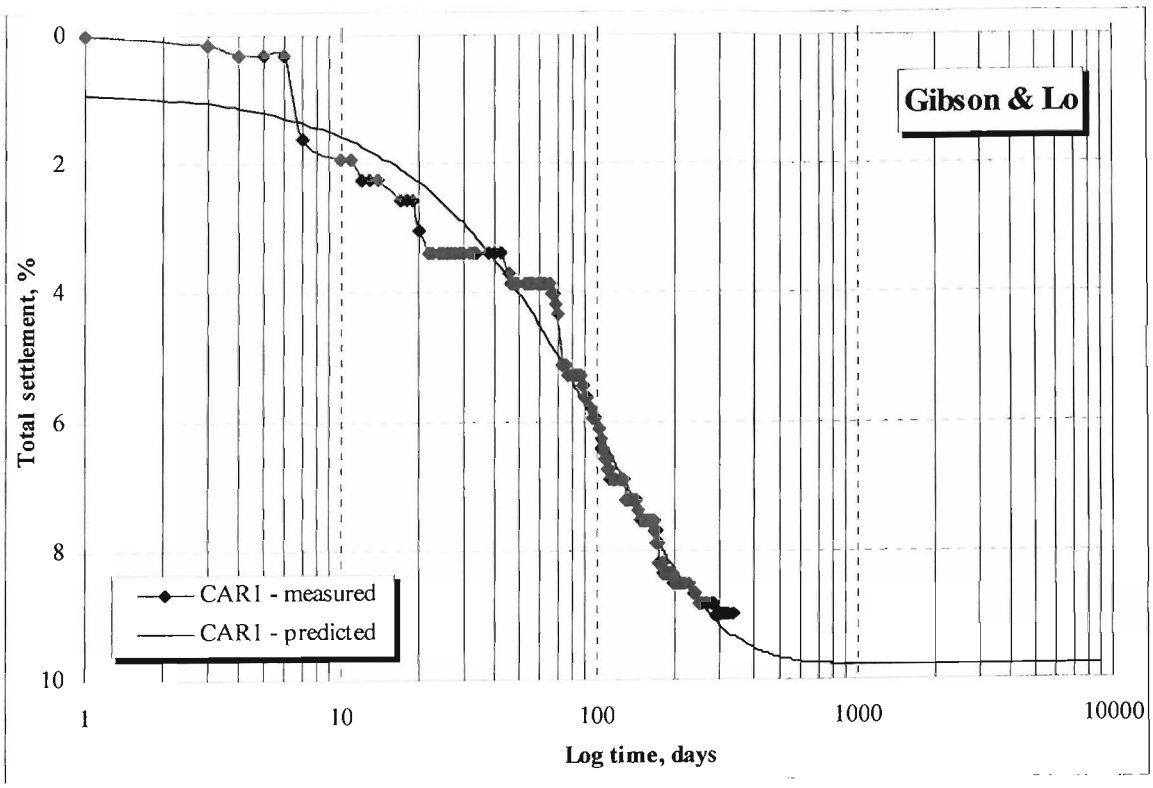

Figure 8.7. Estimated settlement by Gibson & Lo model (1961) for CAR1 - 50kPa (AG waste sample).

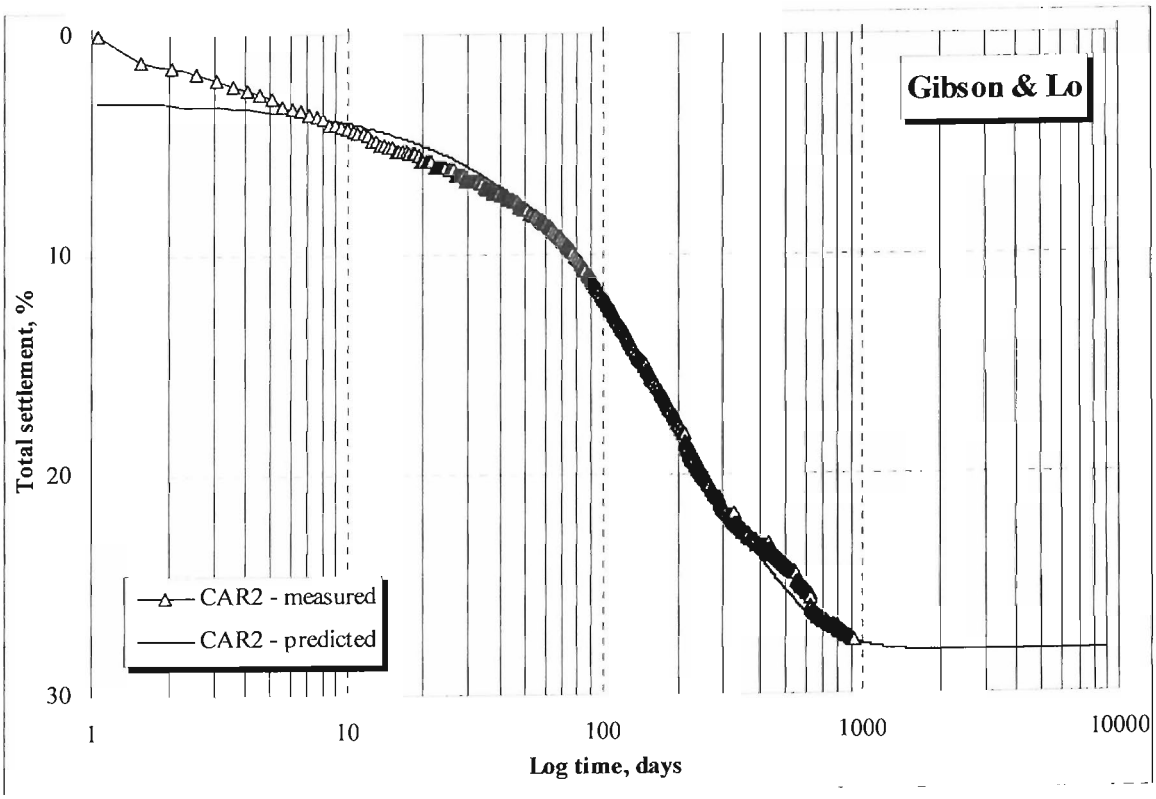

Figure 8.8. Estimated settlement by Gibson & Lo model (1961) for CAR2 - 150kPa (FR waste sample).

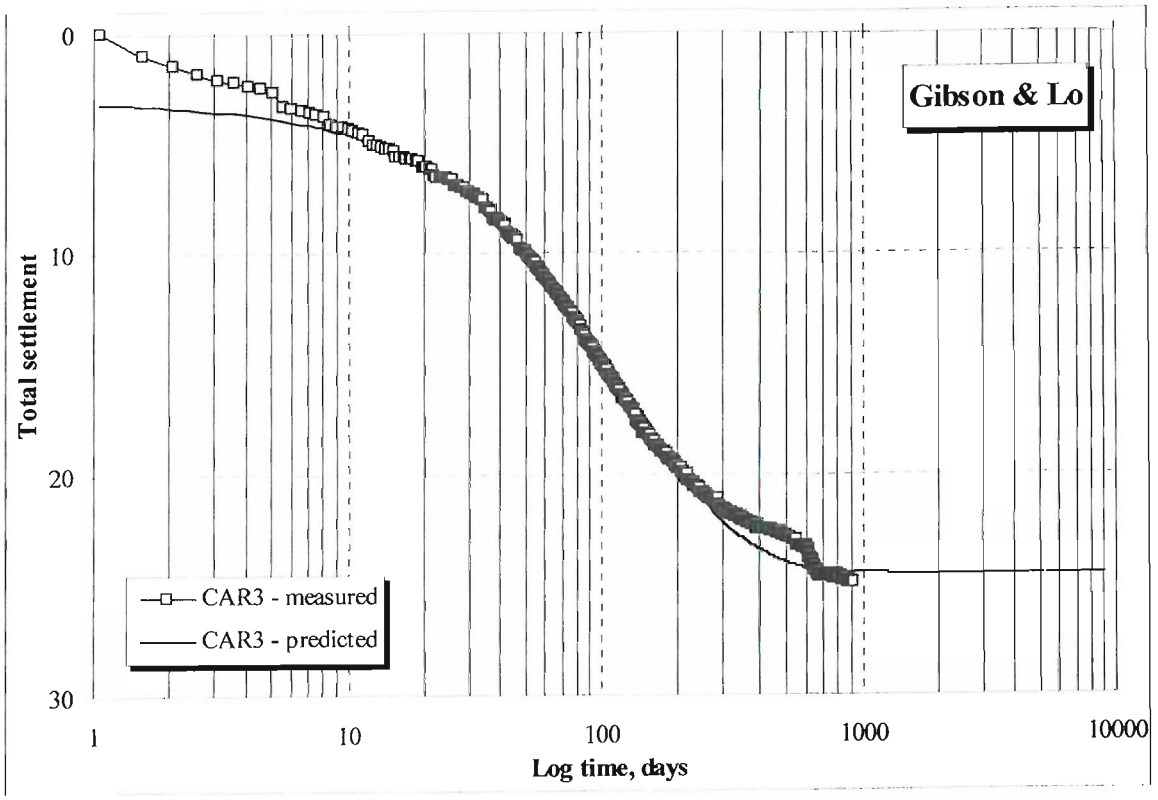

Figure 8.9. Estimated settlement by Gibson & Lo model (1961) for CAR3 - 50kPa (FR waste sample).

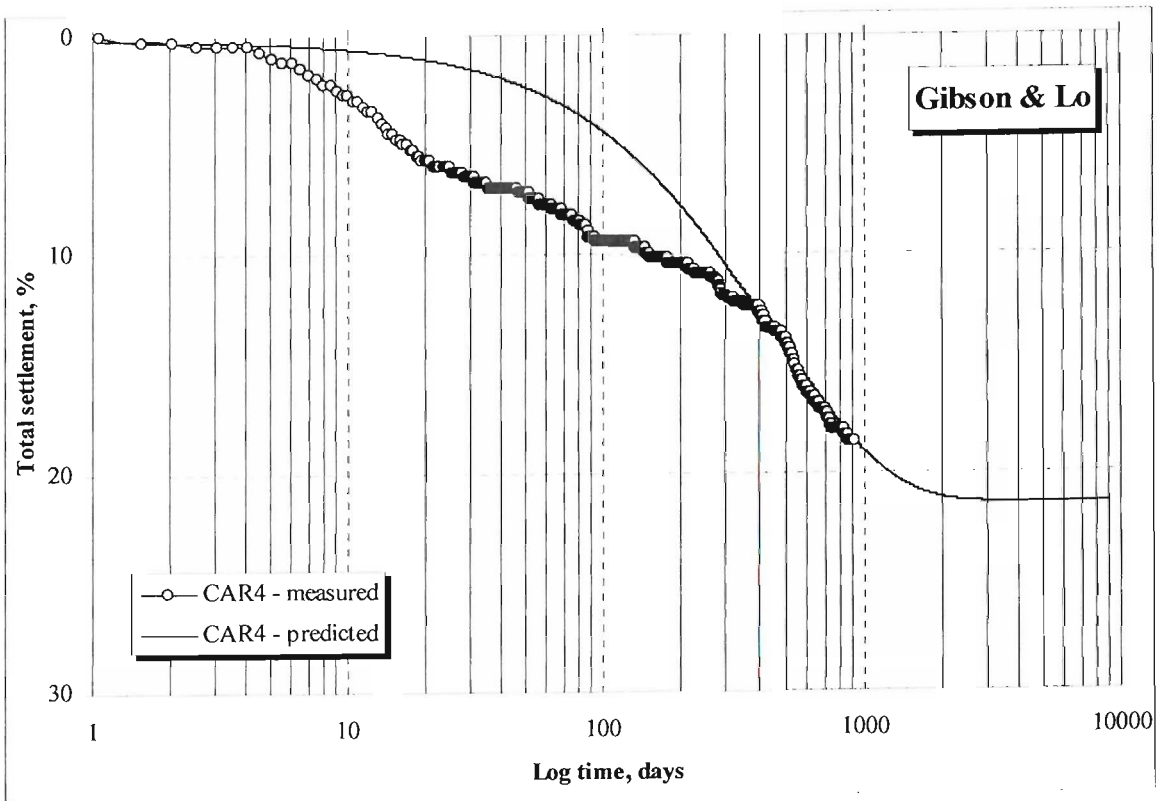

Figure 8.10. Estimated settlement by Gibson & Lo model (1961) for CAR4 - 50kPa (FR waste sample - control).

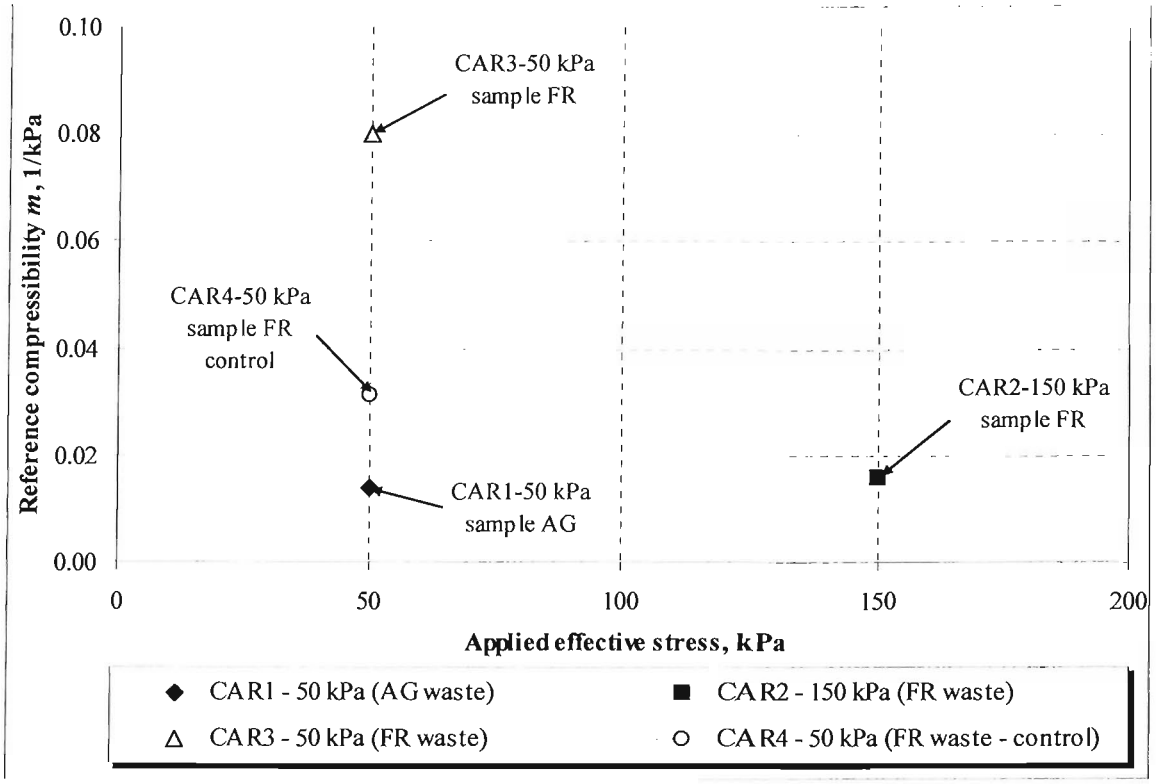

Figure 8.11. Relationship between applied stress and reference compressibility *m*.

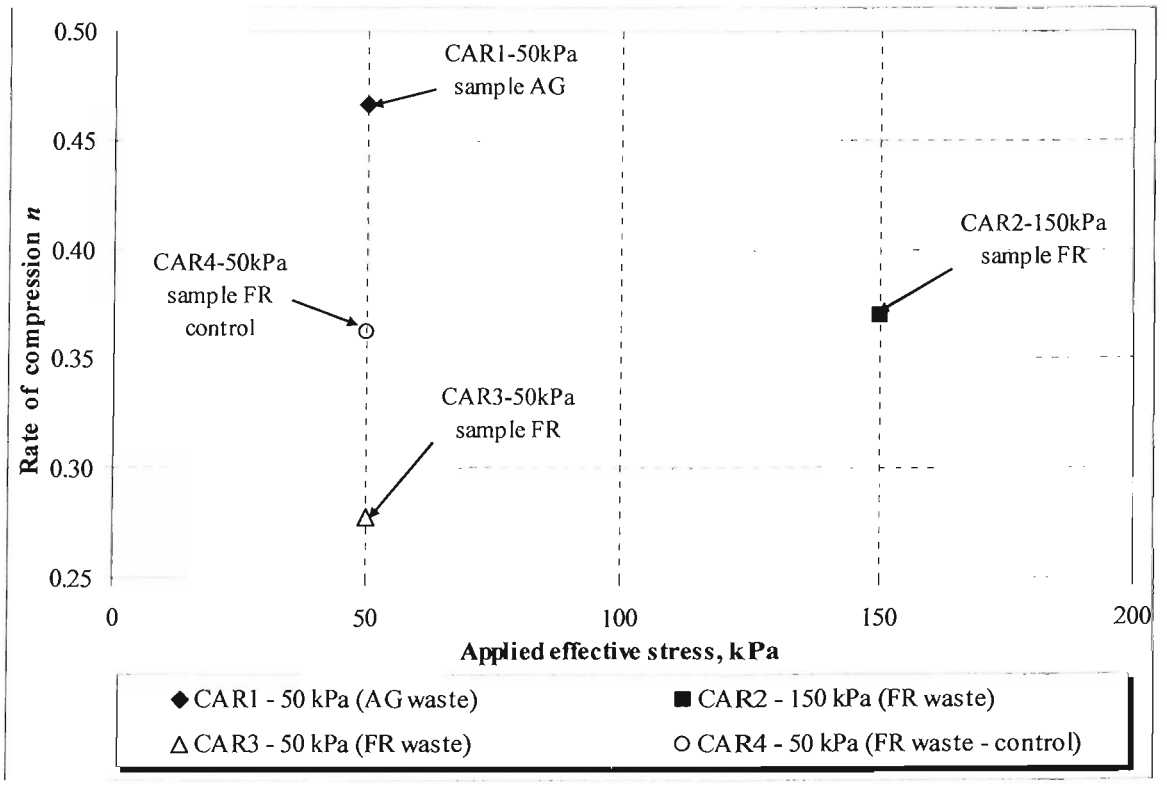

Figure 8.12. Relationship between applied stress and rate of compression *n*.

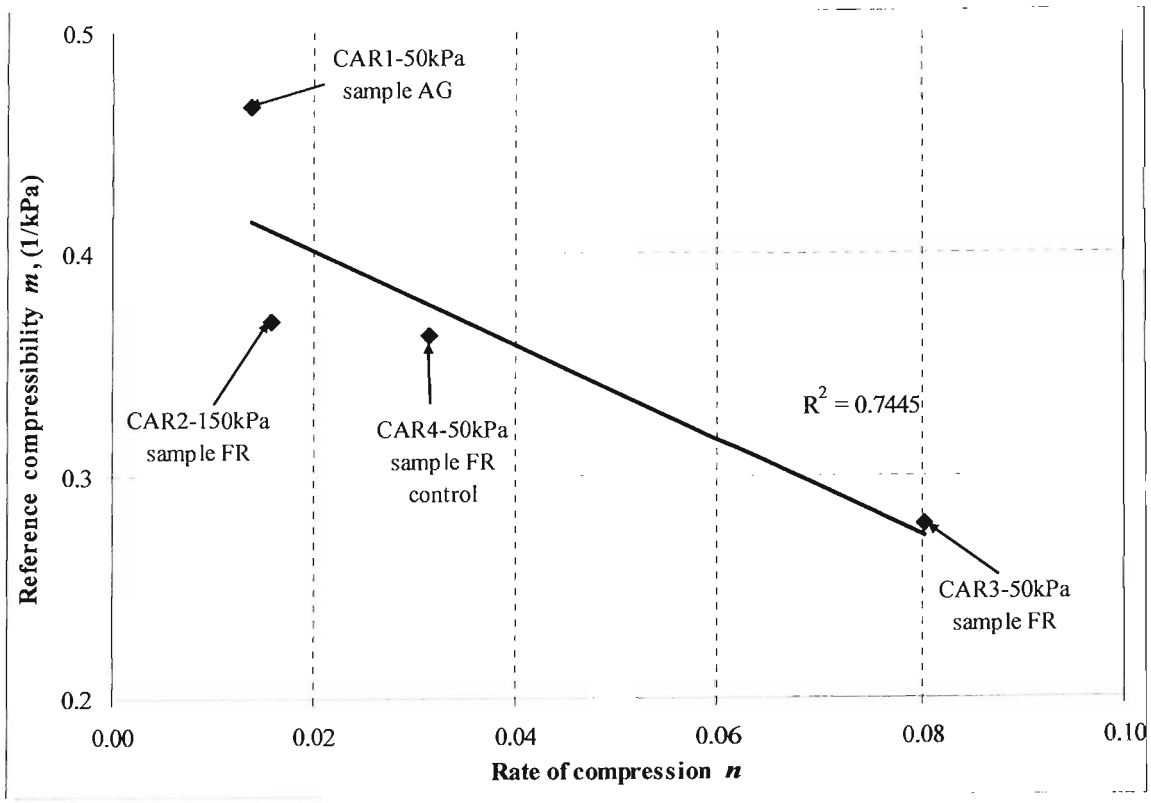

Figure 8.13. Correlation between reference compressibility *m* and rate of compression *n*.

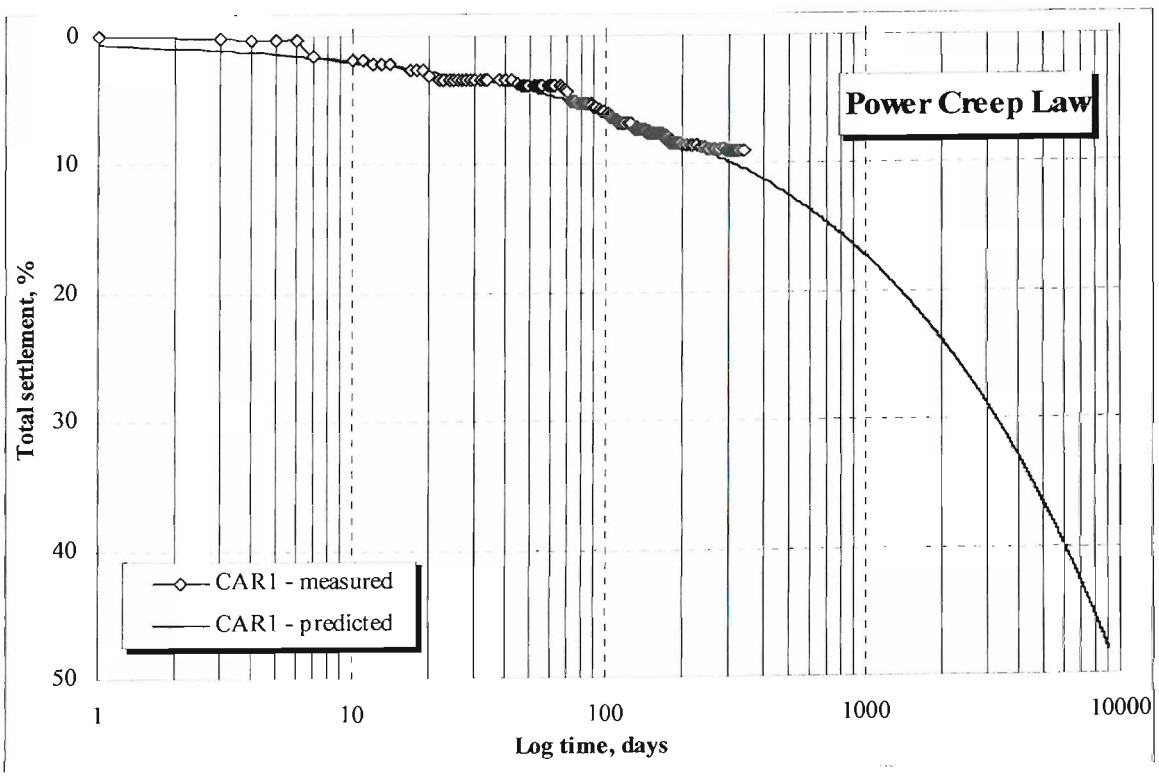

Figure 8.14. Estimated settlement by Power Creep Law (Edil *et al.*, 1990) for CAR1 - 50kPa (AG waste sample).

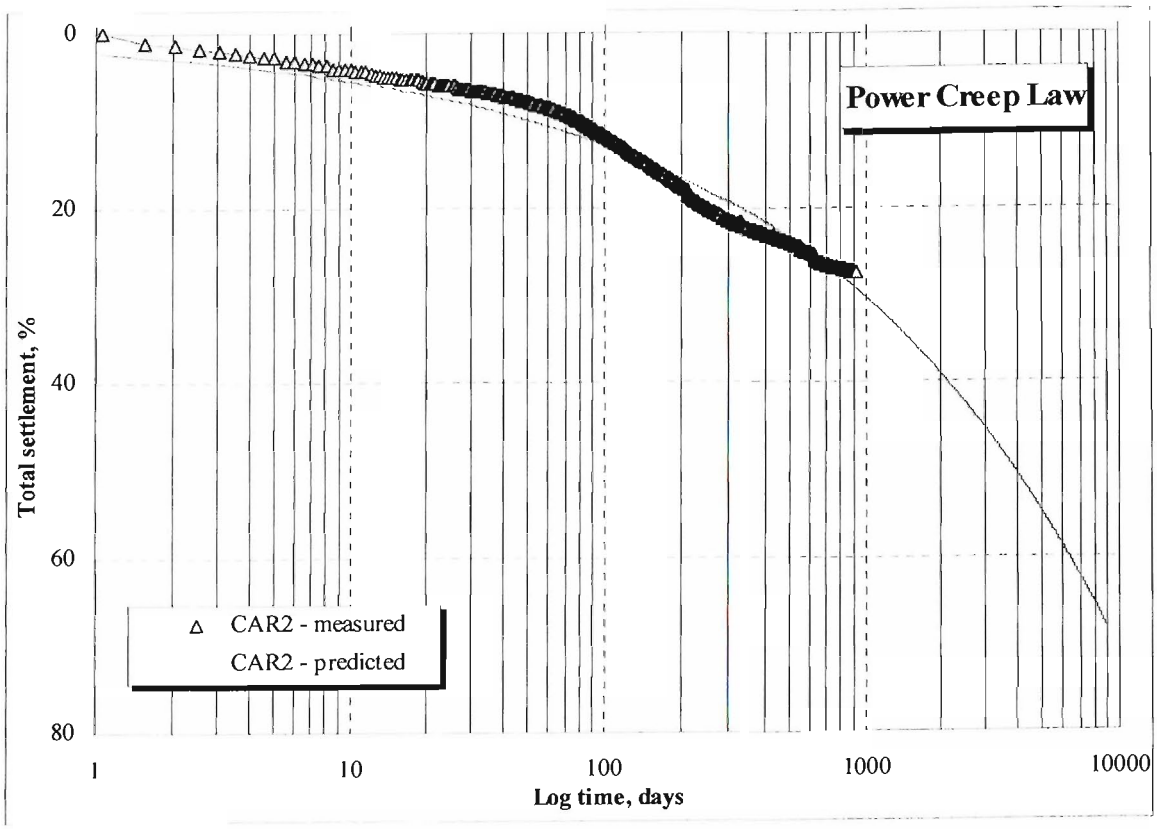

Figure 8.15. Estimated settlement by Power Creep Law (Edil *et al.*, 1990) for CAR2 - 150kPa (FR waste sample).

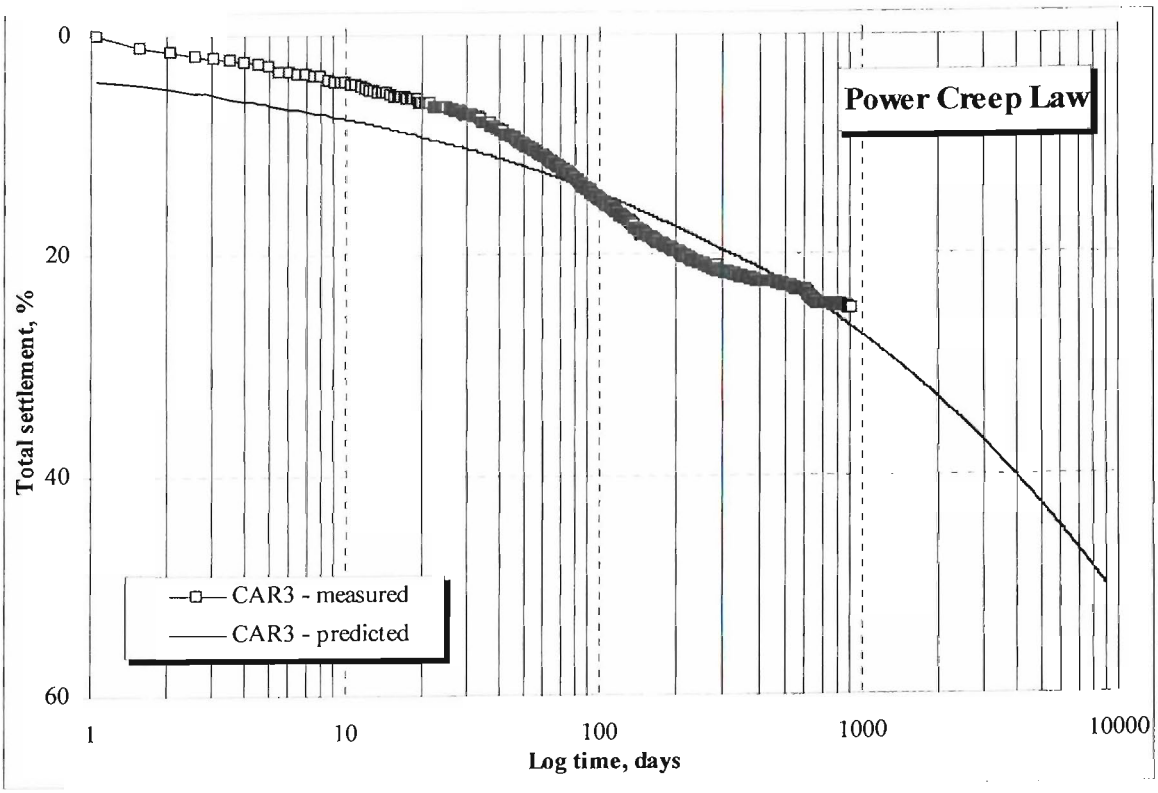

Figure 8.16. Estimated settlement by Power Creep Law (Edil *et al.*, 1990) for CAR3 - 50kPa (FR waste sample).

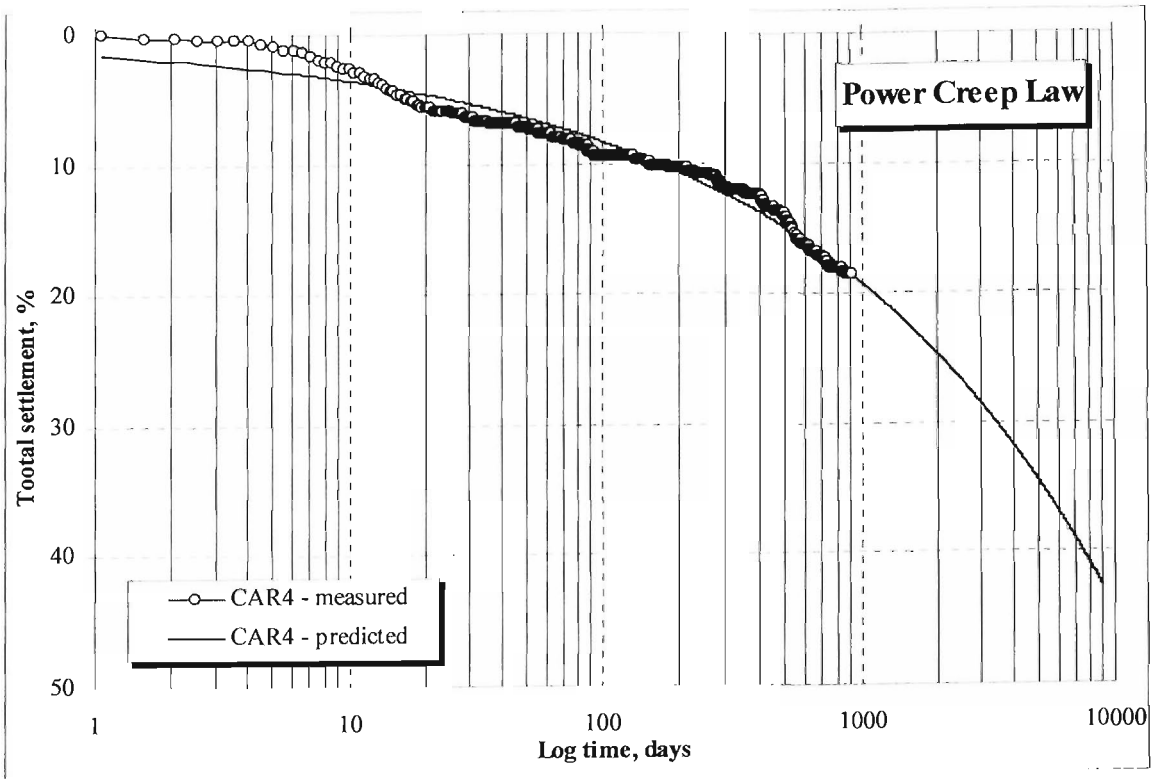

Figure 8.17. Estimated settlement by Power Creep Law (Edil *et al.*, 1990) for CAR4 - 50kPa (FR waste sample - control).

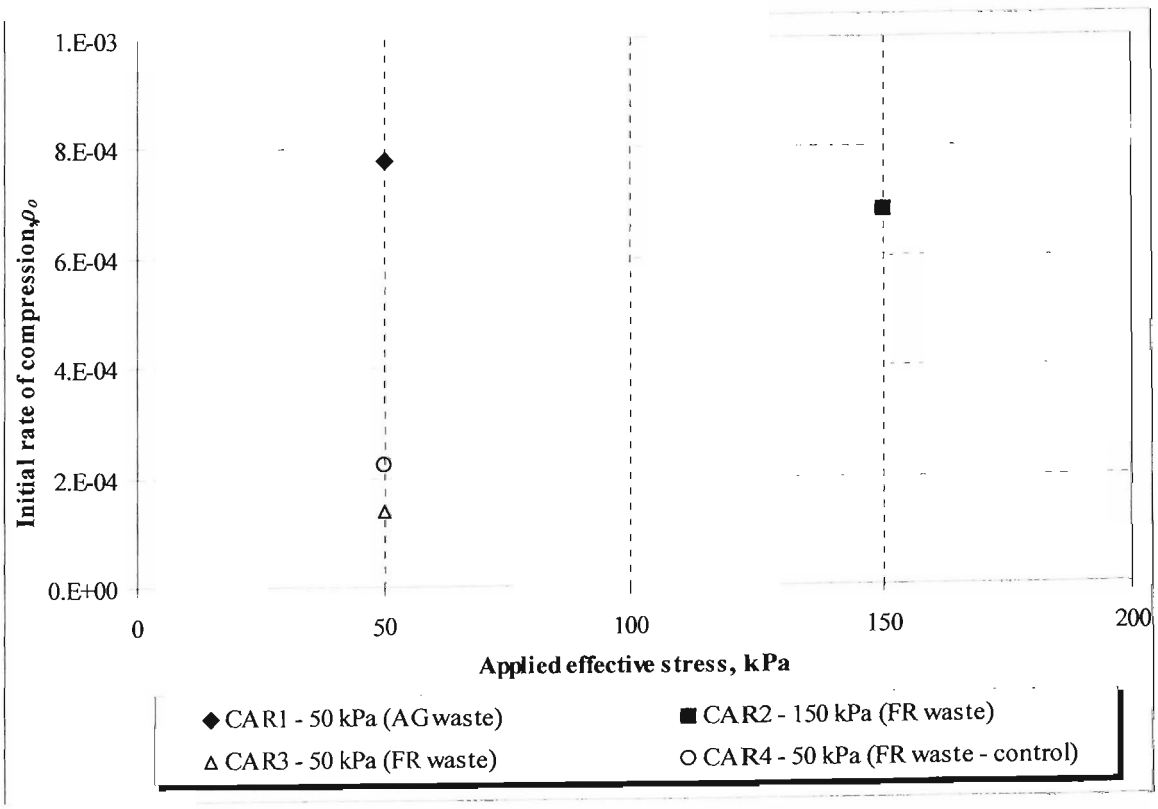

Figure 8.18. Relationship between applied stress and initial rate of compression ρ_o.

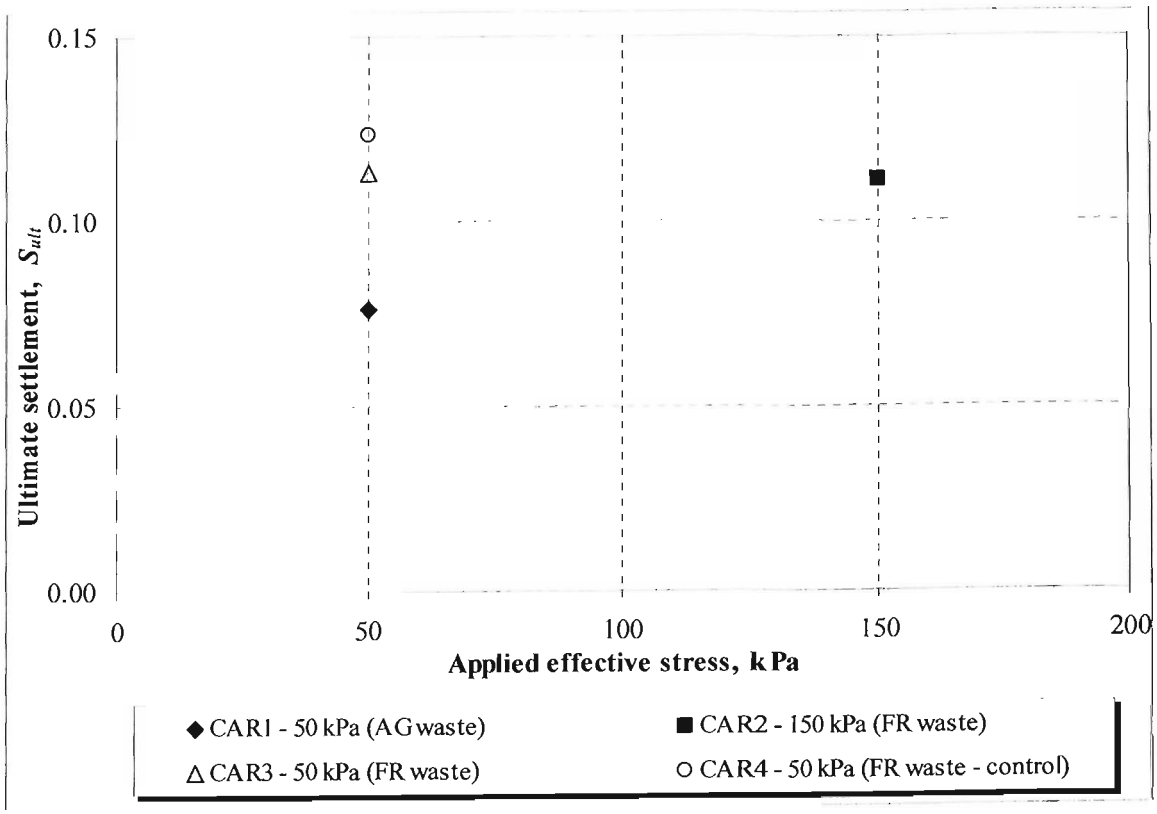

Figure 8.19. Relationship between applied stress and ultimate settlement S_{ult}.

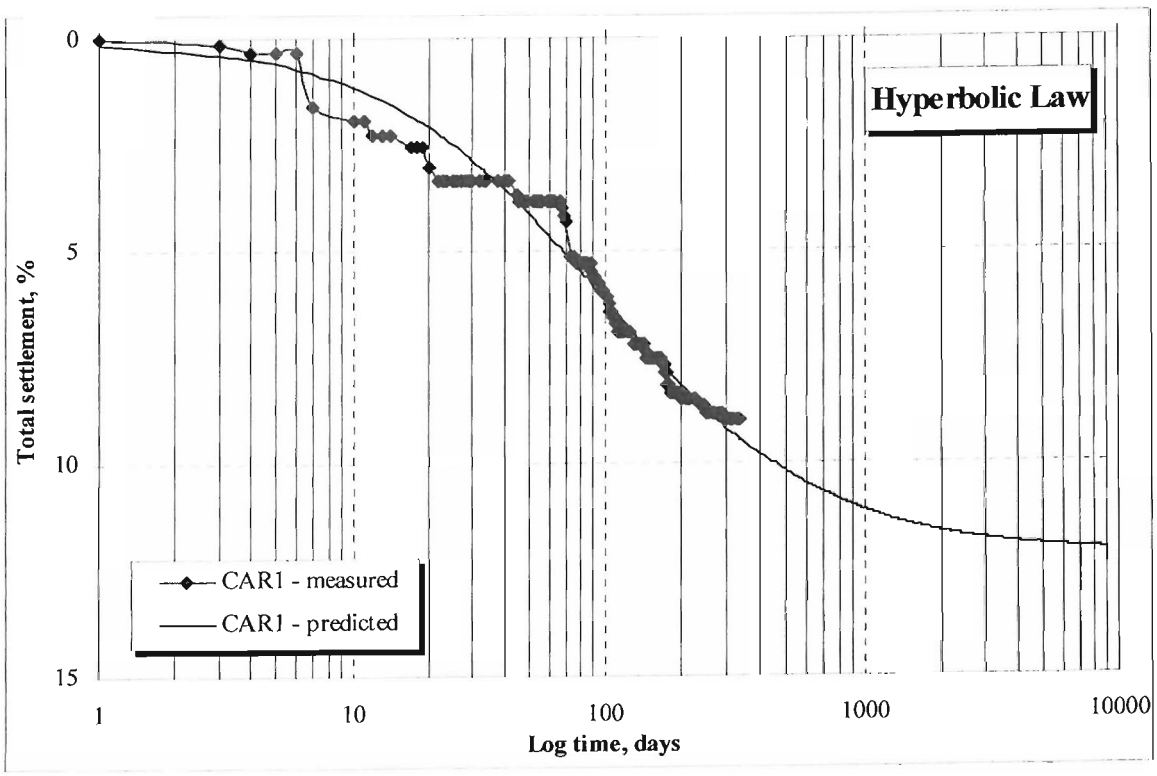

Figure 8.20. Estimated settlement by Hyperbolic Law (Ling *et al.*, 1998) for CAR1 - 50kPa (AG waste sample).

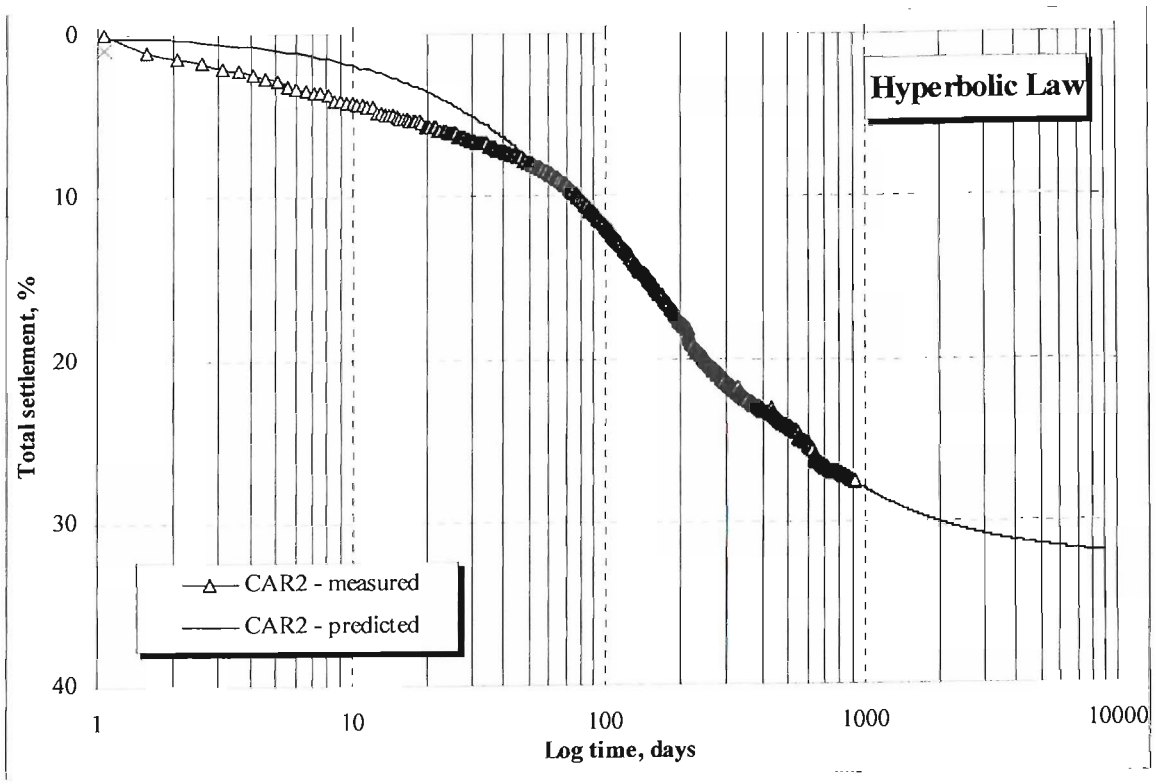

Figure 8.21. Estimated settlement by Hyperbolic Law (Ling *et al.*, 1998) for CAR2 - 150kPa (FR waste sample).

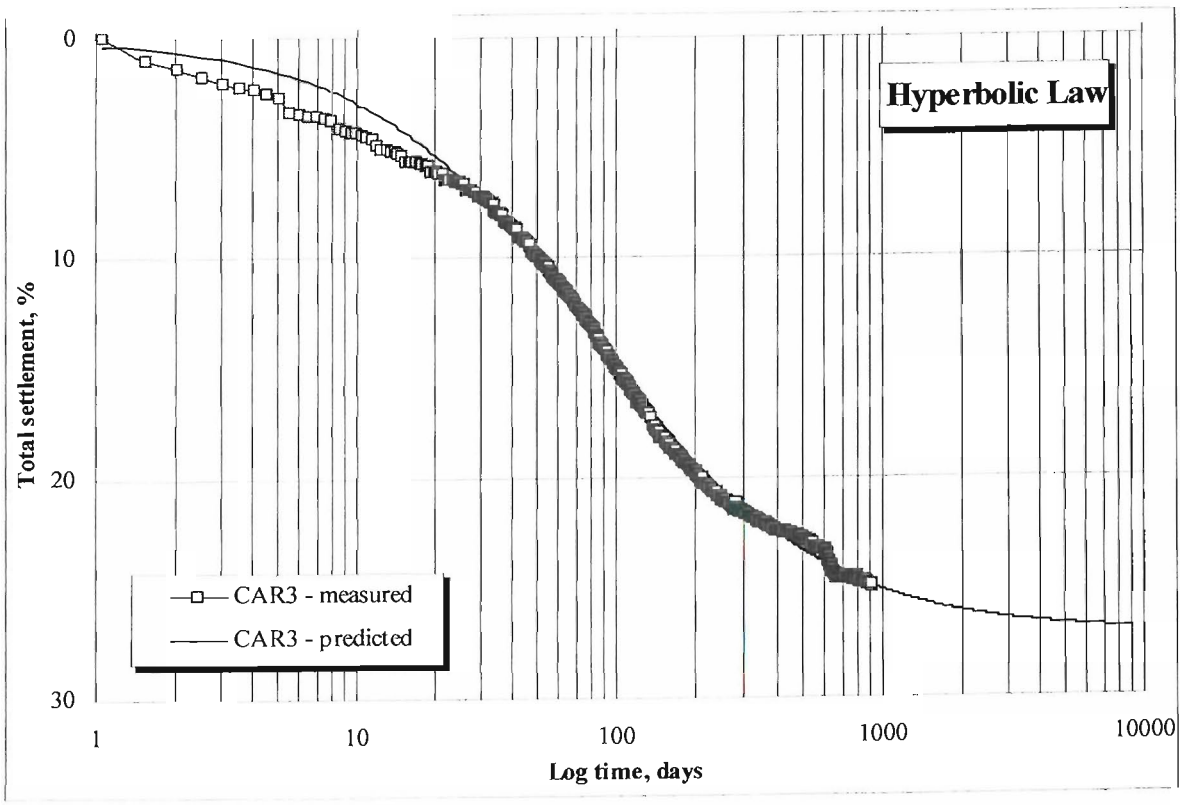

Figure 8.22. Estimated settlement by Hyperbolic Law (Ling *et al.*, 1998) for CAR3 - 50kPa (FR waste sample).

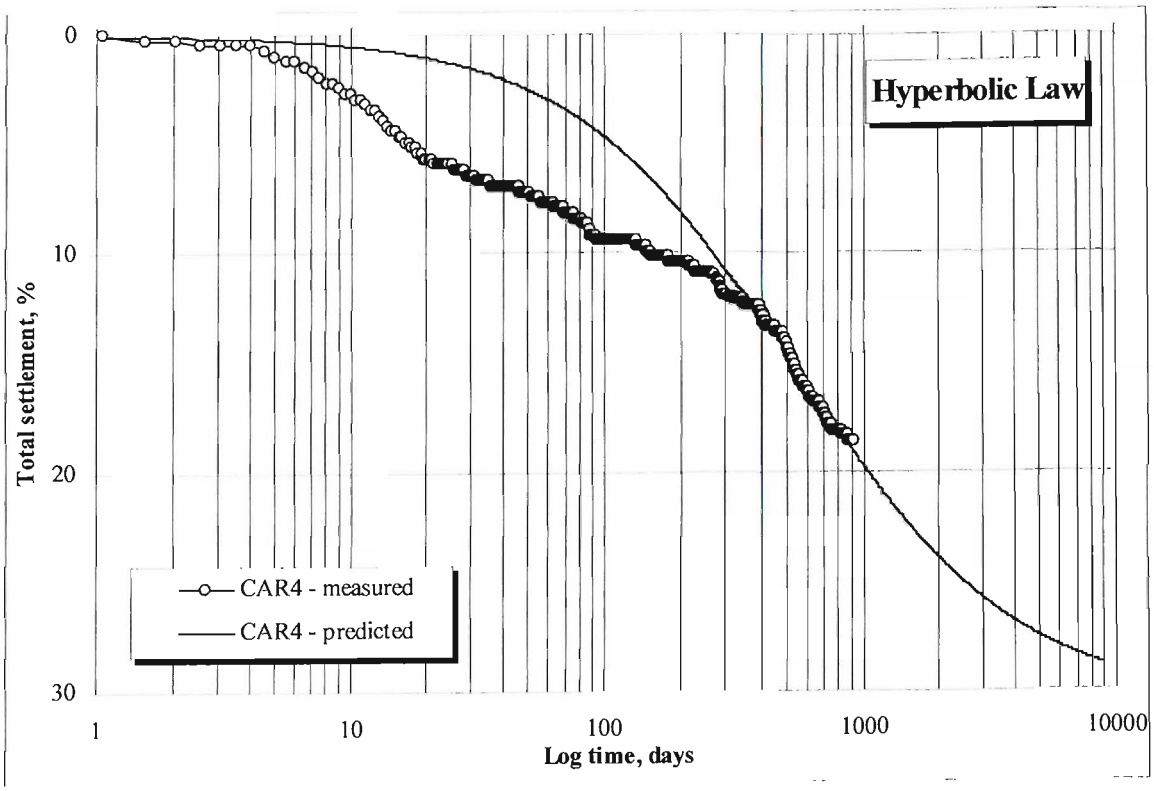

Figure 8.23. Estimated settlement by Hyperbolic Law (Ling *et al.*, 1998) for CAR4 - 50kPa (FR waste sample - control).

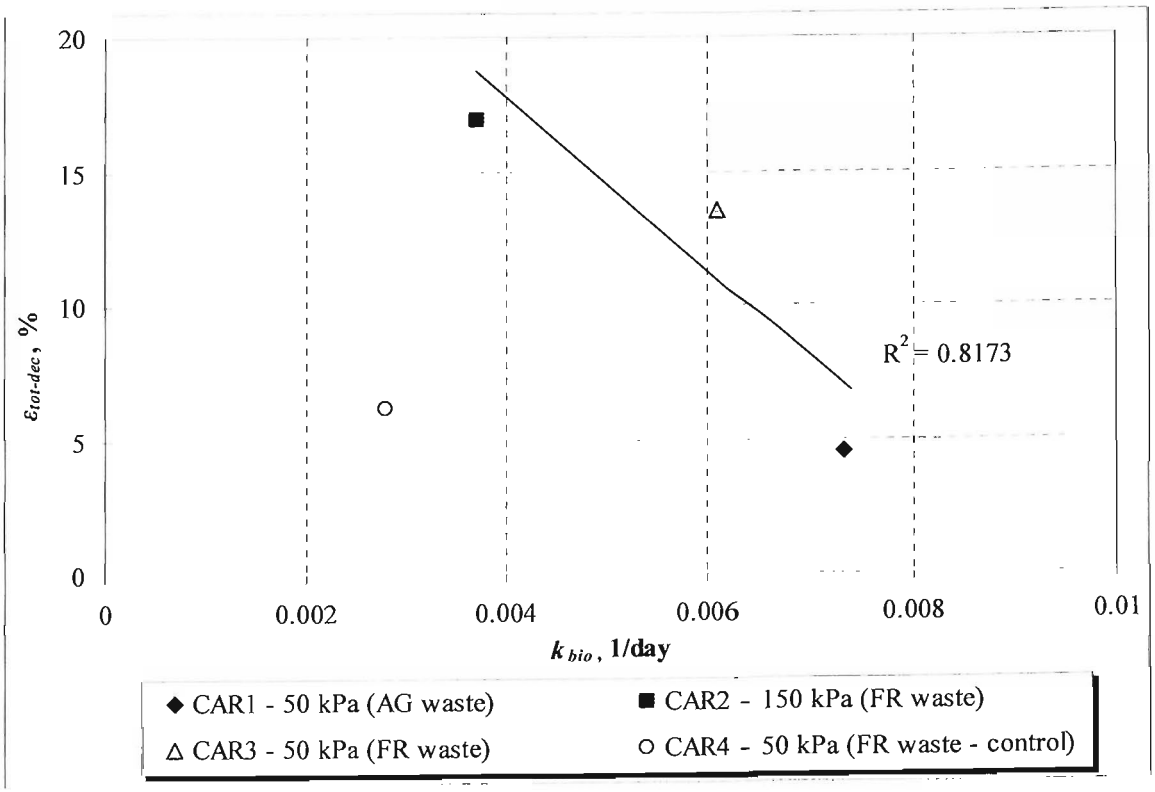

Figure 8.24. Relationship between Park & Lee (1997 & 2002[a]) model parameters.

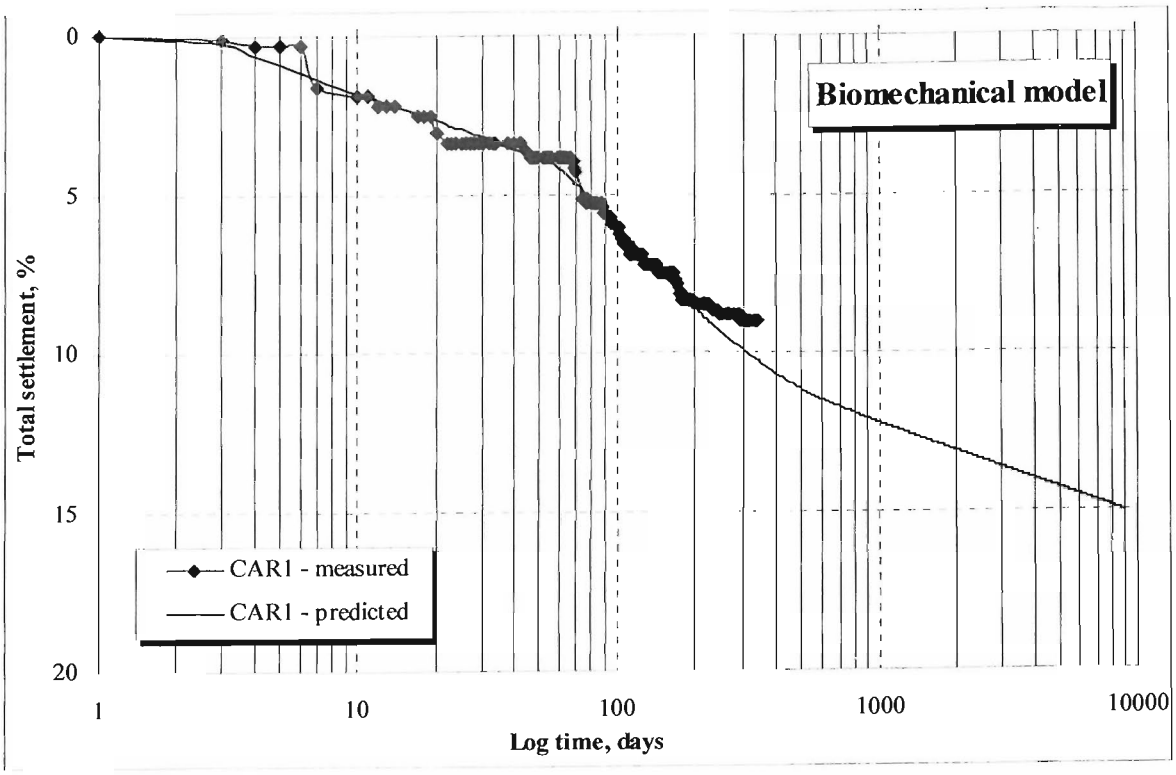

Figure 8.25. Estimated settlement by biomechanical model (Park & Lee, 1997, 2002) for CAR1 - 50kPa (AG waste sample).

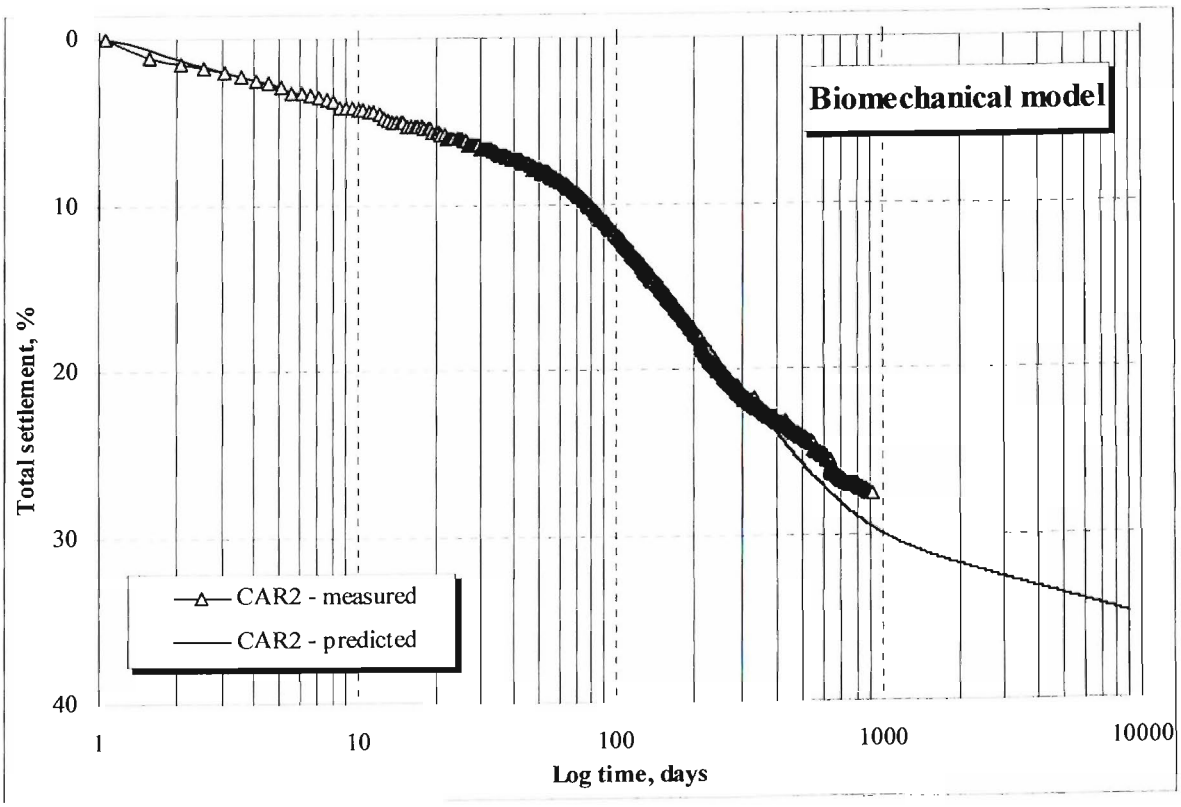

Figure 8.26. Estimated settlement by biomechanical model (Park & Lee, 1997, 2002) for CAR2 - 150kPa (FR waste sample).

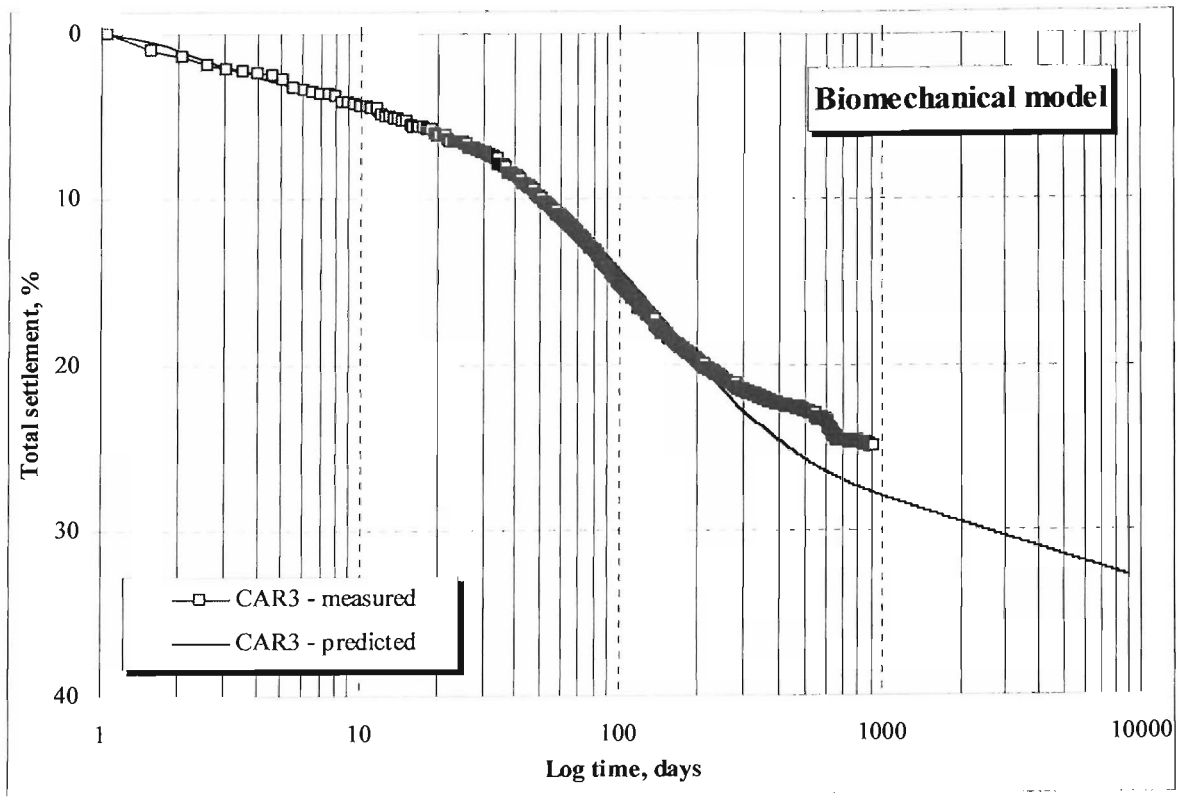

Figure 8.27. Estimated settlement by biomechanical model (Park & Lee, 1997, 2002) for CAR3 - 50kPa (FR waste sample).

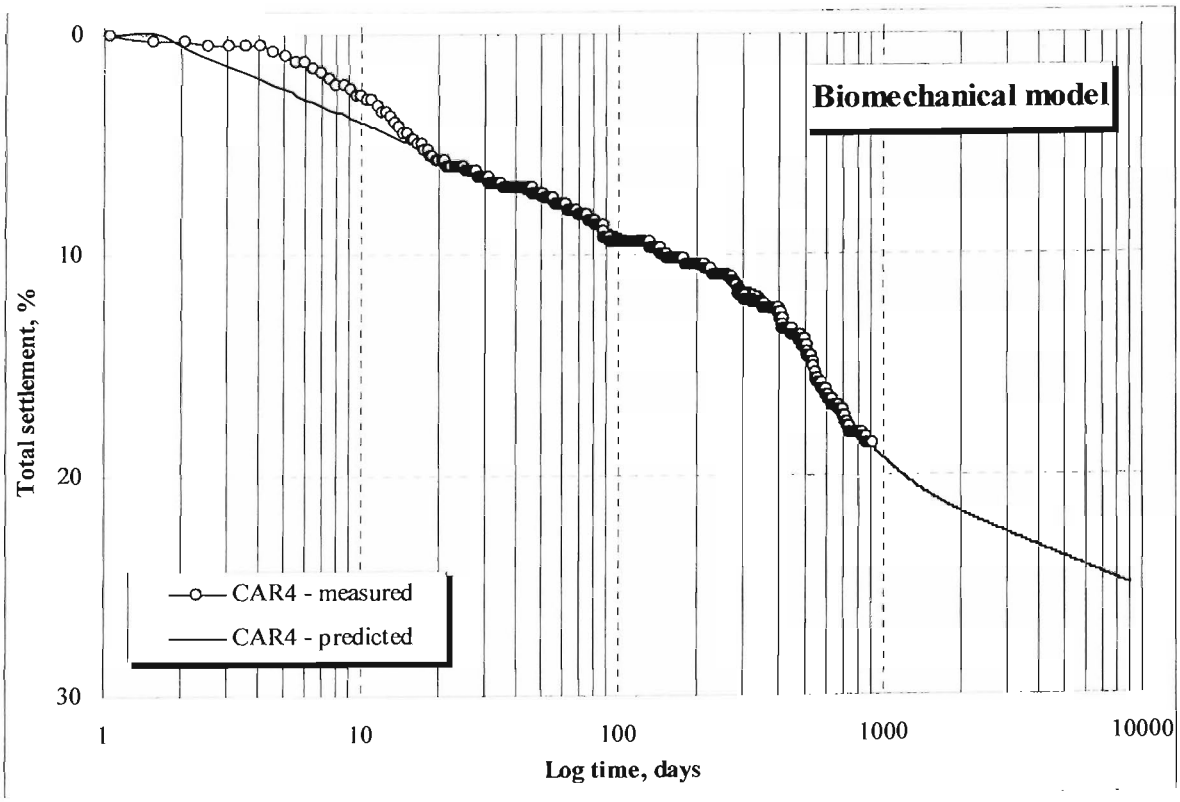

Figure 8.28. Estimated settlement by biomechanical model (Park & Lee, 1997, 2002) for CAR4 - 50kPa (FR waste sample - control).

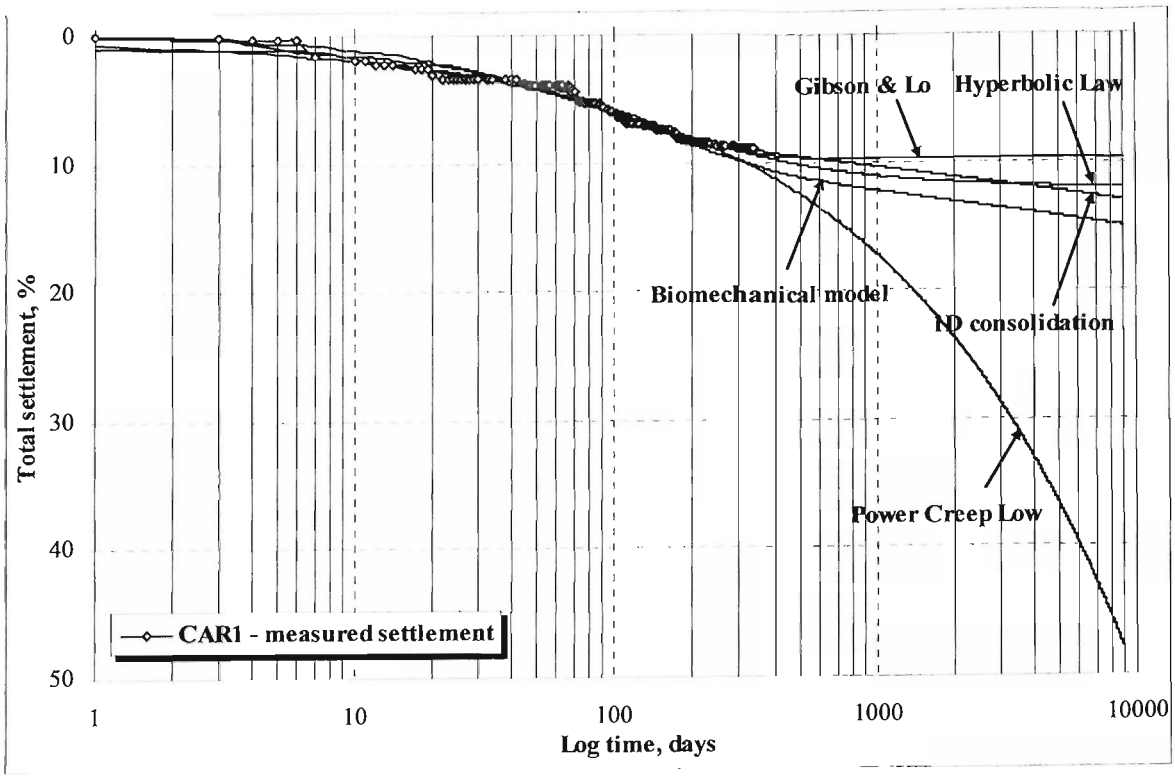

Figure 8.29. Settlement prediction curves for CAR1 - 50kPa (AG waste sample).

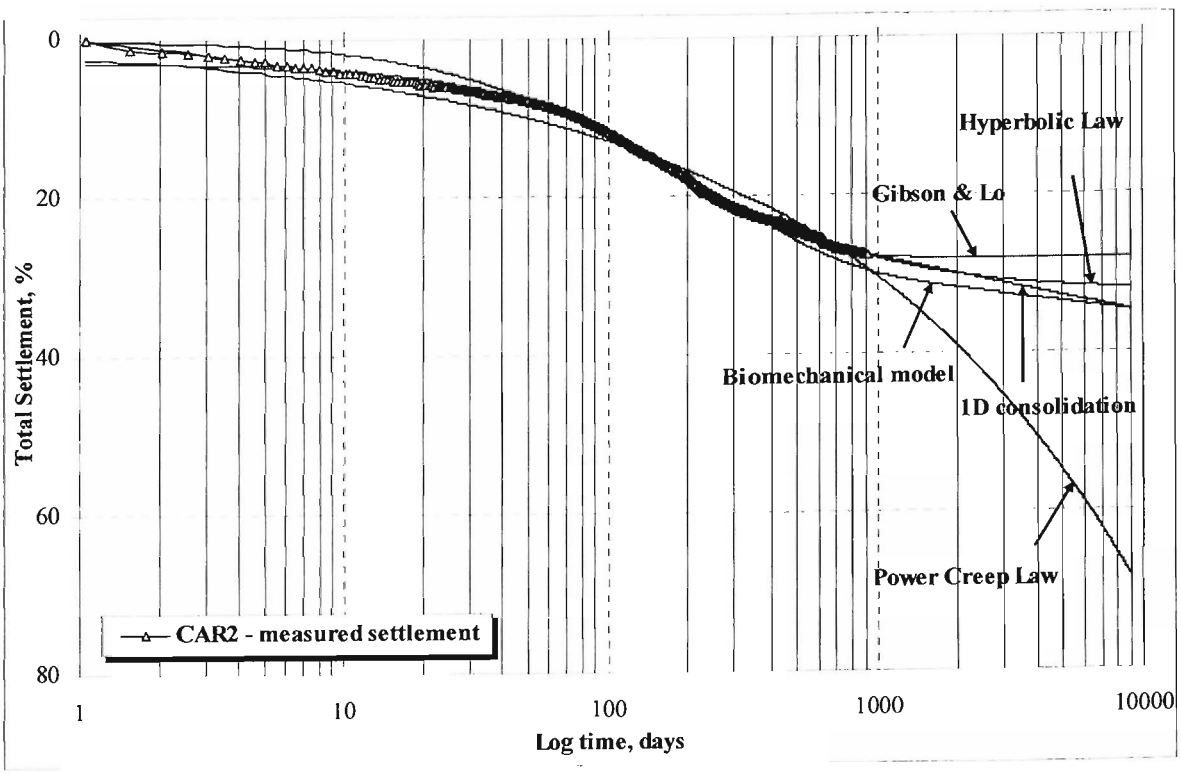

Figure 8.30. Settlement prediction curves for CAR2 - 150kPa (FR waste sample).

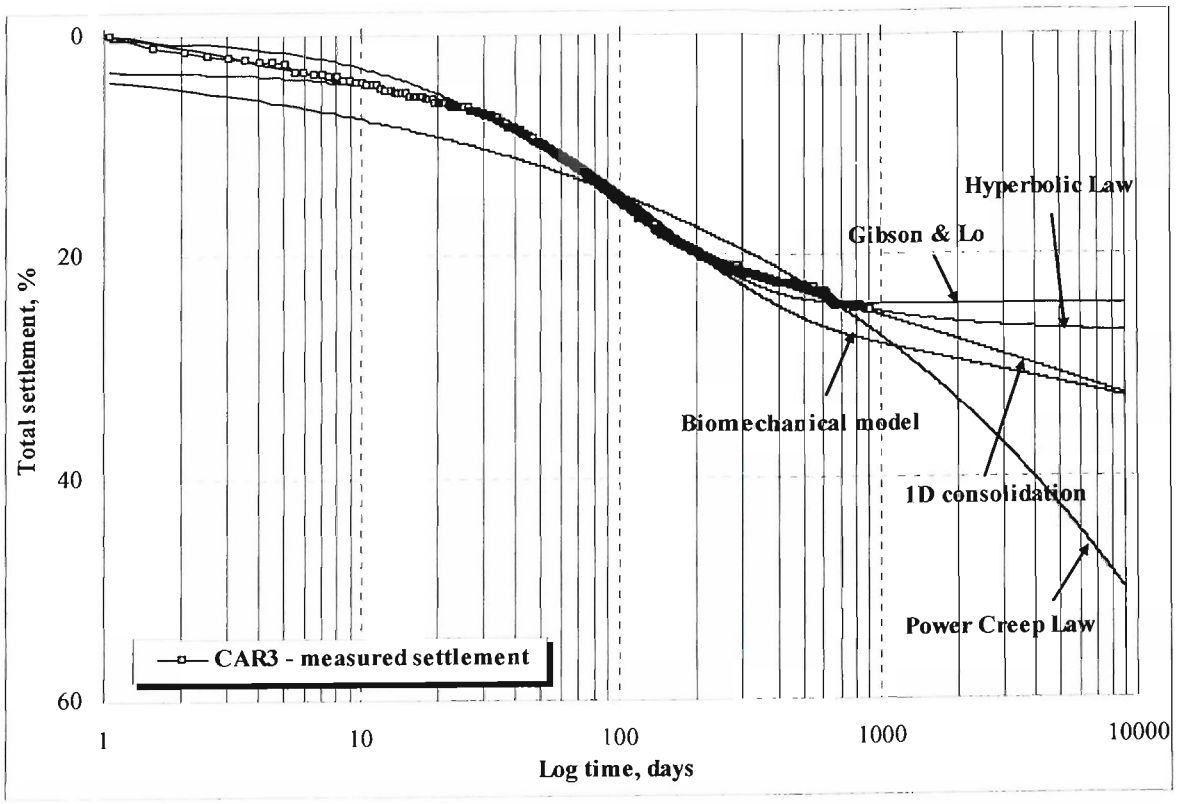

Figure 8.31. Settlement prediction curves for CAR3 - 50kPa (FR waste sample).

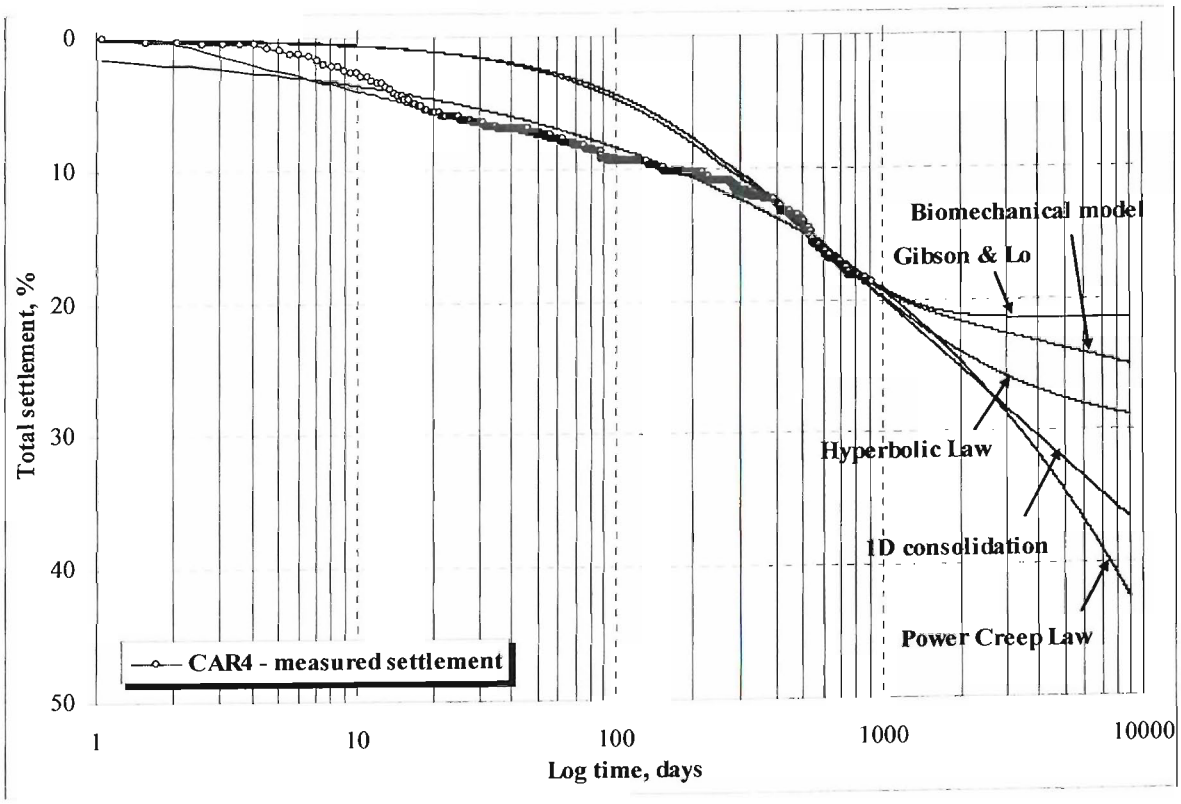

Figure 8.32. Settlement prediction curves for CAR4 - 50kPa (FR waste sample - control).

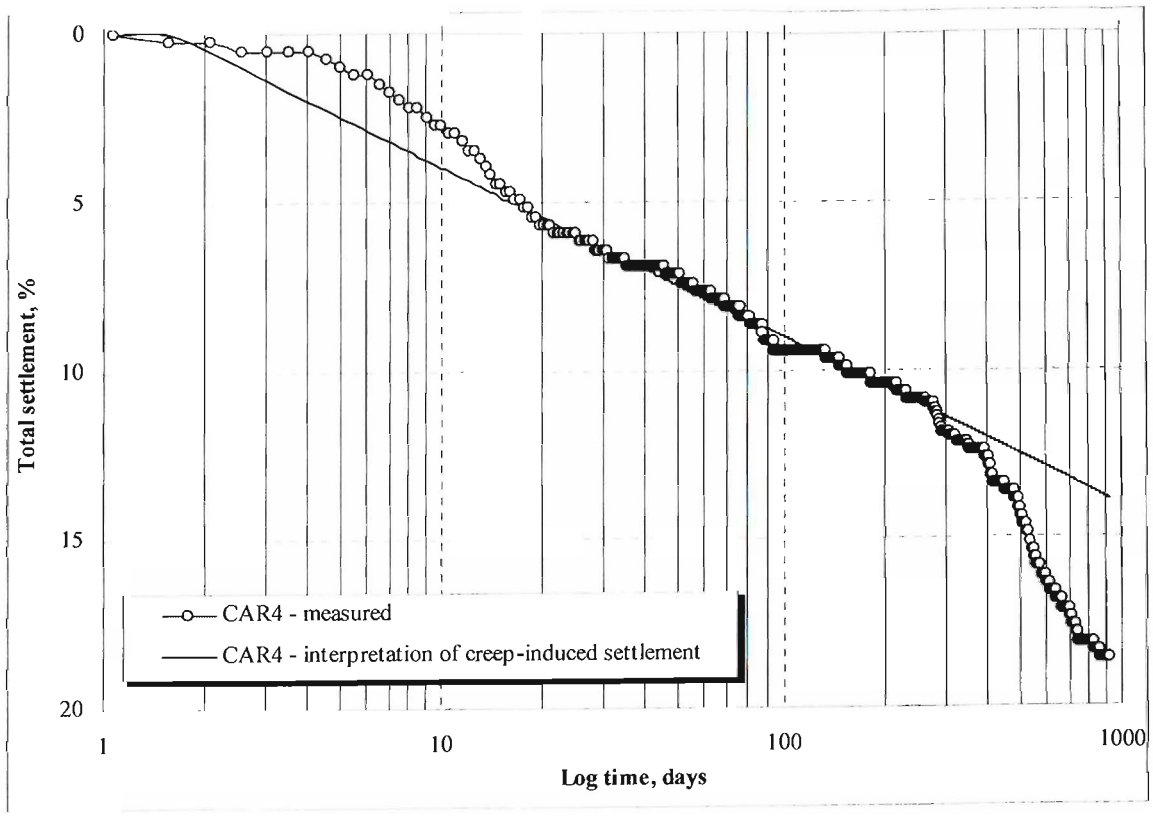

Figure 8.33. Interpretation of settlement data in CAR4 to establish values of creep-induced settlement.

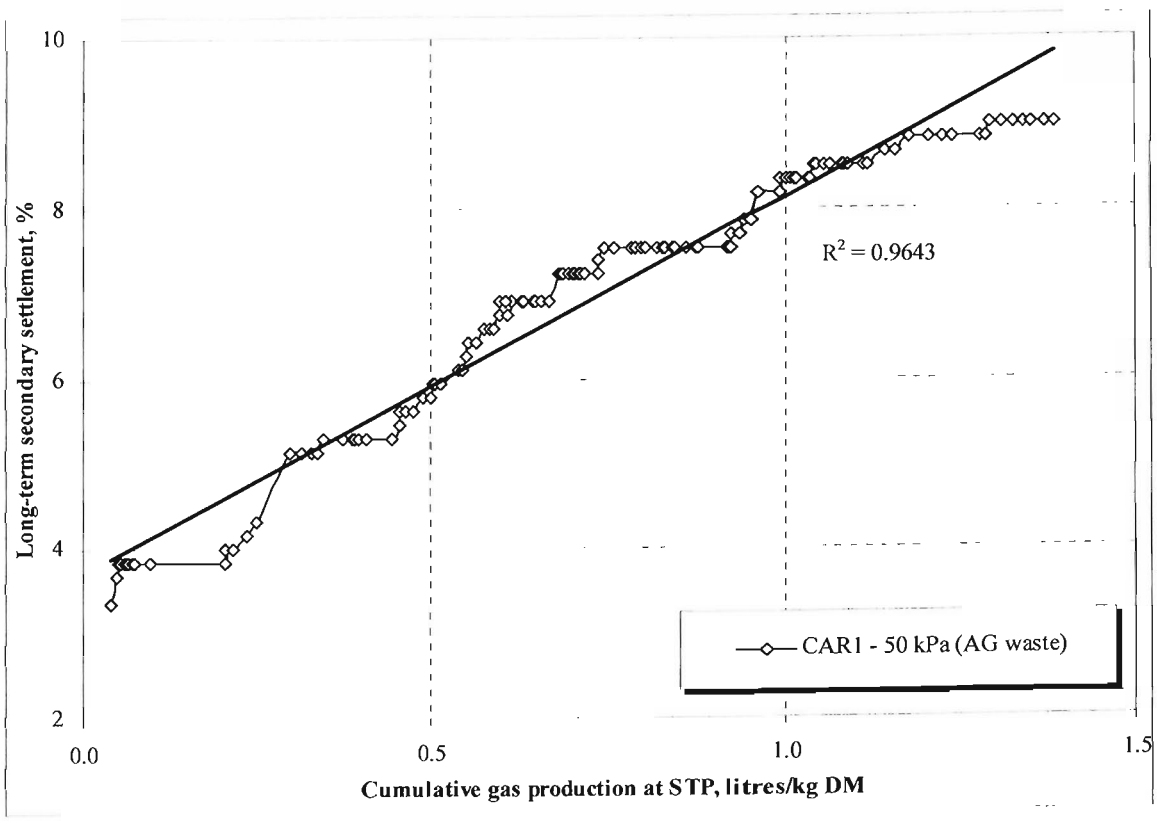

Figure 8.34. Correlation between gas production and long-term secondary settlement for CAR1 (AG waste).

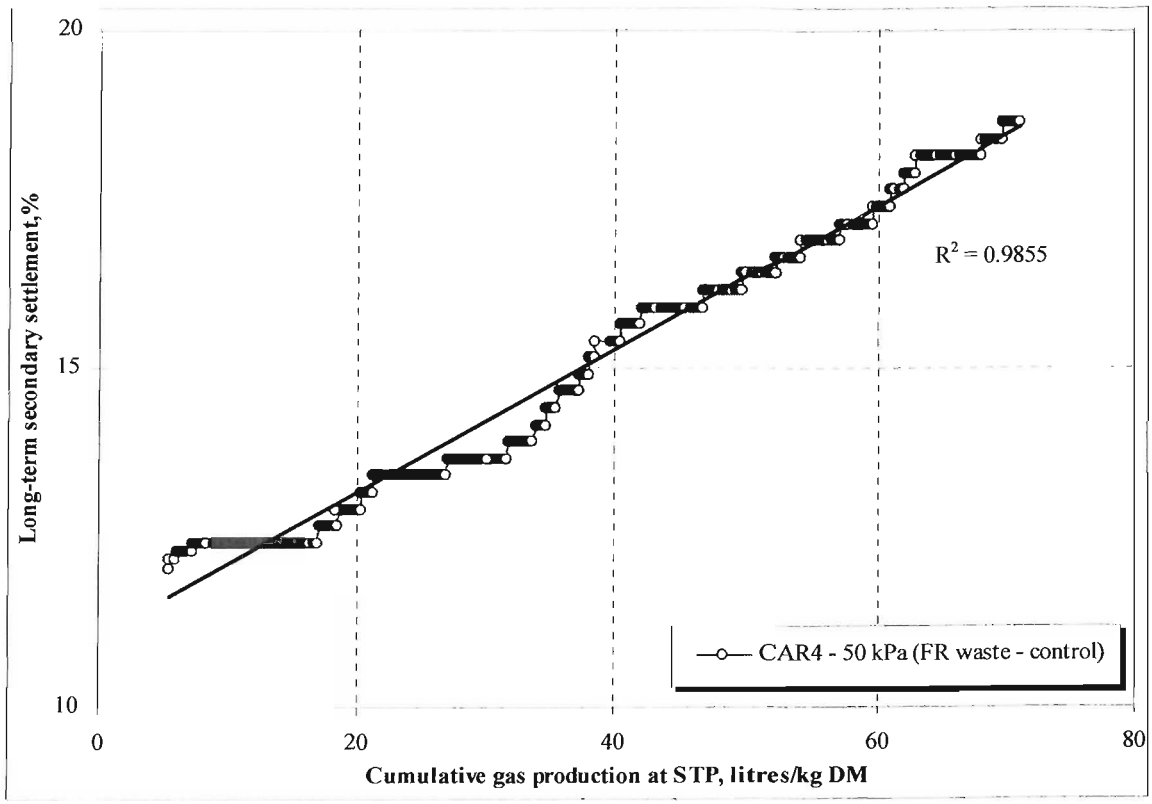

Figure 8.35. Correlation between gas production and long-term secondary settlement for CAR4 (FR waste - control).

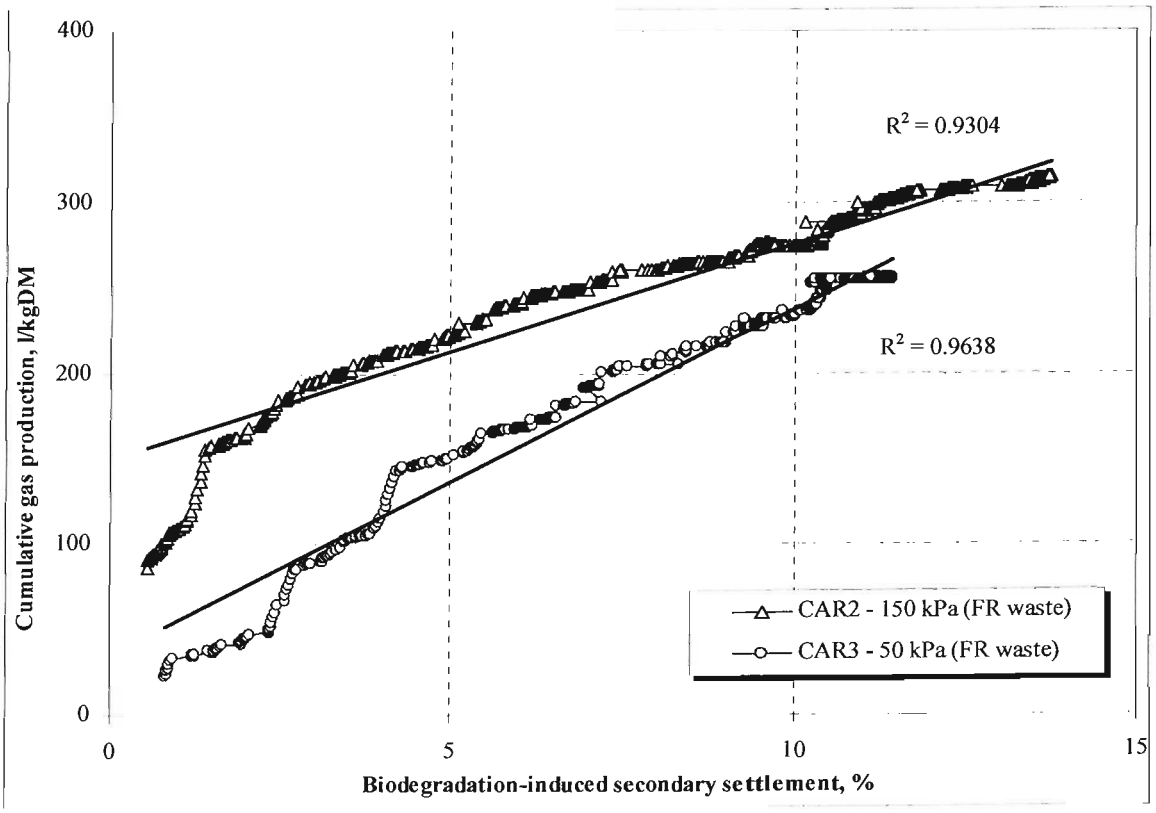

Figure 8.36. Correlation between gas production and settlement due to biodegradation for CARs 2 & 3 (FR waste).

Chapter 9

Conclusions and future work

9.1. Conclusions

The biodegradation of solid waste materials is major cause of secondary settlement in landfills and has a significant impact on the post-closure performance of landfill capping systems. This may in turn lead to water ingress and enhanced leachate generation, significantly increasing the risk of harm to the environment. Laboratory scale experiments were conducted to estimate waste settlement rates under different operational-management practices including leachate recirculation and the addition of synthetic methanogenic mineral media and an anaerobic microbial seed culture. A detailed characterisation of the waste and its associated chemical and physical properties was a key component of the study. The following conclusions have been drawn from this work in accordance with the stated aims given in section 1.2:

9.1.1. Review of previous work on secondary settlement of landfills

The models based on soil mechanics (Sowers, 1973; Janbu, 1989; Yen and Scanlon, 1975; Coumoulos and Koryalos, 1997; Bjarngard and Edgers, 1990) captured the major elements of primary and secondary compression in degradable material. However, a number of disadvantages were identified in the use of these models and include: lack of standardization of time parameters, which makes it difficult for any comparison between other similar models to be made; unsatisfactory model calibration in cases of waste fill with a complex history; and considerable variation in the secondary compression index $C_{\alpha\varepsilon}$. Some of the models rapidly reached constant settlements, and exhibited limitations if the settlements persisted at a significant level (Gibson and Lo, 1961; Ling et al., 1998). In contrast, the Power Creep model did not allow the determination of a time at which settlement rate stabilized leading to overestimated long-term settlement.

The effect of waste degradation on settlement was modelled by various researches (Edgers *et al.*,1992; Guasconi, 1995; Wall and Zeiss, 1995; Park and Lee, 1997) who identified two stages of delayed compression, the first stage being dominated by mechanical interactions, and the second stage by biological processes generally expressed according to first order kinetics. The major drawback of these models is that the bacterial population is actually an ecosystem, yet the models can only incorporate the growth kinetics of a single species of that population, the methanogens, and therefore underestimates the role of hydrolysis which is considered to be the rate-limiting step in degradation.

Various researchers (Lee et al.,1994; Ling et al., 1998; Edil et al., 1990; El-Fadel and Al-Rashed, 1998; El-Fadel et al., 1999b; Park et al., 2007) effectively simulated the long term settlement of landfills using different predictive models (Gibson and Lo, 1961; Sowers, 1973; Yen and Scanlon, 1975; Edil et al., 1990; Edgers et al., 1990; Bjarngard and Edgers, 1990; Edgers et al., 1990; Park and Lee, 1997; Ling *et al.*; 1998). However, determination of empirical parameters remains a difficult task, especially after time (t_k) where settlement rates start to increase due to degradation. Additional work is needed to relate model parameters to waste composition, density, moisture content, temperature fluctuations and applied stress.

In addition, all large-scale trials to date have been focused on degradation and there has been no large-scale trial or study of factors that influence landfill settlement and the interaction between them. Also the various parameters required for modelling work (e.g., accurate waste composition, waste placement history) are not recorded at normal operating landfills and require significant effort and expense to measure. Since underestimation of settlement can have serious and potentially costly engineering and environmental consequences, accurate prediction of both short-term and degradation controlled long-term behaviour inclusive of the heterogeneous properties of the waste is of great importance.

9.1.2. Determination of the optimum sewage seed addition to be applied in the CARs

The results of the BMP test 1 highlighted the fact that the development of a methanogenic biodegradation potential in the waste material could be hastened utilising a 10% inoculum of anaerobic digester sludge in the liquid medium applied to the waste.

9.1.3. *Influence of the organic fraction of waste, temperature, depth and gas production rate on the rate of secondary settlement under constant applied load*

The total magnitude of settlement in CAR1 (AG waste sample) after 338 days was approximately 9.0%. During the test in CAR1, it was determined that 43% of the total settlement took place within 65 days after loading and a further 57% settlement occurred over a longer period of time due to degradation effects.

The total magnitude of settlement observed in CARs 2 & 3 (FR waste sample) after 919 days into test was 27.6 and 25.0%, respectively. Test cells 2 & 3 exhibited almost identical intermediate secondary compression rates compared to that in the control cell (CAR4) (values between 7.3 and 8.3%), which is thought to be dominated by mechanical interactions due to delayed compression of the wastes and was not linked to biodegradation. An applied stress of 50kPa (5m depth in a landfill) resulted in 17.7% long-term secondary compression in test cell 3 whereas 150kPa (15m depth) caused a 19.3% long-term secondary compression in test cell 2, which was thought to be due to the combined effects of creep and biodegradation.

CAR4 is an interesting and unique control reactor because despite efforts to prevent the onset of biodegradation and methane formation, the control overcame the inhibitory effect of the VFAs and became methanogenic after day 314. CAR4 can only be considered as a control until day 314 where the onset of degradation processes occurred. Therefore after assuming that the control cell (CAR4) remained inhibited over the whole duration of the test and as a result of that the related settlement would have been linear with respect to the logarithm of time (i.e., associated with creep processes only), it was concluded that the amount of settlement which was likely to be caused by compression processes alone was 13.9%.

The long-term secondary settlement exhibited in CARs 2 & 3 was also found to be dependent on applied stress. The increased stress in CAR2 (150 kPa) appeared to lead to a 20% increase in the rates of long-term secondary compression in comparison to CAR3 (50kPa). The dominant cause of long-term settlement in CARs 2 & 3 was due to a major reduction in volume as a result of waste biodegradation. The close similarity of the CARs settlement behaviour to full-scale observations suggests that the test cells can effectively simulate actual landfill settlement.

The total volumes of biogas produced at STP by CARs 1, 2 & 3 were 1.41 litres/kg dry wt. (AG sample), 314.31 litres/kg (FR sample) and 256.03 litres/kg (FR sample), respectively. The organic content of the waste was found to directly affect the volume of the gas produced which in turn directly affected the magnitude of secondary settlement observed in the CARs. However, the gas production curve for cells 2 and 3 was almost identical up to day 80, but then started to diverge and the reason for this have not been established. The results of this study indicate that the reactors filled with fresh waste exhibited greater amounts of settlement than aged waste due to the added effect of biodegradation.

Results also highlight the importance of temperature in promoting stabilisation of the waste. In particular, upon heating CAR1 to a temperature of approximately 35°C at day 65, a noticeable increase in the rate of secondary settlement and gas production was immediately observed. Removal of sulphate and enhanced ammonia production were all immediately increased by the increase in the temperature. This study has shown that by accelerating and enhancing conditions for rapid biodegradation the associated physical, chemical and biological phenomena related to waste settlement can be studied over reduced time-scales.

9.1.4. Changes in chemical composition of the leachate as the waste degrades

The enhanced biodegradative conditions achieved by the various techniques described in section 5.2.3 were found to accelerate the waste biodegradation processes in the CARs and hence the establishment of methanogenic conditions. Four distinct phases were identified from the results obtained of leachate samples taken from CAR2 & CAR3: Phase I: *the acidogenic phase* (0 - 9 days), when the long-chain fatty acids (propionic, butyric, valeric and caproic acids) were the main product and the pH was low (5.5 - 5.8); Phase II: *the acetogenic phase* (10 - 40 days), when the long-chain VFAs were converted to acetate, carbon dioxide and hydrogen, and the biogas production was negligible; Phase III: *the accelerated methanogenic phase* (40 - 140 days), where the maximum biogas production rate was recorded; and Phase IV: *the decelerated methanogenic phase* (140 - 919 days), where the rate of methane production decreased, even though the methane and carbon dioxide concentrations remained constant.

In the CARs, the removal of all the sulphate (at day 65 in CAR1 and at day 65 in CARs 2& 3) in the leachate resulted in a simultaneous increase in the rate of biogas production. In addition, a gradual increase in the ammonium ion concentration to a level of 302.3mg/l (CAR1), 778.3 mg/l (CAR2) and 967.8mg (CAR3) was observed in leachate samples taken form the reactors, indicating that nitrogen existed in quantities in excess of those which could be bound in the cell biomass during the growth of microbial populations in the CARs.

Chemical analysis of leachate samples taken from the CARs showed a gradual decrease in calcium and magnesium ions which is almost certainly due to the precipitation of these elements during biodegradation, although some of these ions could have been adsorbed in the cell biomass during the growth of microbial populations.

Solubility product controls the heavy metals precipitation order as well as the type of solid formation. However, bacterial activities are responsible for producing sulphides and carbonates, which control in general precipitation rate. Immobilisation of *Al*, *Cu*, *Pb*, *Cd*, *Zn*, *Co*, *Ni, Mo* and *Fe* from the soluble phase was completed in CARs 1, 2 & 3 in 66, 30 and 15 days, respectively via form of metabolic uptake due to the establishment of a highly reducing environment and the formation of sulphide from the sulphate reduction. Some soluble metals remained in the CARs, even after 338 (CAR1) and 919 (CARs 2 & 3) days into the test.

9.1.5. Variation in waste chemical composition with depth

Core samples were obtained from the experimental reactors CAR2 and CAR3 to gain further information on the waste chemical composition at the end of the experiment. The results show that the TC utilised in CAR2 as a result of biodegradation was approximately 30% higher that that observed in CAR3. The rate of biodegradation was found to vary with depth. Good statistical correlations were found between: TC content and LOI data (R^2 values between 0.78 and 0.89); and cellulose content and TC content (R^2 values between 0.81 and 0.82). The data shows a very clear variation in waste TC, LOI, NDF, ADF and cellulose with depth in the reactors. However, the reason for this variation has not yet been identified. All these parameters were found to be depth dependant variables.

9.1.6. *Prediction of the rate and potential of MSW biodegradation in the CARs filled with specific type of wastes*

The data from the BMP test 2 indicates that well degraded MSW still contains a significant percentage of slowly degradable organic matter which remains in the waste for a long period of time. It was also found that the parameters NDF, ADF, cellulose and methane potential for the BMP2 test samples were interrelated. The (C+H)/L ratio, in this instance, was found not to correlate with biogas production, and leads to the conclusion that the measured cellulose and hemicellulose content in well degraded samples did not represent total bioavailable carbon.

The data form the BMP test 3 (FR waste sample) shows that the TC analysis is advantageous in terms of accuracy and reproducibility and is a useful measurement as it provides an expression of the amount of waste mineralised by biodegradation process. However, it is not a completely reliable indicator for the prediction the rate and potential of MSW biodegradation. TN, ADL and hemicellulose contents in all BMP3 test reactors proved to be very variable indicators of degradation potential, with relatively small changes in their concentration observed with sample age. The BMP3 test results indicate that changes in values for NDF, ADF, cellulose, (C+H)/L ratio and methane potential for the BMP test samples that have been found are interrelated. Additionally, the best correlation found was between the (C+H)/L ratio and BMP (R^2=0.84), which indicates that measured cellulose and hemicellulose contents in fresh MSW give a realistic assessment of the readily biodegradable carbon. The correlation between all the chemical parameters mentioned above suggests that monitoring only one of these parameters may be sufficient to provide an accurate prediction of the degree of biodegradation and BMP of a fresh MSW sample without extensive monitoring methods.

9.1.7. *Correlation between settlement and biodegradation*

The percentage of settlement observed in CARs 2, 3 & 4 that can be attributed to biodegradation was 13.73%, 11.09% and 4.75%, respectively. These values were found to be lower than values obtained by Coduto and Huitric (1990) (18 - 24%), possibly due to the fact that Coduto and Huitric (1990) determined the ultimate settlement due to biodegradation based on composition of waste typically produced from 1964 to 1981.

For the fresh waste tested in this study (CARs 2, 3 & 4) secondary settlement due to biodegradation was found to be of comparable magnitude to the component of secondary

settlement caused by mechanical creep. The results show that long-term secondary settlement is directly correlated with the amount of biogas produced and hence biodegradation. A very good linear statistical correlation between cumulative biogas generation and long-term secondary settlement was found to exist for CAR1 and CAR4, although the biodegradation rates were observed to be lower than the other cells. In addition, a significant correlation was found between biogas production and biodegradation-induced secondary settlement for the most bioactive test cells (CARs 2 & 3) with R^2 values of 0.93 and 0.96, respectively.

9.1.8. Assessment of the performance of various settlement models

It was found that all models (Sowers, 1973; Gibson and Lo, 1961; Ling *et al.*, 1998; Edil *et al.*, 1990; Park and Lee, 1997 & 2002) closely simulated the observed settlement in the CARs for the test duration with values of the correlation coefficient between 0.954 (Power Creep Law, Edil *et al.*, 1990) and 0.999 (1D consolidation model, Sowers, 1973) depending on the model used and the reactor simulated. In general, the Power Creep Law (Edil *et al.*, 1990) and the biochemical model (Park and Lee, 1997 & 2002) simulated the first stage of secondary settlement well but it overestimated the long-term settlement for all cells by up to 7% and 14%, respectively. The magnitude of this discrepancy was observed to increase as the simulated time period increased. In terms of waste type, all the models used provided a good representation of the settlement data observed for the reactor filled with AG waste sample (CAR1). However, the settlement behaviour of the FR waste sample (CARs 2, 3 & 4) was most closely simulated by the Sowers model (1973), Gibson and Lo model (1961) and Hyperbolic Law (Ling *et al.*, 1998). The estimated settlements over a 25 year period predicted by the Power Creep Law (Edil *et al.*, 1990) was 2 and 5 times greater than that predicted by the Gibson and Lo (1961) model as the power function used caused a divergence at greater timescales.

9.1.9. Generation of good quality data set for the validation of other quantitative models

The data presented in this study is a detailed and extensively monitored laboratory trail on the settlement and biodegradation of MSW. This was based on an experiment involving three CARs each containing approximately 27kg dry weight of shredded fresh MSW. The information provided in this study includes: input and output waste composition; composition of added synthetic leachate; the operational procedure; data on

imposed external variables such as applied load pressure, atmospheric pressure, temperature and recirculation events; and monitoring results of waste settlement, biogas composition, leachate pH and Redox potential and leachate composition over the test duration. The data collected in this study is a good medium term dataset that will provide modellers with the ability to compare their predictions and promote the development of more accurate models.

9.2. Future work

On the basis of the research described in this thesis the following suggestions for future work can be made:

- In order to assess the biodegradability of waste, a standard test methodology is needed. The methodology should propose guidance on: the suitability of various tests commonly used to assess the biodegradability according to waste composition; what is the biodegradation potential of each biodegradable waste constituent determined by each test; and the correlation between biodegradation potential determined for each waste constituent using different tests;
- Further research is needed to evaluate the factors that triggered the establishment of methanogenesis in the control cell even though it was inhibited by adding a mixture of acetic and propionic acid. N-butyrate and n-valerate showed a tendency to accumulate and to prevail over the other measured acids (except acetate and propionate). This requires further verification and suggests that these VFAs may provide a useful indicator of reactor stressing, even at an early stage, when the other indicators (such as TOC concentration and pH) are still within a normal range of values; and
- Further work is required to create a framework by which the various models can be compared. The lack of detailed datasets on the settlement and biodegradation of MSW has made it difficult to identify the drawbacks within the various models and identify problems that require further work without much duplication of effort in the development and calibration of models that describe landfill processes.

References

Ahring, B. K., Sandberg, M., and Angelidaki, I. (1995). Volatile fatty acids as indicators of process imbalance in anaerobic digesters. *Applied Microbiology and Biotechnology* 43, 559 - 565.

Andersen, E. O., Balanko, L. A. L., Lem, J. M., and Davis, D. H. (2004). Field monitoring of the compressibility of MSW and soft alluvium. Proc. Fifth International Conference on Case Histories in Geotechnical Engineering.

Angelidaki, I., and Ahring, B. K. (1994). Anaerobic thermophilic digestion of manure at different ammonia loads: effect of temperature. *Water Research* 28, 727 - 731.

Angelidaki, I., Ellegaard, L., and Ahring, B. K. (1993). A mathematical model for dynamic simulation of anaerobic digestion of complex substrates: focusing on ammonia inhibition *Biotechnology and Bioengineering.* 42, 159-166.

AOAC (1984). *Association of Official Agricultural Chemists.* In: Williams, S. (Ed), Official Methods of Analysis. 14th Ed. AOAC Arlington. VA.

Archer, D. (1988). A basic study of landfill microbiology and biochemistry. Contractor Report ETCU B 1159. ARFC Institute for Food Research, UK. *Water Research*, 6 - 14, 25 - 47.

Asaoka, A. (1978). Observational procedure of settlement prediction. *Soils and Foundations*, 87 - 101.

ASTM (1992). *Standard test method for determining the anaerobic biodegradation potential of organic chemicals.* E1196-92, American Society for Testing and Materials, West Conshohocken, PA.

Atlas, R., and Bartha, R. (1998). *Microbial Ecology: Fundamentals and Applications.* Fourth Ed Benjamin Ca.

Augenstein, D., Yazdani, R., Kieffer, J., and Benemann, J. (2005[a]). Yolo County, California controlled landfill program. A summary of results since 1994. Proc. Sardinia 2005 International Landfill Conference.

Augenstein, D., Yazdani, R., Kieffer, J., and Benemann, J. (2005[b]). Engineering landfills versus in-vessel processes for anaerobic composting and methane recovery from MSW. Proc. Sardinia 2005 International Landfill Conference.

Augenstein, D., Yazdani, R., Mansoubi, A., and Pacey, J. (1999). Yolo County controlled landfill demonstration. Sardinia 99, Seventh International Landfill Symposium, pp. 235 - 242.

Augenstein, D. C., Wise, D. L., Wentworth, R. L., and Cooney, C. L. (1976). Fuel gas recovery from controlled landfilling of municipal waste. *Resource Recovery and Conservation* 2, 103 - 117.

Baird, C. (1995). *Environmental Chemistry.* Ed. WH Freeman and Company, New York.

Baldwin, T. D., Stinson, J., and Ham, R. K. (1998). Decomposition of specific materials buried within sanitary landfills. *Journal of Environmental Engineering* 124 1193 - 1202.

Banfield, F. S., Meek, D. M., and Lowden, G. F. (1978). Manual and automated gas-chromatograph procedures for the determination of volatile fatty acids. Technical report TR 76, Laboratory Services Division, Water Research Centre.

Barlaz, M. A. (1998). Carbon storage during biodegradation of municipal solid waste components in laboratory-scale landfills. *Global Biogeochemical Cycles* 12, 373 - 380.

Barlaz, M. A. (2006). Forest products decomposition in municipal solid waste. *Waste Management & Research* 26, 321 - 333.

Barlaz, M. A., Eleazer, W. E., Odle, W. S., Qian, X., and Wang, Y. S. (1997). Biodegradative analysis of municipal solid waste in laboratory-scale landfills. EPA Project Summary EPA/600/SR-97/071.

Barlaz, M. A., and Ham, R. K. (1993). *Leachate and gas generation.* In: Daniel, D.E. (Ed.), Geotechnical Practice for Waste Disposal. Chapman & Hall. London, pp. 114-136, UK.

Barlaz, M. A., Ham, R. K., and Schaefer, D. M. (1989[a]). Mass balance analysis of anaerobically decomposed refuse. *Journal of Environmental Engineering Division, ASCE* 115, 1088 - 1101.

Barlaz, M. A., Ham, R. K., and Schaefer, D. M. (1990). Methane production from municipal refuse: a review of enhancement techniques and microbial dynamics. *Critical Reviews in Environmental Control, CRC Press* 19, 557 - 584.

Barlaz, M. A., Milke, M. W., and Ham, R. K. (1987). Gas production parameters in sanitary landfill simulators. *Waste Management and Research* 5, 27 - 36.

Barlaz, M. A., Rooker, A. P., Kjeldsen, P., Gabr, M. A., and Borden, R. C. (2002). A Critical Evaluation of Factors Required To Terminate the Post-Closure Monitoring Period at Solid Waste Landfills. *Environmental Science and Technology* 36, 3457 - 3464.

Barlaz, M. A., Schaefer, D. M., and Ham, R. K. (1989[b]). Bacterial population development and chemical characteristics of refuse decomposition in a simulated sanitary landfill. *Applied and Environmental Microbiology* 55, 55 - 65.

Beaven, R. P. (1996). A hydrogeological approach to sustainable landfill design. Harwell Waste Management Symposium: Progress, Practice and Landfill Research. 22nd May, AEA Technology.

Beaven, R. P. (2000). The hydrogeological and geotechnical properties of household waste in relation to sustainable landfilling PhD dissertation. In *Queen Mary and Westfield College, University of London.*

Beaven, R. P., and Powrie, W. (1995). Determination of hydrogeological and geotechnical properties of refuse using a large compression cell. Proc. Sardinia 1995 International Landfill Conference, pp. 745 - 760.

Beaven, R. P., and Walker, A. N. (1997). Evaluation of the total pollution load of MSW. Proc. Sardinia 1997 International Landfill Conference, pp. 57 - 71.

Bialkowski, S. E. (web page). Use of acid distribution in solubility problems. In *http://www.chem.usu.edu/~sbialkow/Classes/3600/alpha/alpha3.html.* last updated 03 August 2004. Department of Chemistry and Biochemistry, Utah State University.

Bingemer, H. G., and Crutzen, P. J. (1987). The production of methane from solid wastes. *Journal of Geophysical Research* 92 2181 - 2187.

Bjarnard, A. B., and Edgers, L. (1990). Settlement of municipal solid waste landfills. Proc. of the 13th Annual Madison Waste Conference, Wisconsin-Madison, pp. 192 - 205.

Bjerrum, L. (1967). Engineering geology of Norwegian normally-consolidated marine clays as related to settlement of buildings. *Geotechnique* 17, 83 -118.

Blakey, N. C. (1991). Enhanced landfill stabilization using sewage sludge. Proc. Sardinia 1991, 3rd International Landfill Symposium, pp. 1367 - 1387.

Bleiker, D. E., Farquahr, G., and McBean, E. (1995). Landfill settlement and the impact on site capacity and refuse hydraulic conductivity. *Waste Management and Research* 13, 533 - 554.

Boetius, A., Ravenschlag, K., Schubert, C., Rickert, D., Widdel, F., Gieseke, A., Amann, R., Bo Barker Jùrgensen, B. J., Witte, U., and Pfannkuche, O. (2000). Marine microbial consortium apparently mediating anerobic oxidation of methane. *Nature* 407, 623 - 626.

Bogner, J. (1990). Controlled study of landfill biodegradation rates using modified BMP assays. *Waste Management and Research* 13, 522 - 554.

Bogner, J. (1992). Anaerobic burial of refuse in landfills: increased atmospheric methane and implications for increased carbon storage. *Ecological Bulletin* 42, 98 - 108.

Bogner, J., and Spokas, K. (1995). *Carbon storage in landfills. In Advances in Soil Scienc, Soil and Global Change*. Eds R. Lal, J. Kimble, E. Levine and B. Stewart. Lewis Publishers Boca Ratan FL, pp 67 - 80.

Bookter, T. J., Asce, A. M., and Ham, R. K. (1982). Stabilization of solid waste in landfills. *Journal of Environmental Engineering* 108, 1089-1100.

Boone, D. R., Chynoweth, D. P., Mah, R. A., Smith, P. H., and Wilkie, A. C. (1993). Ecology and microbiology of biogasification. *Biomass Bioenergy* 5, 191 - 202.

Borowski, W. S., Paull, C. K., and Ussler, W. (1997). Carbon cycling within the upper methanogenic zone of continental rise systems: an example from methane-rich sediments overlying the Blake Ridge gas hydrate deposits. *Marine Chemistry* 57, 299 - 311.

Borowski, W. S., Paull, C. K., and Ussler, W. (1999). Global and local variations of interstitial sulfate gradients in deep-water, continental margin sediments: sensitivity to underlying methane and gas hydrates. *Marine Geology* 159, 131 - 154.

Boutwell, G. P., and Fiore, N. A. (1995). Settlement of clay cover on saturated garbage. Proc. Geoenvironment 2000, pp. 964 - 979.

Bozkurt, S., Aulin, C., Moreno, L., and Neretnieks, I. (1997). Long-term release of toxic metals from waste deposits. In: Christensen, T.,Cossu, R. & Stegmann, R. (eds) Landfill processes and waste pretreatment. Proc. of the Sixth International Landfill Symposium, Sardinia 97, pp. 257-266.

Bozkurt, S., Moreno, L., and Neretnieks, I. (2000). Long-term processes in waste deposits. *Science of the Total Environment* 250, 101 - 121.

Brock, T. D. (1970). *Biology of Microorganisms*. Prentice-Hall, Englewood Cliffs, NJ.

Brune, M., Ramke, H. G., Collins, H. J., and Hanert, H. H. (1991). Incrustation processes in drainage systems of sanitary landfills. Proc. Sardinia 1991 Third International Landfill Symposium, pp. 999 - 1035.

BS. EN 13039:2000 Soil improvers and growing media Determination of a quantity.

BS. EN 12880:2000 Characterization of sludges Determination of dry residue and water content.

Buck, A. L. (1981). New equations for computing vapor pressure and enhancement factor. *Journal of Applied Meteorology* 20, 1527 - 1532.

Buisman, A. S. K. (1936). Results of long duration settlement tests. Proc. 1st International Conference on Soil Mechanics and Foundation Engineering, pp. 103 - 106.

Buivid, M. G., Wise, D. L., Blanchet, M. J., Remedios, E. C., Jenkins, B. M., Boyd, W. F., and Pacey, J. G. (1981). Fuel gas enhancement by controlled landfilling of municipal solid waste. *Resource Recovery and Conservation* 6, 3 - 20.

Burlingame, M. J. (1985). Construction of a Highway on a Sanitary Landfill and Its Long-Term Performance, pp. 34 - 40. Transportation Research Record 1031, Transportation Research Board, Washington, D.C.

Burton, S. A. Q., and Watson-Craik, I. A. (1998). Ammonia and nitrogen fluxes in landfill sites: applicability to sustainable landfilling. *Waste Management and Research* 16, 41 - 53.

Burton, S. A. Q., and Watson-Craik, I. A. (1999). Accelerated landfill refuse decomposition by recirculation of nitrified leachate. Proc. Sardinia 1999 7th International Waste Management and Landfill Symposium, pp. 119 - 126.

Carpentier, W. L., Li, T., Vigneron, V., Mazeas, L., and Bouchez, T. (2006). Methanogenic diversity and activity in municipal solid waste landfill leachates. *Antonie van Leeuwenhoek* 89, 423-434.

Chang, J. C., and Hannon, J. B. (1976). *Settlement Performance of Two Test Highway Embankments on Sanitary Landfills. In: New Horizons in Construction Materials.* Envo Publishing Co., Lehigh Valley, PA.

Chen, A. C., Imachi, H., Sekiguchi, Y., Ohashi, A., and Harada, H. (2003[a]). Archaeal community compositions at different depths (up to 30 m) of a municipal solid waste landfill in Taiwan as revealed by 16S rDNA cloning analyses. *Biotechnology Letters* 25 719 - 724.

Chen, A. C., Ohashi, A., and Harada, H. (2003[b]). Acetate synthesis from H_2/CO_2 in simulated and actual landfill samples. *Environmental Technology* 24, 435 - 443.

Chen, A. C., Ueda, K., Sekiguchi, Y., Ohashi, A., and Harada, H. (2003[c]). Molecular detection and direct enumeration of methanogenic Archaea and methanotrophic Bacteria in domestic solid waste landfill soils. *Biotechnology Letters* 25, 1563 - 1569.

Christensen, A. G., Fischer, E. V., Nielsen, H. N., Nygaard, T., Østergaard, H., Lenschow, S. R., Sørensen, H., Fuglsang, I. A., and Larsen, T. H. (2000). Passive soil vapor extraction of chlorinated solvents using boreholes. In: Physical and Thermal Technologies, Remediation of chlorinated and recalcitrant compounds, The second International Conference on Remediation of Chlorinated and Recalcitrant Compounds.

Christensen, T. H., and Jensen, D. L. (1999). Colloidal and dissolved metals in leachates from four Danish landfills. *Water Research* 33, 2139 - 2147.

Christensen, T. H., and Kjeldsen, P. (1995). Landfill emissions and environmental impact: An introduction in Sardinia '95 Landfill Symposium. Proc. Fifth International Landfill Symposium, Cagliari, Sardinia, Italy.

Christensen, T. H., Kjeldsen, P., and Lindhardt, B. (1996). *Gas generating processes in landfills*, London.

Christopherson, M., and Kjeldsen, P. (2001). Lateral gas transport in soil adjacent to an old landfill: factors governing gas migration. *Waste Management and Research* 19, 144 - 159.

Chynoweth, D. P., Owens, J., O'Keefe, D., Earle, J. F. K., Bosch, G., and Legrand, R. (1992). Sequential batch anaerobic composting of the organic fraction of municipal solid waste. *Water Science and Technology* 25, 327 - 339.

Coduto, D. P., and Huitric, R. (1990). *Monitoring landfill movements using precise instruments. In Geotechnics of waste fills: theory and practice, ASTM STP 1070 pp. 358 – 370*, Philadelphia.

Cossu, R., and Serra, R. (1989). *Effects of codisposal on degradation process. Sanitary landfilling: process, technology and environmental impact.* Christensen, Cossu and Stegmann, Academic press Ltd, London.

Coumoulos, D. G., Karyalos, T. P., Metaxas, I. L., and Gioka, D. A. (1995). Geotechnical investigations at the main landfill of Athens. Proc. Sardinia 1995, 5th International Landfill Symposium, pp. 886 - 895.

Coumoulos, D. G., and Koryalos, T. P. (1997). Prediction of attenuation of landfill settlement rates with time. Proc. 14th International Conference on Soil Mechanics and Foundation Engineering, pp. 1807 - 1811.

Council Directive 98/83/EC on the quality of water intended for human consumption.

Croft, B., Smith, R., Caine, M., Knox, K., White, J., Watson-Craik, I., Young, C., and Ellis, J. (2001). The Brogborough test cells: conclusions from a 14-year field scale landfill gas experiment. Proc. Sardinia 2001 Eighth International Waste Management and Landfill Symposium, pp. 3 - 12.

Daniels, L., Sparling, R., and Sprott, G. D. (1984). The bioenergetics of methanogenesis. *Biochimica et Biophysica Acta* 768, 113 - 163.

De Baere, L., De Vocht, M., Van Assche, P., and Verstraete, W. (1984). Influence of high NaCl and NH4Cl salt levels on methanogenic associations. *Water Research* 5, 543 - 548.

De Renzo, D. J. (1978). *Nitrogen Control and Phosphorous Removal in Sewage Treatment*. Noyes Data Corportation. Park Ridge, New Jersey.

Dixon, N., and Jones, D. R. V. (2005). Engineering properties of municipal solid waste *Geotextiles and Geomembranes* 23, 205 - 233.

Dixon, N., Ng'ambi, S., and Jones, D. R. V. (2004). Structural performance of a steep slope landfill lining system. Proc. of the Institution of Civil Engineers Geotechnical Engineering, pp. 115 - 125.

Drake, H. L., Kusel, K., and Matthies, C. (2002). Ecological consequences of the phylogenetic and physiological diversities of acetogens. *Antonie Van Leeuwenhoek, International Journal of General and Molecular Microbiology* 81, 203 - 213.

Edgers, L., Noble, J. J., and Williams, E. (1992). A biologic model for long term settlement in landfills. Proc. Mediterranean Conference on Environmental Geotechnology, pp. 177 - 184.

Edil, T. B., Fox, P. J., and Lan, L. T. (1991). Observational procedure for settlement of peat. Proc. Geo-Coast 91 Conference, pp. 165 - 170.

Edil, T. B., and Mochtar, N. E. (1981). Prediction of peat settlement. ASCE Proceeding of Symposium: Sedimentation/Consolidation Models.

Edil, T. B., Ranguette, V. J., and Wuellner, W. W. (1990). Settlement of municipal refuse. In Geotechnics of Waste Fills-Theory and Practice, (Landva, A. and Knowles, D., eds.), ASTM STP1070, American Society of Testing and Materials.

Effland, M. J. (1977). Modified procedure to determine acid-insoluble lignin in wood and pulp. *Technical Association of the Pulp and Paper Industry* 60, 143 - 144.

Ehrig, H. J., and Scheelhase, T. (1993). Pollution potential and long term behaviour of sanitary landfills. Proc. Sardinia 1993 International Landfill Conference, pp. 1203-1225.

Eleazer, W. E., Odle, W. S., Wang, Y. S., and Barlaz, M. A. (1997). Biodegradability of municipal solid waste components in laboratory-scale landfills. *Environmental Science and Technology* 31, 911 - 917.

El-Fadel, M., and Al-Rashed, H. (1998). Settlement in municipal solid waste landfills. I. Field scale experiments. II. Mathematical modelling. *Journal of Solid Waste Technology and Management* 25, 89 - 104.

El-Fadel, M., Findikakis, A. N., and Leckie, J. O. (1996). Numerical modelling of generation and transport of gas and heat in landfills. *Waste Management and Research* 14, 483 - 504.

El-Fadel, M., and Khoury, R. (2000). Modelling settlement in MSW landfills: a critical review. *Critical Reviews on Environmental Science and Technology* 30, 327 - 361.

El-Fadel, M., Sadek, S., and Khoury, R. (1999[a]). Simulation of solid waste settlements in laboratory columns. Proc. Sardinia 99, 7th International Landfill Symposium, pp. 521 - 528.

El-Fadel, M., Shazbak, S., Saliby, E., and Leckie, J. (1999[b]). Comparative assessment of settlement models for municipal solid waste landfill applications. *Waste Management and Research* 17, 347 - 368.

Emberton, J. R., and Parker, A. (1987). The problems associated with building on landfill sites. *Waste Management and Research* 5, 473 - 482.

EPA Method 3051A 1998. Microwave assisted acid digestion of sediments, sludges, soils and oils. SW 846, Ch3.2. United States Environmental Protection Agency. Washington, DC.

Fassett, J. B., Leonards, G. A., and Repetto, P. C. (1994). Geotechnical properties of municipal waste and their use in landfill design. Proc. Waste Technology Conference.

Ferry, J. G. (1995). Co dehydrogenase. *Annual Review in Microbiology* 49, 305 - 333.

Findikakis, A. N., and Leckie, J. O. (1979). Numerical simulation of gas flow in sanitary landfills. *Journal of Environmental Engineering ASCE* 105, 927.

Fleming, I. R., Rowe, R. K., and Cullimore, D. R. (1999). Field observations of clogging in a landfill leachate collection systems. *Canadian Geotechnical Journal* 36, 685 - 707

Florencio, L., Field, J. A., and Lettinga, G. (1995). Substrate competition between methanogens and acetogens during the degradation of methanol in UASB reactors. *Water Research* 29, 915.

Flyhammar, P., Tamaddon, F., and Bengtsson, L. (1998). Heavy metals in a municipal solid waste deposition cell. *Waste Management and Research* 16, 403 - 410.

Förstner, U., Colombi, C., and Kistler, R. (1991). *In: Metals and Their Compounds in the Environment.* VCH Publishers Inc., NY, pp. 333 - 355.

Gabr, M. A., Hossain, M. S., and Barlaz, M. A. (2000). Solid waste settlement with leachate recirculation. *Geotechnical News* 18, 50 - 55.

Gabr, M. A., and Valero, S. N. (1995). Geotechnical properties of MSW. *ASTM Geotechnical Testing Journal* 2, 241 - 254.

Gandolla, M., Dugnani, L., Bressi, G., and Acaia, C. (1992). The determination of subsidence effects at municipal solid waste disposal sites. Proc. 6th International Solid Waste Congress and Exhibition, pp. 1 - 17.

Garlanger, J. E. (1972). The consolidation of soils exhibiting creep under constant effective stress. *Geotechnique* 22, 71 - 78.

Gasparini, P. A., Saetti, G. F., and Marastoni, M. (1995). Experimental research on MSW compaction degree and its change with time. Proc. Sardinia 1995, 5th International Waste Management and Landfill Symposium, pp. 833 - 842.

Gerrardi, M. H. (2003). *The microbiology of anaerobic digestion.* Eds. Wiley Publisher.

Gertloff, K. H. (1993). Setzungsanalyse und Setzungsprognose für eine Hausmülldeponie. *Müll and Abfall* 25, 752 - 766.

Gibson, R. E., and Lo, K. Y. (1961). A theory of soils exhibiting secondary compression. *Acta Polytechnica Scandinavica* 296, 1 - 15.

Glasstone, S., Laidler, K., and Eyring, H. (1941). *The theory of rate process.* McGraw-Hill, New York.

Godley, A. R., Graham, A., and K., E. (2005). Estimating biodegradable municipal solid waste diversion from landfill: Screening exercise to evaluate the performance of biodegradable waste test methods. Environment Agency R&D Technical Report P1-513 (EP 0173) phase 1.

Green, D., and Jamenjad, G. (1997). Settlement characteristics of domestic waste. Shear strength of waste and its use in landfill stability analysis. Proc. Conference on Contaminated Ground, British Geotechnical Society, pp. 319 - 324.

Grisolia, M., Gasparini, A., and Saetti, G. F. (1993). Survey of waste compressibility. Proc. Sardinia 1993, 4rd International Landfill Symposium, pp. 1447 - 1456.

Grisolia, M., and Napoleoni, Q. (1995). Deformability of waste and settlements of sanitary landfills. Proc. of World Congress on Waste Management ISWA'95, Wien.

Guasconi, M. (1995). A study of settlement in landfills due to biodegradation, Master thesis. In *New Jersey Institute of Technology, Department of Civil and Environmental Engineering*, pp. 59.

Gulec, S. B., Onay, T. T., and Erdincler, A. (2000). Determination of the remaining stabilization potential of landfilled solid waste by sludge addition. *Water Science and Technology* 42 269 - 276.

Güven, D., Dapena, A., Kartal, B., Schmid, M. C., Maas, B., Van de Pas-Schoonen, K., Sozen, S., Mendez, R., Op den Camp, H. J. M., Jetten, S. M. M., Strous, M., and Schmidt, I. (2005). Propionate oxidation by and methanol inhibition of anaerobic ammonium-oxidizing bacteria. *Applied and Environmental Microbiology* 71, 1066 - 1071.

Ham, R. K. (1988). *Biological and Chemical Processes in Landfills*. Sanitary Landfill Design Manual. Department of Engineering Professional Department, University of Wisconsin-Madison.

Ham, R. K., and Bookter, T. J. (1982). Decomposition of solid waste in test lysimeters. *Journal of Environmental Engineering.* 108, 1147.

Ham, R. K., Fritschel, P. R., and Norman, M. R. (1993[a]). Refuse decomposition at a large lamdfill. Proc. Fourth International Waste Management and Landfill Symposium, pp. 1046 - 1054.

Ham, R. K., Norman, M. R., and Fritschel, P. R. (1993[b]). Chemical characterization of fresh kills landfill refuse and extracts. *Journal of Environmental Engineering* 119, 1176 - 1195.

Hansen, B. (1969). A mathematical model for creep phenomena in clay. Proc. Seventh International Conference on Soil Mechanics and Foundation Engineering, Speciality session 12, pp. 12 - 18.

Hansen, L. B., Finster, K., Fossing, H., and Iversen, N. (1998). Anaerobic methane oxidation in sulfate depleted sediments: effects of sulfate and molybdate addition. *Aquatic Microbial Ecology* 14, 195 - 204.

Hansen, T. L., Schmidt, J. E., Angelidaki, I., Marca, E., Jansen, J. C., Mosbæk, H., and hristensen, T. H. (2004). Method for determination of methane potentials of solid organic waste. *Waste Management* 24, 393 - 400.

Harmon, J. L., Svoronos, S. A., Lyberatos, G., and Chynoweth, D. P. (1993). Adaptive temperature optimization of continuous anaerobic digesters. *Biomass and Bioenergy* 4, 1 - 7.

Hashimoto, A. G., Chen, Y. R., Varel, V. H., and Prior, R. L. (1980). *In: Utilization and Recycle of Agricultural Wastes and Residues*. CRC Press, Boca Raton, FL, 35 - 196.

Hater, G. R. (2000). Leachate recirculation, landfill bioreactor development and data acquisition at waste management. Third Annual LMOP Conference on Landfill Methane Outreach Program.

Hilde, J. L., and reginster, J. (1995). Three years of vertical and horisontal movements in MSW landfill. Proc. Sardinia 1995, 5th International Landfill Symposium, pp. 855 - 860.

Hill, D. T., and Bolte, J. P. (1989). Digester stress as related to iso-butyric and iso-valeric acids. *Biological Wastes* 28, 33 - 37.

Hoehler, T. M., Alperin, M. J., Albert, D. B., and Martens, C. S. (1994). Field and laboratory studies of methane oxidation in an anoxic marine sediment: Evidence for a methanogenic-sulfate reducer consortium. *Global Biogeochemical Cycles* 8, 451 - 463.

Hoeks, F. W. J. M. M., Ten Hoopen, H. J. G., Roels, J. A., and Kuenen, J. G. (1984). Anaerobic treatment of acid water (methane production in sulphate rich environment). *Progr. Ind. Microbiol.* 20, 113 - 119.

Hoeks, J. (1983). Significance of biogas production in waste tips. *Waste Managemant and Research* 1, 323 - 335.

Hossain, M. S., Gabr, M. A., and Barlaz, M. A. (2003). Relationship of compressibility parameters to municipal solid waste decomposition. *ASCE Journal of Geotechnical and Geoenvironmental Engineering* 129, 1151 - 1158.

Huang, L. N., Chen, Y. Q., Zhou, H., Luo, S., Lan, C. Y., and Qu, L. H. (2003). Characterization of methanogenic Archaea in the leachate of a closed municipal solid waste landfill. *FEMS Microbiology and Ecology* 46, 171 -177.

Huang, L. N., Zhou, H., Chen, Y. Q., Luo, S., Lan, C. Y., and Qu, L. H. (2002). Diversity and structure of the archaeal community in the leachate of a full-scale recirculating landfill as examined by direct 16S rRNA gene sequence retrieval. *FEMS Microbiology Letters* 214, 235 - 240.

Hudson, A. P., Beaven, R. P., and Powrie, W. (2001). Interaction of water and gas in saturated household waste in large scale compression cell. Proc. Sardinia 1999, Eighth International Waste Management and Landfill Symposium, pp. 585 - 594.

Hungate, R. E. (1950). The anaerobic mesophilic cellulolytic bacteria. *Bacteriological Reviews* 14, 1.

Huser, B. A., Wuhemann, X., and Zehnder, A. J. B. (1982). Methanothrix-soehhgenii gen-nov-sp-nov, a new acetotrophic non-hydrogen-oxidizing methane bacterium. *Archives of Microbiology* 132, 1 - 9.

Iannotti, E. T., Kafkewitz, D., Wolin, M. J., and Bryant, M. P. (1973). Glucose fermentation products of Ruminococcus albus grown in continuous culture with Vibrio succinogenes: changes caused by interspecies transfer of H2. *Journal of Bacteriology* 114, 1231 - 1240.

ISO. 11465:1995 Soil quality Determination of dry matter and water content on a mass basis Gravimetric method.

Janbu, N., Svanø, G., and Christensen, S. (1989). Back-calculated creep rates from case records. Proc.12th International Conference on Soil Mechanics and Foundation Engineering, Rio, pp. 1809 - 1812.

Jetten, M. S. M., Strous, M., Van de Pas-Schoonen, K. T., Schalk, J., Van Dongen, U. G. J. M., Van de Graaf, A. A., Logemann, S., Muyzer, G., Van Loosdrecht, M. C. M., and Kuenen, J. G. (1999). The anaerobic oxidation of ammonium. *FEMS Microbiology Reviews* 22, 421 - 437.

Jetten, M. S. M., Wagner, M., Fuerst, J., Van Loosdrecht, M., Kuenen, G., and Strous, M. (2001). Microbiology and application of the anaerobic ammonium oxidation ('anammox') process. *Current Opinion in Biotechnology* 12, 283 - 288.

Jung, H. J. G. (1997). Analysis of forage fiber and cell walls in ruminant nutrition. *Journal of Nutrition* 127, 8105 - 8135.

Kalyuzhnyi, S., Fedorovich, V., Lens, P., Hulshoff Pol, L., and Lettinga, G. (1998). Mathematical modelling as a tool to study population dynamics between sulphate reducing and methanogenic bacteria. *Biodegradation* 9, 187 - 199.

Kerby, R., and Zeikus, J. G. (1987). Anaerobic catabolism of formate to acetate and CO_2 by butyribacterium methylotrophicum *Journal of Bacteriology* 169.

Khoury, R., El-Fadel, M., Sadek, S., and Ayoub, G. (2000). Temporal variation of leachate quality in seawater saturated fills. *Advances in Environmental Research* 4, 313 - 323.

Kinman, R. K., Nutini, D. L., Walsh, J. J., Vogt, W. G., Stamm, J., and Rickabaugh, J. (1987). Gas enhancement techniques in landfill simulators. *Waste Management and Research* 5, 13 - 25.

Kitcherside, M. A., Glen, E. F., and Webster, A. J. F. (2000). FibreCap: An improved method for the rapid analysis of fibre in feeding stuffs. *Animal Feed Science and Technology* 86, 125 - 132.

Kjeldsen, P., and Christensen, T. H. (2001). A simple model for the distribution and fate of organic chemicals in a landfill: MOCLA. *Waste Management Research* 19, 201 - 216.

Knox, K. (1999). A review of the Brogborough and Landfill 2000 test cell monitoring data, pp. 231. Environment Agency R & D Technical Report.

Knox, K. (2000). Sustainable landfill in the UK: A review of current knowledge and outstanding R & D needs. Report prepared for the Norlands Foundation and Environmental Services Association Research Trust (ESART).

Knox, K., and Gronow, J. R. (1995). Pilot scale study of denitrification and contaminant flushing during prolonged leachate recirculation. Proc. Sardinia 1995, Fifth International Landfill Symposium, pp. 681 - 690.

Konig, H., and Stetter, K. O. (1982). Isolation and characterization of Methanolobus tindarius, sp. nov., a coccoid methanogen growing only on methanol and methylamines. *Zentralbl. Bakteriol. Parasitenkd. Infektionskr. Hyg. Abt. 1 Orig. Reihe* 3, 478 - 490.

Koppejan, A. W. (1948). A formula combining the Terzaghi load compression relationship and the Buisman secular time effect. Proc. 2nd International Conference on Soil Mechanic and Foundation Engineering, pp. 32 - 38.

Kristjansson, J. K., Schonheit, P., and Thauer, R. K. (1982). Different Ks values for hydrogen of methanogenic bacteria and sulfate reducing bacteria: an explanation for the apparent inhibition of methanogenesis by sulfate. *Archives of Microbiology* 131, 278 - 282.

Kuenen, J. G., and Jetten, M. S. M. (2001). Extraordinary Anaerobic Ammonium-Oxidizing Bacteria. *ASM News* 67, 456 - 463.

Kumar, S. (2000). Settlement prediction for municipal solid waste landfills using Power Creep Law. *Soil and Sediment Contamination* 9, 579-592.

Kungelman, I. J., and McCarty, P. L. (1965). Cation toxicity and stimulation in anaerobic waste treatment. *Journal of Water Pollution and Control Federation* 37, 97 - 115.

Lai, T. E., Nopharatana, A., Pullammanappallil, P. C., and Clarke, W. P. (2001). Cellulolytic activity in leachate during leach-bed anaerobic digestion of municipal solid waste. *Bioresource Technology* 80, 205 - 210.

Landva, A. O., and Clark, J. I. (1990). *Geotechnics of a Waste Fill: Theory and Practice.* Arvid Landva and G. David Knowles, eds. Philadelphia: American Society for Testing and Materials, pp. 86 -103. SEL TD795.7 G46.

Landva, A. O., Clark, J. I., Weisner, W. R., and Burwash, W. J. (1984). Geotechnical engineering and refuse landfills. Proc. Sixth National Conference on Waste Management.

Landva, A. O., Valsangkar, A. J., and Pelkey, S. G. (2000). Lateral earth pressure at rest and compressibility of municipal solid waste. *Canadian Geotechnical Journal* 37, 1157 - 1165.

Leckie, J. O., Pacey, J. G., and Halvadakis, C. (1979). Landfill management with moisture control. *Journal of Environmental Engineering Division, ASCE* 105, 337 - 355.

Lee, B. S., Hwang, K. H., Lee, K. Y., and Lee, H. (1995). Settlement characteristics of municipal wastes. *J. Korean Soc. Civ. Eng.* 15, 1773 - 1782.

Lee, S. R., Lee, C. T., and Park, H. (1994). Large scale laboratory tests for evaluating the effects of organic contents on the landfill settlement characteristics. Proc. 2nd Young Asian Geotechnical Engineers Conference, pp. 233 - 244.

Leonard, M. L., Floom, K. J., and Brown, S. (2000). Estimating method and use of landfill settlement. Proc. GeoDenver 2000 on Environmental Geotechnics, pp. 1 - 15.

Ling, H. I., Leshchinsky, D., Mohri, Y., and Kawabata, T. (1998). Estimation of municipal solid waste landfill settlement. *Journal of Geotechnical and Geoenvironmental Engineering, ASCE* 124, 21 - 28.

Lowe, S. E., Jain, M. K., and Zeikus, J. G. (1993). Biology, ecology, and biotechnological applications of anaerobic bacteria adapted to environmental stresses in temperature, pH, salinity, or substrates *Microbiological Reviews* 57, 451 - 509.

Lowry, J. B., Schlink, L. L., and McSweeney, C. S. (1994). Acid detergent dispersible lignin in tropical grasses. *Journal of the Science of Food and Agriculture* 65, 41 - 50.

Lukas, R. G. (1992). Dynamic compaction engineering considerations, in Grouting, Soil Improvement and Geosynthetics. *Geotechnical Special Publication No. 30, ASCE, New York*, 940 – 953.

Madigan, M. T., Martinko, J. M., and Parker, J. (1997). *Brock Biology of Microorganisms*. Prentice Hall, Upper Saddle River, NJ.

Mah, R. A., and Smith, M. A. (1981). *The methanogenic bacteria.* In: Starr, M.P., Stolp, H., Truper, H.G., Balows, A., Schlegel, M.P. (Eds.),The Prokaryotes, A Handbook on Habitats, Isolation and Identifcation of Bactria. Springer New York.

Manahan, E. S. (1991). *Environmental Chemistry*. Lewis Publishers , Chelsea, Michigan.

Mårtensson, A. M., Aulin, C., Wahlberg, O., and Ågren, S. (1999). Effect of humic substances on the mobility of toxic metals in a mature landfill. *Waste Management & Research* 17, 296 - 304.

McBean, E. A., Rovers, F. A., and Farquhar, G. J. (1995). Solid waste landfill engineering and design. Prentice Hall.

McCarty, P. L. (1964). Anaerobic waste treatment fundamentals, Part III. Toxic materials and their control. *Public Works* 95 91 - 94.

McCarty, P. L., and McKinney, R. E. (1961). Salt toxicity in anaerobic treatment. *Journal of Water Pollution Control Federation* 33 399 - 415.

McFarland, M. J., and Jewell, W. J. (1989). In situ control of sulfide emissions during the thermophilic (55°C) anaerobic digestion process. *Water Research* 23, 1571 - 1577.

Mehta, R., Barlaz, M., Yazdani, R., Augenstein, D., Bryars, M., and Sinderson, L. (2002). Refuse decomposition in the presence and absence of leachate recirculation. *Journal of Environmental Engineering* 128, 228 - 236.

Meissner, H. (1996). Settlements and subsidences under intermediate liners and covers. Proc. 3rd Polish-German Symposium, pp. 7.

Merz, R. C., and Stone, R. (1962). Landfill settlement rates. *Public Works* 93, 103 - 106; 210 - 212.

Micales, J. A., and Skog, K. E. (1997). The decomposition of forest products in landfills. *International Biodeterioration and Biodegradation* 39, 145 - 158.

Misra, U., Singh, S., Singh, A., and Pandey, G. N. (1992). A new temperature controlled digester for anaerobic digestion for biogas production. *Energy Conservation Management* 33, 983 - 986.

Mitchell, R. (1974). *Introduction to Environmental Microbiology.* Prentice-Hall, Englewood Cliffs, New Jersey.

Mori, K., Sparling, R., Hatsu, M., and Takamizawa, K. (2003). Quantification and diversity of the archaeal community in a landfill site. *Canadian Journal of Microbiology* 49, 28 -36.

Mormile, M. R., Gurijala, K. R., Robinson, J. A., Mcinerney, M. J., and Suflita, J. M. (1996). The Importance of Hydrogen in Landfill Fermentations *Applied and Environmental Microbiology. American Society for Microbiology* 62, 1583 - 1588

Mulder, A. (1984). The effect of high sulphate concentrations on the methane fermentation of waste water. *Progress in Industrial Microbiology* 20, 133 - 143.

Noble, J. J., Nair, G. M., and Heestand, J. F. (1989). Some numerical predictions for moisture transport in capped landfills at long times. Proc. 12th Annual Madison Waste Conference, pp. 353 - 366.

Noble, J. J., Nunez-Mc Nally, T., and Tausel, B. (1988). The effects of mass transfer on landfill stabilization rates, pp. 519 - 532.

Noike, T., Endo, G., Chang, J., Yaguchi, J., and Matsumoto, J. (1985). Characteristics of carbohydrate degradation and the rate-limiting step in anaerobic digestion. *Biotechnology and Bioengineering* 27, 1482 - 1489.

Oleszkiewicz, J. A., and Hilton, B. L. (1985). Proc. International Conference on the New Directions and Research in Waste Treatment and Residual Management, pp. 864 - 876.

Omil, F., Bakker, C. D., Hulshoff Pol, L. W., and Lettinga, G. (1997). Effect of pH and low temperature shocks on the competition between sulphate reducing bacteria and methane producing bacteria in UASB Reactors *Environmental Technology* 18, 255 - 264.

Omil, F., Lens, P., Hulshoff Pol, L. W., and Lettinga, G. (1996). Effect of upward velocity and sulphide concentration on volatile fatty acid degradation in a sulphidogenic granular sludge reactor. *Process Biochemistry* 31, 699 - 710.

Onay, T. T., and Pohland, F. G. (2001). Nitrogen and sulfate attenuation in simulated landfill bioreactors. *Water Science and Technology* 44, 367 - 372.

Oonk, H., Van Der Sloot, H. A., Vroon, R., Luning, L., and Woelders, H. (2000). Treatment of mechanical separation organic residues in a landfill-bioreactor.

Oonk, H., and Woelders, H. (1999). Waste treatment at VAM - Wijster: Mechanical separation and treatment of organic residues in bioreactors. Proc. Sardinia 99, 7th International landfill Symposium,, pp. 343 - 350.

Oude Elferik, S. J. W. H., Visser, A., Hulshoff Pol, L., and Stams, A. J. M. (1994). Sulphate reduction in methanogenic bioreactors. *FEMS Microbiological Review* 5, 119 - 136.

Oweis, I. S., and Khera, R. (1986). Criteria for geotechnical construction on sanitary landfills. Proc. of the Symposium on Environmental Geotechnology, Allentown, Pa, pp. 215 - 222.

Palmisano, A. C., Schwab, B. S., and Maruscik, D. A. (1993). Hydrolytic enzyme activity in landfill refuse. *Applied Microbiology and Biotechnology* 38, 828 - 832.

Pankow, J. F. (1991). *Aquatic Chemistry Concepts*. Lewis Publishers, p. 247.

Park, H. I., and Lee, S. R. (1997). Long-term settlement behaviour of landfills with refuse decomposition. *Journal of Solid waste Technology and Management* 24, 159 - 165.

Park, H. I., and Lee, S. R. (2002). Long-term settlement behaviour of MSW landfills with various fill ages. *Waste Management and Research* 20, 259 - 268.

Park, H. I., Lee, S. R., and Do, N. Y. (2002). Evaluation of decomposition effect on long-term settlement prediction for fresh municipal solid waste landfills. *Journal of Geotechnical and Geoenvironmental Engineering* 128, 107 - 118.

Park, H. I., Park, B., Lee, S. R., and Hwang, D. (2007). Parameter evaluation and performance comparison of MSW settlement prediction model in various landfill types. . *Journal of Environmental Engineering* 133, 64 - 72.

Parker, L. J., Powrie, W., and White, J. K. (1999). The measurement of the geotechnical and hydrogeological properties of degrading solid waste. Proc. Sardinia 1999, 7th International Waste Management and Landfill Symposium.

Pohland, F. G. (1975). Accelerated solid waste stabilization and leachate treatment by leachate recycle, through sanitary landfill. *Progress in Water Technology* 7, 753 - 765.

Pohland, F. G. (1991). Fundamental principles and management strategies for landfill codisposal practices. Proc. Sardinia 1991, Third International Landfill Symposium pp. 1445 - 1460.

Pohland, F. G., Al-Yousfi, A. B., and Reinhart, D. R. (2002). *Anaerobic Digestion of Organic Solid Waste in Bioreactor Landfill*. In: Biomethanization of the organic fraction of municipal solid waste. J. Mata-Alvarez (Editor), pp. 303 - 315, IWA.

Pohland, F. G., Al-Yousfi, A. B., and Reinhart, D. R. (2003). *Anaerobic digestion of organic solid waste in bioreactor landfills*. In: Biomethanization of the organic fraction of municipal solid wastes. Eds. J. Mata-Alvarez. London, England: IWA Publ.

Pohland, F. G., and Harper, S. P. (1985). Critical review and summary of leachate and gas production from landfills. EPA/600/2-86/073. US Environmental Protection Agency, Cincinnati.

Pohland, F. G., and Harper, S. R. (1985). Biogas developments in North America, pp. 41 - 82. In: Anaerobic Digestion 1985, China State Biogas Association, Quangzhou, China.

Pohland, F. G., and Kim, J. C. (2000). Microbially mediated attenuation potential of landfill bioreactor systems. *Water Science and Technology* 41, 247 - 254.

Powrie, W. (1997). *Soil Mechanics: Concepts and Applications*. E & FN Spon, 127 - 129.

Powrie, W., and Beaven, R. P. (1999). Hydraulic properties of household waste and implications for landfills. Proc. of the Institution of Civil Engineers, Geotechnical Engineering, pp. 235 - 247.

Qasim, R. S., and Chiang, W. C. (1994). *Sanitary Landfill Leachate:Generation, Control and Treatment*. Eds.Technomic Publishing Co, Lancaster, Pennsylvania, USA.

Rao, S. K., Moulton, L. K. a., and Seals, R. K. (1977). Settlement of refuse landfills. Proc. of the Conference on Geotechnical Practice for Disposal of Solid Waste Materials, ASCE, pp. 574 - 598.

Reddy, K. R., and Bogner, J. E. (2003). Bioreactor landfill engineering for accelerated stabilization of municipal solid waste. Invited Theme Paper on Solid Waste Disposal,. International e-Conference on Modern Trends in Foundation Engineering: Geotechnical, Indian Institute of Technology chalange and solutions, Madras, India, October 2003.

Rees, J. F. (1980). The fate of carbon compounds in the landfill disposal of organic matter. *Journal of Chemical Technology and Biotechnology* 30, 161 - 175.

Reinhart, D. R., and Grosh, C. J. (1998). *Analysis of Florida MSW landfill leachate quality*. Florida Center for Solid and Hazardous Management, Gainesville, FL.

Reuter, E., and Nolte, H. C. (1995). Conception of a stability analysis for large landfills: Case study in Hannover. Proc. Sardinia 1995, 5th International Landfill Symposium, pp. 801 - 812.

Revans, A., Ross, D., Gregory, B., Meadows, M., Harries, C., and Gronow, J. l. (1999). Long-term fate of metals in landfil. Proc. Sardinia 1999, 7th International Waste Management and Landfill Symposium.

Reynolds, T. D., and Richards, P. A. (1996). *Unit Operations and Processes in Environmental Engineering-2nd Edition*. Boston, MA: PWS.

Robinson, H. D. The technical aspects of controlled waste management. A review of the composition of leachates from domestic wastes in landfill sites. Report for the UK Department of the Environment. Waste Science and Research, Aspinwall & Company, Ltd., London, UK, 1995.

Rosentrater, K. A., Flores, R. A., Richard, T. L., and Bern, C. J. (1999). Characterization of agribusiness residues. physical and nutritional properties of corn masa byproduct streams. *Applied Engineering in Agriculture* 15, 515 - 523.

Rovers, F. A., and Farquhar, G. I. (1972). Sanitary landfill study final report: Effect of season on landfill leachate and gas production, Report 8083. Waterloo Research Institute.

Rowe, R. K., Fleming, I. R., Armstong, M. D., Cooke, A. J., Cullimore, D. R., Rittmann, B. E., Bennet, P. T., and Longstaffe, F. J. (1997). Recent advances in understanding the clogging of leachate collection systems. Proc. Sardinia 1997, Sixth International Landfill Symposium, pp. 383 - 390, 397 - 408.

Sadek, S., El-Fadel, M., Khoury, R., and Ayoub, G. (2000). Settlement of seawater saturated waste fills. *Environmental Engineering Science* 17, 81 - 95.

Sánchez-Alciturri, J. M., Palma, J., Sagaseta, C., and Canizal, J. (1995). Three years of deformation monitoring at Meruelo landfill. Proc. Green 1993, Geotechnics Related to the Environment, Bolton, UK, pp. 365 - 371.

Sarsby, R. (2000). *Environmental Geotechnics*. Thomas Telford Ltd., London.

Shimizu (1991). Technical survey of refuse landfill ground in the Port of Tokyo. Proc. Int. Conference on Geotechnical Engineering for Coastal Development, Theory and Practice on Soft Ground, "Geo-Coast 91", Yokohama, pp. 75 - 80.

Siegel, R. A., Robertson, R. J., and Anderson, D. G. (1990). *Slope stability investigations at a landfill in Southern California. In: Geotechnics of waste fills - Theory and practice, ASTM SPT 1070*. Eds. A. Landva and G. D. Knowles.

Sohn, K. C., and Lee, S. (1994). A method for prediction of long term settlement of sanitary landfill. Proc. International Congress on Environmental Geotechnics, pp. 807 - 811.

Sowers, G. F. (1973). Settlement of waste disposal fills. Proc. Eighth International Conference on Solid Mechanics and Foundation Engineering, pp. 207 - 221.

Speece, R. F. (1987). *Nutrient reguirements*. In: D. P. Chynoweth, and R. Isaacson, Anaerobic digestion of biomass, Elsevier Applied Science, Ltd., London, pp. 109 - 128.

Spokas, K., Bogner, J., Chanton, J. P., Morcet, M., Aran, C., Graff, C., Moreau-Le Golvan, Y., and Hebe, I. (2006). Methane mass balance at three landfill sites: What is the efficiency of capture by gas collection systems? *Waste Management* 26, 516 - 525.

Srinath, and Loehr (1974). Ammonia desorption by diffused aeration. *Journal of Water Pollution Control Federation* 46, 1939-1957.

Srivastava, V. (1987). *Net energy*. In: Anaerobic Digestion of Biomass. Eds. D. P. Chynoweth & R. Isaacson, Elsevier Science. London, 219 - 230.

Stamm, J. W., and Walsh, J. J. (1988). Pilot scale evaluation of sludge landfilling: four years of operation. United States Environmental Protection Agency, Cincinatti, Ohio. EPA/600/2-88/027.

Stegmann, R. (1983). New aspects on enhancing biological processes in sanitary landfills. *Waste Management Research* 5, 201 - 211.

Stegmann, R., and Ehrig, H. J. (1989). Enhancement of gas production in sanitary landfill sites - experiences in West Germany. *Resource Recovery of Solid Wastes*, 425 - 434.

Stinson, J. A., and Ham, R. K. (1995). Effect of lignin on the anaerobic decomposition of cellulose as determined through the use of a biochemical methane potential method. *Environmental Science and Technology* 29, 2305 - 2310.

Stoll, U. W. (1971). Mechanical properties of milled domestic trash. National Water Resources Meeting, ASCE, Phoenix.

Strous, M., Fuerst, J. A., Kramer, E. H. M., Logemann, S., Muyzer, G., Van de Pas-Schoonen, K. T., Webb, R., Kuenen, J. G., and Jetten, M. S. M. (1999). Missing lithotroph identified as new planctomycete. *Nature* 400, 446 - 449.

Strous, M., Van Gerven, E., Kuenen, J. G., and Jetten, M. S. M. (1997[a]). Effects of aerobic and microaerobic conditions on anaerobic ammonium-oxidizing (Anammox) sludge. *Applied and Environmental Microbiology* 63, 2446 - 2448a.

Strous, M., Van Gerven, E., Ping, Z., Kuenen, J. G., and Jetten, M. S. M. (1997[b]). Ammonium removal from concentrated waste streams with the Anaerobic Ammonium Oxidation (Anammox) process in different reactor configurations. *Water Research* 31, 1955 - 1962b.

Stulgis, R. P., Soydemir, C., and Telgener, R. J. (1995). Predicting landfill settlement. Proc. International Conference GeoEnvironment 2000, Geotechnical Special Publication, pp. 980 - 991.

Stumm, W., and Morgan, J. J. (1981). *Aquatic Chemistry: An Introduction Emphasizing Chemical Equilibria in Natural Waters*. First edition. John Wiley & Sons, Inc., Canada.

Stumm, W., and Morgan, J. J. (1996). *Aquatic Chemistry*. Third edition, John Wiley & Sons, Inc., pp. 473 - 478, New York, USA.

Suflita, J. M., Gerba, C. P., Ham, R. K., Palmisano, A. C., Rathje, W. L., and Robinson, J. A. (1992). The world's largest landfill. *Environmental Science and Technology* 26, 1486-1495.

Suna Erses, A., and Onay, T. T. (2003). Accelerated landfill waste decomposition by external leachate recirculation from an old landfill cell. *Water Science and Technology* 47, 215 - 222.

Tan, T. S., Inoue, T., and Lee, S. L. (1991). Hyperbolic method for consolidation analysis. *Journal of Geotechnical Engineering* 117, 1723 -1737.

Tchobanoglous, G., Burton, F. L., and Stensel, H. D. (2003). *Wastewater Engineering: Treatment and Reuse*. 4th edition. Boston, Metcalf & Eddy, Inc. Eds. McGraw Hill.

Tchobanoglous, G., Theisen, H., and Vigil, S. (1993). *Integrated Solid Waste Management*. McGraw-Hill Book Company, New York.

Tchobanoglous, G. H., and O'Leary, P. R. (1994). *Landfilling. In: Handbook of Solid Waste Management, Kreith F. (Ed.)*. McGraw-Hill Book Company, New York.

Terzaghi, K. (1925). *Structure and volume of voids of soils*. Pages 10, 11, 12 and part of 13 of Erdbaumechanik auf Bodenphysikalisher Grundlage, translated by A. Casagrande in From Theory to Practice in Soil Mechanics. John Wiley and Sons Eds. 1960, New York.

Terzaghi, K. (1943). *Theoretical Soil Mechanics*. John Wiley and Sons Eds., pp. 510, New York.

Thamdrup, B., and Dalsgaard, T. (2002). Production of N_2 through anaerobic ammonium oxidation coupled to nitrate reduction in marine sediments. *Applied and Environmental Microbiology* 68, 1312 - 1318.

Third, K. A., Sliekers, O., Kuenen, J. G., and Jetten, M. S. M. (2001). The CANON system (Completely Autotrophic Nitrogen-removal Over Nitrite) under ammonium limitation: Interaction and competition between three groups of bacteria. *Systematic and Applied Microbiology* 24, 588 - 596.

Tiedje, J. M. (1988). *Ecology of denitrification and dissimilatory nitrate reduction to ammonium*. In: Biology of Anaerobic Microorganisms. Eds. Zehnder, J.B.A., John Wiley and Sons, NY, pp. 179 - 244.

Tong, X. G., Smith, L. H., and McCarty, P. L. (1990). Methane fermentation of selected lignocellulosic materials. *Biomass* 21, 239 - 255.

Uz, I., Rasche, M. E., Townsend, T., Ogram, A. V., and Lindner, A. S. (2003). Characterization of methanogenic and methanotrophic assemblages in landfill samples Proc. Royal Society Ser. B: Biological Sciences, London, pp. S202 - S205.

Van de Graaf, A. A., De Bruijn, P., Robertson, L. A., Jetten, M. S. M., and Kuenen, J. G. (1997). Metabolic pathway of anaerobic ammonium oxidation on the basis of N-15 studies in a fluidized bed reactor. *Microbiology* 143, 2415 - 2421.

Van Soest, P. J., and Robertson, J. B. (1980). *Systems of analysis for evaluating fibrous feeds*. International Research Development Center, Ottawa, Canada, pp. 49 - 60.

Van Soest, P. J., Robertson, J. B., and Lewis, B. A. (1991). Methods for dietary fiber, neutral-detergent fiber and nonstarch polysaccharides in relation to animal nutrition. *Journal of Dairy Science* 74, 3583 - 3597.

Visser, A., Beeksma, I., Van Der Sloot, H. A., Zee, F., Stams, A. J. M., and Lettinga, G. (1993). Anaerobic degradation of volatile fatty acids at different sulphate concentrations. *Applied Microbiology and Technology* 40, 549 - 556.

Visser, A., Pol, L., and Lettinga, G. (1996). Competition of methanogenic and sulfidogenic bacteria. *Water Science and Technology* 33 99 - 110.

Wall, D. K., and Zeiss, C. (1995). Municipal landfill biodegradation and settlement. *Journal of Environmental Engineering* 121, 214 - 224.

Wang, Y. S., Byrd, C. S., and Barlaz, C. S. (1994). Anaerobic biodegradability of cellulose and hemicellulose in excavated refuse samples using a biochemical methane potential assay. *Journal of Industrial Microbiology* 13, 147 - 153.

Wang, Y. U., Odle, W. S., Eleazer, W. E., and Barlaz, M. A. (1997). Methane potential of food waste and anaerobic toxicity of leachate produced during food waste decomposition. *Waste Management and Research* 15, 149 - 167.

Wardwell, R. E., and Nelson, J. D. (1981). Settlement of sludge landfills with fiber decomposition. Proc. Tenth International Conference for Soil Mechanics and Foundation Engineering, pp. 397 - 401.

Waste Management Paper No 26A (1993). Landfill completion: A technical memorandum providing guidance on assessing the completion of licensed landfill sites. Department of the Environment. HMSO, pp. 47, ISBN 0-11-752807-2, London.

Waste Management Paper No 26B (1995). Landfill design, construction and operation practice. Department of the Environment. ISBN 0-11-753185-5, HMSO, London.

Watts, K. S., and Chalres, J. A. (1999). Settlement characteristics of landfill wastes. Proc. of Institution of Civil Engineers, Geotechnical Engineering, pp. 225 - 233.

Watts, K. S., and Charles, J. A. (1990). Settlement of recently placed domestic refuse landfill. Proc. of the Institution of Civil Engineers, Geotechnical Engineering, pp. 971 - 993.

Watts, K. S., and Charles, J. A. (1993). *Building on fill: geotechnical aspects*. Publisher: BRE Centre for Ground Engineering and Remediation.

Welander, U., Henrysson, T., and Welander, T. (1997). Nitrification of landfill leachate using suspended-carrier biofilm technology. *Water Research* 31, 2351 - 2355.

West, M. E., Brown, K. W., and Thomas, J. C. (1998). Methane production of raw and composted solid wastes in simulated landfill cells *Waste Management and Research*, 430 - 436.

White, J. K., Robinson, J. P., and Ren, Q. (2004). Modelling the biochemical degradation of solid waste in landfills. *Waste Management* 24, 227 - 240.

Williams, P. T. (2002). *Waste Treatment and Disposal*. John Wiley Sons Ltd, England.

Woelders, H., and Oonk, H. (1999). Full-scale demonstration of treatment of MSOR in a bioreactor at VAM in Wijster, pp. 376 - 382.

Wolin, M. J. (1974). Metabolic interactions among intestinal microorganisms. *The Americal Journal of Clinical Nutrition* 27, 1320 - 1328.

Yazdani, R., Dahl, K., Byars, M., Mansoubi, A., and Augenstein, D. (2000). Yolo County Controlled Landfill Bioreactor Project. Yolo County Public Works and I E M, Inc. report to the Urban Consortium Energy Foundation (UUCETF) and the Western Regional Biomass Energy Program.

Yen, B. C., and Scanlon, B. (1975). Sanitary landfill settlement rates. *Journal of Environmental Engineering Division, ASCE* 101, 475 - 487.

York, D., Lesser, N., Bellatty, T., Irsai, E., and Patel, A. (1977). Terminal development on a refuse fill site. Proc. Conference on Geotechnical Practice for Disposal of Solid Waste Materials, Ann Arbor, Michigan, pp. 810 - 830.

Young, A. (1992). The effects of fluctuations in atmospheric pressure on landfill gas migration and composition. *Water Air Soil Pollution* 64, 601 - 616.

Young, L. Y., and Frazer, A. C. (1987). The fate of lignin and lignin derived compounds in anaerobic environments. *Geomicrobiology Journal* 5, 261 - 293.

Yuen, S. T. S., and Styles, J. R. (2000). Settlement and characteristics of waste at a municipal solid waste landfill in Melbourne. Proc. International Conference GeoEng 2000.

Zehnder, A. J., Ingvorsen, K., and Marti, T. (1982). *Microbiology of methanogenic bacteria.* In: Anerobic Digestion. Eds. D. E. Hughes et al., Elsevier Biomedical Press, Amsterdam, NL, pp. 45 - 68.

Zehnder, A. J. B. (1978). Ecology of methane formation. *Water Pollution Microbiology* 2, 349–376.

Zehnder, A. J. B., and Brock, T. D. (1979). Methane formation and oxidation by methanogenic bacteria. *Journal of Bacteriology* 137, 420 - 432.

Zeikus, J. G. (1977). The biology of methanogenic bacteria. *Bacteriological Reviews* 41, 514 - 541.

Zeikus, J. G. (1983). Metabolism of one-carbon compounds by chemotropic anaerobes. *Advances in Microbial Physiology* 24, 215 - 241.

Zeikus[a], J. G. (1980). Chemical and Fuel Production by Anaerobic Bacteria. *Annual Review of Microbiology* 34, 423 - 456.

Zeikus[b], J. G. (1980). Proc. 1st International Symposium on Anaerobic Digestion, pp. 75 - 103.

Zeikus[c], J. G. (1980). *Microbial Populations in Digesters.* In: Anaerobic Digestion. Applied Science Publishers Ltd, London, pp. 61 - 89.

Zinder, S. H. (1993). *Physiological ecology of methanogens.* In: Methanogenesis. Eds. J. G. Ferry, Chapman & Hall, New York, pp. 128 - 206.

Zinder, S. H., and Koch, M. (1984). Non - aceticlastic methanogenesis from acetate: acetate oxidation by a thermophilic syntrophic coculture. *Archives of Microbiology* 138, 263 - 272.

Zinder, S. H., and Mah, R. A. (1979). Isolation and characterization of a thermophilic strain, of Methanosarcina unable to use H_2 - CO_2 for methanogenesis. *Applied Environmental Microbiology* 38, 996 - 1008.

Zoino, W. S. (1974). Stabilizing landfills with surcharge. Proc. Highway Research Board Conference, In: Utilization of sanitary landfill as a foundation for transportation facilities, 23rd January, Washington, D. C.